



Benchmark Systems for Small-Signal Stability Analysis and Control

PREPARED BY THE
Power System Dynamic Performance Committee
Power System Stability Controls Subcommittee
Benchmark Systems for Stability Controls Task Force

THIS PAGE LEFT BLANK INTENTIONALLY

IEEE PES Task Force on Benchmark Systems for Stability Controls

Technical Report

Rodrigo Ramos, Chair

Ian Hiskens, Past Chair

Contributors (*alphabetical*)

Claudio Canizares
Tatiane Fernandes
Edson Gerald Jr.
Luc Gerin-Lajoie
Michael Gibbard
Jonas Kersulis

Roman Kuiava
Leonardo Lima
Fernando de Marco
Nelson Martins
Bikash Pal
Artur Piardi

Jhonatan dos Santos
Dinemayer Silva
Abhinav Singh
Behnam Tamimi
David Vowles

August 12th, 2015

This report documents the work of the IEEE PES Task Force (TF) on Benchmark Systems for Stability Controls. The following sections present the objectives of the TF, the guidelines used to select the benchmarks, a brief description of each benchmark system so the reader can select the most suitable system for the intended application, the input data and results for each benchmark system, and a set of conclusions.

Detailed descriptions of each system are also presented in the Appendices to this report and in the website¹ created by this Task Force to share the data and simulation results related to the benchmark systems.

¹ This website is provisionally available at the web address <http://www.sel.eesc.usp.br/ieee>, but it will be transferred to the PSDP web server as soon as the Task Force work is complete.

1. Index	
2. Scope of Work	4
3. Context	4
4. Choice and Validation of the Benchmark Systems	5
5. Data Sets for the Benchmark Systems.....	14
5.1. Data for the 3MIB System	14
5.2. Data for the Brazilian 7-bus Equivalent Model.....	35
5.3. Data for the 2-area (4-generator) system	54
5.4. Data for the 39-bus (New England) System	66
5.5. Data for the Simplified Australian 14-Generator Model.....	80
5.6. Data for the 68-bus (NETS/NYPS) System	95
6. References.....	114
Appendix A - Report on the Simplified Australian 14-Generator Model by Profs. David Vowles and Michael Gibbard.....	A.1
Appendix B - Report on the Simplified Australian 14-Generator Model by Prof. Claudio Canizares and Dr. Behnam Tamimi.....	B.1
Appendix C - Report on the 2-area (4-generator) system by Dr. Leonardo Lima and Dinemayer Silva	C.1

Appendix D - Report on the New England Test System by Prof. Ian Hiskens and Jonas Kersulis.....D.1

Appendix E - Report on the New England Test System by Luc Gerin-LajoieE.1

2. Scope of Work

The objective of this TF is to develop a set of benchmark models that could be used by the research community on small signal stability analysis and control to compare small-signal stability analysis methods and algorithms, as well as to compare different power system stabilizer (PSS) tuning procedures. These benchmarks highlight a number of practical aspects and issues that should be observed while proposing a new tuning procedure for the PSSs (or a new type of power oscillation damper (POD) to enhance the poor damping of the electromechanical oscillations exhibited in each system without adversely impacting other oscillatory modes and other aspects of the system transient response.

3. Context

For many decades, the problem of ensuring adequate damping to the electromechanical oscillations [1] that are typical of large interconnected power systems has attracted the attention of engineers and researchers alike. The classical Power System Stabilizer (PSS), which generates damping torques through the modulation of the excitation level of synchronous generators [2], has been the industry practice for many decades. Many variants of the early phase compensators that were employed in the 1970s have been proposed along this period to cope with or avoid specific technical problems [3].

The classical PSS with a properly tuned phase compensation [4], [5] is still the most cost-effective approach for improving electromechanical oscillation damping and is, therefore, the accepted standard. New control techniques, either in terms of the control loop to be used or the applied tuning technique should be compared with this well-established structure and tuning practice.

The advances in robust control theory have also contributed with a number of alternative proposals to enhance the damping of electromechanical oscillations by supplementary control acting through the Automatic Voltage Regulator (AVR) of synchronous machines [6]. Controllers with structures that are different from the classical lead-lag network that characterizes a PSS have been named Power Oscillation Dampers (PODs) [3], although classical phase compensators, when applied to FACTS devices [7] for the same purpose, have also been referred to as PODs.

Several proposals for advanced PODs or even for tuning techniques for classical PSSs can be found in the literature (see, for instance, [8], [9], and [10]). Many of them claim superior performances for their proposed controllers as compared to those achieved with classical PSSs in terms of robustness, either with respect to changes in the operating point or to nonlinear behaviors in the power system response (or both).

However, the comparisons made to support these claims are based on results for different test systems and damping controller criteria. They often focus on a feature in which the proposed POD is indeed superior to the classical PSS, but neglect other essential practical requirements. These requirements include, for instance, the provision of adequate damping for

multiple modes, non-detrimental interactions with other controllers in the system and control and protection features that do not induce saturation on the PSS output or on the field voltage.

As discussed in the previous paragraphs, there is a clear need for a set of benchmark systems to provide a common basis of comparison among new PSS or POD design alternatives. The next section describes the criteria used to select the benchmark systems and the guidelines to be followed when proposing a new tuning procedure or damping controller structure.

4. Choice and Validation of the Benchmark Systems

Test systems comprising a Single Machine connected to an Infinite Bus (SMIB) have been extensively used for the study of PSS design to damp electromechanical oscillations [1]. The SMIB model very effectively considers the practical aspects related to the field commissioning of stabilizers, since it is quite difficult to perform staged tests that would excite oscillations modes other than the intra-plant and local modes [11]. Despite being an excellent starting point for the analysis of electromechanical oscillations (due to its simplicity, which allows a clear understanding of the underlying principle that gives rise to these oscillations), the simplifications inherent to the SMIB model lead to well-documented limitations when dealing with different aspects of the electromechanical oscillations in a large interconnected power system [10].

The current challenges in this area include the coordination of multiple damping controllers, the damping enhancement for multiple modes and dealing with controllability issues when considering multiple scenarios, for example. Therefore, the guidelines used for the choice of the benchmark systems address the above issues as well as the following:

- a) Each chosen benchmark system must have unique characteristics and present a challenge from the viewpoint of small signal stability analysis and control that would not be apparent or properly captured by a SMIB model. Additionally, a controller must be proposed to overcome this challenge without compromising other relevant aspects from practice;
- b) The addition of a proposed controller to a system under expansion should be made in coordination with the previously existing controllers. However, the simultaneous design of several controllers will rarely be required in practice, so the approaches that propose the design or tuning of one or two controllers are considered closer to practice and of higher interest;
- c) The proposed controllers must deal with the multiple modes that exist in multi-machine systems and, therefore, SMIB models are not adequate to present new controller proposals on such control design coordination. The benchmarks must therefore have multiple machines and exhibit a combination of local and inter-area modes to be damped by the proposed controllers. Other types of modes (such as intra-plant ones, for example) can also be present in the models to better reflect the system conditions from practice;
- d) When the system is subjected to a small perturbation, the damping action of the controller must be evident with respect to the open-loop case, while avoiding saturation of the controller output and of the field voltage. For this reason, each benchmark must be provided with at least one set of nonlinear simulation results of the system response to a not so small perturbation, and the simulation results must

include the responses of rotor angle (or speed), damping controller output and field voltage.

In order to better focus on the damping control issue, small-scale test systems were chosen to keep the benchmarks simple and easy to handle, while still maintaining the characteristics that are of interest to actual practice. Robustness with respect to changes in the operating point and to nonlinear behavior excited by large disturbances, although a mandatory feature for any proposed controller, have unfortunately not been considered in most of the proposed systems: only one of the benchmark systems has multiple generation and load dispatch scenarios.

Based on these guidelines, six benchmark systems are presented in this report, covering different aspects of practical interest to electromechanical oscillation damping control. To elevate these systems to benchmark status, their computer models were simulated, whenever possible, in at least two commercial-grade software and the results of these simulations were compared. When a satisfactory level of agreement was achieved between these results, the system was considered to be a validated benchmark. Unavoidable discrepancies between the results from the different simulators (due to the different generator and controller models available in different software, for example) were highlighted and their probable source discussed.

Reports on these validation processes, as well as the complete set of data for each of the benchmark systems, can be found (provisionally) at the URL <http://www.sel.eesc.usp.br/ieee/> [12]. For brevity, this URL will be referred to as "the TF website" in the remainder of this report. The TF website also provides a set of data files describing the component models for the benchmark systems (generators and their respective controllers, as well as for the network data) which were used to obtain the described simulation results. It is, however, worth emphasizing that this TF does not recommend or endorse the use of any specific component model or simulation software to perform the small-signal stability analyses or the nonlinear simulations in order to reproduce the reported results. The recommendation is to choose, within the set of models available in the software of choice, that one which exhibits the closer match to the reported results.

Based on the above-mentioned guidelines, the benchmark systems validated by this Task Force are summarized in Table 4.1 and briefly presented in the following subsections, so readers can select the most suitable one for the purposes of their work. The systems are listed in ascending order according to their respective number of buses.

Table 4.1: Description of the benchmark systems

System	Buses	Generators	Feature
#1	6	3	Simultaneous damping of intra-plant, local (inter-plant) and inter-area modes
#2	7	5	Poor controllability due to zeros in the vicinity of the critical electromechanical mode
#3	11	4	Simultaneous damping of local and inter-area modes in a system with a highly symmetrical structure

#4	39	10	Coordination of multiple stabilizers to damp electromechanical modes within a control area
#5	59	14	Simultaneous damping of local and inter-area modes of a longitudinal system considering multiple operating conditions
#6	68	16	Coordination of multiple stabilizers to damp multiple local and inter-area modes

4.1. The Three-Machine versus Infinite-Bus System (3MIB)

The 3-machine-infinite bus (3MIB) benchmark system shown in Figure 4.1 is comprised of 6 buses and 3 generators. It was proposed in [11] to show the effectiveness of power system stabilizers to simultaneously contribute to the damping of electromechanical modes of different nature, ranging from the intra-plant to the inter-area modes in terms of frequency.

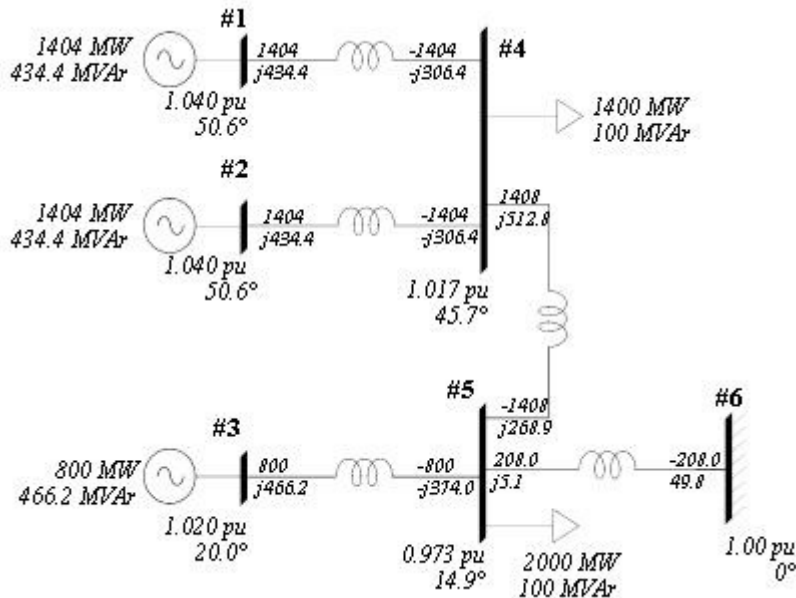


Figure 4.1: The Three-Machine Infinite-Bus system (3MIB)

In the given operating point, three electromechanical modes are clearly identified from the system eigensolution, which can be classified into intra-plant (oscillation between generators #1 and #2), inter-plant (generators #1 and #2 oscillating against generator #3), and inter-area (the three generators oscillating coherently against the infinite bus, with the infinite bus considered to be the equivalent representation of an external area).

Detailed small-signal stability results are given [13], while nonlinear results are presented in [14]. Power flow results are given for a single operating point. Including other operating points, for the assessment of control design robustness, are recommended by the TF for future work.

4.2. The Brazilian 7-Bus Equivalent Model

This 7-bus, 5-machine equivalent model of the South-Southeastern Brazilian system configuration in the late 1980's, disregarding the large HVDC Itaipu transmission system, has been used in several small-signal stability related works (an example is reference [10]). All of its synchronous generators are described by fifth-order models and have first-order automatic voltage regulator models. The single-line diagram for this system is depicted in Figure 4.2. Bus 7 represents an equivalent of the southeastern part of the system.

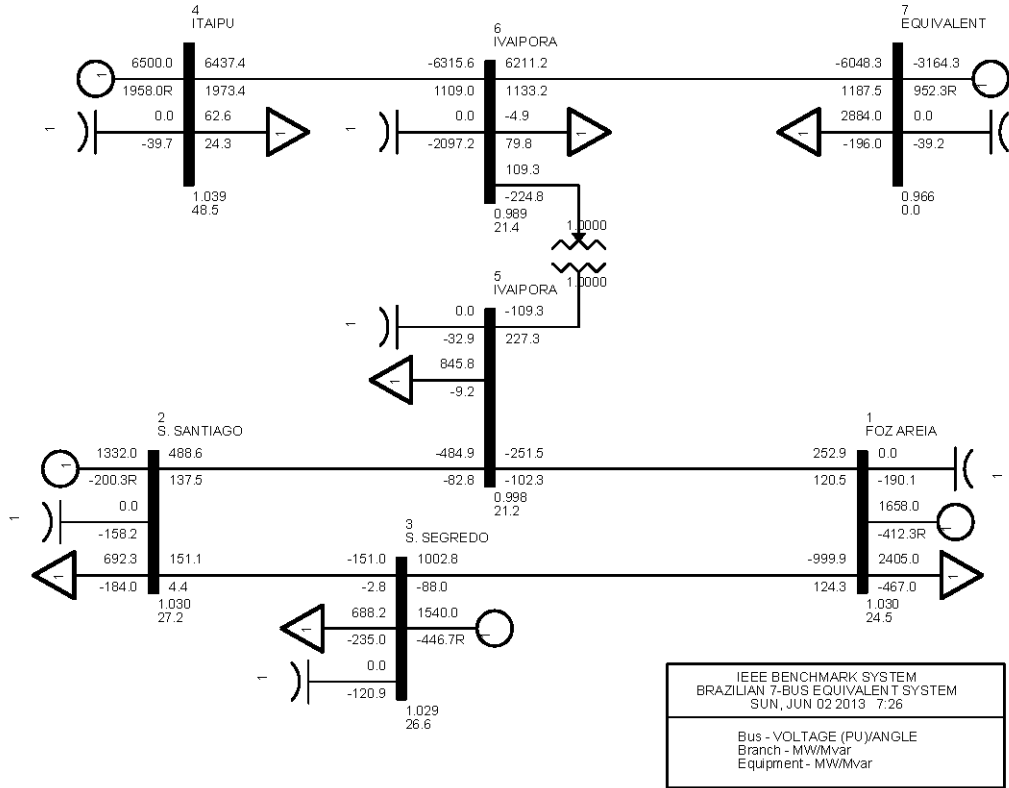


Figure 4.2: The Brazilian 7-bus equivalent system

This system highlights a modal controllability problem that may exist in multi-machine systems, in which a single generator, despite having the largest magnitude of the transfer function residue [15], [16] (thus a relatively good modal observability and controllability), might be unable to provide enough damping via excitation control to a poorly-damped inter-area mode. In this benchmark system, this single control-loop impossibility arises due to the presence of a poorly-damped complex-conjugate pair of zeros in the single-input, single-output (SISO) transfer function associated with the PSS transfer function at the Itaipu plant. The root-locus shows branches starting at the open-loop unstable poles and approaching the transfer function zeros as the PSS gain is increased². One possible solution is to install a PSS at a second machine, in order to eliminate the problematic SISO transfer function zeros, and thus allow the PSS at the Itaipu machine to move the unstable open-loop pole further into the left-half of the complex plane [17].

² The ends of these root-locus branches are defined by the mentioned zeroes that are located close to the imaginary axes of the s-plane in such a way that the closed loop poles, for whatever PSS gain and phase compensation, result poorly damped.

4.3. The Two-Area, 4-Generator System

The two-area, 4-generator system is very well-suited for the study of concepts related to the different nature of local and inter-area modes. The one-line diagram for this system is shown in Figure 4.3.

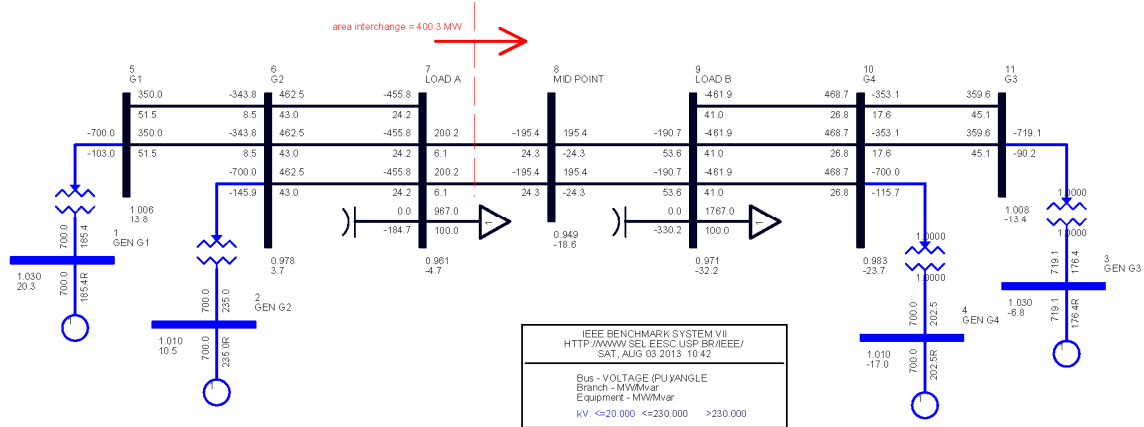


Figure 4.3: The 2-area, 4-generator system

This test system first appeared in [18] and then in several other works including [16], where this system is very well documented.

The symmetric structure and the easy modeling of its components, coupled with the conceptually clear results produced, contributed to the pervasive use of this system in small-signal stability analysis work. The system is comprised by Area 1, located to the left of the dashed red line (shown in Figure 4.3), and by Area 2, located to the right of the same red dashed line. The two local modes, related to areas 1 and 2, respectively, can have almost identical frequencies (depending on the power flow conditions, among other factors [18]). The inter-area mode for this system involves Area 1 oscillating against Area 2 at a lower frequency and, under certain circumstances, can only be properly damped by a suitable coordination of PSS tunings or by the addition of other types of controller structures to the system.

Due to its highly symmetrical topology, the eigenstructure of this system reveals a clear separation among the eigenvalues, eigenvectors and participation factors related to the local and inter-area modes. Therefore, the modes can be easily related to their respective invariant subspaces in the state-space model, and thus it is also straightforward to apply perturbations that predominantly excite one of these modes at a time [3].

While this system symmetry contributes to simplifying the description of the concepts involved in small-signal stability analysis, it must be emphasized that such a feature will seldom be seen in real, large-scale systems. It is therefore important to have in mind the use of the 2-area, 4 generator system should be limited to cases for proof-of-concept or illustration of a particular feature. Successful results obtained when using this system should not automatically lead to claims about real-life systems, which will certainly not exhibit this level of symmetry.

4.4. The 39-bus (New England) System

The New England test system has been extensively used in the power system dynamics literature, as far back as in [19], and possibly even before that. The system has 39 buses, 9 generators and 1 equivalent generator that represents the New York system to which the New England system is interconnected [20], [21]. The TF website provides the system data for a base case, together with results of small-signal analysis and nonlinear simulations.

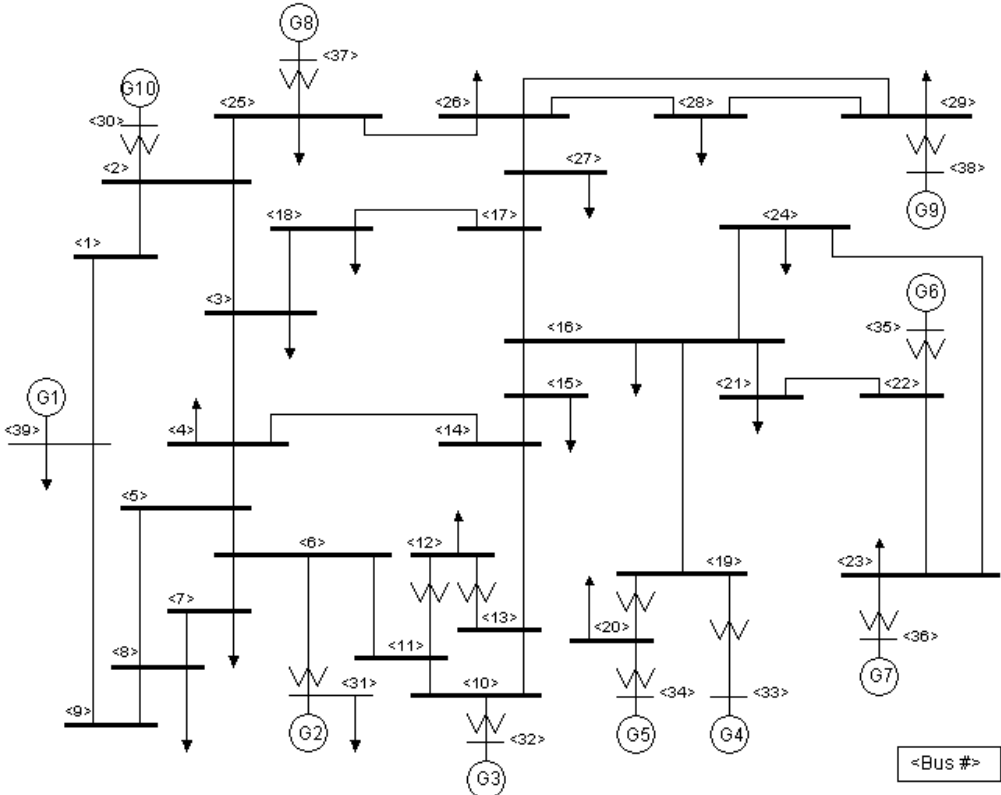


Figure 4.4: The New England system

Figure 4.4 presents the one-line diagram of the New England system. Almost all electromechanical modes in this system have a local or regional nature, except for one that represents the oscillation of all generators within the New England Area (generators 2 to 10) against the equivalent generator representing the New York Area (generator 1). This last-mentioned mode has the lowest frequency and should be regarded as a New England versus New York inter-area mode, with all generators within New England area oscillating coherently, against the New York equivalent (generator 1).

This system does not present much of a challenge from the small signal stability viewpoint and is included mostly for historical reasons and for the sake of verifying the compatibility among different software. The emphasis of the presented results is on avoiding detrimental interactions among the multiple PSSs that have to provide adequate damping for both the local mode of their respective generators and the inter-area mode.

4.5. The Simplified Australian 14-Generator Model

The simplified 14 generator model of the southern and eastern Australian system is representative of the longitudinal Australian system that extends for some 5000 km from Pt. Lincoln in South Australia to Cairns in far north Queensland. The one-line diagram of this 50 Hz system is shown in Figure 4.5. It is characterized by four weakly connected regions resulting in three inter-area modes of oscillation as well as 10 local area modes. Without PSSs many of these modes are either unstable or inadequately damped. The system also includes five Static Var Compensators (SVCs) and a series compensated transmission line. The generators are represented by 5th or 6th order models. Two basic types of excitation systems are employed from IEEE Std 421.5(2005) [4]: static excitation system ST1A and rotating ac exciter AC1A.

Base cases for six different system operating conditions representing a range of system loading and interconnection power flow conditions are provided. The six cases are prudently chosen to encompass a set of normal operating conditions; this leads to the resulting P-V_r characteristics that forms the basis of the conventional PSS tuning procedure [22], [23] which is adopted and demonstrated in this benchmark. This is done because the robustness of stabilizers for a wide range of operating conditions is essential. Thus, this benchmark system provides a firm basis on which alternative advanced stabilizer tuning procedures can be assessed.

Appendix A of this report provides a comprehensive description of the benchmark system including the following:

1. A description of the benchmark system and the base case scenarios.
2. A description of the theoretical basis for the benchmark PSS tuning procedure that was employed together with the P-V_r characteristics [22], [23] for each of the 14 generators in each of the six base cases.
3. A comparison between the 13 electromechanical modes with the PSSs in- and out-of-service for each base case.
4. Listing of all network, generator and controller parameters sufficient for both small-signal and transient stability analysis.
5. Verification of the small-signal model of the six base case scenarios by comparison of small-disturbance step responses obtained with two different software packages.
6. A comprehensive set of transient stability studies conducted to demonstrate that with the benchmark PSSs in-service the six base case scenarios are transiently stable for all credible contingencies involving a two-phase to ground fault and associated de-energization of the faulted transmission element.
7. A list of references.

The TF website [12] provides the following data.

1. The power flow data for each of the six base cases;
2. The dynamic data of the system for small-signal stability and transient stability analysis;
3. State-space models and associated eigenanalysis results of the system with the PSSs in- and out-of-service for two of the six base cases;
4. Time-series data from small-disturbance step-response simulations;
5. Time-series data from transient-stability simulations;

Appendix A also describes the formats in which all data mentioned in the previous lists are available.

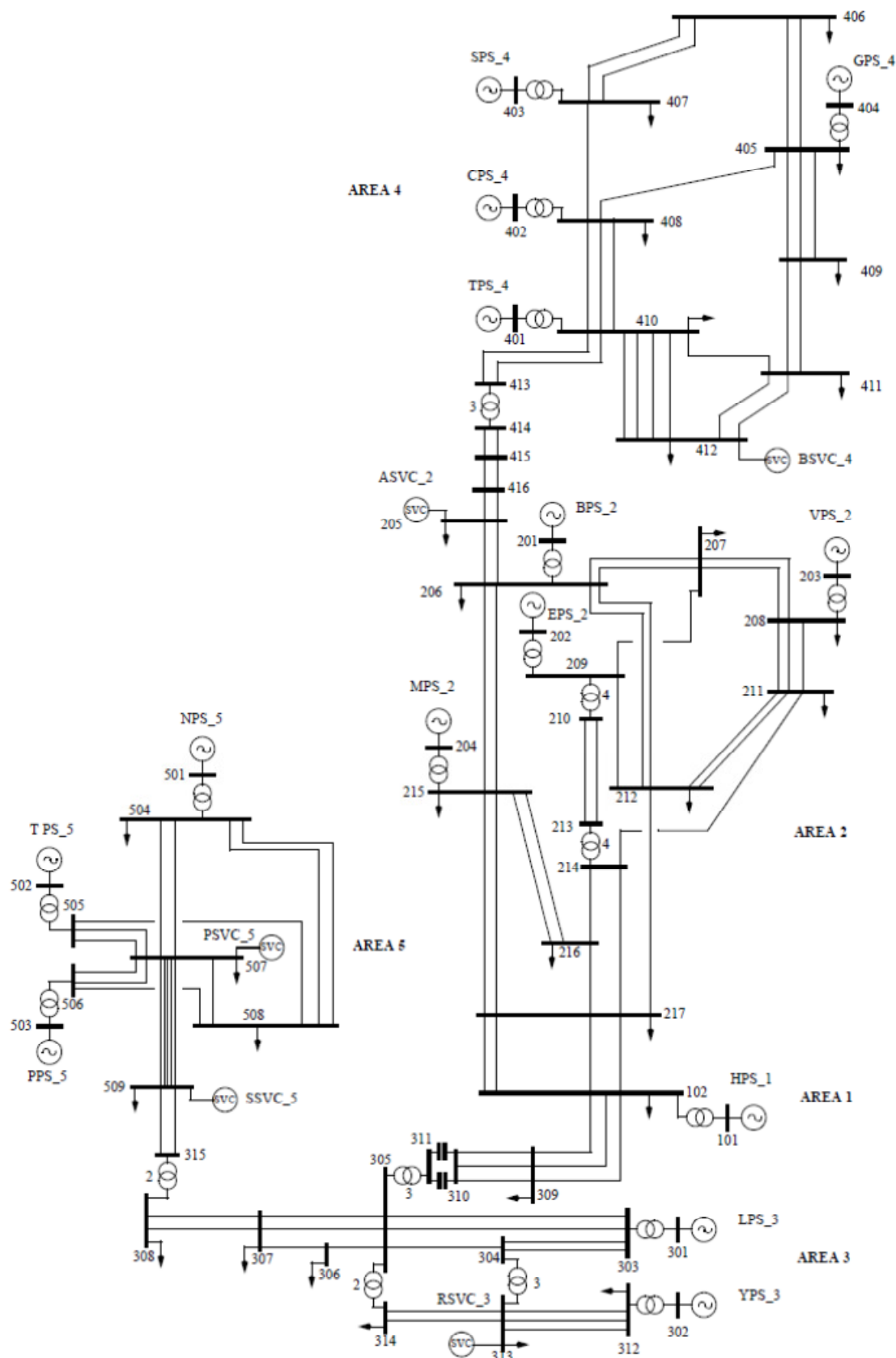


Figure 4.5: Simplified 14-generator model of the South and East Australian Power System

4.6. The 68-bus (New England/New York Interconnection) System

The 68-bus system is a reduced order equivalent of the inter-connected New England test system (NETS) and New York power system (NYPS), with five geographical regions out of which NETS and NYPS are represented by a group of generators, whereas the power import from each of the three other neighboring areas are approximated by equivalent generator models, as shown in Figure 4.6. This model was created after the 1965 blackouts and represents part of the power network of that region in the 1970s.

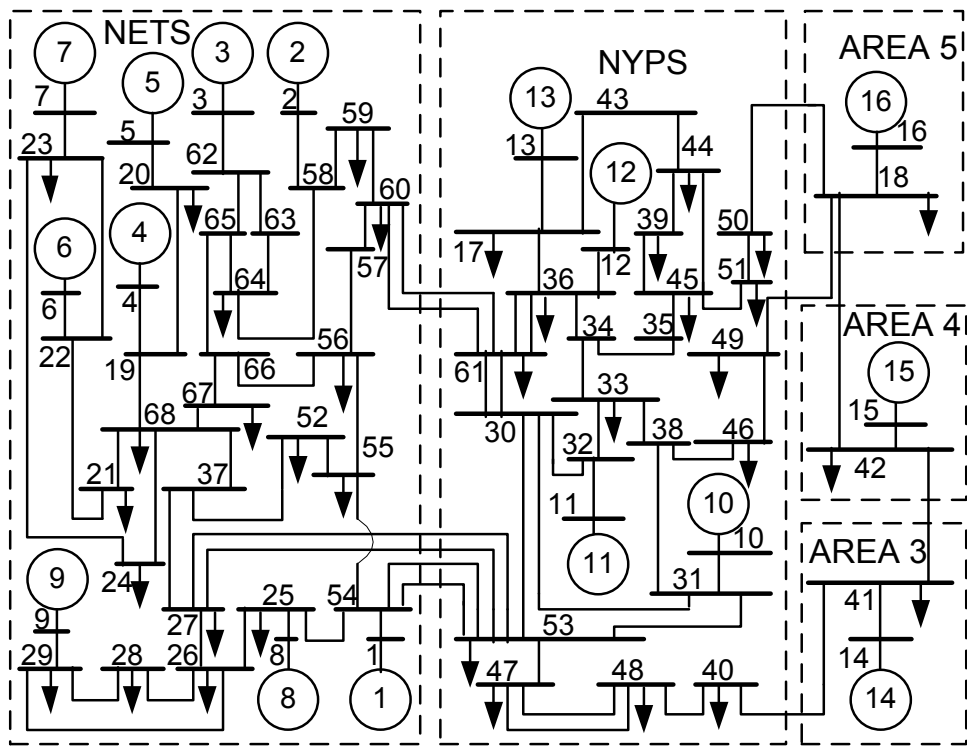


Figure 4.6: The 68-bus system

There are three major tie-lines between NETS and NYPS (connecting buses 60-61, 53-54 and 27-53). All the three tie-lines are double-circuit lines. Generators G1 to G12 have IEEE Std 421.5(2005) [4] DC4B excitation systems, except for G9, which has an ST1A static excitation system. There are four inter-area modes present in the system, and all of them have a high participation from the mechanical states of G14, G15 and G16.

The challenge in this system resides in the difficulty to damp its local and inter-area modes simultaneously. An interesting research problem for this system is whether it is possible to get adequate damping for the inter-area modes without relying on PODs for FACTS devices [8].

5. Data Sets for the Benchmark Systems

5.1. Data for the 3MIB System

5.1.1. Power Flow Data

The power flow solution is printed in Figure 5.1, over the one-line diagram of the system. The bus data, including the voltage magnitudes and angles from the power flow solution, are shown in Table 5.1. The transmission line data is shown in Table 5.2. The data is provided in percent considering a system MVA base of 100 MVA. The generator step-up transformers (GSU) are explicitly represented in the case. Table 5.3 presents the GSU data, on system MVA base (100 MVA).

There are two loads, directly connected to the high-voltage buses 4 and 5. A large load was added to bus 6 to ensure that the equivalent machine at the infinite bus is a generator (injecting power into the grid), although this is probably unnecessary and the results would be practically the same with the infinite bus absorbing power from the grid. The associated data is given in Table 5.4.

These loads are represented, in the dynamic simulation, with a combination of constant power, constant current and constant admittance characteristics for the active power and reactive power, as shown in Table 5.4. The power flow data for this system is given in Table 5.5.

Table 5.1: Bus Data and Voltages from the Power Flow Solution

Bus Number	Bus Name	Base kV	Bus type	Voltage (pu)	Angle (deg)
1	GENERATOR 1	18.0	PV	1.0400	50.57
2	GENERATOR 2	18.0	PV	1.0400	50.57
3	GENERATOR 3	18.0	PV	1.0200	20.05
4	PLANT HV 1	500.0	PQ	1.0169	45.69
5	PLANT HV 2	500.0	PQ	0.9728	14.87
6	INFINITE BUS	500.0	swing	1.0000	0.00

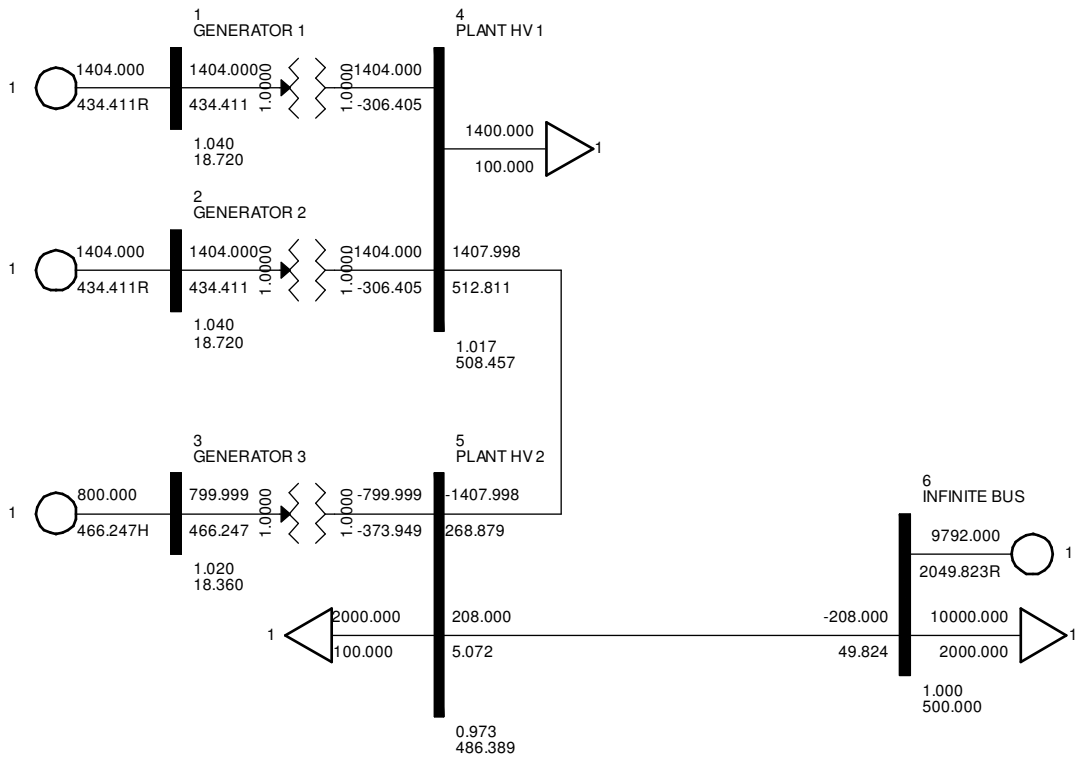


Figure 5.1: One-line Diagram and Power Flow Solution of Benchmark Model #1

Table 5.2: Transmission Line Data (100 MVA Base)

From Bus	To Bus	ckt id	R (%)	X (%)	Charging (%)
4	5	1	0.00	3.6	0.0
5	6	1	0.00	12.0	0.0

Table 5.3: Generator Step- Up Transformer Data (100 MVA Base)

From Bus	To Bus	R (%)	X (%)	MVA Base	tap (pu)
1	4	0	0.641	1560	1
2	4	0	0.641	1560	1
3	5	0	1.12	890	1

Table 5.4: Load Data

Bus	Bus Loads		ZIP Load Parameters	
	P (MW)	Q (MVar)	P	Q
4	1400	100	80% I 20% Z	100% Z
5	2000	100	100% P	100% Z
6	10000	2000	100% P	100% P

Table 5.5: Power Flow Solution Printout

BUS	1 GENERATOR 1	18.000	CKT	MW	MVAR	MVA	%	1.0400PU	50.57	X---	LOSSES	--X
FROM	GENERATION			1404.0	434.4R	1469.7	94	18.720KV		MW	MVAR	
TO	4 PLANT HV 1	500.00	1	1404.0	434.4	1469.7		1.0000LK		0.00	128.01	
BUS	2 GENERATOR 2	18.000	CKT	MW	MVAR	MVA	%	1.0400PU	50.57	X---	LOSSES	--X
FROM	GENERATION			1404.0	434.4R	1469.7	94	18.720KV		MW	MVAR	
TO	4 PLANT HV 1	500.00	1	1404.0	434.4	1469.7	94	1.0000LK		0.00	128.01	
BUS	3 GENERATOR 3	18.000	CKT	MW	MVAR	MVA	%	1.0200PU	20.05	X---	LOSSES	--X
FROM	GENERATION			800.0	466.2H	926.0	104	18.360KV		MW	MVAR	
TO	5 PLANT HV 2	500.00	1	800.0	466.2	926.0	104	1.0000LK		0.00	92.30	
BUS	4 PLANT HV 1	500.00	CKT	MW	MVAR	MVA	%	1.0169PU	45.69	X---	LOSSES	--X
								508.46KV		MW	MVAR	
TO	LOAD-PQ			1400.0	100.0	1403.6						
TO	1 GENERATOR 1	18.000	1	-1404.0	-306.4	1437.0		1.0000UN		0.00	128.01	
TO	2 GENERATOR 2	18.000	1	-1404.0	-306.4	1437.0	92	1.0000UN		0.00	128.01	
TO	5 PLANT HV 2	500.00	1	1408.0	512.8	1498.5				0.00	781.69	
BUS	5 PLANT HV 2	500.00	CKT	MW	MVAR	MVA	%	0.9728PU	14.87	X---	LOSSES	--X
								486.39KV		MW	MVAR	
TO	LOAD-PQ			2000.0	100.0	2002.5						
TO	3 GENERATOR 3	18.000	1	-800.0	-373.9	883.1	99	1.0000UN		0.00	92.30	
TO	4 PLANT HV 1	500.00	1	-1408.0	268.9	1433.4				0.00	781.69	
TO	6 INFINITE BUS500.00	1		208.0	5.1	208.1				0.00	54.90	
BUS	6 INFINITE BUS500.00	CKT		MW	MVAR	MVA	%	1.0000PU	0.00	X---	LOSSES	--X
FROM	GENERATION			9792.0	2049.8R10004.3	10	500.00KV			MW	MVAR	
TO	LOAD-PQ			10000.0	2000.0	10198.0						
TO	5 PLANT HV 2	500.00	1	-208.0	49.8	213.9				0.00	54.90	

5.1.2. Dynamic Data

The generator model used to represent the salient pole units (generators 1 and 2) is shown in the block diagram in Figure 5.2. This is a 5th order dynamic model with the saturation function represented as a geometric (exponential) function. Similarly, the generator model to represent the round rotor unit (generator 3) is in the block diagram in Figure 5.3. This is a 6th order dynamic model with the saturation function represented as a geometric (exponential) function. The corresponding parameters for these models can be found in Table 5.6 and Table 5.7, respectively.

Table 5.6: Dynamic Model Data for the Salient Pole Units

PARAMETERS				
Description		Symbol	Value	Unit
Rated apparent power		MBASE	1560	MVA
d-axis open circuit transient time constant		T' _{do}	5.10	s
d-axis open circuit sub-transient time constant		T'' _{do}	0.060	s
q-axis open circuit sub-transient time constant		T'' _{qo}	0.094	s
Inertia		H	4.50	MW.s/MVA
Speed damping		D	0	pu
d-axis synchronous reactance		X _d	0.89	pu
q-axis synchronous reactance		X _q	0.66	pu
d-axis transient reactance		X' _d	0.36	pu
sub-transient reactance		X'' _d = X'' _q	0.29	pu
Leakage reactance		X _ℓ	0.28	pu
Saturation factor at 1.0 pu voltage		S(1.0)	0.087	—
Saturation factor at 1.2 pu voltage		S(1.2)	0.257	—

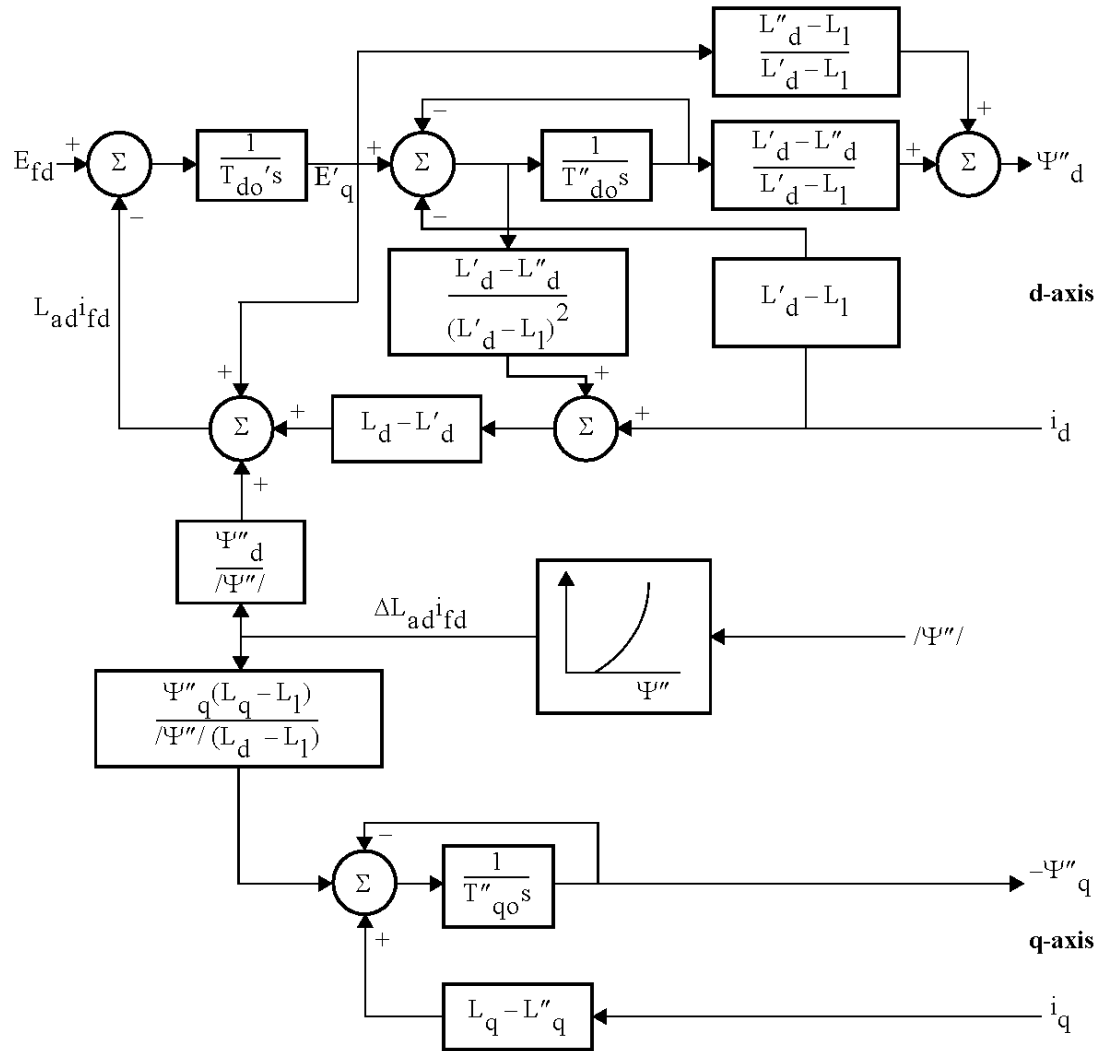


Figure 5.2: Block Diagram for the Salient Pole Machine Model

Table 5.7: Dynamic Model Data for the Round Rotor Units

PARAMETERS				
Description	Symbol	Value	Unit	
Rated apparent power	MBASE	890	MVA	
d-axis open circuit transient time constant	T'_{do}	5.30	s	
d-axis open circuit sub-transient time constant	T''_{do}	0.048	s	
q-axis open circuit transient time constant	T'_{qo}	0.62	s	
q-axis open circuit sub-transient time constant	T''_{qo}	0.066	s	
Inertia	H	3.90	MW.s/MVA	
Speed damping	D	0	pu	
d-axis synchronous reactance	X_d	1.72	pu	
q-axis synchronous reactance	X_q	1.679	pu	
d-axis transient reactance	X'_d	0.488	pu	

q-axis transient reactance	X'_q	0.80	pu
sub-transient reactance	$X''_d = X''_q$	0.337	pu
Leakage reactance	X_ℓ	0.266	pu
Saturation factor at 1.0 pu voltage	$S(1.0)$	0.0001	-
Saturation factor at 1.2 pu voltage	$S(1.2)$	0.001	-

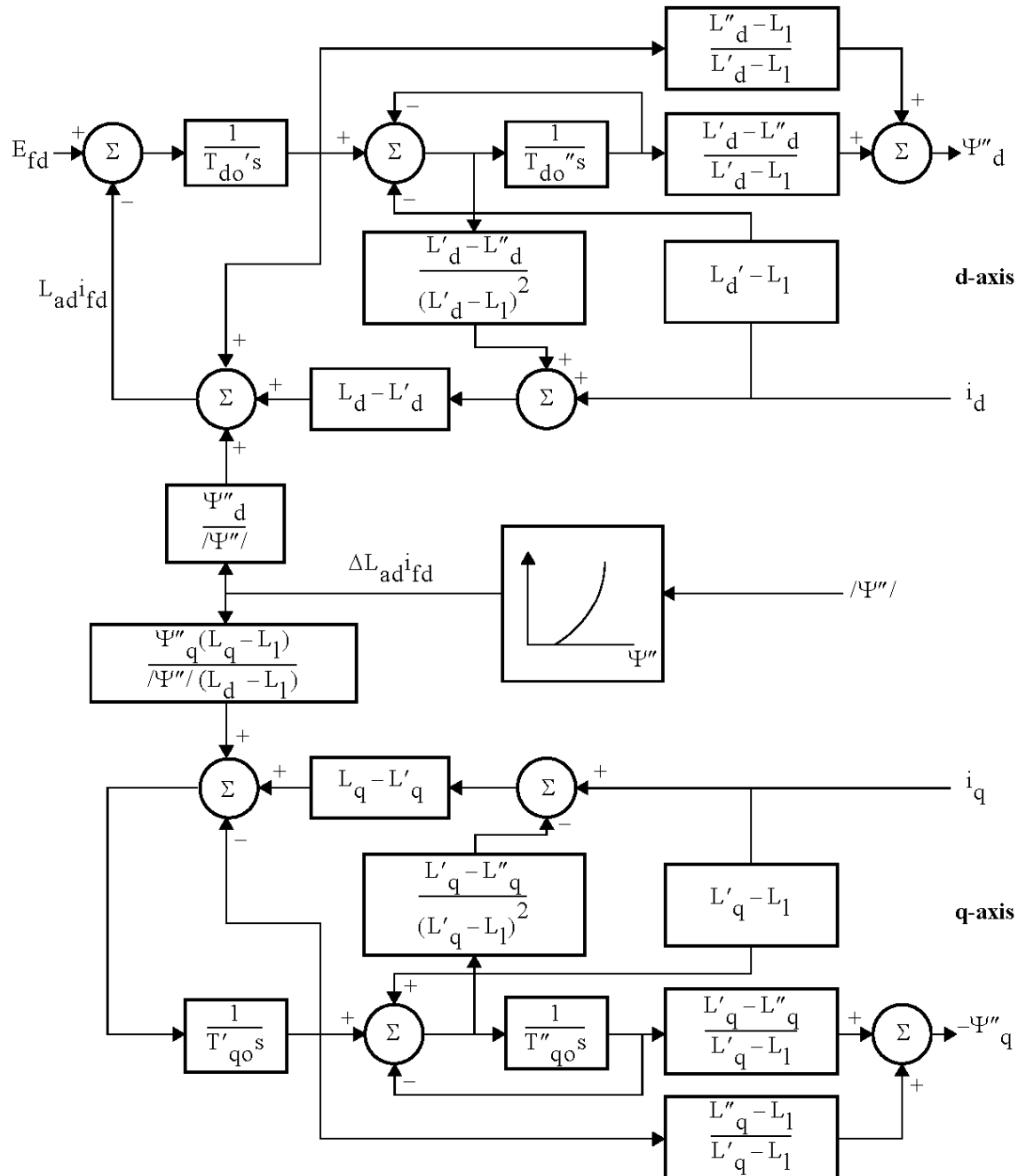


Figure 5.3: Block Diagram for the Round Rotor machine model

The details associated with the representation of the saturation of the generators should not significantly impact the results of a small-signal (linearized) analysis of the system performance. On the other hand, the proper representation of saturation is extremely important for transient stability and the determination of rated and ceiling conditions (minimum and maximum generator field current and generator field voltage) for the excitation system. The calculated rated field current for this generator model is 2.75 pu (considering 0.80 rated power factor). This calculation comprises the initialization of the generator model at full (rated) power output, considering their rated power factor.

The excitation systems are represented by a simple first order model, for which the block diagram is shown in Figure 5.1. The parameters for the model are presented in Table 5.8. Note that the Transient Gain Reduction (TGR) is not used, so $T_A = T_B = 1$.

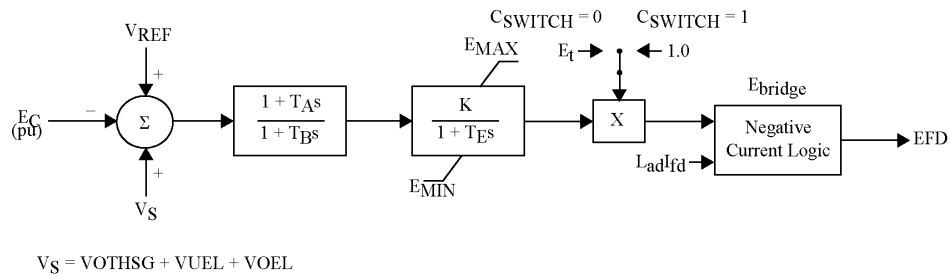


Figure 5.4: Block Diagram for the Excitation System model

Table 5.8: Dynamic Model Data for the Excitation Systems

PARAMETERS			
Description	Symbol	Value	Unit
Transient Gain Reduction	T_A/T_B	1	s
TGR block 2 numerator time constant	T_B	1	s
AVR steady state gain	K_A	100^{\dagger}	pu
AVR equivalent time constant	T_E	0.05	s
Min. AVR output	V_{Rmin}	-5	pu
Max. AVR output	V_{Rmax}	5	pu
excitation power supply option	C_{SWITCH}	$1^{\ddagger\ddagger}$	-
negative field capability	r_C/r_{fd}	$0^{\ddagger\ddagger\ddagger}$	-

Notes:

[†] AVR gains for generators 1 and 2 are $K_A=100$; for Generator 3 the gain is $K_A = 150$.

[‡] The parameter “ C_{SWITCH} ” determines if the excitation system is bus-fed ($C_{SWITCH}=0$) or independently fed ($C_{SWITCH}=1$). The excitation systems are represented as independently fed.

^{††} The excitation system is represented with negative field current capability.

The IEEE Std. 421.5(2005) model PSS1A, which is shown in Figure 5.5, is used to represent the power system stabilizers. The parameters for this model are presented in Table 5.9. The output limits were set to $\pm 5\%$, while the logic to switch off the PSS for voltages outside a normal operation range has been ignored (parameters V_{CU} and V_{CL} set to zero).

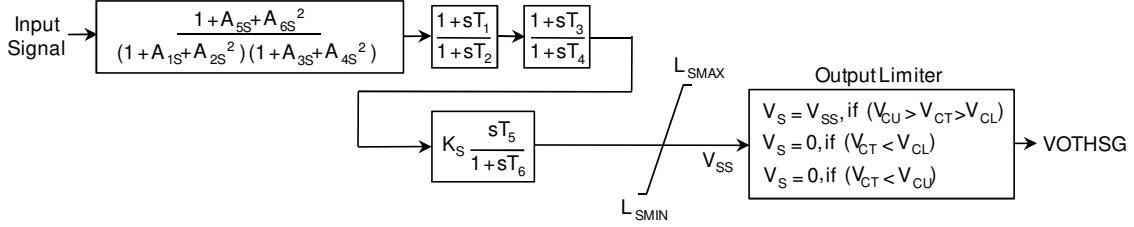


Figure 5.5: Block Diagram for the PSS1A model

Table 5.9: Parameters for the PSS1A Power System Stabilizers

PARAMETERS				
Description	Symbol	Value	Unit	
2 nd order denominator coefficient	A ₁	0.641		
2 nd order denominator coefficient	A ₂	0		
2 nd order numerator coefficient	A ₃	0		
2 nd order numerator coefficient	A ₄	0		
2 nd order denominator coefficient	A ₅	0.158		
2 nd order denominator coefficient	A ₆	0		
1 st lead-lag numerator time constant	T ₁	0.142	s	
1 st lead-lag denominator time constant	T ₂	0.014	s	
2 nd lead-lag numerator time constant	T ₃	0.142	s	
2 nd lead-lag denominator time constant	T ₄	0.014	s	
Washout block numerator time constant	T ₅	3	s	
Washout block denominator time constant	T ₆	3	s	
PSS gain	K _S	35	pu	
PSS max. output	L _{Smax}	0.05	pu	
PSS min. output	L _{Smin}	-0.05	pu	
Upper voltage limit for PSS operation	V _{Cu}	0	pu	
Lower voltage limit for PSS operation	V _{Cl}	0	pu	

5.1.3. Selected Results and Validation

The results presented in the following correspond to eigenstructure calculations and time-domain simulations of different disturbances performed with the PSS/E [24] and PacDyn/ANATEM [25], [26] software packages.

Regarding eigenstructure calculation, the complete set of eigenvalues for the system without PSSs, calculated with PSS/E program LSYSAN [24] and PacDyn [25], are presented in Figure 5.6.a. Figure 5.6.b is an enlarged view of Figure 5.6.a in the region of the electromechanical modes. The speed mode-shapes of the three electromechanical modes calculated by both programs are shown in Figure 5.7. The mode-shapes calculated by LSYSAN had been normalized by the respective elements of highest magnitude.

The comparison of results in Figure 5.6 and Figure 5.7 shows a good matching of the electromechanical modes and their respective speed mode-shapes calculated by the different software.

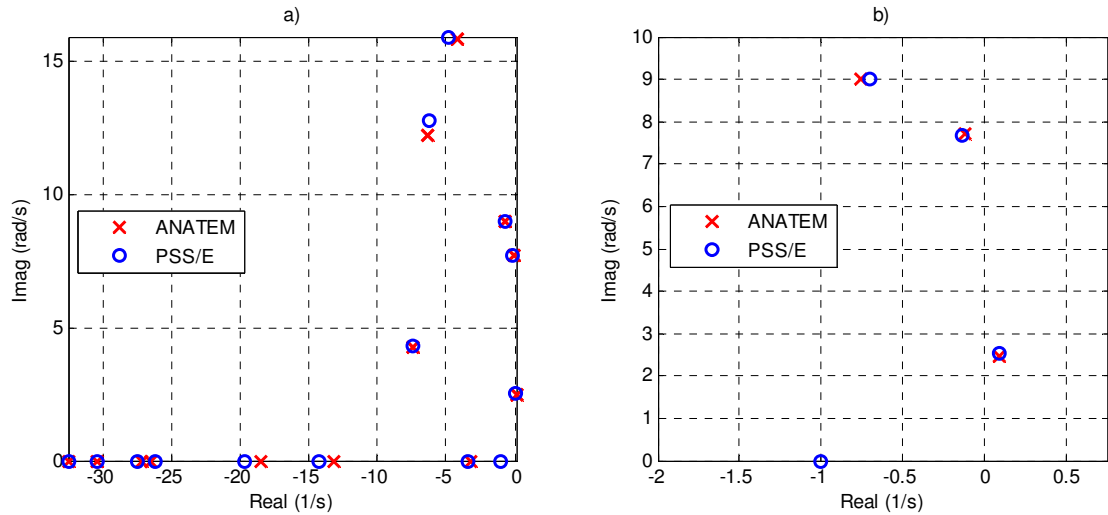


Figure 5.6: Comparison of Eigenvalues Calculated with PSS/E Program LSYSAN [24] and PacDyn [25].
a) Complete set of eigenvalues; b) Enlarged view in the region of the electromechanical modes.

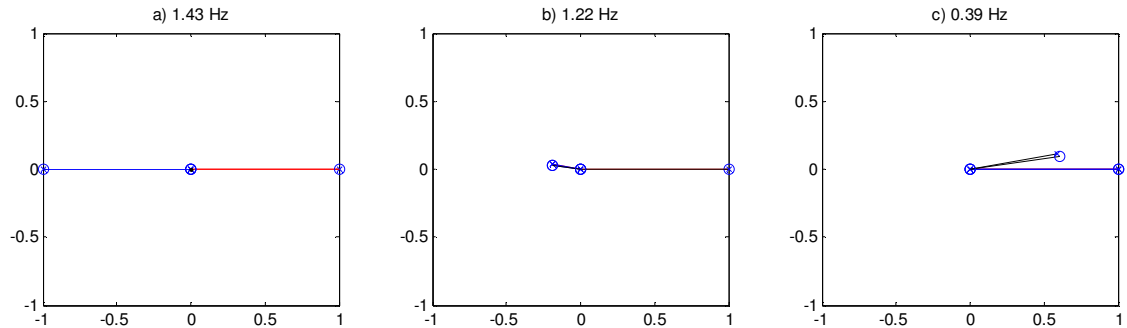


Figure 5.7: Comparison of the Speed Mode-shapes Calculated with PSS/E Program LSYSAN (x) and PacDyn (o).

Regarding the mode shape figures in Figure 5.7:

- a) the 1.43 Hz intraplant mode shows the rotors of Gen 1 and Gen 2 oscillating against each other;
- b) the 1.22 Hz interplant mode is characterized by the coherent oscillation of Gen 1 and Gen 2 generators oscillating against Gen 3. Gen 3 oscillates with a larger magnitude since it has a lighter inertia and capacity as compared to the combined inertia of Gen 1 and Gen2; and
- c) the 0.39 Hz interarea mode is characterized by the coherent oscillation of all three generators against the "infinite bus" placed at bus 6.

Figure 5.8 is reproduced from [11] (Fig. 22 in [11]) and shows the phase compensation requirements for a PSS installed at generator #1 of the 3MIB benchmark system in order to best damp its three electromechanical modes of different frequencies and nature. This figure also shows that the PSS phase compensation requirements for these different modes can be individually computed from three independent SMIB system models that share the same generator and controller data but have different tie line impedances and local load values. Advocating the use of this simpler set of SMIB results (results from "a SMIB family") for

preliminary PSS tuning in multimachine systems is basically the essence of [11], which is just, on its turn, a ready-to-use automated version of the classic GEP method [1].

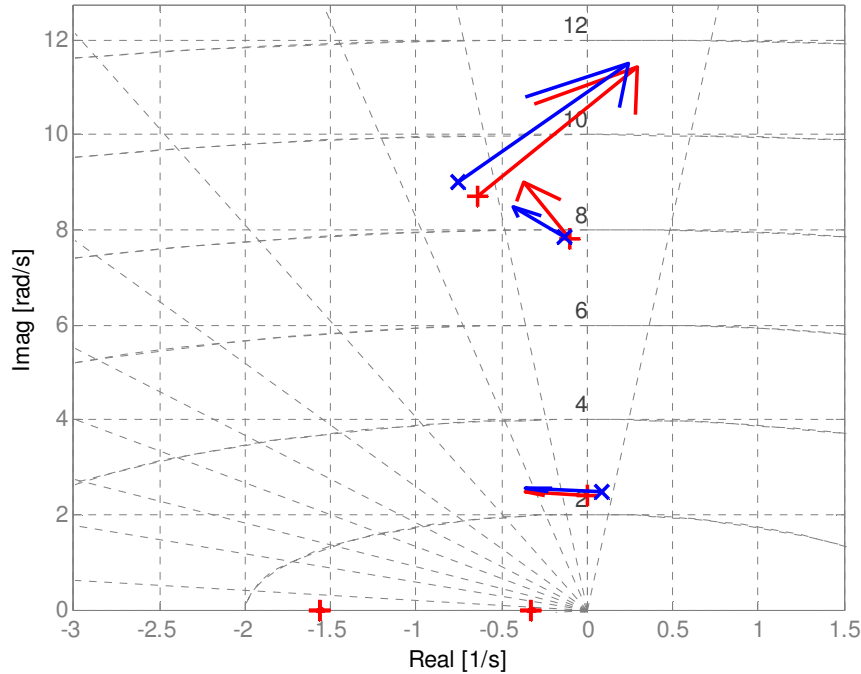


Figure 5.8: Electromechanical poles and their residues of the $(\Delta\omega/\Delta V_{ref})$ transfer function of generator #1 calculated with no PSS (blue \times : multimachine system results; red $+$: synthetic system results).

Figure 5.9 is also taken from [11] and shows the departure angles of the root locus for the PSS loop considering an incremental gain change in a properly phase-tuned PSS. Again, the incremental results for the multimachine system (3MIB benchmark) are equivalent to the combined incremental results from the 3 SMIB systems (the SMIB family).

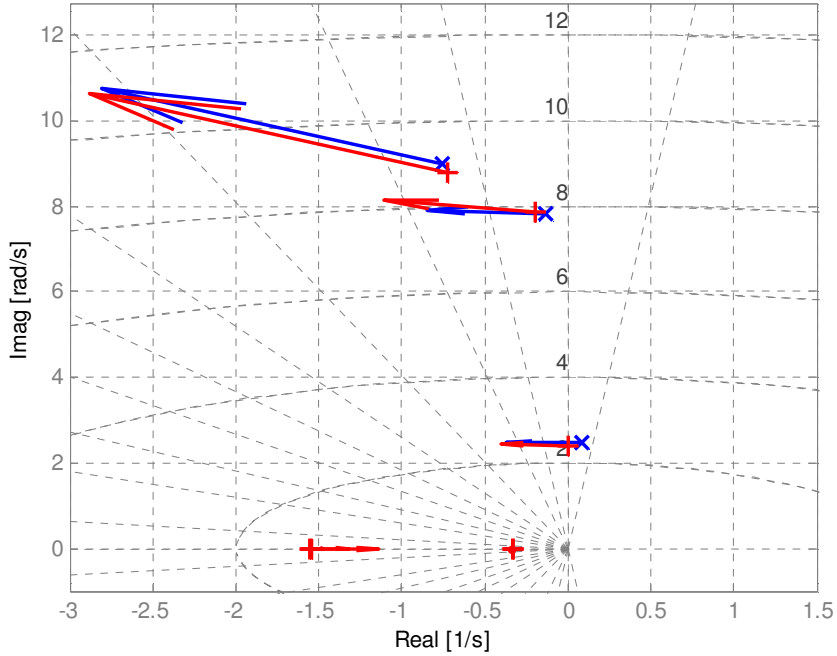


Figure 5.9: Electromechanical poles and their residues of the $(\Delta PSS_{output}/\Delta V_{ref})$ transfer function of generator #1 when equipped with stabilizer.

Figure 5.10 displays the electromechanical poles and their residues of the $(\Delta\omega/\Delta V_{ref})$ and $(\Delta PSS_{output}/\Delta V_{ref})$ transfer functions of generator #3. The speed based PSS at generator #3 has two blocks leading 50° at 3.5 Hz, one block lagging 35° at 0.3 Hz, and a wash out block with a time constant of 3 s. It is verified that the intraplant mode between generators #1 and #2 is insensitive to changes in the gain of generator #3. The sensitivity of the interplant mode to changes in the gain of the PSS at generator #3 is relatively large, and therefore generator #3 is the most suitable for damping this mode because it belongs to the smaller area among the two areas that oscillate against each other at this frequency.

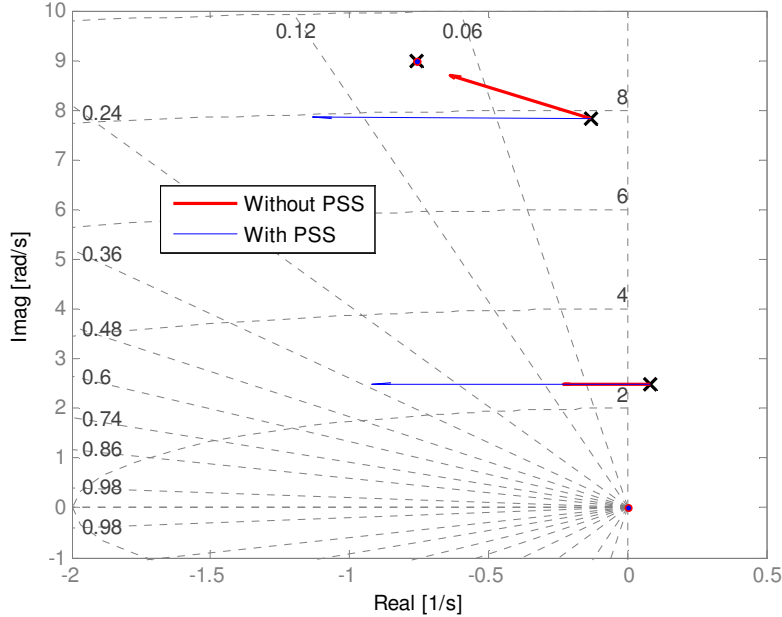


Figure 5.10: Electromechanical poles and their residues of the $(\Delta\omega/\Delta V_{ref})$ and $(\Delta PSS_{output}/\Delta V_{ref})$ transfer functions of generator #3.

An additional result is shown in Figure 5.11, where incremental gain PSSs, with proper phase-tuning circuits, have been added to all three generators. A detailed analysis of this figure is quite instructive for the interested reader. Figure 5.11 shows that the combined effect of the three PSSs positively damps the three modes, and that there is no adverse interaction between damping actions from the various PSSs. It allows to verify that the intraplant mode is damped only by generators 1 & 2, while the other two modes have their damping levels dependent on the combined effort from all three PSSs.

Sensitivities in Figure 5.11 were calculated as the sum of the residues of the $(\Delta PSS_{output}/\Delta V_{ref})$ transfer functions of the three generators. For each mode, the sensitivities are practically in phase, and therefore the magnitude of the total sensitivity is approximately equal to the sum of the sensitivities of the individual generators. Figure 1.4 does not allow to compare the relative magnitudes of the sensitivities for different modes, since the sensitivities were normalized independently for each mode by the calculation software.

Figure 5.12 displays the sensitivities of the electromechanical modes calculated from the shifts of these modes when the gains of all PSSs are changed from 0 to 0.1 pu. The interarea mode is less sensitive to changes in the gains of the three PSSs than the intraplant and the interplant modes. The angles of the sensitivities in Figure 5.12 match those of the sensitivities in Figure 5.11.

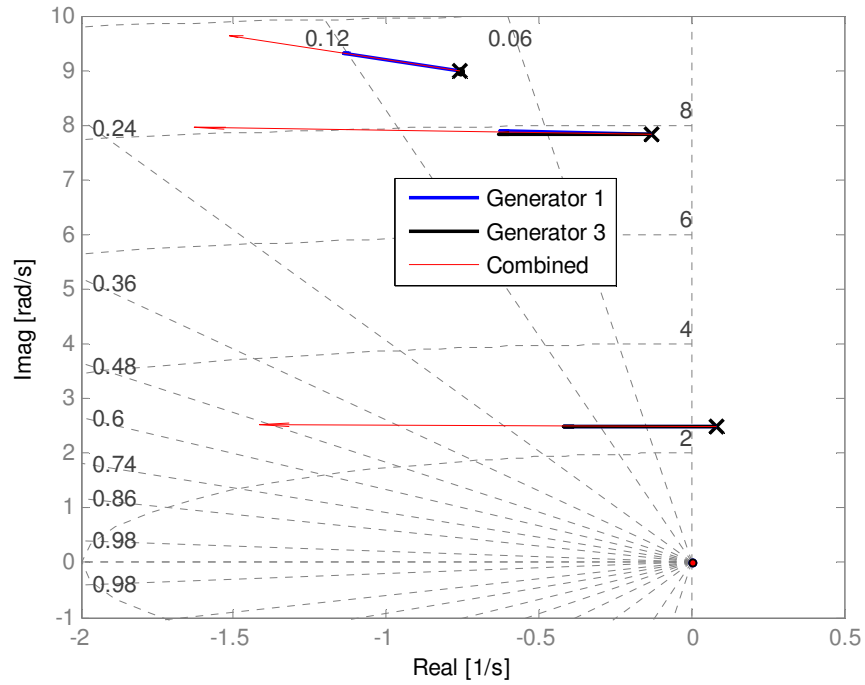


Figure 5.11: Residues of the ($\Delta PSS_{output}/\Delta V_{ref}$) transfer functions of the three generators for each electromechanical mode, and combined sensitivities.

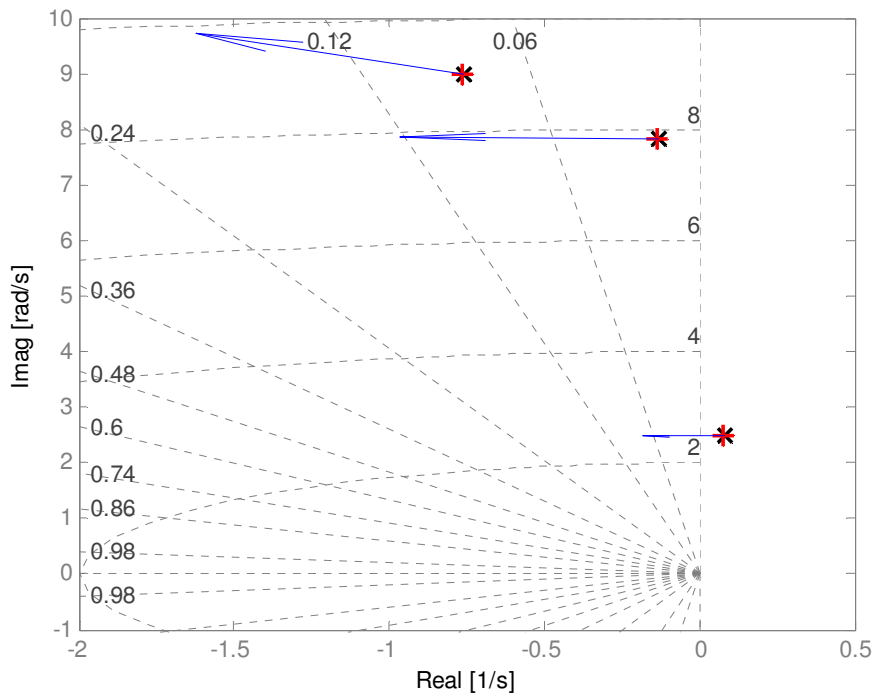


Figure 5.12: Sensitivities of the electromechanical modes to simultaneous changes in the gains of the three PSSs.

With respect to the time-domain simulations, the comparison was made between the results of PSS/E [24] and ANATEM [26]. The main objective associated with the selection of the disturbances was to assess the system damping and the effectiveness of the proposed stabilizers in providing damping to these oscillations.

The first set of simulations comprise the connection of a 50 MVar reactor at the point of interconnection of the generators with the large system (bus #5) through the tie-line at $t = 1.0$ second. The reactor is disconnected 100 ms later, without any changes in the system topology. This is a very small disturbance, and as such leads to results that are essentially a linear system response. Furthermore, given the location where the disturbance is applied, it tends to excite primarily the inter-area oscillation, with all three generators coherently oscillating against the infinite bus.

For the case with no PSSs, the active power output of all generators is compared in Figure 5.13, while their respective rotor speeds are compared in Figure 5.14. When the PSSs are in service, the active power output of all generators is compared in Figure 5.15, whereas their respective rotor speeds are compared in Figure 5.16.

The second set of simulations correspond to simultaneous changes in the excitation system voltage references of all generator units, applied at $t = 1.0$ second. A step change of +3% of the initial voltage was applied to V_{ref} of the AVR associated to generator G1, at the same time that steps of -1% and -2% were applied to the reference voltages of the AVRs associated with generators G2 and G3, respectively.

These changes in voltage references were selected in order to cause a relatively small impact to the inter-area oscillation mode while exciting the intra-plant mode (between generators 1 and 2) and the local mode (generators 1 and 2 oscillating against generator 3).

Once again, for the case with no PSSs, the active power outputs of all generators are compared in Figure 5.17, while their respective rotor speeds are compared in Figure 5.18. For the case with the PSSs in service, the active power outputs of all generators are compared in Figure 5.19, whereas their respective rotor speeds are compared in Figure 5.20.

From the comparative results presented in this section, one may conclude that the two software packages provide satisfactorily matching results and, thus, this benchmark system can be considered to be validated by this Task Force.

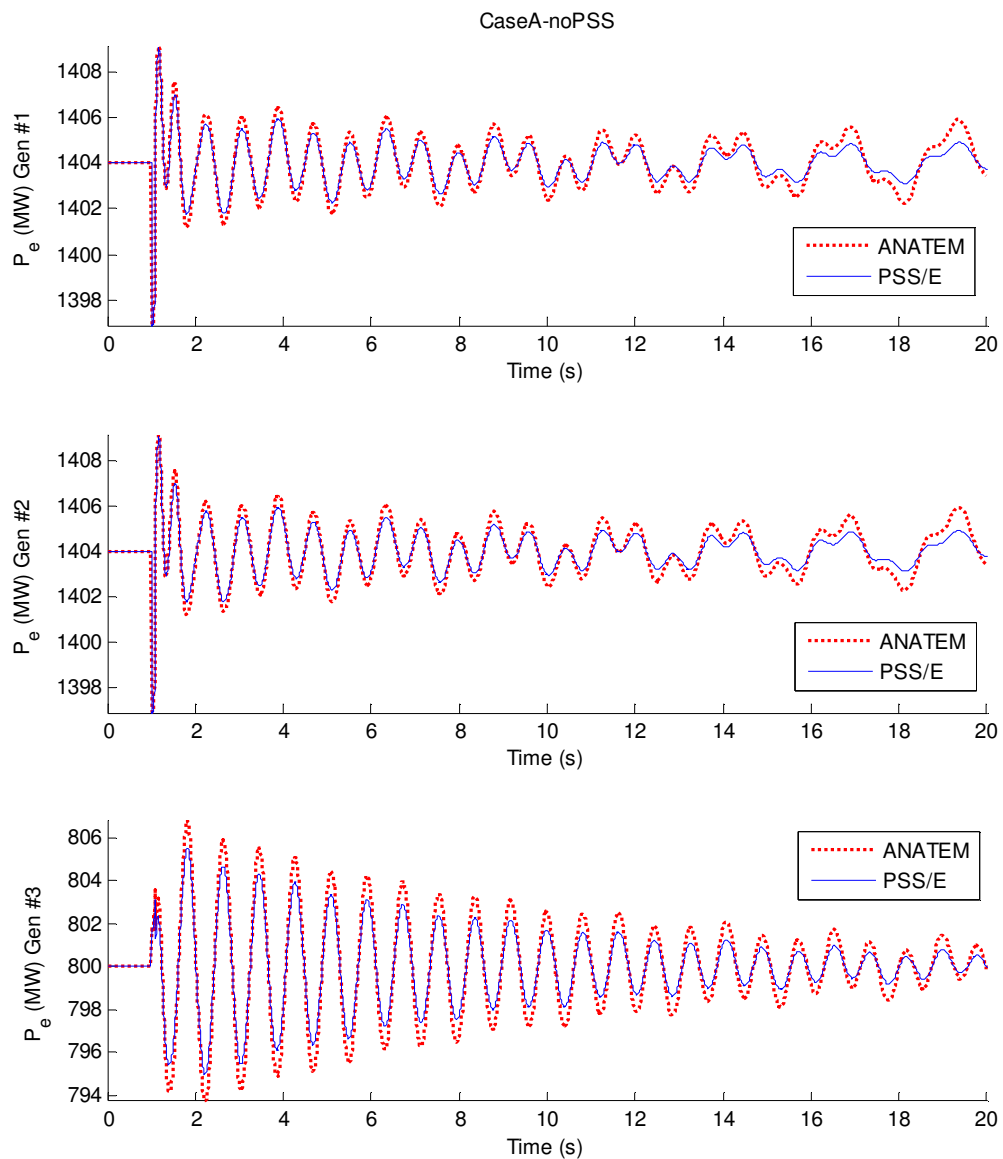


Figure 5.13: Response to a Temporary Connection of a 50 MVar Reactor to Bus #5 (Generator Active Power, no PSS)

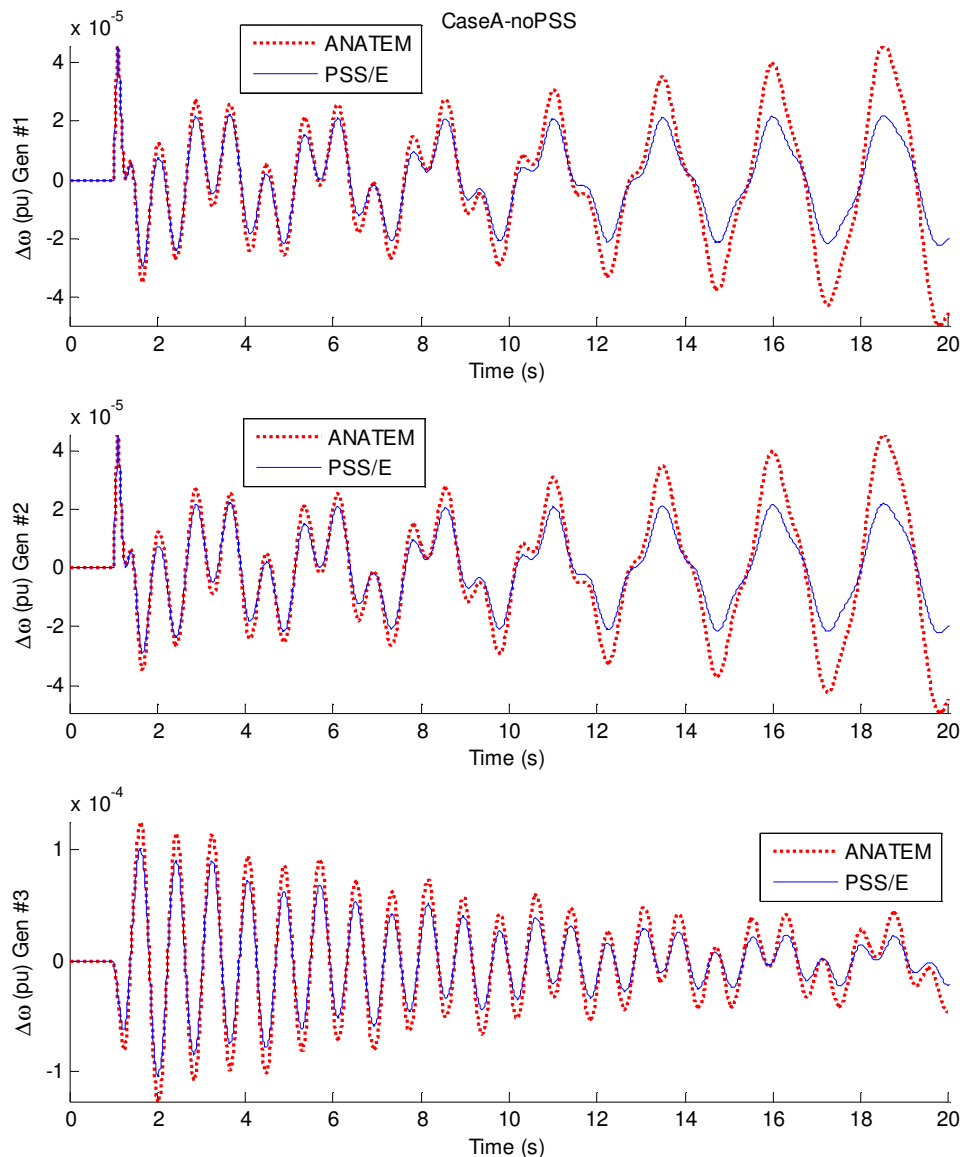


Figure 5.14: Response to a Temporary Connection of a 50 MVAr Reactor to Bus #5 (Generator Speed, no PSS)

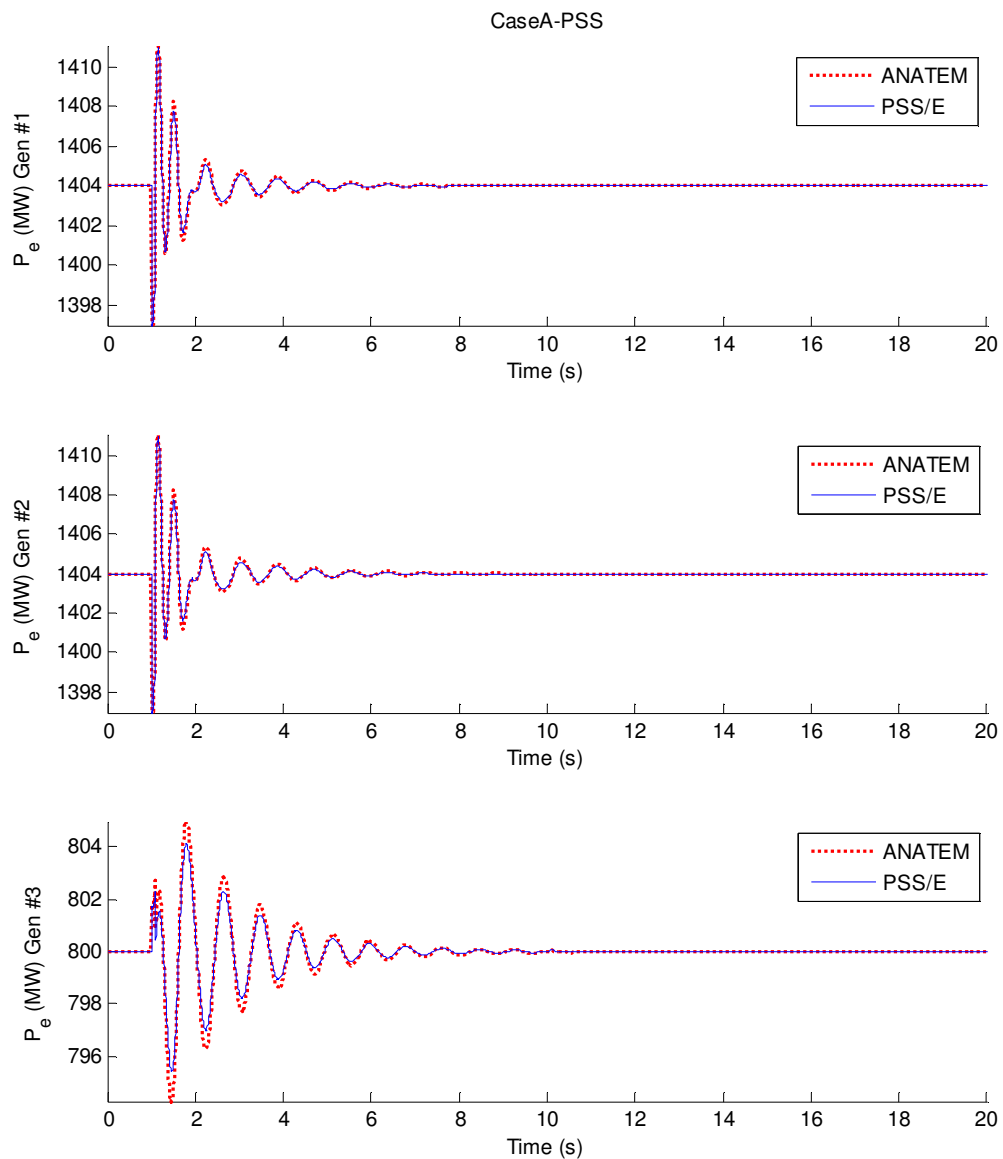


Figure 5.15: Response to a Temporary Connection of a 50 MVAr Reactor to Bus #5 (Generator Active Power, with PSS)

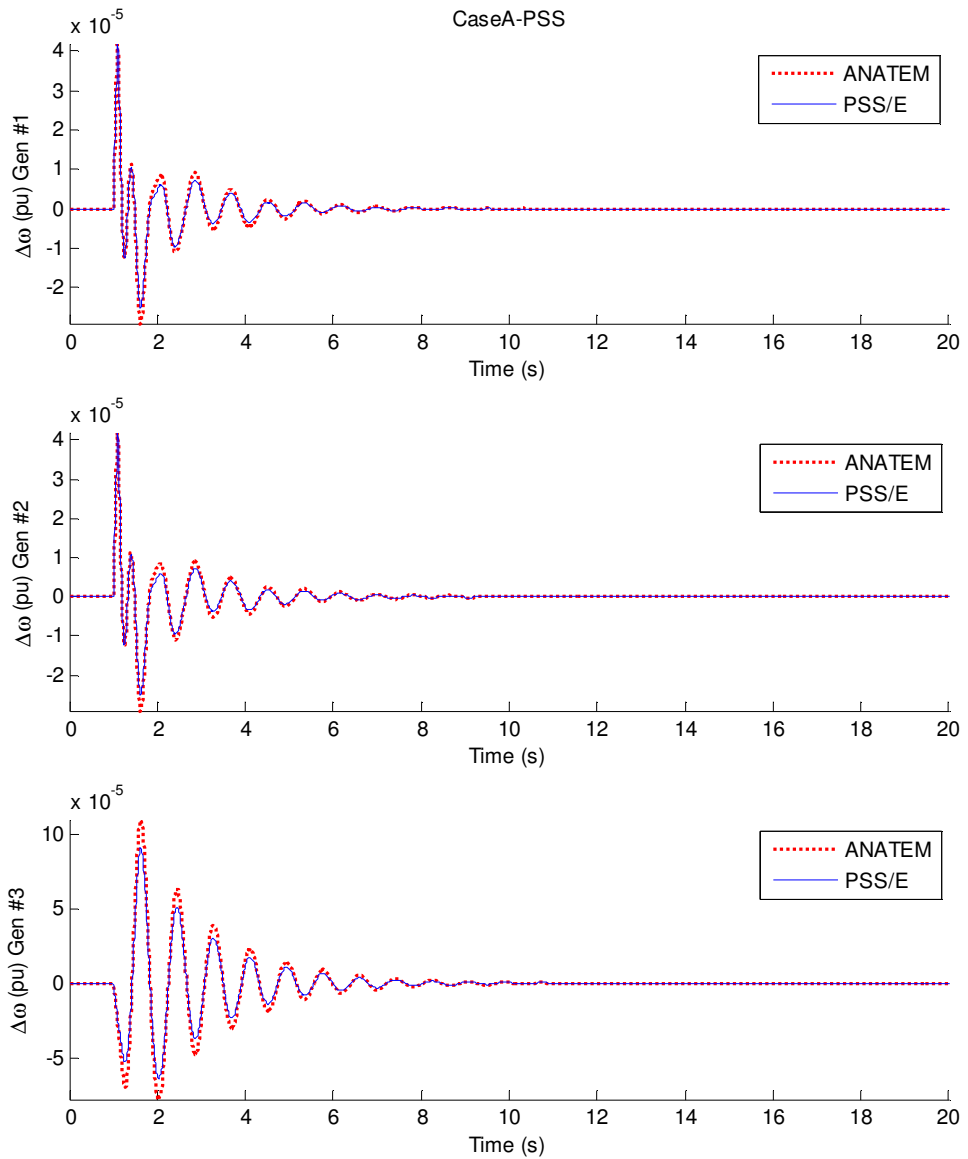


Figure 5.16: Response to a Temporary Connection of a 50 MVAr Reactor to Bus #5 (Generator Speed, with PSS)

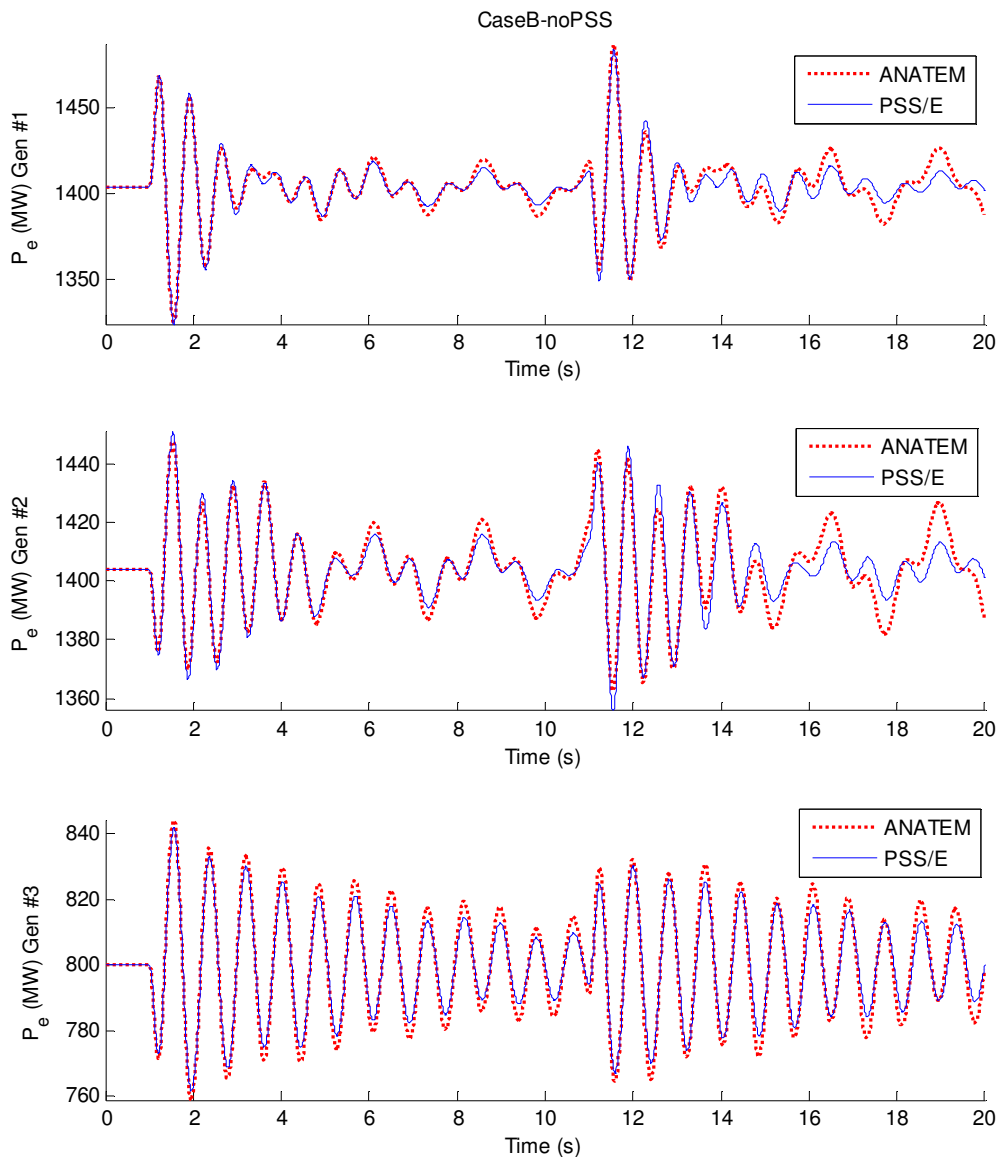


Figure 5.17: Response to steps applied to the reference voltages of the AVRs (Generator Power, no PSS)

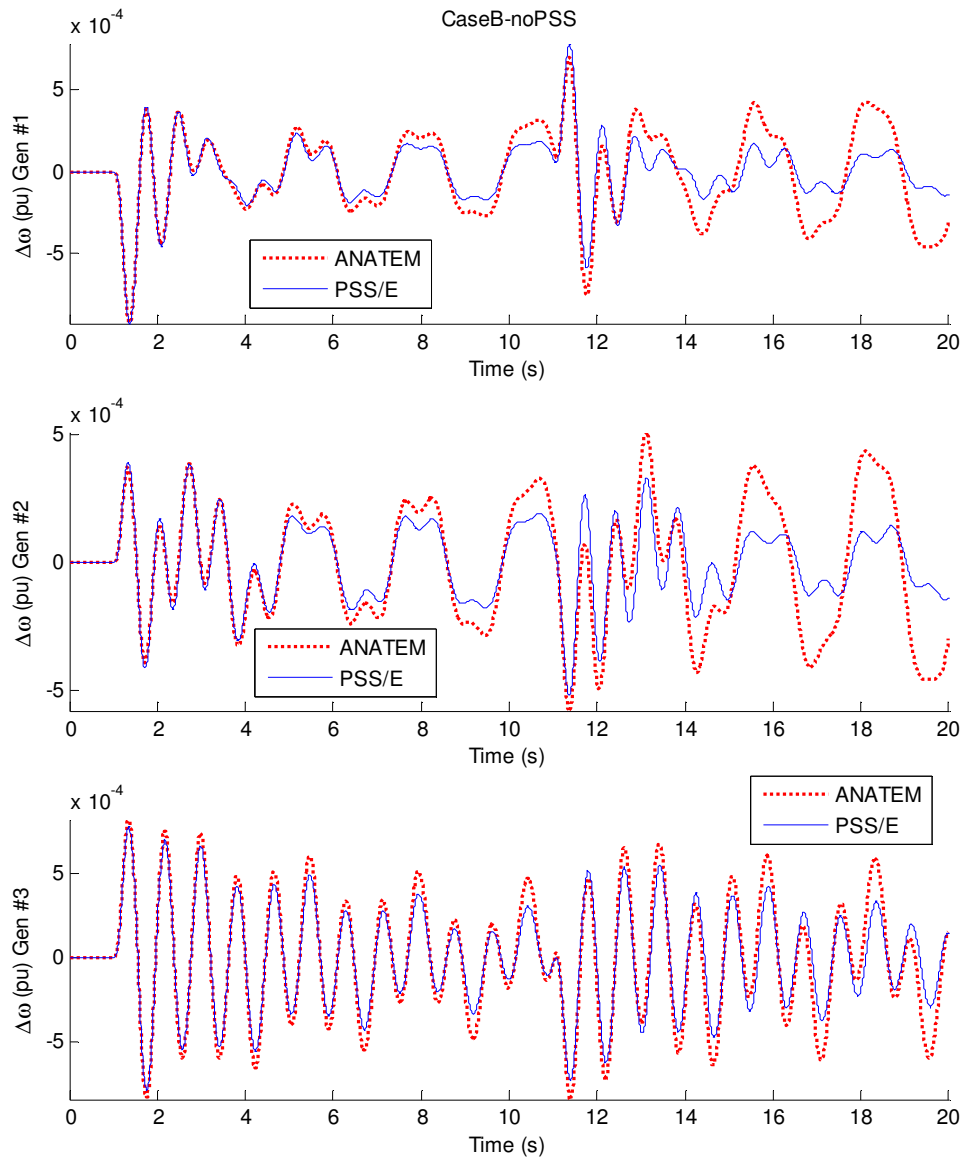


Figure 5.18: Response to steps applied to the reference voltages of the AVRs (Generator Speeds, no PSS)

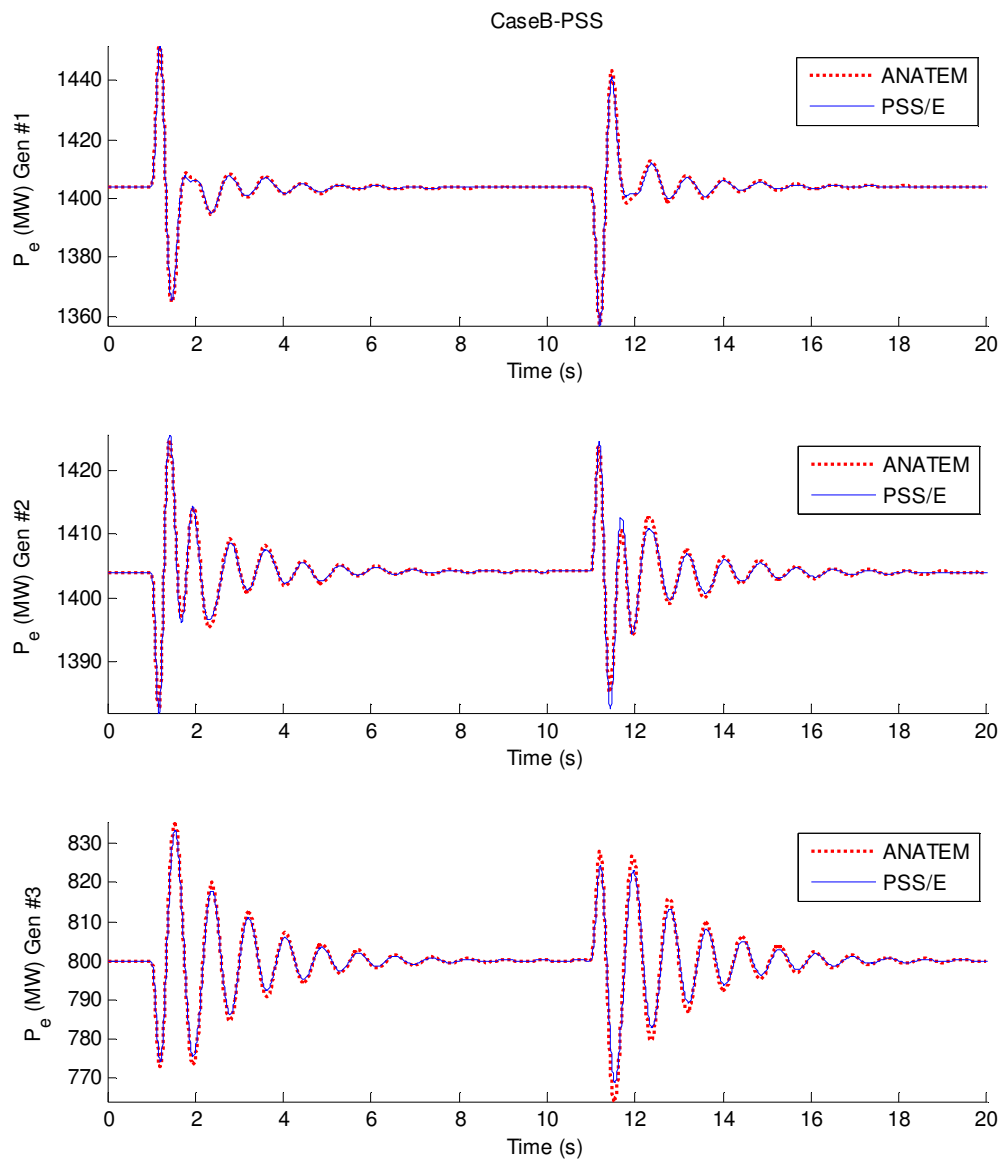


Figure 5.19: Response to steps applied to the reference voltages of the AVRs (Generator Power, with PSS)

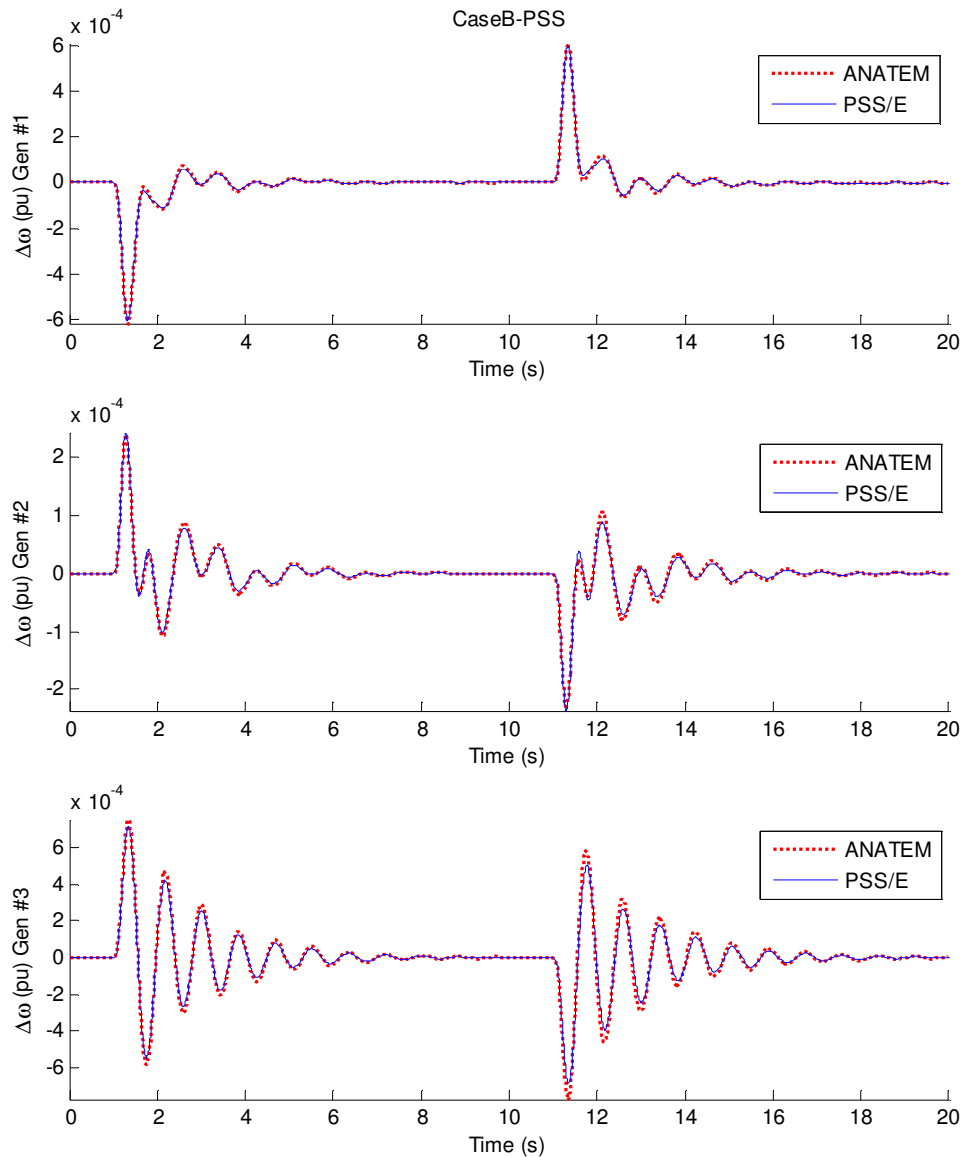


Figure 5.20: Response to steps applied to the reference voltages of the AVR (Generator Speed, with PSS)

5.2. Data for the Brazilian 7-bus Equivalent Model

5.2.1. Power Flow Data

The system one line diagram is shown in Figure 5.21, where the line power flows are also indicated. The bus voltage magnitudes and angles from the power flow solution, for the single condition analyzed in this report, are shown in Table 5.10.

The bus load data are given in Table 5.11 (where the negative loads indicate active or reactive generation). These load values were computed at the power flow solution, being represented, in the dynamic simulation, with a constant current characteristic for the active power components and a constant admittance characteristic for the reactive power components (100%I, 100%Z for P and Q, respectively).

The bus shunt elements are listed in Table 5.12, where the MVAR values for the capacitors relate to nominal voltage conditions (1.0 pu voltage).

The transmission line data is listed in Table 5.13 and given in per unit on the system MVA base of 1,000 MVA. The lines are represented by series (RL) impedances. The capacitive chargings of these lines have been compounded with the bus reactors and are accounted for in the shunt data of Table 5.12.

The transformer data is given in per unit on system MVA base (1,000 MVA) in Table 5.14. The generators step-up transformers (GSU) are not represented in the case.

A complete report from the power flow solution report for this system is given in Table 5.15.

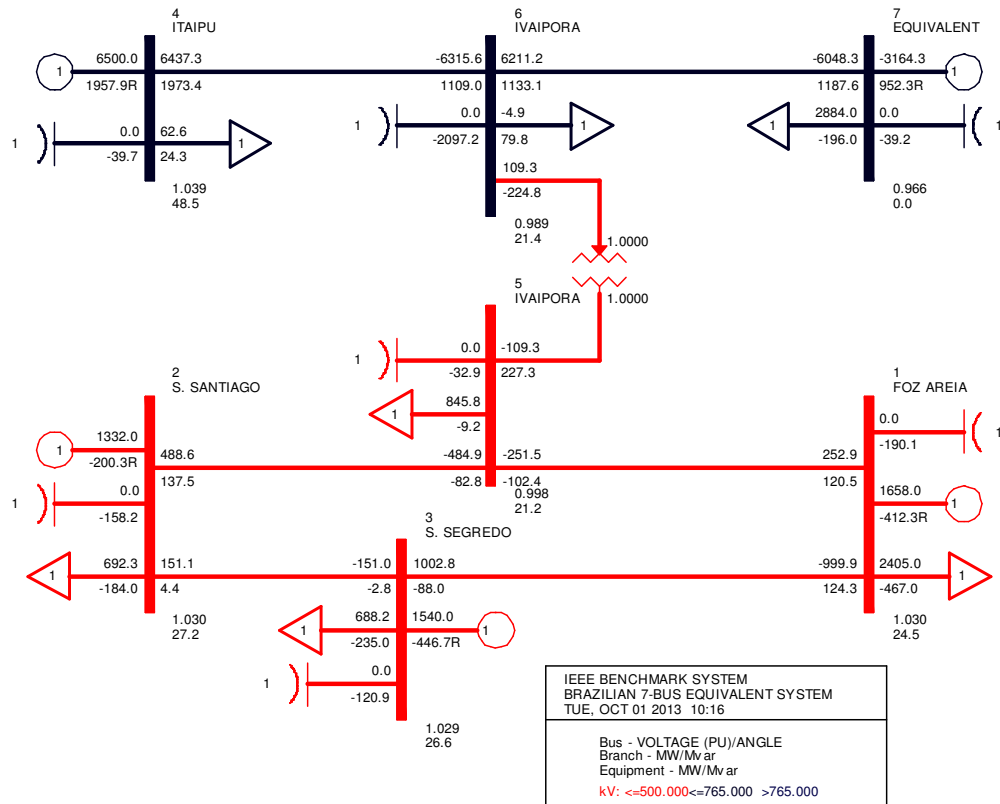


Figure 5.21: One-line diagram of Benchmark Model #2

Table 5.10: Bus Data (Including Voltage and Angle from the Power Flow Solution)

Bus Number	Bus Name	Base kV	Bus type	Voltage (pu)	Angle (deg)
1	FOZ AREIA	500.0	PV	1.0300	24.53
2	S. SANTIAGO	500.0	PV	1.0300	27.22
3	S. SEGREDO	500.0	PV	1.0290	26.60
4	ITAIPU	765.0	PV	1.0390	48.45
5	IVAIPORA	500.0	PQ	0.9984	21.20
6	IVAIPORA	765.0	PQ	0.9895	21.45
7	EQUIVALENT	765.0	swing	0.9660	0.00

Table 5.11: Bus Loads

Bus Number	P (MW)	Q (Mvar)
1	2405.0	-467.0
2	692.3	-184.0
3	688.2	-235.0
4	62.6	24.3
5	845.8	-9.2
6	-4.9	79.8
7	2884.0	-196.0

Table 5.12: Shunt Data

Bus Number	Bus Name	Base kV	G-Shunt (MW)	B-Shunt (Mvar)
1	FOZ AREIA	500.0	0.0	179.2
2	S. SANTIAGO	500.0	0.0	149.1
3	S. SEGREDO	500.0	0.0	114.2
4	ITAIPU	765.0	0.0	36.8
5	IVAIPORA	500.0	0.0	33.0
6	IVAIPORA	765.0	0.0	2142.0
7	EQUIVALENT	765.0	0.0	42.0

Table 5.13: Transmission Line Data (1,000 MVA Base)

From Bus	To Bus	R (pu)	X (pu)	Charging (pu)
1	3	0.003	0.038	0.0
1	5	0.019	0.245	0.0
2	3	0.005	0.076	0.0
2	5	0.015	0.225	0.0
4	6	0.0029	0.0734	0.0
6	7	0.004	0.057	0.0

Table 5.14: Transformer Data (1,000 MVA Base)

From Bus	To Bus	R (pu)	X (pu)	tap (pu)
5	6	0.0	0.039	1.0

Table 5.15: Power Flow Solution Printout

X-----	FROM BUS	-----X	AREA	VOLT	GEN	LOAD	SHUNT	X-----	TO BUS	-----X
TRANSFORMER										
BUS#	X--	NAME	--X	BASKV	ZONE	PU/KV	ANGLE	MW/MVAR	MW/MVAR	BUS# X-- NAME --X BASKV AREA CKT
MW										
MVAR										
1 FOZ AREIA	500.00	1	1.0300	24.5	1658.0	2405.0	0.0			
999.9	124.3			1	515.00	-412.3R	-467.0	-190.1	3 S. SEGREDO	500.00 1 1 -
252.9	120.5								5 IVAIPIORA	500.00 1 1
2 S. SANTIAGO	500.00	1	1.0300	27.2	1332.0	692.3	0.0			
151.1	4.4			1	515.00	-200.3R	-184.0	-158.2	3 S. SEGREDO	500.00 1 1
488.6	137.5								5 IVAIPIORA	500.00 1 1
3 S. SEGREDO	500.00	1	1.0290	26.6	1540.0	688.2	0.0			
1002.8	-88.0			1	514.50	-446.7R	-235.0	-120.9	1 FOZ AREIA	500.00 1 1
151.0	-2.8								2 S. SANTIAGO	500.00 1 1 -
4 ITAPIU	765.00	2	1.0390	48.5	6500.0	62.6	0.0			
6437.4	1973.4			1	794.84	1958.0R	24.3	-39.7	6 IVATPORA	765.00 2 1

5.2.2. Dynamic Data

The generator model shown in the block diagram of Figure 5.2 is used to represent all five generators of this benchmark system. The model parameters corresponding to these five generators are presented in Table 5.16 and Table 5.17. Rotor speed mechanical damping D is set to zero for all generators, which is usually the case when using sub-transient generator models. Table 5.16 and Table 5.17 also present the calculated rated field current (considering 0.80 rated power factor). This calculation comprises the initialization of the generators models at full (rated) power output, considering their rated power factor. The values given to the saturation factors S(1.0) and S(1.2) shown in Table 5.16 and Table 5.17 are equivalent to neglecting saturation effects.

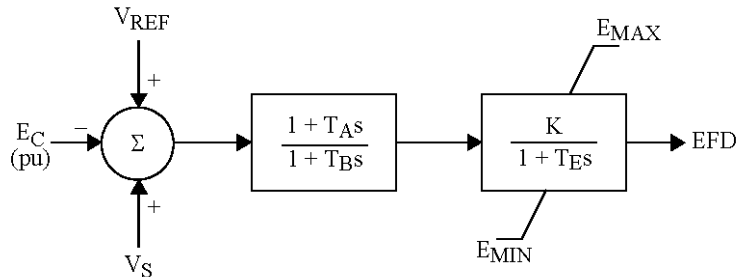
Table 5.16: Dynamic Model Data for the Salient Pole Units 1 and 2

Parameters			Buses	
Description	Symbol	Unit	1 FOZ AREIA	2 S. SANTIAGO
Rated apparent power	MBASE	MVA	1900	1400
d-axis open circuit transient time constant	T'_{do}	s	5.0	5.0
d-axis open circuit sub-transient time constant	T''_{do}	s	0.053	0.053
q-axis open circuit sub-transient time constant	T''_{qo}	s	0.123	0.123
Inertia	H	MW.s/MVA	4.5	4.5
Speed damping	D	pu	0.0	0.0
d-axis synchronous reactance	X_d	pu	0.85	0.85
q-axis synchronous reactance	X_q	pu	0.7	0.7
d-axis transient reactance	X'_d	pu	0.3	0.3
sub-transient reactance	$X''_d = X''_q$	pu	0.2	0.2
Leakage reactance	X_f	pu	0.15	0.15
Saturation factor at 1.0 pu voltage	S(1.0)	—	0.001	0.001
Saturation factor at 1.2 pu voltage	S(1.2)	—	0.01	0.01
Rated field current	IFD _{rated}	pu	1.66	1.66

Table 5.17: Dynamic Model Data for the Salient Pole Units 3, 4 and 7

Parameters		Buses		
Symbol	Unit	3 S. SEGREDO	4 ITAIPU	7 EQUIVALENT
MBASE	MVA	1944	6633	6000
T'_{do}	s	5.0	7.6	8.0
T''_{do}	s	0.06	0.09	0.09
T''_{qo}	s	0.09	0.19	0.2
H	MW.s/MVA	4.5	5.07	5.0
D	pu	0.0	0.0	0.0
X_d	pu	0.88	0.9	1.0
X_q	pu	0.69	0.68	0.7
X'_d	pu	0.3	0.3	0.3
$X''_d = X''_q$	pu	0.2	0.24	0.25
X_f	pu	0.15	0.18	0.18
S(1.0)	—	0.001	0.001	0.001
S(1.2)	—	0.01	0.01	0.01
IFD _{rated}	pu	1.68	1.70	1.79

All five generators have identical excitation systems that will be represented by the same dynamic model, shown in Figure 5.22. The parameters for the model are presented in Table 5.18. The limits E_{\max} and E_{\min} are set to reasonably large values, so they should not impact small-signal stability results. Prime-mover and speed-governor effects are not represented.



$$V_S = VOTHSG + VUEL + VOEL$$

Figure 5.22: Block Diagram for the Excitation Systems

This benchmark system considers power system stabilizers (PSS) in all machines except the machine connected to bus #7 (EQUIVALENT). All PSSs are derived from rotor speed deviation and have the same structure, comprising two lead-lag blocks, one wash-out block, and a gain.

Table 5.18: Data for the Excitation System model

Parameters				
Description	Symbol	Value	Unit	
TGR block 1 transient gain	TA/TB	1	–	
TGR block 1 denominator time constant	TB	1	s	
Exciter gain	K	30	pu	
Exciter time constant	TE	0.05	s	
Max. AVR output	Emin	-4	pu	
Min. AVR output	Emax	5	pu	

The IEEE Std. 421.5(2005) model PSS1A will be used to represent all four power system stabilizers, and is shown in Figure 5.5. The PSS parameters for the corresponding generators are given in Table 5.19. It should be noted that the parameters A1 to A6 are set in a way that leads to the whole filter block to be bypassed.

The output limits were set to $\pm 10\%$, while the logic to switch off the PSS for voltages outside a normal operation range has been ignored (parameters V_{CU} and V_{CL} set to zero).

Table 5.19: Parameters for the four PSSs

Parameters	Buses

Description	Symbol	Unit	1, 2, 3	4
2 nd order denominator coefficient	A ₁	–	0	0
2 nd order denominator coefficient	A ₂	–	0	0
2 nd order numerator coefficient	A ₃	–	0	0
2 nd order numerator coefficient	A ₄	–	0	0
2 nd order denominator coefficient	A ₅	–	0	0
2 nd order denominator coefficient	A ₆	–	0	0
1 st lead-lag numerator time constant	T ₁	s	0.30	0.52
1 st lead-lag denominator time constant	T ₂	s	0.075	0.065
2 nd lead-lag numerator time constant	T ₃	s	0.30	0.52
2 nd lead-lag denominator time constant	T ₄	s	0.075	0.065
Washout block numerator time constant	T ₅	s	3	3
Washout block denominator time constant	T ₆	s	3	3
PSS gain	K _S	pu	10	16
PSS max. output	L _{Smax}	pu	0.1	0.1
PSS min. output	L _{Smin}	pu	-0.1	-0.1
Upper voltage limit for PSS operation	V _{CU}	pu	0	0
Lower voltage limit for PSS operation	V _{CL}	pu	0	0

5.2.3. Selected Results and Validation

The results presented in the following correspond to eigenvalue calculations and time-domain simulations of different disturbances performed with the PSS/E [24] and PacDyn/ANATEM [25], [26] software packages.

For the linearized analyses, the system eigenvalues calculated with both software for the cases with no PSS, with PSS at generator #4 only, and with PSS at all generators (except the equivalent at bus #7) are presented from Figure 5.23 to Figure 5.27.

The PSS/E modal analysis results were generated with PSS/E auxiliary program PSSPLT, which estimates the dominant modal components of an oscillatory response (thus requiring the choice of an output variable for the estimation process) by the Prony method [24].

In the case with no PSS, good matching is observed for the electromechanical modes. In the last two cases (with PSS), the results obtained with PSSPLT highly depend on the processed signal, as expected, since these estimation methods work better with responses involving poorly damped oscillations.

The good matching observed in the time domain simulations of the two software for the cases with PSS practically confirm that the numerical differences observed in their eigenvalue/modal analyses are due to the imprecisions inherent to the estimation process.

System with no PSS

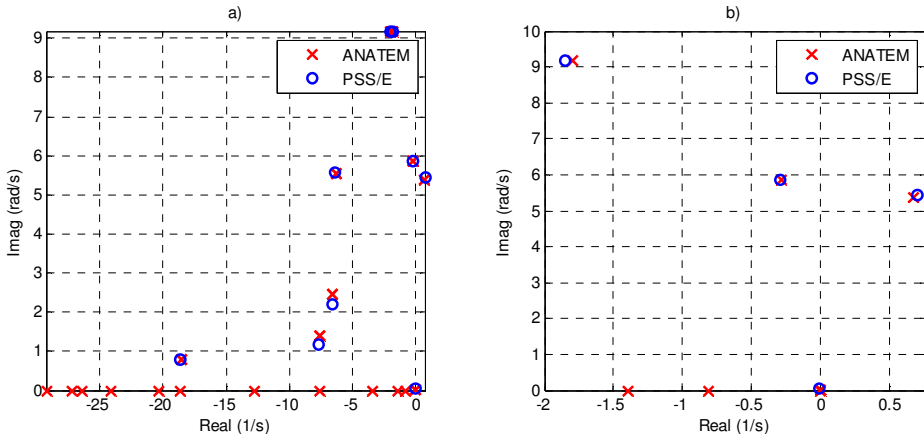


Figure 5.23: : Eigenvalues calculated with PSS®E Program PSSPLT (using Itaipu active power signal) and PacDyn for the system with no PSS. a) Complete spectrum of eigenvalues; b) Enlarged view of the spectrum to highlight the electromechanical modes.

System with PSS at generator #4

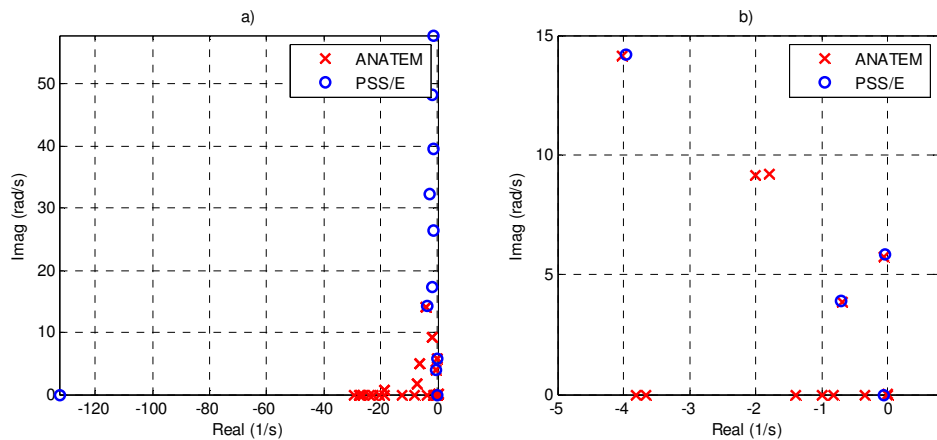


Figure 5.24: Eigenvalues calculated with PSS®E Program PSSPLT (using Itaipu active power signal) and PacDyn for the system with PSS at generator #4 (Itaipu). a) Complete spectrum of eigenvalues; b) Enlarged view of the spectrum to highlight the electromechanical modes.

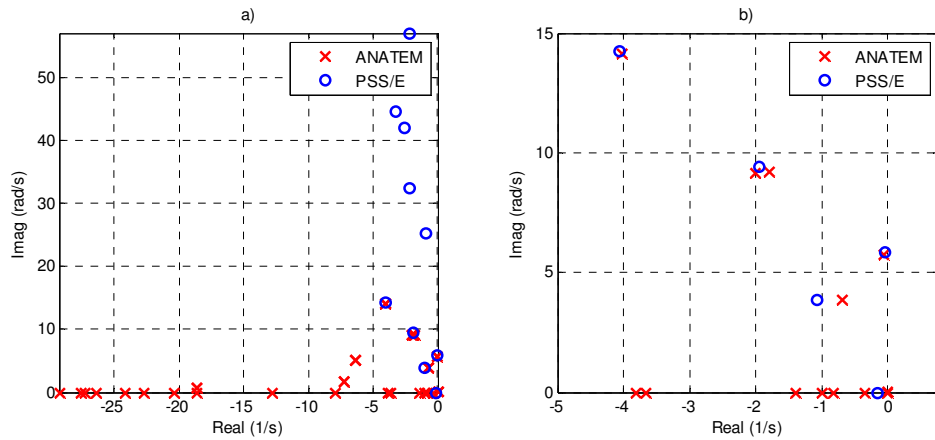


Figure 5.25: Eigenvalues Calculated with PSS®E Program PSSPLT (using S. Santiago active power signal) and PacDyn for the system with PSS at generator #4 (Itaipu). a) Complete spectrum of eigenvalues; b) Enlarged view of the spectrum to highlight the electromechanical modes.

System with PSS at all generators

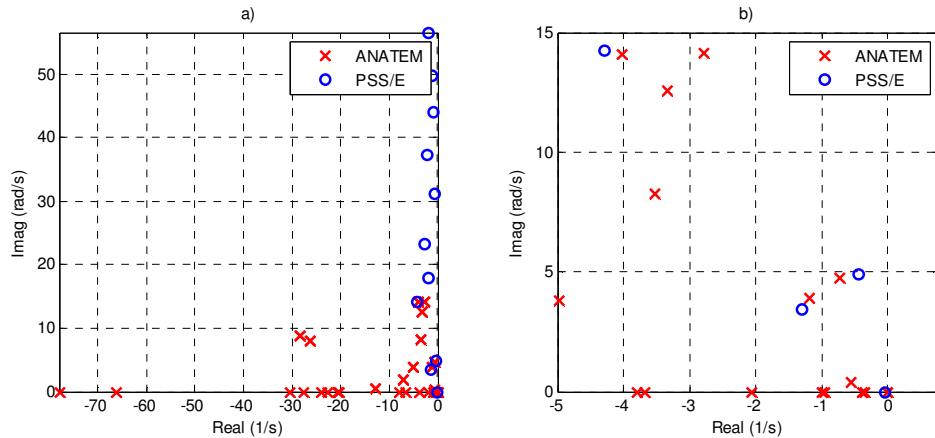


Figure 5.26: Eigenvalues calculated with PSS®E Program PSSPLT (using Itaipu active power signal) and PacDyn for the system with PSS at all generators. a) Complete spectrum of eigenvalues; b) Enlarged view of the spectrum to highlight the electromechanical modes.

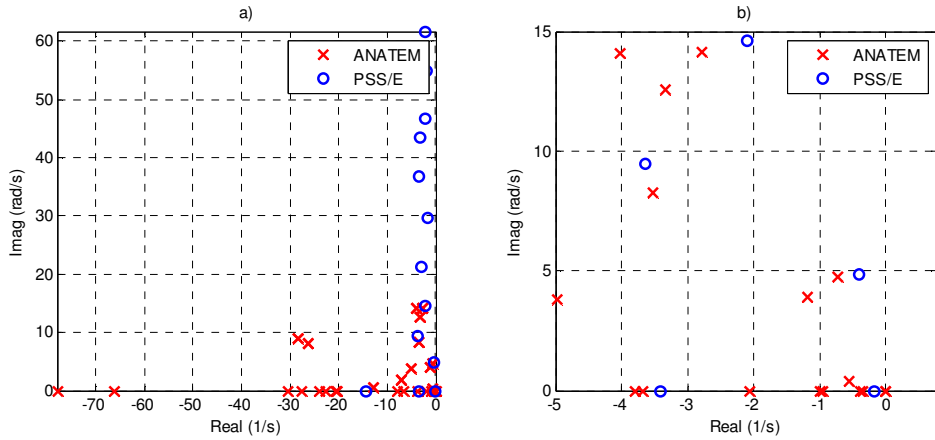


Figure 5.27: Eigenvalues Calculated with PSS®E Program PSSPLT (using S. Santiago active power signal) and PacDyn for the system with PSS at all generators. a) Complete spectrum of eigenvalues; b) Enlarged view of the spectrum to highlight the electromechanical modes.

For the time-domain simulations, two disturbances were selected to generate the results for the comparative analyses between the software. Both disturbances excite the unstable interarea mode of 0.85 Hz. Results are again presented for the system without PSS, with PSS at Itaipu only, and with PSS at all generators except the equivalent (at bus #7).

The first set of simulations comprises the connection of a 500 Mvar reactor at the Ivaiporã 765 kV bus (bus #6) at $t = 1.0$ second. The reactor is disconnected 100 ms later, without any further changes in the system topology. This set of simulations will be referred to as Case A and its corresponding comparative analysis is presented from Figure 5.28 to Figure 5.32.

The second set of simulations corresponds to a 2% step in voltage reference at the Itaipu machine (bus #4), applied at $t = 1.0$ second. The step is removed (i.e., a -2% step is applied) at $t = 11.0$ seconds. This set of simulations will be referred to as Case B and its corresponding comparative analysis is presented from Figure 5.33 to Figure 5.37.

The matching observed between the time-domain simulation results obtained from these two software, as seen from Figure 5.28 to Figure 5.37, allows concluding that this benchmark system has been validated.

Case A: 500 MVar Reactor Applied to Bus #6

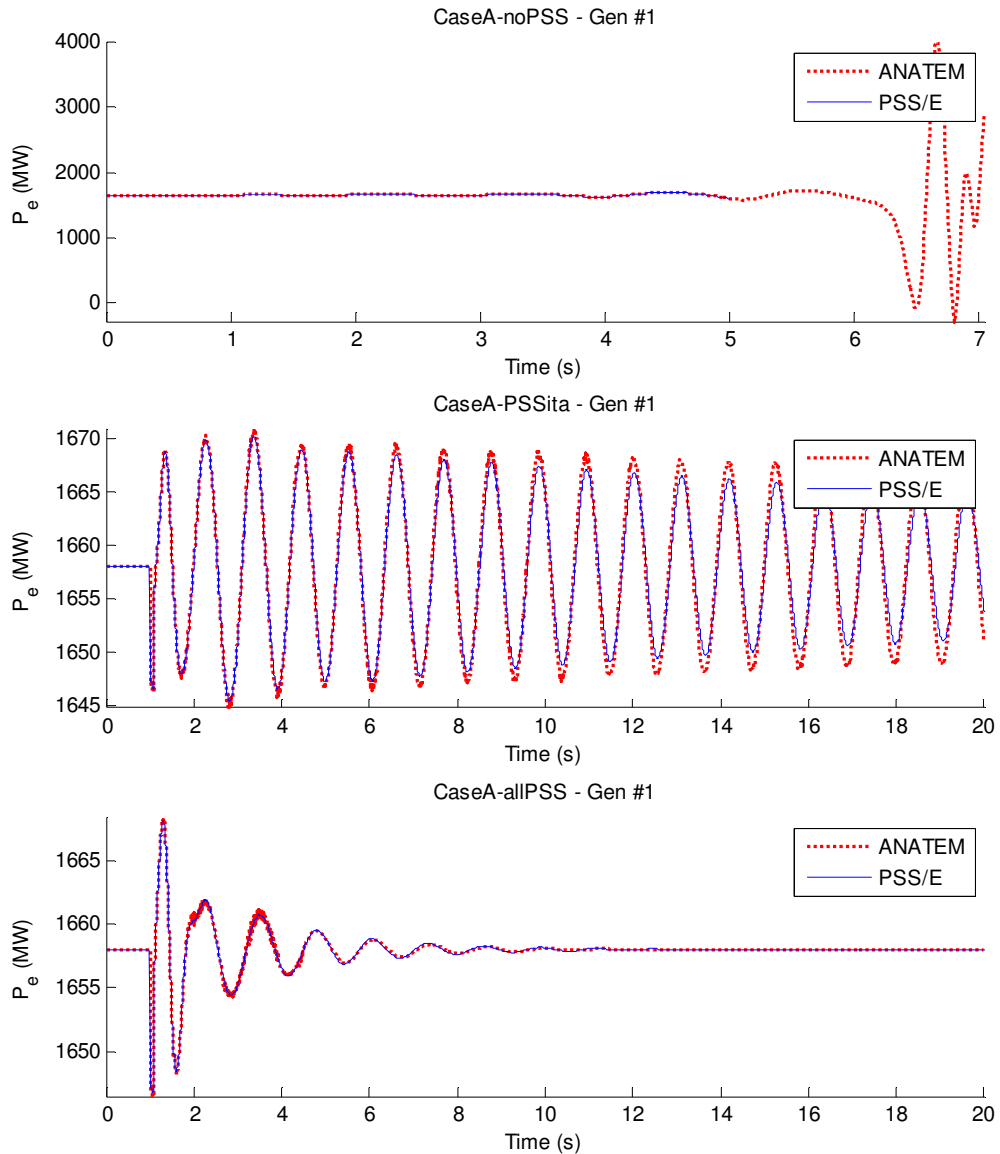


Figure 5.28: Output power Response of Generator #1 to a 500 MVar Reactor Temporarily Connected to Bus #6. Top: no PSS; Center: PSS at Itaipu; Bottom: PSS at four generators.

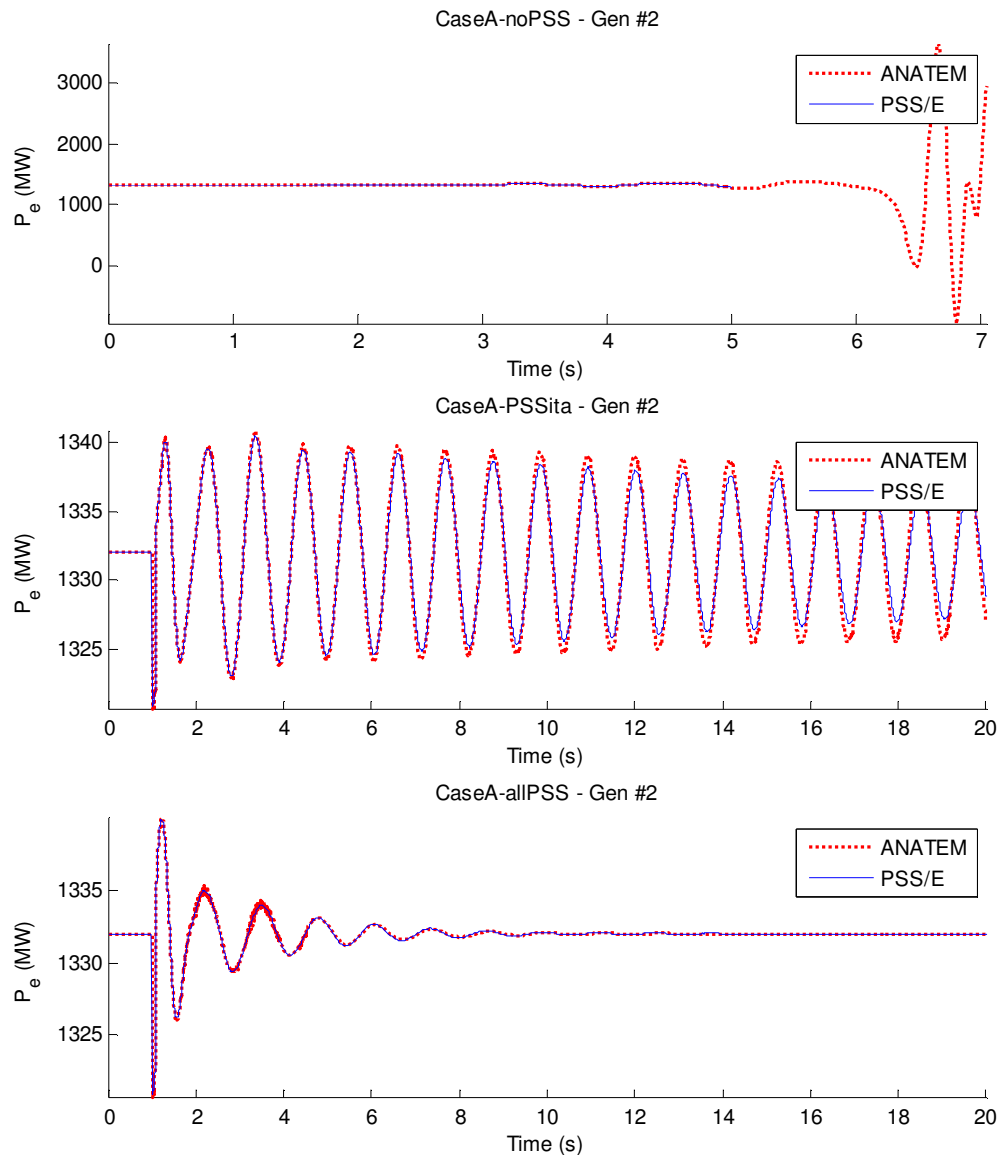


Figure 5.29: Output power Response of Generator #2 to a 500 MVAr Reactor Temporarily Connected to Bus #6. Top: no PSS; Center: PSS at Itaipu; Bottom: PSS at four generators.

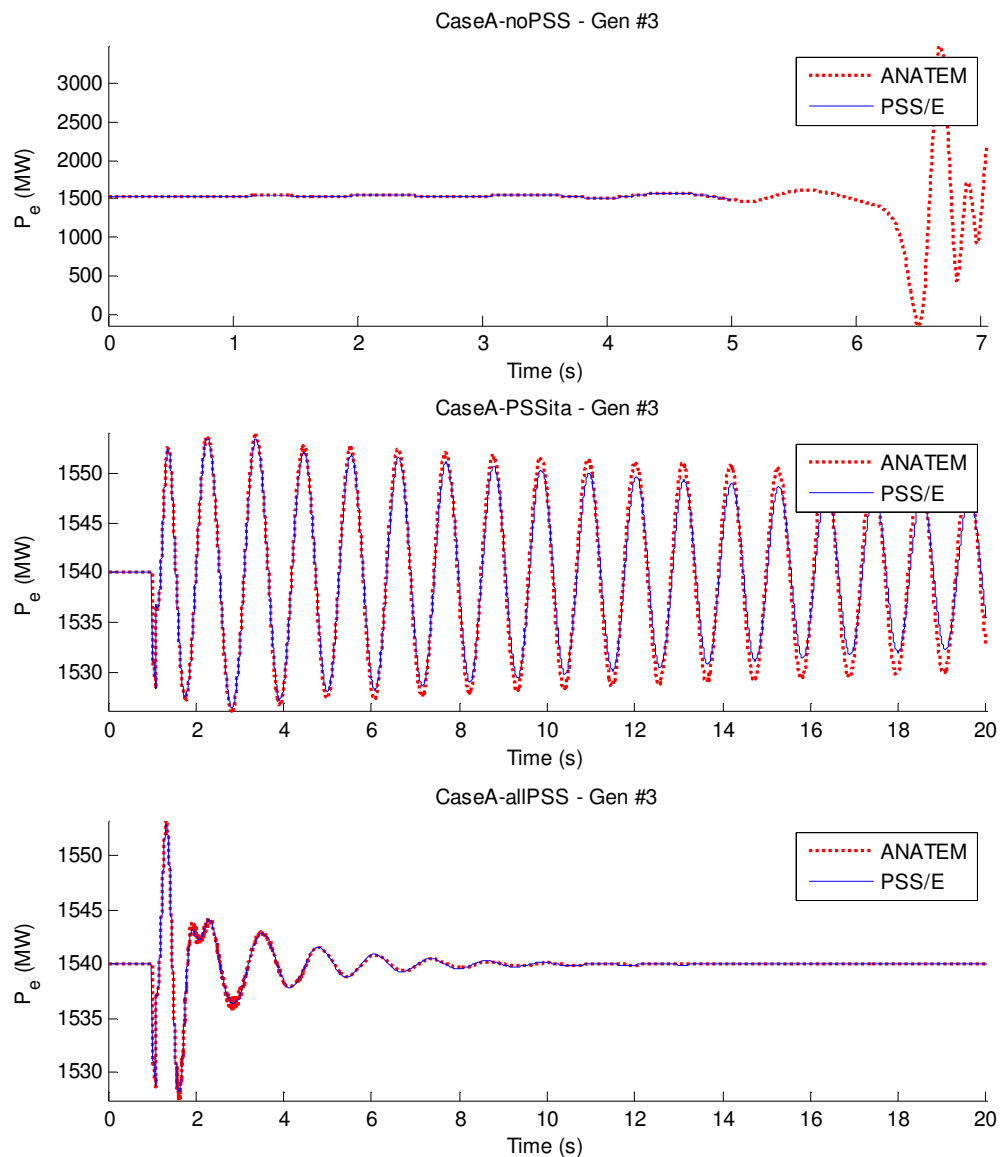


Figure 5.30: Output power Response of Generator #3 to a 500 MVAr Reactor Temporarily Connected to Bus #6. Top: no PSS; Center: PSS at Itaipu; Bottom: PSS at four generators.

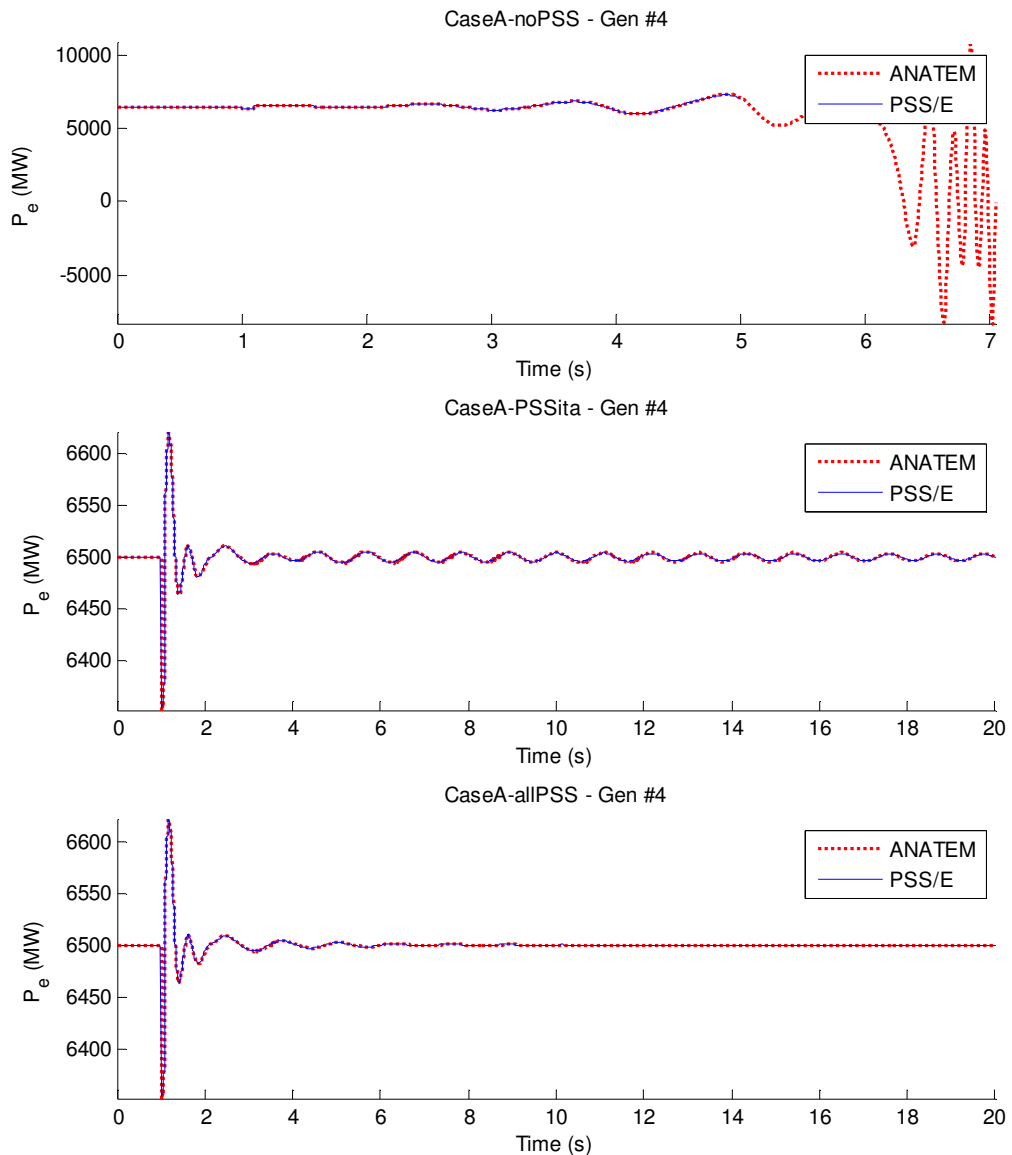


Figure 5.31: Output power Response of Generator #4 to a 500 MVAr Reactor Temporarily Connected to Bus #6. Top: no PSS; Center: PSS at Itaipu; Bottom: PSS at four generators.

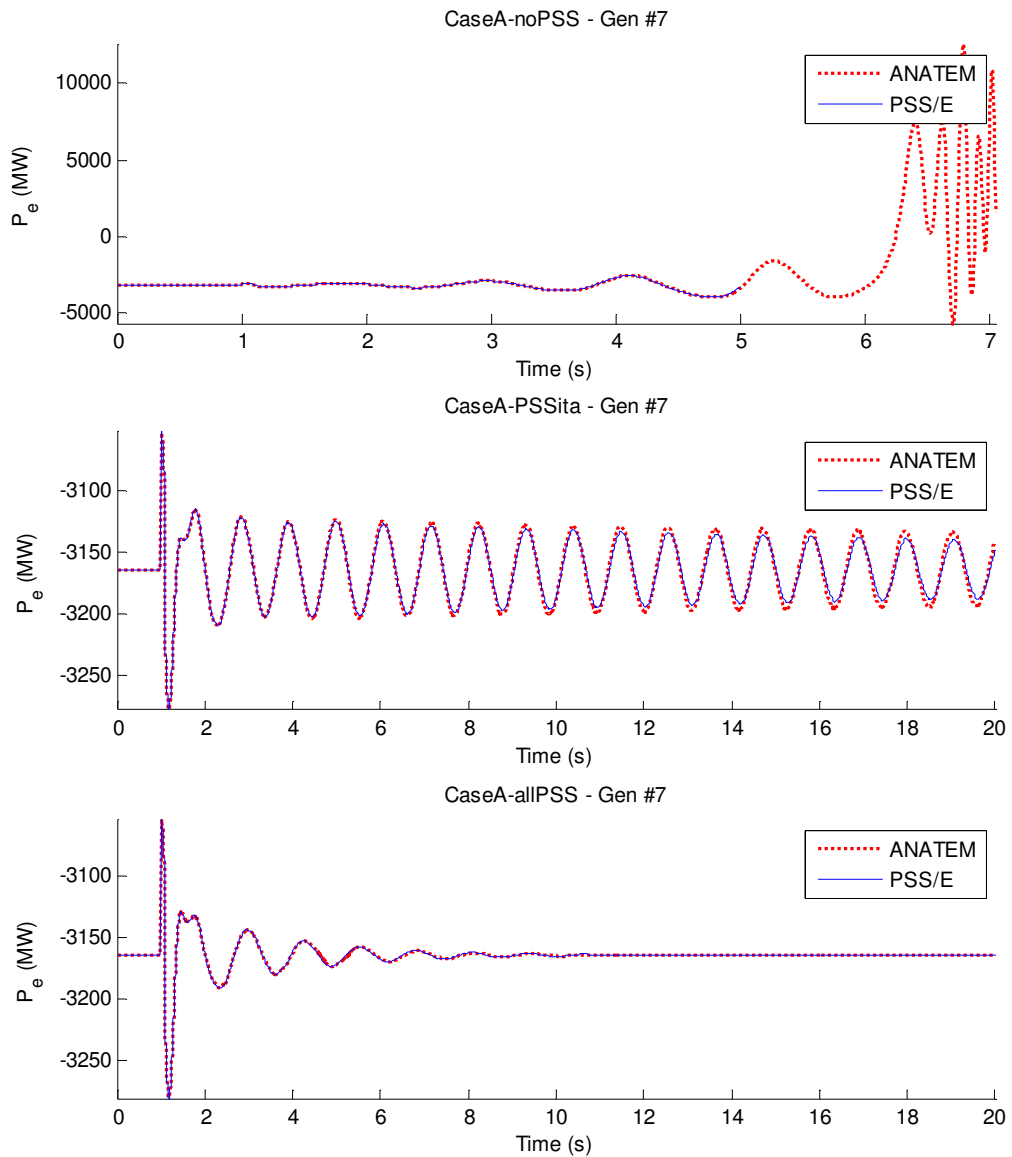


Figure 5.32: Output power Response of Generator #7 to a 500 MVAr Reactor Temporarily Connected to Bus #6. Top: no PSS; Center: PSS at Itaipu; Bottom: PSS at four generators.

Case B: Step applied to the AVR reference of Generator #4

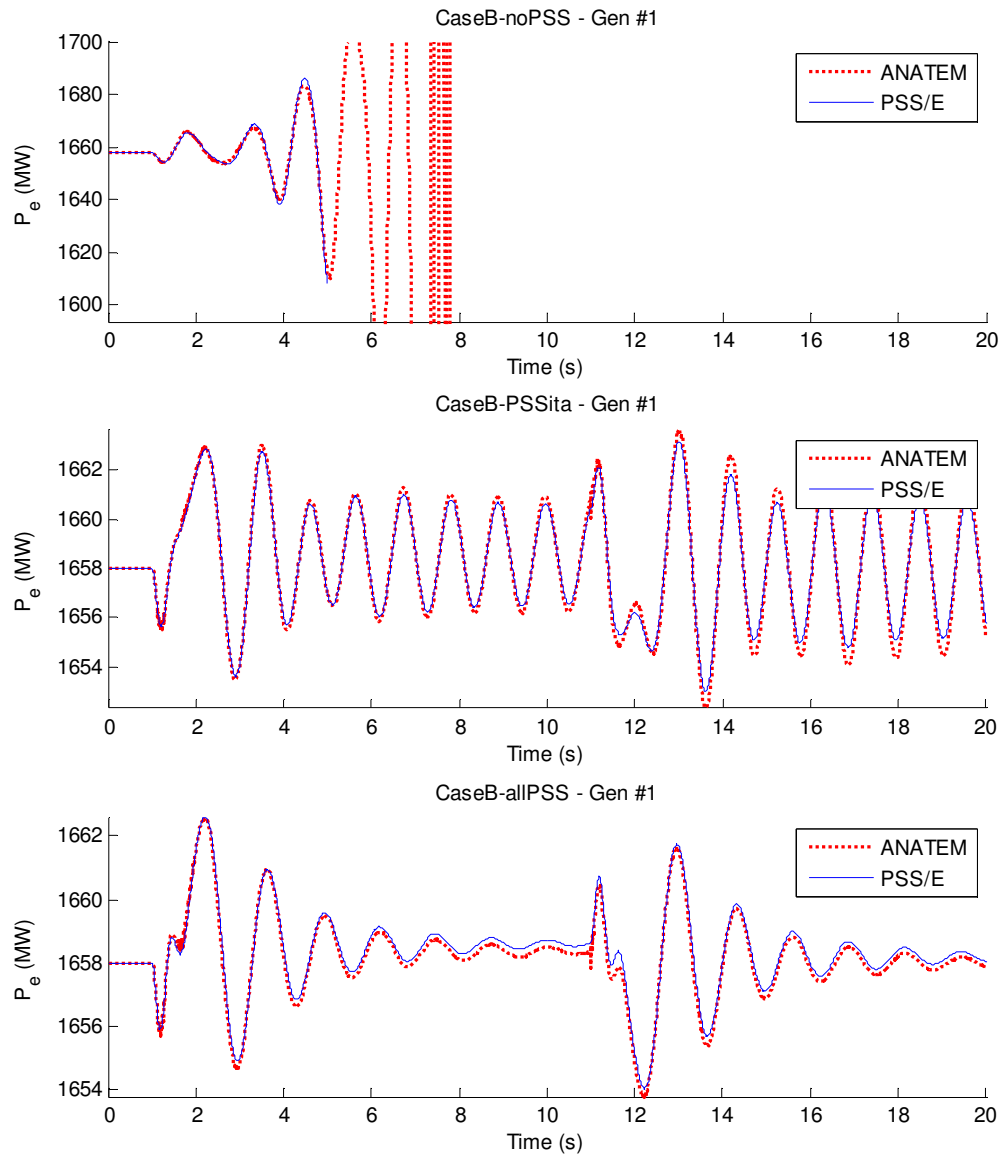


Figure 5.33: Output power response of Generator #1 to step applied to the AVR reference of Generator #4. Top: no PSS; Center: PSS at Itaipu; Bottom: PSS at four generators.

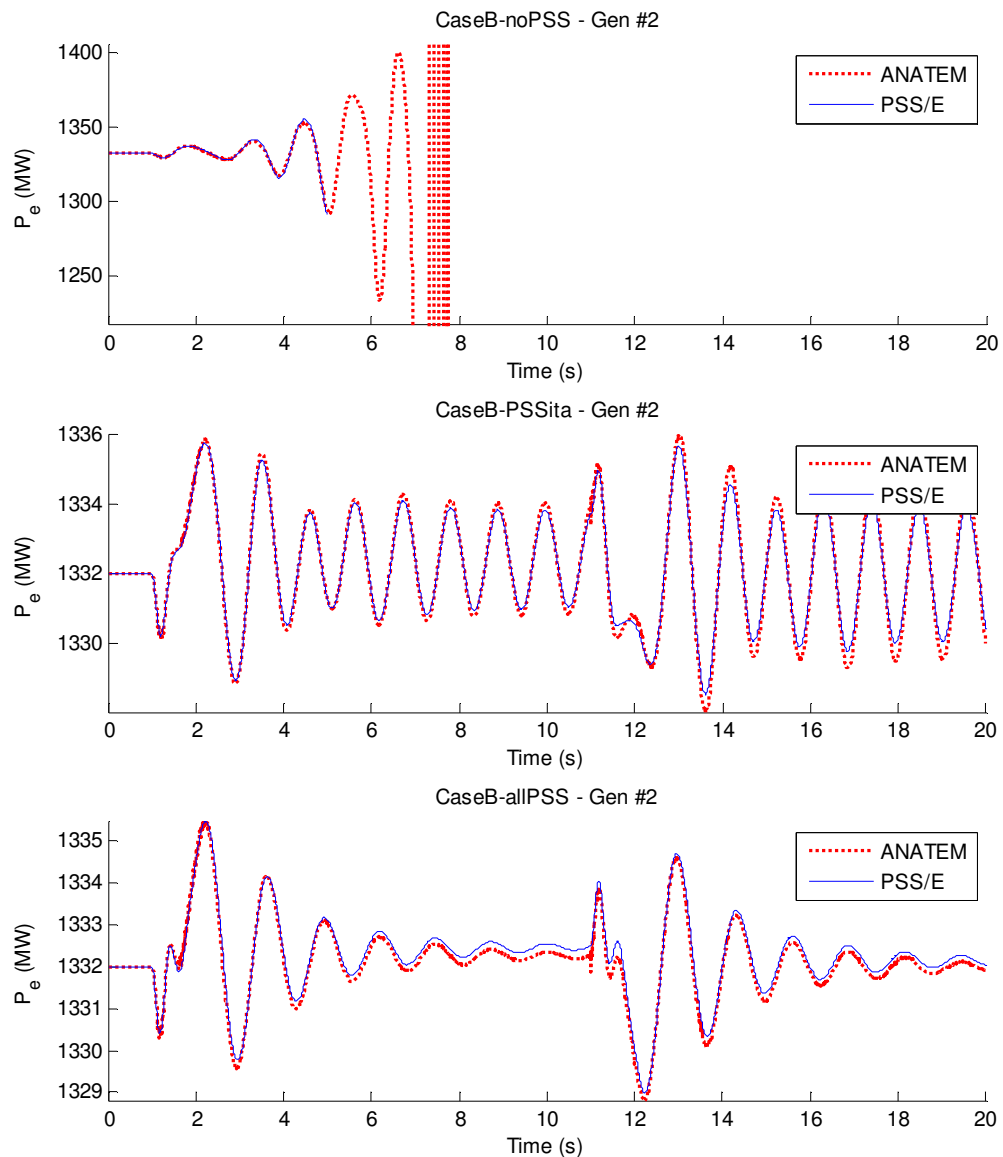


Figure 5.34: Output power response of Generator #2 to step applied to the AVR reference of Generator #4. Top: no PSS; Center: PSS at Itaipu; Bottom: PSS at four generators.

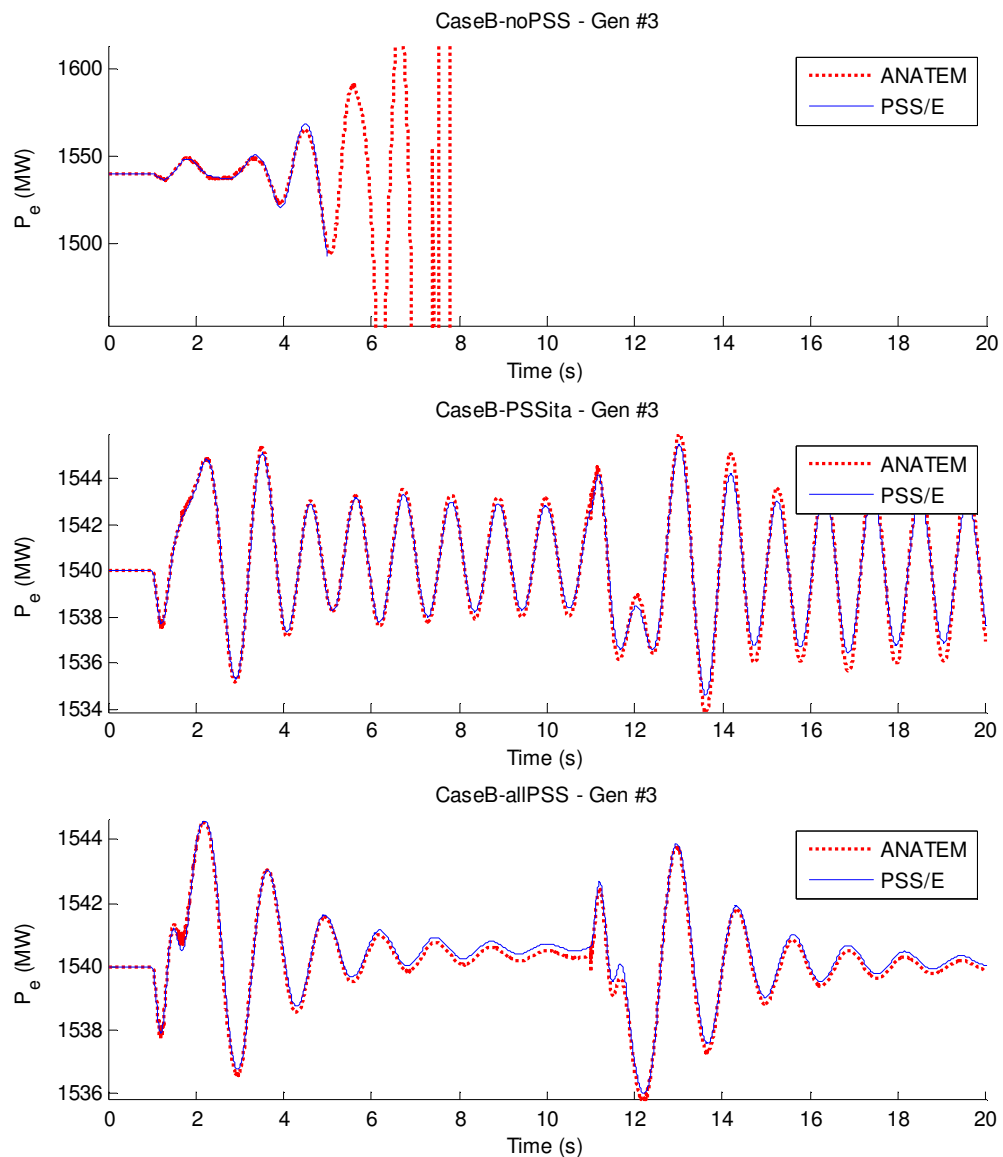


Figure 5.35: Output power response of Generator #3 to step applied to the AVR reference of Generator #4. Top: no PSS; Center: PSS at Itaipu; Bottom: PSS at four generators.

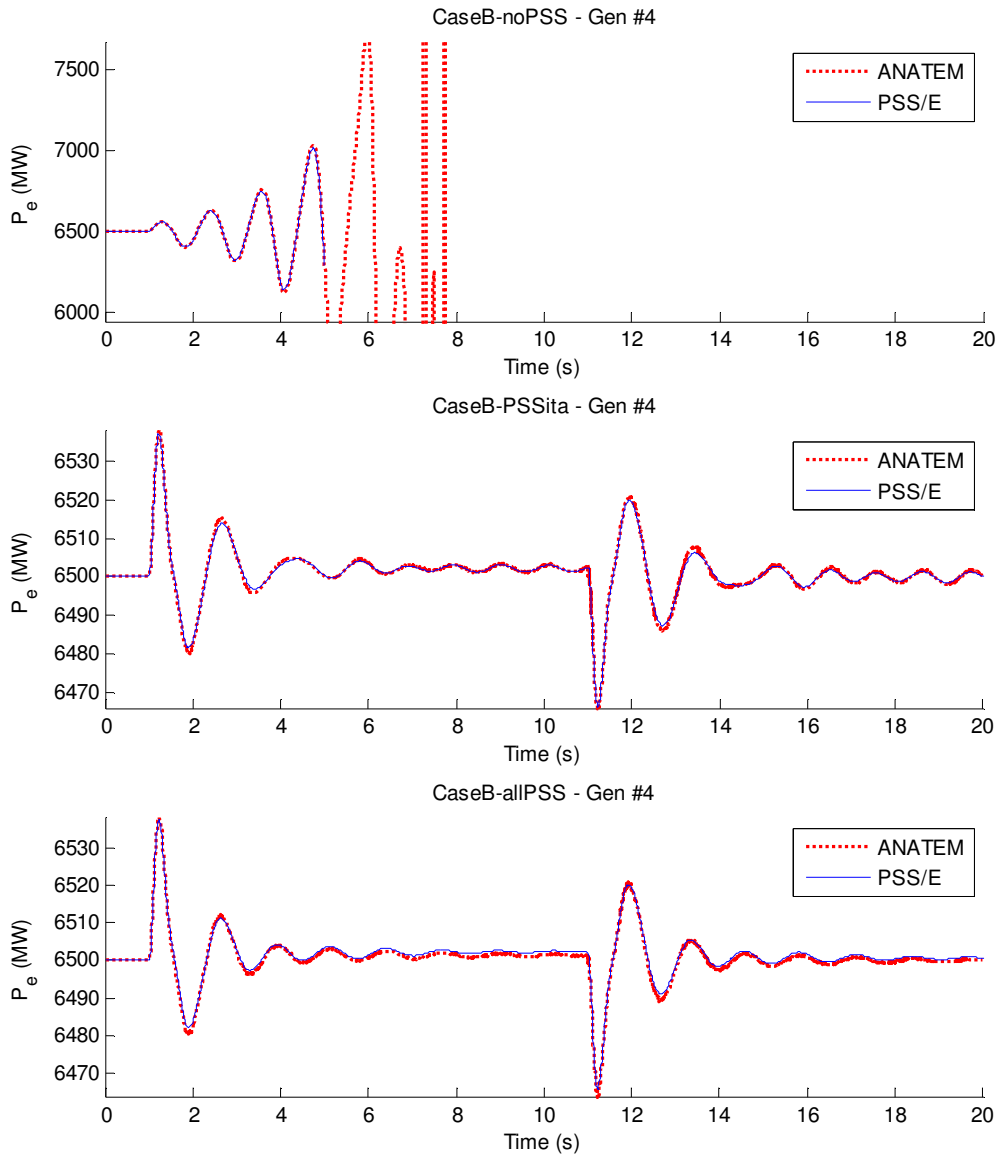


Figure 5.36: Output power response of Generator #4 to step applied to the AVR reference of Generator #4. Top: no PSS; Center: PSS at Itaipu; Bottom: PSS at four generators.

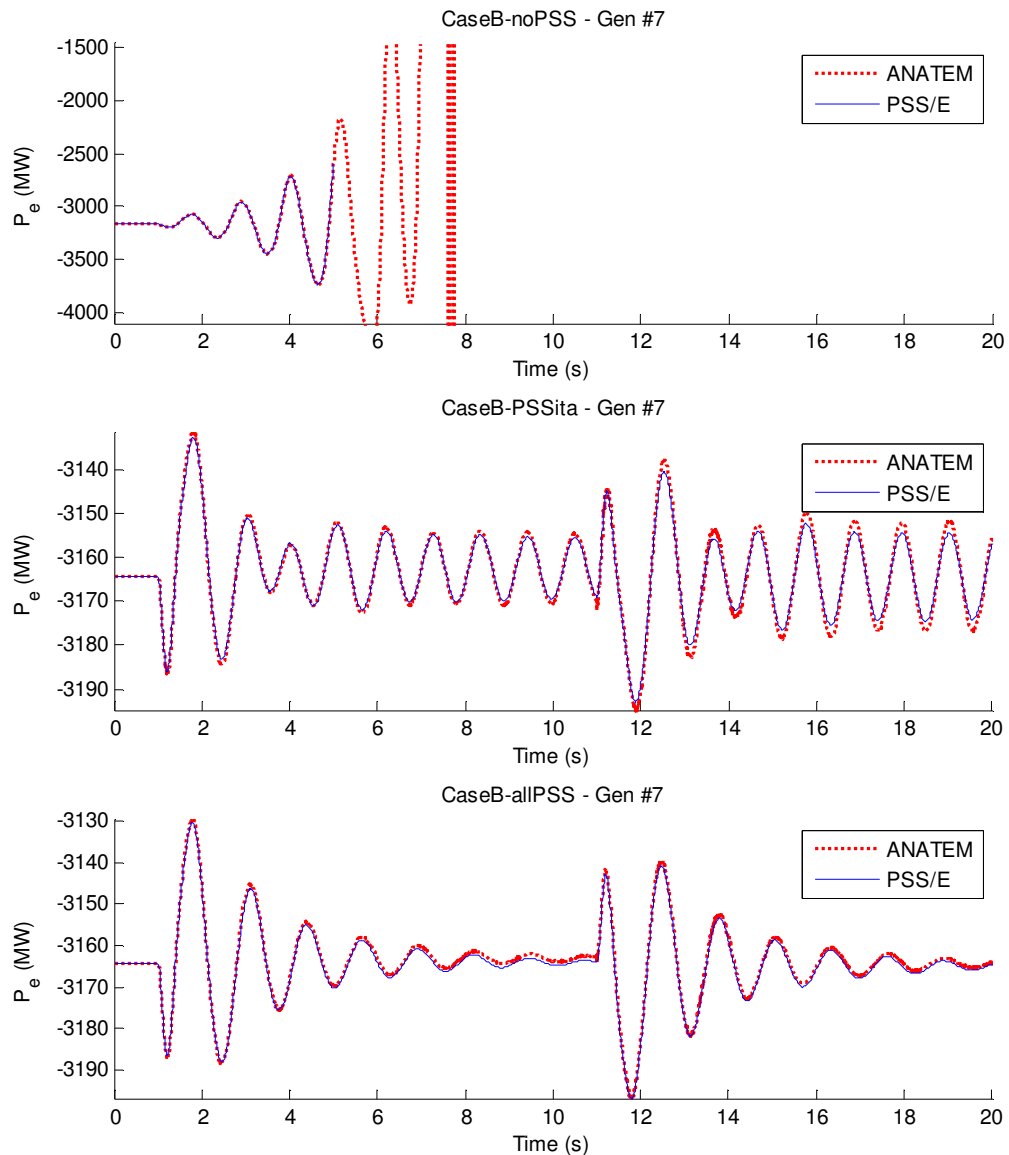


Figure 5.37: Output power response of Generator #7 to step applied to the AVR reference of Generator #4. Top: no PSS; Center: PSS at Itaipu; Bottom: PSS at four generators.

5.3. Data for the 2-area (4-generator) system

5.3.1. Power Flow Data

For the 2-area (4-generator) system, the one-line diagram (together with one respective power flow solution) is shown in Figure 5.38, with the one line diagram of the system. The bus data, including the voltage magnitudes and angles from this power flow solution, are shown in Table 5.20.

The transmission line data is shown in Table 5.21. The data is provided in percent considering a system MVA base of 100 MVA. All transmission lines are 230 kV lines. The lines are represented by π sections and the charging shown in Table 5.21 corresponds to the total line charging.

The only difference regarding the data as presented in [16] is the introduction of multiple parallel circuits, so results considering weaker transmission system conditions might be investigated.

The generator step-up transformers (GSU) are explicitly represented in the case. The GSUs are all rated 900 MVA and have a leakage reactance of 15% on the transformer base. Winding resistance and magnetizing currents are neglected. Table 5.22 presents the GSU data.

There are two loads, directly connected to the 230 kV buses 7 and 9. The associated data is given in Table 5.23. These loads are represented, in the dynamic simulation, with a constant current characteristic for the active power and a constant admittance characteristic for the reactive power ($100\%I$, $100\%Z$ for P and Q, respectively).

Capacitor banks are also connected to the 230 kV buses 7 and 9. The values for these capacitors at nominal voltage (1.0 pu voltage) are shown in Table 5.24.

The complete output report with all power flows for this system is given in Table 5.25.

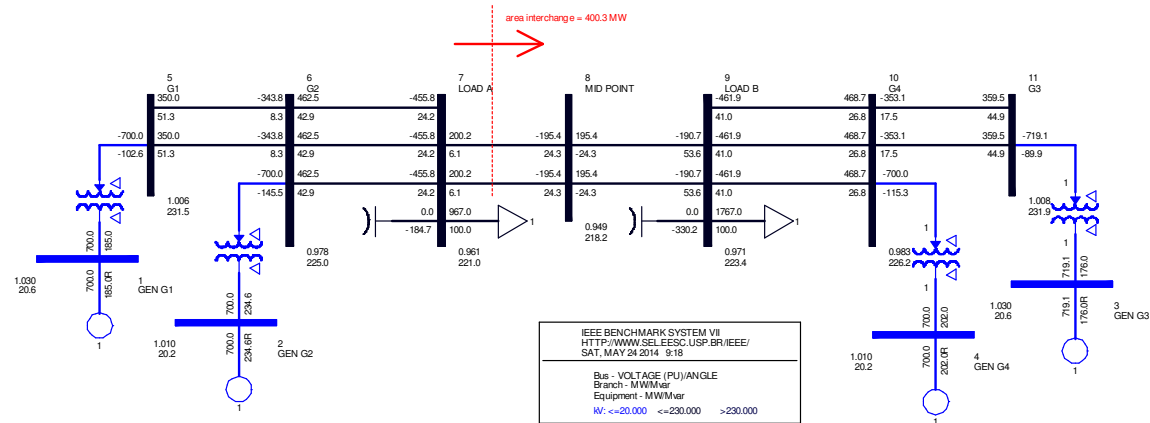


Figure 5.38: One-line Diagram of the 2-area, 4-generator system (with power flow solution)

Table 5.20: Bus Data and Power Flow Solution

Bus Number	Bus Name	Base kV	Bus type	Voltage (pu)	Angle (deg)
1	GEN G1	20.0	PV	1.0300	20.07
2	GEN G2	20.0	PV	1.0100	10.31
3	GEN G3	20.0	swing	1.0300	-7.00
4	GEN G4	20.0	PV	1.0100	-17.19
5	G1	230.0	PQ	1.0065	13.61
6	G2	230.0	PQ	0.9781	3.52
7	LOAD A	230.0	PQ	0.9610	-4.89
8	MID POINT	230.0	PQ	0.9486	-18.76
9	LOAD B	230.0	PQ	0.9714	-32.35
10	G4	230.0	PQ	0.9835	-23.94
11	G3	230.0	PQ	1.0083	-13.63

Table 5.21: Transmission Line Data

From Bus	To Bus	ckt id	R (%)	X (%)	Charging (%)	Length (km)
5	6	1	0.50	5.0	2.1875	25
5	6	2	0.50	5.0	2.1875	25
6	7	1	0.30	3.0	0.5833	10
6	7	2	0.30	3.0	0.5833	10
6	7	3	0.30	3.0	0.5833	10
7	8	1	1.10	11.0	19.2500	110
7	8	2	1.10	11.0	19.2500	110
8	9	1	1.10	11.0	19.2500	110
8	9	2	1.10	11.0	19.2500	110
9	10	1	0.30	3.0	0.5833	10
9	10	2	0.30	3.0	0.5833	10
9	10	3	0.30	3.0	0.5833	10
10	11	1	0.50	5.0	2.1875	25
10	11	2	0.50	5.0	2.1875	25

Table 5.22: Generator Step- Up Transformer Data (on Transformer MVA Base)

From Bus	To Bus	R (%)	X (%)	MVA Base	tap (pu)
1	5	0	15	900	1
2	6	0	15	900	1
3	11	0	15	900	1
4	10	0	15	900	1

Table 5.23: Load Data

Bus	P (MW)	Q (MVar)
7	967	100
9	1767	100

Table 5.24: Capacitor Bank Data

Bus	Q (MVar)
7	200
9	350

Table 5.25: Power Flow Results

X---- FROM BUS ---X VOLT		GEN	LOAD	SHUNT	X---- TO BUS -----X	TRANSFORMER				
BUS#	X-- NAME --X PU/KV	ANGLE	MW/MVAR	MW/MVAR	MW/MVAR	BUS#	X-- NAME --X CKT	MW	MVAR	RATIO
1 GEN G1	1.0300	20.1	700.0	0.0	0.0	-----				
	20.600		185.0R	0.0	0.0	5 G1	1	700.0	185.0	1.000UN
2 GEN G2	1.0100	10.3	700.0	0.0	0.0	-----				
	20.200		234.6R	0.0	0.0	6 G2	1	700.0	234.6	1.000UN
3 GEN G3	1.0300	-7.0	719.1	0.0	0.0	-----				
	20.600		176.0R	0.0	0.0	11 G3	1	719.1	176.0	1.000UN
4 GEN G4	1.0100	-17.2	700.0	0.0	0.0	-----				
	20.200		202.0R	0.0	0.0	10 G4	1	700.0	202.0	1.000UN
5 G1	1.0065	13.6	0.0	0.0	0.0	-----				
	231.49		0.0	0.0	0.0	1 GEN G1	1	-700.0	-102.6	1.000LK
						6 G2	1	350.0	51.3	
						6 G2	2	350.0	51.3	
6 G2	0.9781	3.5	0.0	0.0	0.0	-----				
	224.97		0.0	0.0	0.0	2 GEN G2	1	-700.0	-145.5	1.000LK
						5 G1	1	-343.8	8.3	
						5 G1	2	-343.8	8.3	
						7 LOAD A	1	462.5	42.9	
						7 LOAD A	2	462.5	42.9	
						7 LOAD A	3	462.5	42.9	
7 LOAD A	0.9610	-4.9	0.0	967.0	0.0	-----				
	221.04		0.0	100.0	-184.7	6 G2	1	-455.8	24.2	
						6 G2	2	-455.8	24.2	
						6 G2	3	-455.8	24.2	
						8 MID POINT	1	200.2	6.1	
						8 MID POINT	2	200.2	6.1	
8 MID POINT	0.9486	-18.8	0.0	0.0	0.0	-----				
	218.18		0.0	0.0	0.0	7 LOAD A	1	-195.4	24.3	
						7 LOAD A	2	-195.4	24.3	
						9 LOAD B	1	195.4	-24.3	
						9 LOAD B	2	195.4	-24.3	
9 LOAD B	0.9714	-32.4	0.0	1767.0	0.0	-----				
	223.42		0.0	100.0	-330.2	8 MID POINT	1	-190.7	53.6	
						8 MID POINT	2	-190.7	53.6	
						10 G4	1	-461.9	41.0	
						10 G4	2	-461.9	41.0	
						10 G4	3	-461.9	41.0	
10 G4	0.9835	-23.9	0.0	0.0	0.0	-----				
	226.20		0.0	0.0	0.0	4 GEN G4	1	-700.0	-115.3	1.000LK
						9 LOAD B	1	468.7	26.8	
						9 LOAD B	2	468.7	26.8	

						9 LOAD B	3	468.7	26.8
						11 G3	1	-353.1	17.5
						11 G3	2	-353.1	17.5
11 G3	1.0083	-13.6	0.0	0.0	0.0				
	231.90		0.0	0.0	0.0	3 GEN G3	1	-719.1	-89.9
						10 G4	1	359.5	44.9
						10 G4	2	359.5	44.9

5.3.2. Dynamic Data

All generation units are considered identical and will be represented by the same dynamic models and parameters, with exception of the inertias.

The generator model to represent the all units is given in the block diagram in Figure 5.3. The corresponding parameters for this model can be found in Table 5.26.

Table 5.26: Dynamic Model Data for Round Rotor Units

PARAMETERS				
Description		Symbol	Value	Unit
Rated apparent power	M _{BASE}	666.7	MVA	
d-axis open circuit transient time constant	T' _{do}	8.0	s	
d-axis open circuit sub-transient time constant	T" _{do}	0.03	s	
q-axis open circuit transient time constant	T' _{qo}	0.4	s	
q-axis open circuit sub-transient time constant	T" _{qo}	0.05	s	
Inertia	H	†	MW.s/MVA	
Speed damping	D	0	pu	
d-axis synchronous reactance	X _d	1.8	pu	
q-axis synchronous reactance	X _q	1.70	pu	
d-axis transient reactance	X' _d	0.3	pu	
q-axis transient reactance	X' _q	0.55	pu	
sub-transient reactance	X" _d = X" _q	0.25	pu	
Leakage reactance	X _ℓ	0.20	pu	
Saturation factor at 1.0 pu voltage	S(1.0)	0.0392	—	
Saturation factor at 1.2 pu voltage	S(1.2)	0.2672	—	

Notes:

[†] Units 1 and 2 have inertias $H = 6.50$, while units 3 and 4 have inertias $H = 6.175$

The block diagram of the Excitation System Model DC1A [4] is shown in Figure 5.39. The TGR will be implemented by the lead-lag block with parameters T_C and T_B , so the parameters T_{C1} , T_{B1} , K_F and T_F are not applicable and have been set accordingly. Similarly, the generator field current limit represented by the parameters K_{LR} and I_{LR} is not considered in the results presented in this report. The parameters for the ST1A model are presented in Table 5.28.

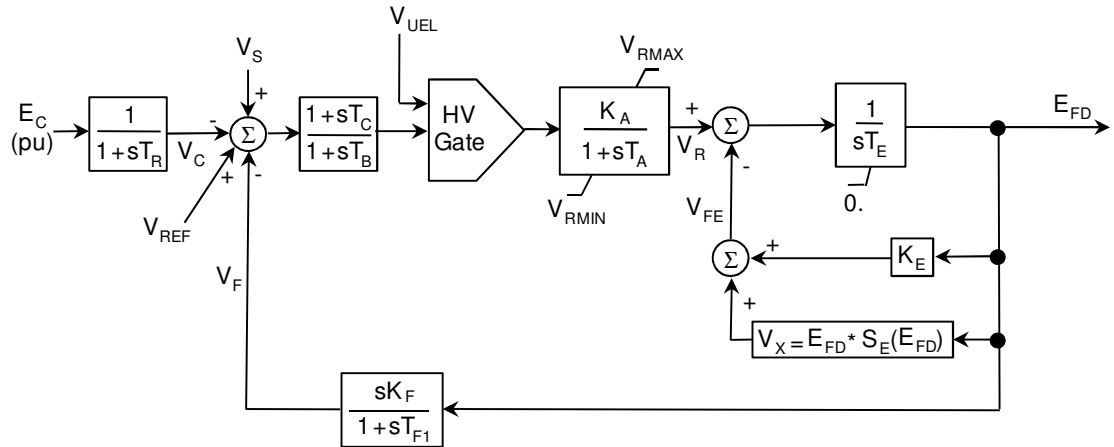


Figure 5.39: Block Diagram for the Excitation System Model DC1A

Table 5.27: Dynamic Model Data for DC Rotating Excitation System Model DC1A

PARAMETERS			
Description	Symbol	Value	Unit
Voltage transducer time constant	\$T_R\$	0.05	s
AVR steady state gain	\$K_A\$	\$20^\dagger\$	pu
AVR equivalent time constant	\$T_A\$	0.055	s
TGR block 1 denominator time constant	\$T_B\$	0	s
TGR block 2 numerator time constant	\$T_C\$	0	s
Max. AVR output	\$V_{Rmax}\$	5	pu
Min. AVR output	\$V_{Rmin}\$	-3	pu
Exciter feedback time constant	\$K_E\$	1	pu
Exciter time constant	\$T_E\$	0.36	s
Stabilizer feedback gain	\$K_F\$	0.125	pu
Stabilizer feedback time constant	\$T_{F1}\$	1.8	s
Exciter saturation point 1	\$E_1\$	\$3^\dagger\$	pu
Exciter saturation factor at point 1	\$S_E(E_1)\$	0.1	-
Exciter saturation point 2	\$E_2\$	4	pu
Exciter saturation factor at point 2	\$S_E(E_2)\$	0.3	-

The block diagram of the Excitation System Model ST1A [4] is shown in Figure 5.40. The TGR will be implemented by the lead-lag block with parameters \$T_C\$ and \$T_B\$, so the parameters \$T_{C1}\$, \$T_{B1}\$, \$K_F\$ and \$T_F\$ are not applicable and have been set accordingly. Similarly, the generator field current limit represented by the parameters \$K_{LR}\$ and \$I_{LR}\$ is not considered in the results presented in this report. The parameters for the ST1A model are presented in Table 5.28.

The limits (parameters $V_{I\max}$, $V_{I\min}$, $V_{A\max}$, $V_{A\min}$, $V_{R\max}$ and $V_{R\min}$) in the model were set to typical values corresponding to the expected ceilings of such static excitation system. These limits are irrelevant for the small-signal analysis of the system dynamic response. On the other hand, these limits are a critical part of the model and the expected response of the excitation system following large system disturbances such as faults.

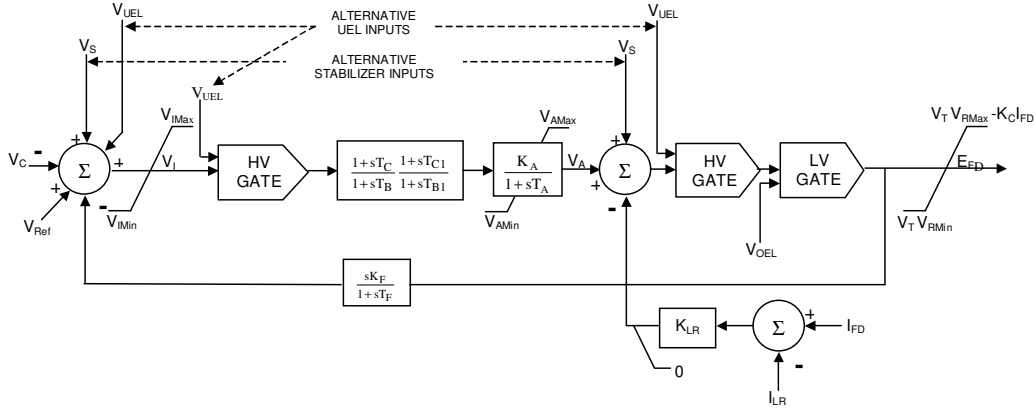


Figure 5.40: Block Diagram for the Excitation System Model ST1A

Table 5.28: Dynamic Model Data for Static Excitation System Model ST1A

PARAMETERS			
Description	Symbol	Value	Unit
Voltage transducer time constant	T_R	0.01	s
Max. voltage error	$V_{I\max}$	99	pu
Min. voltage error	$V_{I\min}$	-99	pu
TGR block 1 numerator time constant	T_C	1	s
TGR block 1 denominator time constant	T_B	10	s
TGR block 2 numerator time constant	T_{C1}	0	s
TGR block 1 denominator time constant	T_{B1}	0	s
AVR steady state gain	K_A	200	pu
Rectifier bridge equivalent time constant	T_A	0	s
Max. AVR output	$V_{A\max}$	4	pu
Min. AVR output	$V_{A\min}$	-4	pu
Max. rectifier bridge output	$V_{R\max}$	4	pu
Min. rectifier bridge output	$V_{R\min}$	-4	pu
Commutation factor for rectifier bridge	K_C	0	pu
Stabilizer feedback gain	K_F	0	pu
Stabilizer feedback time constant	T_F	1	s
Field current limiter gain	K_{LR}	0	pu
Field current instantaneous limit	I_{LR}	3	pu

The IEEE Std. 421.5(2005) model PSS1A will be used to represent the power system stabilizers. The block diagram corresponding to this model is shown in Figure 5.5. The parameters for the PSS1A model are presented in Table 5.29. The output limits were set to $+/- 5\%$, while the logic to switch off the PSS for voltages outside a normal operation range has been ignored (parameters V_{CU} and V_{CL} set to zero).

Table 5.29: Dynamic Model Data for Power System Stabilizer Model PSS1A

PARAMETERS			
Description	Symbol	Value	Unit
2 nd order denominator coefficient	A ₁	0	
2 nd order denominator coefficient	A ₂	0	
2 nd order numerator coefficient	A ₃	0	
2 nd order numerator coefficient	A ₄	0	
2 nd order denominator coefficient	A ₅	0	
2 nd order denominator coefficient	A ₆	0	
1 st lead-lag numerator time constant	T ₁	0.05	s
1 st lead-lag denominator time constant	T ₂	0.02	s
2 nd lead-lag numerator time constant	T ₃	3	s
2 nd lead-lag denominator time constant	T ₄	5.4	s
Washout block numerator time constant	T ₅	10	s
Washout block denominator time constant	T ₆	10	s
PSS gain	K _S	20	pu
PSS max. output	L _{Smax}	0.05	pu
PSS min. output	L _{Smin}	-0.05	pu
Upper voltage limit for PSS operation	V _{CU}	0	pu
Lower voltage limit for PSS operation	V _{CL}	0	pu

5.3.3. Selected Results and Validation

The results presented in the following correspond to eigenvalue calculations and time-domain simulations of disturbances in the AVR references, for different system configurations (with and without power system stabilizers) performed with the PSS/E [24] and PacDyn/ANATEM [25], [26] software packages.

Based on reference [16], the cases that were considered for evaluation of the 2-area (4-generator) system are the following:

Case 1: All generators in manual control (constant generator field voltage);

Case 2: DC1A model for the excitation system with $K_a = 20$;

Case 3: DC1A model for the excitation system with $K_a = 200$;

Case 4: ST1A model for the excitation system (with TGR);

Case 5: ST1A model for the excitation system (without TGR);

Case 6: ST1A model for the excitation system without TGR and with PSS1A.

Not all of these cases, however, were taken into account in the comparative analysis performed for benchmarking this system. To avoid the presentations of an unnecessarily large

set of results in this section (taking into account that the set of eigenvalues for the 2-area (4-generator) system is larger than the previous ones), only the results related to the ST1A excitation system (Cases 4, 5, and 6) were included in this comparative analysis.

Furthermore, only the electromechanical oscillations will be compared, to keep this section of the report focused on the main aspect covered by this Task Force. However, the interested reader is referred to Appendix C of this report for a much more detailed set of results for this system, produced using PSS/E.

The reader will notice that Case 2 is not present in reference [16]. It was deliberately introduced in Appendix C with the objective of showing the effect of a higher AVR gain on the DC1A excitation system model. In order to do so, the AVR gain was increased tenfold with respect to the parameters of Table 5.27. This is the main reason why all the 6 cases that were considered for evaluation of the system are listed at the beginning of this section.

Regarding the eigenvalue calculations, the mode comparisons were made for case 5, and are shown in Table 5.30. When the PSS/E and PacDyn results are compared, the imaginary parts exhibit a close match for all modes, although the same cannot be said for the real parts. However, it is interesting to see that, regarding these real parts, the LSYSAN program for PSS/E provides a reasonable approximation to the ones calculated by PacDyn for the local modes, while for the inter-area modes a better match with PacDyn is obtained when the PSS/E plotting package PSSPLT is used. For a more detailed explanation on how both LSYSAN and PSSPLT work, the reader is referred to Section 3.8 of Appendix C to this report.

It is also noticeable that the eigenvalues provided in reference [16] are not as close to the ones calculated/estimated by PacDyn and PSS/E. This is easily explained by the fact that a quite simple model (consisting of a single first order block) is used to represent the excitation system in [16], while the full ST1A standard model of Figure 5.40 is used to obtain the results shown in the other columns of Table 5.30.

Table 5.30: Comparison of electromechanical modes provided by different sources for the 2-area (4-generator) system.

Source of Results \ Oscillation Mode	Reference [16]	PSS/E (LSYSAN)	PSS/E (PSSPLT)	PacDyn
Local Mode - Area 1 (G1 X G2)	-0.490±j7.15	-0.660±j7.29	-0.575±j7.06	-0.639±j7.08
Local Mode - Area 2 (G3 X G4)	-0.496±j7.35	-0.656±j7.09	Not Provided	-0.639±j7.28
Inter-Area Mode (G1+G2 X G3 +G4)	0.031±j3.84	0.006±j3.84	0.038±j3.82	0.022±j3.82

With respect to the time-domain simulations, the disturbances applied in all simulation cases correspond to simultaneous changes in voltage references in all generator units, applied at t=1.0 second. The applied step changes are depicted in Table 5.31.

Table 5.31: Perturbations applied for the nonlinear simulations of the 2-area (4-generator) system.

GENERATOR	STEP IN V_{ref}
G1	+3%
G2	-1%
G3	-3%
G4	+1%

These changes in voltage reference were selected in order to excite not only the inter-area oscillation mode but also the other electromechanical modes in the system.

A relatively fast (high initial response) ST1A excitation system was used to produce the following results. Figure 5.41 shows the comparison of speed deviations for all generating units obtained by PSS/E and ANATEM in Case 4, when an AVR with transient gain reduction is used and the PSS is not active. Under the same conditions, the active power outputs of all generating units were compared in Figure 5.42.

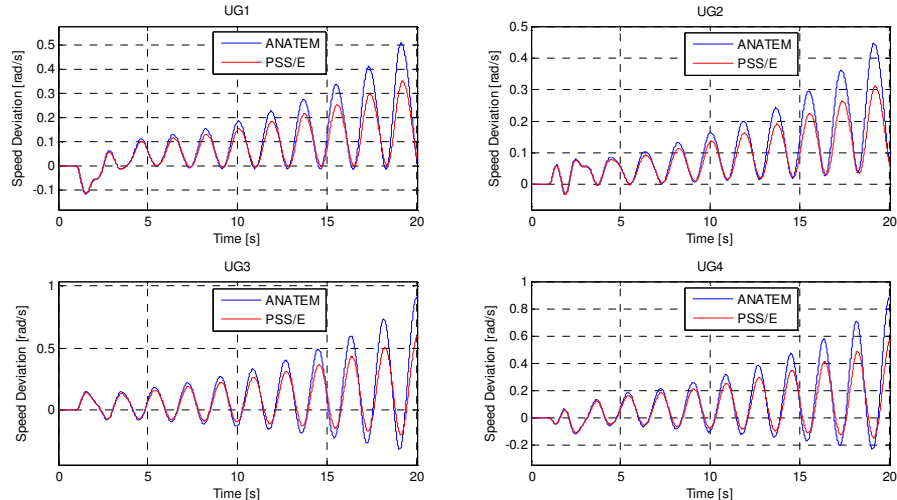


Figure 5.41: Response of the rotor speed deviations for all four generators to the applied perturbation (Case 4: ST1A excitation system, with TGR and without PSS).

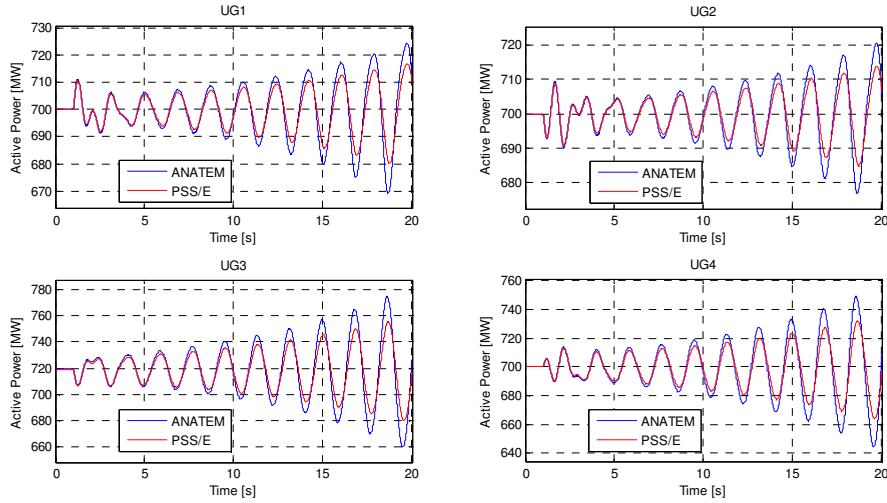


Figure 5.42: Response of the active power outputs for all four generators to the applied perturbation (Case 4: ST1A excitation system, with TGR and without PSS).

For Case 5 (in which the only difference from Case 4 is the absence of the TGR block), Figure 5.43 and Figure 5.44. show the comparison of speed deviations and active power outputs for all generating units obtained by PSS/E and ANATEM.

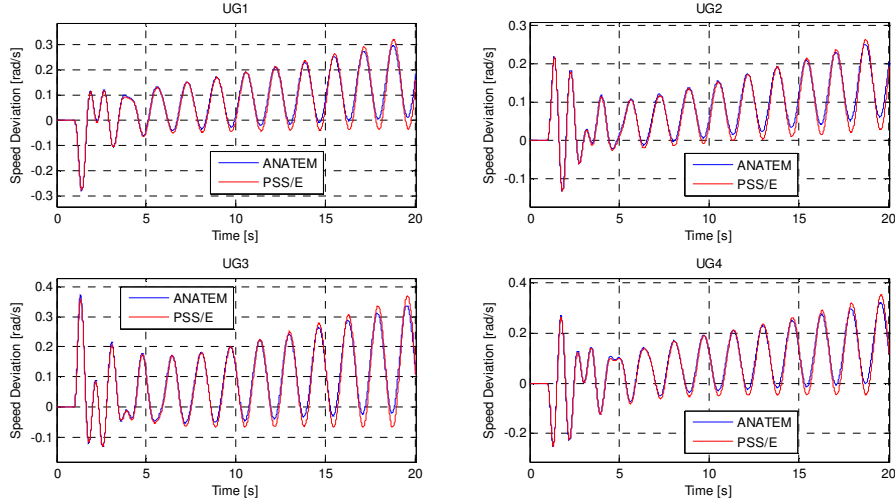


Figure 5.43: Response of the rotor speed deviations for all four generators to the applied perturbation (Case 5: ST1A excitation system, without TGR and without PSS).

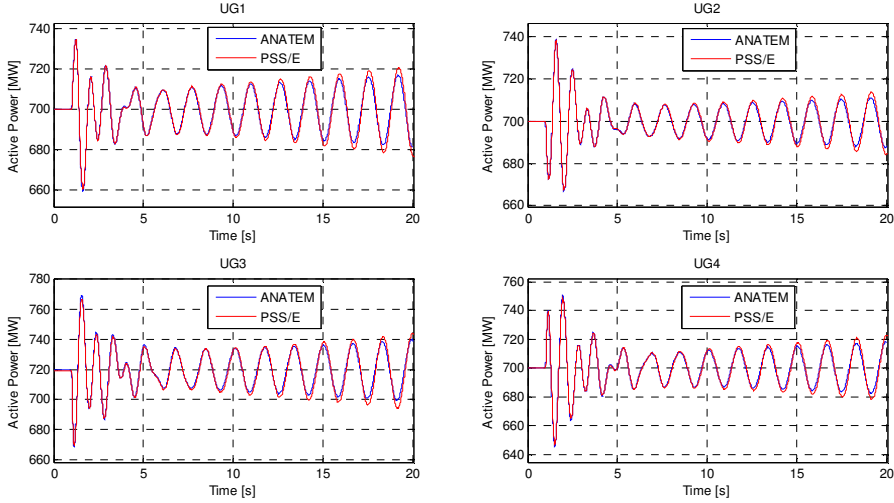


Figure 5.44: Response of the active power outputs for all four generators to the applied perturbation (Case 5: ST1A excitation system, without TGR and without PSS).

It is possible to see, by comparison of Figure 5.41 and Figure 5.43 (or Figure 5.42 and Figure 5.44) that the deviations with respect to the equilibrium conditions are larger in the simulations with the TGR block. Considering that these are two simulations of perturbations applied under unstable conditions (and, thus, the deviations grow larger as the time progresses), the most likely reasons for the differences observed in the PSS/E results with respect to the ones provided by ANATEM are produced by a combination of nonlinear effects, different integration methods and differences in the representation of damping.

The statement in the previous paragraph is reinforced by the results shown for a stable case. For Case 6, (in which a well-tuned PSS ensures the system steady-state is a stable equilibrium), Figure 5.45 shows the comparison of speed deviations and Figure 5.46 shows the comparison of active power outputs for all generating units.

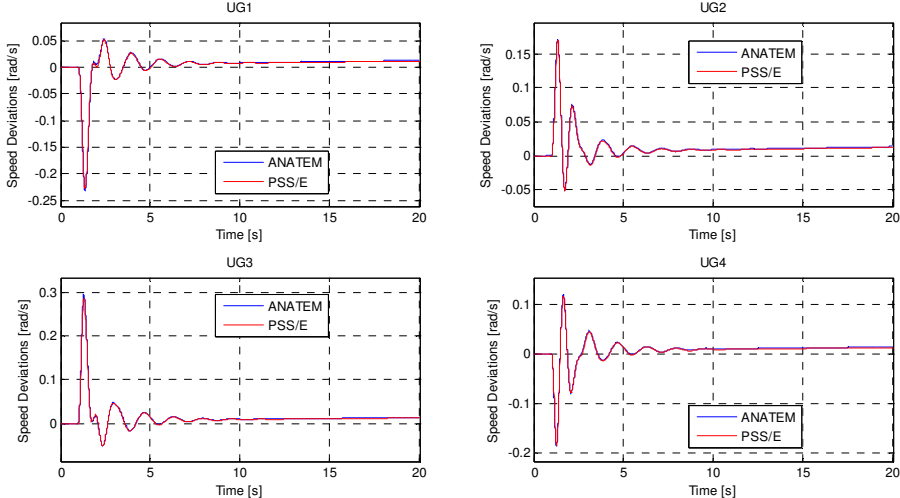


Figure 5.45: Response of the rotor speed deviations for all four generators to the applied perturbation (Case 6: ST1A excitation system, without TGR and with PSS).

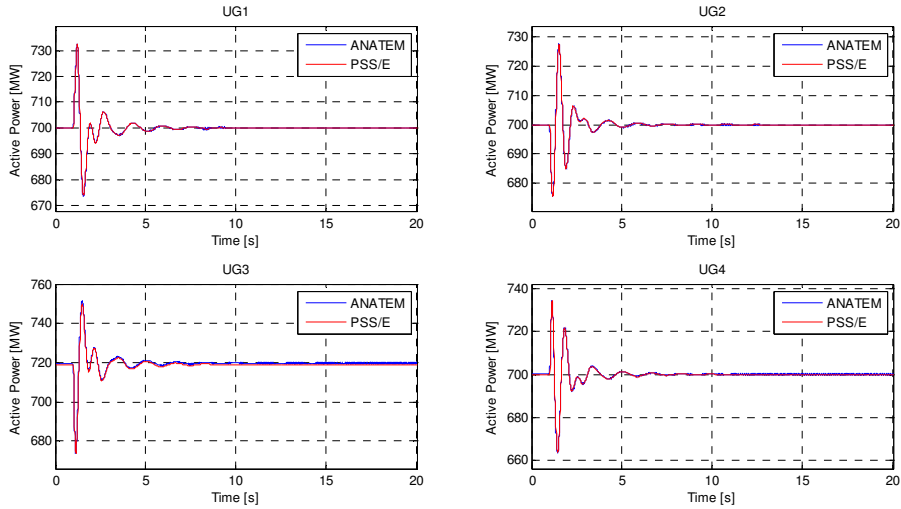


Figure 5.46: Response of the active power outputs for all four generators to the applied perturbation (Case 6: ST1A excitation system, without TGR and with PSS).

The nearly perfect match exhibited in Figure 5.45 and Figure 5.46, associated to the arguments given in the previous paragraph, allow the conclusion that this benchmark has been validated.

Finally, it is important to mention once again that, to avoid the presentations of an unnecessarily large set of results in this section, only the results related to the ST1A excitation system were included in the comparative analysis performed for benchmarking this system. The reader is referred to Appendix C for a complete set of simulations of all six cases defined in this report, using PSS/E and adding some extra information.

5.4. Data for the 39-bus (New England) System

As stated in Subsection 3.5, the 39-bus system (widely known and referred to as the New England Test System) first appeared in Volume 1 of EPRI Report EL-2348 [19] which contained, at the time of its publication, the state-of-the-art in the analysis of electromechanical oscillations using eigenvalue calculations. Due to the advancements, particularly in computational speed and memory, the simulation models used in [19] no longer reflect the best practices for representing synchronous generators and associated controllers in power system studies [27], [4].

Since the publication of [19], this system has been extensively used in several types of studies with different objectives, the vast majority of them being related to small-signal stability analysis and control. Even modified versions of this system have appeared in the literature (different system topologies and the inclusion of FACTS devices are a few examples of such modifications). As a result, there are several versions of the New England Test System published in the power system literature where this system is referred to as the "New England Interconnected Power System".

For the purpose of benchmarking this system, this Task Force has made a choice to be faithful to its original source of data [19]. This choice was motivated by the historical value that the New England Test System has, which is strongly associated to the development of researches in the small-signal stability analysis and control fields. Making this choice, however, implies that it is no longer possible to use [27] as the source of dynamic models for the benchmarking process, given that [19] does not provide, for example, data for the subtransient components (impedances and time constants) of the generator models), given the described limitations in the selected models for the synchronous generators and associated controllers.

In summary, this disclaimer was added prior to the description of the data and results for the New England Test System to justify the previously mentioned choice (related to the historical value of this system) and explain the fact that its presentation (mainly with respect to dynamic models) will be made in a different format with respect to the one adopted for the other benchmark systems.

Furthermore, this Task Force has received only one contribution in which the time-domain simulations are performed with the nonlinear models described in [19] (which corresponds to Appendix D to this report). Therefore, it was not possible to perform a validation study with these results. Most commercial software such as [24] or [26], for example, do not have built-in models that can produce comparable results to the ones presented in Appendix D (with respect to the time-domain simulations).

On the other hand, the Task Force has indeed received a contribution using a commercial software described in [25], which is capable of reproducing the results obtained by the eigenvalue calculations presented in Appendix D using its built-in models. As the reader will notice, the match between the two sets of results is very satisfactory. Therefore, for the purpose of validating the New England Test System, only the eigenvalue analysis will be used.

Another contribution received by this Task Force was produced in a software that employs EMTP-type instead of phasor-based simulations. The results of this contribution are fully described in Appendix E, and also added to this section of the report. The main feature of this contribution is a set of time-domain simulations showing the response of the system to a

perturbation in the set-points of the voltage regulators. These simulation results complement the eigenvalue analysis on which the benchmark validation was grounded.

5.4.1. Power Flow Data

The one-line diagram for the New England Test System was already shown in Figure 4.4 but is repeated here in Figure 5.47 for convenience.

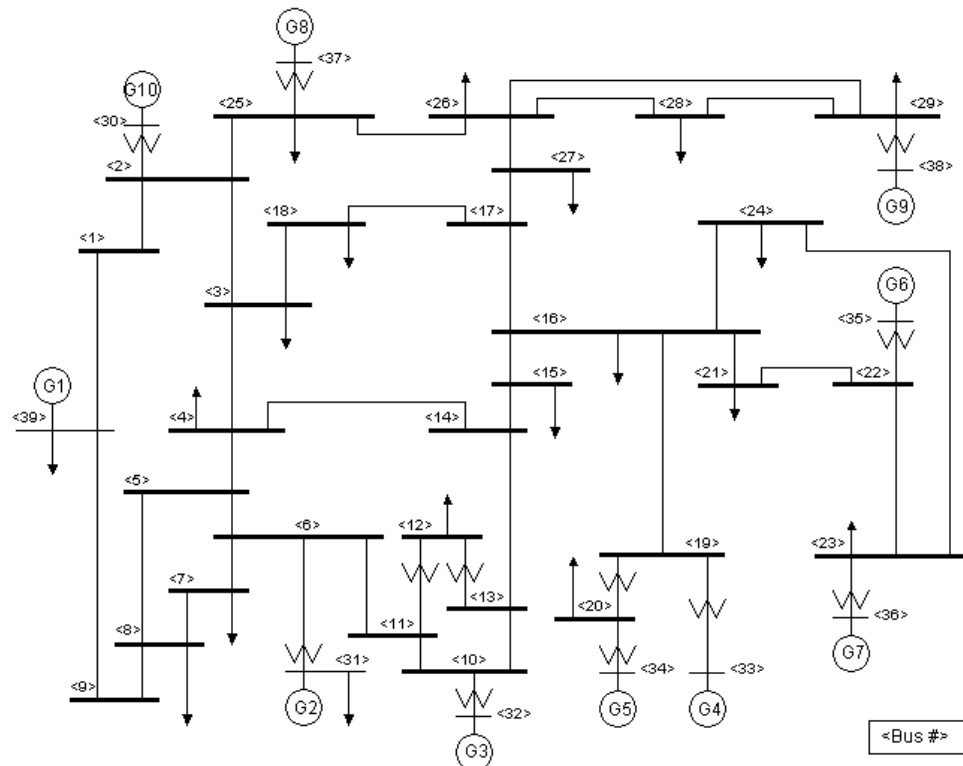


Figure 5.47: The New England system (repeated).

The bus data, including the voltage magnitudes and angles from the power flow solution, are shown in Table 5.32. All data in this section of the report are referred to the system bases of 100 MVA and 100 kV. Load data is also included in Table 5.32, and all loads are represented by constant impedances. A more complete version of Table 5.32 can be found in Appendix D to this report, which includes line flows.

The transmission line data is shown in Table 5.33. The data is provided in per unit using the previously mentioned system bases. The lines are represented by π sections and the susceptances shown in Table 5.33 correspond to the total line charging. The generators step-up transformer data is also given in per unit on system bases, as can be seen in Table 5.34. Table 5.35 brings the same type of data for the other transformers in the system. More details on the power flow data and calculations for this system can be seen in Appendix D to this report.

Table 5.32: Power flow results for the New England Test System.

Bus	V[pu]	Angle[Deg]	Generation		Load	
			P[MW]	Q[MVAR]	P[MW]	Q[MVAR]
1	1.047	-8.4	0.0	0.0	0.0	0.0
2	1.049	-5.8	0.0	0.0	0.0	0.0
3	1.030	-8.6	0.0	0.0	322.0	2.4
4	1.004	-9.6	0.0	0.0	500.0	184.0
5	1.005	-8.6	0.0	0.0	0.0	0.0
6	1.008	-7.9	0.0	0.0	0.0	0.0
7	0.997	-10.1	0.0	0.0	233.8	84.0
8	0.996	-10.6	0.0	0.0	522.0	176.0
9	1.028	-10.3	0.0	0.0	0.0	0.0
10	1.017	-5.4	0.0	0.0	0.0	0.0
11	1.013	-6.3	0.0	0.0	0.0	0.0
12	1.000	-6.2	0.0	0.0	7.5	88.0
13	1.014	-6.1	0.0	0.0	0.0	0.0
14	1.012	-7.7	0.0	0.0	0.0	0.0
15	1.015	-7.7	0.0	0.0	320.0	153.0
16	1.032	-6.2	0.0	0.0	329.4	32.3
17	1.034	-7.3	0.0	0.0	0.0	0.0
18	1.031	-8.2	0.0	0.0	158.0	30.0
19	1.050	-1.0	0.0	0.0	0.0	0.0
20	0.991	-2.0	0.0	0.0	628.0	103.0
21	1.032	-3.8	0.0	0.0	274.0	115.0
22	1.050	0.7	0.0	0.0	0.0	0.0
23	1.045	0.5	0.0	0.0	274.5	84.6
24	1.037	-6.1	0.0	0.0	308.6	-92.2
25	1.058	-4.4	0.0	0.0	224.0	47.2
26	1.052	-5.5	0.0	0.0	139.0	17.0
27	1.038	-7.5	0.0	0.0	281.0	75.5
28	1.051	-2.0	0.0	0.0	206.0	27.6
29	1.050	0.7	0.0	0.0	283.5	26.9
30	1.048	-3.3	250.0	147.6	0.0	0.0
31	0.982	0.0	520.8	198.2	9.2	4.6
32	0.983	2.6	650.0	204.7	0.0	0.0
33	0.997	4.2	632.0	109.6	0.0	0.0
34	1.012	3.2	508.0	165.3	0.0	0.0
35	1.049	5.6	650.0	210.6	0.0	0.0
36	1.064	8.3	560.0	102.9	0.0	0.0
37	1.028	2.4	540.0	0.2	0.0	0.0
38	1.027	7.8	830.0	23.2	0.0	0.0
39	1.030	-10.1	1000.0	87.8	1104.0	250.0

Table 5.33: Transmission Line Data

From Bus	To Bus	R (p.u.)	X (p.u.)	B (p.u.)
1	2	0.0035	0.0411	0.6987
1	39	0.001	0.025	0.75
2	3	0.0013	0.0151	0.2572
2	25	0.007	0.0086	0.146
3	4	0.0013	0.0213	0.2214
3	18	0.0011	0.0133	0.2138
4	5	0.0008	0.0128	0.1342
4	14	0.0008	0.0129	0.1382
5	6	0.0002	0.0026	0.0434
5	8	0.0008	0.0112	0.1476
6	7	0.0006	0.0092	0.113
6	11	0.0007	0.0082	0.1389
7	8	0.0004	0.0046	0.078
8	9	0.0023	0.0363	0.3804
9	39	0.001	0.025	1.2
10	11	0.0004	0.0043	0.0729
10	13	0.0004	0.0043	0.0729
13	14	0.0009	0.0101	0.1723
14	15	0.0018	0.0217	0.366
15	16	0.0009	0.0094	0.171
16	17	0.0007	0.0089	0.1342
16	19	0.0016	0.0195	0.304
16	21	0.0008	0.0135	0.2548
16	24	0.0003	0.0059	0.068
17	18	0.0007	0.0082	0.1319
17	27	0.0013	0.0173	0.3216
21	22	0.0008	0.014	0.2565
22	23	0.0006	0.0096	0.1846
23	24	0.0022	0.035	0.361
25	26	0.0032	0.0323	0.513
26	27	0.0014	0.0147	0.2396
26	28	0.0043	0.0474	0.7802
26	29	0.0057	0.0625	1.029
28	29	0.0014	0.0151	0.249

Table 5.34: Generator Step- Up Transformer Data

From Bus	To Bus	R (p.u.)	X (p.u.)	Tap (p.u.)
6	31	0	0.025	1.007
10	32	0	0.02	1.007

19	33	0.0007	0.0142	1.007
20	34	0.0009	0.018	1.009
22	35	0	0.0143	1.025
23	36	0.0005	0.0272	1
25	37	0.0006	0.0232	1.025
2	30	0	0.0181	1.025
29	38	0.0008	0.0156	1.025

Table 5.35: Transformer Data

From Bus	To Bus	R (p.u.)	X (p.u.)	Tap (p.u.)
12	11	0.0016	0.0435	1.006
12	13	0.0016	0.0435	1.006
19	20	0.0007	0.0138	1.006

5.4.2. Dynamic Data

All generators in the New England Test System are represented by a 4th order model, given that the available data in [19] is related to this model. As previously mentioned, a different format will be used here for presentation of the model for the generators. The following equations describe this 4th order model.

$$\dot{\delta} = \omega \quad (1)$$

$$\dot{\omega} = \frac{1}{M} (T_{mech} - (I_i I_q + \varphi_q I_d) - D\omega) \quad (2)$$

$$\dot{E}'_q = \frac{1}{T'_{do}} (-E'_q - (x_a - x'_d) I_d + E_f a) \quad (3)$$

$$\dot{E}'_d = \frac{1}{T'_{qo}} (-E'_d - (x_q - x'_q) I_q) \quad (4)$$

All generators in this system are equipped with automatic voltage regulators (AVRs) and power system stabilizers (PSSs). The same controller models are used for all generators, and the corresponding parameters for each of them are presented in the following. Figure 5.48 presents the AVR model while Figure 5.49 presents the PSS model used in the mentioned implementations. The reader can see that they are simplified versions of the currently adopted models standardized in [4].

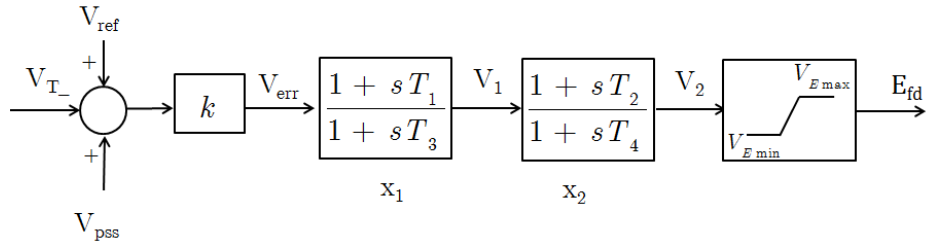


Figure 5.48: Automatic voltage regulator model for all generators in the New England Test System.

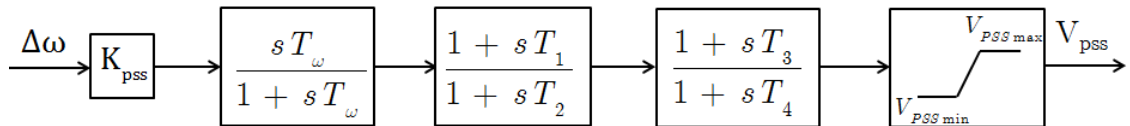


Figure 5.49: Power system stabilizer model for all generators in the New England Test System.

The data for the generators are given in Table 5.36, while the AVR and PSS data are given in Table 5.37 and Table 5.38. With respect to Table 5.36, the per unit conversion from H to M associated with ω is in radians per second, leading to $H = 2M / (120\pi)$, so the value of M that must be used in equations (1) to (4) can be calculated from this relation.

Table 5.36: Generator data for the New England Test System.

Unit No.	H	R _a	x' _d	x' _q	x _d	x _q	T' _{do}	T' _{qo}	x _I
1	500	0	0.006	0.008	0.02	0.019	7	0.7	0.003
2	30.3	0	0.0697	0.17	0.295	0.282	6.56	1.5	0.035
3	35.8	0	0.0531	0.0876	0.2495	0.237	5.7	1.5	0.0304
4	28.6	0	0.0436	0.166	0.262	0.258	5.69	1.5	0.0295
5	26	0	0.132	0.166	0.67	0.62	5.4	0.44	0.054
6	34.8	0	0.05	0.0814	0.254	0.241	7.3	0.4	0.0224
7	26.4	0	0.049	0.186	0.295	0.292	5.66	1.5	0.0322
8	24.3	0	0.057	0.0911	0.29	0.28	6.7	0.41	0.028
9	34.5	0	0.057	0.0587	0.2106	0.205	4.79	1.96	0.0298
10	42	0	0.031	0.008	0.1	0.069	10.2	0	0.0125

Table 5.37: AVR data for the New England Test System.

Unit No.	T _R	K _A	T _A	T _B	T _C	V _{setpoint}	Efd _{Max}	Efd _{Min}
1	0.01	200.0	0.015	10.0	1.0	10.300	5.0	-5.0
2	0.01	200.0	0.015	10.0	1.0	0.9820	5.0	-5.0
3	0.01	200.0	0.015	10.0	1.0	0.9831	5.0	-5.0
4	0.01	200.0	0.015	10.0	1.0	0.9972	5.0	-5.0
5	0.01	200.0	0.015	10.0	1.0	10.123	5.0	-5.0

6	0.01	200.0	0.015	10.0	1.0	10.493	5.0	-5.0
7	0.01	200.0	0.015	10.0	1.0	10.635	5.0	-5.0
8	0.01	200.0	0.015	10.0	1.0	10.278	5.0	-5.0
9	0.01	200.0	0.015	10.0	1.0	10.265	5.0	-5.0
10	0.01	200.0	0.015	10.0	1.0	10.475	5.0	-5.0

Table 5.38: PSS data for the New England Test System.

Unit No.	K	T _w	T ₁	T ₂	T ₃	T ₄	V _{PSS,Max}	V _{PSS,Min}
1	1.0/(120π)	10.0	5.0	0.60	3.0	0.50	0.2	-0.2
2	0.5/(120 π)	10.0	5.0	0.40	1.0	0.10	0.2	-0.2
3	0.5/(120 π)	10.0	3.0	0.20	2.0	0.20	0.2	-0.2
4	2.0/(120 π)	10.0	1.0	0.10	1.0	0.30	0.2	-0.2
5	1.0/(120 π)	10.0	1.5	0.20	1.0	0.10	0.2	-0.2
6	4.0/(120 π)	10.0	0.5	0.10	0.5	0.05	0.2	-0.2
7	7.5/(120 π)	10.0	0.2	0.02	0.5	0.10	0.2	-0.2
8	2.0/(120 π)	10.0	1.0	0.20	1.0	0.10	0.2	-0.2
9	2.0/(120 π)	10.0	1.0	0.50	2.0	0.10	0.2	-0.2
10	1.0/(120 π)	10.0	1.0	0.05	3.0	0.50	0.2	-0.2

5.4.3. Selected Results and Validation

This Task Force received three sets of contributions: one MATLAB-based implementation from a group affiliated to the University of Michigan at Ann Arbor (which was the base for the validation process), one PacDyn implementation from a group affiliated to the University of São Paulo and one EMTP-RV [28] implementation from a researcher affiliated to Hydro-Québec. The MATLAB-based and EMTP-RV implementations are described in Appendices D and E to this report.

As previously mentioned, the validation process will rely on eigenvalue calculations to ensure the results produced by the PacDyn implementation exhibit a satisfactory match when compared to the ones produced by the MATLAB-based implementation. Since the focus of this Task Force is on electromechanical modes, the highly satisfactory match with respect to this type of oscillations will be highlighted initially, and then the whole set of eigenvalues will be compared to ensure the two implementations are fully compatible. Results of the EMTP-RV implementation are also shown together with the MATLAB-based and PacDyn ones, but these results do not exhibit the same level of compatibility observed for the latter.

For this 10-generator system, there are 9 modes identified as being of an electromechanical nature. The following tables will present the eigenvalues associated to them calculated by the three previously mentioned implementations, so the reader can observe how closely they match. Table 5.39 presents the comparison of modes labeled #1, #2 and #3, while modes #4, #5 and #6 and modes #7, #8 and #9 are compared in Table 5.40 and Table 5.41, respectively.

Table 5.39: Eigenvalues related to modes #1, #2 and #3 for the New England Test System.

	Mode #1		Mode #2		Mode #3	
Source	Real	Imag	Real	Imag	Real	Imag
Matlab	-2.553	10.566	-1.849	10.028	-1.582	8.550
Pacdyn	-2.553	10.569	-1.850	10.197	-1.582	8.550
EMTP	-2.15	9.75	-2.48	9.63	-1.53	8.21

Table 5.40: Eigenvalues related to modes #4, #5 and #6 for the New England Test System.

	Mode #4		Mode #5		Mode #6	
Source	Real	Imag	Real	Imag	Real	Imag
Matlab	-2.563	8.671	-1.863	7.439	-1.312	7.108
Pacdyn	-2.561	8.670	-1.864	7.447	-1.312	7.108
EMTP	-2.88	8.89	-0.49	7.42	-1.70	7.10

Table 5.41: Eigenvalues related to modes #7, #8 and #9 for the New England Test System.

	Mode #7		Mode #8		Mode #9	
Source	Real	Imag	Real	Imag	Real	Imag
Matlab	-1.844	7.081	-1.523	6.318	-0.498	3.682
Pacdyn	-1.864	7.082	-1.522	6.316	-0.498	3.682
EMTP	-1.66	6.54	-0.86	6.07	-0.43	3.86

The comparison between the MATLAB-based and PacDyn results can be seen graphically in Figure 5.50. It becomes clear that the match is satisfactory enough to support the claim that, under the special circumstances that were described at the beginning of this section, this benchmark is validated.

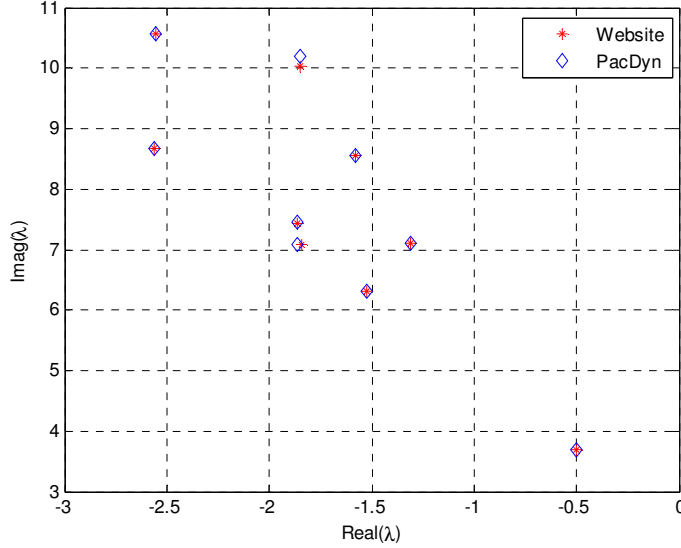


Figure 5.50: Graphical comparison of the electromechanical modes calculated in Matlab and PacDyn for the New England Test System.

To add extra information to this section, a comparison between the full sets of eigenvalues resulting from the MATLAB-based and PacDyn implementations is given in Table 5.42. One can see that the modes that are not of an electromechanical nature also exhibit a very good match, which adds up to support the claim of benchmark validation

Table 5.42: Comparison between full sets of eigenvalues (Matlab-based and PacDyn implementations) for the New England Test System.

Eigenvalues (Matlab-based implementation)				Eigenvalues (PacDyn implementation)			
Real	Imag	f(Hz)	$\zeta(\%)$	Real	Imag	f(Hz)	$\zeta(\%)$
-0.4505	0.6750	0.107	-55.514	-0.4504	0.6750	0.1074	55.504
-0.4861	0.6278	0.100	-61.222	-0.4860	0.6279	0.0999	61.206
-0.4812	0.6084	0.097	-62.035	-0.4810	0.6085	0.9685	62.009
-0.6901	0.8108	0.129	64.813	-0.6901	0.8108	0.1290	64.815
-0.5780	0.6705	0.107	-65.293	-0.5877	0.6705	0.1067	65.918
-0.7928	0.8127	0.129	-69.831	-0.7934	0.8126	0.1293	69.863
-4.4830	4.1880	0.666	73.074	-4.4828	4.1863	0.6663	73.086
-0.8648	0.7743	0.123	74.505	-0.8647	0.7743	0.1232	74.498
-2.9562	2.5076	0.399	76.260	-2.9575	2.5070	3.8771	76.281
-2.0436	1.6338	0.260	78.107	-2.0440	1.6330	0.2599	78.126
-1.2040	0.9107	0.145	79.755	-1.2043	0.9106	0.1449	79.767
-4.3350	2.9883	0.475	82.333	-4.3349	2.9876	0.4755	82.339
-5.7301	3.6713	0.584	84.200	-5.7306	3.6730	0.5846	84.191
-12.618	6.6283	1.055	88.528	-12.616	6.6329	1.0557	88.513
1.4761	0.5231	0.083	94.256	-1.4753	0.5228	0.0832	94.257
-4.3697	1.5310	0.244	94.375	-4.3692	1.5311	0.2437	94.373
-1.0444	0.2387	0.038	97.486	-1.0445	0.2387	0.0380	97.486

Eigenvalues (Matlab-based implementation)				Eigenvalues (PacDyn implementation)			
Real	Imag	f(Hz)	$\zeta(\%)$	Real	Imag	f(Hz)	$\zeta(\%)$
-19.993	1.2699	0.202	99.799	-19.992	1.2724	0.2025	99.798
-104.59	0.0	0.0	100.0	---	---	---	---
-103.78	0.0	0.0	100.0	-103.78	0.0	0.0	100.0
-102.68	0.0	0.0	100.0	-102.68	0.0	0.0	100.0
-102.27	0.0	0.0	100.0	-102.27	0.0	0.0	100.0
-102.13	0.0	0.0	100.0	---	---	---	---
-101.90	0.0	0.0	100.0	-101.90	0.0	0.0	100.0
-101.33	0.0	0.0	100.0	-101.33	0.0	0.0	100.0
-101.32	0.0	0.0	100.0	-101.32	0.0	0.0	100.0
-101.31	0.0	0.0	100.0	-101.31	0.0	0.0	100.0
-100.90	0.0	0.0	100.0	-100.90	0.0	0.0	100.0
-72.869	0.0	0.0	100.0	-72.858	0.0	0.0	100.0
-65.987	0.0	0.0	100.0	-65.989	0.0	0.0	100.0
-65.936	0.0	0.0	100.0	---	---	---	---
-65.797	0.0	0.0	100.0	-65.798	0.0	0.0	100.0
-65.165	0.0	0.0	100.0	-65.166	0.0	0.0	100.0
-64.250	0.0	0.0	100.0	-64.249	0.0	0.0	100.0
-63.948	0.0	0.0	100.0	-63.949	0.0	0.0	100.0
-63.535	0.0	0.0	100.0	-63.535	0.0	0.0	100.0
-61.774	0.0	0.0	100.0	-61.774	0.0	0.0	100.0
-59.612	0.0	0.0	100.0	-59.612	0.0	0.0	100.0
-32.118	0.0	0.0	100.0	-32.136	0.0	0.0	100.0
-13.988	0.0	0.0	100.0	-13.981	0.0	0.0	100.0
-7.3691	0.0	0.0	100.0	-7.3691	0.0	0.0	100.0
-7.1480	0.0	0.0	100.0	-7.1480	0.0	0.0	100.0
-5.8943	0.0	0.0	100.0	-5.8945	0.0	0.0	100.0
-5.5374	0.0	0.0	100.0	-5.5392	0.0	0.0	100.0
-2.8327	0.0	0.0	100.0	-2.8327	0.0	0.0	100.0
-2.0263	0.0	0.0	100.0	-2.0263	0.0	0.0	100.0
-1.5315	0.0	0.0	100.0	-1.5315	0.0	0.0	100.0
-1.4500	0.0	0.0	100.0	-1.4501	0.0	0.0	100.0
-1.0995	0.0	0.0	100.0	-1.0996	0.0	0.0	100.0
-0.9758	0.0	0.0	100.0	-0.9758	0.0	0.0	100.0
-0.9592	0.0	0.0	100.0	-0.9592	0.0	0.0	100.0
-0.9066	0.0	0.0	100.0	-0.9065	0.0	0.0	100.0
-0.1920	0.0	0.0	100.0	-0.1616	0.0	0.0	100.0
-0.1007	0.0	0.0	100.0	-0.1007	0.0	0.0	100.0
-0.1003	0.0	0.0	100.0	-0.1003	0.0	0.0	100.0
-0.1002	0.0	0.0	100.0	-0.1002	0.0	0.0	100.0
-0.1001	0.0	0.0	100.0	-0.1001	0.0	0.0	100.0
-0.1000	0.0	0.0	100.0	-0.1000	0.0	0.0	100.0
-0.1000	0.0	0.0	100.0	-0.1000	0.0	0.0	100.0

Eigenvalues (Matlab-based implementation)				Eigenvalues (PacDyn implementation)			
Real	Imag	f(Hz)	$\zeta(\%)$	Real	Imag	f(Hz)	$\zeta(\%)$
-0.1000	0.0	0.0	100.0	-0.1000	0.0	0.0	100.0

One significant difference that the reader may notice between the two implementations compared in Table 5.42 is the existence of 3 real modes in the Matlab-based implementation that are not present in the PacDyn counterpart. Although it was not possible to determine the exact reason for this, all of them are well-damped modes and do not interfere with the electromechanical dynamics. Further investigation is needed to determine the source of this minor discrepancy between the two implementations.

Finally, although the validation of the New England Test System does not involve time-domain simulations of the corresponding nonlinear equations, results for these simulations using both Matlab and EMTP-RV are available for download at the Task Force website. Furthermore, comparative plots of the time domain responses of the electrical power outputs of all generators to step inputs of +5% in the voltage reference set-points of all AVR, applied at $t = 1$ s and removed at $t = 1.1$ s, are shown in the plots of Figure 5.51 to Figure 5.60.

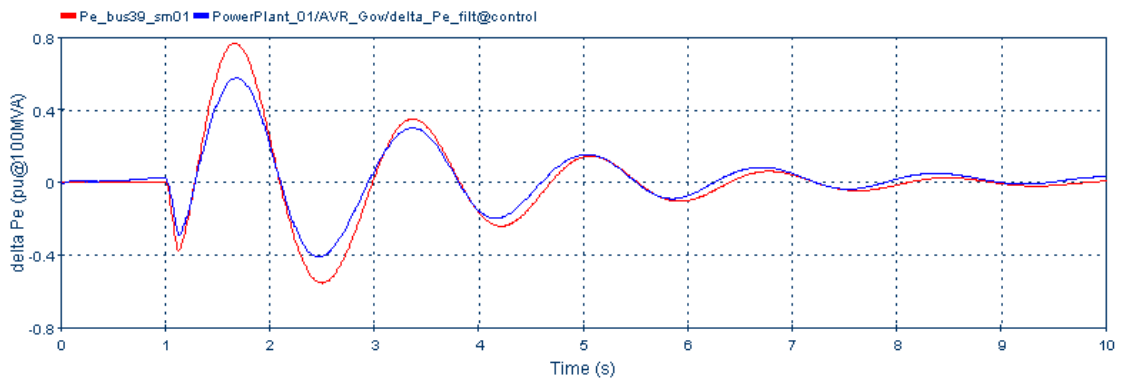
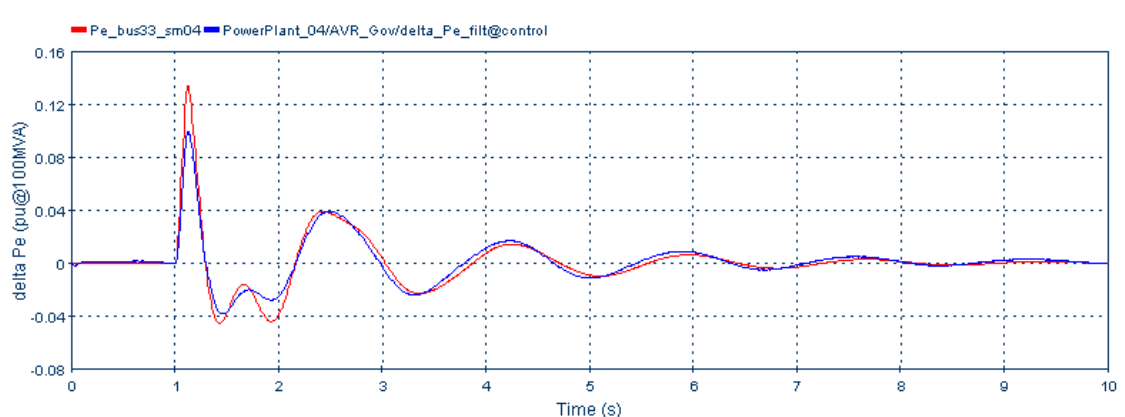
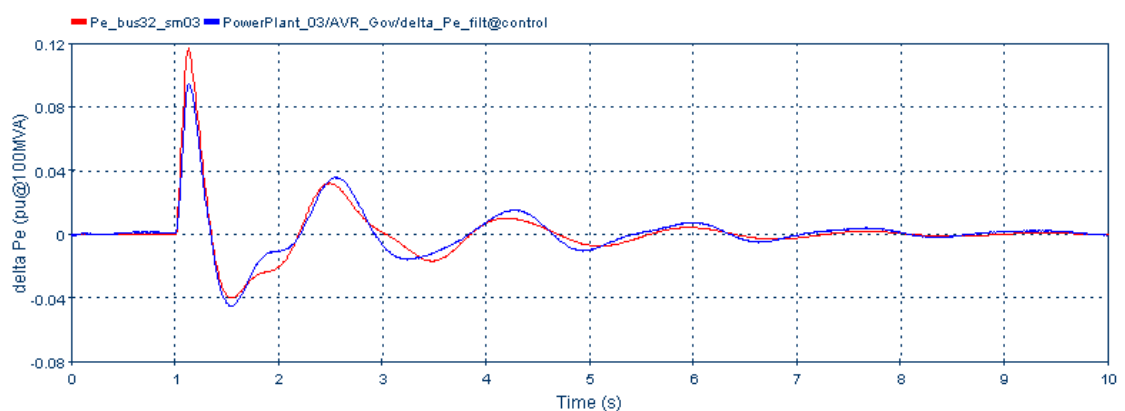
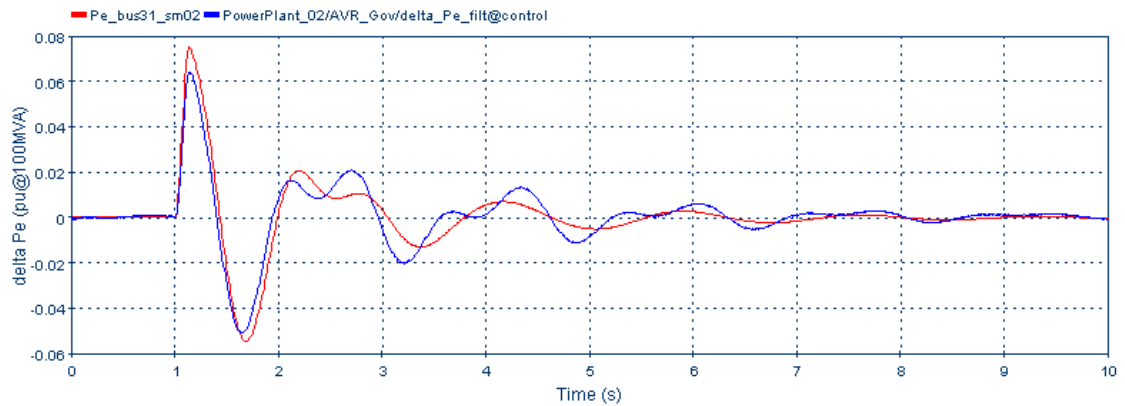


Figure 5.51: Electrical power output of generator 1 for a +5% step in all AVR setpoints - Pacdyn (red) versus EMTP (blue) comparison.



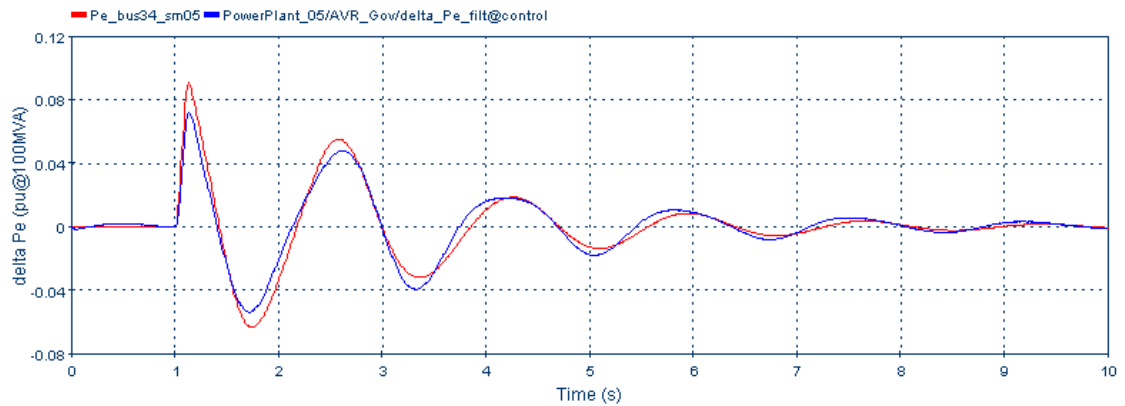


Figure 5.55: Electrical power output of generator 5 for a +5% step in all AVR setpoints - Pacdyn (red) versus EMTP (blue) comparison.

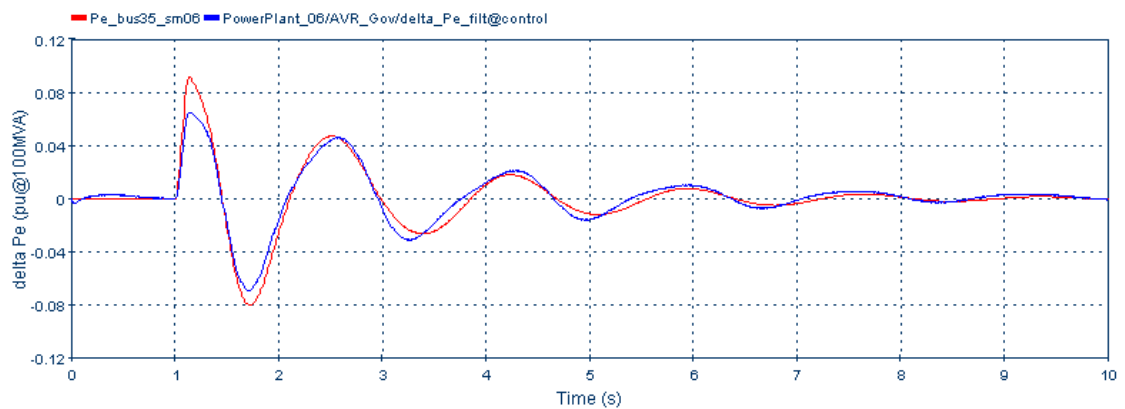


Figure 5.56: Electrical power output of generator 6 for a +5% step in all AVR setpoints - Pacdyn (red) versus EMTP (blue) comparison.

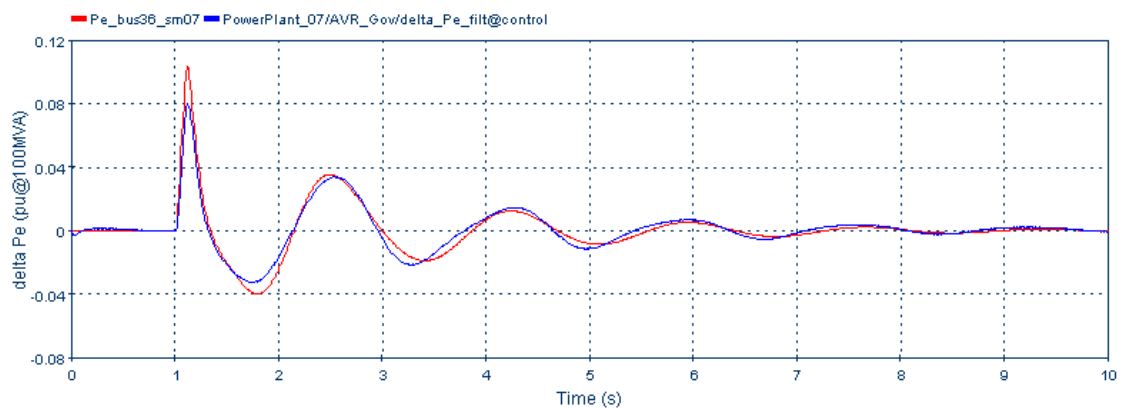


Figure 5.57: Electrical power output of generator 7 for a +5% step in all AVR setpoints - Pacdyn (red) versus EMTP (blue) comparison.

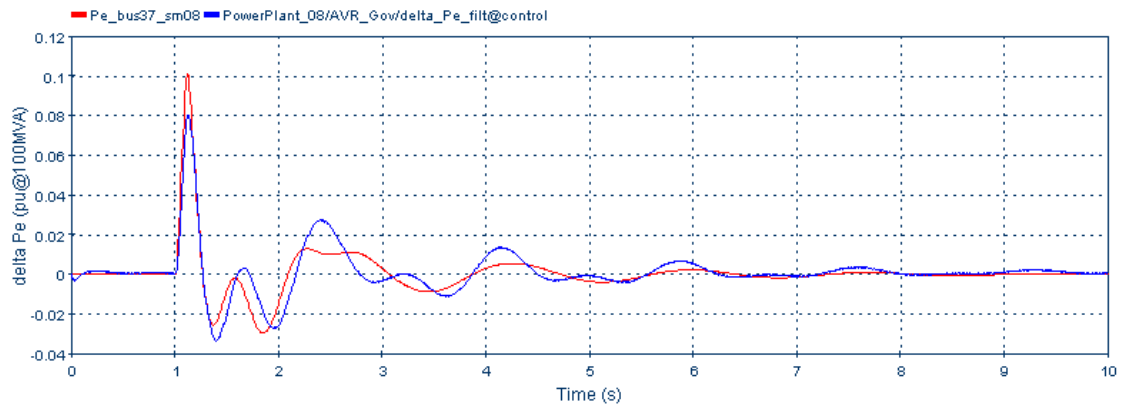


Figure 5.58: Electrical power output of generator 8 for a +5% step in all AVR setpoints - Pacdyn (red) versus EMTP (blue) comparison.

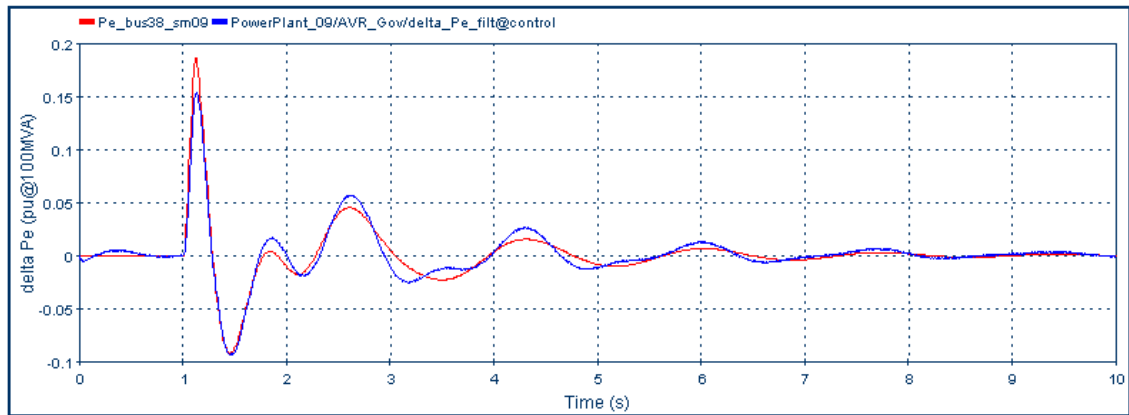


Figure 5.59: Electrical power output of generator 9 for a +5% step in all AVR setpoints - Pacdyn (red) versus EMTP (blue) comparison.

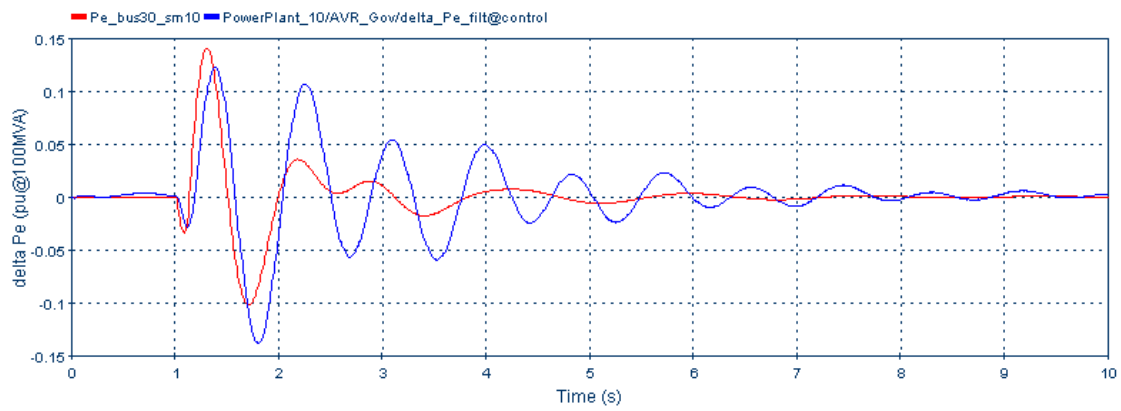


Figure 5.60: Electrical power output of generator 10 for a +5% step in all AVR setpoints - Pacdyn (red) versus EMTP (blue) comparison.

5.5. Data for the Simplified Australian 14-Generator Model

The simplified 14-generator model of the southern and eastern Australian power system is depicted in Figure 4.5. As mentioned in Section 3.6, six base case scenarios representing an encompassing set of normal operating conditions is provided. Therefore, to avoid the provision of the associated large volume of power flow and dynamic data for the models in the main body of the report and to avoid the possibility of transcription errors the reader is referred to the Appendix of this report which includes a comprehensive description of the benchmark system. Power flow and dynamic data as well as eigenanalysis results and time-series data from small-disturbance step responses and transient stability analysis are provided on [12]. The reader is referred to Appendix V of Appendix A to this report for further details about the data provided on [12].

5.5.1. Power Flow Data

Power flow data for the six base case scenarios of the benchmark system are listed in Appendix I.1 of Appendix A to this report. Power flow data files are also provided for the six operating conditions on [12] in a format described in Appendix I.1 along with power flow solution report files for the six base case scenarios.

5.5.2. Dynamic Data

Dynamic data for the Simplified Australian 14-Generator Model are provided in Appendix I.2 of Appendix A to this report. The dynamic data files for both small-signal and transient stability analysis for the six base cases are provided on [12] in formats described in Appendix I.2 of Appendix A.

5.5.3. Selected Results and Validation

a) Small-signal stability model results and validation

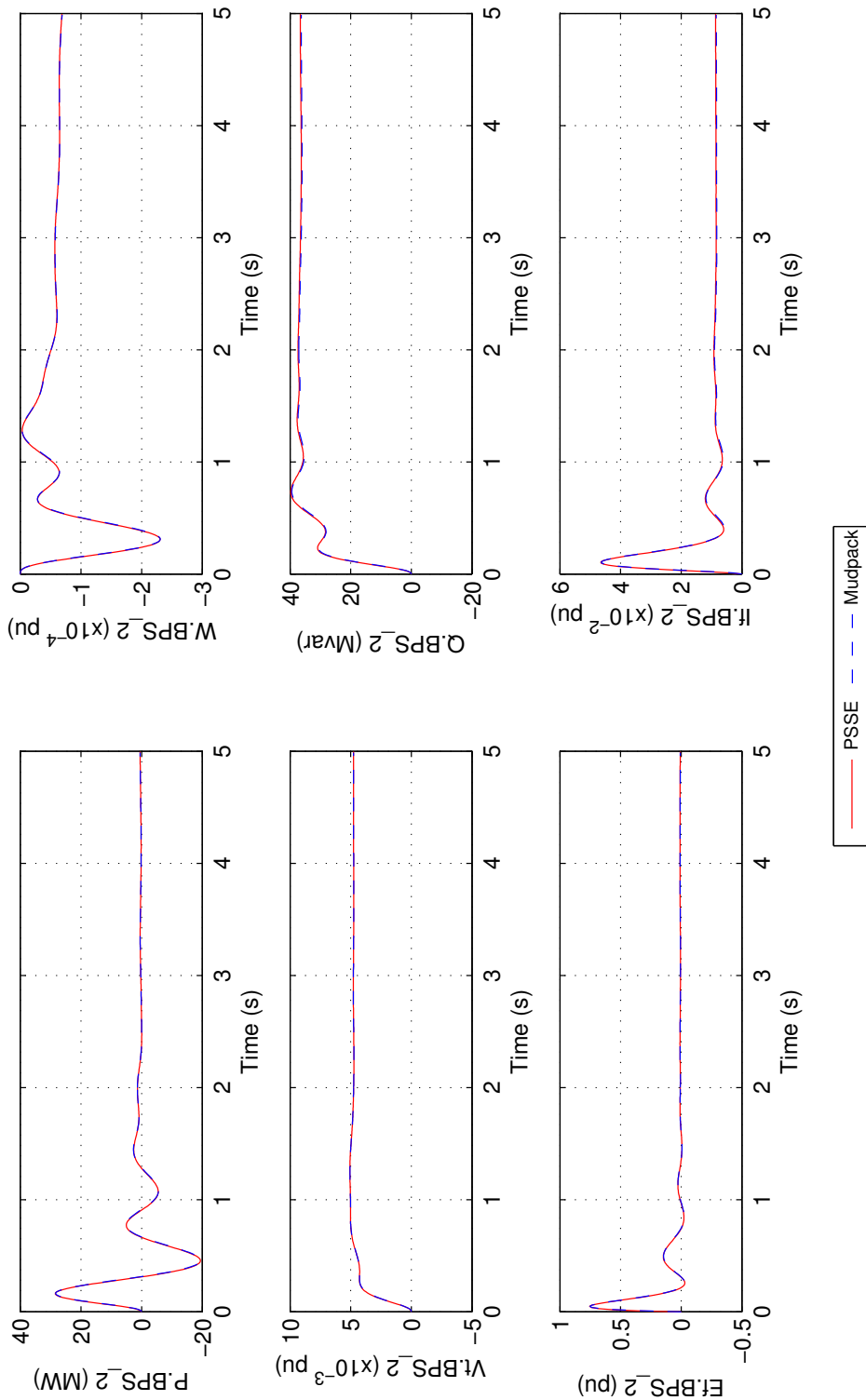
The developers of the simplified 14-generator model of the southern and eastern Australian system have implemented the model in the Mudpack [29] and PSS[®]/E [24] software packages. As explained in Appendix III of Appendix A to this report, a comprehensive set of small-disturbance step response studies have been conducted in these two packages. The responses of selected variables obtained with the respective packages are compared to verify the small-signal dynamic performance for this benchmark system. The step-response studies are conducted only for those scenarios with the PSSs in-service. This is because with the PSSs out-of-service the system is unstable and consequently the non-linear behavior of the system will play a significant role in the PSS[®]/E step responses as the oscillations grow in amplitude.

For each generator a +0.5% step-change in the AVR voltage reference is applied and the perturbations in the generator power output, rotor-speed, stator voltage, reactive power output, field current and field voltage are compared. These studies verify the local modes in which the perturbed generator participates significantly. A typical voltage-reference step-response

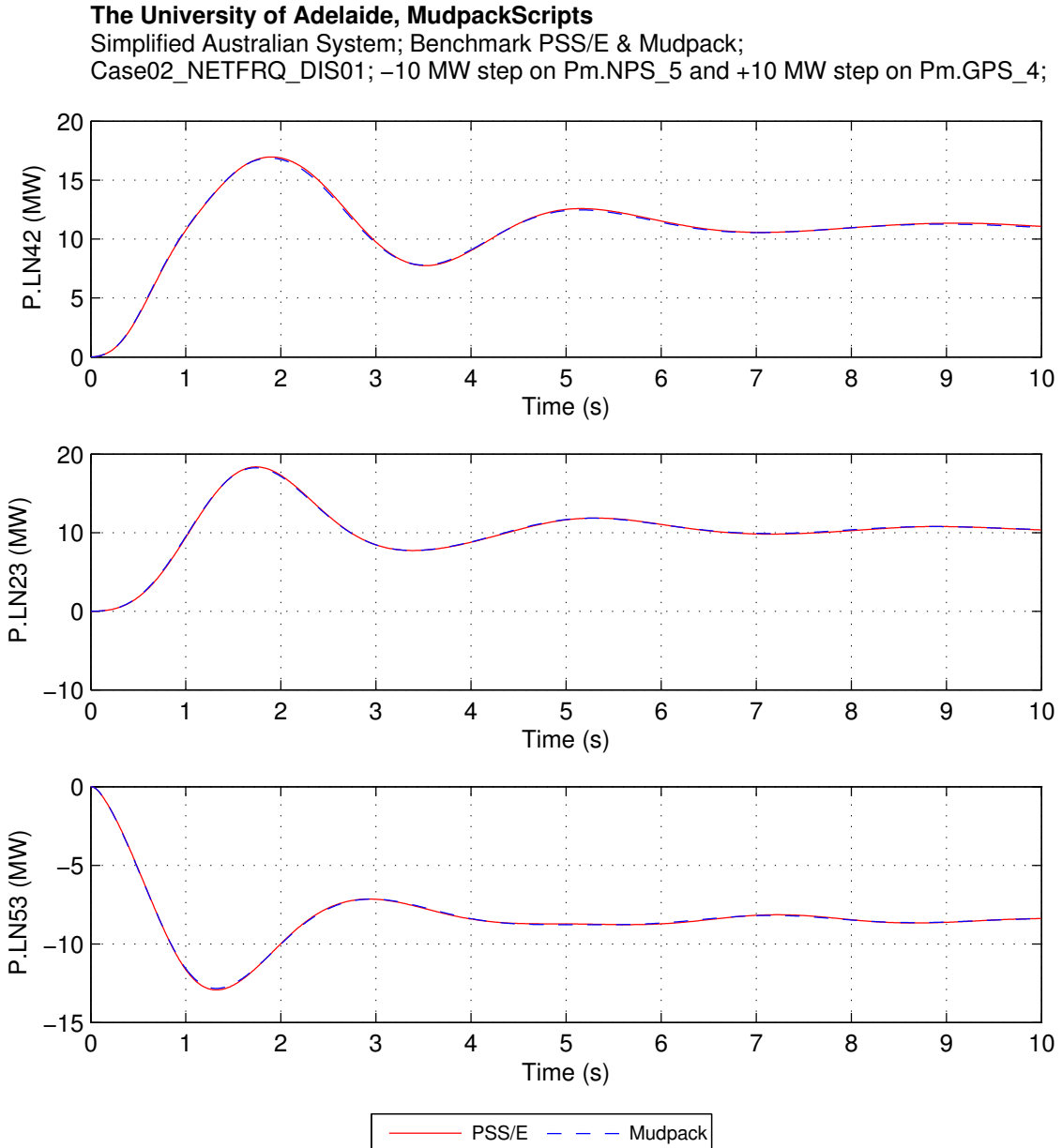
comparison is presented in Figure 5.61 for generator BPS_2 for case 2. The figure shows the typically very close agreement between the PSS®/E and Mudpack implementations of the benchmark system.

Inter-area modes of oscillation are excited by applying perturbations in the mechanical power inputs of two widely separated generators in the respective simulation packages. Power flows in inter-regional transmission corridors obtained with the respective simulation packages are compared to verify the inter-area modal characteristics of the benchmark system. Figure 5.62 shows the typically very close agreement between the inter-area modal characteristics in the PSS®/E and Mudpack implementations of the 14-generator benchmark system.

The University of Adelaide, Mudpack Scripts
 Simplified Australian System; Case02_VrefStep_BPS_2;
 Benchmark PSS/E & Mudpack; 0.5% step on Vref.BPS_2;



File: CMP_Case02_VrefStep_BPS_2.eps
 Thu, 30-Jan-2014 19:07:28



File: CMP_Case02_NETFRQ_DIS01.eps
 Mon, 17-Feb-2014 14:57:53

Figure 5.62: Case 2. Benchmark comparison between PSS®/E (with NETFRQ = 1) and Mudpack. Step change in mechanical power input of +10 MW applied to GPS_4 and a compensating change of -10 MW applied to NPS_5. Power flow in the interconnectors between areas 2 & 4 (P.LN42); areas 2 & 3 (P.LN23) and areas 5 & 3 (P.LN53) are compared.

The tuning of PSSs in this benchmark system is based on the P-V_r characteristics [22], [23] of the generators computed with the Mudpack software package. In Appendix III.3 of Appendix A to this report the developers of the 14-generator model have verified the computation of these P-V_r characteristics by comparison with those computed with PSS®/E for each generator in study case 2. Figure 5.63 shows for generator BPS_2 the typically very close agreement between the P-V_r characteristics computed using Mudpack and PSS®/E. Note that in order to

highlight any differences between the characteristics in the range of electromechanical modal frequencies the magnitude characteristics are displayed in absolute units, rather than in dB.

These results demonstrate that the implementation of the electromagnetic behavior of the generator models and of the AVR/exciter models in the respective simulation packages are practically identical.

To the authors knowledge the PSS[®]/E software package does not include built-in facilities for computation of frequency-responses. A tool, AUPSSEFRTOOL, developed at Adelaide University as a PSS[®]/E “plug-in” has been used to compute the P-Vr characteristics within the PSS[®]/E program. A paper describing this tool is in preparation at time of writing. It should be mentioned that the accuracy of the frequency responses computed in PSS[®]/E are sensitive to the integration time-step and to the amplitude of the sinusoidal perturbation applied to the voltage-reference.

The University of Adelaide, MudpackScripts

Simplified 14 generator model of the SE Australian system. Case 2.

PVr characteristic for BPS_2. Benchmark comparison between Mudpack & PSS/E.

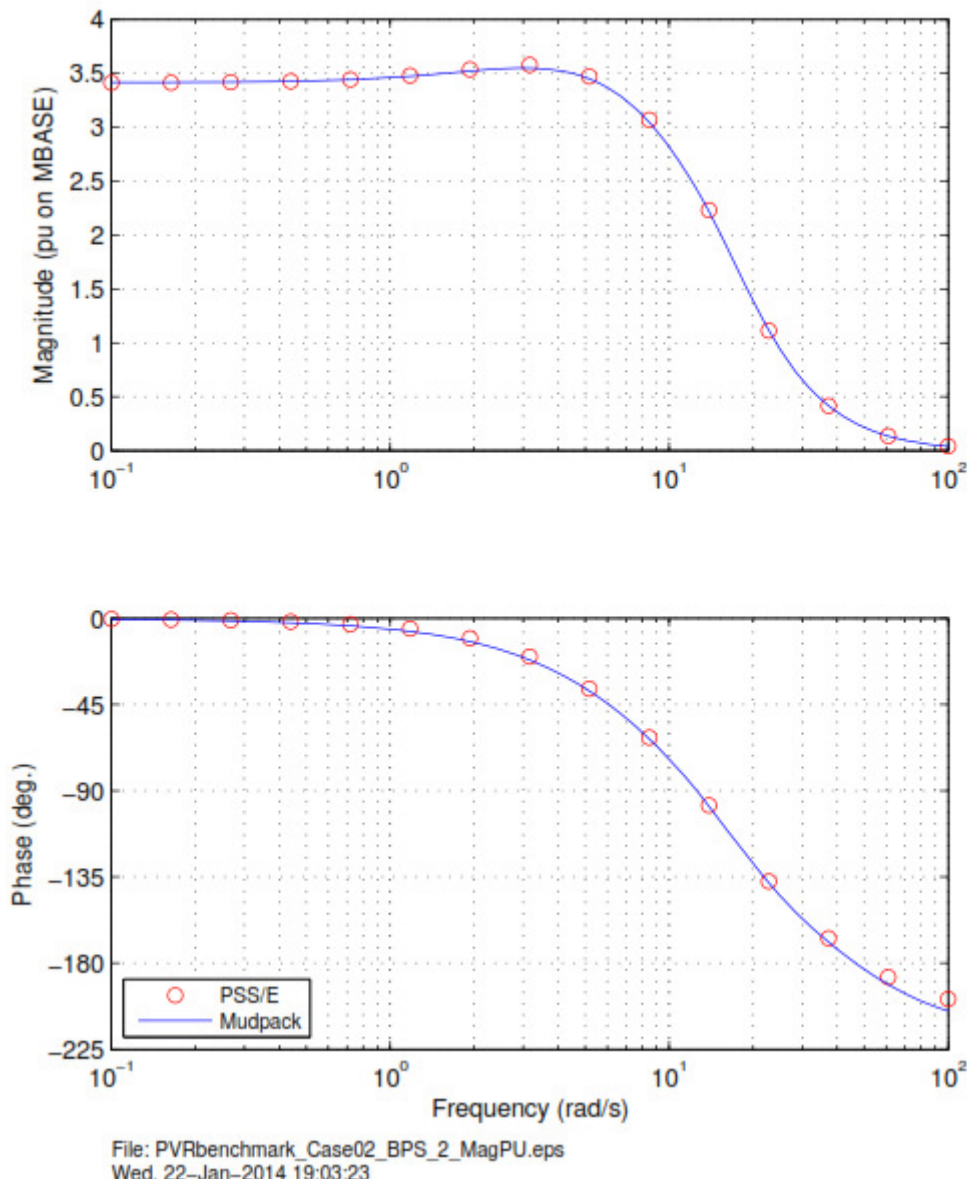


Figure 5.63: Comparison of P-Vr characteristics computed by Mudpack and PSS®/E for generator BPS_2 in case 2.

The simplified 14-generator model of the southern and eastern Australian system has been implemented by researchers at the University of São Paulo, Brazil using the ANAREDE [30] power flow package and the PacDyn [25] small-signal stability analysis software package. The electromechanical modes obtained with the PacDyn package for all six cases with the stabilizers in- and out-of-service are compared in Figure 5.64 with those obtained with the Mudpack package to validate the key eigenanalysis results. The effectiveness of the benchmark PSSs in damping the electromechanical modes of oscillation for all six operating scenarios is evident. It is also clear from this figure that the electromechanical modal behavior of the PacDyn and Mudpack implementations of the model are practically identical.

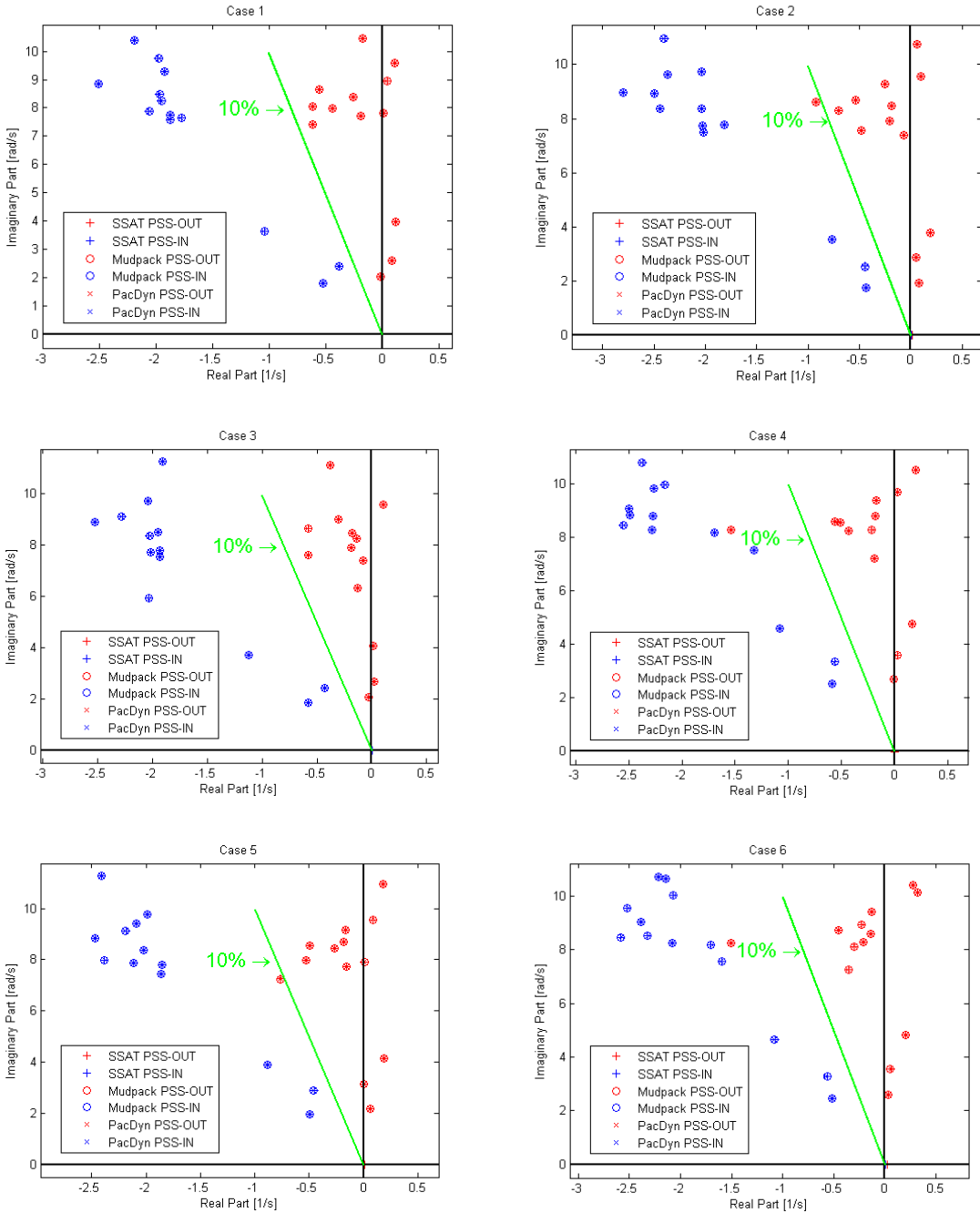


Figure 5.64: Electromechanical modes of oscillation of the simplified 14-generator model of the southern and eastern Australian power system model obtained with Mudpack, PacDyn and SSAT with the PSSs in- and out-of-service for cases 1 to 6.

b) Transient stability results and validation

Under the Australian National Electricity Rules [31] which apply to the operation of the southern and eastern Australian power system three-phase faults on the transmission network are not considered to be credible contingencies (except under exceptional circumstances).

Rather, for planning purposes solid two-phase to ground faults are generally treated as the most severe form of credible contingency. In order to allow the researcher to reflect this practice in their analysis of the simplified 14-generator model of the southern and eastern Australian system the negative and zero sequence impedance data for the network is provided in Appendix II of the Appendix to this report. Based on this data the equivalent fault impedances required to represent two-phase to ground faults can be computed.

As detailed in Appendix IV of Appendix A to this report the developers of the 14-generator model used their PSS[®]/E implementation of the model to conduct a comprehensive set of transient stability studies on the six base cases with the PSSs in-service. These studies verify that the system is transiently stable for all two-phase to ground faults cleared by de-energization of the faulted transmission element in the applicable primary protection time. Since this benchmark system does not include turbine / governor models contingencies involving the loss of generation or load not considered.

Researchers at the University of São Paulo, Brazil have implemented the Simplified Australian 14-Generator Model in the ANATEM transient-stability analysis package [26]. Furthermore, researchers at the University of Waterloo, Canada have also performed the same implementation using TSAT, the transient stability tool contained in the DSAT [32] software package. Comparisons between selected transient-stability simulations conducted with the PSS[®]/E, ANATEM and TSAT for study case 2 have been conducted.

The figures in the remaining of this section compare responses obtained with the respective model implementations due to solid two-phase to ground faults applied adjacent to selected buses on the transmission network, mainly in those related to high-voltage sides of step-up transformers. The faults are cleared by de-energizing the circuit in 100 ms.

The responses of the active power output (P), terminal voltage (V_t) and field voltage (E_{fd}) of generators GPS_4, TPS_4, BPS_2, and EPS_2 to a fault on bus #209 are shown, respectively, in Figure 5.65, Figure 5.66, and Figure 5.67. The same structure of presentation is followed for a fault on bus #303, with responses for generators LPS_3, HPS_1, EPS_2, and TPS_5 shown in Figure 5.68, Figure 5.69, and Figure 5.70, respectively. Similarly, for a fault on bus #506, the responses for generators NPS_5, PPS_5, YPS_3, and NPS_2 are shown, respectively, in Figure 5.71, Figure 5.72, and Figure 5.73.

The final set of simulations shows the responses of the susceptances (B) and the terminal voltages (V_t) of the SVCs in the system to faults applied and cleared in the same manner as the ones described previously for the generators. Responses of ASVC_2 and BSVC_4 to a fault on bus #209 are shown in Figure 5.74, while responses of RSVC_3 and SSVC_5 to a fault on bus #303 and responses of PSVC_5 and ASVC_2 to a fault on bus #506 are shown in Figure 5.75 and Figure 5.76, respectively.

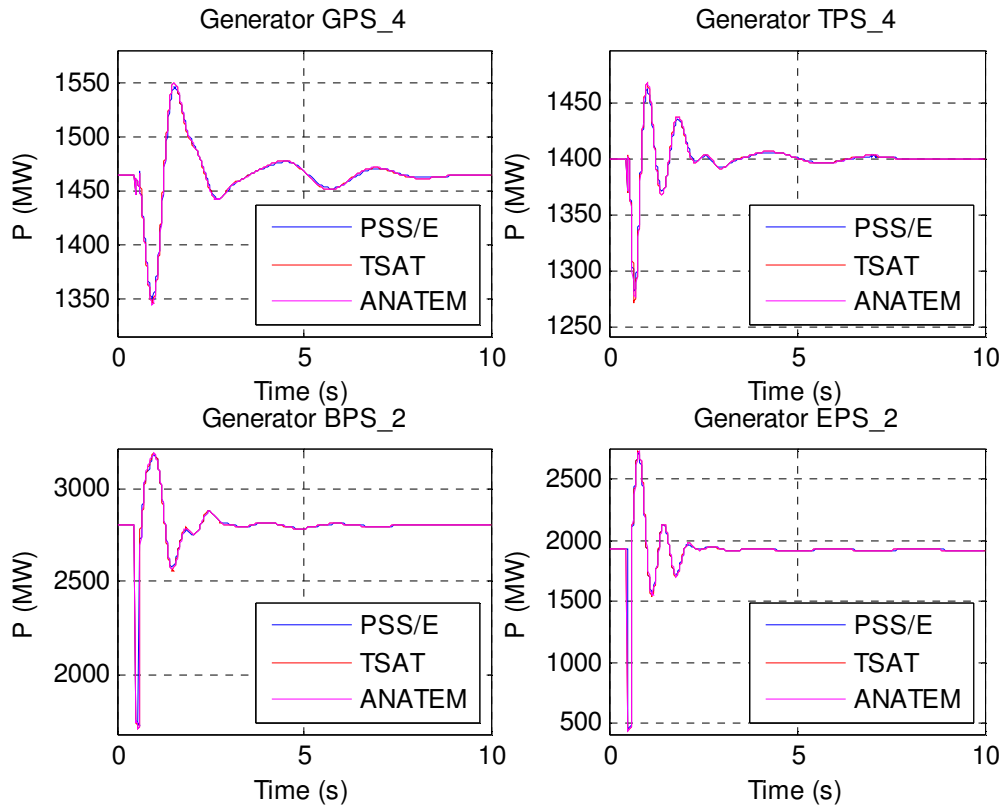


Figure 5.65: Responses of active power outputs (P) of selected generators to a fault on bus #209.

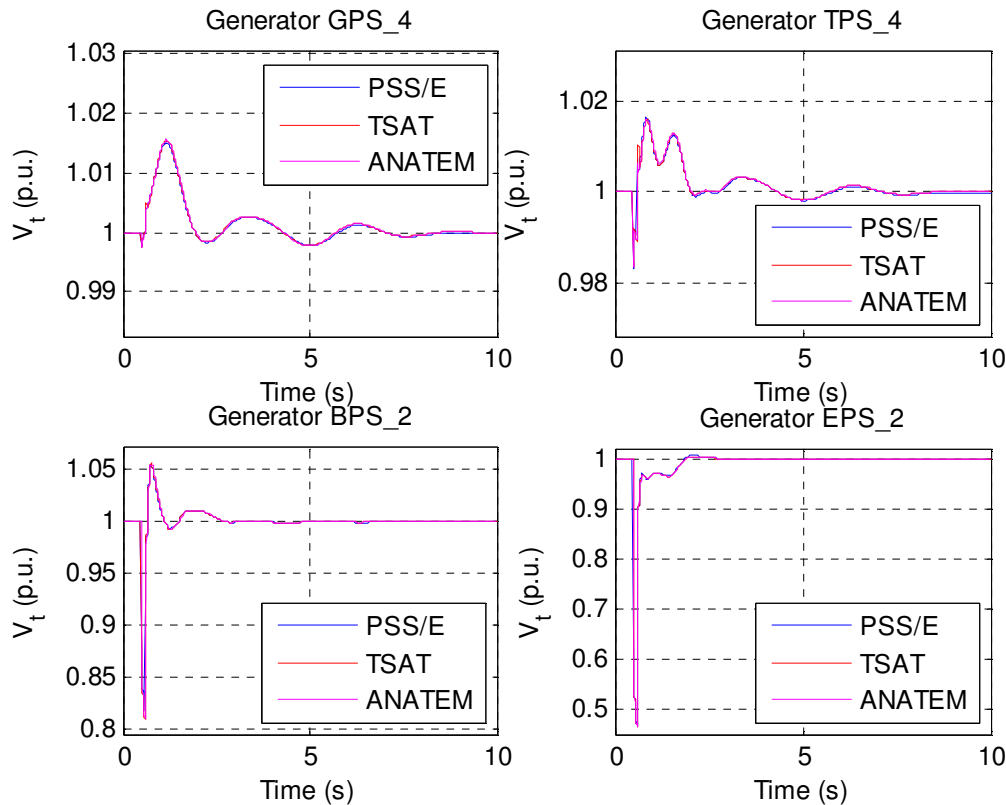


Figure 5.66: Responses of terminal voltages (V_t) of selected generators to a fault on bus #209.

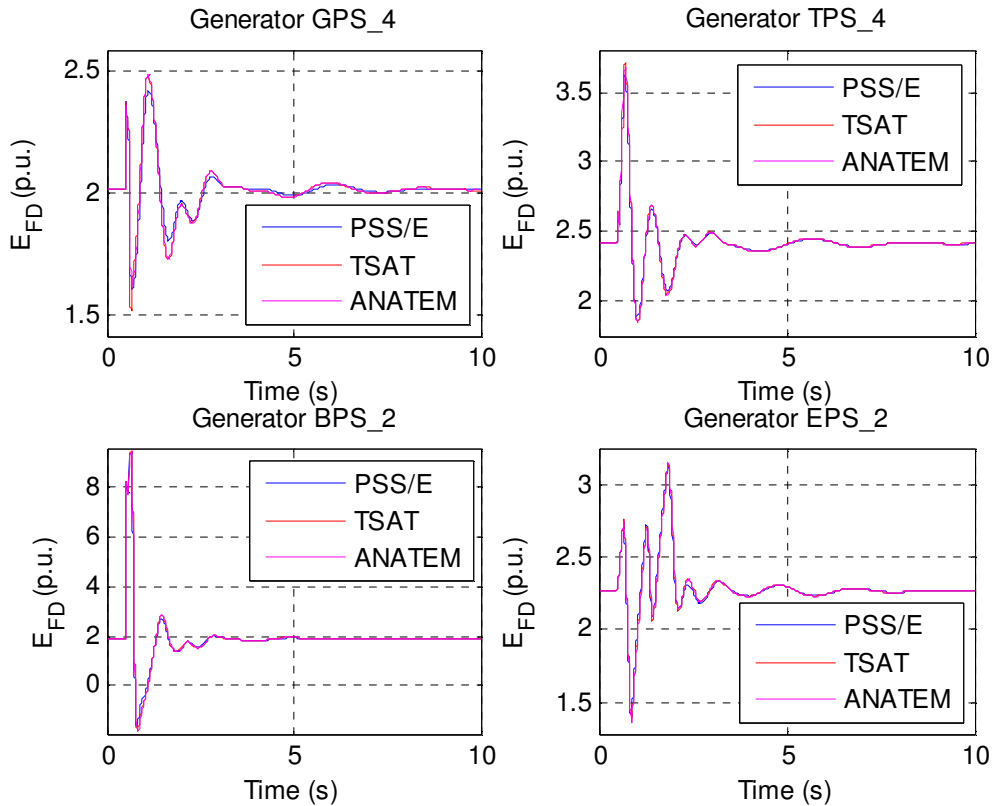


Figure 5.67: Responses of field voltages (E_{fd}) of selected generators to a fault on bus #209.

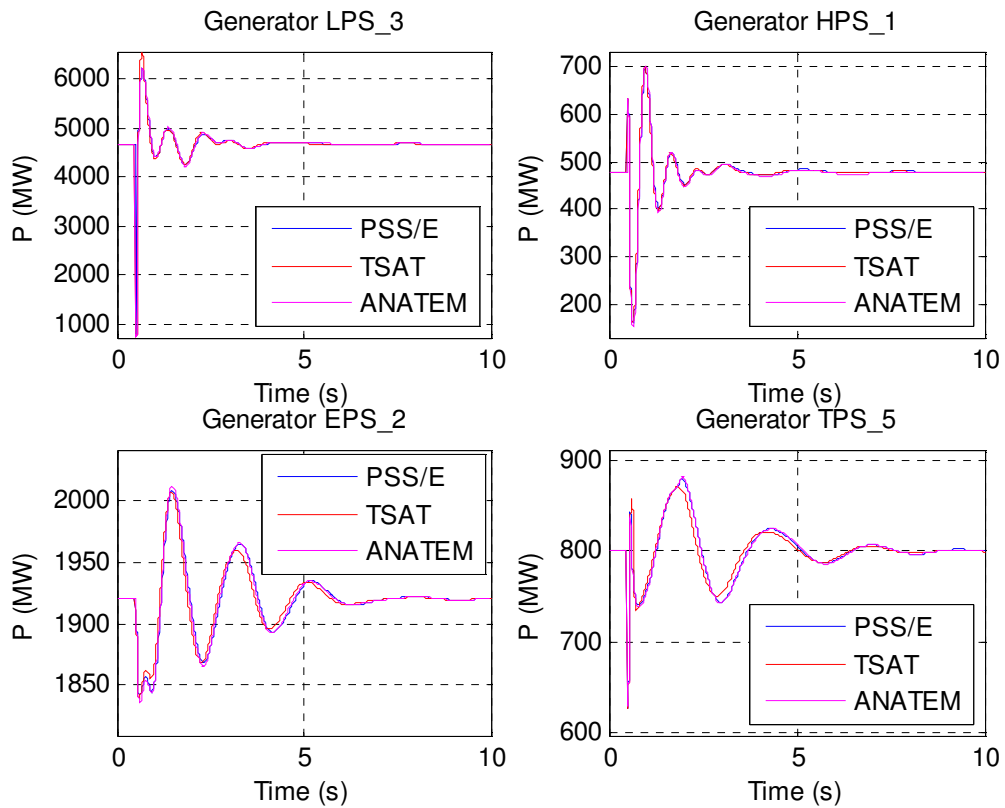


Figure 5.68: Responses of active power outputs (P) of selected generators to a fault on bus #303.

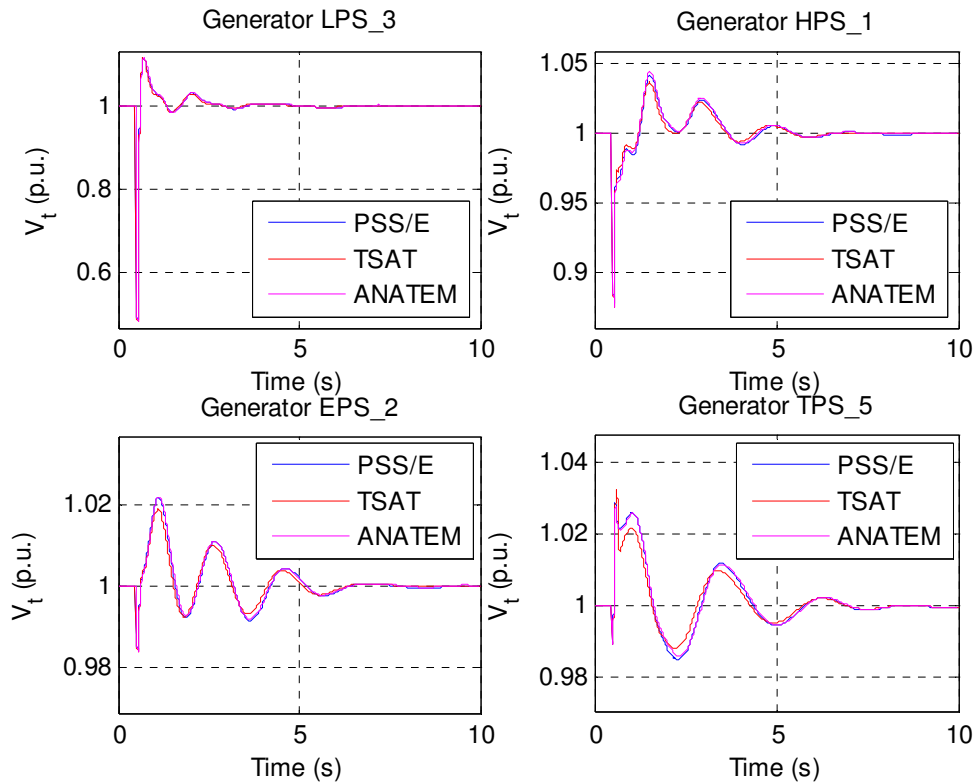


Figure 5.69: Responses of terminal voltages (V_t) of selected generators to a fault on bus #303.

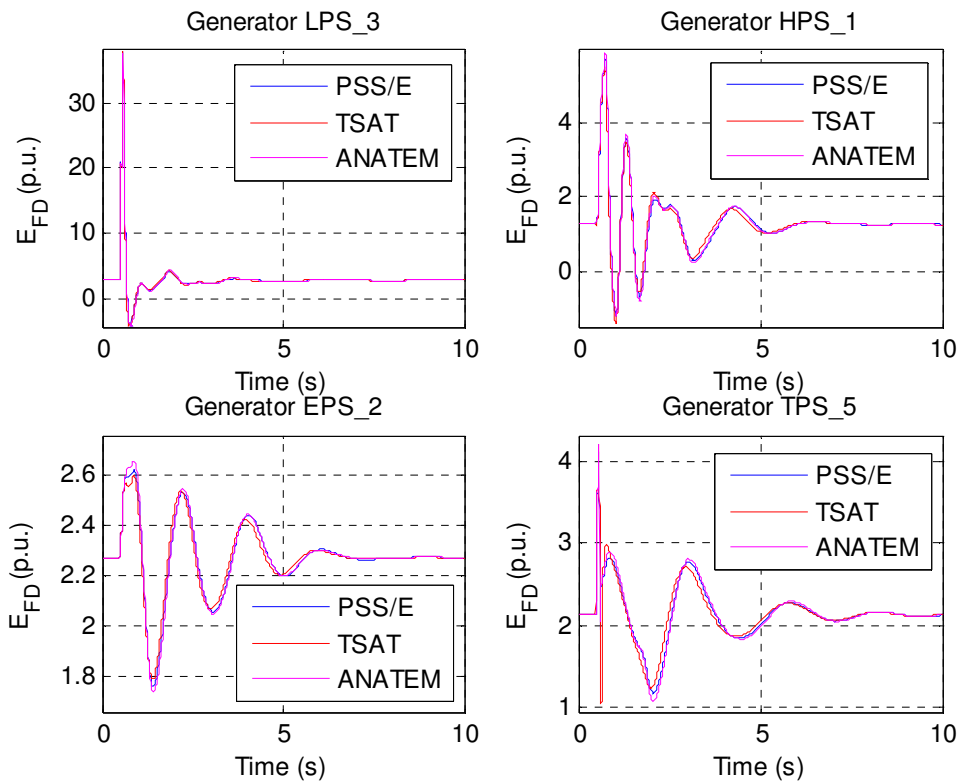


Figure 5.70: Responses of field voltages (E_{FD}) of selected generators to a fault on bus #303.

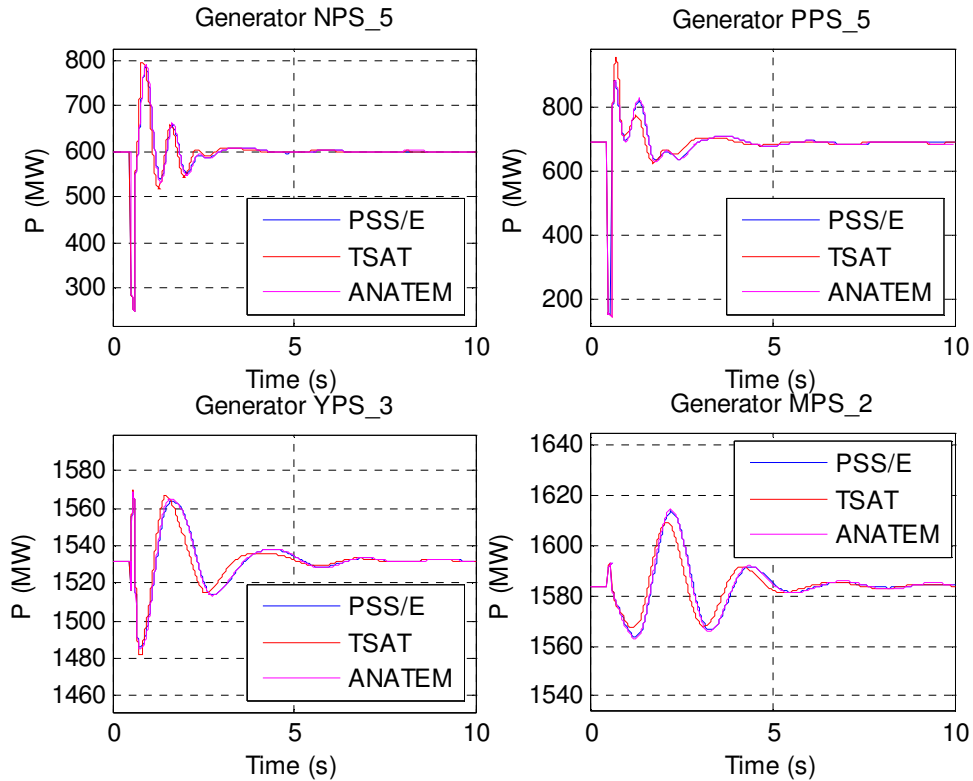


Figure 5.71: Responses of active power outputs (P) of selected generators to a fault on bus #506.

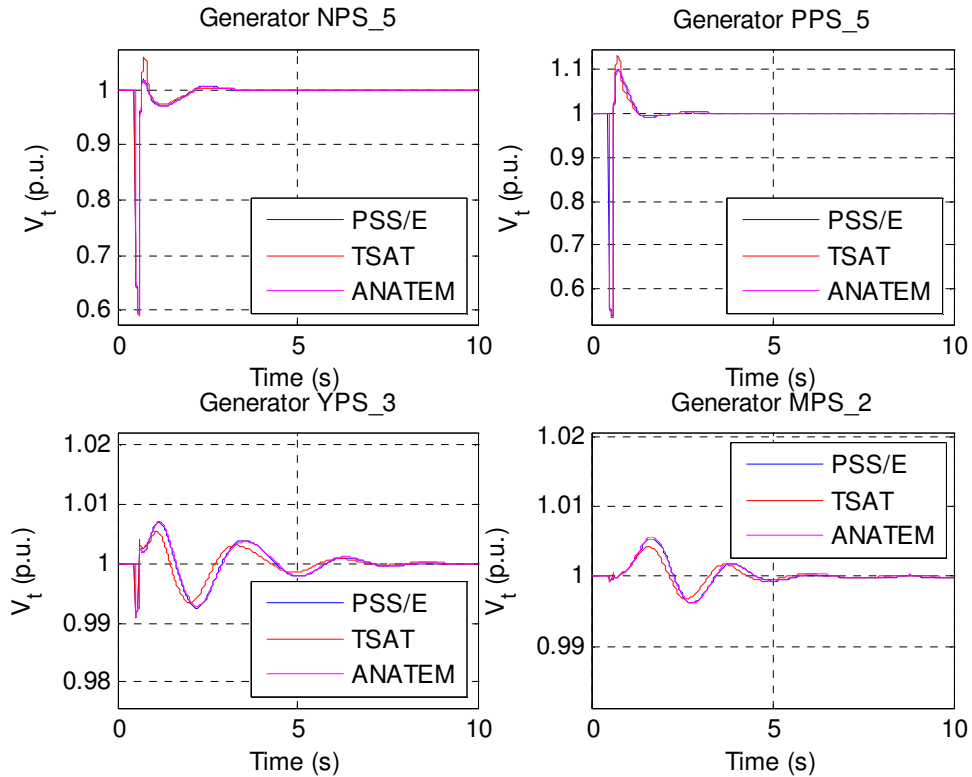


Figure 5.72: Responses of terminal voltages (V_t) of selected generators to a fault on bus #506.

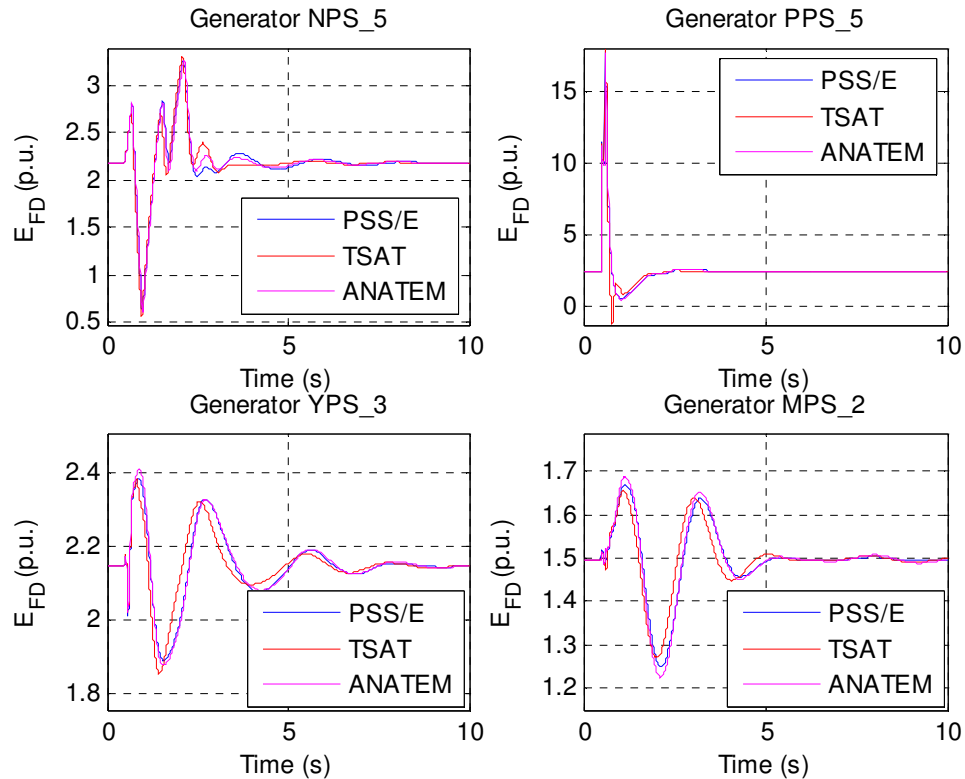


Figure 5.73: Responses of field voltages (E_{FD}) of selected generators to a fault on bus #506.

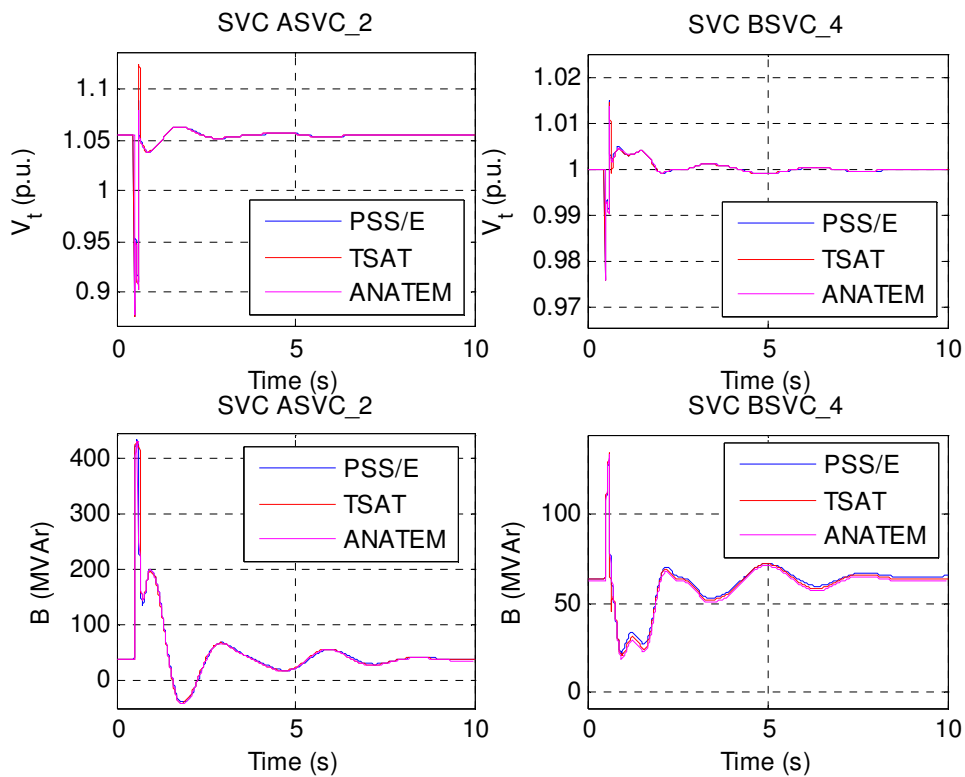


Figure 5.74: Responses of SVCs susceptances (B) and terminal voltages (V_t) to a fault on bus #209.

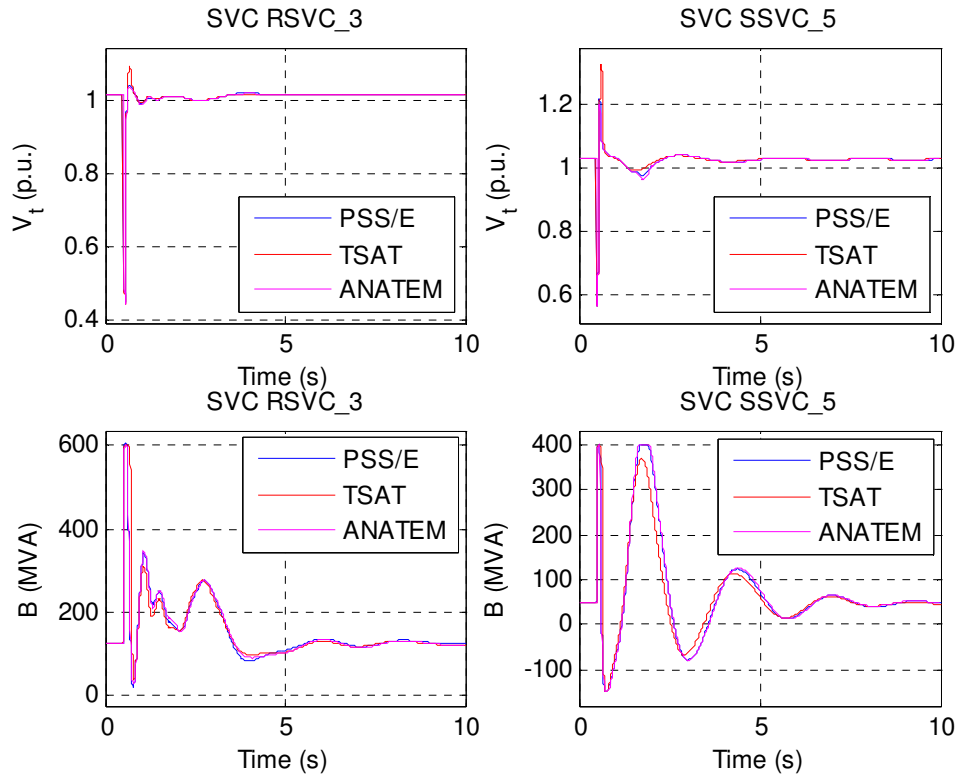


Figure 5.75: Responses of SVCs susceptances (B) and terminal voltages (V_t) to a fault on bus #303.

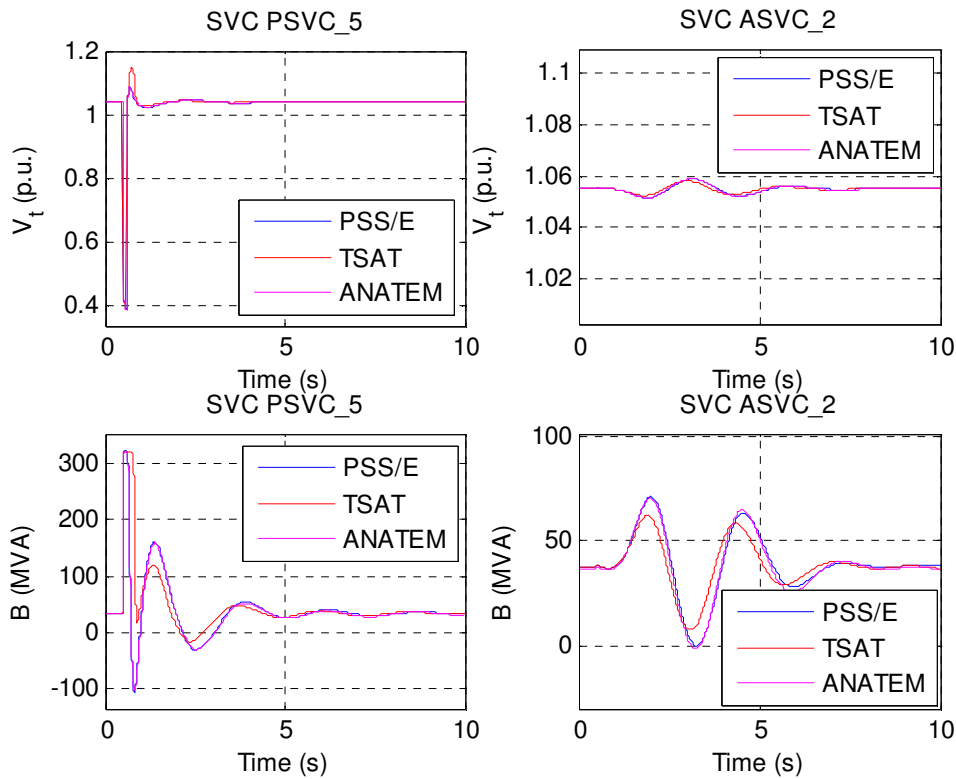


Figure 5.76: Responses of SVCs susceptances (B) and terminal voltages (V_t) to a fault on bus #506.

It is possible to observe in Figure 5.74, Figure 5.75, and Figure 5.76 that there are slight differences in the responses of the SVCs simulated in TSAT with respect to the ones simulated

in PSS/E and ANATEM. The source of these discrepancies has been identified as a difference in the built-in model of the SVC limiters: it is possible to create identical models for these limiters using PSS/E and ANATEM, while for TSAT it would require an extra work that is out of the scope of this Task Force. This difference in the behavior of the SVCs also explains some minor differences observed from Figure 5.65 to Figure 5.73, when comparing the results from TSAT with the ones from PSS/E and ANATEM. A complete report on the TSAT implementation made by the group led by Prof. Claudio Canizares can be found in Appendix B to this report.

In spite of the small differences mentioned in the previous paragraphs - and taking into account that: a) the responses of PSS/E and ANATEM exhibit a perfect agreement, from the viewpoint of visual inspection (i.e., disregarding irrelevant numerical differences); and b) the source of discrepancies from the previously mentioned results with respect to the TSAT outputs has been clearly identified; it is possible to conclude that this benchmark has been validated using the criteria established by this Task Force.

5.6. Data for the 68-bus (NETS/NYPS) System

5.6.1. Power Flow Data

The one line diagram of the system adopted by this Task Force as the 68-bus system is shown in Figure 5.77. The bus data, including the voltage magnitudes and angles from the power flow solution, are shown in Table 5.43 and Table 5.44.

The transmission line data is shown in Table 5.45 and Table 5.46. The data is provided in per unit considering a system MVA base of 100 MVA. The lines are represented by π sections and the charging shown in Table 5.45 and Table 5.46 corresponds to the total line charging.

The transformers (GSU) are explicitly represented in the case. The GSUs are all rated 900 MVA and have a leakage reactance of 15% on the transformer base. Winding resistance and magnetizing currents are neglected. Table 5.47 presents the GSU data.

For both load flow calculation and dynamic simulations, constant admittance characteristics were admitted for all loads. The corresponding load details are given in Table 5.48.

The complete power flow solution for this system is given in Table 5.49.

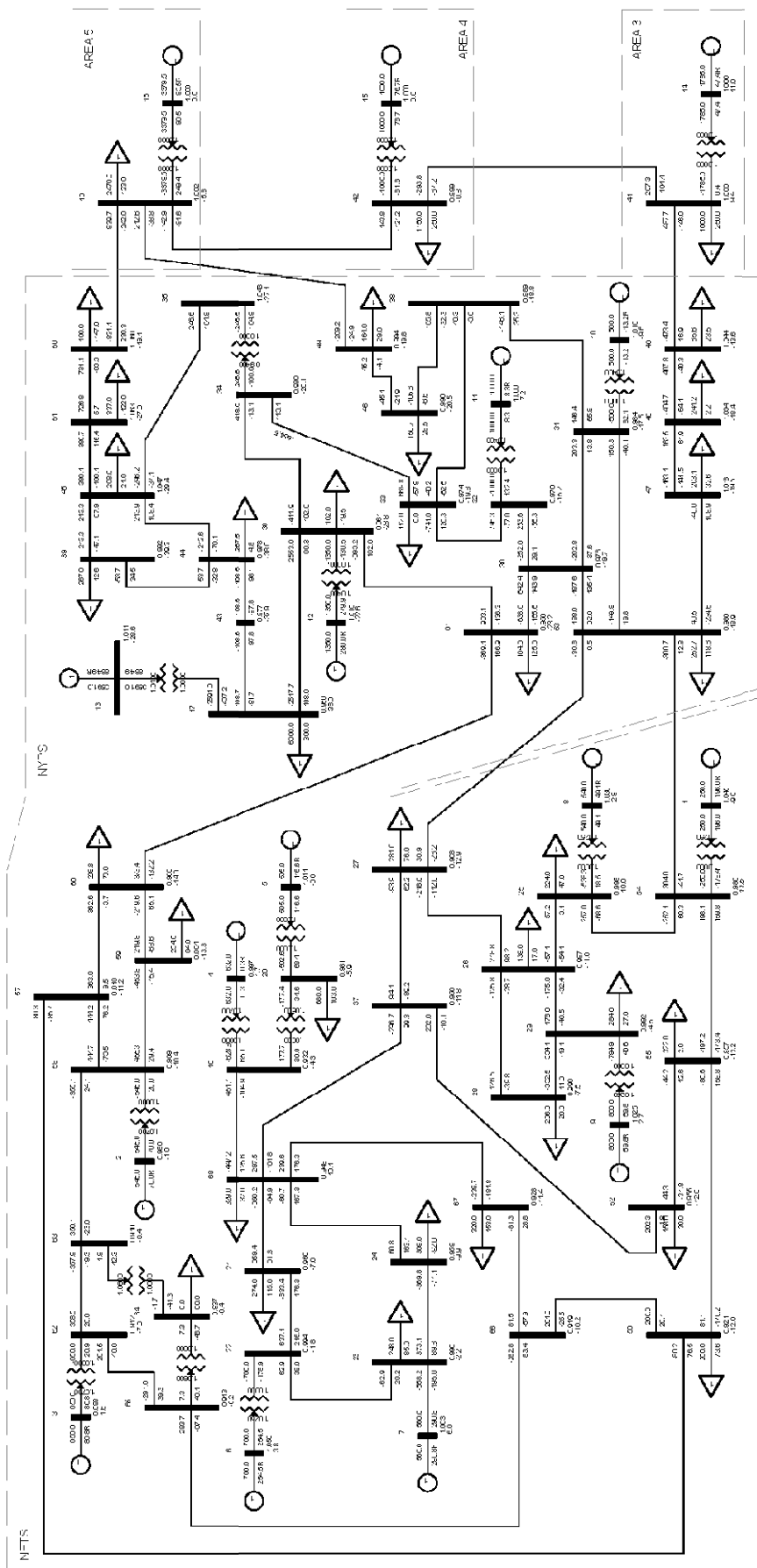


Figure 5.77: One-line Diagram of the 68-bus system (with power flow solution)

Table 5.43: Bus Data and Power Flow Solution

Bus Number	Type	Voltage (pu)	Angle (deg)
1	PV	1.0450	-8.9521
2	PV	0.9800	-0.9796
3	PV	0.9830	1.6167
4	PV	0.9970	1.6725
5	PV	1.0110	-0.6235
6	PV	1.0500	3.8466
7	PV	1.0630	6.0348
8	PV	1.0300	-2.8368
9	PV	1.0250	2.6566
10	PV	1.0100	-9.64
11	PV	1.0000	-7.2206
12	PV	1.0156	-22.6264
13	PV	1.0110	-28.6487
14	PV	1.0000	10.9625
15	PV	1.0000	0.0172
16	slack	1.0000	0
17	PQ	0.9499	-36.0217
18	PQ	1.0023	-5.8053
19	PQ	0.9320	-4.2592
20	PQ	0.9806	-5.8703
21	PQ	0.9603	-7.0498
22	PQ	0.9937	-1.7969
23	PQ	0.9961	-2.1565
24	PQ	0.9587	-9.8725
25	PQ	0.9981	-9.9953
26	PQ	0.9869	-11.0152
27	PQ	0.9679	-12.8529
28	PQ	0.9897	-7.4925
29	PQ	0.9921	-4.5422
30	PQ	0.9762	-19.7057
31	PQ	0.9838	-17.46
32	PQ	0.9699	-15.2335
33	PQ	0.9738	-19.754
34	PQ	0.9801	-26.1115
35	PQ	1.0431	-27.0843
36	PQ	0.9607	-28.8224
37	PQ	0.9555	-11.7838
38	PQ	0.9890	-18.7555
39	PQ	0.9916	-39.2852
40	PQ	1.0443	-13.6368
41	PQ	0.9997	9.4277
42	PQ	0.9990	-0.8432
43	PQ	0.9765	-37.9036
44	PQ	0.9775	-37.9812
45	PQ	1.0471	-29.3591

Table 5.44: Bus Data and Power Flow Solution (continued from Table 4.30)

Bus Number	Type	Voltage (pu)	Angle (deg)
46	PQ	0.9903	-20.5281
47	PQ	1.0184	-19.4936
48	PQ	1.0338	-18.3724
49	PQ	0.9936	-19.8169
50	PQ	1.0603	-19.0506
51	PQ	1.0634	-27.2854
52	PQ	0.9545	-12.8292
53	PQ	0.9864	-18.9331
54	PQ	0.9857	-11.5328
55	PQ	0.9571	-13.2137
56	PQ	0.9209	-11.9551
57	PQ	0.9102	-11.2088
58	PQ	0.9090	-10.3982
59	PQ	0.9038	-13.3067
60	PQ	0.9062	-14.0326
61	PQ	0.9557	-23.2176
62	PQ	0.9122	-7.3078
63	PQ	0.9097	-8.366
64	PQ	0.8367	-8.3731
65	PQ	0.9128	-8.1807
66	PQ	0.9194	-10.1869
67	PQ	0.9280	-11.4256
68	PQ	0.9483	-10.0671

Table 5.45: Transmission Line Data on a 100 MVA base

From Bus Number	To Bus Number	Id	resistance (pu)	reactance (pu)	total charging (pu)
7	23	1	0.0005	0.0272	0
17	36	1	0.0005	0.0045	0.32
17	43	1	0.0005	0.0276	0
18	42	1	0.004	0.06	2.25
18	49	1	0.0076	0.1141	1.16
18	50	1	0.0012	0.0288	2.06
19	68	1	0.0016	0.0195	0.304
21	22	1	0.0008	0.014	0.2565
21	68	1	0.0008	0.0135	0.2548
22	23	1	0.0006	0.0096	0.1846
23	24	1	0.0022	0.035	0.361
24	68	1	0.0003	0.0059	0.068
25	26	1	0.0032	0.0323	0.531
25	54	1	0.007	0.0086	0.146
26	27	1	0.0014	0.0147	0.2396
26	28	1	0.0043	0.0474	0.7802
26	29	1	0.0057	0.0625	1.029
27	37	1	0.0013	0.0173	0.3216
27	53	1	0.032	0.32	0.41
28	29	1	0.0014	0.0151	0.249
30	31	1	0.0013	0.0187	0.333
30	32	1	0.0024	0.0288	0.488
30	53	1	0.0008	0.0074	0.48
30	61	1	0.00095	0.00915	0.58
31	38	1	0.0011	0.0147	0.247
31	53	1	0.0016	0.0163	0.25
32	33	1	0.0008	0.0099	0.168
33	34	1	0.0011	0.0157	0.202
33	38	1	0.0036	0.0444	0.693
34	36	1	0.0033	0.0111	1.45
35	45	1	0.0007	0.0175	1.39
36	61	1	0.0011	0.0098	0.68
37	52	1	0.0007	0.0082	0.1319
37	68	1	0.0007	0.0089	0.1342
38	46	1	0.0022	0.0284	0.43
39	44	1	0	0.0411	0
39	45	1	0	0.0839	0
40	41	1	0.006	0.084	3.15
40	48	1	0.002	0.022	1.28
41	42	1	0.004	0.06	2.25
43	44	1	0.0001	0.0011	0
44	45	1	0.0025	0.073	0
45	51	1	0.0004	0.0105	0.72
46	49	1	0.0018	0.0274	0.27

Table 5.46: Transmission Line Data on a 100 MVA base (continued from Table 4.32)

From Bus Number	To Bus Number	Id	resistance (pu)	reactance (pu)	total charging (pu)
47	48	1	0.00125	0.0134	0.8
47	53	1	0.0013	0.0188	1.31
50	51	1	0.0009	0.0221	1.62
52	55	1	0.0011	0.0133	0.2138
53	54	1	0.0035	0.0411	0.6987
54	55	1	0.0013	0.0151	0.2572
55	56	1	0.0013	0.0213	0.2214
56	57	1	0.0008	0.0128	0.1342
56	66	1	0.0008	0.0129	0.1382
57	58	1	0.0002	0.0026	0.0434
57	60	1	0.0008	0.0112	0.1476
58	59	1	0.0006	0.0092	0.113
58	63	1	0.0007	0.0082	0.1389
59	60	1	0.0004	0.0046	0.078
60	61	1	0.0023	0.0363	0.3804
62	63	1	0.0004	0.0043	0.0729
62	65	1	0.0004	0.0043	0.0729
65	66	1	0.0009	0.0101	0.1723
66	67	1	0.0018	0.0217	0.366
67	68	1	0.0009	0.0094	0.171

Table 5.47: Transformer Data (on 100 MVA Base, tap on the “from” side)

From Bus Number	To Bus Number	Id	resistance (pu)	reactance (pu)	tap (pu)
1	54	1	0	0.0181	1.025
2	58	1	0	0.025	1.07
3	62	1	0	0.02	1.07
4	19	1	0.0007	0.0142	1.07
5	20	1	0.0009	0.018	1.009
6	22	1	0	0.0143	1.025
8	25	1	0.0006	0.0232	1.025
9	29	1	0.0008	0.0156	1.025
10	31	1	0	0.026	1.04
11	32	1	0	0.013	1.04
12	36	1	0	0.0075	1.04
13	17	1	0	0.0033	1.04
14	41	1	0	0.0015	1
15	42	1	0	0.0015	1
16	18	1	0	0.003	1
20	19	1	0.0007	0.0138	1.06
34	35	1	0.0001	0.0074	0.946
63	64	1	0.0016	0.0435	1.06
65	64	1	0.0016	0.0435	1.06

Table 5.48: Load Data

Bus Number	P (MW)	Q (Mvar)
17	6000	300
18	2470	123
20	680	103
21	274	115
23	248	85
24	309	-92
25	224	47
26	139	17
27	281	76
28	206	28
29	284	27
33	112	0
36	102	-19.46
39	267	12.6
40	65.63	23.53
41	1000	250
42	1150	250
44	267.55	4.84
45	208	21
46	150.7	28.5
47	203.12	32.59
48	241.2	2.2
49	164	29
50	100	-147
51	337	-122
52	158	30
53	252.7	118.56
55	322	2
56	200	73.6
59	234	84
60	208.8	70.8
61	104	125
64	9	88
67	320	153
68	329	32

Table 5.49: Power Flow Results

FROM BUS#	VOLT PU	ANGLE	GEN MW/MVAR	LOAD MW/MVAR	TO			TRANSFORMER		
					BUS#	CKT	MW	MVAR	RATIO	
1	1.0450	-9.0	250.0 196.0R	0.0 0.0	54	1	250.0	196.0	1.025LK	
2	0.9800	-1.0	545.0 70.0R	0.0 0.0	58	1	545.0	70.0	1.070LK	
3	0.9830	1.6	650.0 80.8R	0.0 0.0	62	1	650.0	80.8	1.070LK	
4	0.9970	1.7	632.0 0.3R	0.0 0.0	19	1	632.0	0.3	1.070LK	
5	1.0110	-0.6	505.0 116.6R	0.0 0.0	20	1	505.0	116.6	1.009LK	
6	1.0500	3.8	700.0 254.5R	0.0 0.0	22	1	700.0	254.5	1.025LK	
7	1.0630	6.0	560.0 290.8H	0.0 0.0	23	1	560.0	290.8		
8	1.0300	-2.8	540.0 49.1R	0.0 0.0	25	1	540.0	49.1	1.025LK	
9	1.0250	2.7	800.0 59.8R	0.0 0.0	29	1	800.0	59.8	1.025LK	
10	1.0100	-9.6	500.0 -13.2R	0.0 0.0	31	1	500.0	-13.2	1.040LK	
11	1.0000	-7.2	1000.0 8.3R	0.0 0.0	32	1	1000.0	8.3	1.040LK	
12	1.0156	-22.6	1350.0 280.0R	0.0 0.0	36	1	1350.0	279.9	1.040LK	
13	1.0110	-28.6	3591.0 884.9R	0.0 0.0	17	1	3591.0	884.9	1.040LK	
14	1.0000	11.0	1785.0 47.4R	0.0 0.0	41	1	1785.0	47.4	1.000LK	
15	1.0000	0.0	1000.0 76.7R	0.0 0.0	42	1	1000.0	76.7	1.000LK	
16	1.0000	0.0	3379.5 93.5R	0.0 0.0	18	1	3379.5	93.5	1.000LK	
17	0.9499	-36.0	0.0 0.0	6000.0 300.0	13	1	-3591.0	-407.2	1.000UN	
					36	1	-2517.7	198.9		
					43	1	108.7	-91.7		
18	1.0023	-5.8	0.0 0.0	2470.0 123.0	16	1	-3379.5	249.4	1.000UN	
					42	1	-142.9	-91.6		
					49	1	212.6	-38.8		
					50	1	839.7	-242.0		
19	0.9320	-4.3	0.0 0.0	0.0 0.0	4	1	-628.8	65.1	1.000UN	
					20	1	177.7	39.9	1.000UN	
					68	1	451.1	-104.9		
20	0.9806	-5.9	0.0 0.0	680.0 103.0	5	1	-502.6	-68.4	1.000UN	
					19	1	-177.4	-34.6	1.060LK	
21	0.9602	-7.0	0.0 0.0	274.0 115.0	22	1	-633.4	-176.3		
					68	1	359.4	61.3		
22	0.9937	-1.8	0.0 0.0	0.0 0.0	6	1	-700.0	-178.9	1.000UN	
					21	1	637.1	216.9		
					23	1	62.9	-38.0		
23	0.9961	-2.2	0.0 0.0	248.0 85.0	7	1	-558.2	-195.0		
					22	1	-62.9	20.2		
					24	1	373.1	89.8		
24	0.9587	-9.9	0.0 0.0	309.0 -92.0	23	1	-369.8	-71.1		
					68	1	60.8	163.1		
25	0.9981	-10.0	0.0 0.0	224.0 47.0	8	1	-538.3	18.5	1.000UN	
					26	1	57.2	3.1		
					54	1	257.0	-68.6		

Table 6 (cont.): PSS/E Power Flow Results

Table 6 (cont.): PSS/E Power Flow Results

5.6.2. Dynamic Data

The generator model to represent the round rotor units is shown in the block diagram of Figure 5.3. The details associated with the representation of the saturation of the generators should not dramatically interfere with the results of a small-signal (linearized) analysis of the system performance. On the other hand, the proper representation of saturation is extremely important for transient stability and the determination of rated and ceiling conditions (minimum and maximum generator field current and generator field voltage) for the excitation system.

The calculated rated field current for this generator model is 2.75 pu (considering 0.80 rated power factor). This calculation comprises the initialization of the generator model at full (rated) power output, considering their rated power factor.

The parameters and other data for the dynamic models of the generators are given in the sequence, from Table 5.50 to Table 5.52.

Table 5.50: Dynamic Model Data for Round Rotor Units 1 and 2

PARAMETERS		GENERATOR		
Description	Symbol	1	2	Unit
Rated apparent power	M _{BASE}	600	600	MVA
d-axis open circuit transient time constant	T' _{do}	10.2	10.2	s
d-axis open circuit sub-transient time constant	T'' _{do}	0.05	0.05	s
q-axis open circuit transient time constant	T' _{qo}	1.5	1.5	s
q-axis open circuit sub-transient time constant	T'' _{qo}	0.035	0.035	s
Inertia	H	7	7	MW.s/MVA
Speed damping	D	0	0	pu
d-axis synchronous reactance	X _d	0.6	0.6	pu
q-axis synchronous reactance	X _q	0.414	0.414	pu
d-axis transient reactance	X' _d	0.186	0.186	pu
q-axis transient reactance	X' _q	0.25	0.25	pu
sub-transient reactance (X'' _d =X'' _q)	X''	0.15	0.15	pu
Leakage reactance	X _l	0.075	0.075	pu
Saturation factor at 1.0 pu voltage	S(1.0)	0.001	0.001	—
Saturation factor at 1.2 pu voltage	S(1.2)	0.01	0.01	—

Table 5.51: Dynamic Model Data for Round Rotor Units from 3 to 9

Table 5.52: Dynamic Model Data for Round Rotor Units from 10 to 16

The block diagram of the excitation system model DC4B [4] is shown in Figure 5.78. The parameters for the model are presented in Table 5.53. This model and these parameters apply to the excitation systems of generators 1 to 12.

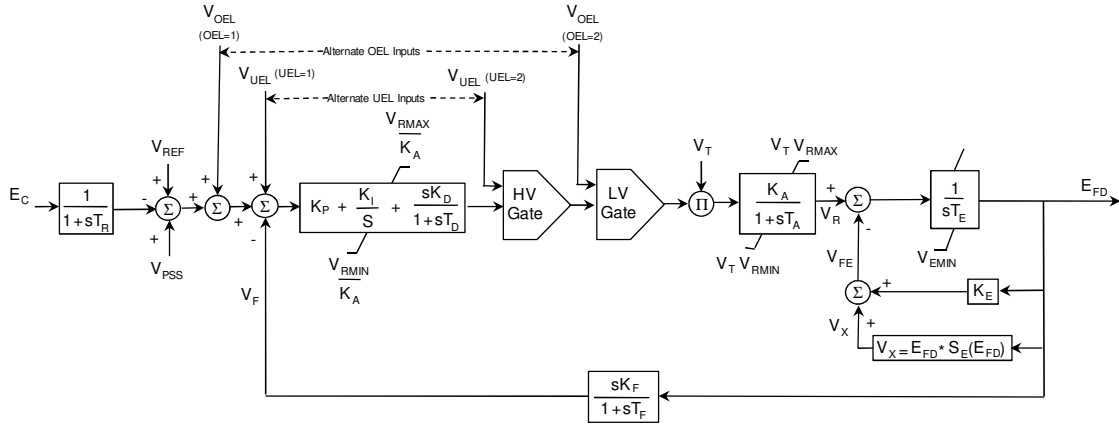


Figure 5.78: Block Diagram for the Excitation System Model DC4B

Table 5.53: Dynamic Model Data for DC Rotating Excitation Systems DC4B

PARAMETERS			
Description	Symbol	Value	Unit
Voltage transducer time constant	\$T_R\$	0.01	s
AVR proportional gain	\$K_P\$	200	pu
AVR integral gain	\$K_I\$	50	pu
AVR derivative gain	\$K_D\$	50	pu
AVR derivative time constant	\$T_D\$	0.01	s
Max. AVR output	\$V_{Rmax}\$	10	pu
Min. AVR output	\$V_{Rmin}\$	-10	pu
thyristor bridge equivalent gain	\$K_A\$	1	pu
thyristor bridge equivalent time constant	\$T_A\$	0.02	s
Exciter feedback time constant	\$K_E\$	1	pu
Exciter time constant	\$T_E\$	0.785	s
Stabilizer feedback gain	\$K_F\$	0	pu
Stabilizer feedback time constant	\$T_F\$	1.0	s
Minimum exciter output	\$V_{Emin}\$	0	
Exciter saturation point 1	\$E_1\$	3.9267	pu
Exciter saturation factor at point 1	\$S_E(E_1)\$	0.07	-
Exciter saturation point 2	\$E_2\$	5.2356	pu
Exciter saturation factor at point 2	\$S_E(E_2)\$	0.91	-

The block diagram of the exciter model ST1A is shown in Figure 5.40. The transient gain reduction will be implemented by the lead-lag block with parameters \$T_C\$ and \$T_B\$, so the parameters \$T_{C1}\$, \$T_{B1}\$, \$K_F\$ and \$T_F\$ are not applicable and have been set accordingly. Similarly, the

generator field current limit represented by the parameters K_{LR} and I_{LR} is not considered in the results presented in this report. The parameters for the this model are presented in .

The limits (parameters $V_{I_{max}}$, $V_{I_{min}}$, $V_{A_{max}}$, $V_{A_{min}}$, $V_{R_{max}}$ and $V_{R_{min}}$) in the model were set to typical values corresponding to the expected ceilings of such static excitation system. These limits are irrelevant for the small-signal analysis of the system dynamic response. On the other hand, these limits are a critical part of the model and the expected response of the excitation system following large system disturbances such as faults.

Table 5.54: Dynamic Model Data for Static Excitation Systems ST1A

PARAMETERS			
Description	Symbol	Value	Unit
Voltage transducer time constant	T_R	0.01	s
Max. voltage error	$V_{I_{max}}$	99	pu
Min. voltage error	$V_{I_{min}}$	-99	pu
TGR block 1 numerator time constant	T_C	1	s
TGR block 1 denominator time constant	T_B	1	s
TGR block 2 numerator time constant	T_{C1}	1	s
TGR block 1 denominator time constant	T_{B1}	1	s
AVR steady state gain	K_A	200	pu
Rectifier bridge equivalent time constant	T_A	0.01	s
Max. AVR output	$V_{A_{max}}$	5	pu
Min. AVR output	$V_{A_{min}}$	-5	pu
Max. rectifier bridge output	$V_{R_{max}}$	5	pu
Min. rectifier bridge output	$V_{R_{min}}$	-5	pu
Commutation factor for rectifier bridge	K_C	0	pu
Stabilizer feedback gain	K_F	0	pu
Stabilizer feedback time constant	T_F	1	s
Field current limiter gain	K_{LR}	0	pu
Field current instantaneous limit	I_{LR}	3	pu

The IEEE Std. 421.5(2005) model PSS1A will be used to represent the power system stabilizers. The block diagram of this model is shown in Figure 5.5. The parameters for the PSSs used in this study are presented in Table 5.55.

The output limits were set to $\pm 5\%$, while the logic to switch off the PSS for voltages outside a normal operation range has been ignored (parameters V_{CU} and V_{CL} set to zero).

Table 5.55: Dynamic Model Data for Power System Stabilizers PSS1A

PARAMETERS				
Description	Symbol	Unit 9	††	Unit
2 nd order denominator coefficient	A_1	0	0.04	
2 nd order denominator coefficient	A_2	0	0	
2 nd order numerator coefficient	A_3	0	0	
2 nd order numerator coefficient	A_4	0	0	
2 nd order denominator coefficient	A_5	0	0.15	

2 nd order denominator coefficient	A ₆	0	0	
1 st lead-lag numerator time constant	T ₁	0.09	0.15	s
1 st lead-lag denominator time constant	T ₂	0.02	0.04	s
2 nd lead-lag numerator time constant	T ₃	0.09	0.15	s
2 nd lead-lag denominator time constant	T ₄	0.02	0.04	s
Washout block numerator time constant	T ₅	10	15	s
Washout block denominator time constant	T ₆	10	15	s
PSS gain	K _S	12	20	pu
PSS max. output	L _{Smax}	0.20	0.20	pu
PSS min. output	L _{Smin}	-0.05	-0.05	pu
Upper voltage limit for PSS operation	V _{CU}	0	0	pu
Lower voltage limit for PSS operation	V _{CL}	0	0	pu

5.6.3. Selected Results and Validation

The first set of results presented for the 68-bus system are a comparison between the eigenvalues (focused on the range of electromechanical modes) generated in Matlab/Simulink [33] and in the PacDyn/ANATEM package [34]. The following plots show that the match between the results of these two software packages is quite satisfactory, and the complete set of input and output data for this comparison can be found at the TF website.

Figure 5.79 shows the eigenvalue comparison for the case where the generators are not equipped with PSSs. It can be seen that three modes are unstable and 9 other modes are poorly damped (considering a minimum acceptable damping of 5%).

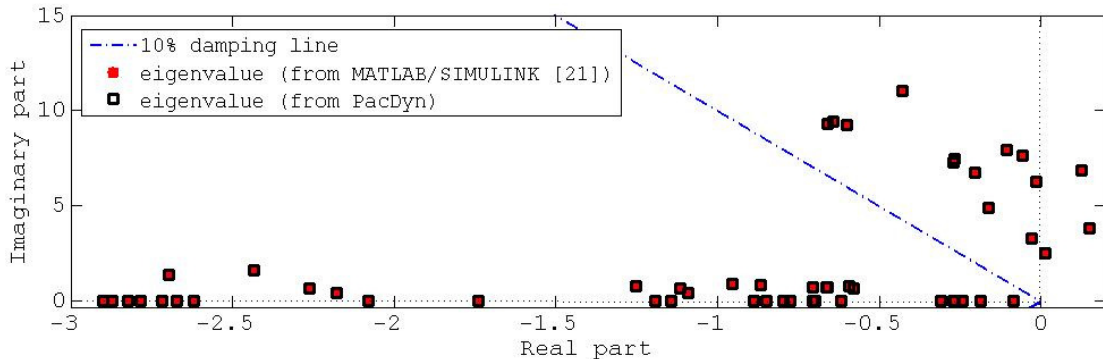


Figure 5.79: Eigenvalues (calculated from MATLAB/SIMULINK [21] and PacDyn [34]) for the case where the generators are not equipped with PSSs.

If only one PSS is in service at Generator 9, the comparative results can be seen in Figure 5.80. It is now possible to see that this single PSS can stabilize most of the modes that were unstable with no damping control at all in the system. However, an unstable inter-area mode still remains in the system. Furthermore, there are several poorly damped modes in this case, indicating that PSS are needed in the other generators to adequately damp the electromechanical oscillations in this system.

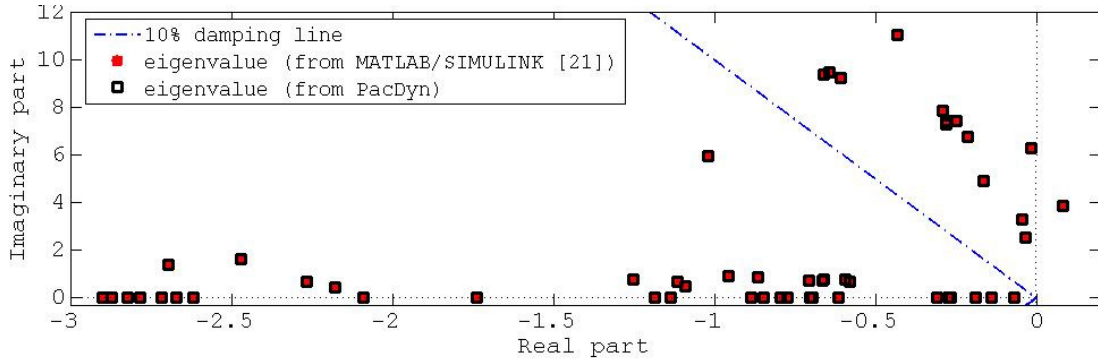


Figure 5.80: Eigenvalues (calculated from MATLAB/SIMULINK [21] and PacDyn [34]) for the case where only generator in bus 9 is equipped with PSS.

For the case where PSSs are placed and tuned for Generators from 1 to 12, the results can be seen in Figure 5.81. In this case, it is possible to see that there are still two inter-area underdamped modes remaining in the system eigenstructure. This is due to the fact that no PSSs were placed in the equivalent generators that represent areas 3, 4 and 5.

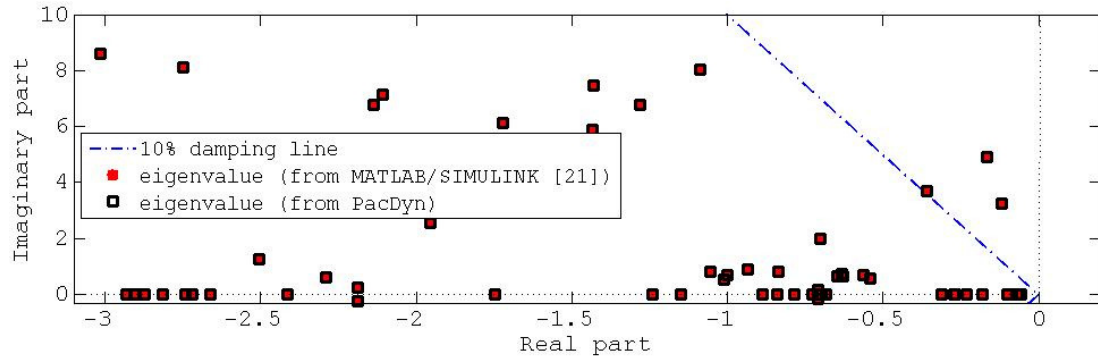


Figure 5.81: Eigenvalues (calculated from MATLAB/SIMULINK [21] and PacDyn [34]) for the case where the generators in the buses 1 to 12 are equipped with PSSs.

To provide more than 5% of damping to the poorly damped modes in Figure 5.81 since there is no access to the detailed structure of areas 3, 4 and 5, it is necessary to rely on different types of damping controllers, such as PODs for FACTS devices, for example. The interested reader can find examples of these PODs in [8].

Nonlinear time-domain simulations were carried out to validate the results of the linear analyses, so the reader can assess the effectiveness of the proposed stabilizers in providing damping to these oscillations directly with a time-domain plot. For the time-domain simulations, only the cases with no PSSs and with PSSs in Generators from 1 to 12 were compared, given that it was found that only one PSS in Generator 9 does not adequately stabilize the system.

The first set of simulations comprise the connection of a 50 MVAr reactor at bus #3 at $t = 1.0$ s. The reactor is disconnected at $t = 11.0$ s, and the system returns to its original topology. The total simulation time was 10s and the integration step was 0.008s. The angle of generator

16 was taken as a reference for angle differences. The relative rotor slips for generators 3, 9 and 15 (in relation to generator 16) are presented in Figure 5.82 to Figure 5.87, were the results obtained from ANATEM [34] are compared with the ones obtained from MATLAB/SIMULINK [33].

Figure 5.82 shows the time-domain plot of the response of Generator 3 to the disturbance described in the previous paragraph. It can be seen that the insertion of this reactor is a very small disturbance, and as such leads to results that correspond to a predominantly linear response of the system. Furthermore, it is also possible to see (mainly in Figure 5.84) that this perturbation excites the poorly damped inter-area modes, and that the system needs extra damping sources to exhibit a well-damped behavior.

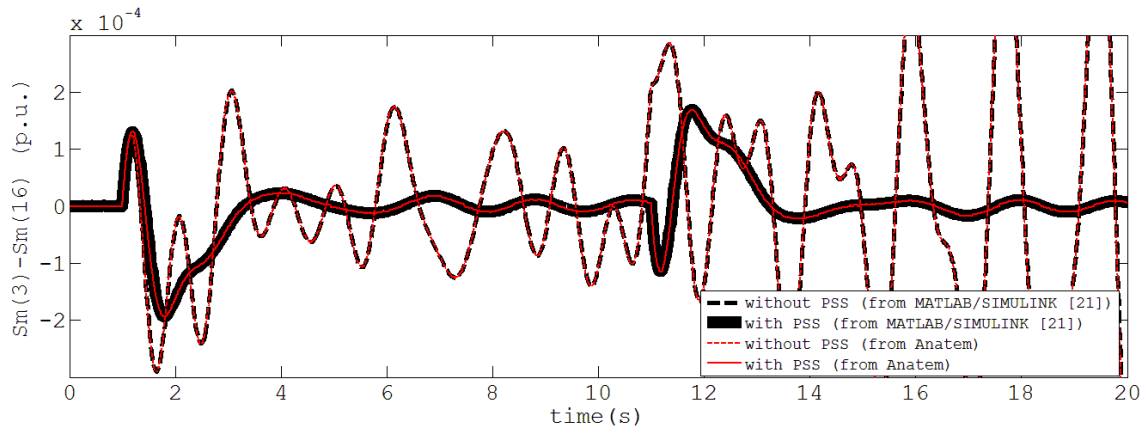


Figure 5.82: Relative rotor slips for G3 for the perturbations in bus #3.

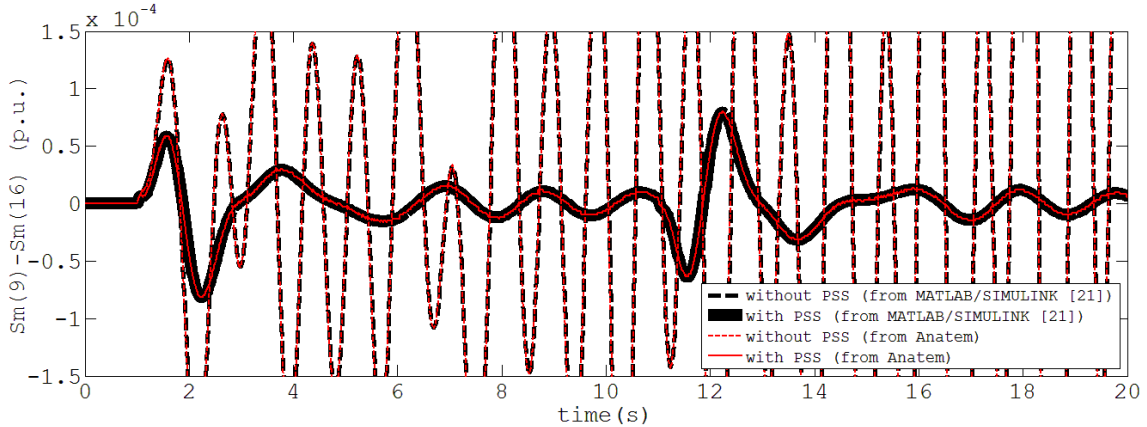


Figure 5.83: Relative rotor slips for G9 for the perturbations in bus #3.

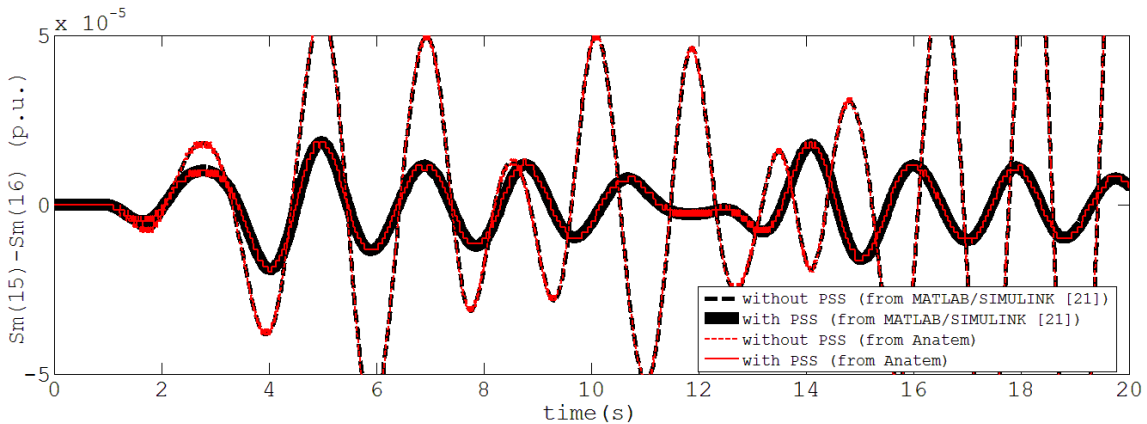


Figure 5.84: Relative rotor slips for G15 for the perturbations in bus #3.

The second set of simulations correspond to simultaneous changes in the voltage references of selected generators. For the case shown in this report, the perturbation consisted in a 2% step in Vref of Generator 3 at $t = 1.0\text{s}$ and a -2% step in the same Vref at $t = 11\text{s}$.

It is possible to see in Figure 5.85, Figure 5.86 and Figure 5.87 that, although the applied disturbance tends to excite primarily the oscillation associated to the local mode of Generator 3, it also excites the poorly damped inter-area oscillation. This can be seen mainly in Figure 5.87, and reinforces the need for the application of PODs to this system.

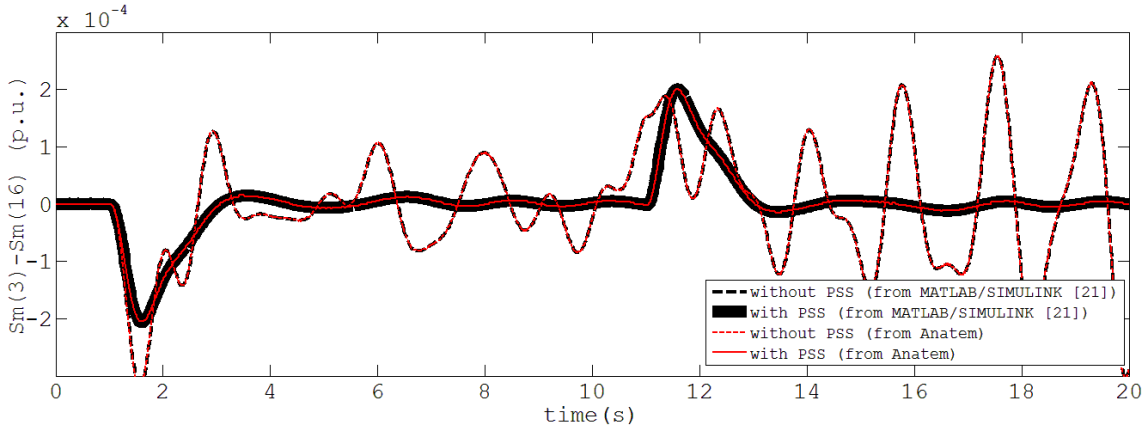


Figure 5.85: Relative rotor slips of G3 for steps in its own AVR setpoint.

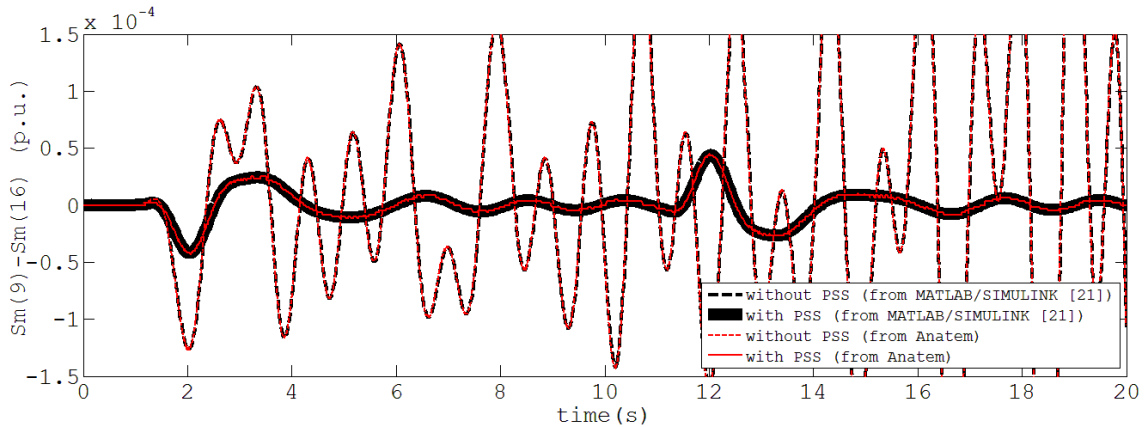


Figure 5.86: Relative rotor slips of G9 for steps in the AVR setpoint of G3.

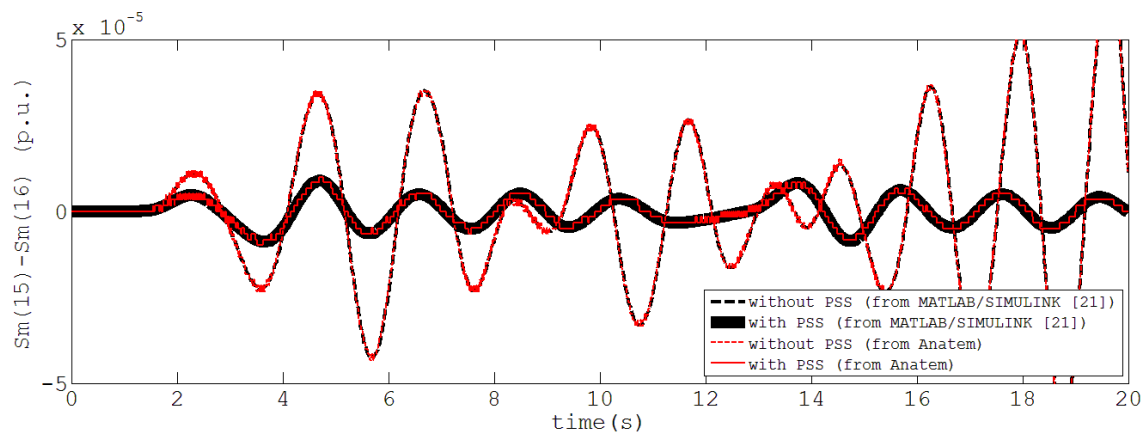


Figure 5.87: Relative rotor slips of G15 for steps in the AVR setpoint of G3.

6. References

- [1] F. P. DeMello and C. Concordia, "Concepts of Synchronous Machine Stability as Affected by Excitation Control," *IEEE Transactions on Power Apparatus and Systems*, Vols. PAS-88, no. 4, pp. 316 - 329, 1969.
- [2] E. V. Larsen and D. A. Swann, "Applying Power System Stabilizers - Parts I, II and III," *IEEE Transactions on Power Apparatus and Systems*, Vols. PAS-100, no. 6, pp. 3017 - 3046, 1981.
- [3] G. Rogers, Power System Oscillations, New York: Kluwer Academic Publishers, 2000.
- [4] "IEEE Recommended Practice for Excitation System Models for Power System Stability Studies," IEEE Standard 421.5(2005), 2006.
- [5] Excitation Systems Subcommittee, Energy Development and Power Generation Committee, ""IEEE Tutorial Course on Power System Stabilization via Excitation Control", IEEE/PES Technical Publication 09TP250," 2009. [Online]. Available: <http://resourcecenter.ieee-pes.org/publications/tutorials/ieee-tutorial-course-power-system-stabilization-via-excitation-control/>.
- [6] L. Fan, "Review of Robust Feedback Control Applications in Power Systems," in *Proceedings of the Power Systems Conference and Exposition*, Seattle, 2009.
- [7] N. G. Hingorani and L. Gyugyi, Understanding FACTS: Concepts and Technology of Flexible AC Transmission Systems, New York: IEEE Press, 2000.
- [8] B. Pal and B. Chaudhuri, Robust Control in Power Systems, New York: Springer Science+Business Media, 2005.
- [9] R. A. Ramos, L. F. C. Alberto and N. G. Bretas, "A New Methodology for the Coordinated Design of Robust Decentralized Power System Damping Controllers," *IEEE Transactions on Power Systems*, vol. 19, no. 1, pp. 444 - 454, 2004.
- [10] G. E. Boukarim, S. Wang, J. H. Chow, G. N. Taranto and N. Martins, "A Comparison of Classical, Robust and Descentralized Control Designs for Multiple Power System Stabilizers," *IEEE Transactions on Power Systems*, vol. 15, no. 4, pp. 1287 - 1292, 2000.
- [11] F. J. De Marco, N. Martins and J. C. R. Ferraz, "An Automatic Method for Power System Stabilizers Phase Compensation Design," *IEEE Transactions on Power Systems*, vol. 28, no. 2, pp. 997 - 1007, 2013.
- [12] Website of the IEEE PES Task Force on Benchmark Models for Stability Controls, 8 August 2015 [Online] Available: <http://www.sel.eesc.usp.br/ieee/> (provisional).
- [13] F. J. de Marco and N. Martins, "Report on the Three-Machine Infinite-Bus (3MIB) System," (Working Paper) 29 July 2013. [Online]. Available:

- [http://www.sel.eesc.usp.br/ieee/.](http://www.sel.eesc.usp.br/ieee/)
- [14] F. J. de Marco, L. T. G. Lima e N. Martins, "Comparison Report – PSS/E versus ANATEM/PacDyn: Results for Benchmark #1- The Three-Machine versus Infinite-Bus System," (Working Paper) 2 July 2014. [Online]. Available: <http://www.sel.eesc.usp.br/ieee/>.
- [15] N. Martins e L. T. G. Lima, "Determination of suitable locations for power system stabilizers and static VAR compensators for damping electromechanical oscillations in large scale power systems," *IEEE Transactions on Power Systems*, vol. 5, pp. 1455-1469, 1990.
- [16] P. Kundur, *Power System Stability and Control*, New York: McGraw-Hill, 1994.
- [17] N. Martins, H. J. C. P. Pinto and L. T. G. Lima, "Efficient Methods for Finding Transfer Function Zeros of Power Systems," *IEEE Transactions on Power Systems*, vol. 7, pp. 1350-1361, 1992.
- [18] M. Klein, G. Rogers and P. Kundur, "A Fundamental Study of Inter-Area Oscillations," *IEEE Transactions on Power Systems*, vol. 6, no. 3, pp. 914 - 921, 1991.
- [19] Electrical Power Research Institute, "EPRI Report EL-2348, "Phase II - Frequency-Domain Analysis of Low Frequency Oscillations in Large Electric Power Systems - Volume 1: Basic Concepts, Mathematical Models and Computing Methods"," April 1982. [Online]. Available: <http://www.eprisearch.com/search/Pages/results.aspx?k=EL-2348-V1>. [Acesso em 2 February 2015].
- [20] R. T. Byerly, D. E. Sherman and R. J. Bennon, "Phase II: Frequency Domain Analysis of Low Frequency Oscillations in Large Power Systems," EPRI EL-2348 Project 744-1 Final Report - Volume 1, Pittsburgh, 1982.
- [21] M. A. Pai, *Energy Function Analysis for Power System Stability*, Boston: Kluwer Academic Publishers, 1989.
- [22] M. J. Gibbard, "Co-ordinated design of multimachine power system stabilisers based on damping torque concepts," *IEE Proceedings C Generation, Transmission and Distribution*, vol. 135, pp. 276-284, 1988.
- [23] M. J. Gibbard, "Robust design of fixed-parameter power system stabilisers over a wide range of operating conditions," *IEEE Transactions on Power Systems*, vol. 6, pp. 794-800, 1991.
- [24] SIEMENS-PTI, "PSS/E 32.0 Online Documentation," 8 August 2015. [Online]. Available: <http://www.energy.siemens.com/hq/en/services/power-transmission-distribution/power-technologiesinternational/software-solutions/pss-e.htm>.
- [25] CEPEL, "PacDyn Online Documentation," 8 August 2015. [Online]. Available: <http://www.pacdyn.cepel.br/>

- [26] CEPEL, "ANATEM Users Manual V10.04.06 (in Portuguese)," 8 August 2015. [Online]. Available: <http://www.anatem.cepel.br/>
- [27] "IEEE Guide for Synchronous Generator Modeling Practices and Applications in Power System Stability Analyses", IEEE Std. 1110(2002), November, 2003.
- [28] EMTP-RV, "EMTP-RV 2.6. EMTP-EMTPWorks Online Documentation," 8 August 2015. [Online] Available: http://emtp.com/software_for_power_systems_transients
- [29] D. J. Vowles e M. J. Gibbard, "Mudpack User Manual: Version 10S-02," School of Electrical and Electronic Engineering, The University of Adelaide, April 2013.
- [30] CEPEL, "ANAREDE online documentation," 8 August 2015. [Online]. Available: <http://www.anarede.cepel.br/>
- [31] Australian National Electricity Rules, Version 60, 8 August 2015 [Online]. Available: <http://www.aemc.gov.au/Electricity/National-Electricity-Rules/Current-Rules.html>.
- [32] Powertech, "DSA Tools Reference Manual," 8 August 2015. [Online]. Available: <http://www.dsatools.com>.
- [33] A. K. Singh and P. Bikash, "Report on the 68-bus, 16-machine, 5-area System," (Working Paper), 3 December 2013 [Online] Available: www.sel.eesc.usp.br/ieee/.
- [34] R. Kuiava, T. C. d. C. Fernandes, M. R. Mansour e R. A. Ramos, "Report on the 68-bus system using PacDyn/ANATEM," 20 June 2014 [Online] Available: www.sel.eesc.usp.br/ieee/.
- [35] P. M. Anderson and R. G. Farmer, Series Compensation of Power Systems, Encinitas: PBL SH! Inc., 1996.

A.1

Appendix A - Report on the Simplified Australian 14-Generator Model by Profs. David Vowles and Michael Gibbard

IEEE PES Task Force on Benchmark Systems for Stability Controls

Simplified 14-Generator Model of the South East Australian Power System:

**(Including implementations in Mudpack for small-signal analysis
and PSS[®]/E for transient-stability analysis)**

14 June 2014

Mike Gibbard & David Vowles

**Power Systems Dynamics Group
School of Electrical and Electronic Engineering
The University of Adelaide, South Australia**

1 Introduction

The purpose of this document is to provide a test system which can be used as a test bed for the small-signal analysis and design of power system stabilisers (PSSs) and other controllers *in a multi-machine power system*.

Frequently papers are published in which the performance of PSSs designed using a new ‘advanced’ method is compared to that of PSSs designed using so-called ‘conventional’ techniques. Often the ‘conventional’ PSSs employed in such papers do not represent a properly-designed ‘conventional’ PSS. In the following a sound basis for a ‘conventional’ PSS design is outlined and its performance demonstrated. It is a tuning method used in practice by a number of organisations.

An important aspect of the design of PSSs for use on practical systems is that PSSs should contribute to the damping of inter-area, local-area and intra-station modes. This aspect is seldom tested adequately in most ‘advanced’ design methods because:

- a single-machine infinite-bus test system is typically employed by the proponent; it does not reveal the damping performance of the proposed PSS over the full range of modal frequencies likely to be encountered in practice, i.e. from the low frequency inter-area modes (~ 1.5 rad/s) to the higher local / intra-station frequencies ($12+$ rad/s);
- the contributions to modal damping by the proposed PSS are not validated over a wide range of operating conditions encountered in practice, light to peak load, for normal and contingency operation, etc.;
- the models of AVR/excitation systems employed in the proponent’s system are often very simple. In practice such models may be third or higher order.

For designs of advanced PSSs to be credible for practical application, the proponents should demonstrate the above issues have been adequately addressed. An aim of the 14-generator test system is to provide researchers and developers with a system possessing the features highlighted above, i.e. a range of modal frequencies, a range of operating conditions, and higher-order avr/excitation system models.

Each generator in the 14-machine system is in fact an aggregated equivalent generator representing a power station (PS) of between 2 to 12 units. While the generators in each station could have been individually represented, this adds an additional level of complexity and increases system size, moreover, it is not warranted for the primary purpose of this document.

Included in [Appendix I](#) is a complete set of power flow and small-signal dynamics data that allows an interested party (i) to replicate the results provided using that party’s loadflow and small-signal dynamics analysis packages, (ii) to cross-check results obtained by the party with those presented here, (iii) to insert in a Matlab environment the party’s own controller, etc., into the power system for the analysis being conducted for research purposes.

A large-signal model of the system has been developed to allow transient stability analysis. As summarized in [Section 9](#) the data for the large-signal model is presented in [Appendix II](#) in a format amenable to use with the PSS[®]/E [1] transient-stability program. Benchmarking studies in

[Appendix III](#) show that the small-disturbance performance of the PSS[®]/E implementation of the model is in close agreement with that of the original Mudpack implementation. A comprehensive set of transient stability studies are conducted in [Appendix IV](#) using the PSS[®]/E implementation of the model. It is found that the system is transiently stable for a comprehensive set of two-phase to ground faults across all six base case scenarios.

2 Caveats

The model of the power system used in this document is *loosely* based on the southern and eastern Australian networks. Therefore,

- it does not accurately represent any particular aspect of those networks;
- the model should not be used to draw any conclusions relating to the actual performance of the networks comprising the southern and eastern Australian grid, either for any normal or any hypothetical contingency condition;
- the model is suitable for educational purposes / research-oriented analysis only.

3 Information provided

The following data are provided. Refer to [Appendix V](#) for details of information provided in electronic format.

- The load flow data and results files in PSS[®]/E format together with the associated data tables for six normal operating conditions. These cover peak, medium and light load conditions with various inter-area power transfers and directions of flow.
- Tables of the parameters for the generators, SVCs, excitation systems and PSSs for use in both the small- and large-signal analysis of the dynamic performance of the system.
- The P-Vr frequency response characteristics of the generators over the range of operating conditions. These are presented in graphical form (on machine base).
- Tables of the rotor modes of oscillation for the six cases with PSSs in- and out-of-service.
- Matlab *.mat files of the state-space model matrices (i.e. ABCD matrices), eigenvalues, eigenvectors and participation factors for two of the six cases with the PSSs both in- and out-of-service.
- Small-disturbance step-response analysis results in comma-separated-value (*.csv) and Matlab (*.mat) formats for a selection of scenarios computed by both Mudpack and PSS[®]/E.
- Transient-stability time-domain analysis results in comma-separated-value (*.csv) and Matlab (*.mat) formats for a selection of faults computed by PSS[®]/E.
- A rudimentary Matlab function is also provided to allow the user to compare their own time-response results (small- or large-signal) with those provided.

4 The Simplified System

The simplified 14-generator, 50 Hz system is shown in [Figure 1](#). It represents a long, linear system as opposed to the more tightly meshed networks found in Europe and the USA. For convenience, it has been divided into 5 areas in which areas 1 and 2 are more closely coupled electrically. There are in essence 4 main areas and hence 3 inter-area modes, as well as 10 local-area modes. Without PSSs many of these modes are unstable.

In order to tune generator PSSs in practice an encompassing range of normal operating conditions and contingencies are considered. In the data provided in the Appendices, however, only six normal conditions are used for illustrative purposes. The operating conditions, system loads and major inter-area flows are listed in [Table 1](#).

Table 1 Six normal steady-state operating conditions

	<u>Case 1</u>	<u>Case 2</u>	<u>Case 3</u>	<u>Case 4</u>	<u>Case 5</u>	<u>Case 6</u>
<u>Load Condition</u>	Heavy	Medium-heavy	Peak	Light	Medium	Light
Total generation (MW)	23030	21590	25430	15050	19060	14840
Total load (MW)	22300	21000	24800	14810	18600	14630
<u>Inter-area flows</u>	(North to south)	(South to north)	(Hydro to N & S)	(Area 2 to N & S)	(N & S to pumping)	(~Zero transfers)
Area 4 to Area 2 (MW)	500	-500	-500	-200	300	0
Area 2 to Area 1 (MW)	1134	-1120	-1525	470	740	270
Area 1 to Area 3 (MW)	1000	-1000	1000	200	-200	0
Area 3 to Area 5 (MW)	500	-500	250	200	250	0

The schedules of generation for the six cases are listed in [Appendix I, Table 8](#). Note that the number of generating units on-line in certain power stations (designated *PS_#, e.g. HPS_1) can vary considerably over the range of operating conditions.

5 Power flow analysis

Data for the power flow analysis of the six normal operating conditions given in [Table 1](#) is supplied in [Appendix I.1](#). Included in [Appendix I.1](#) are relevant results of the analysis such as reactive outputs of generators and SVCs, together with tap positions on generator and network transformers. This information permits the power flows to be set up on any power flow platform and the results checked against those provided in this document.

The power flow data is also provided in Siemens-PTI PSS®/E version 29 format¹. These files for the six operating conditions are accessible from the web site in [Appendix V.1](#).

-
1. The specification of the Siemens-PTI PSS®/E version 29 power flow raw data format is available by application from Siemens-PTI at the following web-site <http://w3.usa.siemens.com/smartgrid/us/en/transmission-grid/products/grid-analysis-tools/transmission-system-planning/Pages/PSSERawDataFormat.aspx>

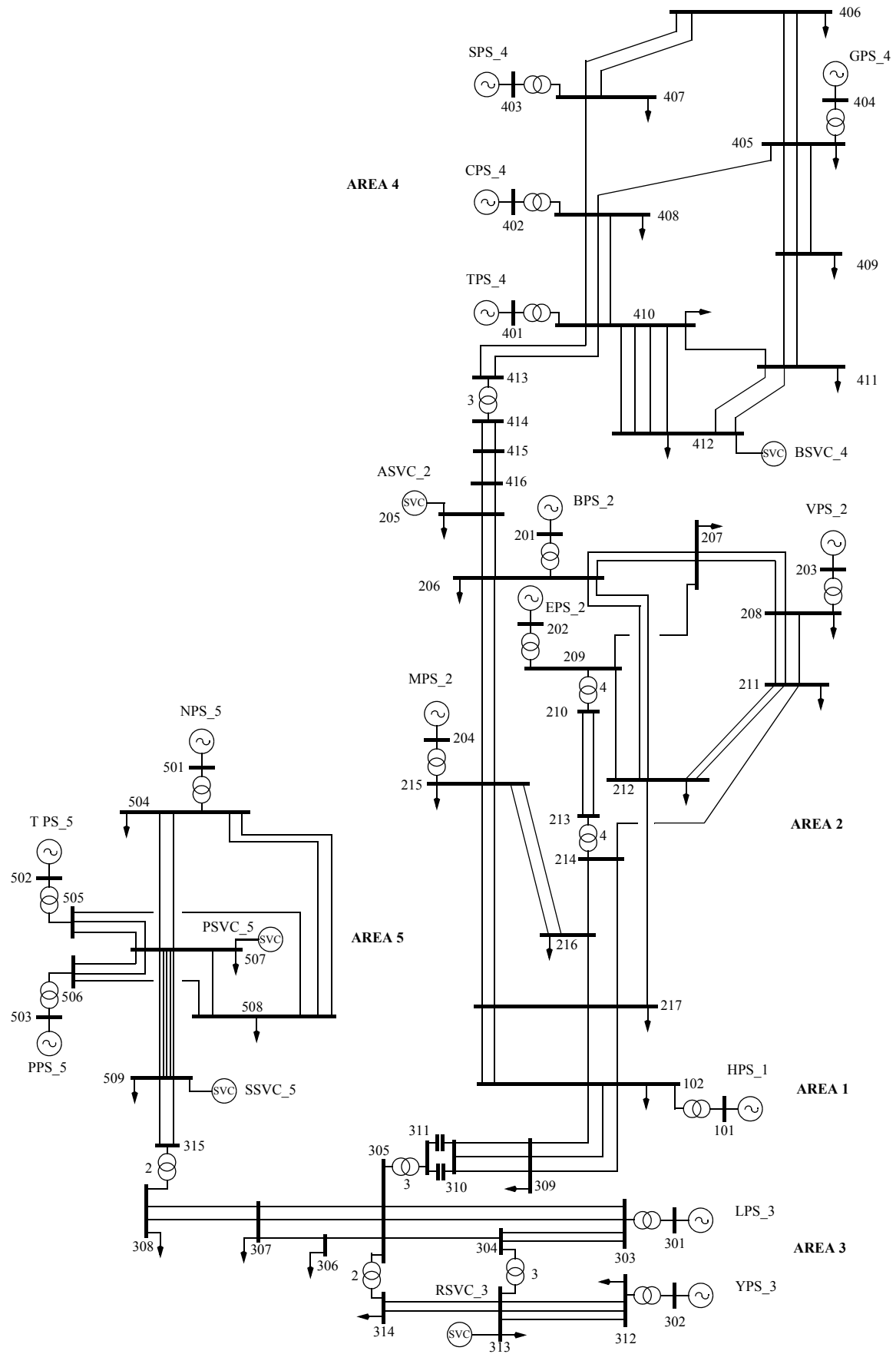


Figure 1 Simplified 14-generator, 50 Hz system.

6 Design of PSSs based on the P-Vr Method for multi-machine systems

6.1 Introduction

Comparisons between conventional PSS design methods such as the ‘GEP’, ‘P-Vr’ - and a method based on residues - for multi-machine power systems are discussed in [7] and [11]. A comparison of the P-Vr and GEP methods and their features are provided in Table 21 of Appendix I.4.

6.2 Concepts based on an ideal PSS

Consider the idealised shaft dynamics of the simplified generator model shown in Figure 2. Assume that a feedback loop can be added from the rotor speed signal $\Delta\omega$ to the torque signal ΔP_d - as shown in Figure 2 - such that $\Delta P_{ds} = k \Delta\omega$. It is clear that increasing the gain k has the same effect as increasing the *inherent damping torque coefficient* k_d [13], that is, enhancing the damping of rotor oscillations. The block with gain k represents an ideal PSS that induces on the rotor a torque of electro-magnetic origin proportional to speed perturbations. The gain k , like k_d , is a *damping torque coefficient* which we call the *damping gain* of the PSS. (The difference between the latter gain and the conventional ‘PSS gain’ is discussed shortly.) The goal in the design of a practical PSS is to achieve the same result, the damping gain being adjusted to meet the specifications on the damping for the rotor modes of oscillation. Framed in this context, the damping gain k of a practical PSS expressed in per unit on machine base becomes a meaningful quantity.

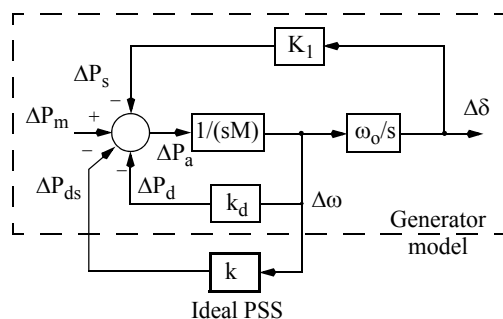


Figure 2 The ideal PSS, represented by a damping gain k , introduces a pure damping torque on the rotor of a simplified generator model.

6.3 Theoretical background

The design of the compensating transfer function (TF) for the PSS of generator i in a multi-machine power system is based on the so-called P-Vr TF of generator i . This is the TF from the AVR voltage reference input, ‘Vr’, on generator i to the torque of electromagnetic origin (or electrical power output, ‘P’) on that generator, calculated with the shaft dynamics of *all* machines disabled [2], [3]. In the following, $\Delta V_{ri}(s)$ and $\Delta P_{ei}(s)$ are perturbations in the reference voltage and the electrical torque, respectively. (For small disturbances the per-unit perturbations in electrical power and electrical torque are identical.)

The frequency response of the P-Vr TF, $H_{PVri}(s) = \Delta P_{ei}(s)/\Delta V_{ri}(s)$, is easily calculated. To disable the shaft dynamics of all machines the rows and/or columns of all generator speed states are eliminated in the ABCD matrices of the linearized state equations of the system. The

frequency response(s) $\Delta P_{ei}(j\omega_f)/\Delta V_{ri}(j\omega_f)$ are then calculated over the range of rotor modal frequencies (typically 1.5 to 12 rad/s).

The TF $H_{PSSI_i}(s)$ of a PSS is typically of the form $k_i G_i(s)$. When the transfer functions of the PSS compensation block $G_{ci}(s)$, and the wash-out and low-pass filters, $G_{Wi}(s)$ and $G_{LPi}(s)$ respectively, are added the PSS TF takes the form,

$$H_{PSSI_i}(s) = k_i G_i(s) = k_i G_{ci}(s) \cdot G_{Wi}(s) \cdot G_{LPi}(s). \quad (1)$$

Alternatively, considering the typical forms of the relevant TFs, the PSS TF is

$$H_{PSSI_i}(s) = k_i G_i(s) = k_i \cdot \left[\frac{sT_W}{1+sT_W} \cdot \frac{1}{k_c} \cdot \frac{(1+c_1s+c_2s^2)(1+sT_{a1})\dots}{(1+sT_{b1})\dots(1+sT_1)(1+sT_2)\dots} \right] \quad (2)$$

where, for generator i , T_W is the time constant of the washout filter; $k_c, c_1, c_2, T_{a1}, \dots, T_{b1}, \dots$ are the parameters of the compensation TF $G_{ci}(s)$ determined in the design procedure described below, and T_1, T_2, \dots are the time constants of the low-pass filter. The corner frequencies of the washout and low-pass filters are selected such that the phase shifts introduced at the frequencies of the rotor modes are negligible. The PSS TF must be proper.

Note that, in the context of (2), the gain k_i has been referred to as the ‘*damping gain*’ of the PSS. If the washout filter is ignored the ‘dc’ gain of the PSS TF is k_i/k_c ; *conventionally this is referred to as the ‘PSS Gain’*. However, the PSS gain k_i/k_c has little meaning as k_c is machine and system dependent.

The compensation TF $G_{ci}(s)$ is designed to achieve the desired *left-shift* in the relevant modes of rotor oscillation. The damping gain k_i (on machine base) of the PSS determines the *extent* of the left-shift. The aim of the design procedure is to introduce on the generator shaft a damping torque (a torque proportional to machine speed); this causes the modes of rotor oscillation to be shifted to the left in the s -plane. Thus the ideal TF between speed $\Delta\omega_i$ and the electrical damping torque perturbations ΔP_{ei} due to the PSS over the range of complex frequencies of the rotor modes should be

$$D_{ei} = \Delta P_{ei}(s)/\Delta\omega_i(s)|_{PSSI_i}, \quad (3)$$

where D_{ei} is a damping torque coefficient (e.g. as is k in Figure 2) and - for design purposes - is a real number (p.u. on machine base). The TF $G_{ci}(s)$ compensates in *magnitude as well as phase* for the P-Vr TF $H_{PVri}(s)$ of machine i . With rotor speed being used as the input signal to the PSS, whose output is $\Delta V_{si}(s)$, the expression (3) for D_{ei} can be written:

$$D_{ei} = \frac{\Delta P_{ei}(s)}{\Delta V_{si}(s)} \cdot \frac{\Delta V_{si}(s)}{\Delta \omega_i(s)} = H_{PVri}(s)[k_i G_{ci}(s)]; \quad (4)$$

hence, rearranging (4), we find

$$[k_i G_{ci}(s)] = D_{ei}/(H_{PVri}(s)). \quad (5)$$

It follows from an examination of (5) that $k_i = D_{ei}$ and $G_{ci}(s) = 1/(H_{PVri}(s))$. As in the case of the simplified generator model of Figure 2, the gain k_i of the PSS can thus also be considered to be a damping torque coefficient. The practical, proper TF for the i -th PSS is that of (2), i.e.:

$$[k_i G_i(s)] = k_i \{1/(PVR_i(s))\} \{\text{washout \& low-pass filters}\}$$

where $PVR_i(s)$ is the *synthesized form* of P-Vr characteristic, $H_{PVri}(s)$. As most rotor modes are relatively lightly damped, s can be replaced by $j\omega_f$ and conventional frequency response methods can be employed in the design procedure. In practice, the aim of a design is to ensure that, over the range of frequencies of rotor oscillations, the magnitude response of the RHS of (3) is flat with zero or slightly lagging phase shift. This means that the PSS introduces an almost pure damping torque over the frequency range of the rotor modes. Because of the more-or-less invariant nature of the TF $H_{PVri}(s)$ over a wide range of operating conditions, fixed-parameter PSSs tend to be robust [5].

Note that speed appears to be the ideal stabilizing signal because the damping torque induced on the shaft of the generator by the associated PSS is related to speed through a simple gain. Moreover, this gain being a damping torque coefficient has practical significance, e.g. a damping gain k_i of 20 pu on machine rating can typically be considered a moderate gain setting for a speed-PSS. A practical form of the “speed-PSS” is the “Integral-of-accelerating-power PSS” for which the design procedure outlined above is applicable.

The approach to the design of speed-PSSs can be adapted to the design of power-input PSSs. If the perturbations in mechanical power are negligible over the frequency range of interest the equation of motion of the unit’s shaft can be written $\Delta\omega(s) = -\Delta P_{ei}(s)/(2Hs)$ [13]; $\Delta\omega$ is then the input to the speed-PSS.

7 The P-Vr characteristics of the 14 generators and the associated synthesized characteristics

For each of the generators the P-Vr characteristics are determined for the six power flow cases as shown in Figure 3 to Figure 16. These characteristics were calculated using Mudpack, a software package for the analysis of the small-signal dynamic performance and control of large power systems [14].

It should be noted in this analysis that the operating conditions on which the load flows, and therefore the P-Vr characteristics, are based are normal operating conditions. In practice, the P-Vr characteristics for a relevant set of contingency conditions are also considered when determining the synthesized characteristic.

The synthesized P-V_r characteristic for each generator is derived based on the following:

- The modal frequency range of interest is 1.5 to 12 rad/s.
- The synthesized characteristic is a best fit of the P-V_r characteristics for the range of cases examined over the modal frequency range 1.5 to 12 rad/s. The ‘best fit’ characteristic is considered to be that characteristic which lies in the middle of the magnitude and phase bands formed by the P-V_r characteristics. If particular P-V_r characteristics tend lie outside the bands formed by the majority of the characteristics, the synthesized P-V_r is offset towards the band formed by the majority (e.g. see [Figure 12](#)).
- Less phase lead at the inter-area model frequencies may be required than that provided by the synthesized TF based on P-V_r characteristic [\[11\]](#). It can be accommodated by a gain-lag-lead transfer function block or by adjusting the synthesized transfer function at the inter-area frequencies. This feature has the effect of increasing the damping of the inter-area modes, however, it is not incorporated in following analysis.

The P-V_r characteristics for the 14 generators, shown in [Figure 3](#) to [Figure 16](#), are in per unit on the machine rating given in [Table 8](#).

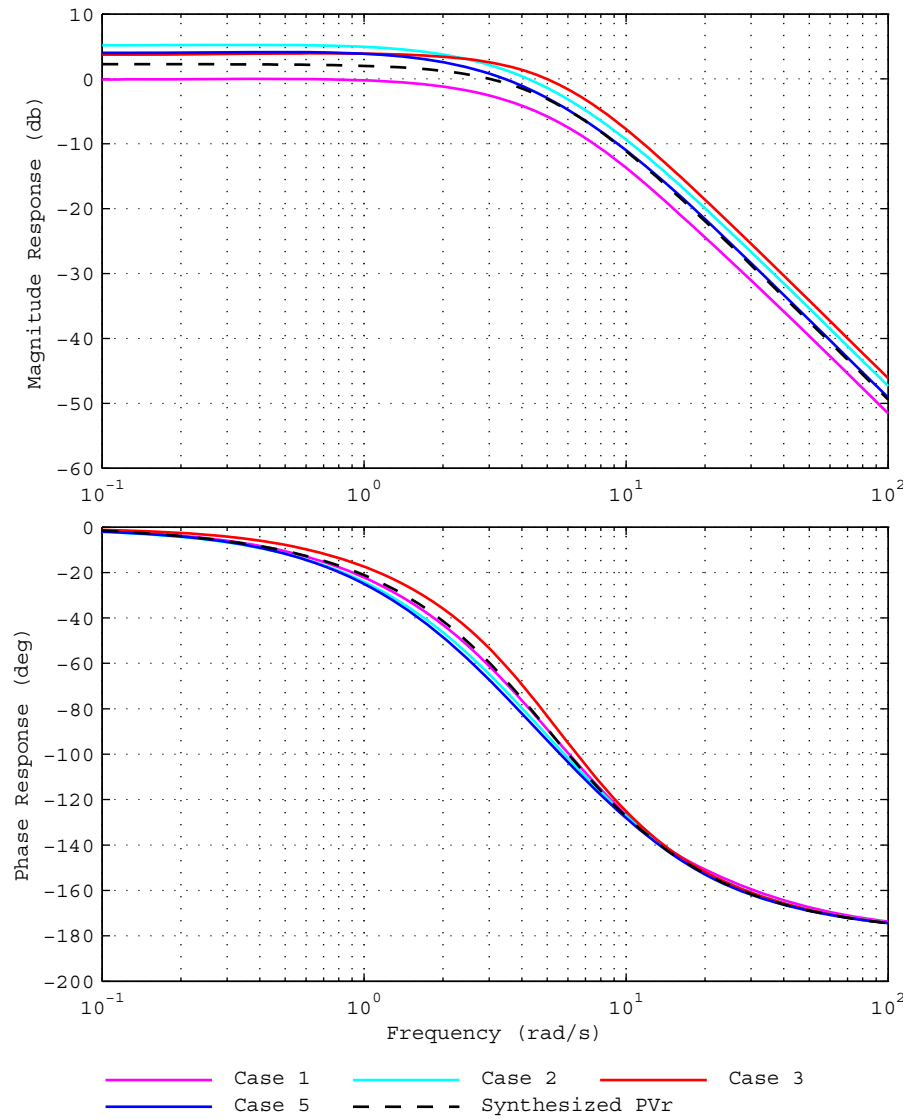


Figure 3 P-Vr characteristics, calculated and synthesized ($PVR(s)$), for generator HPS_1.
(In cases 4 & 6 the PSS is switched off as it is operating as a synchronous compensator.)

$$PVR(s) = 1.3/(1 + s0.373 + s^2 0.0385)$$

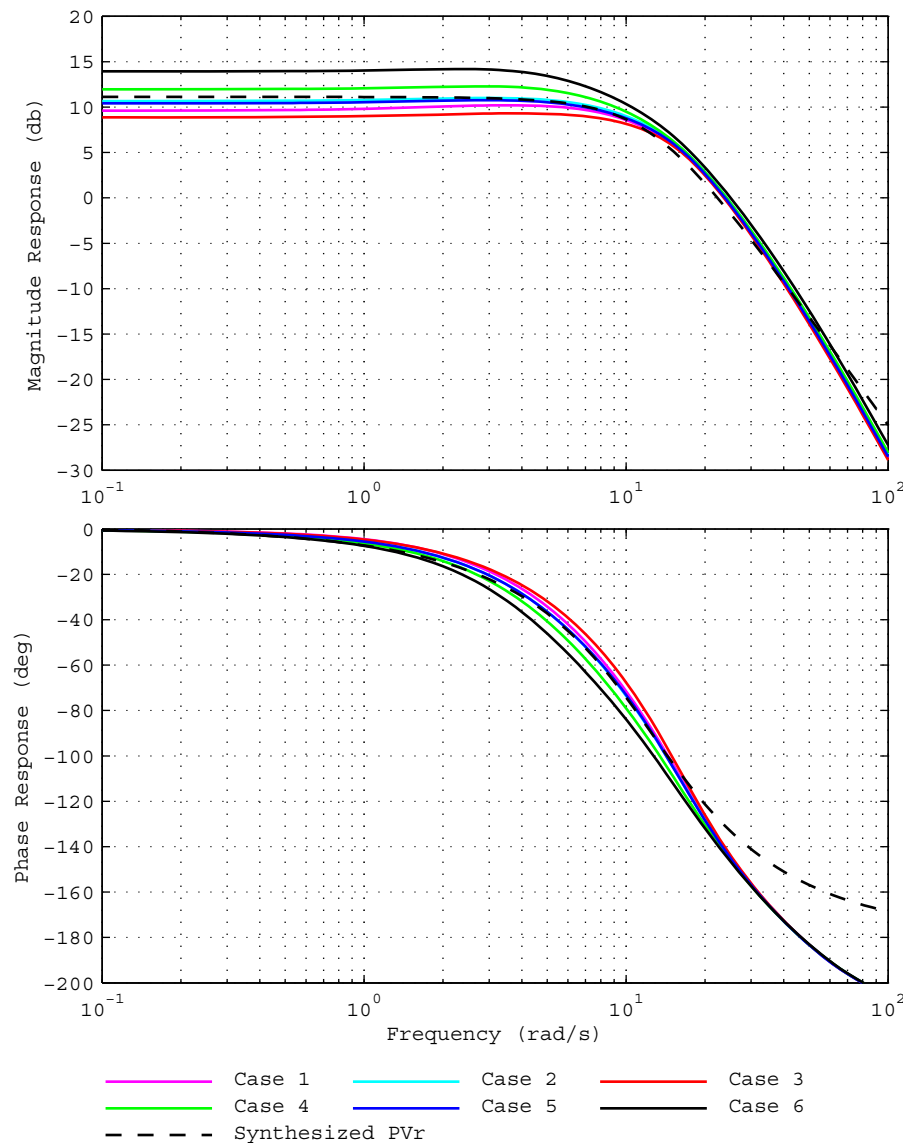


Figure 4 P-Vr characteristics, calculated and synthesized ($PVR(s)$), for generator BPS_2.

$$PVR(s) = 3.6/(1 + s0.128 + s^2 0.0064)$$

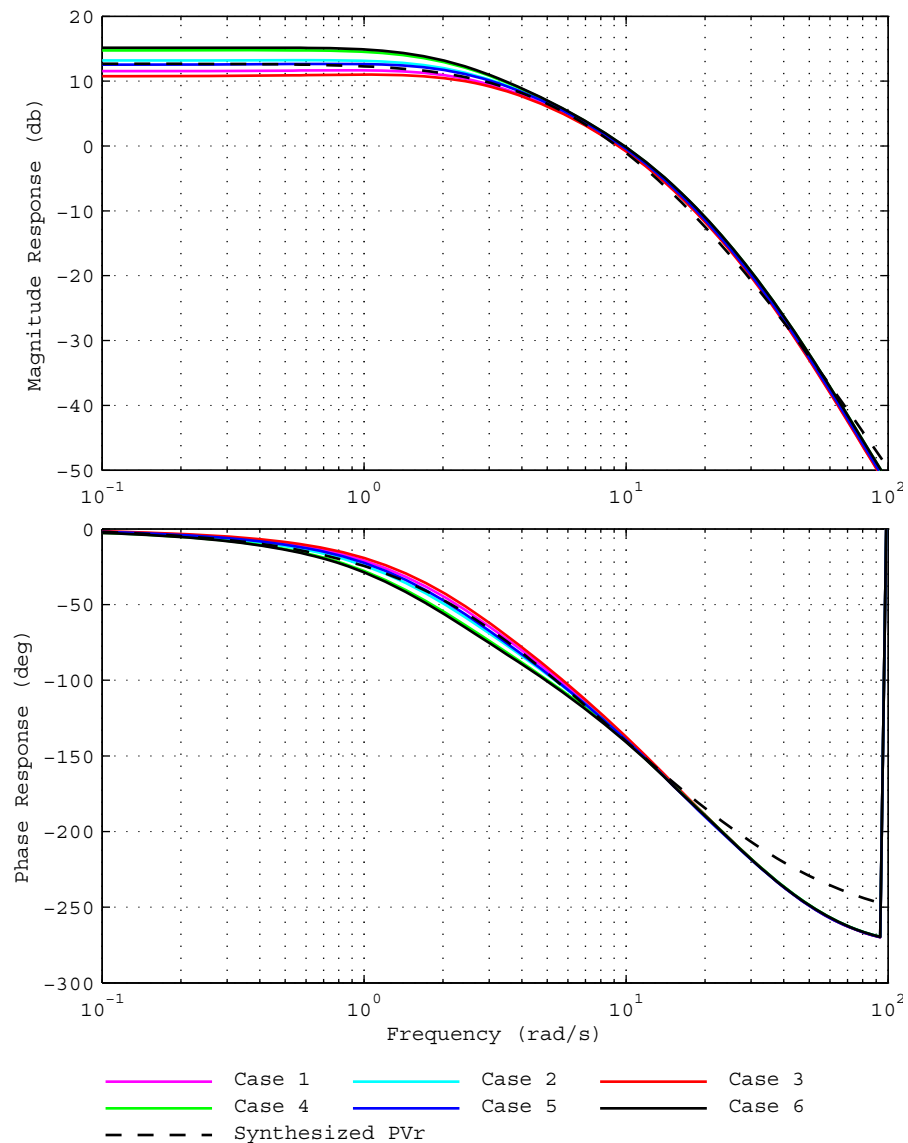


Figure 5 P-Vr characteristics, calculated and synthesized ($PVR(s)$), for generator EPS_2.

$$PVR(s) = 4.3 / [(1 + s0.286)(1 + s0.111)(1 + s0.040)]$$

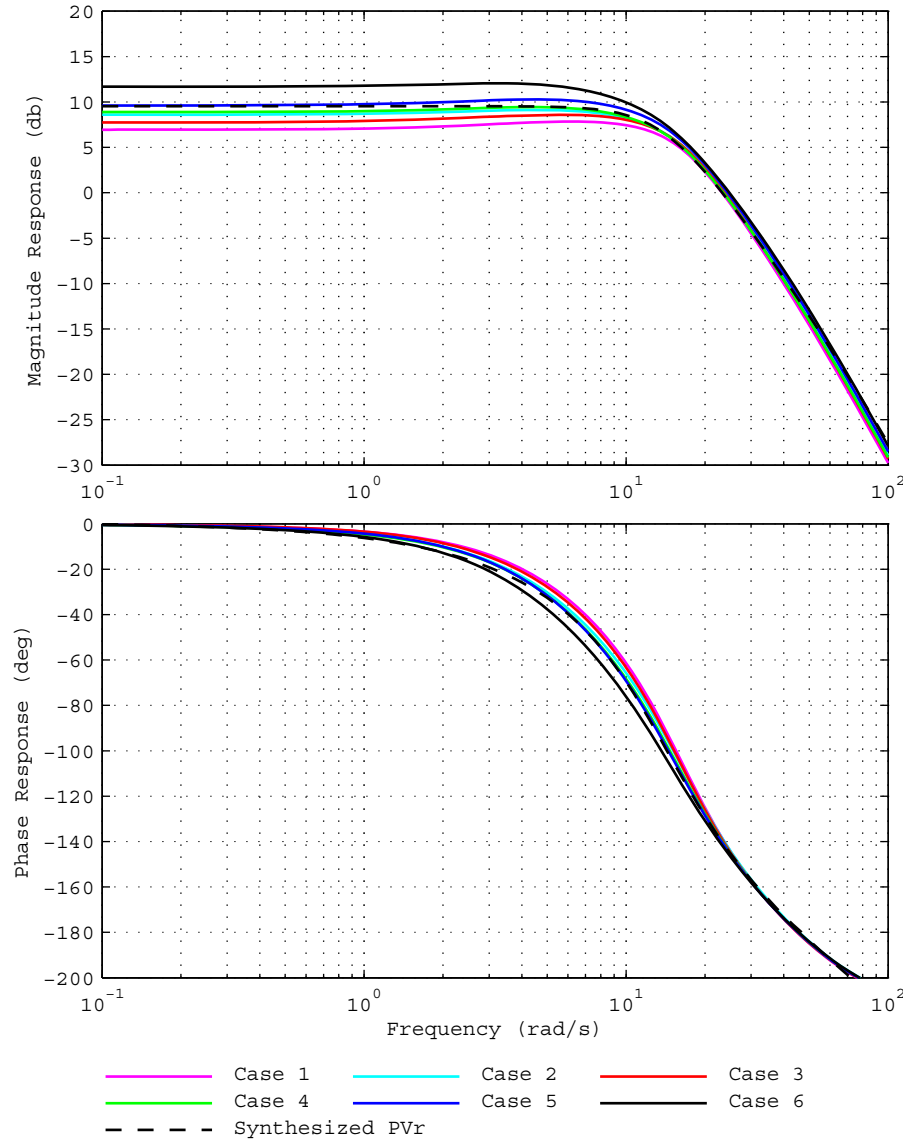


Figure 6 P-V_r characteristics, calculated and synthesized ($PVR(s)$), for generator MPS_2.

$$PVR(s) = 3.0 / [(1 + s0.01)(1 + s0.1 + s^20.0051)]$$

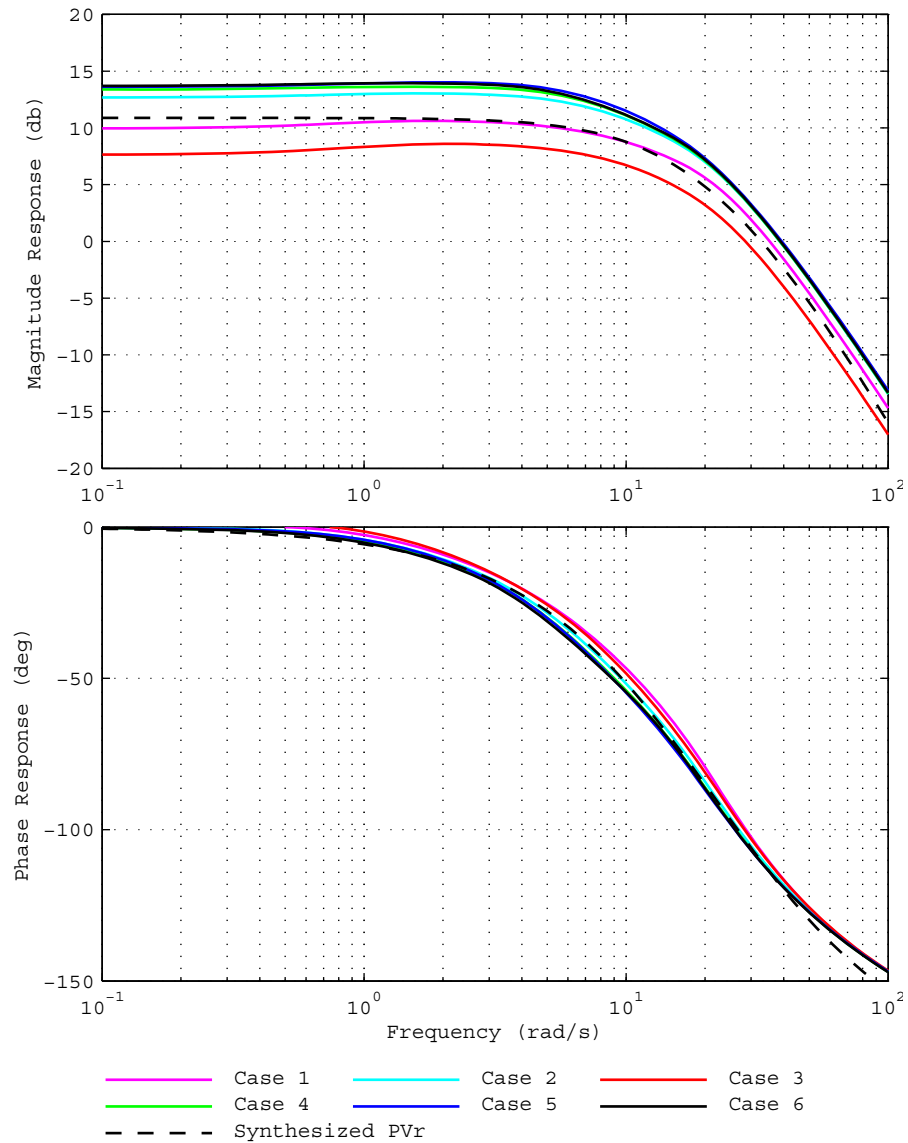


Figure 7 P-Vr characteristics, calculated and synthesized ($PVR(s)$), for generator VPS_2.

$$PVR(s) = 3.5 / [(1 + s0.0292)(1 + s0.0708)]$$

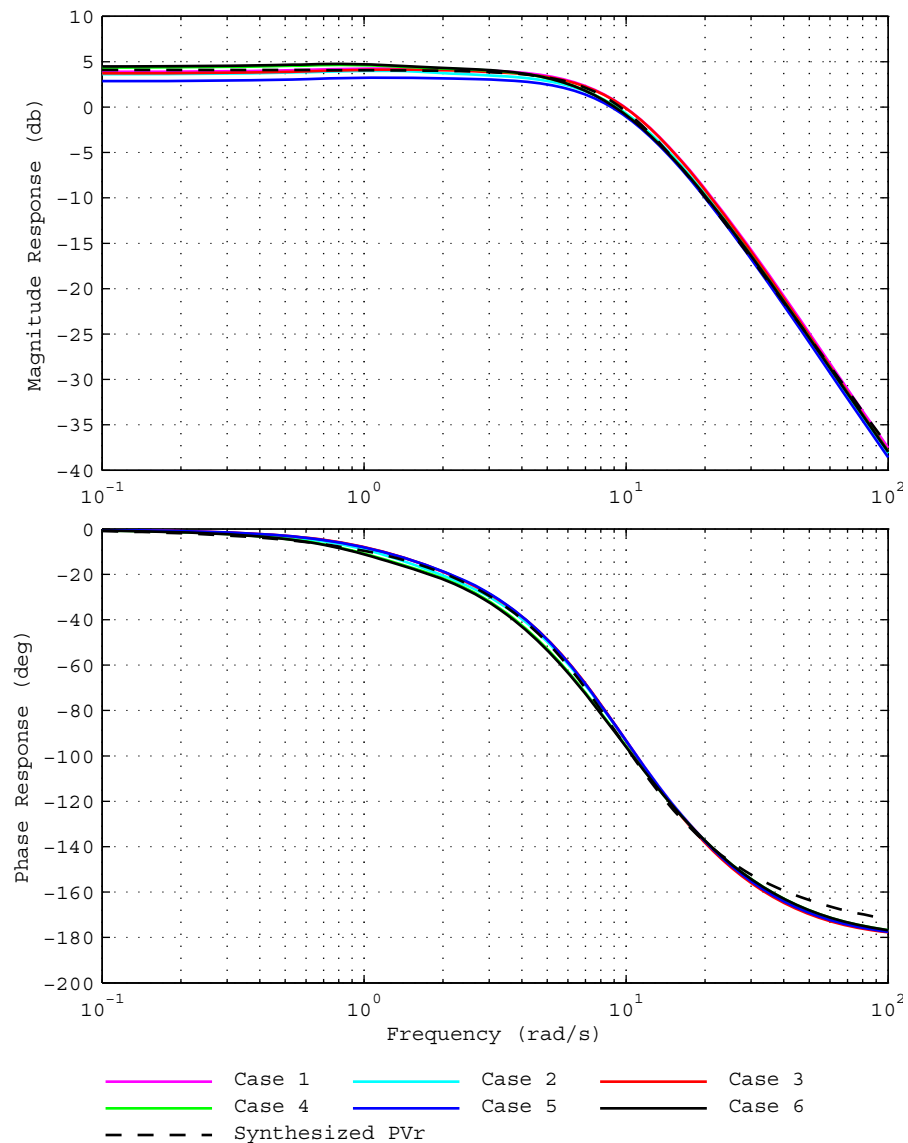


Figure 8 P-Vr characteristics, calculated and synthesized ($PVR(s)$), for generator LPS_3.

$$PVR(s) = 1.6/(1 + s0.168 + s^2 0.0118)$$

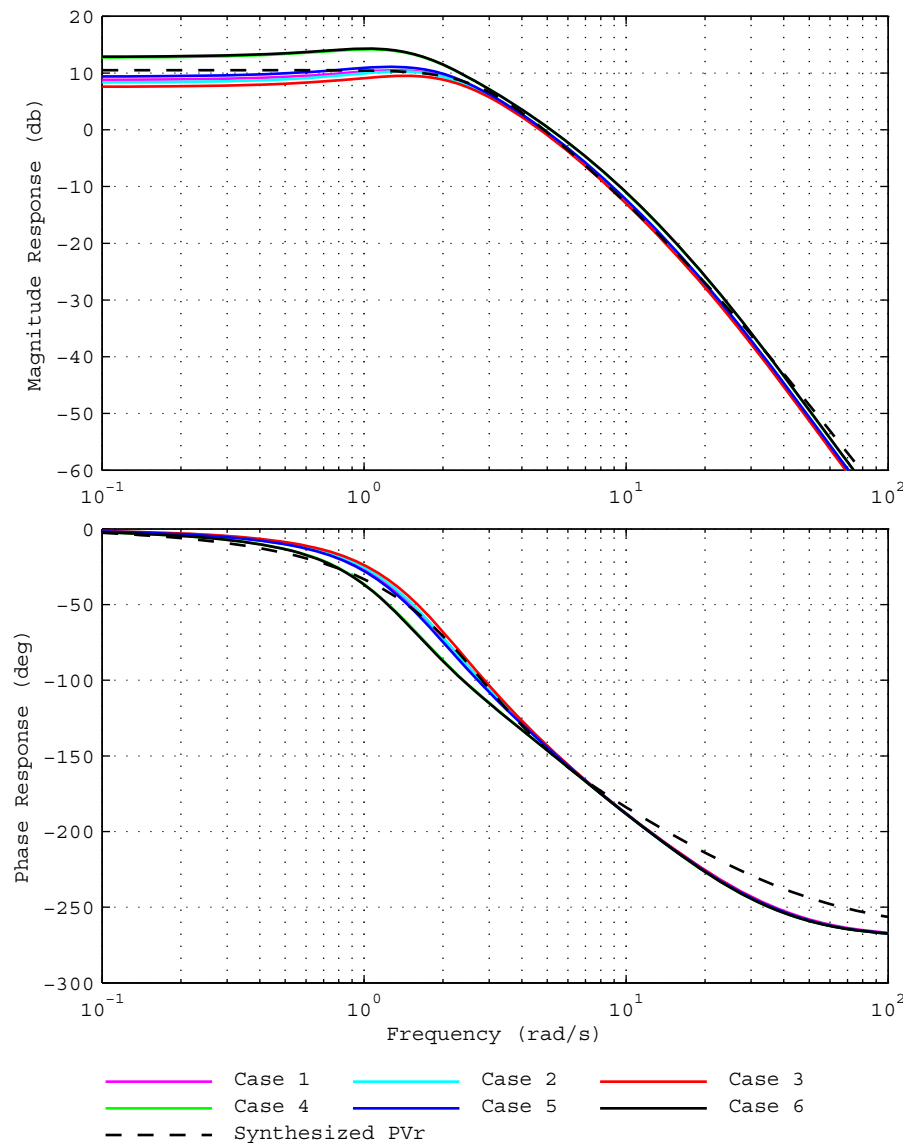


Figure 9 P-Vr characteristics, calculated and synthesized ($PVR(s)$), for generator YPS_3

$$PVR(s) = 3.35 / [(1 + s0.05)(1 + s0.509 + s^20.132)]$$

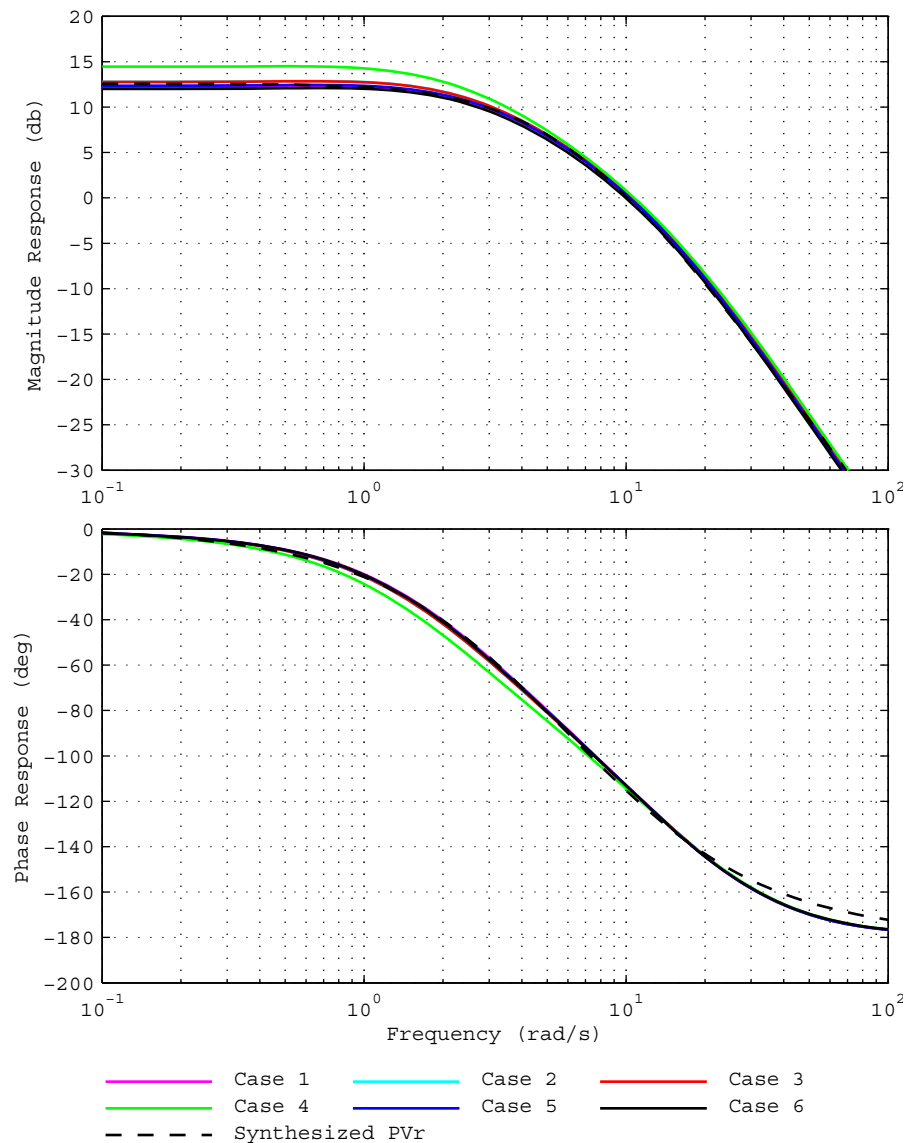


Figure 10 P-Vr characteristics, calculated and synthesized ($PVR(s)$), for generator CPS_4.

$$PVR(s) = 4.25 / [(1 + s0.278)(1 + s0.100)]$$

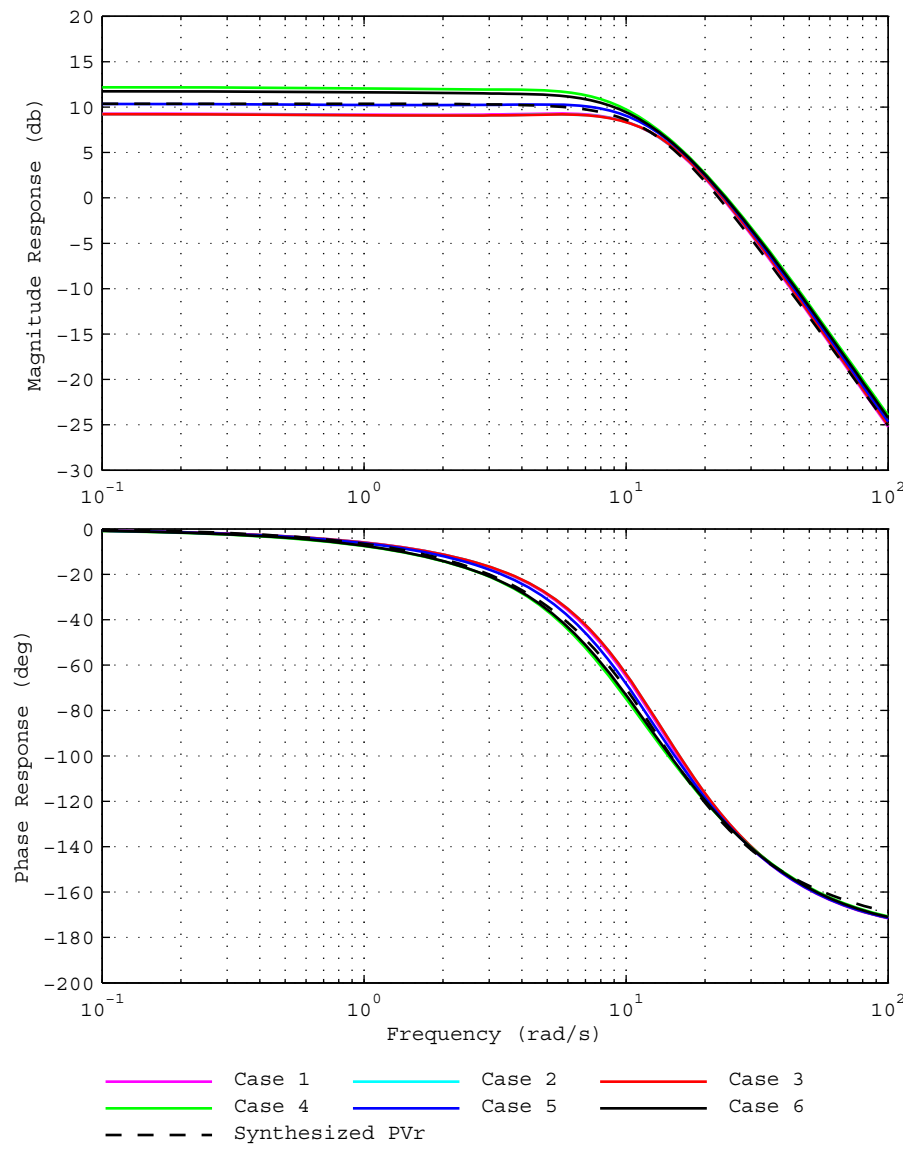


Figure 11 P-Vr characteristics, calculated and synthesized ($PVR(s)$), for generator GPS_4.

$$PVR(s) = \frac{3.3}{(1 + s0.115 + s^2 0.00592)}$$

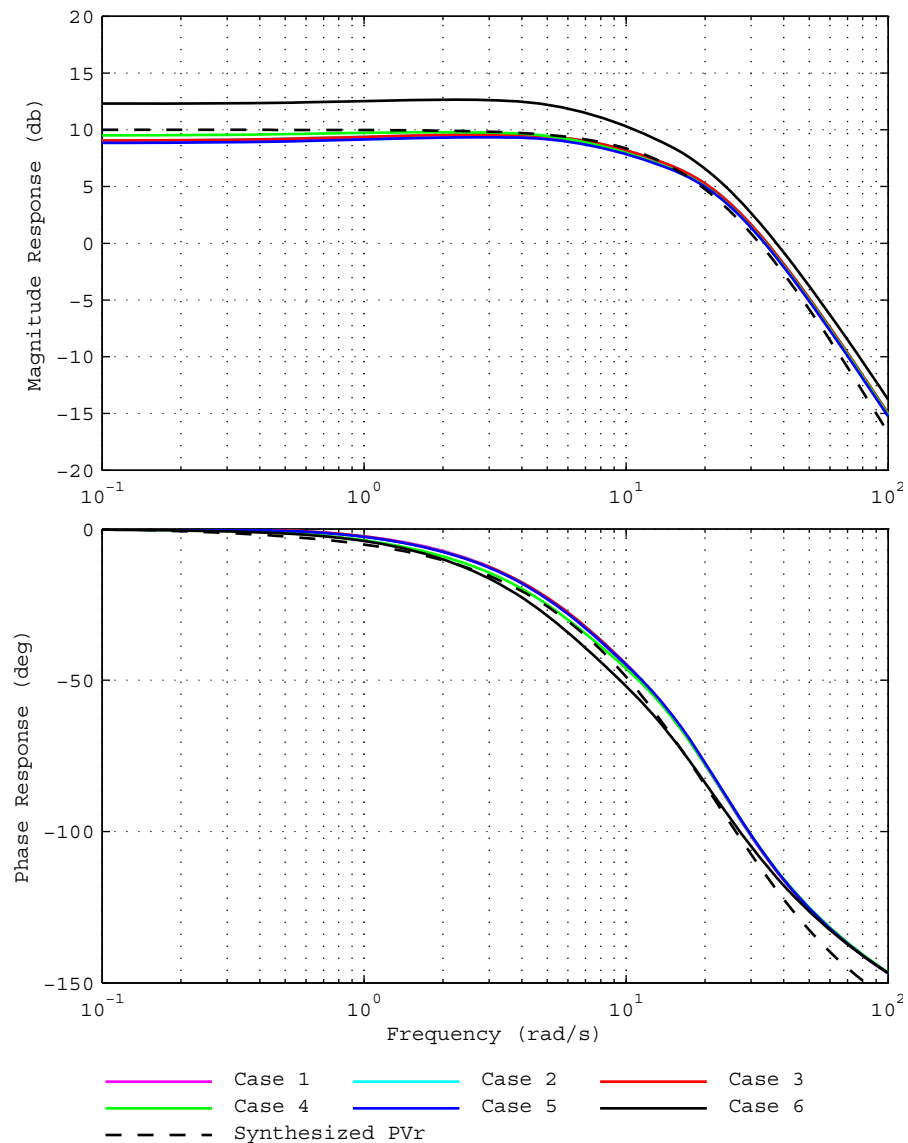


Figure 12 P-Vr characteristics, calculated and synthesized ($PVR(s)$), for generator SPS_4.
The synthesized P-Vr characteristic is weighted towards those of Cases 1 to 5.

$$PVR(s) = 3.16 / (1 + s0.0909 + s^2 0.00207)$$

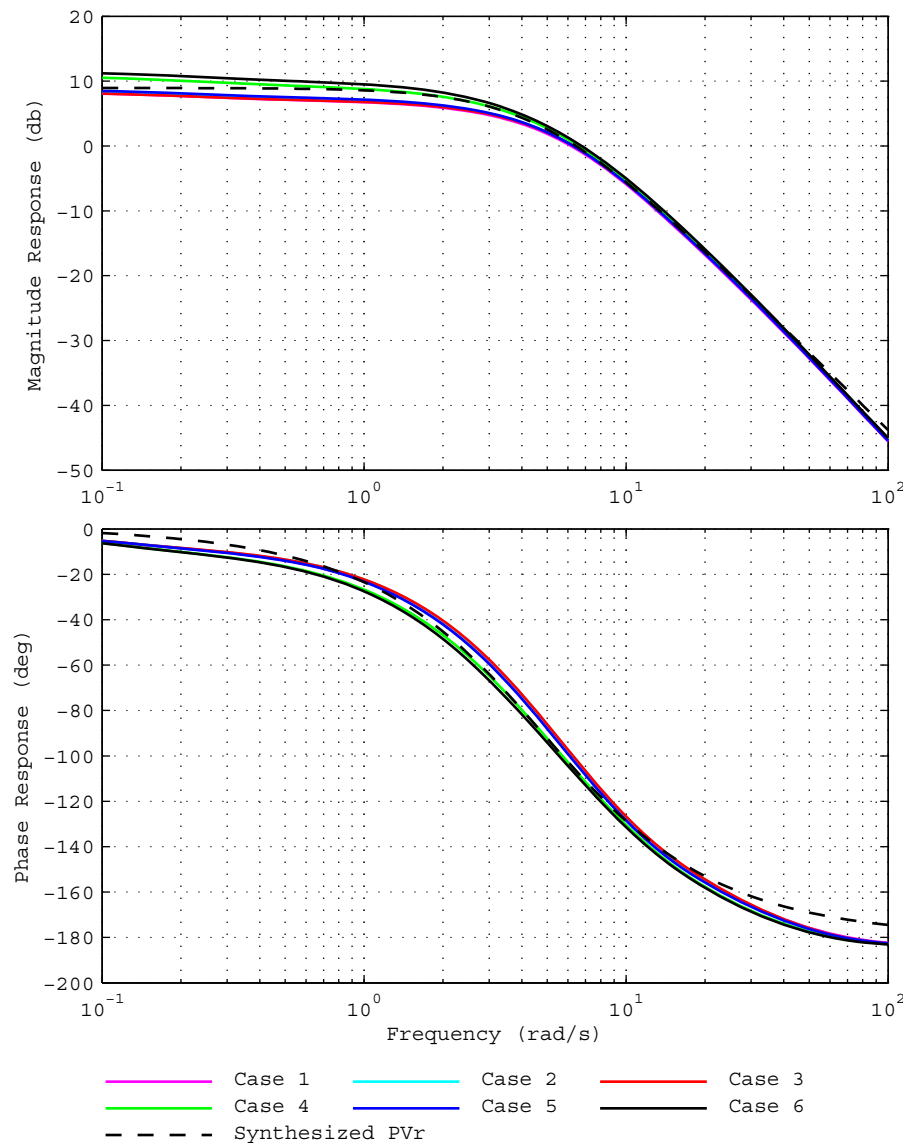


Figure 13 P-Vr characteristics, calculated and synthesized ($PVR(s)$), for generator TPS_4.

$$PVR(s) = 2.8 / [(1 + s0.208)(1 + s0.208)]$$

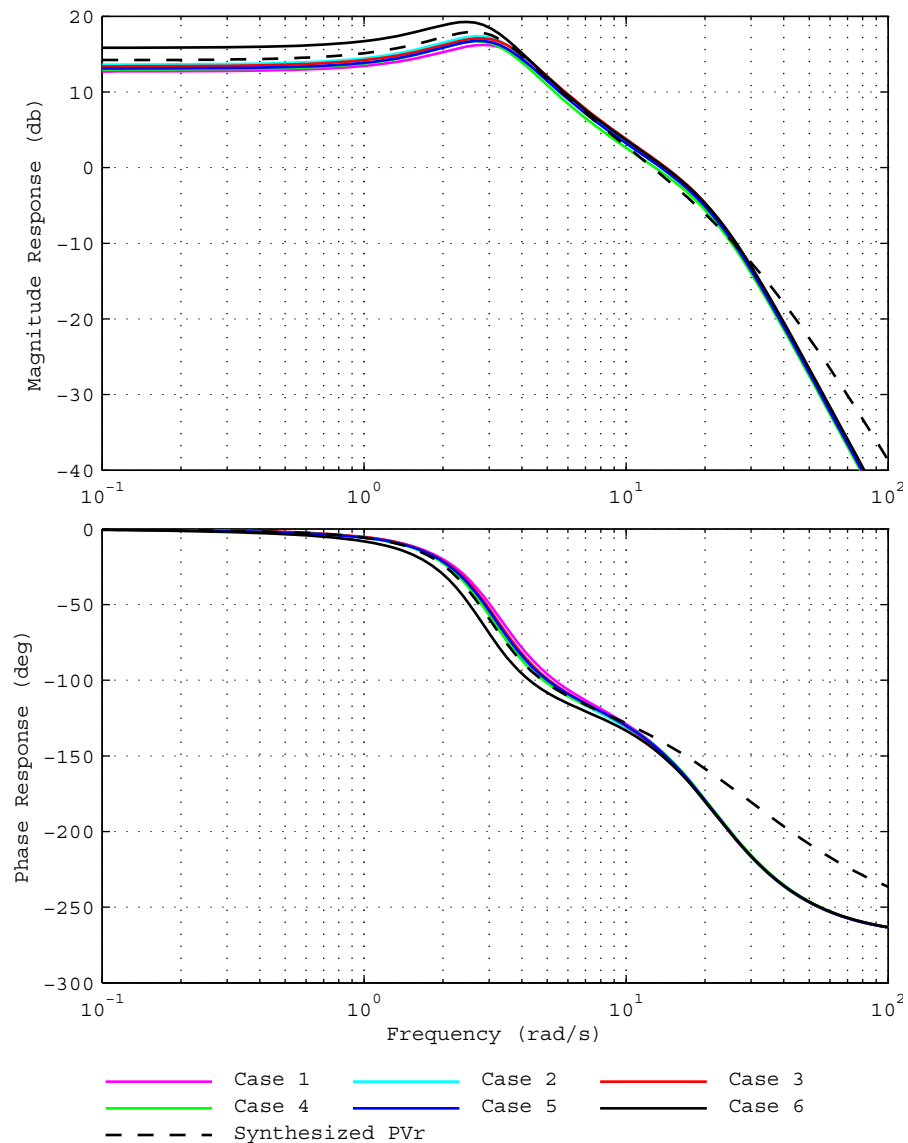


Figure 14 P-Vr characteristics, calculated and synthesized ($PVR(s)$), for generator NPS_5.

$$PVR(s) = 5.13(1 + s0.300)/[(1 + s0.033)^2(1 + s0.300 + s^20.111)]$$

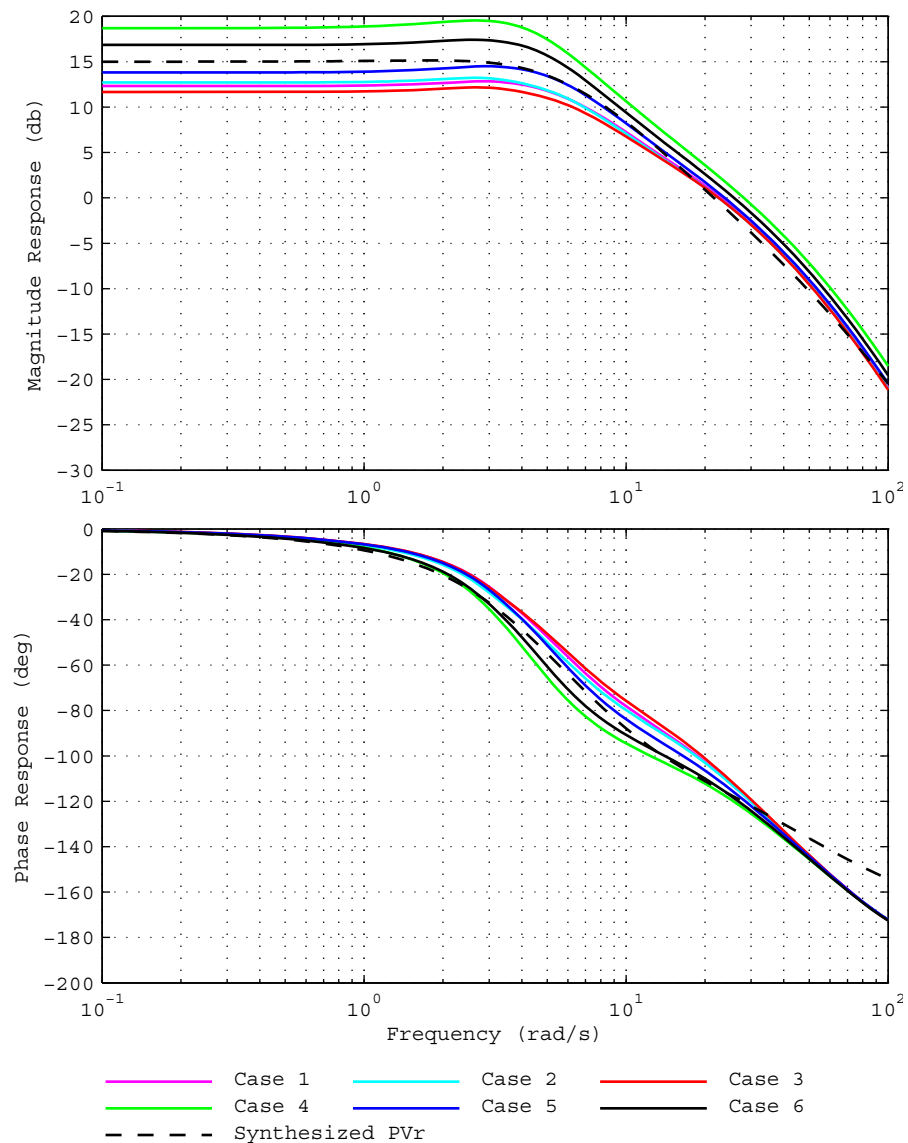


Figure 15 P-Vr characteristics, calculated and synthesized ($PVR(s)$), for generator PPS_5.

$$PVR(s) = \frac{5.62(1 + s0.350)(1 + s0.0667)}{(1 + s0.020)(1 + s0.167)(1 + s0.187)(1 + s0.200)}$$

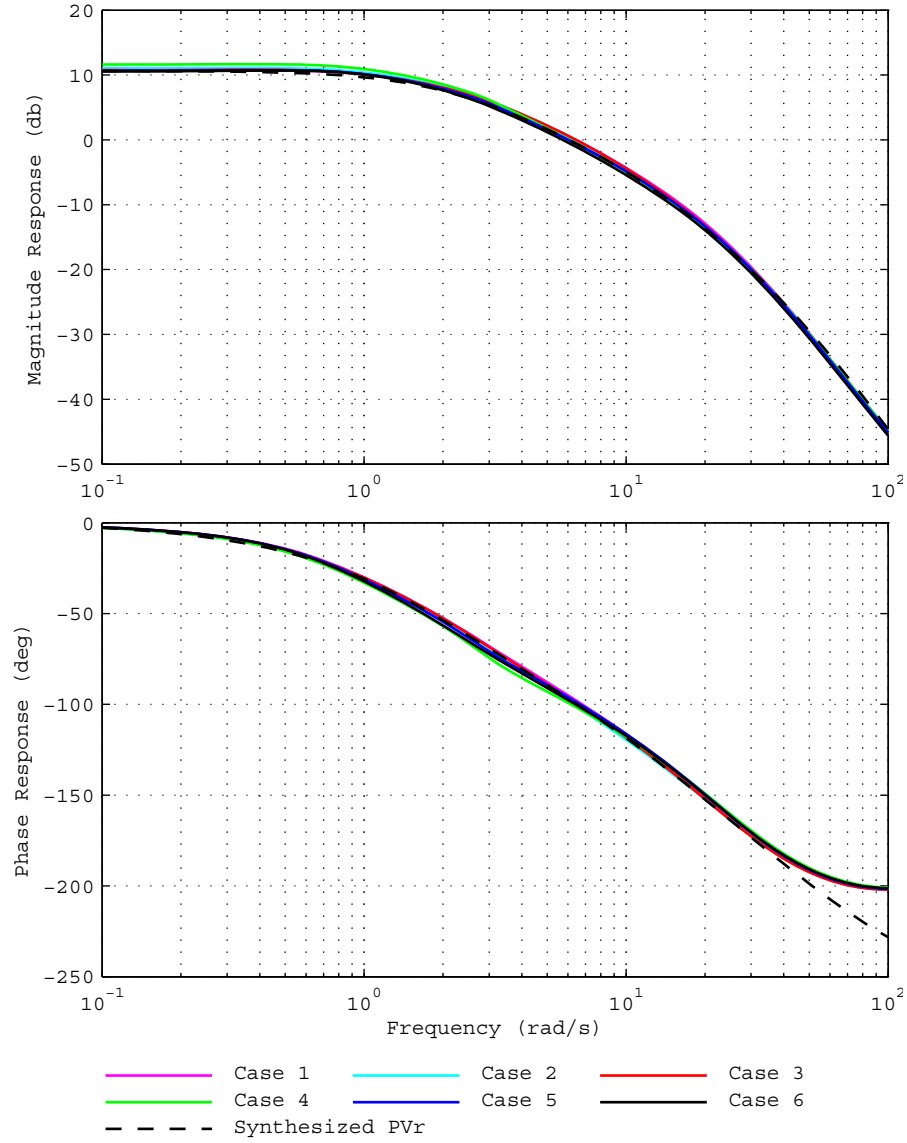


Figure 16 P-Vr characteristics, calculated and synthesized ($PVR(s)$) , for generator TPS_5.

$$PVR(s) = 3.4 / [(1 + s0.500)(1 + s0.0588)(1 + s0.0167)]$$

8 Results of small-signal analysis for the six cases

Please note the Caveats listed in [Section 2](#) before interpreting these results.

For each of the six cases the rotor modes of oscillation without and with all PSSs in service are listed in [Table 2](#) to [Table 7](#).

In [Figure 17](#) is shown the plot of the electro-mechanical modes for Case 1 as the PSS damping gains on all generators are increased from zero (no PSSs in service) to 30 pu in 5 pu steps. Note that the modes shift more or less directly into the left-half of the s -plane. Without the special compensation referred to in [Section 7](#) for the inter-area modes, the frequencies of the inter-area modes tend to decrease relatively more than the local-area modes due to the effects of interactions [6], [11]; the damping of the inter-area modes is also poorer.

Table 2 Rotor modes. Case 1: PSSs out and in service. (Damping gains 20pu on rating)

Case1: No PSSs			Case 1: All PSS in service		
Real	Imag	Damping Ratio	Real	Imag	Damping Ratio
-0.175	10.442	0.017	-2.193	10.386	0.207
0.109	9.583	-0.011	-1.978	9.742	0.199
0.041	8.959	-0.005	-1.926	9.293	0.203
-0.557	8.634	0.064	-2.505	8.858	0.272
-0.260	8.368	0.031	-1.953	8.261	0.230
-0.612	8.047	0.076	-1.971	8.490	0.226
-0.439	7.965	0.055	-1.875	7.756	0.235
0.014	7.812	-0.002	-1.777	7.643	0.226
-0.189	7.724	0.024	-2.061	7.872	0.253
-0.617	7.425	0.083	-1.878	7.588	0.240
0.115	3.970	-0.029	-1.044	3.640	0.276
0.088	2.601	-0.034	-0.385	2.402	0.158
-0.016	2.028	0.008	-0.522	1.798	0.279

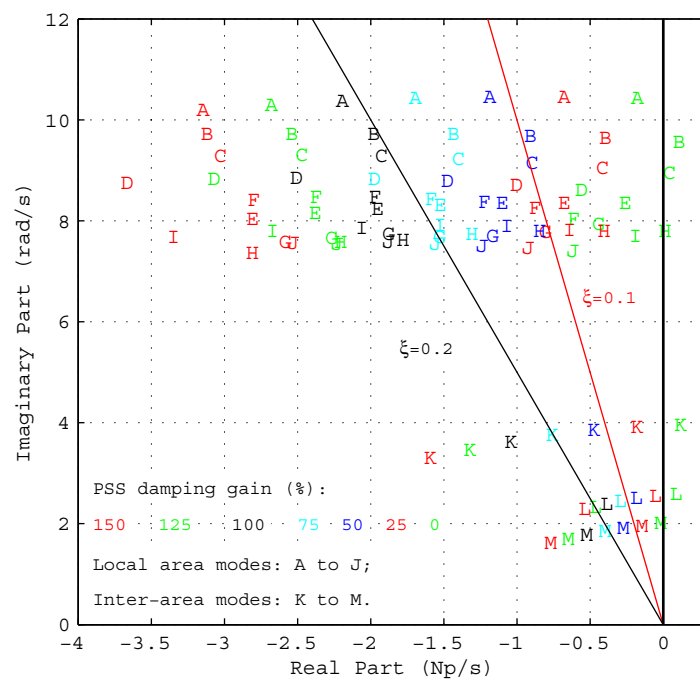


Figure 17 Rotor modes for Case 1 as the PSS damping gain on each generator is increased from zero (no PSSs in service) to 30 pu (150%) in 5 pu (25%) steps.
(100% gain is equivalent to PSS damping gain $D_e=20$ pu on machine base)

Table 3 Rotor modes. Case 2: PSSs out and in service. (Damping gains 20pu on rating)

Case 2: No PSSs			Case 2: All PSS in service		
Real	Imag	Damping Ratio	Real	Imag	Damping Ratio
0.066	10.743	-0.006	-2.403	10.964	0.214
0.101	9.563	-0.011	-2.038	9.725	0.205
-0.250	9.261	0.027	-2.370	9.644	0.239
-0.922	8.613	0.106	-2.805	8.962	0.299
-0.534	8.669	0.062	-2.494	8.936	0.269
-0.184	8.482	0.022	-2.039	8.379	0.236
-0.700	8.293	0.084	-2.442	8.370	0.280
-0.208	7.929	0.026	-2.029	7.739	0.254
-0.065	7.385	0.009	-2.021	7.490	0.261
-0.485	7.570	0.064	-1.814	7.772	0.227
0.193	3.772	-0.051	-0.769	3.537	0.212
0.054	2.863	-0.019	-0.447	2.542	0.173
0.081	1.915	-0.042	-0.431	1.759	0.238

Table 4 Rotor modes. Case 3: PSSs out and in service. (Damping gains 20pu on rating)

Case 3: No PSSs			Case 3: All PSS in service		
Real	Imag	Damping Ratio	Real	Imag	Damping Ratio
-0.377	11.109	0.034	-1.909	11.244	0.167
0.101	9.563	-0.011	-2.037	9.724	0.205
-0.301	9.019	0.033	-2.278	9.100	0.243
-0.583	8.660	0.067	-2.519	8.914	0.272
-0.182	8.476	0.021	-2.025	8.376	0.235
-0.140	8.256	0.017	-1.948	8.492	0.224
-0.191	7.909	0.024	-2.011	7.727	0.252
-0.076	7.381	0.010	-1.932	7.535	0.248
-0.576	7.625	0.075	-1.933	7.800	0.241
-0.131	6.314	0.021	-2.030	5.909	0.325
0.011	4.076	-0.003	-1.119	3.707	0.289
0.020	2.670	-0.007	-0.428	2.418	0.174
-0.032	2.050	0.015	-0.580	1.860	0.298

Table 5 Rotor modes. Case 4: PSSs out and in service. (Damping gains 20pu on rating)

Case 4: No PSSs			Case 4: All PSS in service . [†]		
Real	Imag	Damping Ratio	Real	Imag	Damping Ratio
0.197	10.484	-0.019	-2.374	10.774	0.215
0.030	9.665	-0.003	-2.163	9.951	0.212
-0.173	9.369	0.018	-2.269	9.813	0.225
-1.541	8.276	0.183	-1.695	8.169	0.203
-0.178	8.779	0.020	-2.272	8.793	0.250
-0.561	8.581	0.065	-2.496	9.064	0.266
-0.211	8.278	0.025	-2.554	8.445	0.289
-0.508	8.522	0.060	-2.492	8.826	0.272
-0.431	8.211	0.052	-2.280	8.279	0.265
-0.190	7.200	0.026	-1.319	7.494	0.173
0.165	4.743	-0.035	-1.080	4.581	0.229
0.023	3.573	-0.007	-0.563	3.322	0.167
-0.009	2.678	0.003	-0.589	2.513	0.228

..[†] PSS of HPS_1 is OFF as it operates as a synchronous compensator in this case

Table 6 Rotor modes. Case 5: PSSs out and in service. (Damping gains 20pu on rating)

Case 5: No PSSs			Case 5: All PSS in service		
Real	Imag	Damping Ratio	Real	Imag	Damping Ratio
0.181	10.940	-0.017	-2.409	11.257	0.209
0.086	9.570	-0.009	-1.988	9.762	0.200
-0.163	9.171	0.018	-2.093	9.395	0.217
-0.182	8.696	0.021	-2.187	9.119	0.233
-0.496	8.554	0.058	-2.471	8.828	0.270
-0.263	8.452	0.031	-2.024	8.382	0.235
-0.524	7.975	0.066	-2.382	7.969	0.286
0.008	7.896	0.000	-1.853	7.809	0.231
-0.157	7.736	0.020	-2.116	7.865	0.260
-0.765	7.241	0.105	-1.858	7.449	0.242
0.191	4.152	-0.046	-0.884	3.902	0.221
0.006	3.122	-0.002	-0.457	2.889	0.156
0.059	2.154	-0.027	-0.497	1.957	0.246

Table 7 Rotor modes. Case 6: PSSs out and in service. (Damping gains 20pu on rating)

Case 6: No PSSs			Case 6: All PSS in service ... [†]		
Real	Imag	Damping Ratio	Real	Imag	Damping Ratio
0.276	10.390	-0.027	-2.217	10.708	0.203
0.318	10.138	-0.031	-2.142	10.652	0.197
-0.129	9.423	0.014	-2.069	10.017	0.202
-0.233	8.920	0.026	-2.522	9.541	0.256
-0.455	8.738	0.052	-2.381	9.023	0.255
-0.136	8.578	0.016	-2.320	8.506	0.263
-0.213	8.285	0.026	-2.579	8.453	0.292
-1.507	8.237	0.180	-1.701	8.168	0.204
-0.301	8.128	0.037	-2.076	8.242	0.244
-0.359	7.250	0.049	-1.598	7.553	0.207
0.200	4.810	-0.041	-1.078	4.644	0.226
0.054	3.552	-0.015	-0.565	3.298	0.169
0.036	2.597	-0.014	-0.520	2.451	0.207

...[†] PSS of HPS_1 is OFF as it operates as a synchronous compensator in this case.

9 Transient stability analysis

A large-signal model of the system has been developed to allow transient stability analysis. The data for the large-signal model is presented in [Appendix II](#) in a format amenable to use with the PSS[®]/E transient-stability program. Since, at this stage, the model does not include representation of the generator turbine / governing systems this large signal is unsuitable for analysing loss of generation / load events.

The small-disturbance performance of the PSS[®]/E implementation of the simplified 14-generator model has been thoroughly benchmarked with the original Mudpack implementation of the model in [Appendix III](#). With appropriate setting of PSS[®]/E simulation parameters there is close agreement between the respective simulation packages.

A comprehensive set of transient stability studies are conducted in [Appendix IV](#). It is found that the system is transiently stable for a comprehensive set of two-phase to ground faults across all six base case scenarios. (Note that in accord with the Australian National Electricity Rules [18] two-phase to ground faults are considered to be the most severe *credible* contingency for voltages at and above 220 kV; the risk of solid three-phase to ground faults is, except under extraordinary circumstances, considered to be so low to be non-credible.)

10 Acknowledgements

The authors are most grateful for advice and assistance of Dr. Leonardo Lima in their development of the PSS[®]/E dynamics data set for the model. Some of the ideas on data presentation contained in his draft report have been employed in this report.

During the development of this and earlier versions of the 14-generator model of the Australian system we have been grateful for the opportunity to collaborate with Prof. Rodrigo Ramos and some of his students, particularly Dr. Rodrigo Salim, in their benchmarking of our model with the PacDyn software package.

We thank researchers who have identified errors or unrealistic parameter values in the model. We endeavour to address such matters, at least by notifying users of the deficiencies in reports such as this and, hopefully, over time correcting the model data and associated results.

11 References

- [1] *PSS[®]/E Version 32, Program Operation Manual*: Siemens, June 2009.
Siemens-PTI PSS[®]/E web address:
<http://w3.usa.siemens.com/smartgrid/us/en/transmission-grid/products/grid-analysis-tools/transmission-system-planning/Pages/transmission-system-planning.aspx>
- [2] Gibbard, M.J. "Coordinated design of multi-machine power system stabilisers based on damping torque concepts". Proceedings IEE, Pt.C, Vol.135, July 1988, pp.276-284.
- [3] Gibbard, M.J. "Robust design of fixed-parameter power system stabilisers over a wide range of operating conditions". IEEE Transactions on Power Systems, Vol. 6, No. 2, May 1991, pp 794-800.
- [4] Pourbeik, P. and Gibbard, M.J., "Damping and synchronising torques induced on generators by FACTS stabilizers in multi-machine power systems", IEEE Transactions on Power Systems, Vol. 11, no. 4, Nov. 1996, pp. 1920-1925.
- [5] Pourbeik, P. and Gibbard, M.J., "Simultaneous coordination of Power-System Stabilizers and FACTS device stabilizers in a multi-machine power system for enhancing dynamic performance", IEEE Transactions on Power Systems, Vol. 13, no. 2, May 1998, pp. 473-479.
- [6] Gibbard, M.J., Vowles, D.J. and Pourbeik, P., "Interactions between, and effectiveness of, power system stabilizers and FACTS stabilizers in multi-machine systems", IEEE Transactions on Power Systems, Vol. 15, no. 2, May 2000, pp. 748-755. (In February 2001 this paper received the Prize Paper Award for 2000 from the Power System Dynamic Performance Committee of the IEEE PES.)
- [7] CIGRE Technical Brochure no. 166 prepared by Task Force 38.02.16, "Impact of Interactions among Power System Controls", published by CIGRE in August 2000.
- [8] Gibbard, M.J. and Vowles, D.J., "Discussion of 'The application of Power System Stabilizers to multi-generator plant", IEEE Transactions on Power Systems. Vol. 15, no. 4, Nov. 2000, pp. 1462-1464.
- [9] Gibbard, M.J., Martins, N., Sanchez-Gasca, J.J., Uchida, N., Vittal, V. and Wang, L., "Recent Applications in Linear Analysis Techniques", IEEE Transactions on Power Systems. Vol. 16, no. 1, Feb. 2001, pp. 154-162.
- [10] Pourbeik, P., Gibbard, M.J. and Vowles, D.J., "Proof of the equivalence of residues and induced torque coefficients for use in the calculation of eigenvalue shifts", IEEE Power Engineering Review, Power Engineering Letters, Vol. 22, no.1, Jan. 2002, pp. 58-60.
- [11] Gibbard, M.J. and Vowles, D.J., "Reconciliation of methods of compensation for PSSs in multimachine systems", IEEE Transactions on Power Systems. Vol. 19, no. 1, Feb. 2004, pp. 463-472.
- [12] E.V. Larsen and D.A. Swann, "Applying power system stabilizers: Part I - III", IEEE Transactions PAS, Vol. 100, pp. 3017-3046, 1981.

- [13] P. Kundur, *Power System Stability and Control*, McGraw-Hill, Inc., 1994.
- [14] Vowles, D.J. and Gibbard, M.J., “Mudpack - a software package for the analysis of the small-signal dynamic performance and control of large electric power systems”, School of Electrical & Electronic Engineering, The University of Adelaide, South Australia.
- [15] IEEE Committee Report, “Static VAr compensator models for power flow and dynamic performance simulation,” *Power Systems, IEEE Transactions on*, vol. 9, pp. 229-240, 1994.
- [16] IEEE Recommended Practice for Excitation System Models for Power System Stability Studies, IEEE Standard No:421.5-2005, ISBN:0-7381-4787-7.
- [17] IEEE Committee Report, “Excitation System Models for Power System Stability Studies,” *Power Apparatus and Systems, IEEE Transactions on*, vol. PAS-100, pp. 494-509, 1981.
- [18] [Australian] *National Electricity Rules, Version 60*.
Available: <http://www.aemc.gov.au/Electricity/National-Electricity-Rules/Current-Rules.html>

Appendix I Data

Please note the Caveats listed in [Section 2](#) before using this data.

I.1 Steady-state analysis

Table 1 (repeated) Six normal steady-state operating conditions

	<u>Case 1</u> Load	<u>Case 2</u> Load	<u>Case 3</u> Load	<u>Case 4</u> Load	<u>Case 5</u> Load	<u>Case 6</u> Load
<u>Load Condition</u>	Heavy	Medium-heavy	Peak	Light	Medium	Light
Total generation MW	23030	21590	25430	15050	19060	14840
Total load MW	22300	21000	24800	14810	18600	14630
<u>Inter-area flows</u>	(North to south)	(South to north)	(Hydro to N & S)	(Area 2 to N & S)	(N & S to pumping)	(~Zero transfers)
Area 4 to Area 2 MW	500	-500	-500	-200	300	0
Area 2 to Area 1 MW	1134	-1120	-1525	470	740	270
Area 1 to Area 3 MW	1000	-1000	1000	200	-200	0
Area 3 to Area 5 MW	500	-500	250	200	250	0

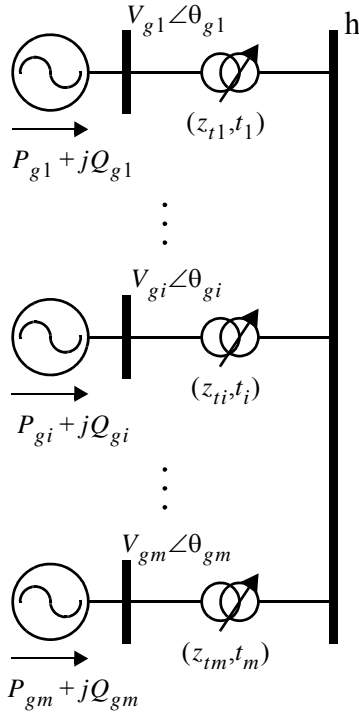
Table 8 Generation conditions for six loadflow cases. (Voltage at all generator buses is 1.0 pu in all cases.)

Power Station / Bus # Rating Rated power factor	<u>Case 1</u> No. units MW Mvar	<u>Case 2</u> No. units MW Mvar	<u>Case 3</u> No. units MW Mvar	<u>Case 4:</u> No. units MW Mvar	<u>Case 5:</u> No. units MW Mvar	<u>Case 6:</u> No. units MW Mvar
HPS_1 / 101 12 x 333.3 MVA 0.9 power factor lag	4 75.2 77.9	3 159.6 54.4	12 248.3 21.8	2 0 -97.4 Syn.Cond	3 -200.0 -26.0 Pumping	2 0 -102.2 Syn. Cond
BPS_2 / 201 6 x 666.7 MVA 0.9 power factor lag	6 600.0 95.6	5 560.0 38.9	6 550.0 109.1	4 540.0 -30.8	5 560.0 38.7	3 560.0 -53.5
EPS_2 / 202 5 x 555.6 MVA 0.9 power factor lag	5 500.0 132.7	4 480.0 60.5	5 470.0 127.6	3 460.0 -2.5	4 480.0 67.2	3 490.0 -7.3
VPS_2 / 203 4 x 555.6 MVA 0.9 power factor lag	4 375.0 132.8	3 450.0 82.4	2 225.0 157.0	3 470.0 9.4	2 460.0 83.1	3 490.0 3.7

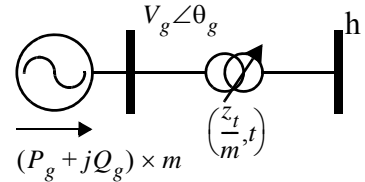
Power Station / Bus # Rating Rated power factor	<u>Case 1</u> No. units MW Mvar	<u>Case 2</u> No. units MW Mvar	<u>Case 3</u> No. units MW Mvar	<u>Case 4:</u> No. units MW Mvar	<u>Case 5:</u> No. units MW Mvar	<u>Case 6:</u> No. units MW Mvar
MPS_2 / 204 6 x 666.7 MVA 0.9 power factor lag	6 491.7 122.4	4 396.0 17.8	6 536.0 96.5	4 399.3 -43.6	4 534.4 55.2	3 488.6 -61.2
LPS_3 / 301 8 x 666.7 MVA 0.9 power factor lag	7 600.0 142.3	8 585.0 141.1	8 580.0 157.6	6 555.0 16.6	8 550.0 88.1	6 550.0 9.4
YPS_3 / 302 4 x 444.4 MVA 0.9 power factor lag	3 313.3 51.5	4 383.0 63.3	4 318.0 49.6	2 380.0 -9.3	3 342.0 43.8	2 393.0 -6.9
TPS_4 / 401 4 x 444.4 MVA 0.9 power factor lag	4 350.0 128.7	4 350.0 116.5	4 350.0 123.2	3 320.0 -21.9	4 346.0 84.9	3 350.0 -32.6
CPS_4 / 402 3 x 333.3 MVA 0.9 power factor lag	3 279.0 59.3	3 290.0 31.4	3 290.0 32.0	2 290.0 -2.4	3 280.0 45.4	3 270.0 4.7
SPS_4 / 403 4 x 444.4 MVA 0.9 power factor lag	4 350.0 52.3	4 350.0 47.2	4 350.0 47.3	3 320.0 14.2	4 340.0 46.3	2 380.0 25.2
GPS_4 / 404 6 x 333.3 MVA 0.9 power factor lag	6 258.3 54.5	6 244.0 39.8	6 244.0 40.0	3 217.0 -3.5	5 272.0 50.4	3 245.0 3.9
NPS_5 / 501 2 x 333.3 MVA 0.9 power factor lag	2 300.0 25.3	2 300.0 -8.8	2 300.0 6.5	2 280.0 -52.5	2 280.0 -35.2	1 270.0 -42.2
TPS_5 / 502 4 x 250 MVA 0.8 pf lag	4 200.0 40.1	4 200.0 53.0	4 180.0 48.8	3 180.0 -1.8	4 190.0 0.1	4 200.0 -9.7
PPS_5 / 503 6 x 166.7 MVA 0.9 power factor lag	4 109.0 25.2	5 138.0 36.9	6 125.0 32.6	1 150.0 2.2	2 87.0 3.5	2 120.0 -11.2

As mentioned in the introduction, in this report, the online generators within each of the 14 power-plants are each replaced by an aggregated equivalent generator. While the generators in each station could have been individually represented, this adds an additional level of complexity and increases system size, moreover, it is not warranted for the primary purpose of this document. If the researcher intends to investigate intra-plant dynamic performance for a particular power plant they can readily modify the `power_flow` and `dynamics` data to individually represent each on-line unit within the plant. In general, a power plant has n identical generating units of which $m \leq n$ are online. If $m = 0$ the entire power-plant is off-line. It is also assumed that each of the n generator step-up transformers is identical. The steady-state operating conditions of each of the m online units are assumed to be identical. For the purpose of analysing any disturbance external to the power plant; or any disturbance which is applied identically to all on-line units within the plant we can aggregate the m on-line units to form a single equivalent unit as illustrated in [Figure 18](#). For such disturbances the dynamic performance of the system in which the

generating plant is replaced by a single equivalent unit is identical to that of the system with the original m identical on-line units. Of course, the $m-1$ intra-plant modes of oscillation do not exist in the single composite representation, however, these modes are not excited by such disturbances.



One line diagram of power-plant with m individual online generators.



One line diagram of power-plant with single aggregated equivalent generator to represent the m online generators.

Notes:

- (a) Generator terminal voltages, angles and power generation are identical: $V_{g1} = \dots = V_{gi} = \dots = V_{gm} = V_g$ pu; $\theta_{g1} = \dots = \theta_{gi} = \dots = \theta_{gm} = \theta_g$ deg; $P_{g1} = \dots = P_{gi} = \dots = P_{gm} = P_g$ MW; and $Q_{g1} = \dots = Q_{gi} = \dots = Q_{gm} = Q_g$ Mvar. The MVA base of each of the m generators is MBASE.
- (b) For the aggregate equivalent generator the terminal voltage and angle is V_g pu and θ_g deg respectively. The real and reactive power output is $(m \times P_g)$ MW and $(m \times Q_g)$ Mvar respectively. The MVA base of the aggregate generator is $(m \times MBASE)$ MVA.
- (c) The impedance and tap position of each generator transformer is identical: $z_{t1} = \dots = z_{ti} = \dots = z_{tm} = z_t = r_t + jx_t$ pu on system MVA base; and $t_1 = \dots = t_i = \dots = t_m = t$ pu;
- (d) The impedance and tap position of the aggregate equivalent generator transformer is $(r_t + jx_t)/m$ pu on system MVA base; and t pu respectively.
- (e) Usually, generator model parameters are specified on the generator MVA base. If so then it is unnecessary to modify the values of the generator parameters. Otherwise, the user must convert the parameters of the equivalent generator model from per-unit on $(m \times MBASE)$ to the base required by their simulation program.

Figure 18 Formulation of a single aggregated equivalent generator to represent m online generators in a power-plant.

Table 9 SVC ratings and operating conditions for loadflow Cases 1 to 6.

SVC name / BusNo.	Reactive Power Range (MBASE)	Qmax	Qmin	Case 1	Case 2	Case 3	Case 4	Case 5	Case 6
				Voltage Mvar	Voltage Mvar	Voltage Mvar	Voltage Mvar	Voltage Mvar	Voltage Mvar
<u>Mvar @ 1.0 pu voltage</u>									
ASVC_2 / 205	650.0	430.0	-220.0	1.055 -68.3	1.055 41.8	1.02 -5.2	1.045 -39.3	1.045 -118.3	1.045 -29.4
RSVC_3 / 313	800.0	600.0	-200.0	1.015 71.4	1.015 129.4	1.015 158.8	1.015 86.7	1.015 54.9	1.015 54.2
BSVC_4 / 412	1430.0	1100.0	-330.0	1.000 58.2	1.000 63.9	1.000 83.8	1.000 -52.2	1.000 22.8	1.000 -0.2
PSVC_5 / 507	500.0	320.0	-180.0	1.015 22.6	1.040 36.8	1.043 18.0	1.010 -4.0	1.015 13.8	1.000 -3.7
SSVC_5 / 509	550.0	400.0	-150.0	1.030 10.6	1.027 50.2	1.050 -63.4	1.030 -109.3	1.030 -123.8	1.030 -109.3

Table 10 Transmission Line Parameters: Values per circuit.

From bus / to bus	Line No.	Line r+jx; b (pu on 100MVA)		
102 217	1,2	0.0084	0.0667	0.817
102 217	3,4	0.0078	0.0620	0.760
102 309	1,2	0.0045	0.0356	0.437
102 309	3	0.0109	0.0868	0.760
205 206	1,2	0.0096	0.0760	0.931
205 416	1,2	0.0037	0.0460	0.730
206 207	1,2	0.0045	0.0356	0.437
206 212	1,2	0.0066	0.0527	0.646
206 215	1,2	0.0066	0.0527	0.646
207 208	1,2	0.0018	0.0140	0.171
207 209	1	0.0008	0.0062	0.076
208 211	1,2,3	0.0031	0.0248	0.304
209 212	1	0.0045	0.0356	0.437
210 213	1,2	0.0010	0.0145	1.540
211 212	1,2	0.0014	0.0108	0.133
211 214	1	0.0019	0.0155	0.190
212 217	1	0.0070	0.0558	0.684
214 216	1	0.0010	0.0077	0.095
214 217	1	0.0049	0.0388	0.475
215 216	1,2	0.0051	0.0403	0.494
215 217	1,2	0.0072	0.0574	0.703
216 217	1	0.0051	0.0403	0.494

From bus / to bus	Line No.	Line r+jx; b (pu on 100MVA)		
303 304	1,2	0.0020	0.0280	0.740
303 305	1,2	0.0011	0.0160	1.700
304 305	1	0.0003	0.0040	0.424
305 306	1	0.0002	0.0030	0.320
305 307	1,2	0.0003	0.0045	0.447
306 307	1	0.0001	0.0012	0.127
307 308	1,2	0.0023	0.0325	3.445
309 310	1,2,3	0.0135	0.1070	0.5827
310 311	1,2	0.0000	-0.0337	0.000
312 313	1,2,3	0.0060	0.0450	0.300
313 314	1,2	0.0010	0.0100	0.260
315 509	1,2	0.0070	0.0500	0.190
405 406	1,2	0.0039	0.0475	0.381
405 408	1	0.0054	0.0500	0.189
405 409	1,2,3	0.0180	0.1220	0.790
406 407	1,2	0.0006	0.0076	0.062
407 408	1	0.0042	0.0513	0.412
408 410	1,2,3	0.0165	0.1920	0.673
409 411	1,2	0.0103	0.0709	0.460
410 411	1	0.0043	0.0532	0.427
410 412	1 to 4	0.0043	0.0532	0.427
410 413	1,2	0.0040	0.0494	0.400
411 412	1,2	0.0012	0.0152	0.122
414 415	1,2	0.0020	0.0250	0.390
415 416	1,2	0.0037	0.0460	0.730
504 507	1,2	0.0230	0.1500	0.560
504 508	1,2	0.0260	0.0190	0.870
505 507	1,2	0.0016	0.0170	0.030
505 508	1	0.0025	0.0280	0.170
506 507	1,2	0.0016	0.0170	0.030
506 508	1	0.0030	0.0280	0.140
507 508	1	0.0020	0.0190	0.090
507 509	1-6	0.0900	0.6600	0.300
<p>Notes:</p> <p>(a) System frequency is 50 Hz.</p> <p>(b) In Version 4 the number of parallel circuits between the following pairs of buses were increased:</p> <ul style="list-style-type: none"> 303-304: 1 to 2 ckt 309-310: 2 to 3 ckt 312-313: 1 to 3 ckt. 313-314: 1 to 2 ckt 505-507: 1 to 2 ckt 506-507: 1 to 2 ckt 507-509: 2 to 6 ckt <p>If the number of parallel circuits between a pair of nodes is changed from m to n then the per-circuit impedance and susceptance ($r + jx, b$) is changed to $((r + jx)*n/m, b*m/n)$. Consequently, the aggregate impedance and susceptance between the pair of nodes is unchanged.</p>				

Table 11 Transformer Ratings and Reactance.

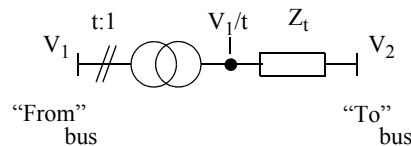
Buses		Number	Rating, each Unit (MVA)	Reactance per transformer	
From	To			% on Rating	per unit on 100MVA
101	102	ng	333.3	12.0	0.0360
201	206	ng	666.7	16.0	0.0240
202	209	ng	555.6	16.0	0.0288
203	208	ng	555.6	17.0	0.0306
204	215	ng	666.7	16.0	0.0240
209	210	4	625.0	17.0	0.0272
213	214	4	625.0	17.0	0.0272
301	303	ng	666.7	16.0	0.0240
302	312	ng	444.4	15.0	0.0338
304	313	2	500.0	16.0	0.0320
305	311	3	333.3	12.0	0.0360
305	314	2	700.0	17.0	0.0243
308	315	2	370.0	10.0	0.0270
401	410	ng	444.4	15.0	0.0338
402	408	ng	333.3	17.0	0.0510
403	407	ng	444.4	15.0	0.0338
404	405	ng	333.3	17.0	0.0510
413	414	3	750.0	6.0	0.0080
501	504	ng	333.3	17.0	0.0510
502	505	ng	250.0	16.0	0.0640
503	506	ng	166.7	16.7	0.1000

Notes:

(a) System frequency is 50 Hz.

(b) n_g - Generator/transformer unit; in-service if associated generator is on-line. (Thus, if n_g generator units are on-line then the impedance of the aggregated generator step-up transformer is x_t/n_g where x_t is the impedance of a single generator step-up transformer.)**Table 12** Switched Shunt Capacitor / Reactor banks (C/R) in service, Cases 1-6 (Mvar)

Bus Number	<u>Case 1</u>	<u>Case 2</u>	<u>Case 3</u>	<u>Case 4</u>	<u>Case 5:</u>	<u>Case 6:</u>
211	-	-	100 C	-	-	-
212	400 C	150 C	150 C	400 C	400 C	400 C
216	300 C	150 C	150 C	300 C	300 C	300 C
409	60 C	60 C				
411	30 C	30 C				
414	30 R	30 R				
415	60 R	60 R				
416	60 R	90 R				
504	-	90 R	90 R	-	-	-



Taps-ratio convention employed

Figure 19 Transformer Taps Convention

The transformer tap ratios listed in [Table 13](#) are based upon the convention shown in [Figure 19](#).

Table 13 Transformer Tap Ratios for Loadflow Cases 1 to 6

Buses		Case 1	Case 2	Case 3	Case 4	Case 5	Case 6
From	To						
101	102	0.939	0.948	0.948	1.000	1.000	1.000
201	206	0.943	0.948	0.939	1.000	0.971	1.010
202	209	0.939	0.948	0.939	1.000	0.971	1.010
203	208	0.939	0.948	0.939	1.000	0.971	1.010
204	215	0.939	0.948	0.939	1.000	0.971	1.010
209	210	0.976	0.990	0.976	0.976	0.976	0.976
213	214	1.000	1.000	1.000	1.000	1.000	1.000
301	303	0.939	0.935	0.930	1.000	0.961	1.000
302	312	0.952	0.952	0.952	1.000	0.961	1.000
304	313	0.961	0.961	0.948	0.961	0.961	0.961
305	311	1.000	1.000	1.000	1.000	1.000	1.000
305	314	1.000	1.000	1.000	1.000	1.000	1.000
308	315	1.000	0.960	1.000	1.000	1.000	1.000
401	410	0.939	0.939	0.939	1.000	0.952	1.010
402	408	0.952	0.952	0.952	1.000	0.952	1.000
403	407	0.952	0.952	0.952	1.000	0.952	1.000
404	405	0.952	0.952	0.952	1.000	0.952	1.000
413	414	1.000	1.000	1.000	1.000	1.015	1.000
501	504	0.952	0.952	0.952	1.000	0.985	1.015
502	505	0.962	0.930	0.930	1.000	0.995	1.020
503	506	0.962	0.930	0.930	1.000	0.985	1.020

For simplicity, loads are assumed to behave as constant impedances in the small- and large-signal analysis.

Table 14 Busbar Loads (P MW, Q Mvar) for Cases 1 to 6

	Case 1		Case 2		Case 3		Case 4		Case 5		Case 6	
Bus No.	P	Q	P	Q	P	Q	P	Q	P	Q	P	Q
102	450	45	380	38	475	50	270	30	340	35	270	30
205	390	39	330	33	410	40	235	25	290	30	235	25
206	130	13	110	11	140	15	80	10	100	10	80	10
207	1880	188	1600	160	1975	200	1130	120	1410	145	1110	120
208	210	21	180	18	220	25	125	15	160	20	125	15
211	1700	170	1445	145	1785	180	1060	110	1275	130	1035	110
212	1660	166	1410	140	1740	180	1000	110	1245	125	1000	110
215	480	48	410	40	505	50	290	30	360	40	290	30
216	1840	184	1565	155	1930	200	1105	120	1380	140	1105	120
217	1260	126	1070	110	1320	140	750	80	940	95	750	80
306	1230	123	1230	123	1450	150	900	90	1085	110	900	90
307	650	65	650	65	770	80	470	50	580	60	470	50
308	655	66	655	66	770	80	620	100	580	60	620	100
309	195	20	195	20	230	25	140	15	170	20	140	15
312	115	12	115	12	140	15	92	10	105	15	92	10
313	2405	240	2405	240	2840	290	1625	165	2130	220	1625	165
314	250	25	250	25	300	30	180	20	222	25	180	20
405	990	99	1215	120	1215	120	730	75	990	100	730	75
406	740	74	905	90	905	90	540	55	740	75	540	55
407	0	0	0	0	0	0	0	0	0	0	0	0
408	150	15	185	20	185	20	110	10	150	15	110	10
409	260	26	310	30	310	30	190	20	260	30	190	20
410	530	53	650	65	650	65	390	40	530	55	390	40
411	575	58	700	70	700	70	420	45	575	60	420	45
412	1255	126	1535	155	1535	155	922	100	1255	130	922	100
504	300	60	200	40	300	60	180	20	225	25	170	20
507	1000	200	710	140	1100	220	640	65	750	75	565	65
508	800	160	520	105	800	160	490	50	600	60	450	50
509	200	40	70	15	100	20	122	15	150	15	117	15

Load Characteristics: Constant Impedance

I.2 Dynamic performance analysis

I.2.1 Generator model parameters (small- and large-signal)

The parameters of the fourteen generators are listed in [Table 15](#). The generator model to which these parameters apply are given in [Section I.5](#). It should be noted that various simulation packages may adopt the same set of generator model parameters but employ different model formulations. Differences in the representation of generator saturation between simulation packages are frequently observed. For that reason, and since generator saturation tends to have a small effect of damping performance, generator saturation has been neglected in this benchmark model.

Table 15 Generator Parameters

Generator	Bus	Order	Rating MVA per Unit	Max. No. of Units	H MWs/MVA	Xa pu	Xd pu	Xq pu	Xd' pu	Tdo' s	Xd" pu	Tdo" s	Xq' pu	Tqo' s	Xq" pu	Tqo" s
HPS_1	101	5	333.3	12	3.60	0.14	1.10	0.65	0.25	8.50	0.25	0.050	-	-	0.25	0.200
BPS_2	201	6	666.7	6	3.20	0.20	1.80	1.75	0.30	8.50	0.21	0.040	0.70	0.30	0.21	0.080
EPS_2	202	6	555.6	5	2.80	0.17	2.20	2.10	0.30	4.50	0.20	0.040	0.50	1.50	0.21	0.060
MPS_2	204	6	666.7	6	3.20	0.20	1.80	1.75	0.30	8.50	0.21	0.040	0.70	0.30	0.21	0.080
VPS_2	203	6	555.6	4	2.60	0.20	2.30	1.70	0.30	5.00	0.25	0.030	0.40	2.00	0.25	0.250
LPS_3	301	6	666.7	8	2.80	0.20	2.70	1.50	0.30	7.50	0.25	0.040	0.85	0.85	0.25	0.120
YPS_3	302	5	444.4	4	3.50	0.15	2.00	1.80	0.25	7.50	0.20	0.040	-	-	0.20	0.250
CPS_4	402	6	333.3	3	3.00	0.20	1.90	1.80	0.30	6.50	0.26	0.035	0.55	1.40	0.26	0.040
GPS_4	404	6	333.3	6	4.00	0.18	2.20	1.40	0.32	9.00	0.24	0.040	0.75	1.40	0.24	0.130
SPS_4	403	6	444.4	4	2.60	0.20	2.30	1.70	0.30	5.00	0.25	0.030	0.40	2.00	0.25	0.250
TPS_4	401	6	444.4	4	2.60	0.20	2.30	1.70	0.30	5.00	0.25	0.030	0.40	2.00	0.25	0.250
NPS_5	501	6	333.3	2	3.50	0.15	2.20	1.70	0.30	7.50	0.24	0.025	0.80	1.50	0.24	0.100
TPS_5	502	6	250.0	4	4.00	0.20	2.00	1.50	0.30	7.50	0.22	0.040	0.80	3.00	0.22	0.200
PPS_5	503	6	166.7	6	7.50	0.15	2.30	2.00	0.25	5.00	0.17	0.022	0.35	1.00	0.17	0.035

Generator reactances in per unit on machine rating as base.
For all generators the stator winding resistance (Ra) and damping torque coefficient (D) are both assumed to be zero.
System frequency is 50 Hz.

I.2.2 Small-signal Excitation System Models and Parameters

Two basic types of excitation systems are employed, ST1A and AC1A [16]. For simplicity exciter saturation, exciter armature reaction and voltage-drop due to rectifier regulation are neglected in the AC1A model. The parameters of the AVR have been tuned to ensure that the open-circuit generator under closed-loop voltage control is stable and satisfies the performance specifications. The small-signal models for the ST1A and AC1A excitation systems are shown in Figures 20 and 21, respectively.

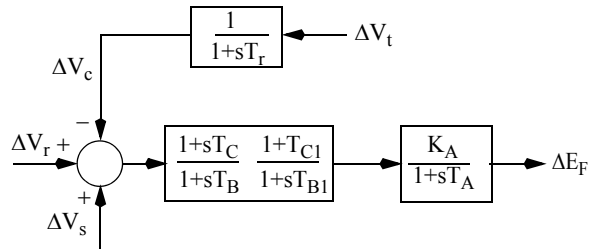


Figure 20 Small-signal model of a type ST1A excitation system.

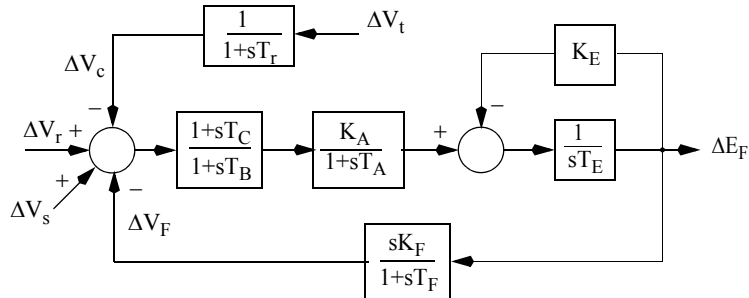


Figure 21 Small-signal model of a type AC1A Excitation System; exciter saturation, the demagnetizing effect of generator field current and the voltage drop due to rectifier regulation are neglected.

Table 16 Small-signal excitation System Model Parameters: 14-generator system

	HPS ₁₀₁ 1 /	BPS ₂₀₁ 2 /	EPS ₂₀₂ 2 /	VPS ₂₀₃ 2 /	MPS ₂₀₄ 2 /	LPS ₃₀₁ 3 /	YPS ₃₀₂ 3 /	TPS ₄₀₁ 4 /	CPS ₄₀₂ 4 /	SPS ₄₀₃ 4 /	GPS ₄₀₄ 4 /	NPS ₅₀₁ 5 /	TPS ₅₀₂ 5 /	PPS ₅₀₃ 5 /
Type	ST1A	ST1A	AC1A	ST1A	ST1A	AC1A	ST1A	ST1A	ST1A	ST1A	AC1A	ST1A	AC1A	ST1A
T _r (s)	0	0	0	0	0	0	0	0.02	0	0	0	0	0	0
K _A (s)	200	400	300	400	400	200	300	300	300	300	250	1000	400	300
T _A (s)	0.10	0.02	0.02	0.01	0.02	0.05	0.05	0.10	0.05	0.01	0.20	0.04	0.50	0.01
T _B (s)	13.25	1.12	0	0.70	1.12	6.42	0	40.0	9.80	0.70	0.0232	0	16.0	0.8
T _C (s)	2.50	0.50	0	0.35	0.50	1.14	0	4.00	1.52	0.35	0.1360	0	1.40	0.2
K _E	-	-	1.0	-	-	-	1.0	0	0	0	0	0	0.05	0
T _E (s)	-	-	1.0	-	-	-	1.333	0	0	0	0	0	0.60	0
K _F	-	-	0.029	-	-	-	0.020	-	-	-	-	1.00	-	-
T _F (s)	-	-	1.0	-	-	-	0.8	-	-	-	-	0.87	-	-

I.2.3 SVC small-signal model and parameters

From a small-signal perspective the SVC is represented as a perturbation in the shunt susceptance ΔB connected to the bus. The susceptance is controlled by a voltage-regulator with SVC current droop as depicted in [Figure 22](#). (Note: In Version 3 and earlier ΔB and $\Delta[Q/V_t]$ were in per-unit on the system MVA base of 100 MVA, whereas now they are in per-unit on the SVC Mvar base. Consequently the base conversion factor K_s is now included in the model. It is emphasized that this change in base has no effect on the dynamic performance of the model.)

An alternative formulation of the SVC model in which the current droop signal is represented implicitly, under the assumption that the perturbation in voltage is “small” compared to the associated perturbation in susceptance, is developed in [Appendix II.2.2](#). The alternative formulation is developed to allow the SVC to be represented in the PSS[®]/E program using one of its built-in SVC models. It is shown in the later appendix that the damping performance of the system with the alternative SVC model formulation is practically identical to that obtained with the SVC model in [Figure 22](#).

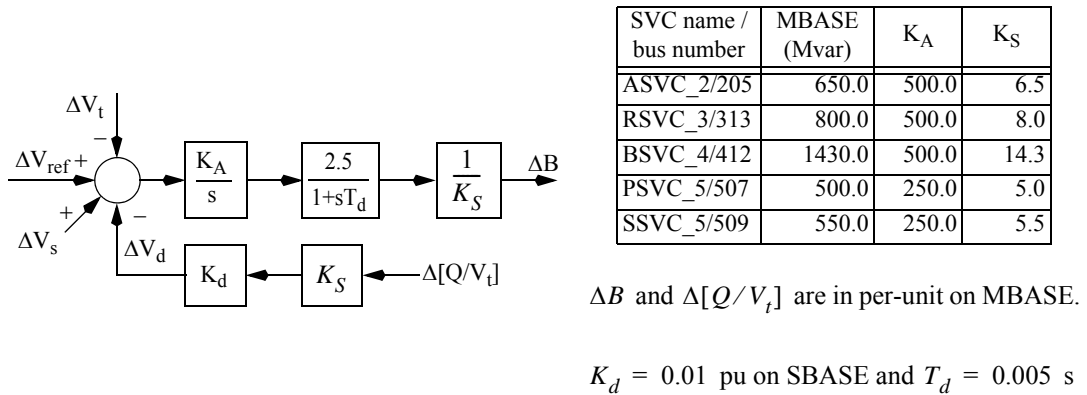


Figure 22 Small-signal model of the SVCs.

I.3 Power System Stabiliser (PSS) Parameters

The structure of the PSS employing a speed-stabilising signal is shown in [Figure 23](#). The design based on the P-Vr method of the block labelled ‘Compensation TF and LP Filter’ has been outlined in [Section 6.3](#).

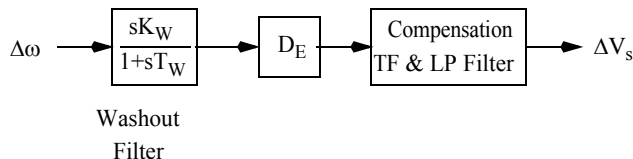


Figure 23 Structure of the PSS for analysis and design purposes

Assuming a single washout filter block is employed, the general form of the PSS TF is given in (2), i.e.

$$H_{PSS}(s) = kG_c(s) = k \cdot \left[\frac{sT_W}{1+sT_W} \cdot \frac{1}{k_c} \cdot \frac{(1+c_1s+c_2s^2)(1+sT_a)\dots}{(1+sT_{b1})\dots(1+sT_1)(1+sT_2)\dots} \right].$$

The ‘Compensation TF & LP Filter’ (which excludes the Washout Filter) in [Figure 23](#) represents a general form of that component in the above PSS TF given by:

$$H_c(s) = K_c \cdot \frac{(1+c_1s+c_2s^2)(1+sT_{a1})\dots}{(1+sT_{b1})\dots(1+sT_1)(1+sT_2)\dots} \quad \text{where } K_c = 1/k_c \quad (6)$$

In the PSS transfer function of [Figure 23](#), (i) the damping gain of the PSS is $k = D_e = 20$ pu on generator MVA rating, and (ii) the washout time constant T_W is 7.5 s.

I.3.1 PSS compensating transfer functions and parameters

Form of the fourth-order TF having real zeros:

$$H_c(s) = K_c \cdot \frac{1+sT_a}{1+sT_e} \cdot \frac{1+sT_b}{1+sT_f} \cdot \frac{1+sT_c}{1+sT_g} \cdot \frac{1+sT_d}{1+sT_h} \quad (7)$$

Table 17 Compensation and LP Filter Parameters for PSS based on (7).

Generator Name / Number	K _c	T _a	T _b	T _c	T _d	T _e	T _f	T _g	T _h
EPS_2 / 202	0.233	0.286	0.111	0.040	0	0.00667	0.00667	0.00667	0
TPS_5 / 502	0.294	0.500	0.0588	0.0167	0	0.00667	0.00667	0.00667	0
PPS_5 / 503	0.178	0.200	0.187	0.167	0.020	0.350	0.0667	0.00667	0.00667

Form of the fourth-order TF having real and complex zeros:

$$H_c(s) = K_c \cdot \frac{1+sT_a}{1+sT_d} \cdot \frac{1+sT_b}{1+sT_e} \cdot \frac{1+as+bs^2}{(1+sT_f)(1+sT_g)} \quad (8)$$

Table 18 Compensation and LP Filter Parameters for PSS based on (8)

Generator Name / Number	K _c	T _a	T _b	a	b	T _d	T _e	T _f	T _g
MPS_2 / 204	0.333	0.010	0	0.10	0.0051	0.00667	0	0.00667	0.00667
YPS_3 / 302	0.298	0.050	0	0.5091	0.1322	0.00667	0	0.00667	0.00667
NPS_5 / 501	0.195	0.033	0.033	0.30	0.1111	0.300	0.00667	0.00667	0.00667

Form of the second-order TF having real zeros:

$$H_c(s) = K_c \cdot \frac{1 + sT_a}{1 + sT_e} \cdot \frac{1 + sT_b}{1 + sT_f} \quad (9)$$

Table 19 Compensation and LP Filter Parameters for PSS based on (9)

Generator Name / Number	K _c	T _a	T _b	T _e	T _f
VPS_2 / 203	0.286	0.0708	0.0292	0.00667	0.00667
TPS_4 / 401	0.357	0.2083	0.2083	0.00667	0.00667
CPS_4 / 402	0.235	0.2777	0.1000	0.00667	0.00667

Form of the second-order TF having a pair of complex zeros:

$$H_c(s) = K_c \cdot \frac{1 + as + bs^2}{(1 + sT_e)(1 + sT_f)} \quad (10)$$

Table 20 Compensation and LP Filter Parameters for PSS based on (10)

Generator Name / Number	K _c	a	b	T _e	T _f
HPS_1 / 101 *	0.769	0.3725	0.03845	0.00667	0.00667
BPS_2 / 201	0.278	0.1280	0.00640	0.00667	0.00667
LPS_3 / 301	0.625	0.1684	0.01180	0.00667	0.00667
SPS_4 / 403	0.316	0.0909	0.002067	0.00667	0.00667
GPS_4 / 404	0.303	0.1154	0.005917	0.00667	0.00667

* Note for HPS_1: PSSs are OFF in Cases 4 and 6. When motoring in Case 5 the sign of the PSS output ΔV_S at the summing junction is negated - or equivalently the PSS gain setting is negated..

I.4 Comparison of P-Vr and GEP methods

Table 21 P-Vr and GEP methods for the design of PSS compensation TFs

Comparison of two methods for the design of the PSS compensation transfer functions		
Feature	P-Vr	GEP [12]
1	Essentially an analytical frequency response approach using small-signal analysis software or Matlab. A wide range of normal and contingency operating conditions occurring on the power system is examined.	Originally a field-based frequency response method for tuning the PSS on a particular generator in a station for the particular operating condition(s) existing at the time.

Comparison of two methods for the design of the PSS compensation transfer functions		
Feature	P-Vr	GEP [12]
2	Calculates magnitude and phase of the P-Vr over the complete range of rotor modes.	Field measurements provide the phase response $\Delta V_{term}/\Delta V_{ref}$ over a frequency range. Higher frequency measurements may be limited by resonances at lightly-damped local-area or intra-station modal frequencies.
3	The shaft dynamics are disabled.	The phase response of the TF $\Delta V_{term}/\Delta V_{ref}$ is close to that of the P-Vr TF because the speed perturbations associated with measurements are small (i.e. the shaft dynamics are virtually disabled).
4	PSS TF synthesized in <i>both</i> magnitude and phase from P-Vr characteristic.	PSS TF is synthesized from phase response.
5	Using magnitude information from P-Vr TF, damping gain k_i is set to provide the left-shift required to satisfy relevant system stability criteria.	The gain setting of the PSS (on site) is determined by increasing the gain until the onset of instability is detected; the gain is set to $1/3^{\text{rd}}$ the latter value.

I.5 Machine Equations

In Table 15 both fifth- and sixth-order generator models are represented; in the fifth-order model the q-axis representation is simplified.

I.5.1 Sixth-order generator model

The following is a sixth-order model of a synchronous generator employed in PSS®/E. In this model the “classically” defined, unsaturated operational-impedance parameters are used [13], section 4.1-2. A linearized form of these equations are provided in small-signal analysis packages such as [14].

Equations of motion:

$$\frac{d\delta}{dt} = \omega_0(\omega - 1), \quad (11)$$

$$2H\omega \frac{d\omega}{dt} = -D\omega(\omega - 1) + P_m - (v_D i_D + v_Q i_Q + r_a i_D^2 + r_a i_Q^2). \quad (12)$$

$$\omega_0 = 2\pi f_0, f_0 \text{ is } 50 \text{ Hz},$$

where δ is the rotor angle (rad), and ω is the shaft speed in per-unit.

The rates of change of voltage behind transient reactance (E'_q and E'_d) and damper winding flux linkages (ψ_{kd} and ψ_{kq}) are given by:

$$\frac{dE'_q}{dt} = \frac{1}{T'_{d0}}(E_{fd} - X_{ad}i_{fd}); \quad (13)$$

$$\frac{d\psi_{kd}}{dt} = \frac{1}{T'_{d0}}(E'_q - \psi_{kd} - (X'_d - x_a)i_d); \quad (14)$$

$$\frac{dE'_d}{dt} = \frac{1}{T'_{q0}}X_{aq}i_{kq}; \quad (15)$$

$$\frac{d\psi_{kq}}{dt} = \frac{1}{T'_{q0}}(E'_d - \psi_{kq} - (X'_q - x_a)i_q). \quad (16)$$

The d- and q-axis components of the generator terminal voltage are:

$$v_d = -r_a i_d + X''_q i_q + \psi''_q, \quad (17)$$

$$v_q = -r_a i_q - X''_d i_d + \psi''_d. \quad (18)$$

The transformer voltages and the speed dependency of the rotational voltages in the stator equations are neglected.

The d- and q-axis components of the stator subtransient flux linkages, ψ''_d and ψ''_q , are:

$$\psi''_d = \left(\frac{X''_d - x_a}{X'_d - x_a} \right) E'_q + \left(\frac{X'_d - X''_d}{X'_d - x_a} \right) \psi_{kd}, \quad (19)$$

$$\psi''_q = \left(\frac{X''_q - x_a}{X'_q - x_a} \right) E'_d + \left(\frac{X'_q - X''_q}{X'_q - x_a} \right) \psi_{kq}. \quad (20)$$

The field current ($I_{fd} = X_{ad}i_{fd}$) is given by:

$$X_{ad}i_{fd} = K_{1d}E'_q + K_{2d}\psi_{kd} + K_{3d}i_d, \quad (21)$$

where

$$K_{1d} = 1 + \frac{(X_d - X'_d)(X'_d - X''_d)}{(X'_d - x_a)^2}, \quad K_{2d} = 1 - K_{1d}, \quad K_{3d} = \frac{(X_d - X'_d)(X''_d - x_a)}{(X'_d - x_a)}. \quad (22)$$

The q-axis excitation is:

$$X_{aq}i_{kq} = K_{1q}E'_d + K_{2q}\psi_{kq} + K_{3q}i_q, \quad (23)$$

where

$$K_{1q} = -\left[1 + \frac{(X_q - X'_q)(X'_q - X''_q)}{(X'_q - x_a)^2} \right], \quad K_{2q} = -(1 + K_{1q}),$$

$$K_{3q} = \frac{(X_q - X'_{\text{q}})(X''_{\text{q}} - x_a)}{(X'_{\text{q}} - x_a)}. \quad (24)$$

I.5.2 Fifth-order generator model

In the fifth-order model, only one damper winding is represented on the quadrature axis. The equations of motion and those for the direct-axis of the generator are therefore the same as for the sixth-order generator model. However, (15) and (16) for the quadrature axis are replaced by:

$$\frac{d\Psi''_{\text{q}}}{dt} = \frac{1}{T''_{q0}} [\Psi''_{\text{q}} - (X_q - X''_{\text{q}}) i_q]; \quad (25)$$

furthermore, the following equation replaces (20), (23) and (24):

$$\Psi_q = \Psi''_{\text{q}} - X''_{\text{q}} i_q. \quad (26)$$

Appendix II Transient stability modelling data

The small-signal model of the simplified 14-generator model of the southern and eastern Australian power system is augmented to allow large-signal (i.e. transient-stability) analysis. The study results in this report are prepared using the Siemens-PTI PSS[®]/E program [1]. Consequently, the large-signal dynamics model data is presented in a format consistent with PSS[®]/E. However, it is expected the data can be readily adapted to other transient-stability programs as well.

II.1 Steady-state analysis data

The power flow data in [Appendix I.1](#) is used as a basis for transient stability analysis.

II.2 Dynamic analysis data

II.2.1 Generator model and parameters

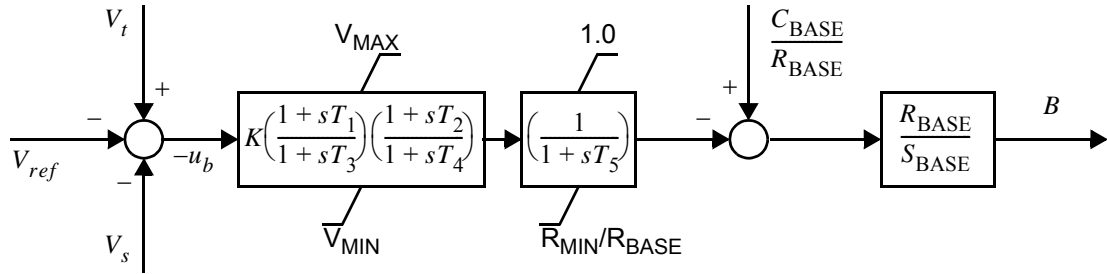
The generator model and parameters in [Appendix I.2.1](#) are used in the transient stability analysis, with the exception of a difference in the formulation of the rotor equations of motion which is described below. In addition, since generator saturation is neglected, the parameters S(1.0) and S(1.2) are both set to zero in the PSS[®]/E data for each generator.

II.2.1.1 *Formulation of the generator rotor-equations of motion*

When using PSS[®]/E it is necessary that the frequency dependence of network parameters is represented by setting the simulation parameter NETFRQ = 1. This ensures a consistent formulation of the generator rotor-equations of motion.

II.2.2 Large-signal SVC model and parameters

To our knowledge there is no standard or built-in model in PSS[®]/E of a SVC with the structure used in the small-signal formulation described in [Appendix I.2.3](#). In the following it is shown that, subject to certain assumptions, the PSS[®]/E ‘CSVGN1’ SVC model has similar small-signal dynamic performance to the model in [Appendix I.2.3](#).



Notes:

- (a) V_{ref} is the external SVC AVR voltage reference input; V_t is the SVC terminal voltage in pu; V_s is the output from an optional power oscillation damper and is not used in the 14 generator system model; B is the SVC susceptance in pu on system MVA base (S_{BASE}).
- (b) R_{BASE} is the maximum value of the SVC inductance (in Mvar @ 1.0 pu voltage) and in the 14 generator system model is equal to the SVC reactive power range $M_{BASE} = Q_{MAX} - Q_{MIN}$ (Mvar) as specified in [Table 9](#), The SVC inductance is assumed to be continuously controllable between R_{MIN} and R_{BASE} (Mvar @ 1.0 pu voltage).
- (c) C_{BASE} is the total SVC capacitance (in Mvar @ 1.0 pu voltage) and in the 14 generator model is equal to the maximum SVC reactive power output Q_{MAX} (Mvar @ 1.0 pu voltage) as specified in [Table 9](#).
- (d) R_{MIN} is the minimum value of the controllable inductance (in Mvar @ 1.0 pu voltage) and is zero for all five SVCs in the 14 generator system model.
- (e) $V_{MAX} = 1.0$ pu and $V_{MIN} = 0.0$ pu and for the 14 generator system model corresponds to the inductance range of the SVC in pu of R_{BASE} .

Figure 24 PSS®/E ‘CSVGN1’ SVC model structure used to represent the five SVCs in transient stability simulations.

Linearizing the PSS®/E ‘CSVGN1’ model we have the following transfer-function from Δu_b to ΔB :

$$\frac{\Delta B(s)}{\Delta u_b(s)} = K \left(\frac{R_{BASE}}{S_{BASE}} \right) \left(\frac{1 + sT_1}{1 + sT_3} \right) \left(\frac{1 + sT_2}{1 + sT_4} \right) \left(\frac{1}{1 + sT_5} \right) \text{ pu on SBASE} \quad (27)$$

Referring to [Figure 22](#) we seek to develop the transfer-function from the perturbation in the voltage-error signal $\Delta u_b = \Delta V_{ref} - \Delta V_t + \Delta V_s$ to the perturbation in the SVC susceptance ΔB .

$$\Delta B(s) = \left(\frac{2.5K_A}{sK_S} \right) \left(\frac{1}{1 + sT_d} \right) \left(\Delta u_b(s) - (K_d K_S) \Delta \left(\frac{Q(s)}{V_t(s)} \right) \right) \text{ pu on MBASE} \quad (28)$$

Now, consider the expression for the SVC current, Q/V_t . Recall that $Q = BV_t^2$ and therefore, $Q/V_t = BV_t$. Linearizing the latter expression and transforming to the Laplace domain yields:

$$\Delta \left(\frac{Q(s)}{V_t(s)} \right) = B_0 \Delta V_t(s) + V_{t0} \Delta B(s) \quad (29)$$

Assuming that the perturbation in susceptance is large when compared to the associated change in voltage we can simplify (29) to:

$$\Delta \left(\frac{Q(s)}{V_t(s)} \right) \approx V_{t0} \Delta B(s) \quad (30)$$

Substituting for $\Delta \left(\frac{Q(s)}{V_t(s)} \right)$ in (28) from the approximation in (30) yields:

$$\Delta B(s) = \left(\frac{2.5K_A}{sK_S} \right) \left(\frac{1}{1+sT_d} \right) (\Delta u_b(s) - (K_d K_S V_{t0}) \Delta B(s)) \quad (31)$$

which, upon rearrangement yields the following transfer-function:

$$\frac{\Delta B(s)}{\Delta u_b(s)} = \frac{1/(K_d K_S V_{t0})}{\left(1 + \left(\frac{1}{2.5K_d K_A V_{t0}} \right) s + \left(\frac{T_d}{2.5K_d K_A V_{t0}} \right) s^2 \right)} \quad (32)$$

Let us now factorize the characteristic equation $1 + \left(\frac{1}{2.5K_d K_A V_{t0}} \right) s + \left(\frac{T_d}{2.5K_d K_A V_{t0}} \right) s^2 = 0$

into the form $(1 + sT_a)(1 + sT_b) = 0$.

$$\text{After defining } a = \frac{1}{2.5K_d K_A V_{t0}} \quad (33)$$

we have $T_a + T_b = a$ and $T_a T_b = aT_d$. Eliminating T_b from the preceding two equations we have the following quadratic equation for T_a : $T_a^2 - aT_a + aT_d = 0$. Taking the largest root we have

$$T_a = \frac{a + \sqrt{a(a - 4T_d)}}{2} \quad (34)$$

$$T_b = a - T_a = \frac{a - \sqrt{a(a - 4T_d)}}{2}$$

Thus, subject to the assumption that $\Delta V_t \ll \Delta B$, the small-signal transfer-function representation of the SVC in Figure 22 is:

$$\frac{\Delta B(s)}{\Delta u_b(s)} = \left(\frac{1}{K_d K_S V_{t0}} \right) \left(\frac{1}{1+sT_a} \right) \left(\frac{1}{1+sT_b} \right) \text{ pu on MBASE.} \quad (35)$$

With minimal loss of accuracy we can set $V_{t0} = 1.0$ pu, thereby avoiding the need to adjust the SVC model parameters with changes in the SVC bus voltage.

Comparing the transfer-function of the small-signal model of the SVC in (35) with that of the PSS®/E ‘CSVGN1’ model in (27) we can see that the ‘CSVGN1’ model can be used to represent the SVC according to the following relationships between the small-signal model parameters and ‘CSVGN1’ model parameters:

Table 22 Transformation from the small-signal SVC model parameters in (35) to the PSS®/E ‘CSVGN1’ model parameters in (27).

PSS®/E ‘CSVGN1’ Parameter	in terms of small-signal model parameters
K	$\left(\frac{1}{K_d K_S V_{t0}} \right)$
T_1	0.0
T_2	0.0
T_3	$T_a = \frac{a + \sqrt{a(a - 4T_d)}}{2}$
T_4	0.0
T_5	$T_b = \frac{a - \sqrt{a(a - 4T_d)}}{2}$
Notes:	
(a) from (35), $a = \frac{1}{2.5K_d K_A V_{t0}}$	
(b) set $V_{t0} = 1.0$ for fixed model parameters.	

Table 23 Parameter values of the PSS[®]/E ‘CSVGN1’ SVC model [1] used in the transient stability studies. (Note that K, T₃ and T₅ are calculated assuming V_{t0} = 1.0 pu)

Parameter	Parameter values for five SVCs in the 14-generator system				
	ASVC_2	RSVC_3	BSVC_4	PSVC_5	SSVC_5
IBUS	205	313	412	507	509
Model Code	‘CSVGN1’	‘CSVGN1’	‘CSVGN1’	‘CSVGN1’	‘CSVGN1’
I	‘1’	‘1’	‘1’	‘1’	‘1’
K	15.384615	12.5	6.993	20.0	18.181818
T ₁	0.0	0.0	0.0	0.0	0.0
T ₂	0.0	0.0	0.0	0.0	0.0
T ₃	0.074641	0.074641	0.074641	0.154833	0.154833
T ₄	0.0	0.0	0.0	0.0	0.0
T ₅	0.005359	0.005359	0.005359	0.005167	0.005167
R _{MIN}	0.0	0.0	0.0	0.0	0.0
V _{MAX}	1.0	1.0	1.0	1.0	1.0
V _{MIN}	0.0	0.0	0.0	0.0	0.0
C _{BASE}	430.0	600.0	1100.0	320.0	400.0

II.2.2.1 Assessment of the effect of the modified SVC model on damping performance

The 13 electromechanical modes for Case 2 with all PSSs in-service with their design damping-gains are listed in Table 24 for two alternative SVC representations. The first is the small-signal representation with SVC-current droop explicitly represented as shown in Figure 22 and the second is the transfer-function in (35) which is derived from the first on the assumption that perturbation in SVC susceptance is large when compared to the associated change in voltage. It is thus clear from this comparison that employing the PSS[®]/E ‘CSVGN1’ model of the SVC in which current droop is implicitly represented will have negligible effect on the damping performance of the system.

Table 24 Comparison of electromechanical modes for Case 2 with two alternative SVC representations.

SVC model with explicit current droop (i.e. Figure 22)		SVC model with implicit current droop (i.e. transfer-function (35))		Difference	
				(3)-(1)	(4)-(2)
Real	Imag	Real	Imag	Real	Imag
Np/s	rad/s	Np/s	rad/s	Np/s	rad/s
(1)	(2)	(3)	(4)	(5)	(6)
-2.403	10.964	-2.403	10.964	0.000	0.000
-2.038	9.725	-2.038	9.725	0.000	0.000
-2.370	9.644	-2.370	9.644	0.000	0.000
-2.805	8.962	-2.805	8.962	0.000	0.000
-2.494	8.936	-2.494	8.936	0.000	0.000
-2.442	8.370	-2.443	8.370	-0.001	0.000
-2.039	8.379	-2.039	8.379	0.000	0.000
-1.814	7.772	-1.813	7.770	0.001	-0.002
-2.021	7.490	-2.021	7.490	0.000	0.000
-2.029	7.739	-2.030	7.738	-0.001	-0.001
-0.769	3.537	-0.769	3.538	0.000	0.001
-0.447	2.542	-0.446	2.545	0.001	0.003

SVC model with explicit current droop (i.e. Figure 22)		SVC model with implicit current droop (i.e. transfer-function (35))		Difference	
				(3)-(1)	(4)-(2)
Real	Imag	Real	Imag	Real	Imag
Np/s	rad/s	Np/s	rad/s	Np/s	rad/s
(1)	(2)	(3)	(4)	(5)	(6)
-0.431	1.759	-0.431	1.760	0.000	0.001

II.2.3 Large-signal excitation system models and data

II.2.3.1 IEEE Std. 421.5-2005 ST1A Model [16]

The PSS®/E ‘ESST1A’ implementation [1] of the IEEE Std 421.5-2005 ST1A excitation system model [16] is employed in the studies conducted in this report. The model data for the control-system block diagram of the PSS®/E ‘ESST1A’ implementation of the model in Figure 25 is presented in Table 25.

The source of power for generator excitation is the generator stator – consequently the limit on the generator field voltage is proportional to the generator stator voltage. The limit V_{RMAX} is specified such that when a three-phase short-circuit is applied to the high-voltage side of the generator step-up transformer the excitation system is able to produce a factor k times the field voltage which is required to produce rated power output at rated (lagging) power factor and a stator voltage of 1.05 pu. The factor k is, with the following exceptions, 1.5. For the LPS_3 generator $k = 4.5$ and for the TPS_5 and PPS_5 generators $k = 3.0$. These latter values of k are considered to be somewhat (probably unrealistically) high. They are set to these values to ensure that the six base cases in this version of the model are transiently stable. V_{RMIN} is set to $-V_{RMAX}$, V_{AMAX} to V_{RMAX} and V_{AMIN} to V_{RMIN} .

II.2.3.2 IEEE Std. 421.5-2005 AC1A Model [16]

The PSS®/E ‘ESAC1A’ implementation [1] of the IEEE Std 421.5-2005 AC1A excitation system model [16] is employed in the studies conducted in this report. The model data for the control-system block diagram of the PSS®/E ‘ESAC1A’ implementation of the model in Figure 26 is presented in Table 26.

The upper limit on the voltage regulator output (V_{AMAX}) is specified as a factor k times the generator field voltage which is required to produce rated power output at rated (lagging) power factor and a stator voltage of 1.05 pu. For generators EPS_2 and NPS_5 k is 2 and for YPS_3 k is 2.75. The lower limit V_{AMIN} is set to $-V_{AMAX}$. The limits V_{RMAX} and V_{RMIN} are disabled by setting them to large positive and negative values respectively.

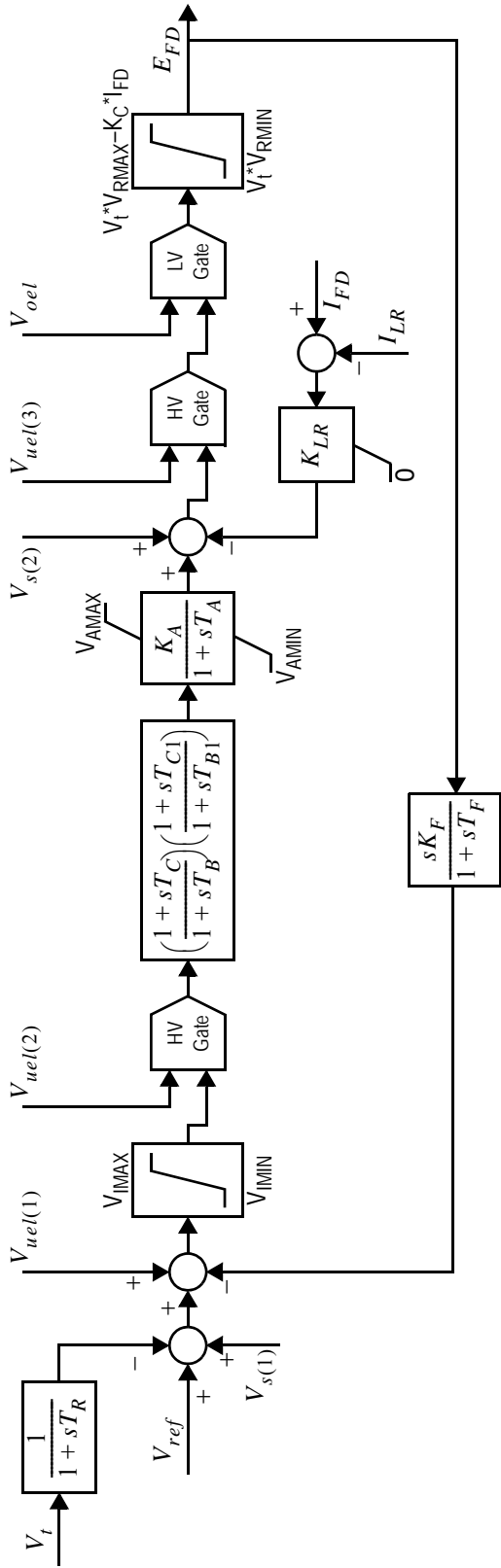


Figure 25 Control-system block diagram of the PSS®/E ‘ESST1A’ implementation [1] of the IEEE Std. 421.5-2005 ST1A model [16] used in the transient-stability studies conducted in this report. (Note: Vs(1) and Vs(2) are alternative inputs from the PSS; Vuel(1), Vuel(2) and Vuel(3) are alternative inputs from the under-excitation-limiter (UEL); and Voel is the input from the over-excitation-limiter. Vt is the generator stator voltage in pu; E_{FD} and I_{FD} are the generator field voltage and current respectively in per-unit as defined in Annex B of [16]) Note that under- and over-excitation limiters are not modelled in this report.

Table 25 Parameter values for the PSS[®]/E ‘ESST1A’ implementation [1] of the IEEE Std. 421.5-2005 ST1A model [16] used in the transient-stability studies conducted in this report.

		Parameter values for generators fitted with ESST1A AVR/exciter models										
Parameter Name		HPS_1	BPS_2	VPS_2	MPS_2	LPS_3	TPS_4	CPS_4	SPS_4	GPS_4	TPS_5	PPS_5
IBUS		101	201	203	204	301	401	402	403	404	502	503
Model/Code	‘ESST1A’	‘ESST1A’	‘ESST1A’	‘ESST1A’	‘ESST1A’	‘ESST1A’	‘ESST1A’	‘ESST1A’	‘ESST1A’	‘ESST1A’	‘ESST1A’	‘ESST1A’
I	‘1’	‘1’	‘1’	‘1’	‘1’	‘1’	‘1’	‘1’	‘1’	‘1’	‘1’	‘1’
UEL ^(a)	1	1	1	1	1	1	1	1	1	1	1	1
VOS ^(b)	1	1	1	1	1	1	1	1	1	1	1	1
T _R (s)	0.0	0.0	0.0	0.0	0.0	0.0	0.0	0.02	0.0	0.0	0.0	0.0
V _{IMAX}	99.0	99.0	99.0	99.0	99.0	99.0	99.0	99.0	99.0	99.0	99.0	99.0
V _{IMIN}	-99.0	-99.0	-99.0	-99.0	-99.0	-99.0	-99.0	-99.0	-99.0	-99.0	-99.0	-99.0
T _C (s)	2.500	0.500	0.350	0.500	1.140	4.000	1.520	0.350	0.136	1.400	0.200	
T _B (s)	13.25	1.12	0.70	1.12	6.42	40.00	9.80	0.70	0.0232	16.0	0.80	
T _{C1} (s)	0.0	0.0	0.0	0.0	0.0	0.0	0.0	0.0	0.0	0.60	0.0	
T _{B1} (s)	0.0	0.0	0.0	0.0	0.0	0.0	0.0	0.0	0.0	0.05	0.0	
K _A	200.0	400.0	300.0	400.0	400.0	300.0	300.0	250.0	400.0	300.0		
T _A (s)	0.10	0.02	0.01	0.02	0.05	0.10	0.05	0.01	0.20	0.50	0.01	
V _{AMAX}	9.5	9.5	10.5	9.5	42.0	13.0	11.0	13.0	11.0	22.0	18.5	
V _{AMIN}	-9.5	-9.5	-10.5	-9.5	-42.0	-13.0	-11.0	-13.0	-11.0	-22.0	-18.5	
V _{RMAX}	9.5	9.5	10.5	9.5	42.0	13.0	11.0	13.0	11.0	22.0	18.5	
V _{RMIN}	-9.5	-9.5	-10.5	-9.5	-42.0	-13.0	-11.0	-13.0	-11.0	-22.0	-18.5	
K _C	0.0	0.0	0.0	0.0	0.0	0.0	0.0	0.0	0.0	0.0	0.0	
K _F	0.0	0.0	0.0	0.0	0.0	0.0	0.0	0.0	0.0	0.0	0.0	
T _F (s)	1.0	1.0	1.0	1.0	1.0	1.0	1.0	1.0	1.0	1.0	1.0	
K _{LR}	0.0	0.0	0.0	0.0	0.0	0.0	0.0	0.0	0.0	0.0	0.0	
I _{LR}	999.0	999.0	999.0	999.0	999.0	999.0	999.0	999.0	999.0	999.0	999.0	

Notes:

- (a) UEL is ignored unless the under-excitation limiter is modelled. UEL = 1 means the output signal from the UEL is connected to Vuel(1); and similarly for UEL = 2 and UEL = 3.
- (b) VOS is ignored unless the PSS is modelled. VOS = 1 means the output signal from the PSS is connected to Vos(1) and similarly for Vos = 2.

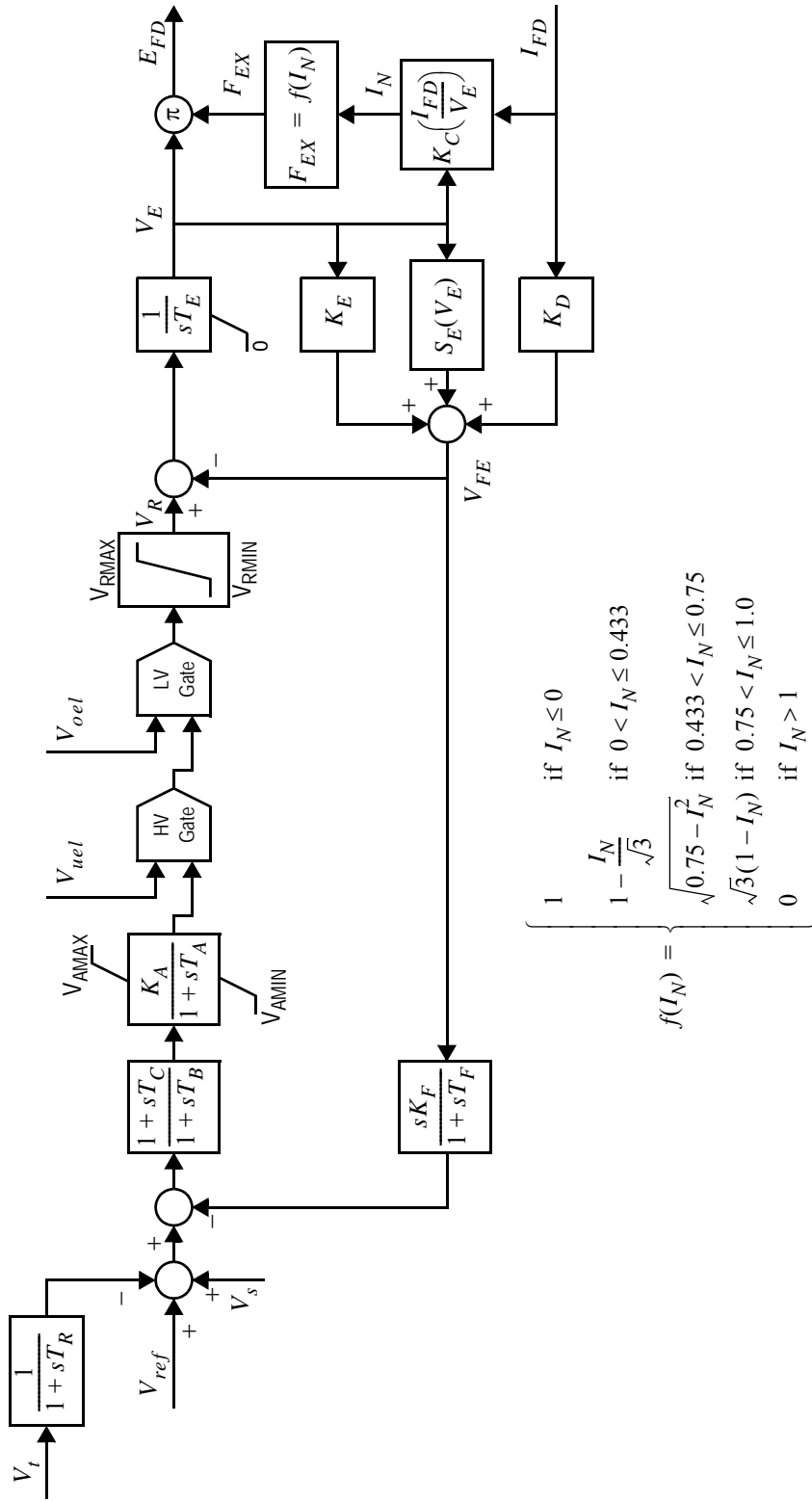


Figure 26 Control-system block diagram of the PSS®/E ‘ESAC1A’ implementation [1] of the IEEE Std. 421.5-2005 AC1A model [16] used in the transient-stability studies conducted in this report. (Note: Vs is the input from the PSS; Vuel is the input from the under-excitation-limiter; and Voel is the input from the over-excitation-limiter. Vt is the generator stator voltage in pu; E_{FD} and I_{FD} are the generator field voltage and current respectively in per-unit as defined in Annex B of [16]. Note that under- and over-excitation limiters are not modelled in this report.)

Table 26 Parameter values for the PSS[®]/E ‘ESAC1A’ implementation [1] of the IEEE Std. 421.5-2005 AC1A model [16] used in the transient-stability studies conducted in this report.

Parameter Name	Parameter values for generators fitted with ESAC1A AVR/exciter models		
	EPS_2	YPS_3	NPS_5
IBUS	202	302	501
Model Code	‘ESAC1A’	‘ESAC1A’	‘ESAC1A’
I	‘1’	‘1’	‘1’
T _R (s)	0.0	0.0	0.0
T _B (s)	0.0	0.0	0.0
T _C (s)	0.0	0.0	0.0
K _A	400.0	200.0	1000.0
T _A (s)	0.02	0.05	0.04
V _{AMAX}	5.5	7.0	5.5
V _{AMIN}	-5.5	-7.0	-5.5
T _E (s)	1.0	1.333	0.87
K _F	0.029	0.02	0.004
T _F (s)	1.0	0.8	0.27
K _C	0.0	0.0	0.0
K _D	0.0	0.0	0.0
K _E	1.0	1.0	1.0
E ₁ ^(a)	0.0	0.0	0.0
S _E (E ₁)	0.0	0.0	0.0
E ₂	0.0	0.0	0.0
S _E (E ₂)	0.0	0.0	0.0
V _{RMAX}	99.0	99.0	99.0
V _{RMIN}	-99.0	-99.0	-99.0
Notes:			
(a) The exciter saturation function is defined by two points, (E ₁ , S _E (E ₁)) and (E ₂ , S _E (E ₂)). In the case of PSS [®] /E exciter saturation is neglected if (E ₁ , S _E (E ₁)) = (0,0) and (E ₂ , S _E (E ₂)) = (0,0). Other programs may have different ways to indicate that exciter saturation is to be neglected.			

II.2.4 Large-signal PSS models and data

II.2.4.1 IEEE 1981 general purpose single-input PSS model [17]

The 1981 report of the IEEE Working Group on Computer Modelling for Excitation Systems [17] recommended a general purpose single-input PSS. This PSS model is implemented in PSS[®]/E as the ‘IEEEEST’ model [1] as shown in the block diagram in Figure 27.

The parameters of the phase-compensation transfer-functions in equations (7) to (10) are transformed to the parameters A₁ to A₆, T₁ to T₆ and K_S of the PSS[®]/E formulation of the PSS transfer-function according to the mappings in Table 27. The parameters for the PSSs contained in Tables 17 to 20 are converted according to the transformations defined in Table 27 to the parameters required by the PSS[®]/E ‘IEEEEST’ model. The resulting PSS[®]/E parameters are listed

in Table 28. Recall from Appendix I.3.1 that for all of the PSSs $T_W = 7.5$ s and $D_e = 20.0$ pu on the machine MVA rating.

Not shown in Figure 27 are the voltage-dependent limits on the output from the PSS[®]/E ‘IEEEEST’ model. These latter limits are disabled by setting the parameters V_{CU} and V_{CL} to zero.

All PSS output limits have been set to +/- 0.1 pu. In this version no attempt has been made to optimize the setting of these limits.

Table 27 Transformation from the PSS parameters in equations (7) to (10) to the PSS parameters in the PSS[®]/E ‘IEEEEST’ PSS model in Figure 27.

PSS [®] /E model Parameter	Eqn. (7)	Eqn. (8)	Eqn. (9)	Eqn. (10)
A_1	$T_g + T_h$	$T_f + T_g$	0.0	$T_e + T_f$
A_2	$T_g \times T_h$	$T_f \times T_g$	0.0	$T_e \times T_f$
A_3	0.0	0.0	0.0	0.0
A_4	0.0	0.0	0.0	0.0
A_5	$T_c + T_d$	a	0.0	a
A_6	$T_c \times T_d$	b	0.0	b
T_1	T_a	T_a	T_a	0.0
T_2	T_e	T_d	T_e	0.0
T_3	T_b	T_b	T_b	0.0
T_4	T_f	T_e	T_f	0.0
T_5			T_W	
T_6			T_W	
K_S			D_e/k_c	

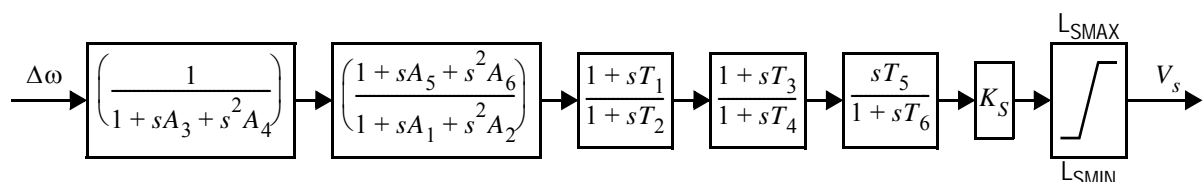


Figure 27 Control-system block diagram of the PSS[®]/E ‘IEEEEST’ implementation [1] of the general-purpose PSS model developed in 1981 by the IEEE Working Group on Computer Modelling for Excitation Systems [17]. This model is used in the transient-stability studies conducted in this report. (Note: $\Delta\omega$ is the rotor-speed perturbation (in pu of synchronous speed) and V_s is the output from the stabilizer which is connected to the AVR reference-input summing junction. The voltage-dependent output limits are not shown and are disabled.)

Table 28 Parameter values for the PSS[®]/E ‘IEEEEST’ implementation [1] of the IEEE 1981 general-purpose PSS model [17] used in the transient-stability studies conducted in this report.

Parameter Name	Parameter Values												
	HPS_1 ^(b)	BPS_2	EPS_2	VPS_2	MPS_2	LPS_3	YPS_3	TPS_4	CPS_4	SPS_4	GPS_4	NPS_5	TPS_5
Eqn / Tab ^(a)	10 / 20	10 / 20	7 / 17	9 / 19	8 / 18	10 / 20	8 / 18	9 / 19	10 / 20	10 / 20	8 / 18	7 / 17	7 / 17
IBUS	101	201	202	203	204	301	302	401	402	403	404	501	502
Model Code	‘IEEEEST’	‘IEEEEST’	‘IEEEEST’	‘IEEEEST’	‘IEEEEST’	‘IEEEEST’	‘IEEEEST’	‘IEEEEST’	‘IEEEEST’	‘IEEEEST’	‘IEEEEST’	‘IEEEEST’	‘IEEEEST’
I	‘1’	‘1’	‘1’	‘1’	‘1’	‘1’	‘1’	‘1’	‘1’	‘1’	‘1’	‘1’	‘1’
ICs	1	1	1	1	1	1	1	1	1	1	1	1	1
IB	0	0	0	0	0	0	0	0	0	0	0	0	0
A ₁	0.01333	0.01333	0.006667	0	0.01333	0.01333	0	0	0.01333	0.01333	0.01333	0.006667	0.01333
A ₂	4.444e-5	4.444e-5	0	0	4.444e-5	4.444e-5	0	0	4.444e-5	4.444e-5	4.444e-5	0	4.444e-5
A ₃	0	0	0	0	0	0	0	0	0	0	0	0	0
A ₄	0	0	0	0	0	0	0	0	0	0	0	0	0
A ₅	0.3725	0.128	0.04	0	0.1	0.1684	0.5091	0	0	0.0909	0.1154	0.3	0.0167
A ₆	0.03845	0.0064	0	0	0.006667	0.006667	0.006667	0	0.006667	0.005917	0.1111	0	0.00334
T ₁	0	0	0.286	0.0708	0.01	0	0.05	0.2083	0.2777	0	0	0.033	0.5
T ₂	0	0	0.006667	0.006667	0	0.006667	0.006667	0	0	0	0	0.006667	0.35
T ₃	0	0	0.111	0.0292	0	0	0	0.2083	0.1	0	0	0.033	0.0588
T ₄	0	0	0.006667	0.006667	0	0	0	0.006667	0.006667	0	0	0.006667	0.0667
T ₅	7.5	7.5	7.5	7.5	7.5	7.5	7.5	7.5	7.5	7.5	7.5	7.5	7.5
T ₆	7.5	7.5	7.5	7.5	7.5	7.5	7.5	7.5	7.5	7.5	7.5	7.5	7.5
K _S	15.38	5.556	4.651	5.714	6.667	12.5	5.97	7.143	4.706	6.329	6.061	3.899	3.559
L _{SMAX}	0.1	0.1	0.1	0.1	0.1	0.1	0.1	0.1	0.1	0.1	0.1	0.1	0.1
L _{SMIN}	-0.1	-0.1	-0.1	-0.1	-0.1	-0.1	-0.1	-0.1	-0.1	-0.1	-0.1	-0.1	-0.1
V _{CU}	0	0	0	0	0	0	0	0	0	0	0	0	0
V _{CL}	0	0	0	0	0	0	0	0	0	0	0	0	0

Notes:

- (a) Eqn / Tab refers respectively to the equation describing the form of the PSS compensation transfer-function and the associated table of parameter values from which the ‘IEEEEST’ model parameters are derived according to the parameter mappings in Table 27.
- (b) The PSS fitted to machine HPS_1 is removed from service in cases 4 & 6 because it is operating as a synchronous condenser; in case 5 the PSS gain KS is negated because it is pumping.

II.3 Network sequence impedance data

In the South East Australian power system three-phase faults on the transmission network are *not* considered to be credible contingencies (except under exceptional circumstances) under the Australian National Electricity Rules [18]. Rather, for planning purposes solid two-phase to ground faults are generally treated as the most severe form of credible contingency. In order to reflect this practice on the simplified 14-generator model of the South East Australian system it is necessary to provide negative and zero sequence impedance data for the network so that the equivalent fault impedances required to represent two-phase to ground faults can be computed.

II.3.1 Transmission lines

It is assumed that the three-phase system is balanced and consequently the negative-sequence impedance of transmission lines are identical to the positive-sequence impedances listed in [Table 10](#). The zero-sequence impedances are deemed to be 2.5 times the corresponding positive-sequence impedance. This multiplying factor is based on “rules-of-thumb” on the relationships between positive- and zero-sequence impedances on page 884 of [13].

Mutual coupling between transmission circuits is neglected.

II.3.2 Transformers

Since it is assumed that the three-phase system is balanced the negative-sequence impedances of the transformers are identical to the positive sequence impedances listed in [Table 11](#).

All generator step-up transformers are assumed to have a delta/grounded-star connection with the delta on the generator side. The neutral of the high-voltage windings is solidly grounded. Consequently, there is no path for the flow of zero-sequence currents from the generator to the network. For the generator step-up transformers the zero-sequence impedances are identical to the corresponding positive-sequence impedances listed in [Table 11](#).

All other network transformers, such as those between buses 315 and 308, are assumed to have a delta/delta connection. The implication is that there is no path for the flow of zero-sequence currents from the delta windings into the lines and thus viewed from either terminal the zero-sequence impedance is infinite. Although three-winding transformers are often employed in practice, it is considered an unnecessary complication for the purpose of this benchmark study system.

II.3.3 Generators

As discussed in Section 13.4.2 (pg. 877) of [13], if only the fundamental frequency component of the negative-sequence current produced by impressing a balanced set of fundamental frequency negative-phase sequence voltages on the stator terminals of a generator is considered the effective negative-sequence reactance of the generator is found to be:

$$X_2 = 2 \frac{X_d'' X_q''}{X_d'' + X_q''} \quad (36)$$

Since we are neglecting saliency of sub-transient reactances (i.e. $X_q'' = X_d''$) it follows that $X_2 = X_d''$. Thus, for the generators, the negative-sequence impedances are identical to the d-axis sub-transient reactances listed in [Table 15](#).

Since we are concerned only with faults on the high-voltage side of the generator step-up transformers; and since the generator step-up transformers have a delta/grounded-star connection the generator zero-sequence impedances of the generators are irrelevant and so we do not propose values for them.

II.3.4 Loads

All loads are represented as an equivalent impedance in the negative-sequence network; and as an infinite impedance in the zero-sequence network.

II.4 Effective negative and zero sequence admittances at network buses

For the purpose of representing an unbalanced fault in a transient stability study it is usual practice to represent the effect of the negative- and zero-sequence networks by their equivalent admittances (Y_2 and Y_0) as seen at the fault location [13]. These admittances (or impedances) are combined depending on the type of fault and the resulting effective fault admittance (Y_{fe}) is connected at the fault location in the detailed positive-phase sequence representation of the network for the duration of the fault. The fault is cleared by removing the effective fault admittance and (possibly) disconnecting the faulted network element (e.g. transmission line or transformer). It should be noted that this study system does not include models of generator turbines and governors and therefore, events involving the loss of generation or load should not be simulated.

The effective fault admittance for a two-phase to ground fault is given by $Y_{fe} = Y_2 + Y_0$; and

$$\text{for a single-phase to ground fault it is: } Y_{fe} = \frac{Y_2 Y_0}{Y_2 + Y_0}.$$

The negative- and zero-sequence admittances seen from all of the high-voltage buses in the system are listed in Tables 29 & 30 respectively for each of the six study cases. These admittances are computed with the PSS®/E program based on the sequence impedance data in Appendix II.3.

The effective fault admittances for a solid two-phase to ground fault at each of the high-voltage buses in the system are listed in Table 31 for the six study cases. This data is intended to assist researchers to benchmark the system model in other simulation tools and, for users who do not have access to software capable of analysing sequence networks.

Table 29 Equivalent negative-sequence admittances at transmission network nodes.

BusID	Equivalent negative sequence admittance (pu on 100 MVA)						Case	
	1	2	3	4	5	6		
	G	B	G	B	G	B	G	B
102	16.965	-79.65	15.725	-70.544	17.434	-147.54	13.45	-61.791
205	7.5511	-30.363	7.0619	-29.959	8.0742	-30.446	6.1675	-29.198
206	24.099	-183.25	23.19	-159.72	25.85	-181.32	20.106	-143.08
207	41.504	-142.34	36.879	-126.18	43.826	-132.26	30.163	-116.81
208	34.256	-137.15	30.856	-118.7	34.781	-114.42	25.995	-113.29
209	29.666	-157.06	27.436	-135.23	32.072	-152.39	22.98	-119.83
210	14.971	-97.353	15.009	-90.226	16.055	-96.267	13.195	-82.264
211	46.608	-113.61	40.68	-103.87	48.316	-106.81	32.791	-97.045
212	42.098	-102.93	37.239	-96.459	44.531	-101.26	29.857	-89.012
213	17.17	-88.871	16.681	-82.937	17.937	-88.755	14.461	-76.967
214	31.477	-103.74	28.791	-95.659	32.733	-104.77	23.933	-88.89
215	23.874	-165.72	21.818	-129.41	23.79	-168.37	18.927	-128.56
216	34.128	-88.128	29.99	-82.114	35.596	-90.964	24.227	-77.37
217	30.531	-90.366	27.086	-82.905	31.634	-103.49	22.385	-77.517
303	32.186	-140.23	30.726	-155.54	33.606	-159.96	27.299	-124.57
304	36.54	-95.185	35.02	-101.49	39.644	-106.24	29.553	-84.939
305	47.209	-101.19	45.86	-108.42	52.707	-113.74	37.169	-90.083
306	41.236	-87.168	39.81	-92.449	45.62	-96.344	32.836	-78.679
307	41.977	-88.051	40.513	-93.493	46.427	-97.458	33.454	-79.374
308	15.482	-39.026	14.359	-39.981	15.854	-40.595	13.868	-36.921
309	12.572	-54.639	12.233	-52.388	12.757	-67.072	11.101	-48.394
310	118.16	-119.98	129.85	-138.51	148.58	-130.97	84.199	-113.25
311	14.278	-62.688	13.185	-63.049	14.415	-68.943	12.74	-57.435
312	13.345	-65.999	12.989	-78.329	14.323	-79.422	10.957	-53.35
313	37.023	-73.143	36.782	-79.3	42.284	-80.882	27.167	-64.75
314	30.037	-70.831	29.026	-75.344	32.999	-77.563	23.24	-63.312
315	8.6531	-29.653	7.2494	-28.361	8.1737	-30.406	7.7893	-28.183
405	17.405	-84.43	20.214	-85.113	20.217	-85.121	14.456	-58.198
406	11.907	-68.179	13.877	-68.548	13.879	-68.551	10.69	-55.563

BusID	Equivalent negative sequence admittance (pu on 100 MVA)					
	Case					
1	2	3	4	5	6	
G	B	G	B	G	B	G
407	10.191	-75.287	11.857	-75.728	11.858	-75.731
408	7.1565	-59.856	7.9054	-60.244	7.9093	-60.253
409	10.429	-30.954	11.448	-31.442	11.453	-31.453
410	23.738	-67.921	27.597	-69.561	27.736	-69.667
411	20.345	-40.669	23.853	-41.424	23.889	-41.461
412	23.206	-43.332	27.478	-43.914	27.529	-43.957
413	6.2368	-32.806	6.5949	-33.126	6.7649	-33.269
414	5.7672	-31.562	6.0586	-31.834	6.2372	-31.981
415	4.8186	-27.582	4.9204	-27.677	5.1492	-27.856
416	4.8979	-25.878	4.7868	-25.761	5.2026	-26.039
504	16.449	-38.182	13.317	-39.793	16.765	-40.769
505	14.636	-54.83	10.25	-54.506	13.952	-58.094
506	14.181	-51.57	10.225	-53.859	14.216	-59.972
507	19.541	-54.41	13.684	-55.491	19.571	-60.109
508	19.041	-47.291	13.762	-48.271	18.908	-51.387
509	6.372	-21.723	4.8856	-21.055	5.4178	-21.97

Table 30 Equivalent zero-sequence admittances at transmission network nodes.

BusID	Case											
	1	2	3	4	5	6						
G	B	G	B	G	B	G	B					
102	1.66334	-124.68	1.6301	-96.752	1.6558	-346.86	1.6275	-68.967	1.6249	-96.727	1.6	-68.845
205	1.2262	-10.016	1.2136	-9.9582	1.2258	-10.015	1.1972	-9.8786	1.2132	-9.9572	1.1741	-9.7606
206	4.8793	-291.8	4.6429	-249.09	4.7078	-290.91	4.5569	-207.07	4.5258	-248.49	4.4645	-164.99
207	10.666	-107.71	9.5677	-101.44	9.5527	-100.16	8.7957	-96.979	8.9301	-96.886	8.6251	-96.22
208	5.5817	-179.14	5.3427	-145.37	5.5978	-113.84	5.0306	-143.86	5.3427	-112.69	4.9157	-143.39
209	4.3886	-212.28	4.1447	-176.31	3.9155	-209.51	4.093	-141.38	3.8607	-174.59	4.0155	-141.07
210	0	0	0	-0	0	0	0	0	0	0	0	0
211	7.458	-68.53	6.9751	-65.831	6.748	-63.469	6.8158	-65.223	6.5425	-62.679	6.7023	-64.775
212	6.7248	-58.269	6.4218	-56.842	6.3896	-56.246	6.2525	-56.149	6.196	-55.491	6.132	-55.65
213	0	0	0	-0	0	0	0	0	0	0	0	0
214	4.7418	-40.019	4.5585	-39.192	4.7095	-39.705	4.4867	-38.902	4.4964	-38.824	4.3831	-38.451
215	3.6439	-280.78	3.5428	-197.01	3.7125	-281.04	3.407	-196.4	3.5187	-196.9	3.3288	-154.36
216	4.7708	-40.306	4.5459	-39.285	4.7831	-40.269	4.4814	-39.024	4.5111	-39.093	4.3287	-38.305
217	5.6728	-50.5	5.2859	-48.647	6.2433	-53.034	4.9161	-46.68	5.2618	-48.521	4.7906	-46.092
303	0	291.55	0	333.33	0	333.33	0	-250	0	333.33	0	-250
304	2.9847	-50.887	3.1198	-52.022	3.1198	-52.022	2.8188	-49.458	3.1198	-52.022	2.8188	-49.458
305	3.2288	-57.702	3.3952	-59.166	3.3952	-59.166	3.0265	-55.87	3.3952	-59.166	3.0265	-55.87
306	2.7379	-46.815	2.8515	-47.773	2.8515	-47.773	2.5974	-45.602	2.8515	-47.773	2.5974	-45.602
307	2.7664	-47.597	2.8832	-48.588	2.8832	-48.588	2.6221	-46.344	2.8832	-48.588	2.6221	-46.344
308	1.0749	-16.172	1.09	-16.285	1.09	-16.285	1.0553	-16.025	1.09	-16.285	1.0553	-16.025
309	2.3346	-22.001	2.1431	-20.94	2.9105	-24.777	1.8751	-19.266	2.1426	-20.939	1.8715	-19.256
310	0.87866	-7.3537	0.85297	-7.2316	0.94362	-7.6393	0.81204	-7.0213	0.85291	-7.2314	0.81153	-7.0201
311	0	0	0	-0	0	0	0	0	0	0	0	0
312	0	-88.739	0	-118.35	0	-118.35	0	-59.18	0	-88.739	0	-59.18
313	2.0803	-20.299	2.3404	-21.516	2.3404	-21.516	1.6754	-18.236	2.0803	-20.299	1.6754	-18.236
314	1.6477	-16.158	1.8087	-16.92	1.8087	-16.92	1.3844	-14.824	1.6477	-16.158	1.3844	-14.824
315	0.37366	-2.7786	0.37449	-2.784	0.37519	-2.7882	0.36865	-2.7317	0.37146	-2.7608	0.36668	-2.7548
405	2.1525	-141.69	2.1525	-141.69	2.1525	-141.69	2.0122	-82.022	2.1525	-122.08	1.9682	-81.597
406	3.6302	-71.835	3.6302	-71.835	3.6302	-71.835	2.8993	-63.28	3.5894	-71.524	2.3291	-53.908

BusID	Equivalent zero sequence admittance (pu on 100 MVA)					
	Case					
1	2	3	4	5	6	
G	B	G	B	G	B	G
407	1.4574	-138.16	1.4574	-138.16	1.2668	-107.08
408	1.7902	-79.409	1.7902	-79.409	1.6737	-59.147
409	2.1169	-16.351	2.1169	-16.351	1.978	-15.783
410	1.0002	-128.22	1.0002	-128.22	0.94342	-98.297
411	2.1582	-26.807	2.1582	-26.807	1.9781	-25.513
412	2.3017	-31.925	2.3017	-31.925	2.0653	-29.987
413	1.0408	-14.303	1.0408	-14.303	0.98054	-13.834
414	0.39389	-4.0498	0.39231	-4.0402	0.39383	-4.0496
415	0.46309	-4.6406	0.46095	-4.6281	0.46301	-4.6404
416	0.6783	-6.3433	0.67397	-6.3199	0.67815	-6.3429
504	7.7156	-55.425	7.9791	-55.638	8.1862	-55.798
505	3.4127	-86.355	3.434	-87.54	3.4618	-88.472
506	3.5219	-66.144	3.5219	-76.144	3.5219	-86.132
507	5.1748	-60.311	5.3215	-62.982	5.4662	-65.197
508	11.301	-45.26	11.478	-46.281	11.628	-47.094
509	0.45004	-3.3764	0.45126	-3.3844	0.45227	-3.3906

Table 31 Equivalent two-phase to ground fault admittances at transmission network nodes.

BusID	Equivalent two phase to ground fault admittance (pu on 100 MVA)						Case
	1	2	3	4	5	6	
G	B	G	B	G	B	G	B
102	18.628	-204.33	17.355	-167.3	19.09	-494.4	15.078
205	8.7773	-40.379	8.2755	-39.917	9.3	-40.461	7.3647
206	28.979	-475.05	27.833	-408.81	30.558	-472.23	24.663
207	52.17	-250.05	46.447	-227.62	53.378	-232.42	38.959
208	39.838	-316.29	36.199	-264.07	40.379	-228.26	31.026
209	34.054	-369.34	31.581	-311.54	35.988	-361.9	27.073
210	14.971	-97.353	15.009	-90.226	16.055	-96.267	13.195
211	54.066	-182.14	47.655	-169.71	55.064	-170.28	39.607
212	48.822	-161.19	43.66	-153.3	50.92	-157.51	36.109
213	17.17	-88.871	16.681	-82.937	17.937	-88.755	14.461
214	36.219	-143.76	33.349	-134.85	37.442	-144.47	28.42
215	27.517	-446.5	25.361	-326.42	27.503	-449.42	22.334
216	38.898	-128.43	34.536	-121.4	40.379	-131.23	28.708
217	36.204	-140.87	32.371	-131.55	37.877	-156.52	27.301
303	32.186	-431.77	30.726	-488.87	33.606	-493.29	27.299
304	39.525	-146.07	38.14	-153.51	42.764	-158.27	32.372
305	50.438	-158.89	49.255	-167.59	56.102	-172.9	40.196
306	43.974	-133.98	42.662	-140.22	48.471	-144.12	35.433
307	44.744	-135.65	43.397	-142.08	49.31	-146.05	36.076
308	16.557	-55.198	15.449	-56.265	16.944	-56.88	14.923
309	14.907	-76.64	14.376	-73.329	15.667	-91.849	12.976
310	119.04	-127.33	130.71	-145.74	149.53	-138.61	85.011
311	14.278	-62.688	13.185	-63.049	14.415	-68.943	12.74
312	13.345	-154.74	12.989	-196.68	14.323	-197.77	10.957
313	39.104	-93.442	39.122	-100.82	44.625	-102.4	28.843
314	31.685	-86.989	30.834	-92.264	34.808	-94.483	24.625
315	9.0268	-32.431	7.6239	-31.145	8.5488	-33.194	8.158
405	19.558	-226.12	22.366	-226.8	22.37	-226.81	16.468
406	15.537	-140.01	17.507	-140.38	17.509	-140.39	13.589

BusID	Equivalent two phase to ground fault admittance (pu on 100 MVA)					
	Case					
1	2	3	4	5	6	
G	B	G	B	G	B	G
407	11.648	-213.45	13.314	-213.89	13.316	-213.89
408	8.9466	-139.26	9.6955	-139.65	9.6994	-139.66
409	12.546	-47.305	13.565	-47.793	13.57	-47.804
410	24.738	-196.14	28.597	-197.78	28.736	-197.89
411	22.504	-67.475	26.011	-68.231	26.048	-68.268
412	25.507	-75.257	29.778	-75.839	29.831	-75.882
413	7.2776	-47.109	7.6357	-47.429	7.8056	-47.571
414	6.1611	-35.611	6.4509	-35.874	6.631	-36.031
415	5.2817	-32.222	5.3813	-32.305	5.6122	-32.496
416	5.5762	-32.221	5.4607	-32.08	5.8808	-32.382
504	24.165	-93.608	21.296	-95.43	24.952	-96.567
505	18.049	-141.19	13.684	-142.05	17.414	-146.57
506	17.703	-117.71	13.746	-130	17.738	-146.1
507	24.716	-114.72	19.005	-118.47	25.038	-125.31
508	30.342	-92.551	25.24	-94.552	30.535	-98.481
509	6.822	-25.099	5.3368	-24.439	5.8701	-25.36

Appendix III Benchmark comparison between Mudpack and PSS[®]/E models of the 14-generator system

The small-signal stability analysis in this report is conducted with Mudpack [14]. Mudpack is an interactive software package for investigating the small-signal dynamic performance of large multi-machine power systems. It forms the linearized differential and algebraic equations of the power system based on an exact analytical evaluation of the partial derivatives of the non-linear system equations, rather than on the numerical estimation methods used in some other tools. Based on the linearized system model Mudpack computes and graphically displays the eigenvalues, mode-shapes, participation factors; computes and graphically displays time- and frequency-responses; computes and graphically displays transfer-function residues and performs a number of other specialized tasks associated with the tuning of stabilizers and investigation of the interactions between stabilizers and generators.

We employ the widely used PSS[®]/E software package [1] for power flow and transient stability analysis.

As a precursor to performing transient stability studies on the simplified 14-generator model of South East Australian power system we establish through a number of benchmark tests that the small-signal performance of the PSS[®]/E model of the system agrees closely with that of the Mudpack model.

As stated in [Appendix II.2.1.1](#) in PSS[®]/E the frequency dependence of network parameters is represented by setting the simulation parameter NETFRQ = 1. This ensures that a consistent formulation of the generator rotor equations of motion in PSS[®]/E.

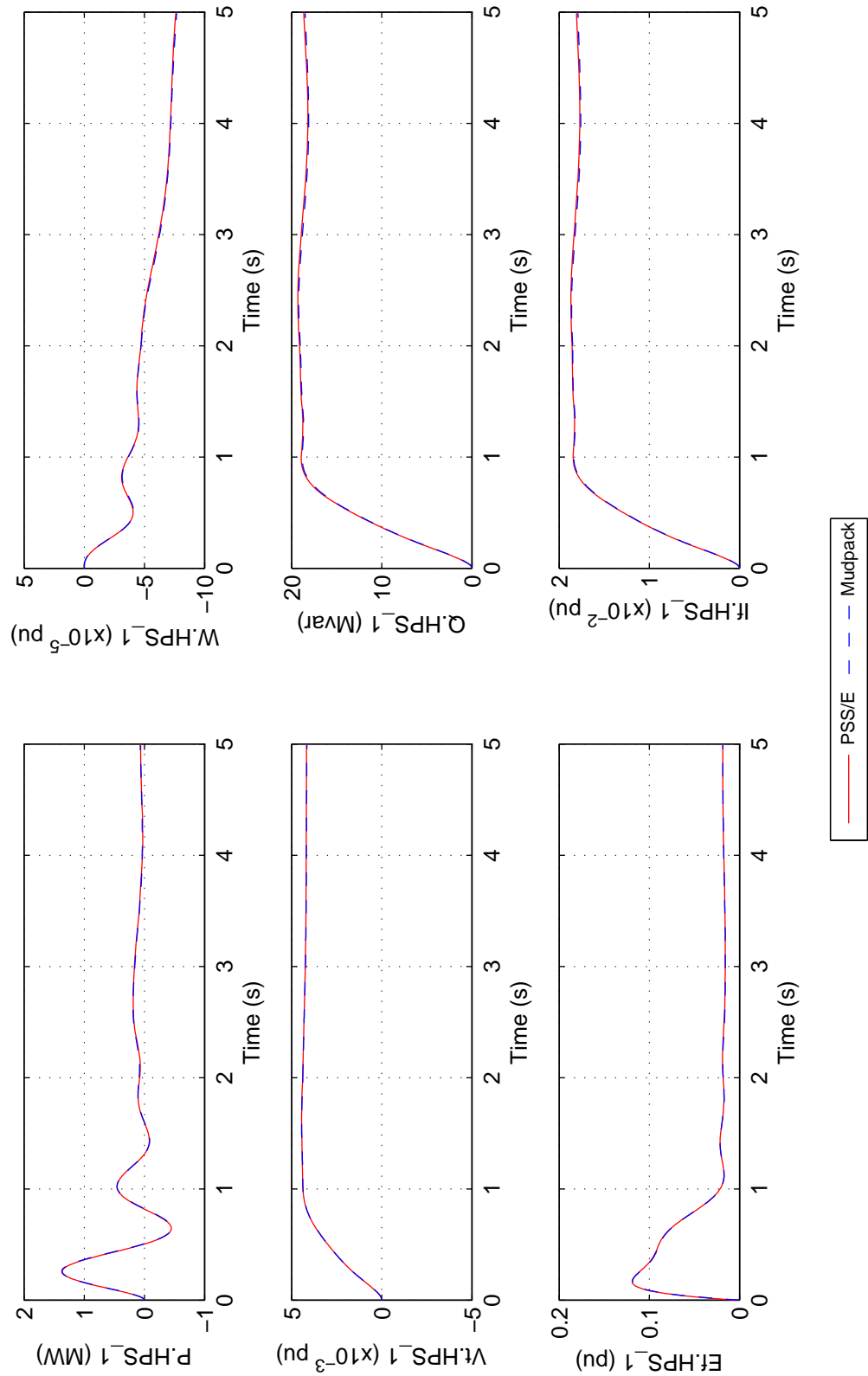
All benchmark studies are conducted with the PSSs in-service with their design damping gain of $D_e = 20$ pu on the machine MVA rating. (Comparison of PSS[®]/E and Mudpack responses with the PSSs out-of-service is ill-advised because the system is unstable without PSSs. Consequently, non-linear behaviour of the system will play a significant role in the PSS[®]/E step responses as the oscillations grow in amplitude.)

III.1 Generator voltage-reference step-responses

For study case 1, with all PSSs in service at their design damping gain of 20.0 pu, a 0.5% step increase in the voltage reference is applied to the AVR of generator HPS_1 and the *perturbations* in the power output (P), rotor-speed (W), stator-voltage (V_t), reactive-power output (Q), generator field voltage (E_f) and generator field current (I_f) are monitored. This test is conducted in both PSS[®]/E and Mudpack. As shown in [Figure 28](#) the responses obtained with the two packages are practically identical. Such voltage-reference step-response tests are useful in verifying that the local mode behaviour obtained with the respective simulation packages are consistent.

Similar tests have been performed for all 14 generators in all six study cases and there is similarly very close agreement between the PSS[®]/E and Mudpack responses. A selection of these results is presented in Figures [29](#) to [41](#). A complete set of the $14 \times 6 = 84$ plots is provided in the form of a PDF file as part of the DataPackage. Furthermore, to aid the reader in benchmarking their own implementation of the model, the step-response time-series data is also provided in the DataPackage for a selection of the voltage-reference step-response tests.

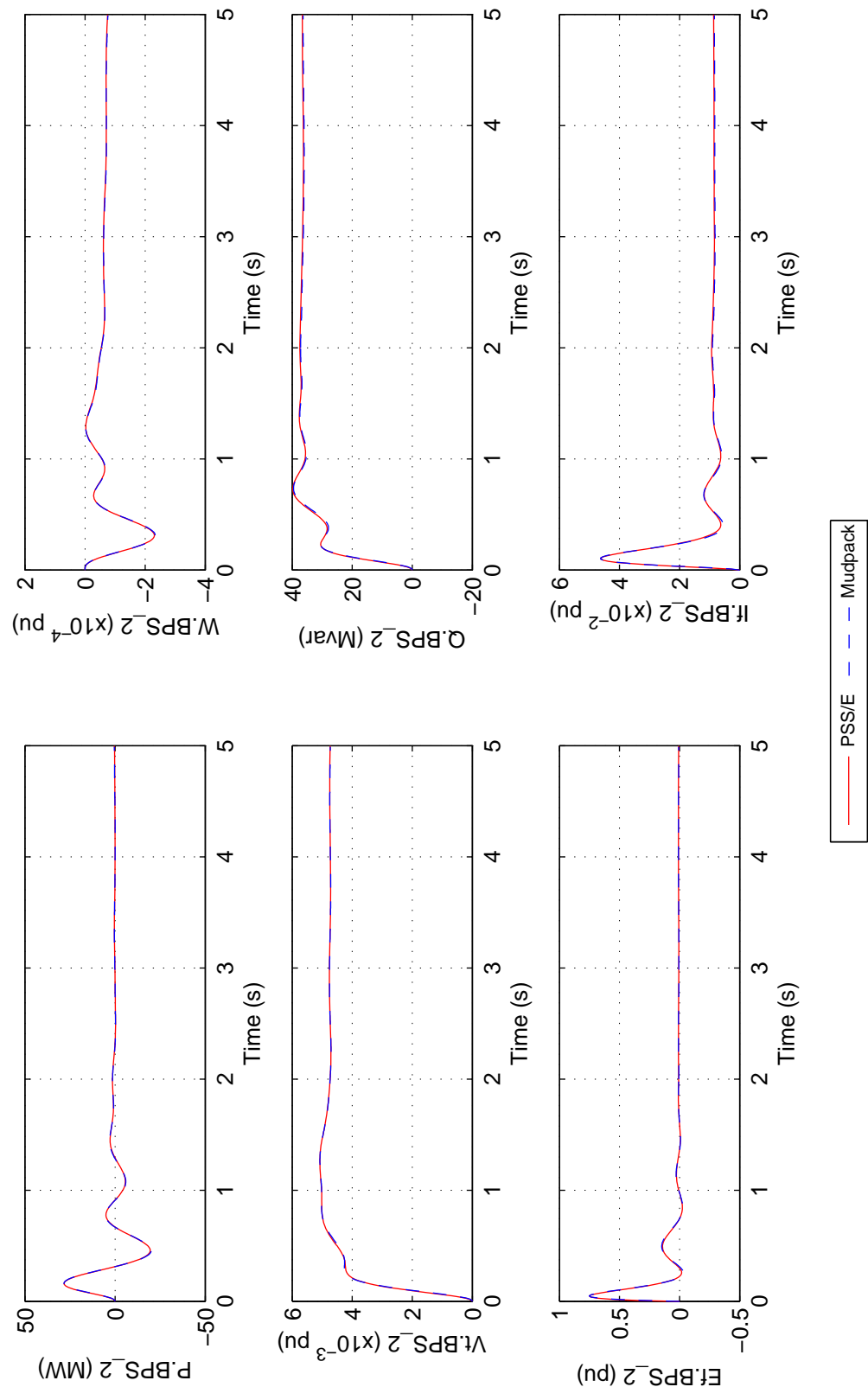
The University of Adelaide, Mudpack Scripts
 Simplified Australian System; Benchmark PSS/E & Mudpack;
 Case01_NETFRQ_VrefStep_HPS_1; 0.5% step on Vref.HPS_1;



File: CMP_Case01_NETFRQ_VrefStep_HPS_1.eps
 Mon, 17-Feb-2014 22:35:15

Figure 28 Case 1, Vref.HPS_1 step-response benchmark comparison between PSS[®]/E (with NETFRQ = 1) and Mudpack. A 0.5% step increase in the voltage-reference of the AVR of generator HPS_1 is applied and the perturbations in the electrical power output (P), rotor-speed (W), stator-voltage (Vt), reactive-power output (Q), generator field-voltage (Ef) and field-current (If) of HPS_1 are compared.

The University of Adelaide, Mudpack Scripts
 Simplified Australian System; Benchmark PSS/E & Mudpack;
 Case02_NETFRQ_VrefStep_BPS_2; 0.5% step on Vref.BPS_2;



File: CMP_Case02_NETFRQ_VrefStep_BPS_2.eps
 Mon, 17-Feb-2014 23:28:53

Figure 29 As for Figure 28 but for Case 2 and generator BPS_2.

The University of Adelaide, Mudpack Scripts
 Simplified Australian System; Benchmark PSS/E & Mudpack;
 Case03_NETFRQ_VrefStep_EPS_2; 0.5% step on Vref.EPS_2;

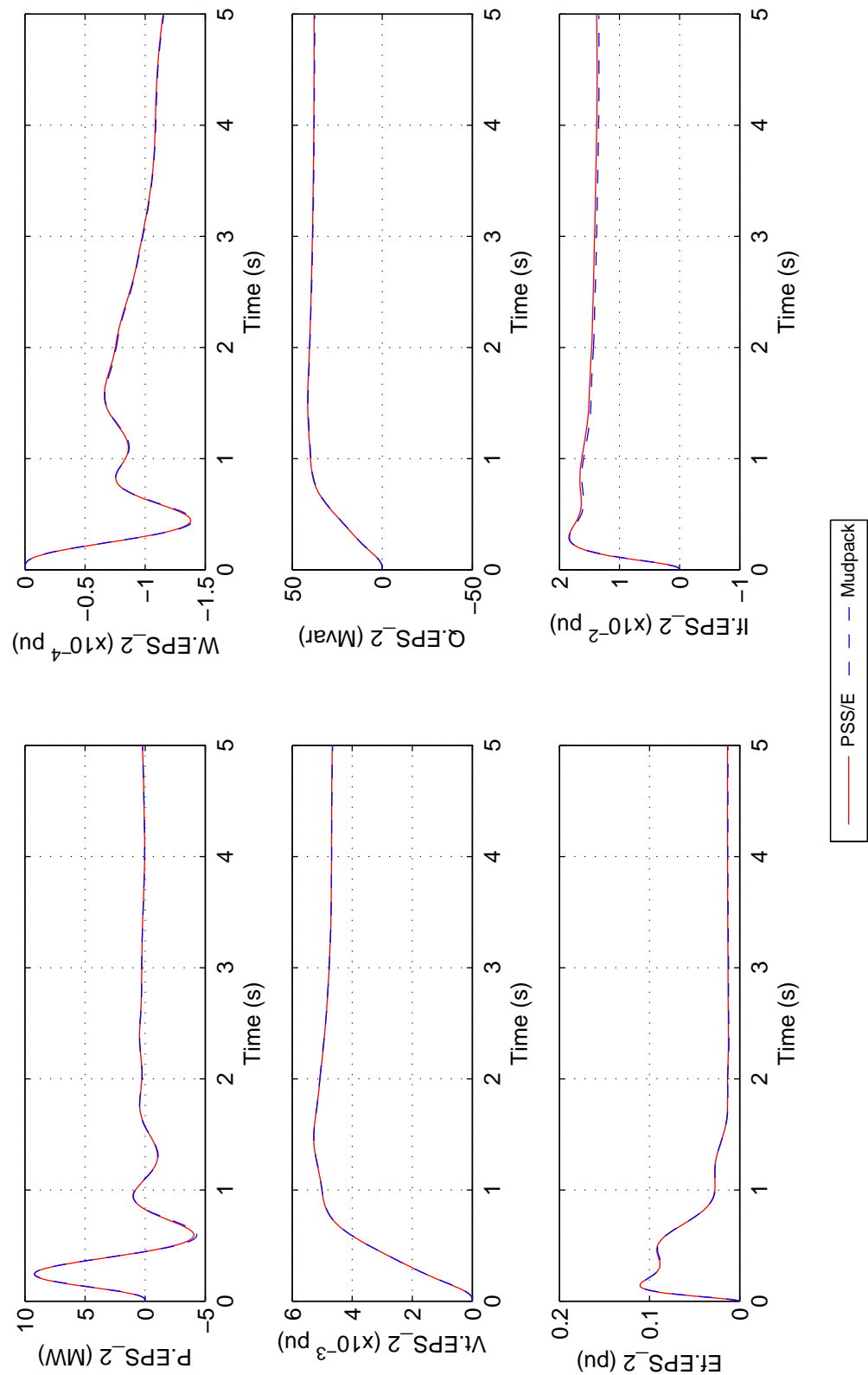


Figure 30 As for Figure 28 but for Case 3 and generator EPS_2.

File: CMP_Case03_NETFRQ_VrefStep_EPS_2.eps
 Tue, 18-Feb-2014 06:38:22

The University of Adelaide, Mudpack Scripts
 Simplified Australian System; Benchmark PSS/E & Mudpack;
 Case04_NETFRQ_VrefStep_VPS_2; 0.5% step on Vref.VPS_2;

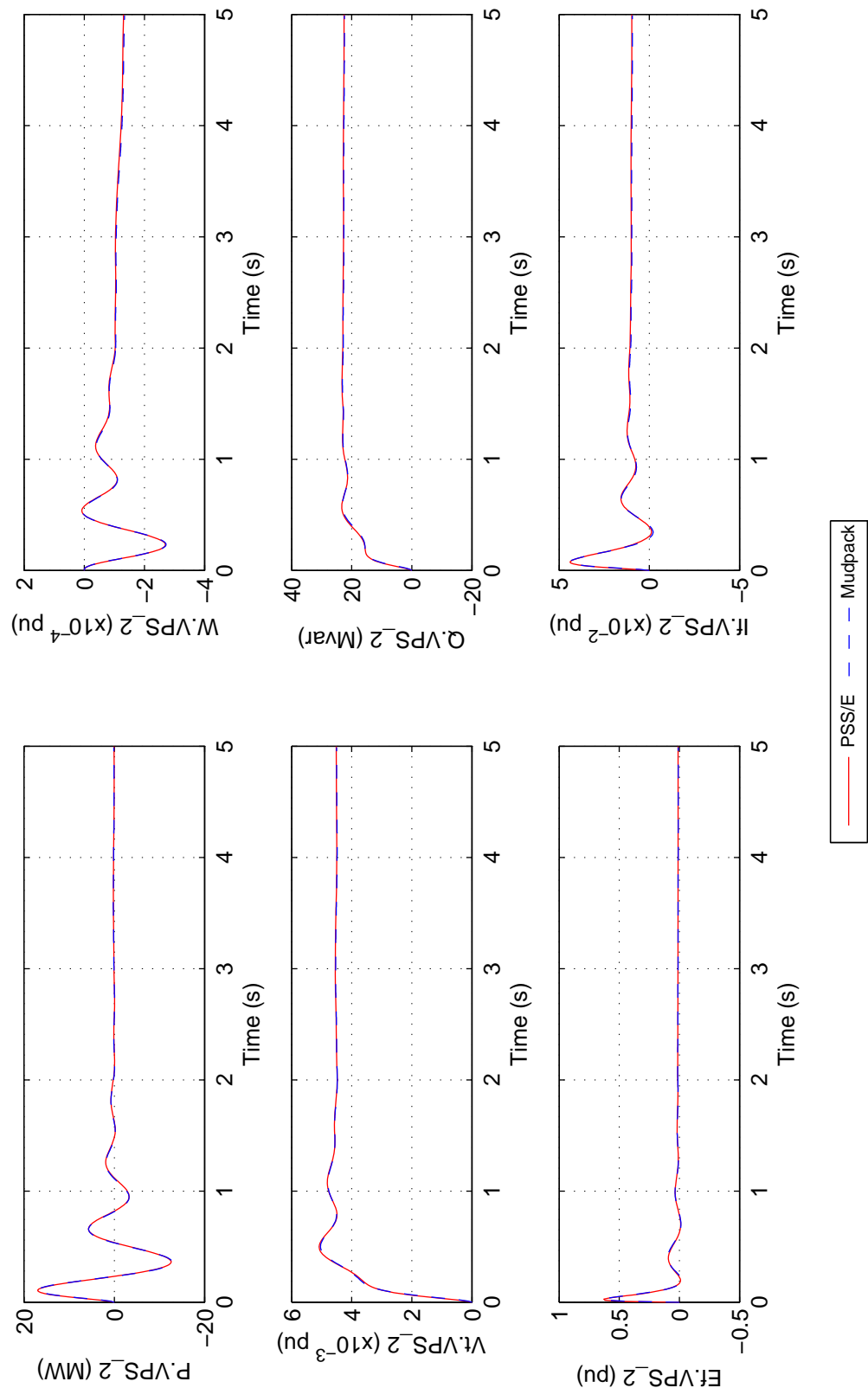
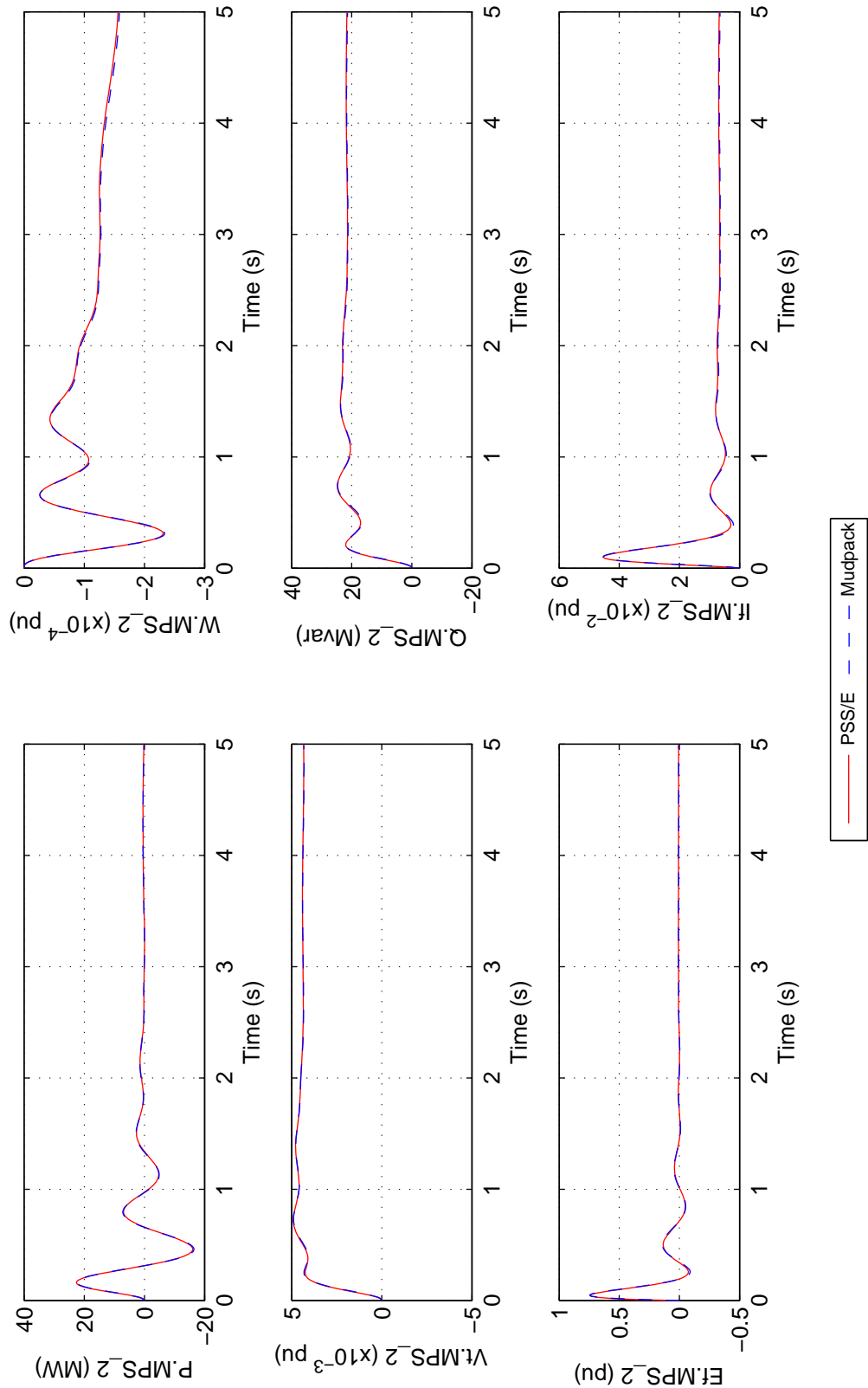


Figure 31 As for Figure 28 but for Case 4 and generator VPS_2.

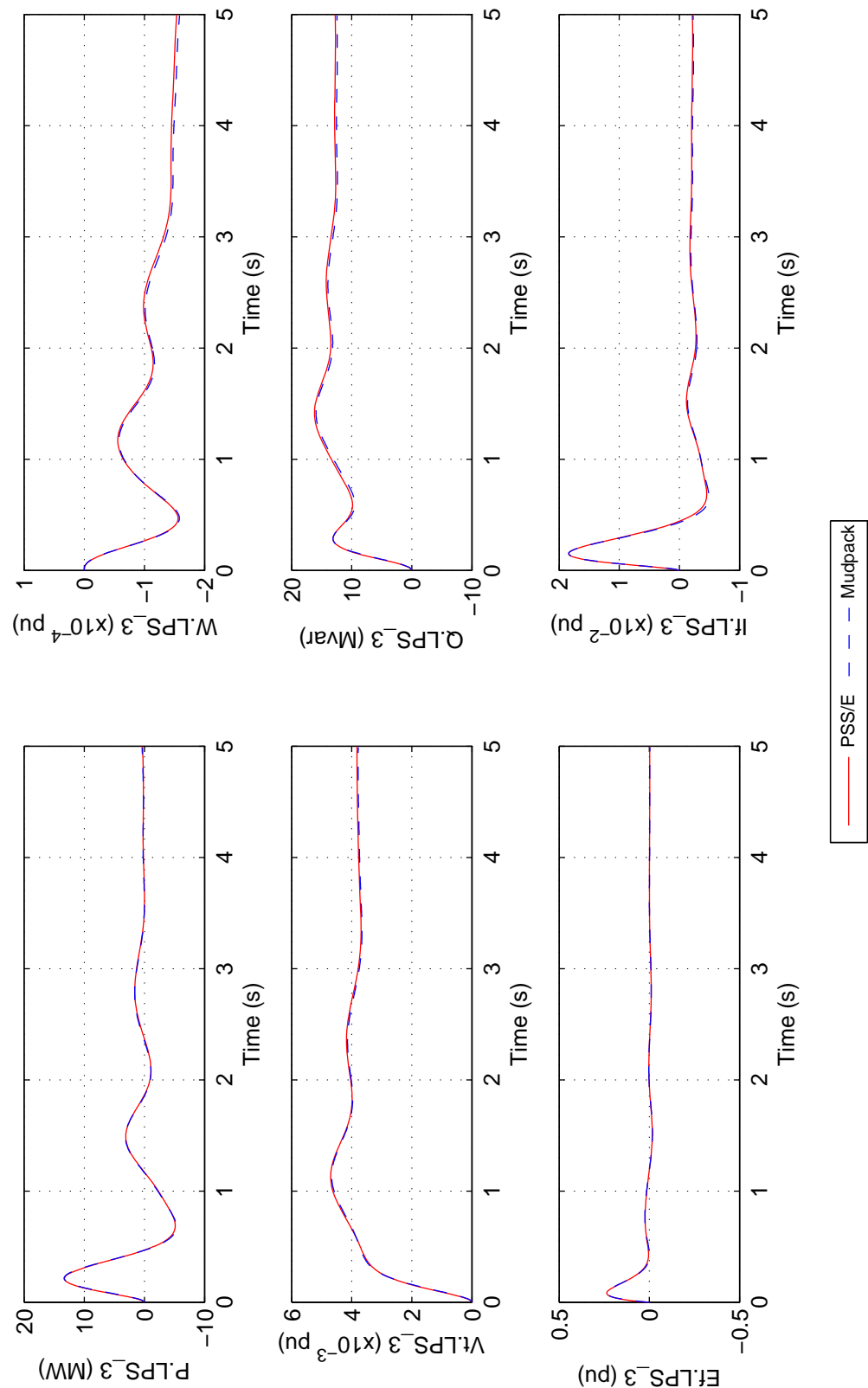
The University of Adelaide, Mudpack Scripts
 Simplified Australian System; Benchmark PSS/E & Mudpack;
 Case05_NETFRQ_VrefStep_MPS_2; 0.5% step on Vref.MPS_2;



File: CMP_Case05_NETFRQ_VrefStep_MPS_2.eps
 Tue, 18-Feb-2014 06:42:11

Figure 32 As for Figure 28 but for Case 5 and generator MPS_2.

The University of Adelaide, Mudpack Scripts
 Simplified Australian System; Benchmark PSS/E & Mudpack;
 Case06_NETFRQ_VrefStep_LPS_3; 0.5% step on Vref.LPS_3;



File: CMP_Case06_NETFRQ_VrefStep_LPS_3.eps
 Tue, 18-Feb-2014 06:44:11

Figure 33 As for Figure 28 but for Case 6 and generator LPS_3.

The University of Adelaide, Mudpack Scripts
 Simplified Australian System; Benchmark PSS/E & Mudpack;
 Case01_NETFRQ_VrefStep_YPS_3; 0.5% step on Vref.YPS_3;

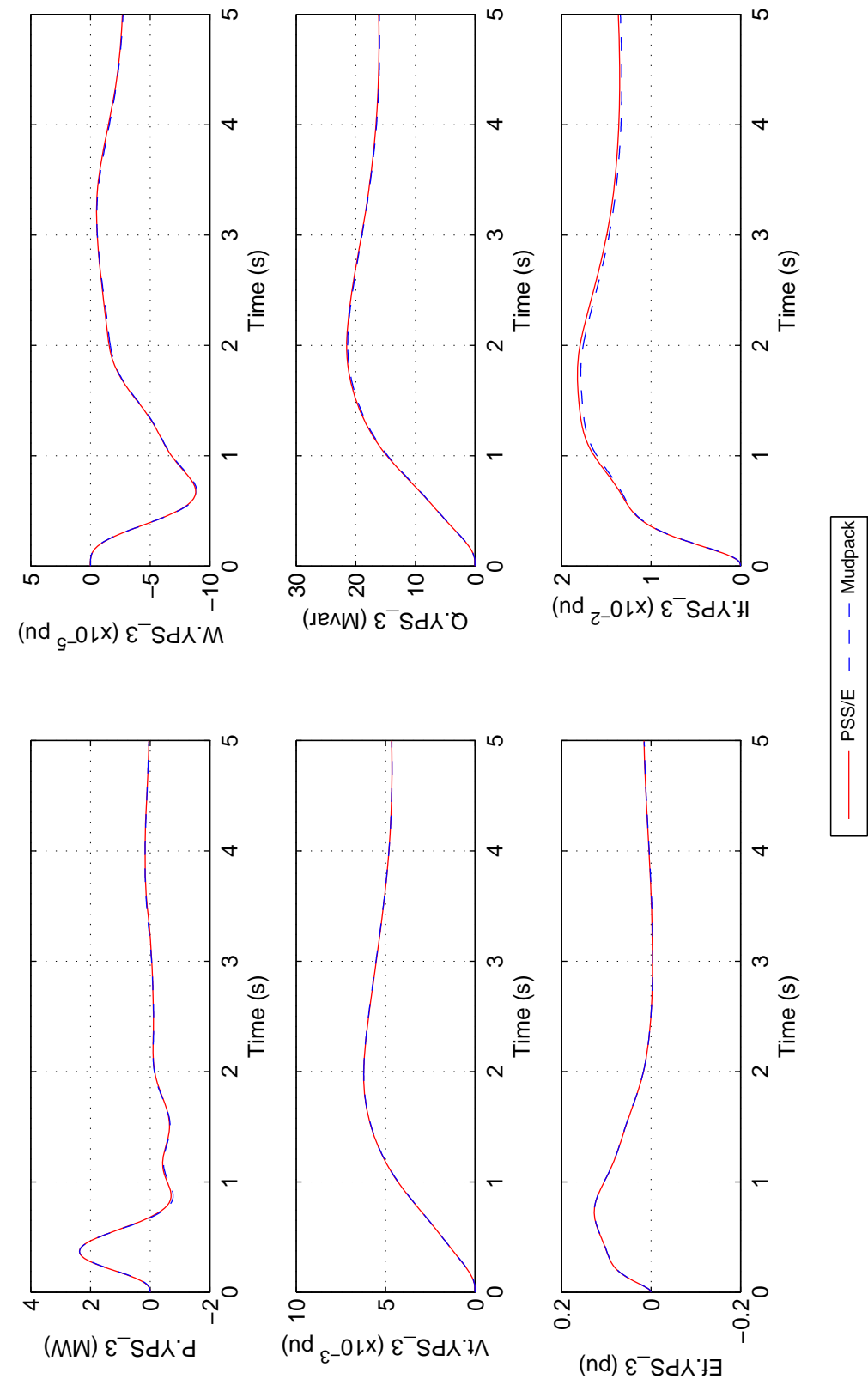
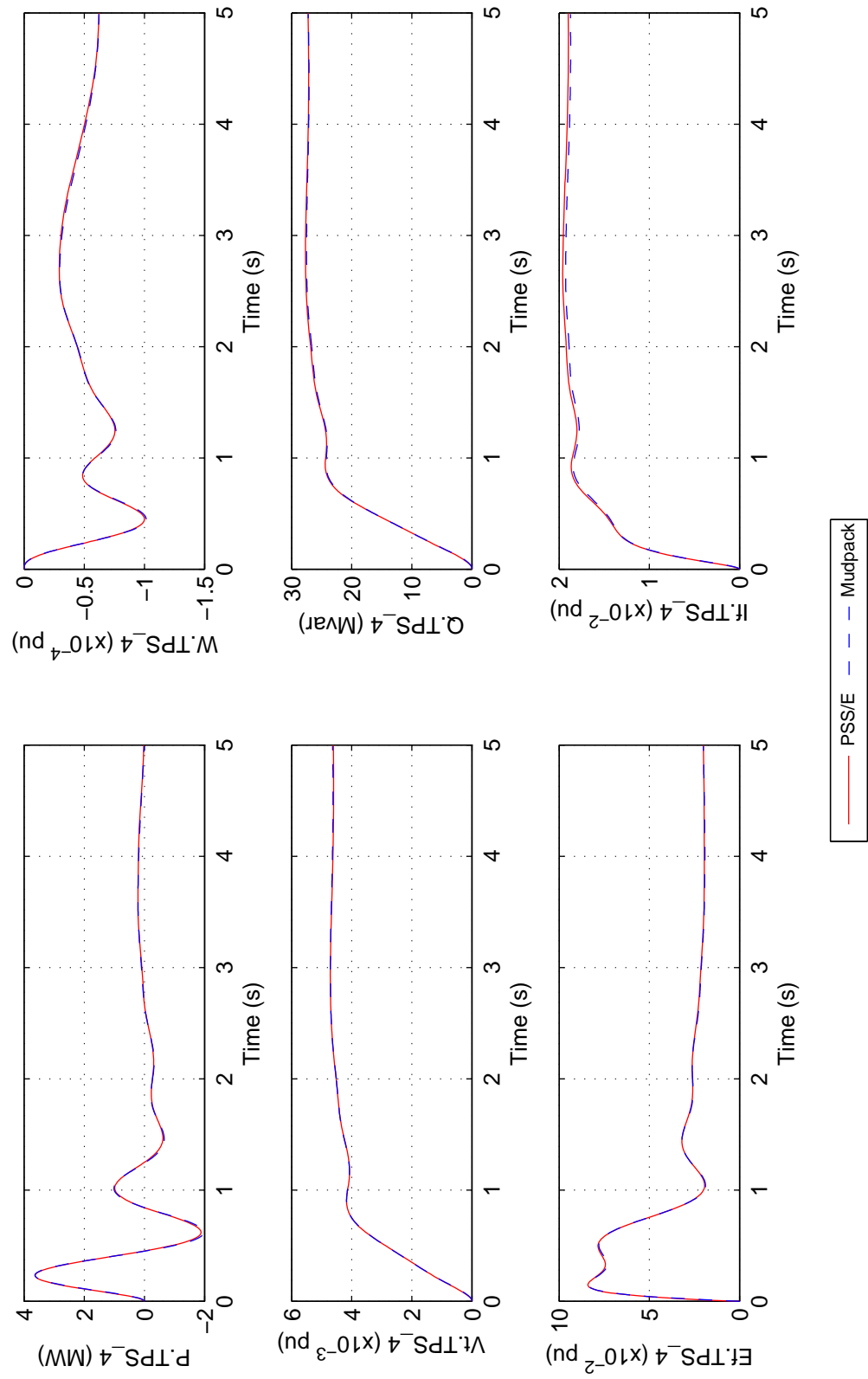


Figure 34 As for Figure 28 but for Case 1 and generator YPS_3.

File: CMP_Case01_NETFRQ_VrefStep_YPS_3.eps
 Mon, 17-Feb-2014 22:57:35

The University of Adelaide, Mudpack Scripts
 Simplified Australian System; Benchmark PSS/E & Mudpack;
 Case02_NETFRQ_VrefStep_TPS_4; 0.5% step on Vref.TPS_4;



File: CMP_Case02_NETFRQ_VrefStep_TPS_4.eps
 Tue, 18-Feb-2014 06:48:02

Figure 35 As for Figure 28 but for Case 2 and generator TPS_4.

The University of Adelaide, Mudpack Scripts
 Simplified Australian System; Benchmark PSS/E & Mudpack;
 Case03_NETFRQ_VrefStep_CPS_4; 0.5% step on Vref.CPS_4;

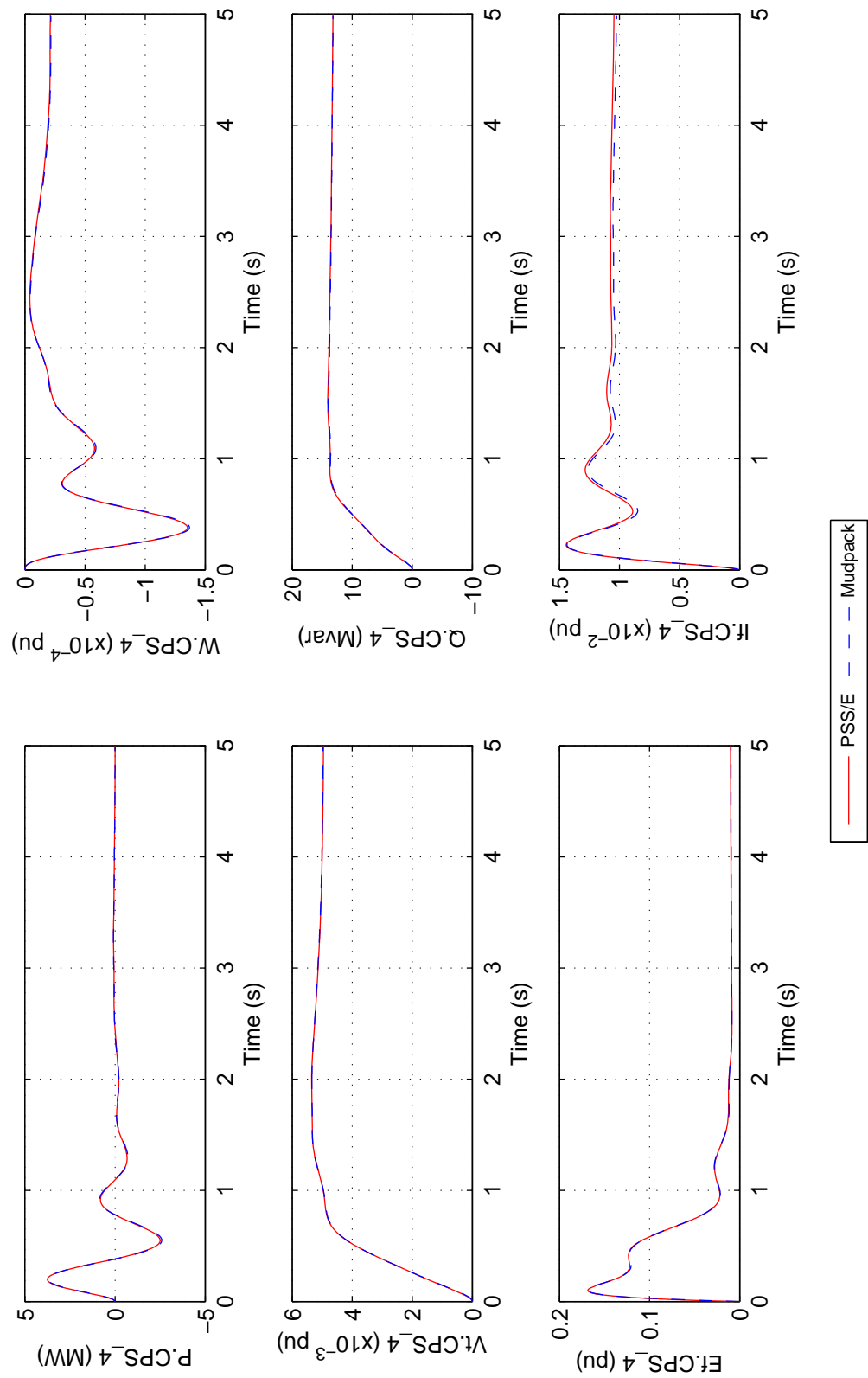
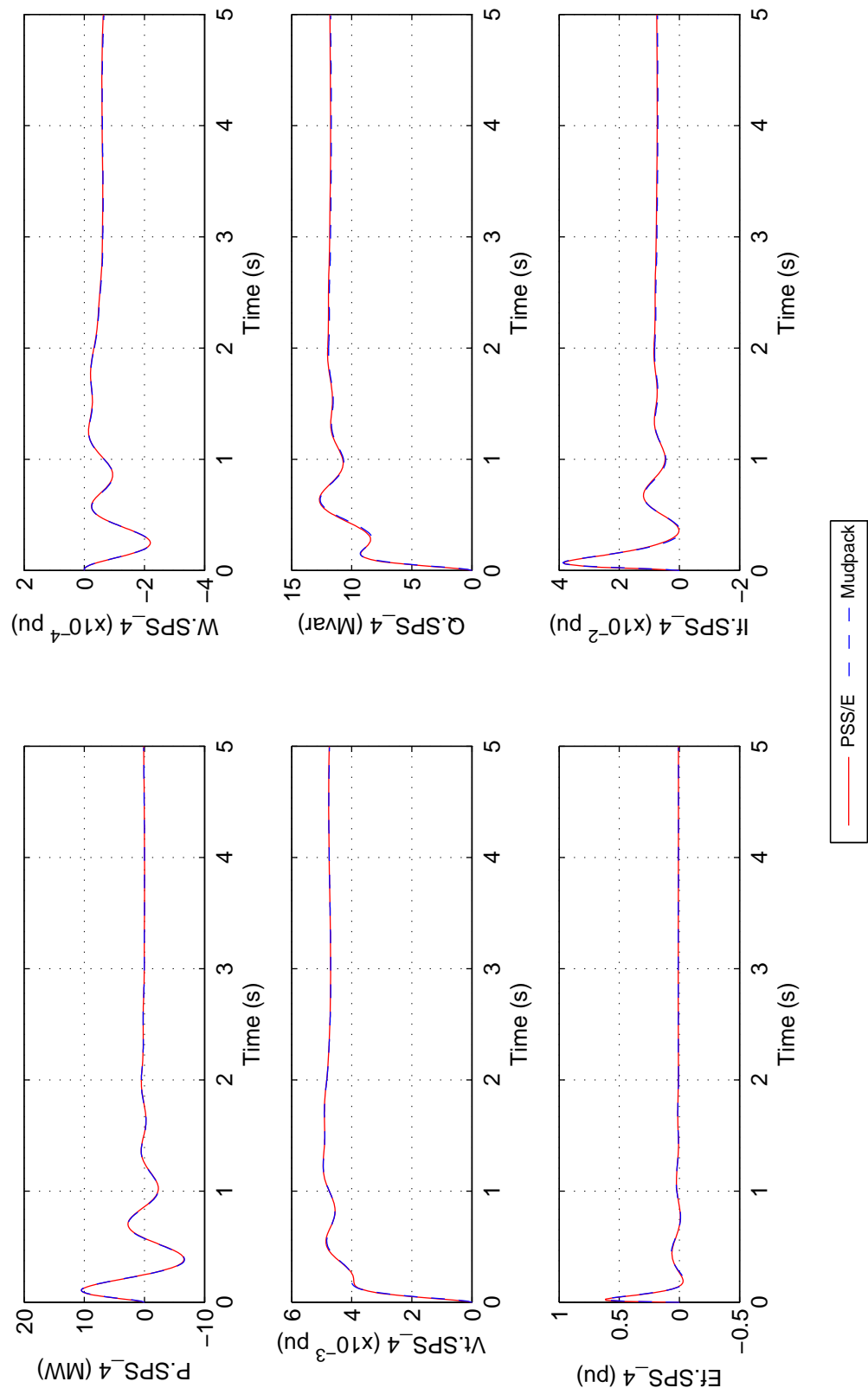


Figure 36 As for Figure 28 but for Case 3 and generator CPS_4.

File: CMP_Case03_NETFRQ_VrefStep_CPS_4.eps
 Tue, 18-Feb-2014 06:50:56

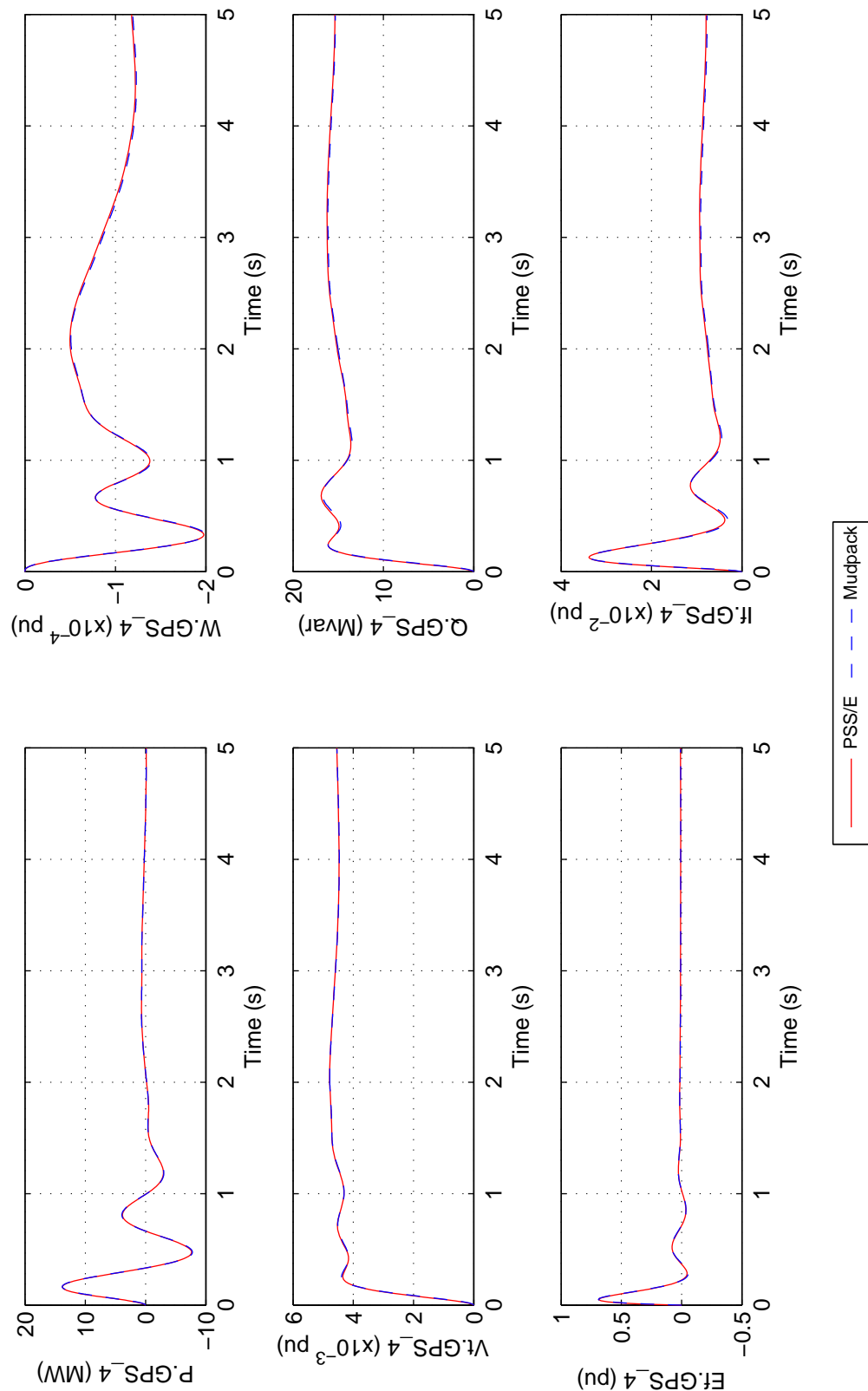
The University of Adelaide, Mudpack Scripts
 Simplified Australian System; Benchmark PSS/E & Mudpack;
 Case04_NETFRQ_VrefStep_SPS_4; 0.5% step on Vref.SPS_4;



File: CMP_Case04_NETFRQ_VrefStep_SPS_4.eps
 Tue, 18-Feb-2014 06:53:12

Figure 37 As for Figure 28 but for Case 4 and generator SPS_4.

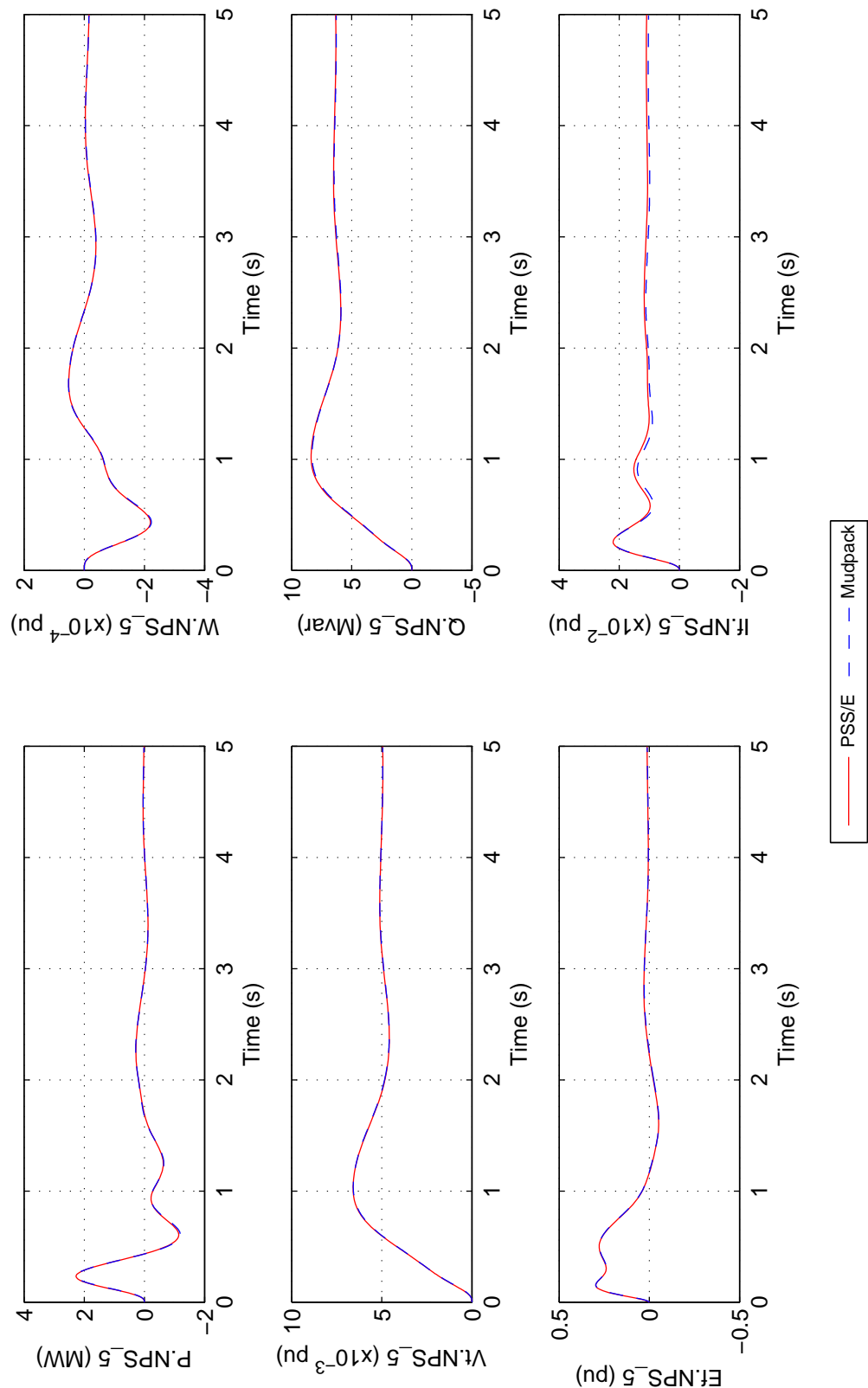
The University of Adelaide, Mudpack Scripts
 Simplified Australian System; Benchmark PSS/E & Mudpack;
 Case05_NETFRQ_VrefStep_GPS_4; 0.5% step on Vref.GPS_4;



File: CMP_Case05_NETFRQ_VrefStep_GPS_4.eps
 Tue, 18-Feb-2014 06:55:09

Figure 38 As for Figure 28 but for Case 5 and generator GPS_4.

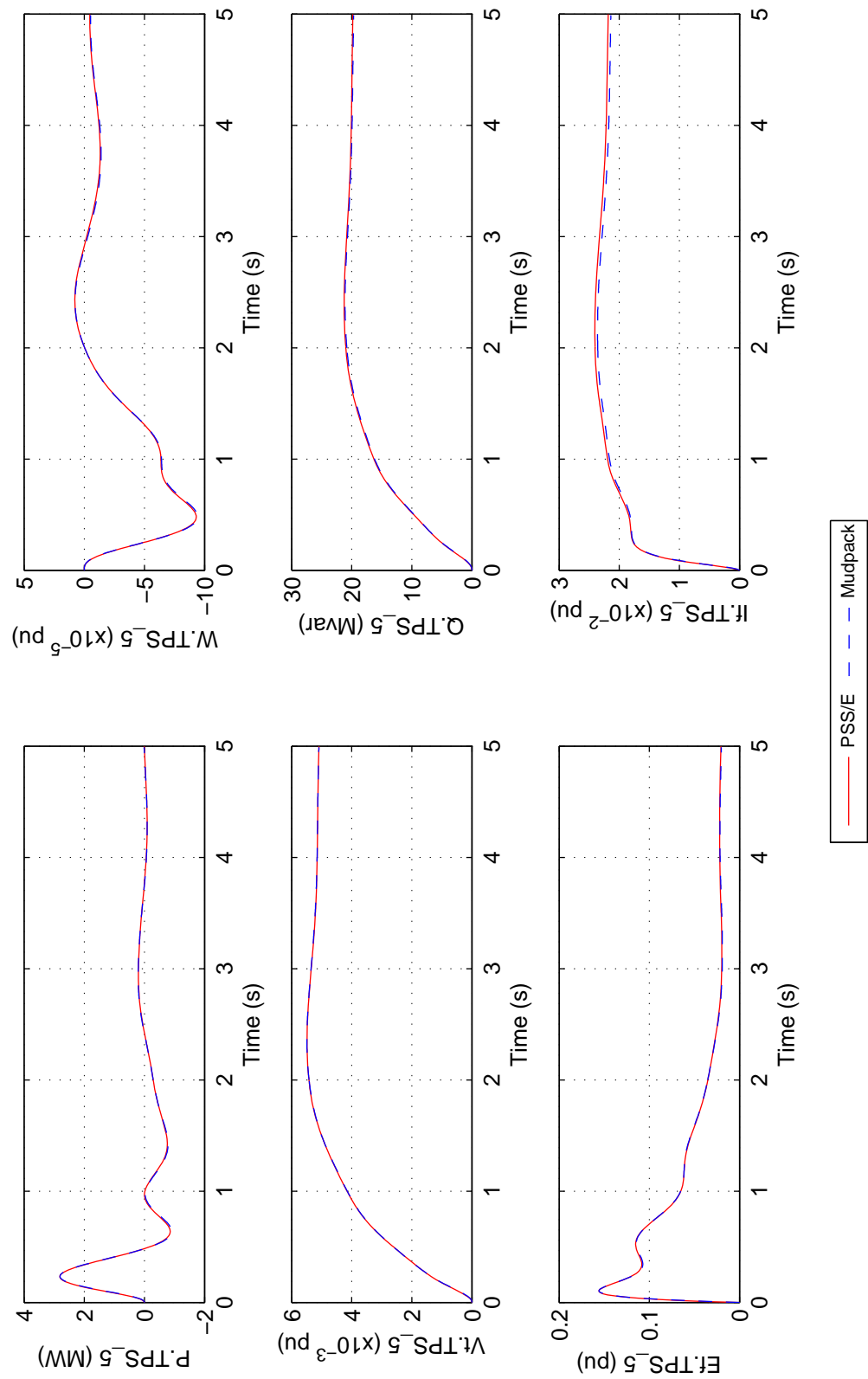
The University of Adelaide, Mudpack Scripts
 Simplified Australian System; Benchmark PSS/E & Mudpack;
 Case06_NETFRQ_VrefStep_NPS_5; 0.5% step on Vref.NPS_5;



File: CMP_Case06_NETFRQ_VrefStep_NPS_5.eps
 Tue, 18-Feb-2014 06:57:07

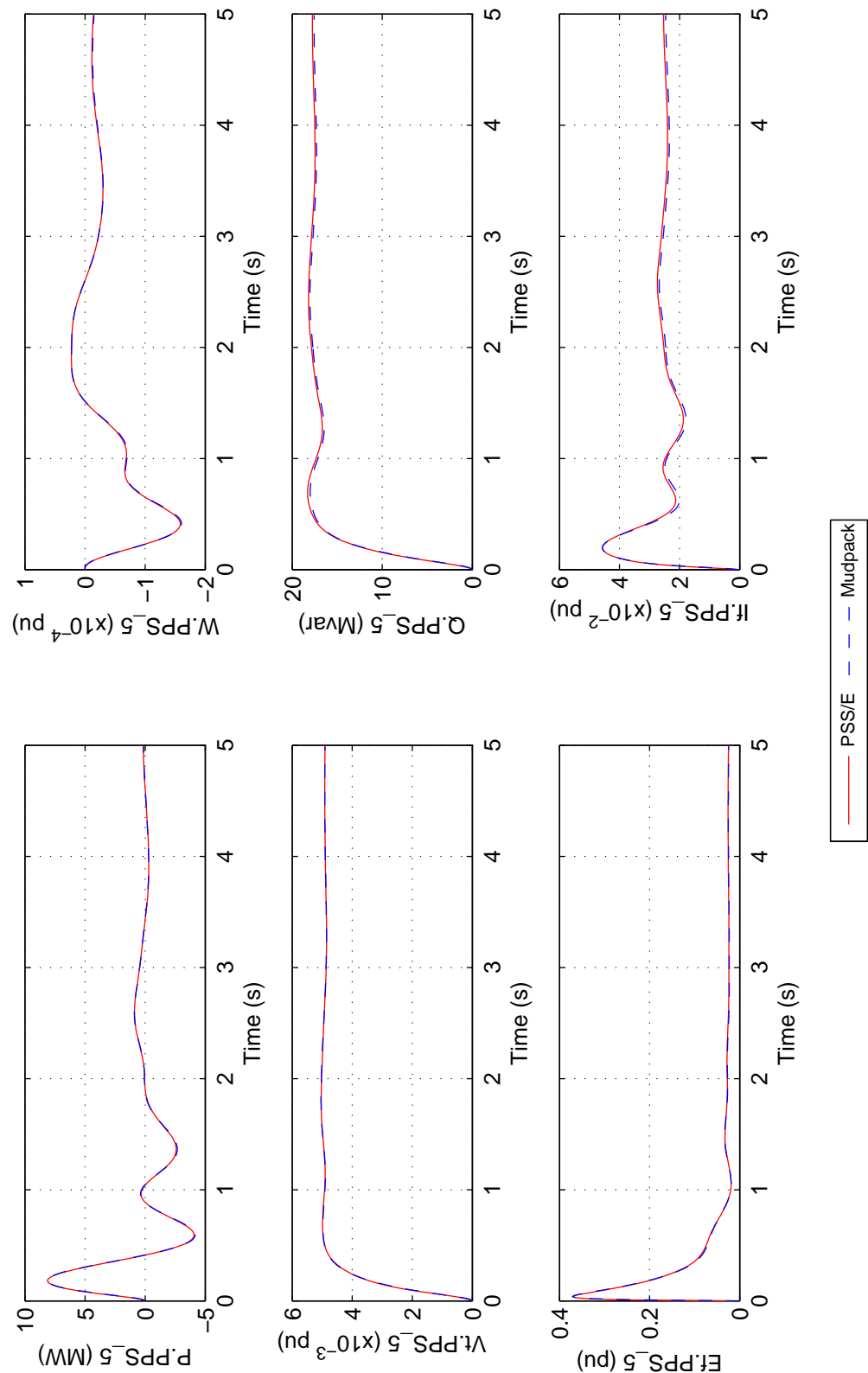
Figure 39 As for Figure 28 but for Case 6 and generator NPS_5.

The University of Adelaide, Mudpack Scripts
 Simplified Australian System; Benchmark PSS/E & Mudpack;
 Case01_NETFRQ_VrefStep_TPS_5; 0.5% step on Vref.TPS_5;



File: CMP_Case01_NETFRQ_VrefStep_TPS_5.eps
 Mon, 17-Feb-2014 23:22:04

The University of Adelaide, Mudpack Scripts
 Simplified Australian System; Benchmark PSS/E & Mudpack;
 Case02_NETFRQ_VrefStep_PPS_5; 0.5% step on Vref.PPS_5;



File: CMP_Case02_NETFRQ_VrefStep_PPS_5.eps
 Tue, 18-Feb-2014 06:58:41

Figure 41 As for Figure 28 but for Case 2 and generator PPS_5.

III.2 Mechanical power step-responses to verify consistency of inter-area modes

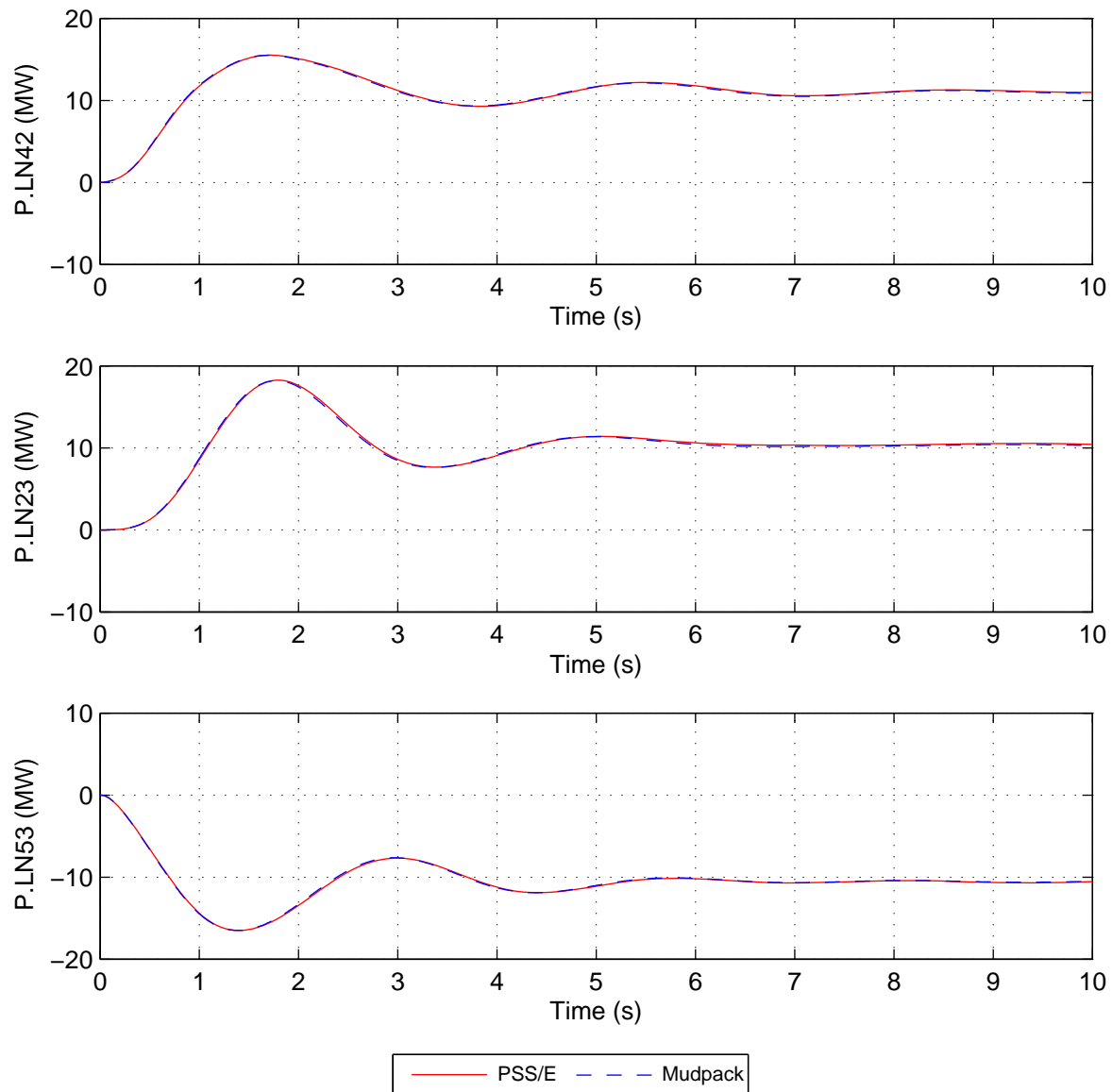
For study case 1, with all PSSs in service at their design damping gain of 20.0 pu, a +10 MW step is applied to the mechanical power input of the GPS_4 machine and a compensating -10 MW step is applied to the NPS_5 machine. Since these two machines are located at either end of the system the interarea modes of oscillation are excited and the power flow in the inter-regional tie-lines contain significant inter-area modal components. Thus, the perturbations in the total line-power flow in the circuits between buses 410 & 413 (P.LN42); 217 & 102 (P.LN23); and 509 & 315 (P.LN53) are monitored. This test, which is conducted in PSS[®]/E and Mudpack, is intended to verify that the inter-area mode behaviour obtained with the respective simulation packages are consistent. As shown in [Figure 42](#) the responses obtained with the two packages are practically identical (with PSS[®]/E NETFRQ = 1).

The results of similar tests conducted for cases 2 to 6 are shown in Figures [43](#) to [47](#) respectively and they reveal similarly very close agreement between the PSS[®]/E and Mudpack responses. The time-series data for these results are also provided in the DataPackage.

The University of Adelaide, MudpackScripts

Simplified Australian System; Benchmark PSS/E & Mudpack;

Case01_NETFRQ_DIS01; -10 MW step on Pm.NPS_5 and +10 MW step on Pm.GPS_4;



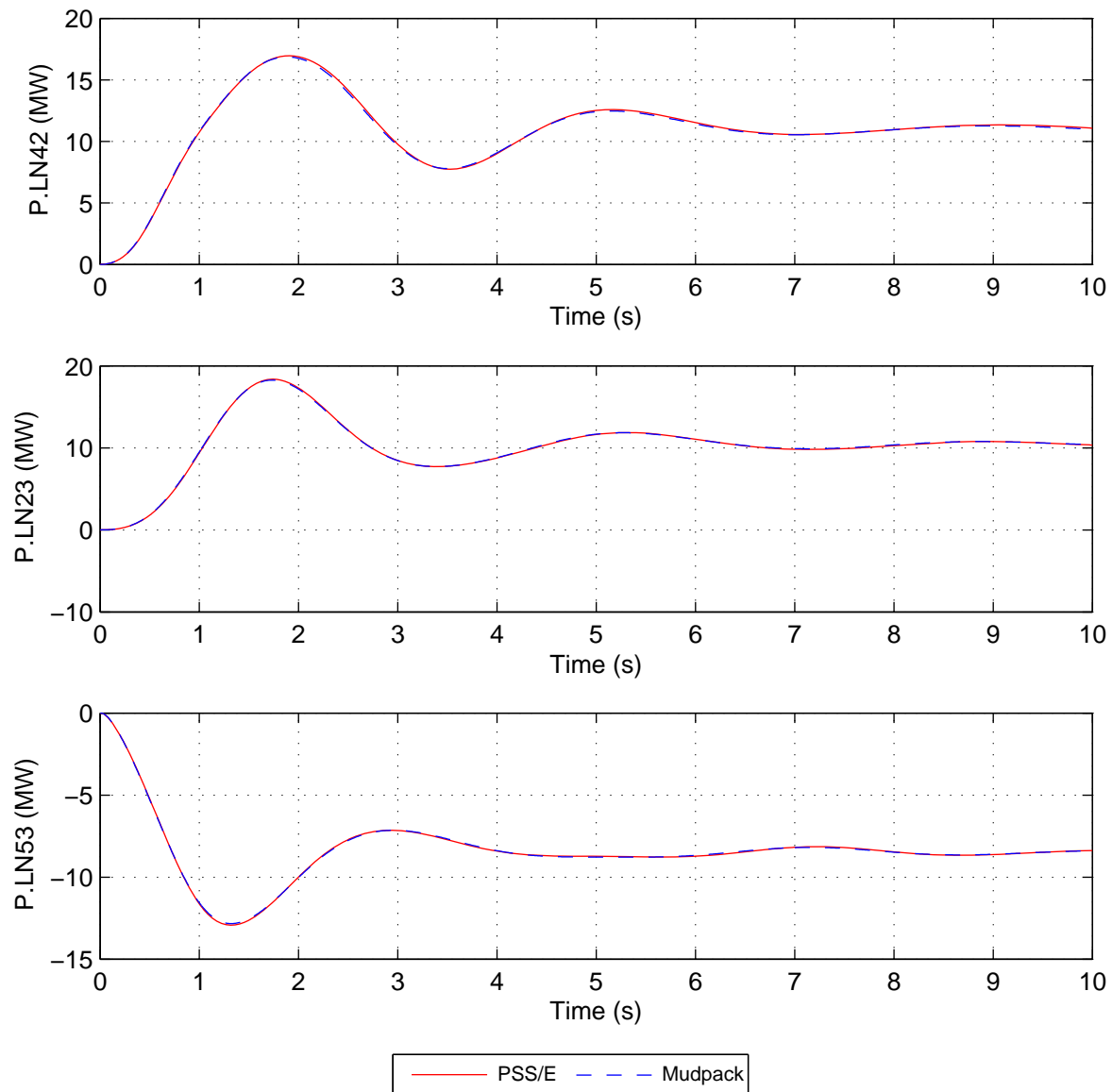
File: CMP_Case01_NETFRQ_DIS01.eps
Mon, 17-Feb-2014 14:56:24

Figure 42 Case 1. Benchmark comparison between PSS[®]/E (with NETFRQ = 1) and Mudpack. Step change in mechanical power input of +10 MW applied to GPS_4 and a compensating change of -10 MW applied to NPS_5. Powerflow in interconnectors between areas 2 & 4 (P.LN42); areas 2 & 3 (P.LN23) and areas 5 & 3 (P.LN53) are compared.

The University of Adelaide, MudpackScripts

Simplified Australian System; Benchmark PSS/E & Mudpack;

Case02_NETFRQ_DIS01; -10 MW step on Pm.NPS_5 and +10 MW step on Pm.GPS_4;



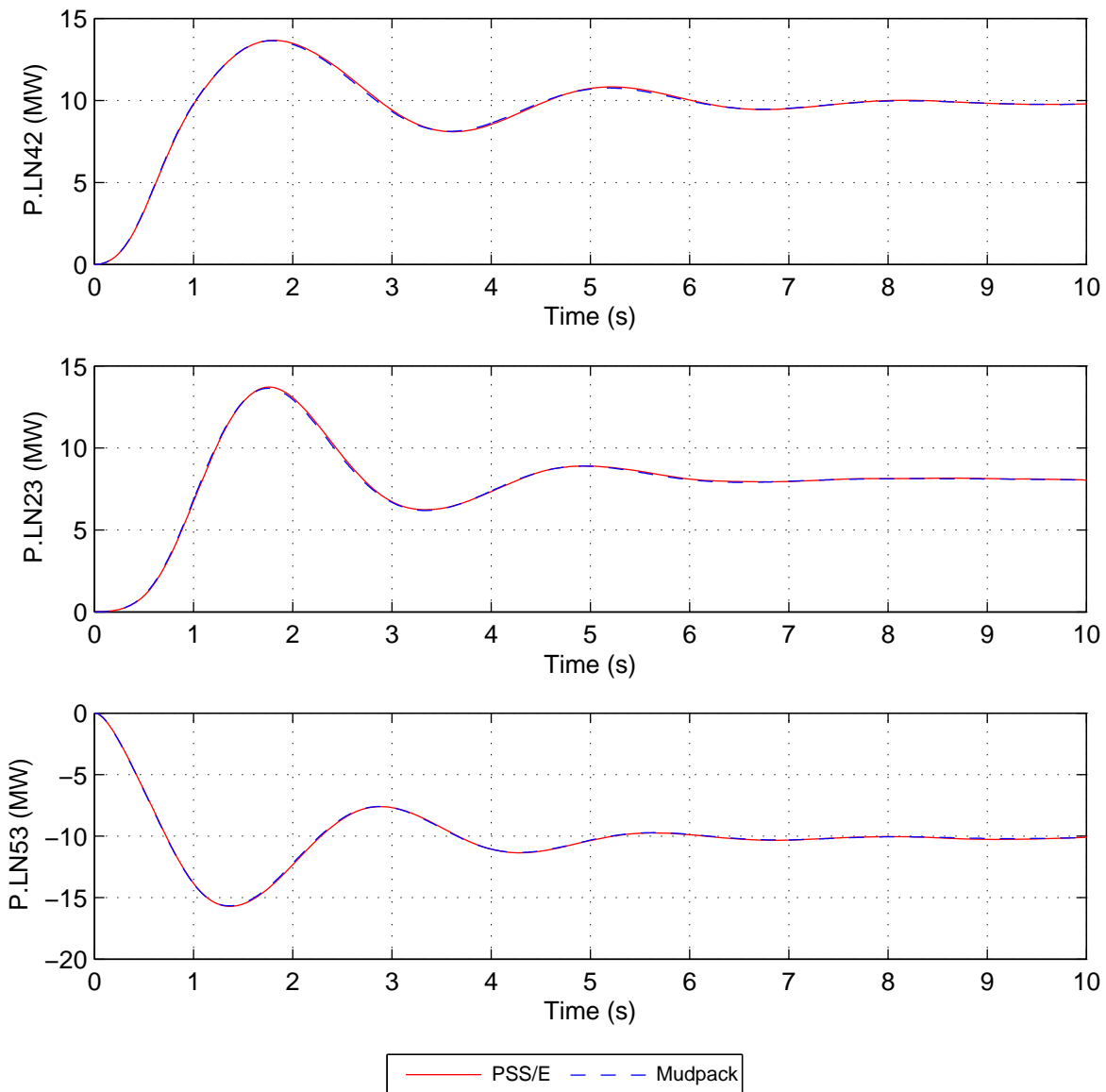
File: CMP_Case02_NETFRQ_DIS01.eps
Mon, 17-Feb-2014 14:57:53

Figure 43 As for [Figure 42](#) but for Case 2.

The University of Adelaide, MudpackScripts

Simplified Australian System; Benchmark PSS/E & Mudpack;

Case03_NETFRQ_DIS01; -10 MW step on Pm.NPS_5 and +10 MW step on Pm.GPS_4;



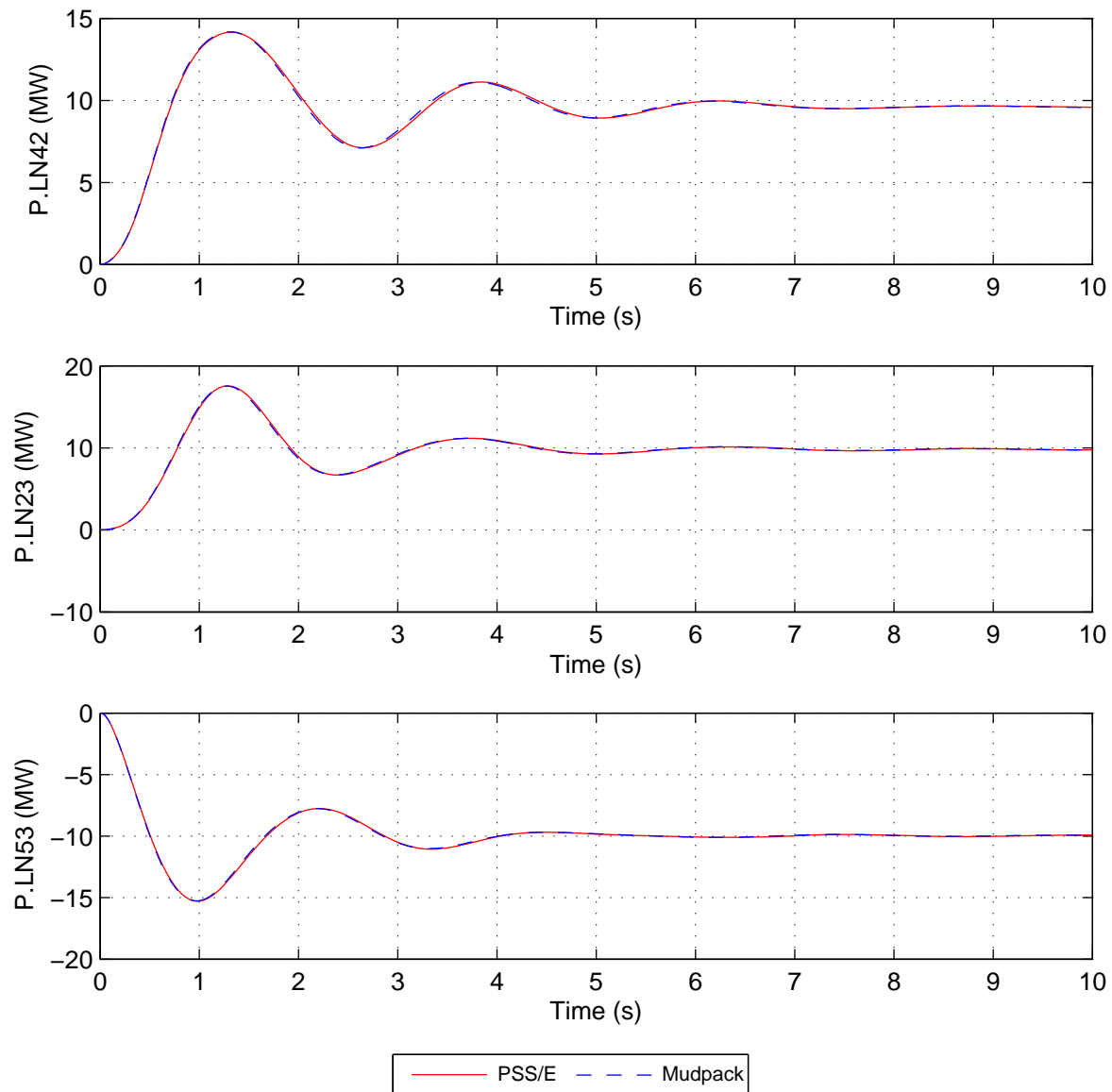
File: CMP_Case03_NETFRQ_DIS01.eps
Mon, 17-Feb-2014 14:59:07

Figure 44 As for [Figure 42](#) but for Case 3.

The University of Adelaide, MudpackScripts

Simplified Australian System; Benchmark PSS/E & Mudpack;

Case04_NETFRQ_DIS01; -10 MW step on Pm.NPS_5 and +10 MW step on Pm.GPS_4;



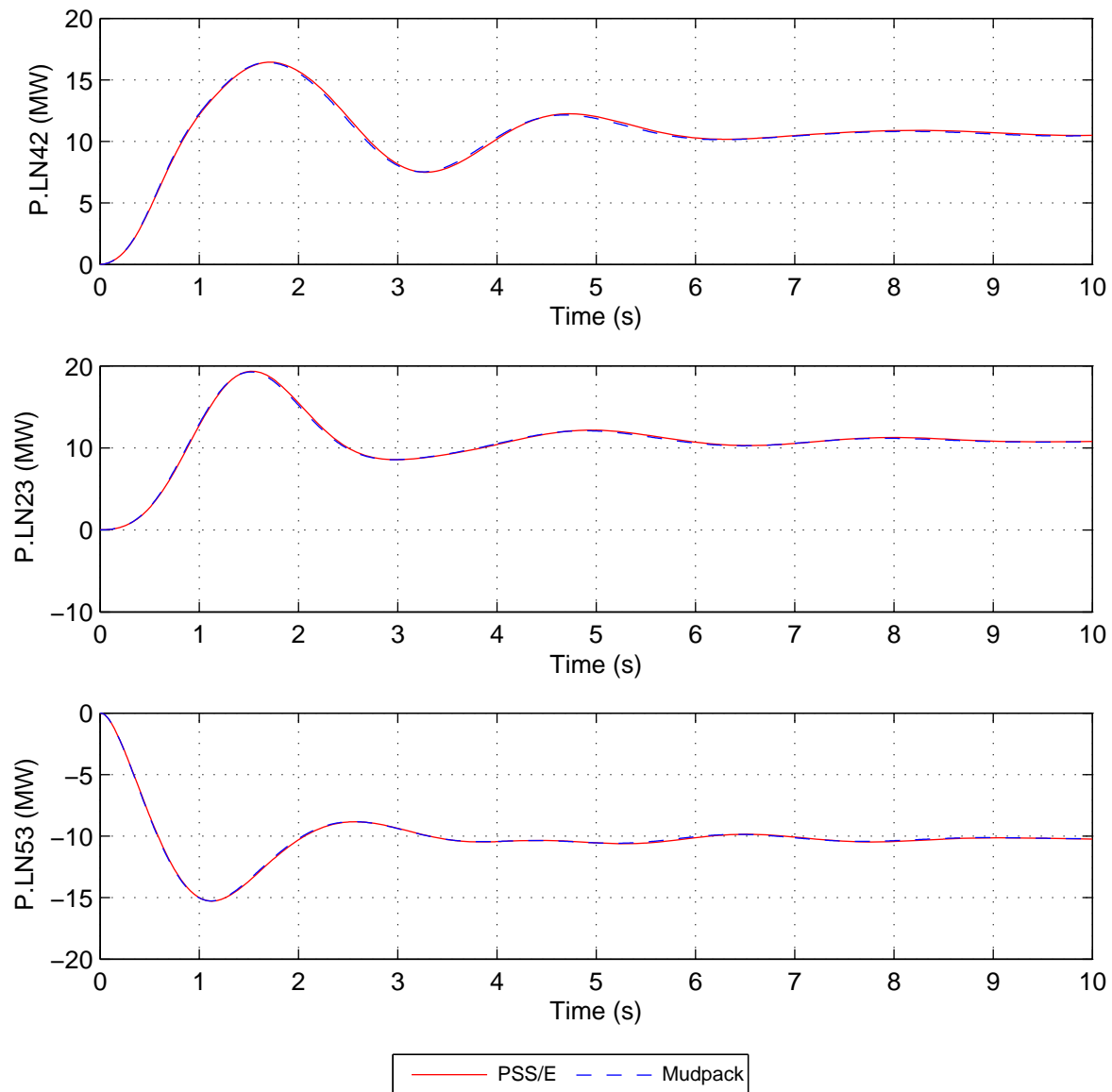
File: CMP_Case04_NETFRQ_DIS01.eps
Mon, 17-Feb-2014 15:00:45

Figure 45 As for [Figure 42](#) but for Case 4.

The University of Adelaide, MudpackScripts

Simplified Australian System; Benchmark PSS/E & Mudpack;

Case05_NETFRQ_DIS01; -10 MW step on Pm.NPS_5 and +10 MW step on Pm.GPS_4;



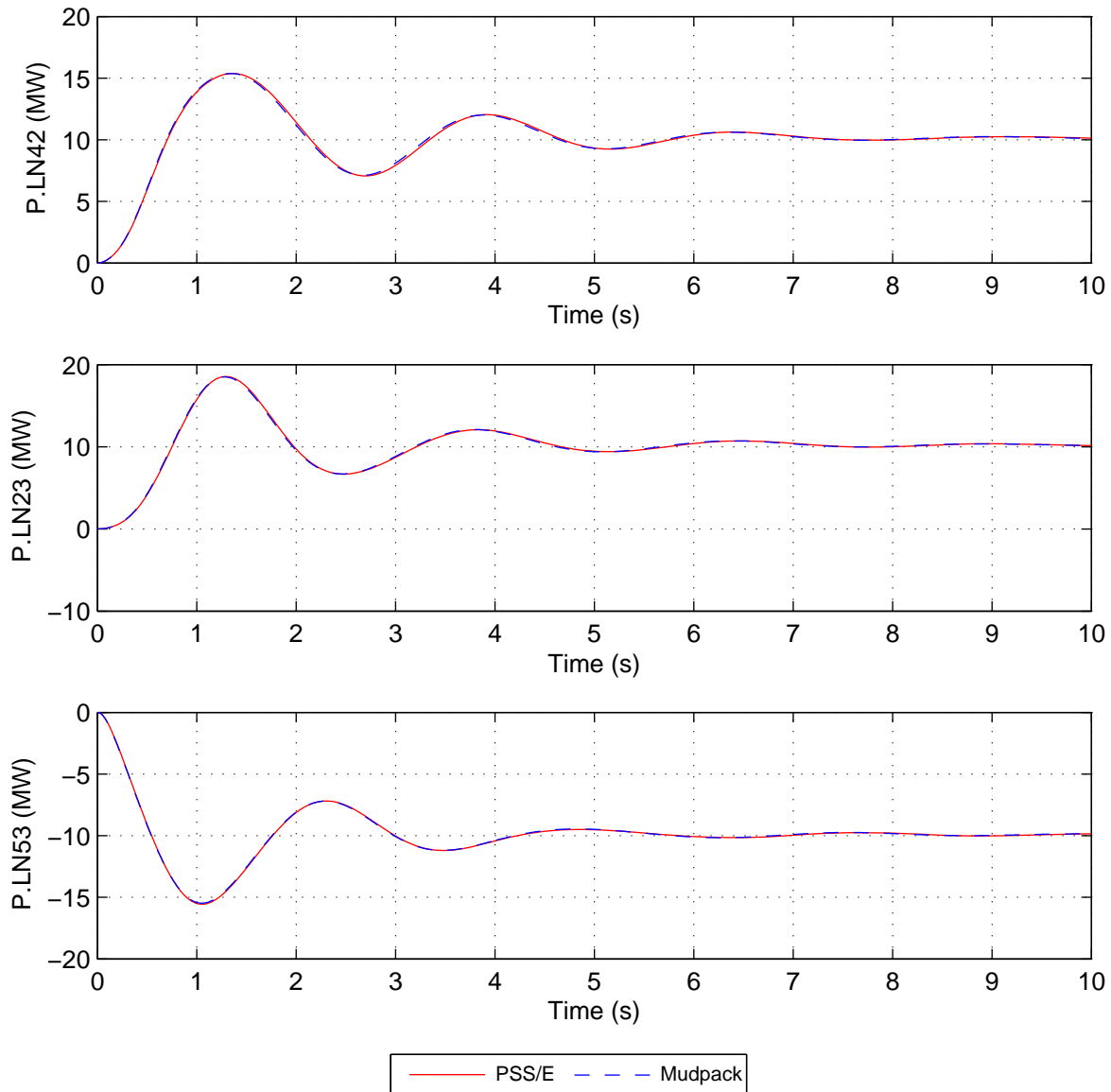
File: CMP_Case05_NETFRQ_DIS01.eps
Mon, 17-Feb-2014 15:02:37

Figure 46 As for [Figure 42](#) but for Case 5.

The University of Adelaide, MudpackScripts

Simplified Australian System; Benchmark PSS/E & Mudpack;

Case06_NETFRQ_DIS01; -10 MW step on Pm.NPS_5 and +10 MW step on Pm.GPS_4;



File: CMP_Case06_NETFRQ_DIS01.eps
Mon, 17-Feb-2014 15:03:54

Figure 47 As for [Figure 42](#) but for Case 6.

III.3 Benchmark comparison of the generator P-V_r characteristics computed by PSS®/E and Mudpack

The P-V_r characteristics of the fourteen generators are computed in PSS®/E for Case 2 and compared in Figures 48 to 61 with the corresponding P-V_r characteristics computed using Mudpack. There is very close agreement between the characteristics computed by the respective packages. In order to highlight any differences between the characteristics in the range of electromechanical modal frequencies the magnitude characteristics are displayed in absolute units, rather than in dB.

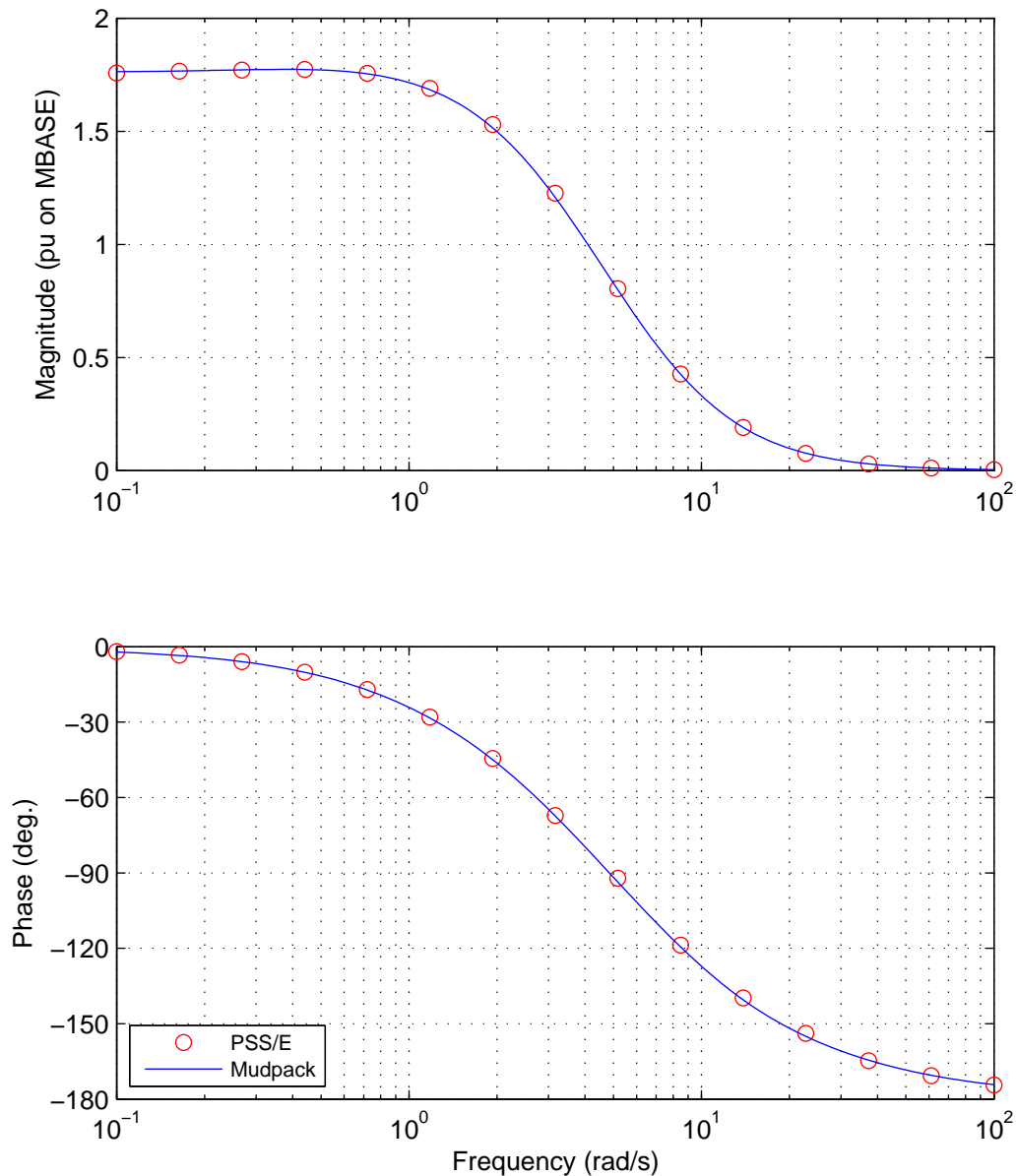
These results demonstrate that the implementation of the electromagnetic behaviour of the generator models and of the AVR/exciter models in the respective simulation packages are practically identical.

To the authors knowledge the PSS[®]/E software package does not include built-in facilities for computation of frequency-responses. A tool, AUPSSEFRTOOL, developed at Adelaide University as a PSS[®]/E “plug-in” has been used to compute the P-Vr characteristics within the PSS[®]/E program. A paper describing this tool is in preparation at time of writing. It should be mentioned at this point that the accuracy of the frequency responses computed in PSS[®]/E are sensitive to the integration time-step and to the amplitude of the sinusoidal perturbation applied to the voltage-reference.

The University of Adelaide, MudpackScripts

Simplified 14 generator model of the SE Australian system. Case 2.

PVr characteristic for HPS_1. Benchmark comparison between Mudpack & PSS/E.



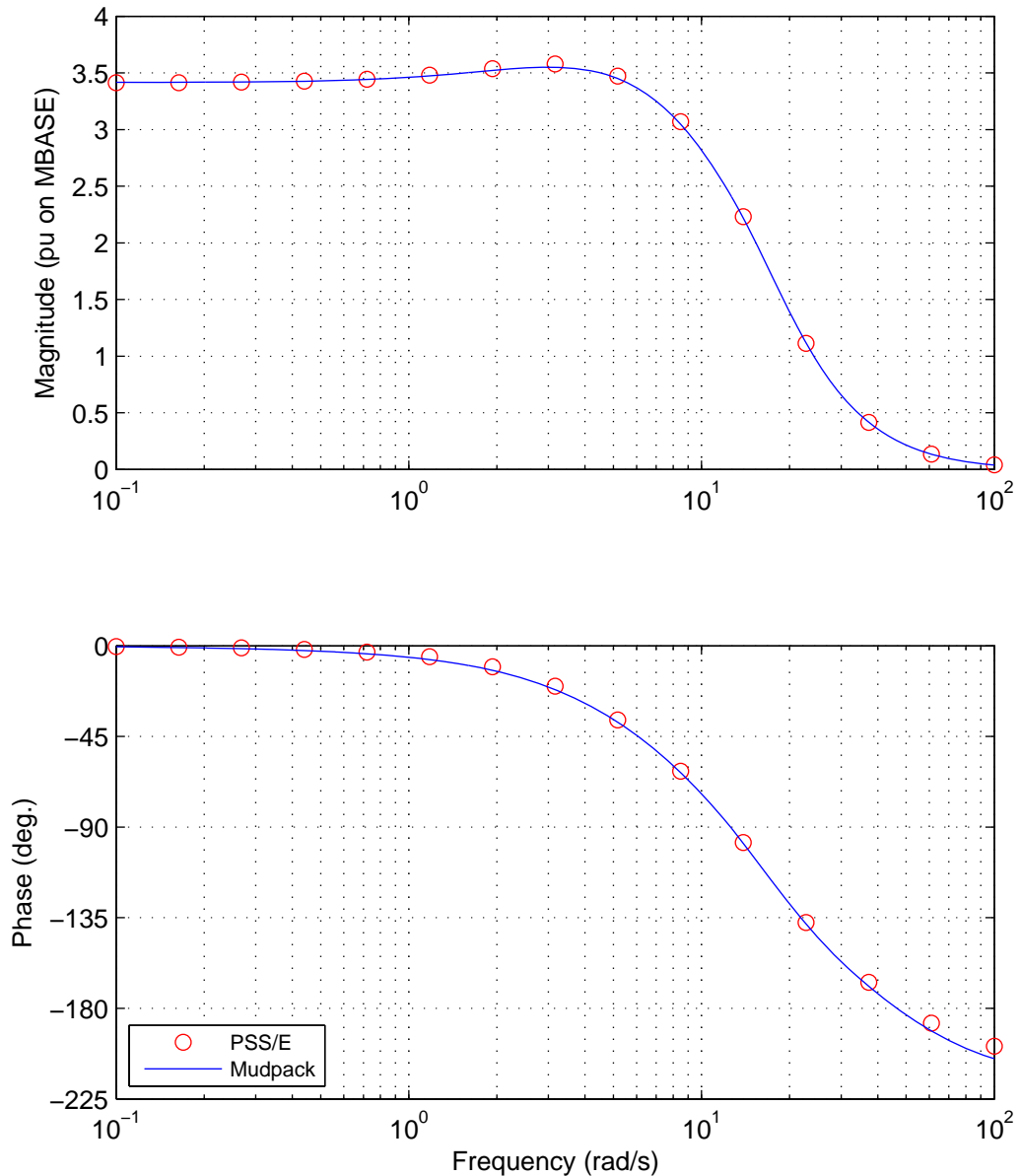
File: PVRbenchmark_Case02_HPS_1_MagPU.eps
Wed, 22-Jan-2014 19:03:13

Figure 48 HPS_1 P-Vr characteristic benchmark comparison between Mudpack and PSS[®]/E.

The University of Adelaide, MudpackScripts

Simplified 14 generator model of the SE Australian system. Case 2.

PVr characteristic for BPS_2. Benchmark comparison between Mudpack & PSS/E.



File: PVRbenchmark_Case02_BPS_2_MagPU.eps

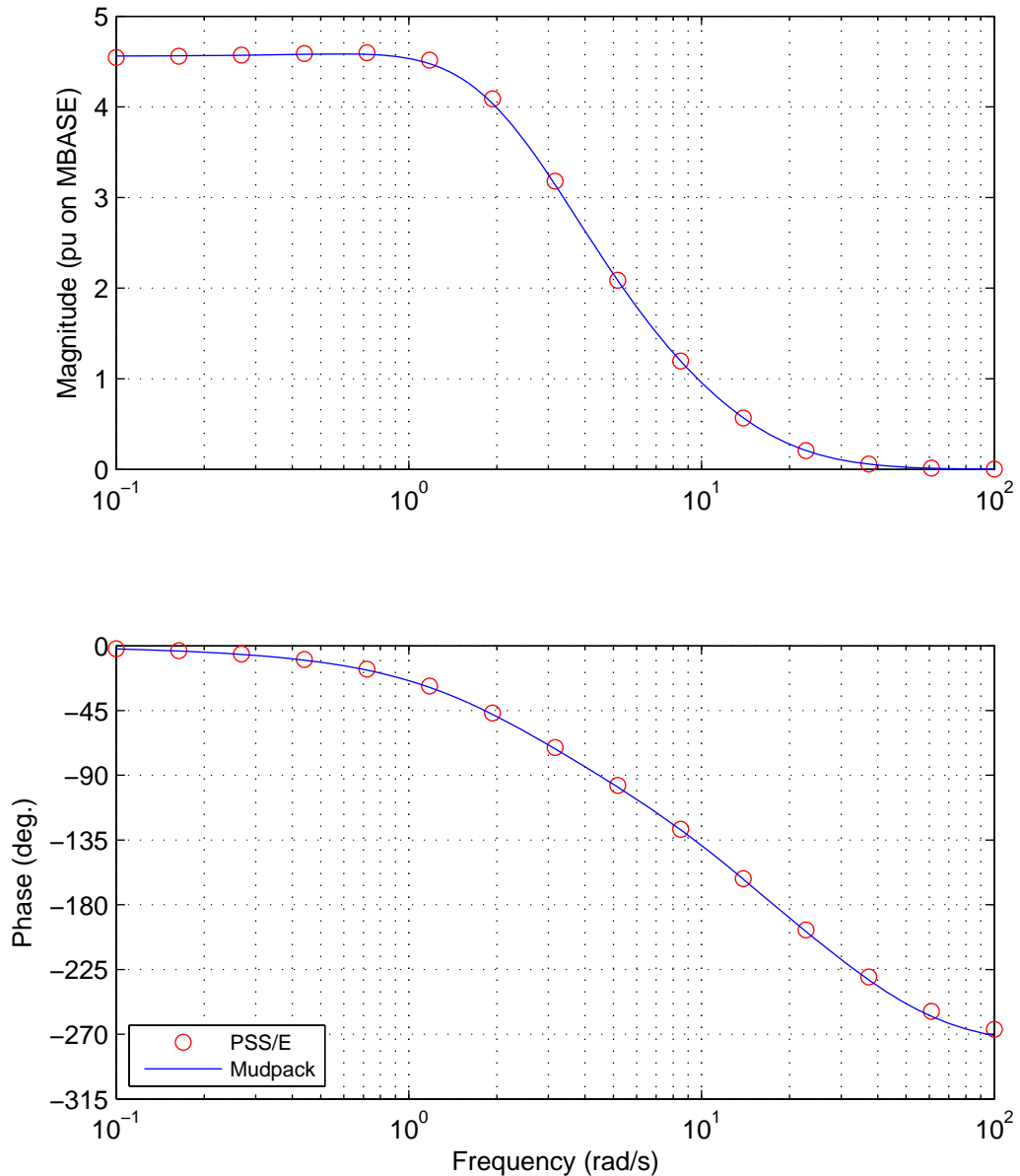
Wed, 22-Jan-2014 19:03:23

Figure 49 As for [Figure 48](#) but for generator BPS_2.

The University of Adelaide, MudpackScripts

Simplified 14 generator model of the SE Australian system. Case 2.

PVr characteristic for EPS_2. Benchmark comparison between Mudpack & PSS/E.



File: PVRbenchmark_Case02_EPS_2_MagPU.eps

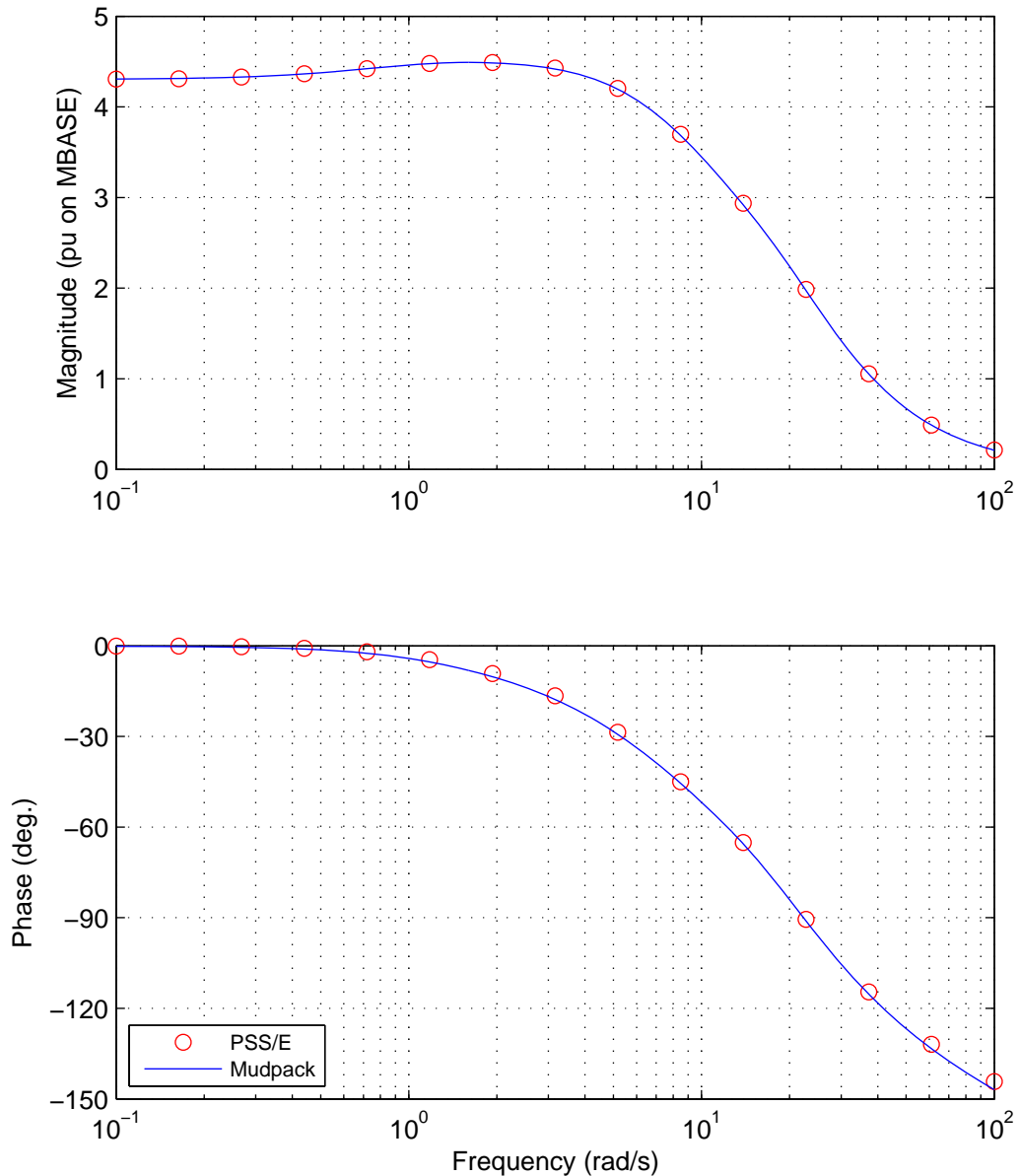
Wed, 22-Jan-2014 19:03:35

Figure 50 As for [Figure 48](#) but for generator EPS_2.

The University of Adelaide, MudpackScripts

Simplified 14 generator model of the SE Australian system. Case 2.

PVr characteristic for VPS_2. Benchmark comparison between Mudpack & PSS/E.



File: PVRbenchmark_Case02_VPS_2_MagPU.eps

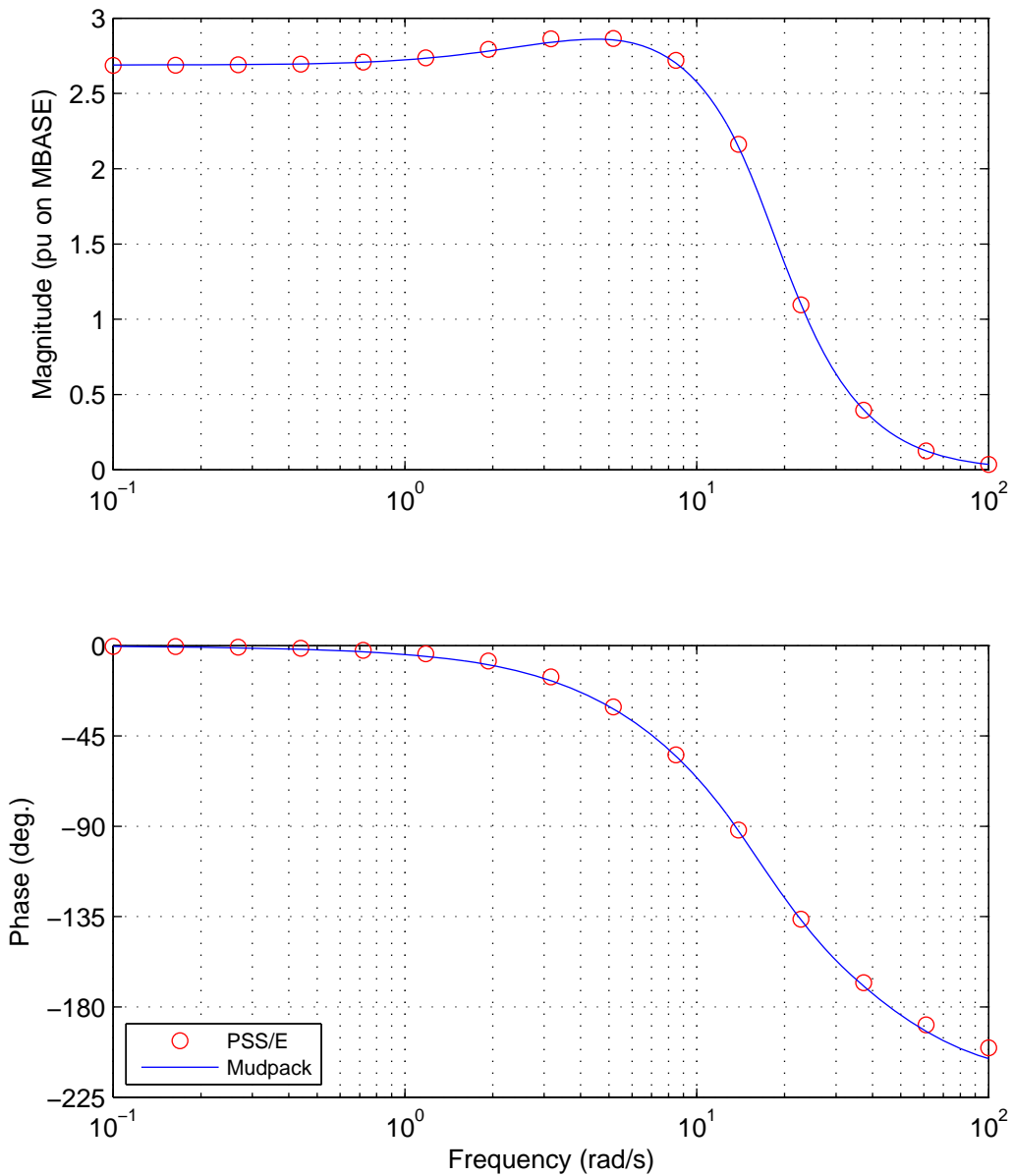
Wed, 22-Jan-2014 19:03:47

Figure 51 As for [Figure 48](#) but for generator VPS_2.

The University of Adelaide, MudpackScripts

Simplified 14 generator model of the SE Australian system. Case 2.

PVr characteristic for MPS_2. Benchmark comparison between Mudpack & PSS/E.



File: PVRbenchmark_Case02_MPS_2_MagPU.eps

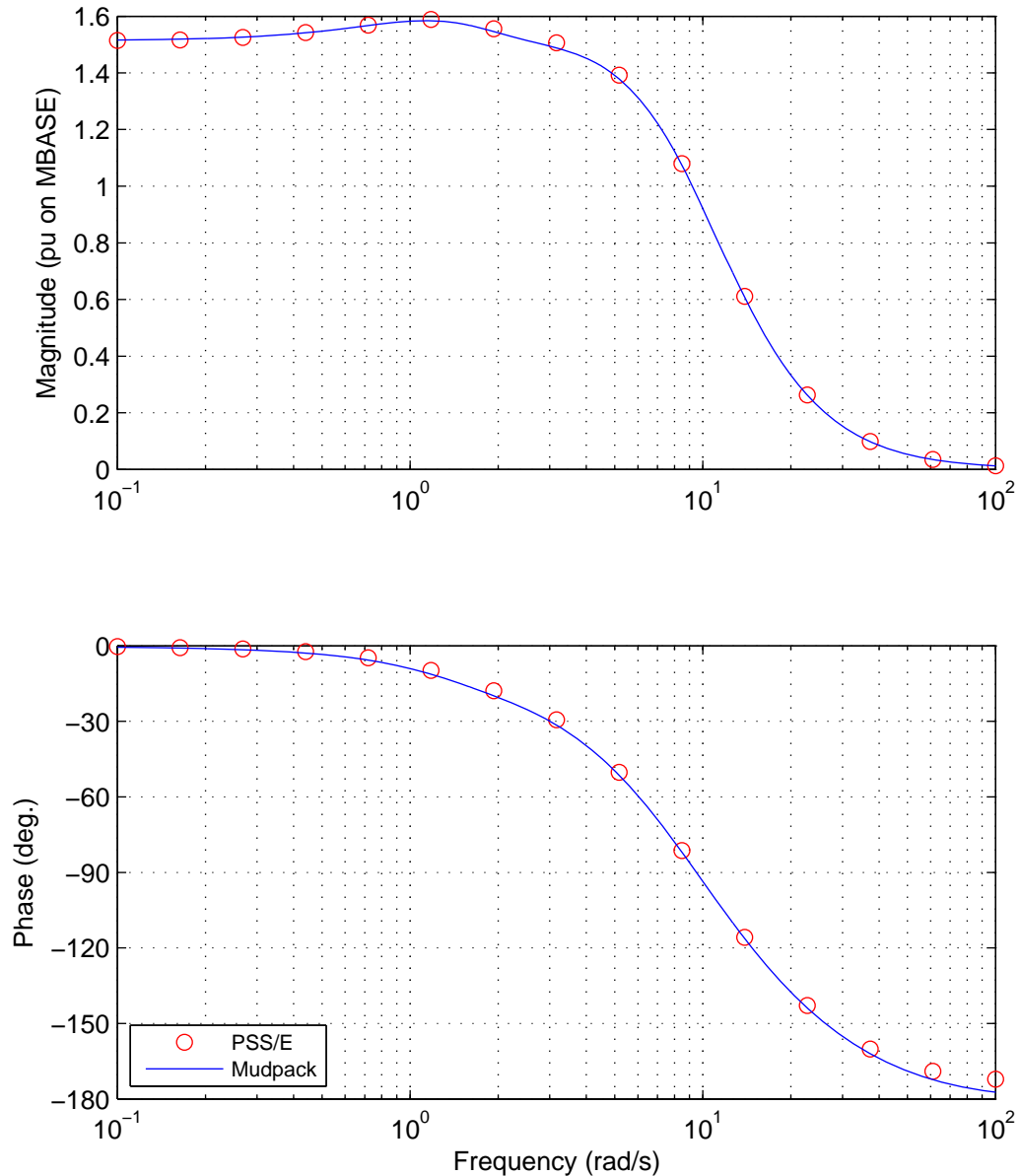
Wed, 22-Jan-2014 19:04:00

Figure 52 As for [Figure 48](#) but for generator MPS_2.

The University of Adelaide, MudpackScripts

Simplified 14 generator model of the SE Australian system. Case 2.

PVr characteristic for LPS_3. Benchmark comparison between Mudpack & PSS/E.



File: PVRbenchmark_Case02_LPS_3_MagPU.eps

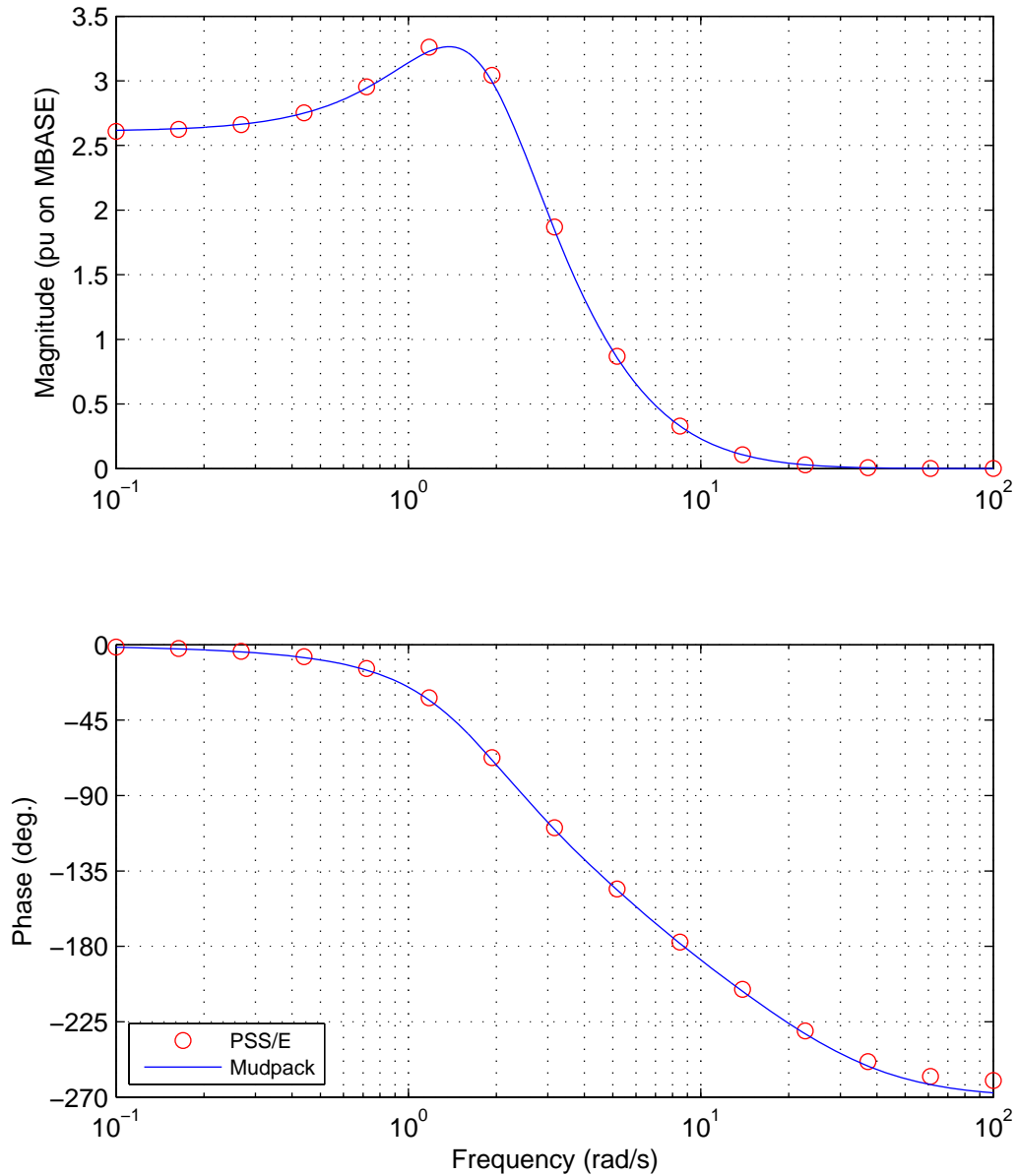
Wed, 22-Jan-2014 19:04:11

Figure 53 As for [Figure 48](#) but for generator LPS_3.

The University of Adelaide, MudpackScripts

Simplified 14 generator model of the SE Australian system. Case 2.

PVr characteristic for YPS_3. Benchmark comparison between Mudpack & PSS/E.



File: PVRbenchmark_Case02_YPS_3_MagPU.eps

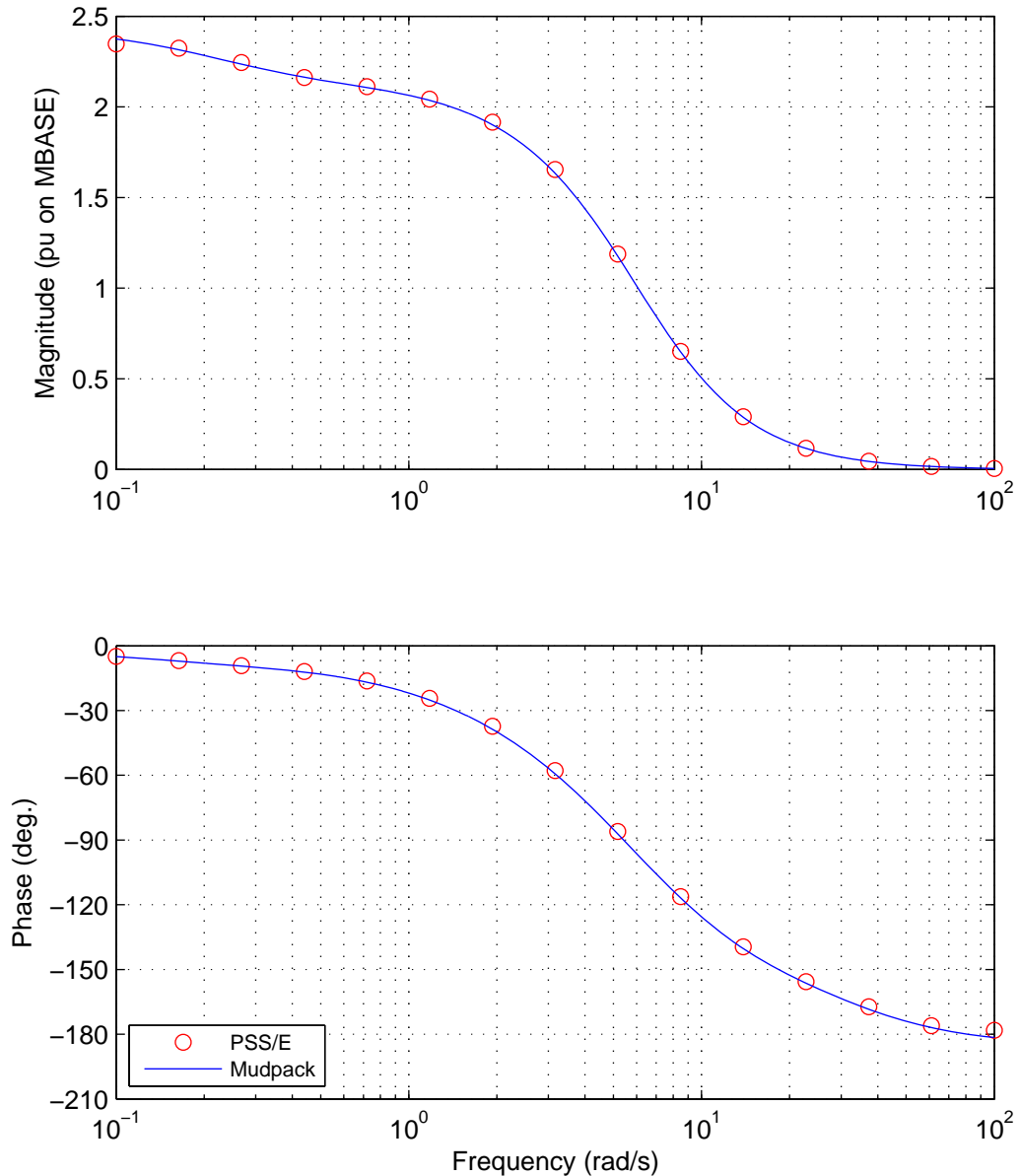
Wed, 22-Jan-2014 19:04:23

Figure 54 As for [Figure 48](#) but for generator YPS_3.

The University of Adelaide, MudpackScripts

Simplified 14 generator model of the SE Australian system. Case 2.

PVr characteristic for TPS_4. Benchmark comparison between Mudpack & PSS/E.



File: PVRbenchmark_Case02_TPS_4_MagPU.eps

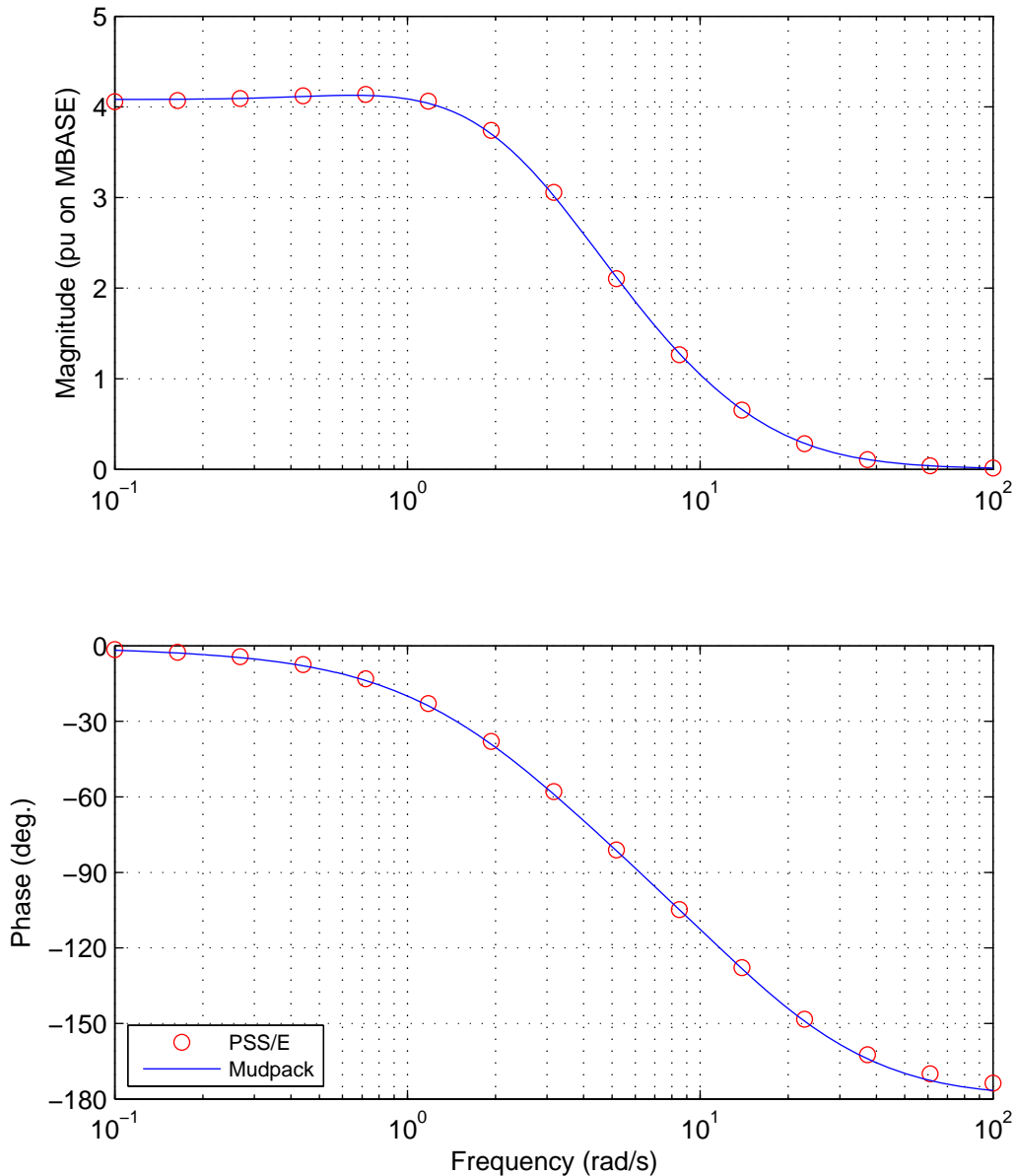
Wed, 22-Jan-2014 19:04:35

Figure 55 As for [Figure 48](#) but for generator TPS_4.

The University of Adelaide, MudpackScripts

Simplified 14 generator model of the SE Australian system. Case 2.

PVr characteristic for CPS_4. Benchmark comparison between Mudpack & PSS/E.



File: PVRbenchmark_Case02_CPS_4_MagPU.eps

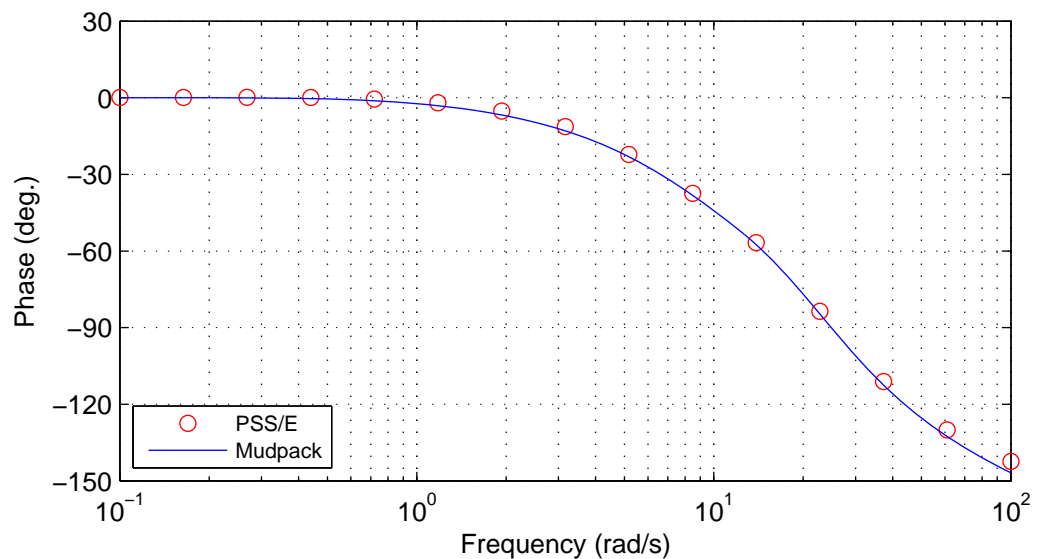
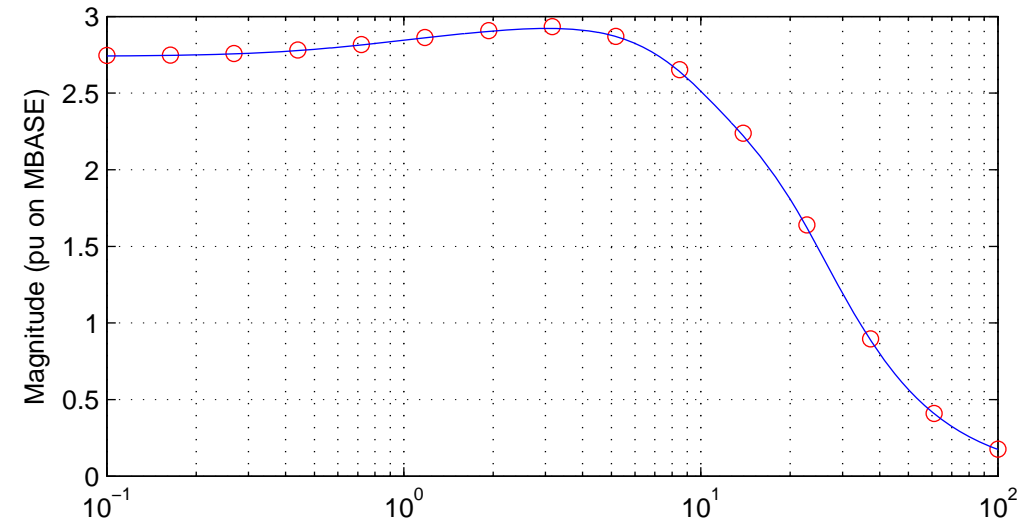
Wed, 22-Jan-2014 19:04:47

Figure 56 As for [Figure 48](#) but for generator CPS_4.

The University of Adelaide, MudpackScripts

Simplified 14 generator model of the SE Australian system. Case 2.

PVr characteristic for SPS_4. Benchmark comparison between Mudpack & PSS/E.



File: PVRbenchmark_Case02_SPS_4_MagPU.eps

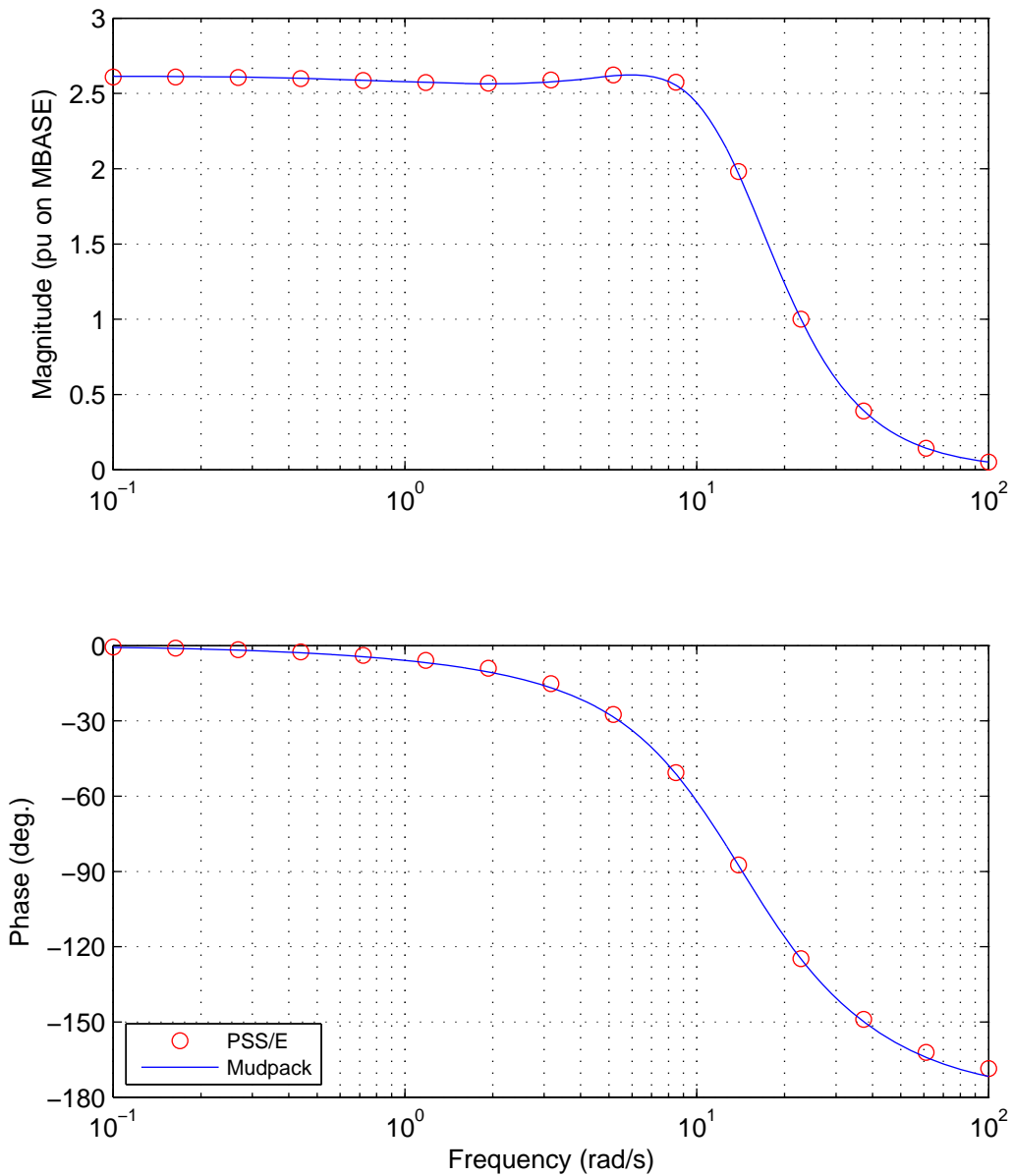
Wed, 22-Jan-2014 19:04:59

Figure 57 As for [Figure 48](#) but for generator SPS_4.

The University of Adelaide, MudpackScripts

Simplified 14 generator model of the SE Australian system. Case 2.

PVr characteristic for GPS_4. Benchmark comparison between Mudpack & PSS/E.



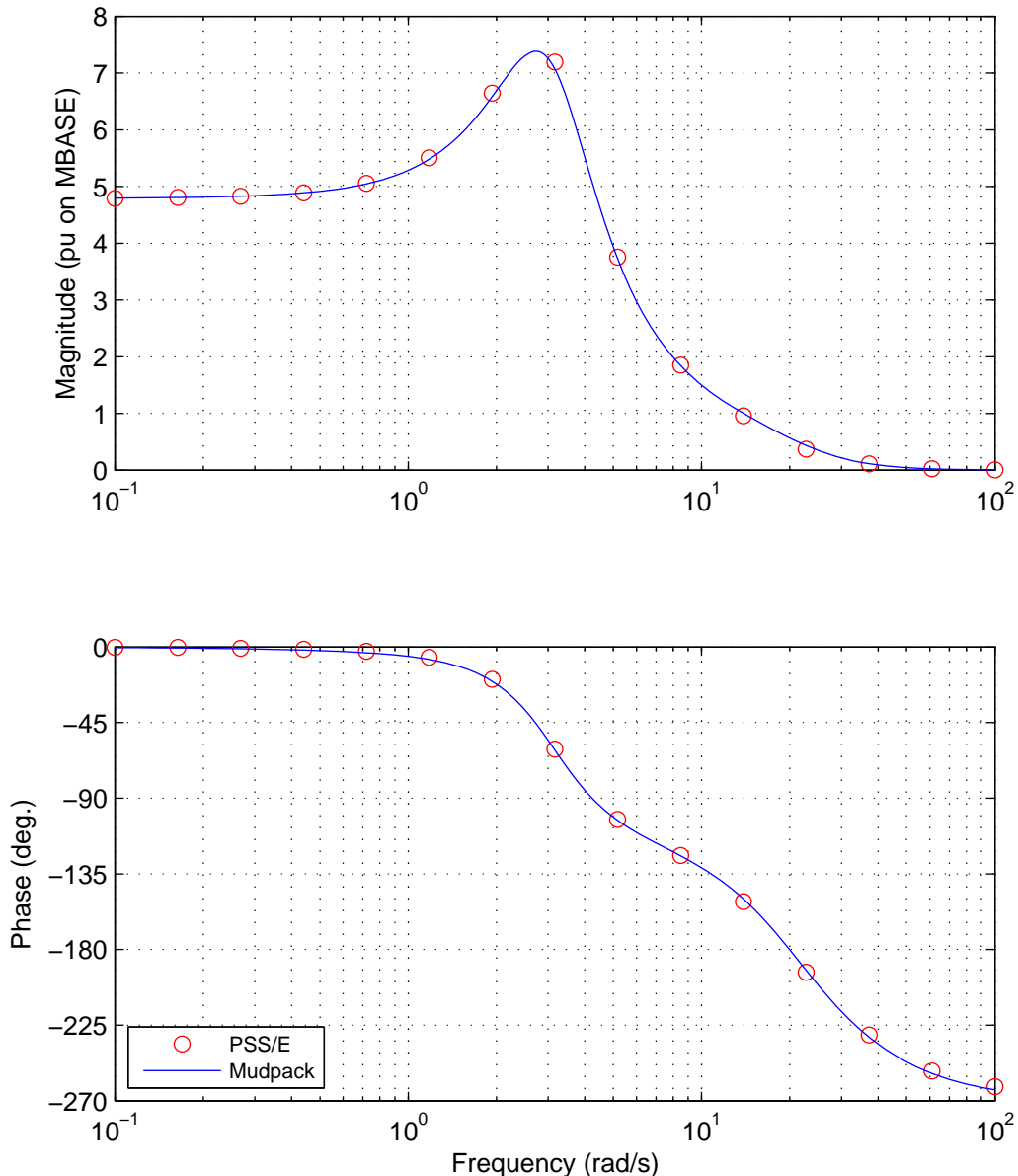
File: PVRbenchmark_Case02_GPS_4_MagPU.eps
Wed, 22-Jan-2014 19:05:12

Figure 58 As for [Figure 48](#) but for generator GPS_4.

The University of Adelaide, MudpackScripts

Simplified 14 generator model of the SE Australian system. Case 2.

PVr characteristic for NPS_5. Benchmark comparison between Mudpack & PSS/E.



File: PVRbenchmark_Case02_NPS_5_MagPU.eps

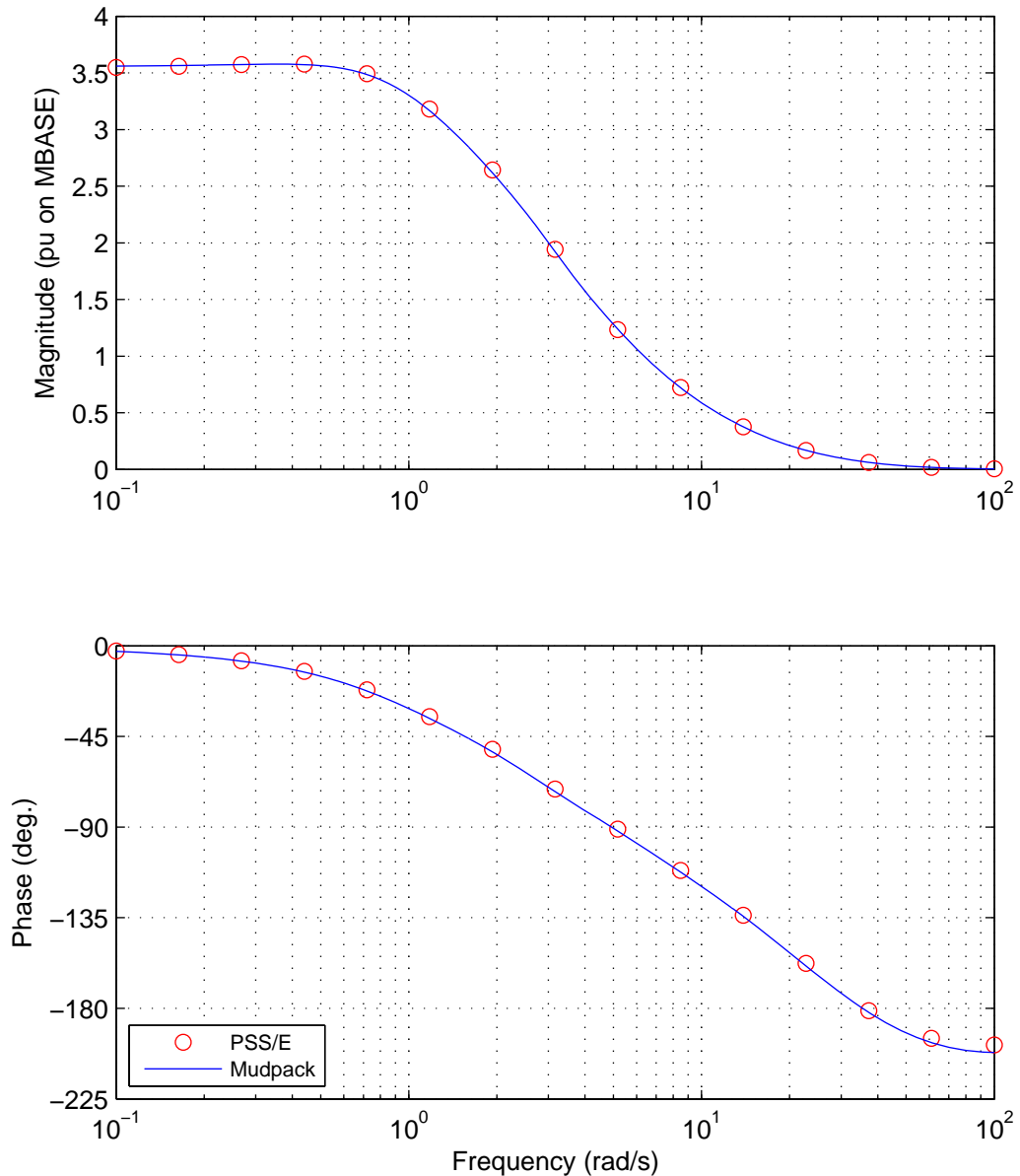
Wed, 22-Jan-2014 19:05:23

Figure 59 As for [Figure 48](#) but for generator NPS_5.

The University of Adelaide, MudpackScripts

Simplified 14 generator model of the SE Australian system. Case 2.

PVr characteristic for TPS_5. Benchmark comparison between Mudpack & PSS/E.



File: PVRbenchmark_Case02_TPS_5_MagPU.eps

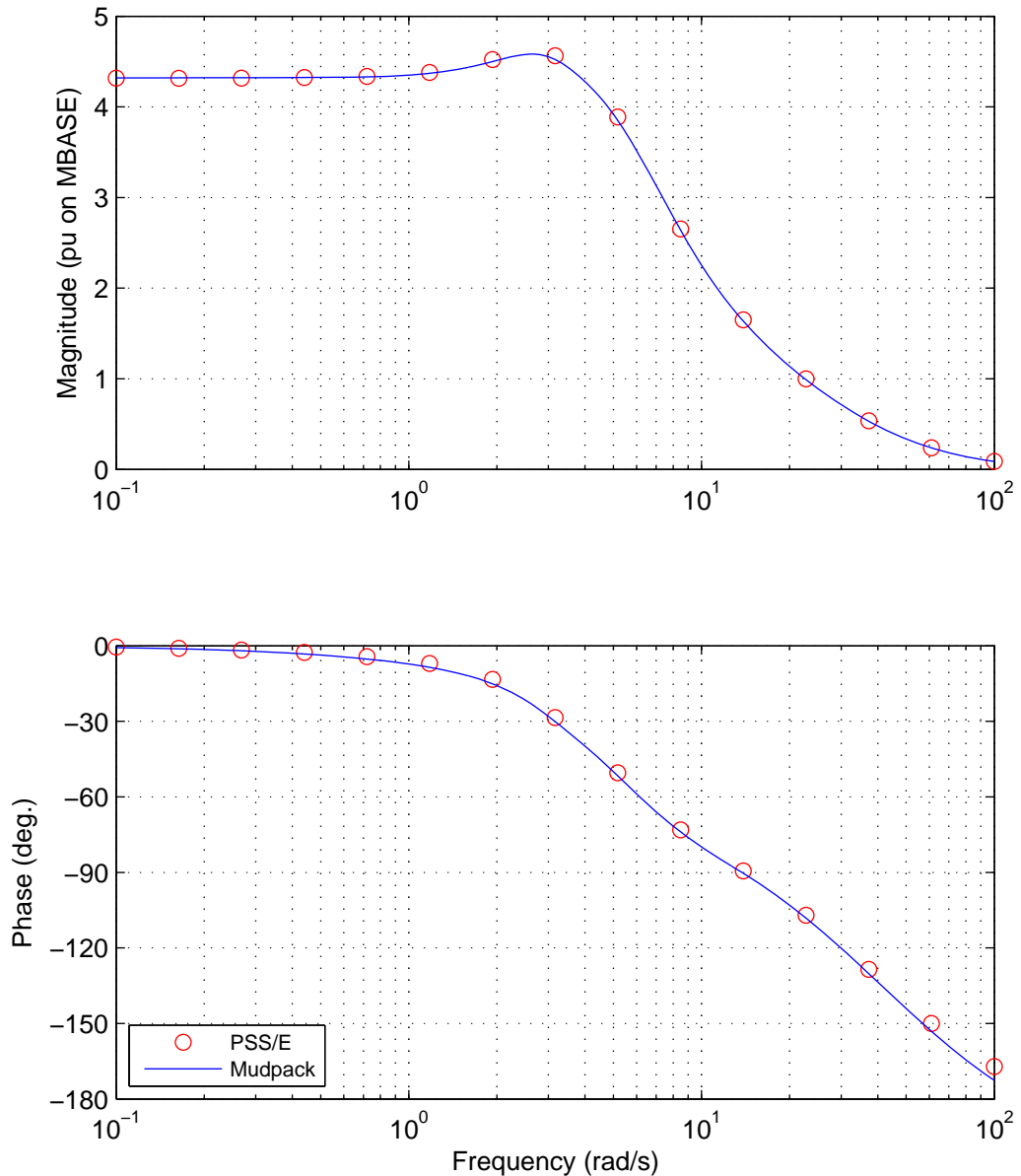
Wed, 22-Jan-2014 19:05:35

Figure 60 As for [Figure 48](#) but for generator TPS_5.

The University of Adelaide, MudpackScripts

Simplified 14 generator model of the SE Australian system. Case 2.

PVr characteristic for PPS_5. Benchmark comparison between Mudpack & PSS/E.



File: PVRbenchmark_Case02_PPS_5_MagPU.eps

Wed, 22-Jan-2014 19:05:47

Figure 61 As for [Figure 48](#) but for generator PPS_5.

Appendix IV PSS[®]/E Transient Stability Analysis

The confirmation in [Appendix III](#) of the very close agreement between the small-signal performance of the PSS[®]/E implementation of the simplified 14-generator model of the South East Australian system and that of the original Mudpack implementation provides a firm basis for analysing the transient stability performance of the model with the PSS[®]/E package. Nevertheless, it is desirable that the transient stability results presented in the following are independently validated in another transient-stability analysis package.

The transient stability studies conducted in this report are with the PSSs in-service with their design damping gains of $D_e = 20.0$ pu on the generator MVA base.

All PSS[®]/E studies are conducted including the frequency dependence of the network parameters (i.e. with NETFRQ = 1).

IV.1 Representation of faults in PSS[®]/E studies

IV.1.1 Type of fault

As mentioned earlier, in the Australian National Electricity Rules (NER) [\[18\]](#), a three-phase to ground fault is not generally considered to be a credible transmission system contingency event for lines operating at or above 220 kV. Rather, solid two-phase to ground faults are normally considered to be the most severe credible type of transmission system fault.

Thus, in accordance with the above practice, when assessing the transient-stability performance of the 14-generator model the response to solid two-phase to ground faults are considered.

As described in [Appendix II.4](#) a two-phase to ground fault at node ‘F’ is represented by connecting an equivalent fault admittance $Y_{fe} = Y_0 + Y_2$ to node ‘F’ in the detailed positive-phase sequence representation of the system. The equivalent fault admittance represents the combined effect of the zero- and negative-phase sequence networks as seen from the fault location.

The equivalent fault admittances for two-phase to ground faults at each high-voltage (≥ 275 kV) node in the system are listed in [Table 31](#) for each of the six study scenarios.

IV.1.2 Fault clearance times

For faults at 275 and 330 kV nodes the fault clearance time (ΔT_c) is 100 ms; for 500 kV faults the clearance time is 80 ms. These clearance times are in accord with the primary protection clearance times specified in Clause S5.1a.8 (Fault clearance times) of the NER [\[18\]](#).

IV.1.3 Fault clearance

Two types of fault clearance are analysed: (i) the fault is cleared by disconnecting the equivalent fault admittance after the elapse of the applicable fault clearance time; (ii) the fault is cleared, after the elapse of the applicable fault clearance time, by simultaneously disconnecting both the equivalent fault admittance and the transmission element (line or transformer) on which the fault is deemed to have occurred.

As mentioned earlier, since the model does not include turbine/governor models events involving the disconnection of generators or loads are not and should not be considered.

IV.2 Two-phase to ground faults on the high-voltage terminals of the generator step-up transformers.

Referring to [Figure 62](#) a two-phase to ground fault at node ‘h’ is analysed.

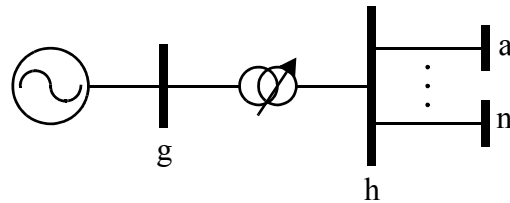


Figure 62 Network for describing faults applied to the high-voltage terminals of generator step-up transformers.

In the first study the application of the fault is represented by connecting the applicable equivalent fault admittance to ‘h’ at time $T_f = 0.5$ s. The fault is then simply cleared at time $T_c = T_f + \Delta T_c$ where ΔT_c is the fault clearance time in [Appendix IV.1.2](#).

In the second study it is assumed that the fault is applied immediately adjacent to bus ‘h’ on the lowest-impedance circuit between nodes ‘h’ and ‘a’. It is cleared by disconnecting both the equivalent fault admittance and the faulted circuit at time $T_c = T_f + \Delta T_c$.

In the third and subsequent studies, faults are successively applied to the remaining circuits connected to ‘h’ with the exception of the generator step-up transformer between nodes ‘g’ and ‘h’.

For each of these faults the responses of the following variables associated with the generator connected to node ‘g’ are displayed: inertia-weighted rotor-angle (DEL), rotor speed perturbation (W), electrical power output (P), stator voltage (V_t), generator field voltage (E_f) and PSS output signal (V_s). Note that the inertia-weighted rotor-angles should not be relied on to provide modal information; rather divergence of this variable provides clear evidence of transient instability.

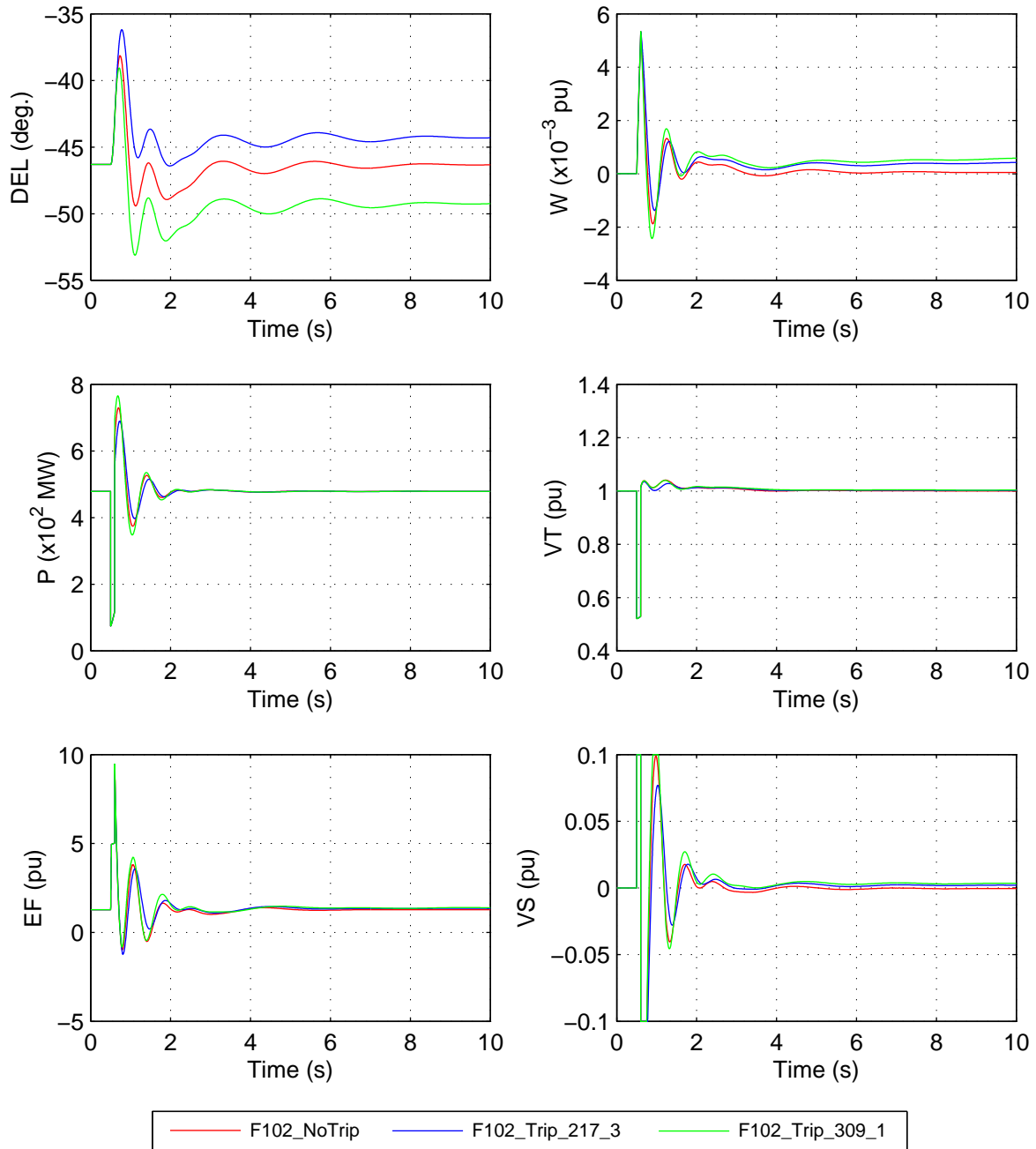
Inspection of the E_f and V_s responses reveals if there is prolonged limiting of the exciter and/or PSS outputs following the fault.

Such studies have been conducted for each of the fourteen generators in each of the six study cases. The results for Case 2 are displayed for each of the fourteen generators in [Figures 63 to 76](#). The time-series data for these results and for the other five cases are provided in the Data-Package (i.e. a total of $6 \times 49 = 294$ studies).

It is found that the system is transiently stable for each of the faults analysed.

The University of Adelaide, MudpackScripts

Simplified 14 generator model of the SE Australian power system;
Case02; Two phase to ground fault at bus 102 for 100ms; Monitor HPS_1 variables.



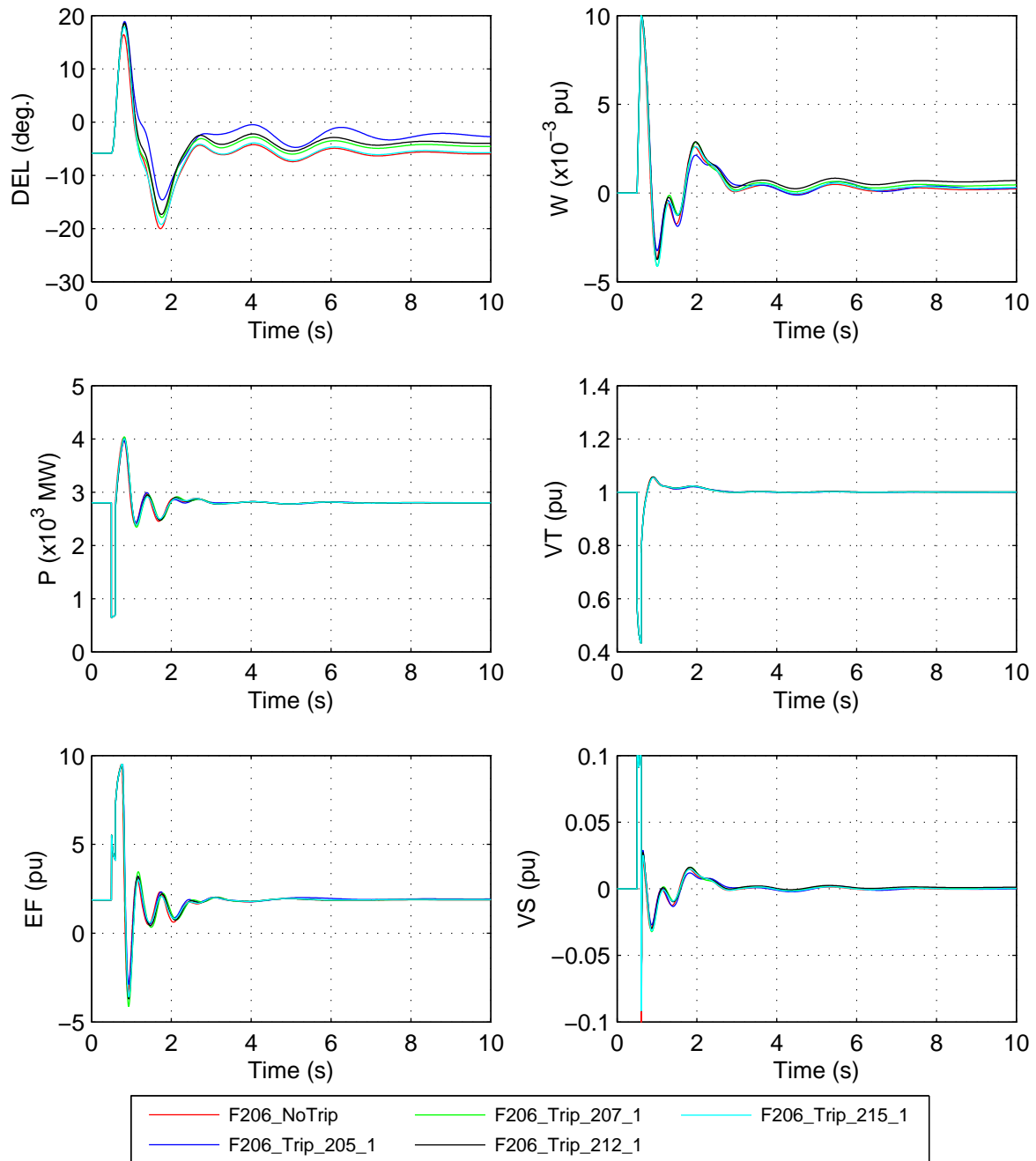
File: FaultStudy_Case02_G101_F102_G101_AllVars.eps
Mon, 17-Feb-2014 21:16:13

Figure 63 Case 2. Two-phase to ground fault applied to the 330 kV bus 102 on the high-voltage side of the HPS_1 generator step-up transformer at $t = 0.5$ s. The fault is cleared 100 ms later.

The responses to the following clearance scenarios are displayed: (i) fault cleared without switching any network elements; (ii) trip circuit 3 between nodes 102 and 217; (iii) trip circuit 1 between nodes 102 and 309. The responses of the following HPS_1 generator variables are displayed: inertia weighted rotor angle (DEL); rotor-speed perturbation (W); electrical power output (P); stator-voltage (Vt); generator field voltage (Ef); PSS output signal (Vs).

The University of Adelaide, MudpackScripts

Simplified 14 generator model of the SE Australian power system;
Case02; Two phase to ground fault at bus 206 for 100ms; Monitor BPS_2 variables.

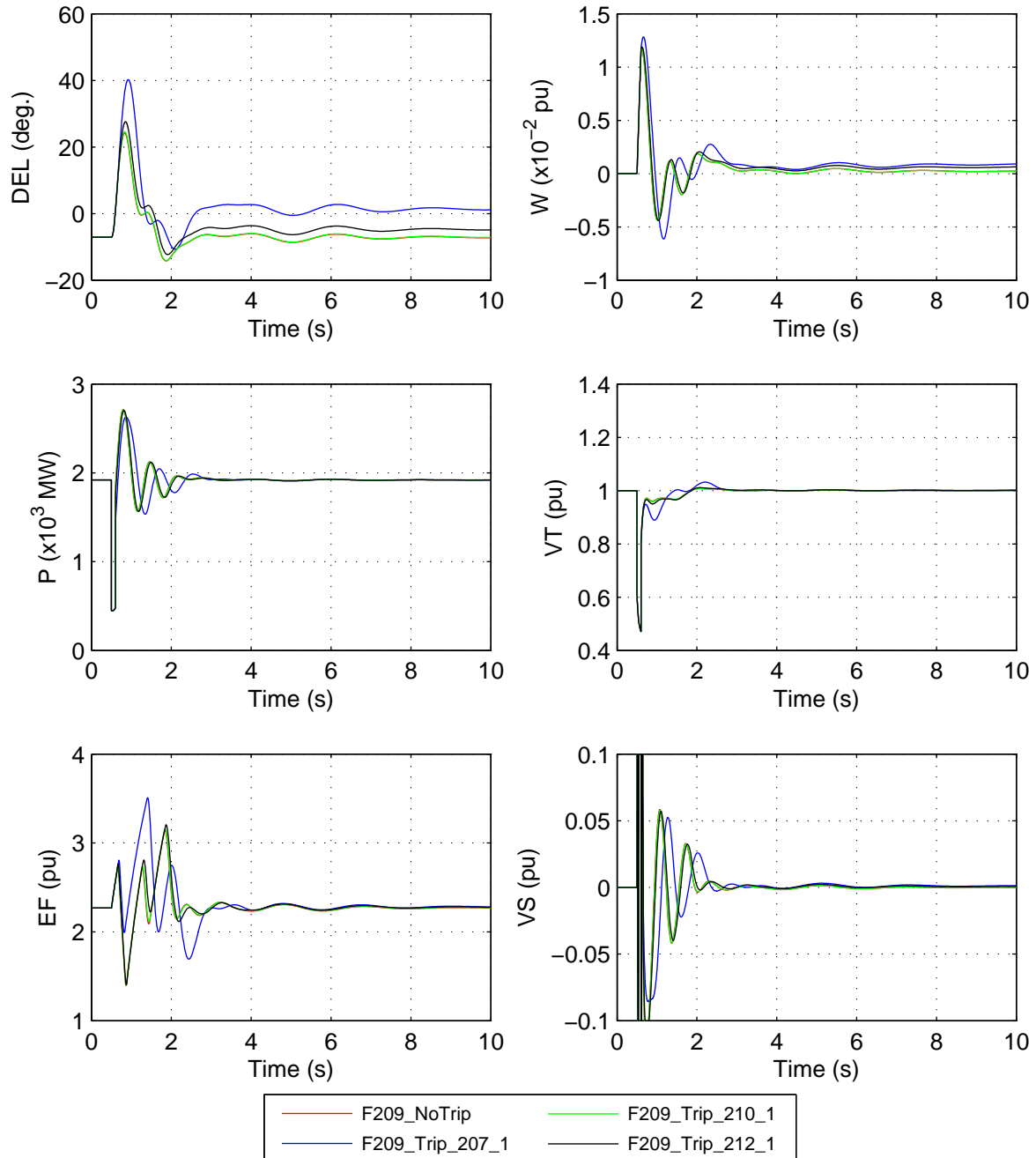


File: FaultStudy_Case02_G201_F206_G201_AllVars.eps
Mon, 17-Feb-2014 21:18:00

Figure 64 Case 2. Similar to [Figure 63](#) but for generator BPS_2 and a fault applied to bus 206.

The University of Adelaide, MudpackScripts

Simplified 14 generator model of the SE Australian power system;
Case02; Two phase to ground fault at bus 209 for 100ms; Monitor EPS_2 variables.

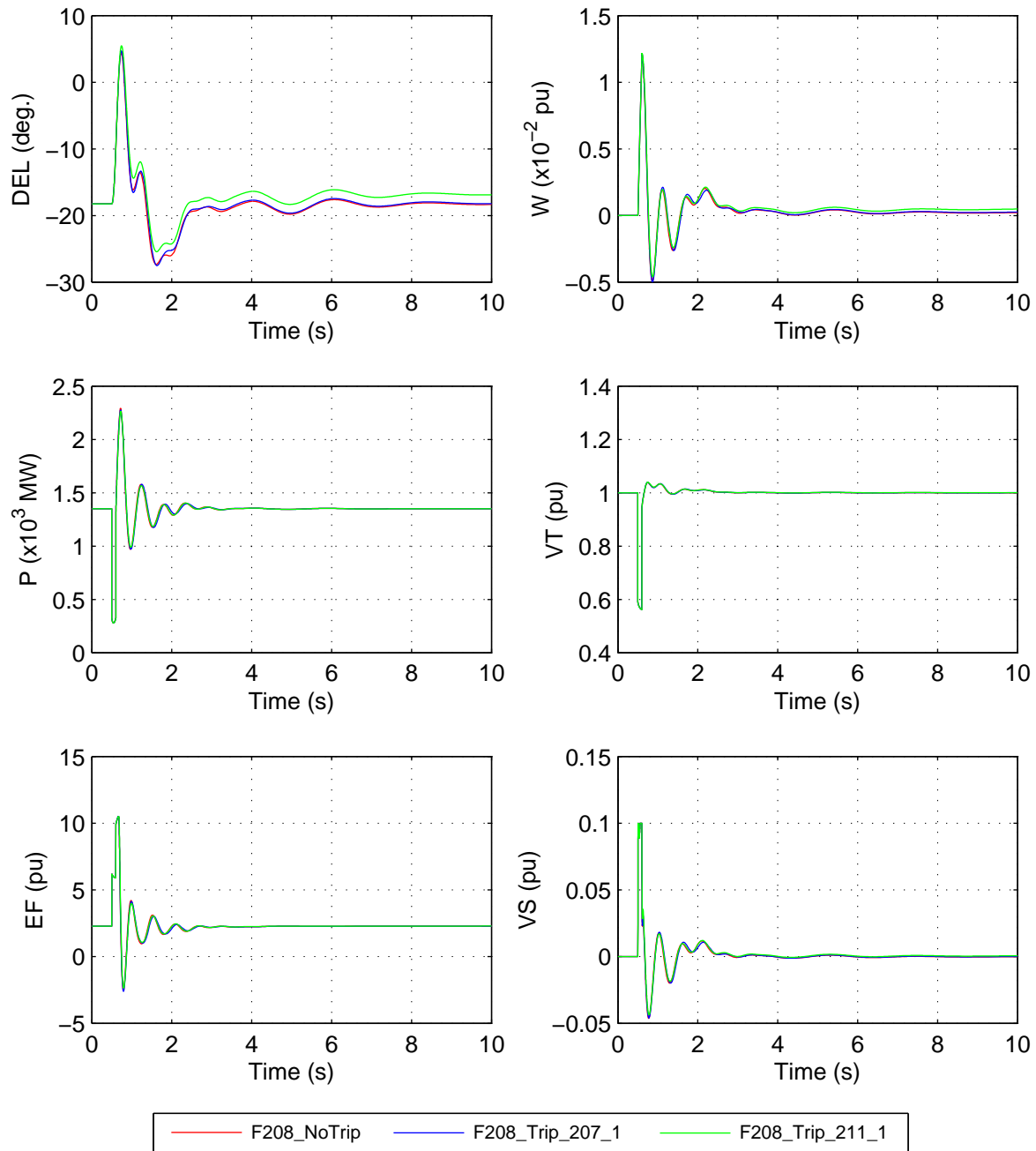


File: FaultStudy_Case02_G202_F209_G202_AllVars.eps
Mon, 17-Feb-2014 21:20:09

Figure 65 Case 2. Similar to [Figure 63](#) but for generator EPS_2 and a fault applied to bus 209.

The University of Adelaide, MudpackScripts

Simplified 14 generator model of the SE Australian power system;
Case02; Two phase to ground fault at bus 208 for 100ms; Monitor VPS_2 variables.

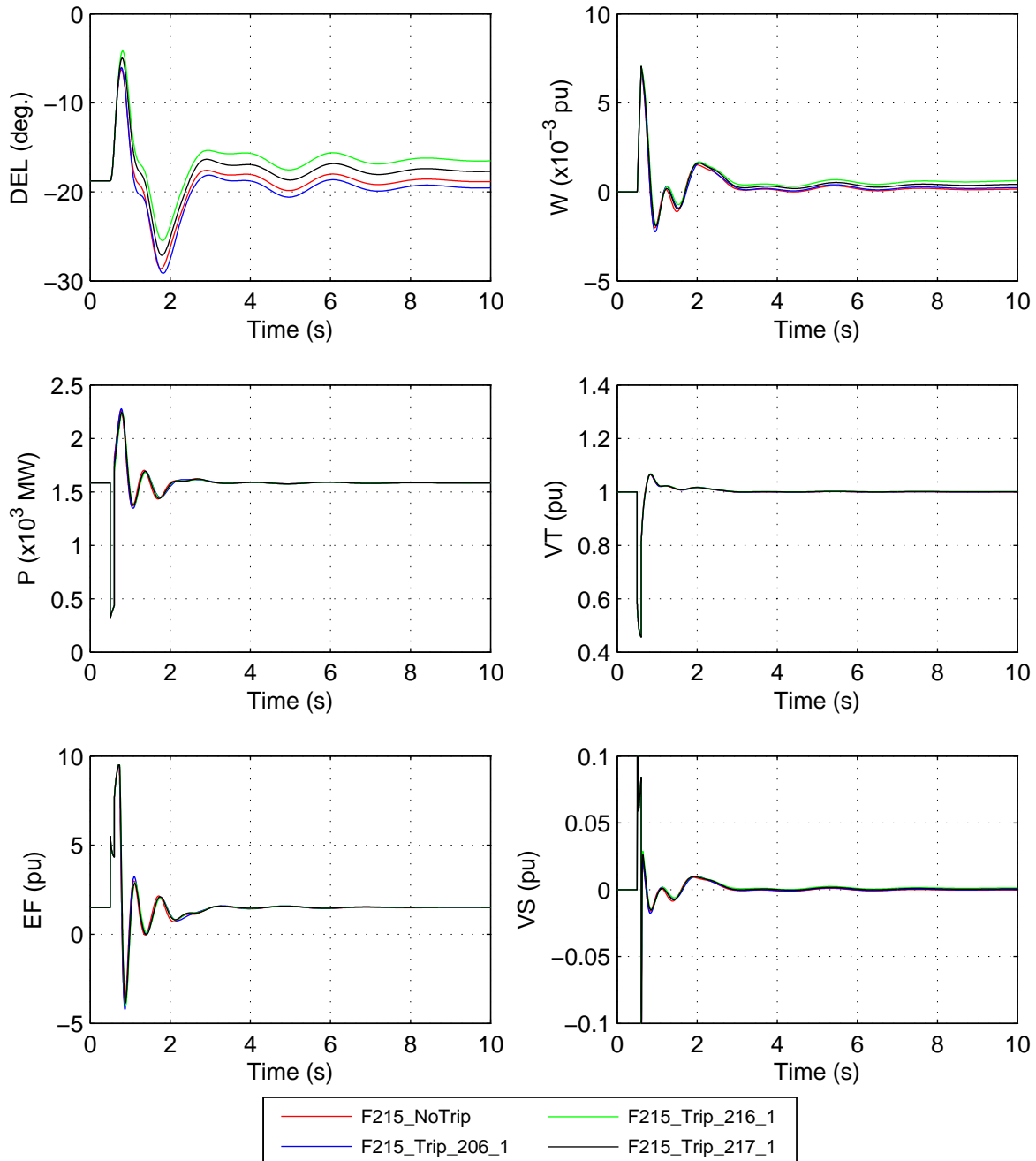


File: FaultStudy_Case02_G203_F208_G203_AllVars.eps
Mon, 17-Feb-2014 21:21:41

Figure 66 Case 2. Similar to [Figure 63](#) but for generator VPS_2 and a fault applied to bus 208.

The University of Adelaide, MudpackScripts

Simplified 14 generator model of the SE Australian power system;
Case02; Two phase to ground fault at bus 215 for 100ms; Monitor MPS_2 variables.

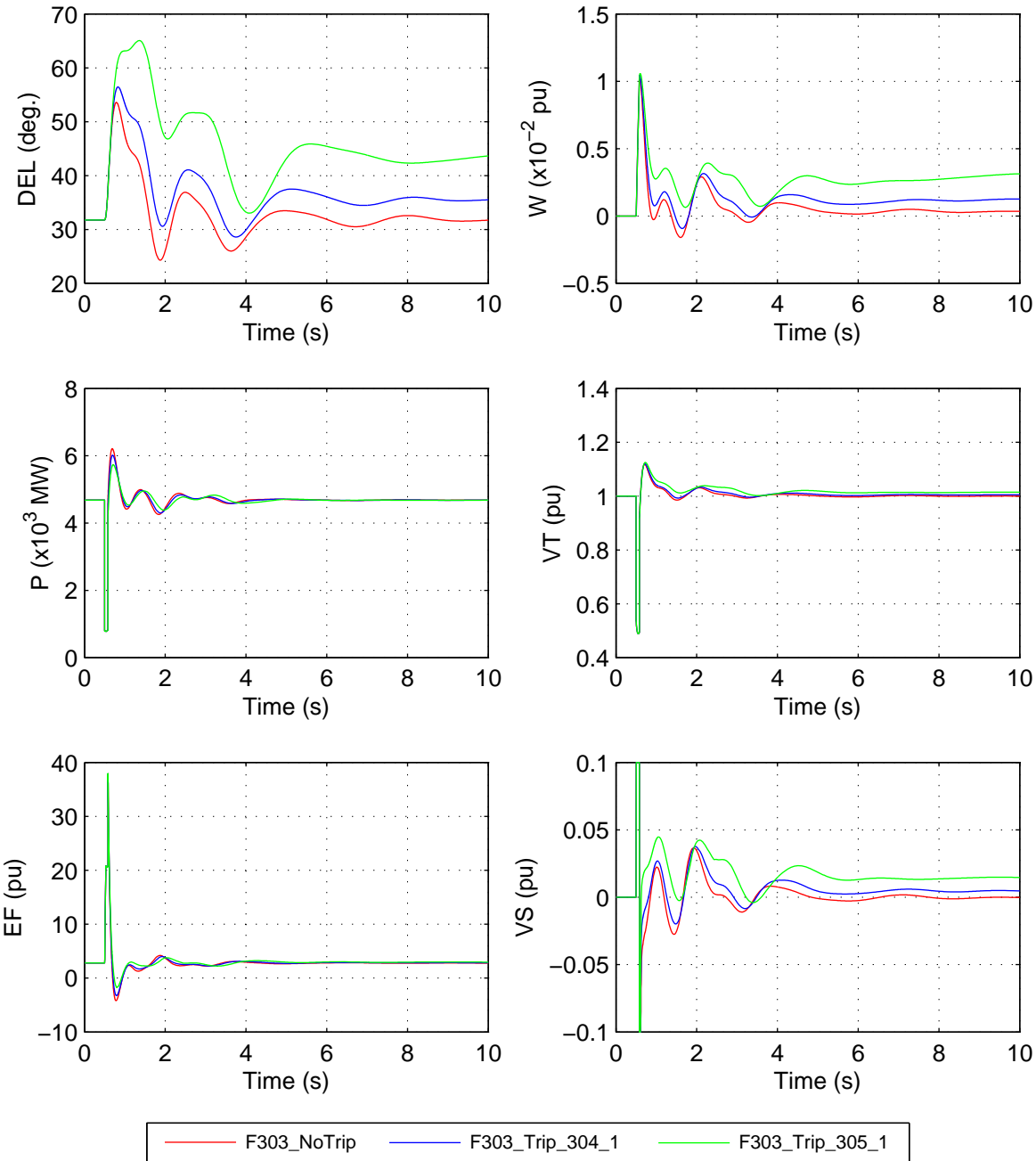


File: FaultStudy_Case02_G204_F215_G204_AllVars.eps
Mon, 17-Feb-2014 21:23:38

Figure 67 Case 2. Similar to [Figure 63](#) but for generator MPS_2 and fault applied to bus 215.

The University of Adelaide, MudpackScripts

Simplified 14 generator model of the SE Australian power system;
Case02; Two phase to ground fault at bus 303 for 80ms; Monitor LPS_3 variables.

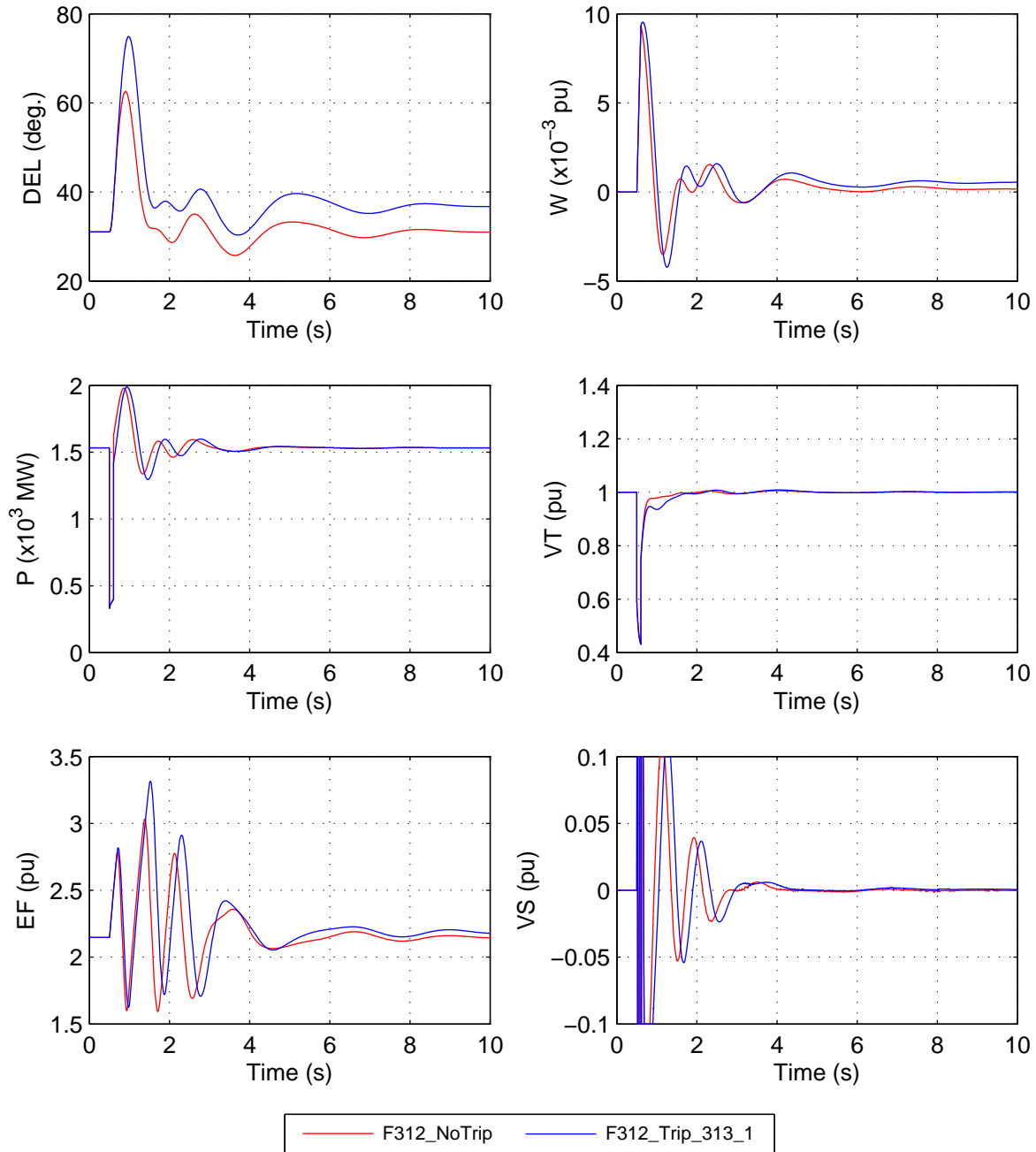


File: FaultStudy_Case02_G301_F303_G301_AllVars.eps
Mon, 17-Feb-2014 21:25:17

Figure 68 Case 2. Similar to [Figure 63](#) but for generator LPS_3 and a fault applied to bus 303.

The University of Adelaide, MudpackScripts

Simplified 14 generator model of the SE Australian power system;
Case02; Two phase to ground fault at bus 312 for 100ms; Monitor YPS_3 variables.

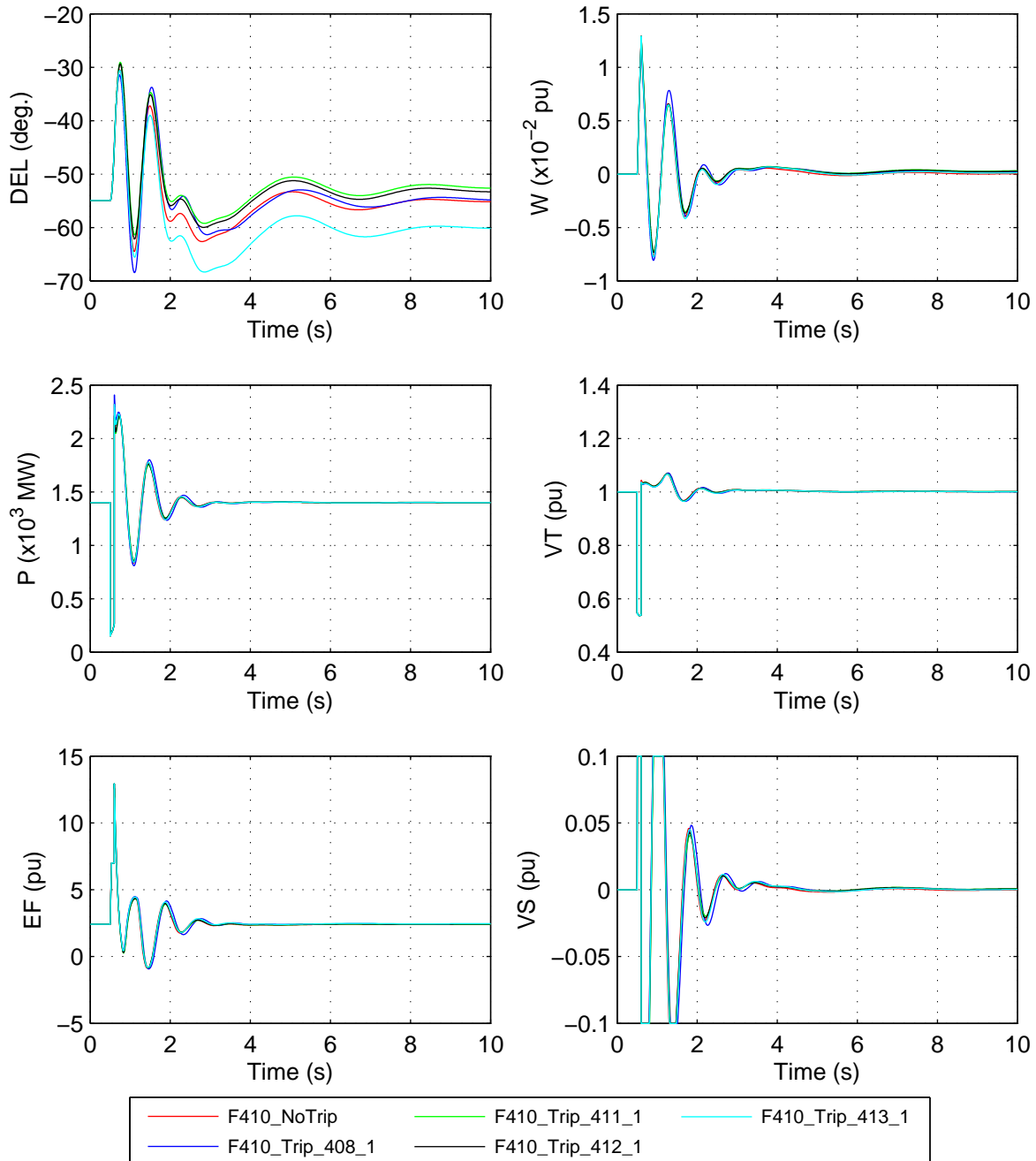


File: FaultStudy_Case02_G302_F312_G302_AllVars.eps
Mon, 17-Feb-2014 21:26:23

Figure 69 Case 2. Similar to [Figure 63](#) but for generator YPS_3 and a fault applied to bus 312.

The University of Adelaide, MudpackScripts

Simplified 14 generator model of the SE Australian power system;
Case02; Two phase to ground fault at bus 410 for 100ms; Monitor TPS_4 variables.

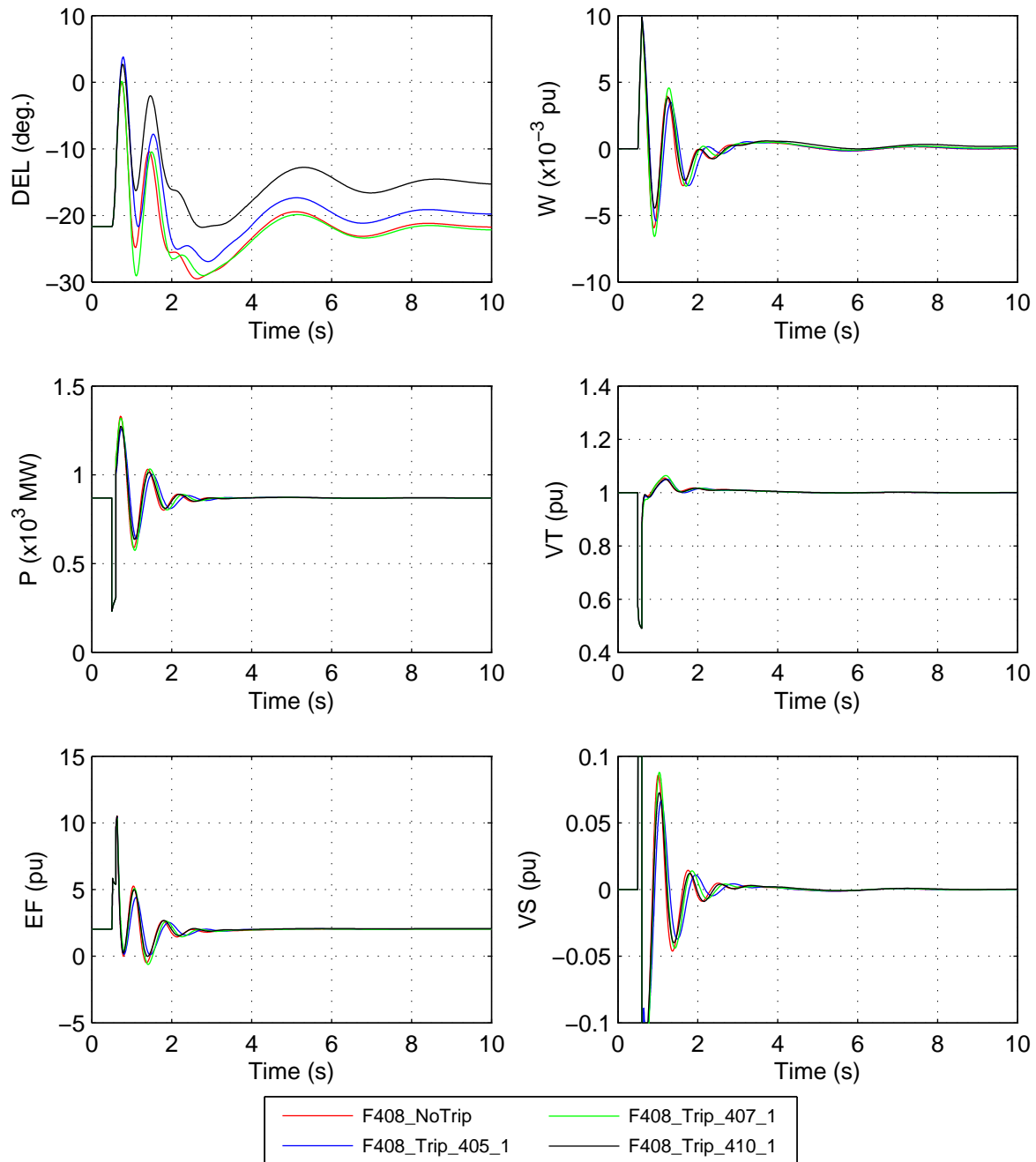


File: FaultStudy_Case02_G401_F410_G401_AllVars.eps
Mon, 17-Feb-2014 21:29:12

Figure 70 Case 2. Similar to [Figure 63](#) but for generator TPS_4 and a fault applied to bus 410.

The University of Adelaide, MudpackScripts

Simplified 14 generator model of the SE Australian power system;
Case02; Two phase to ground fault at bus 408 for 100ms; Monitor CPS_4 variables.

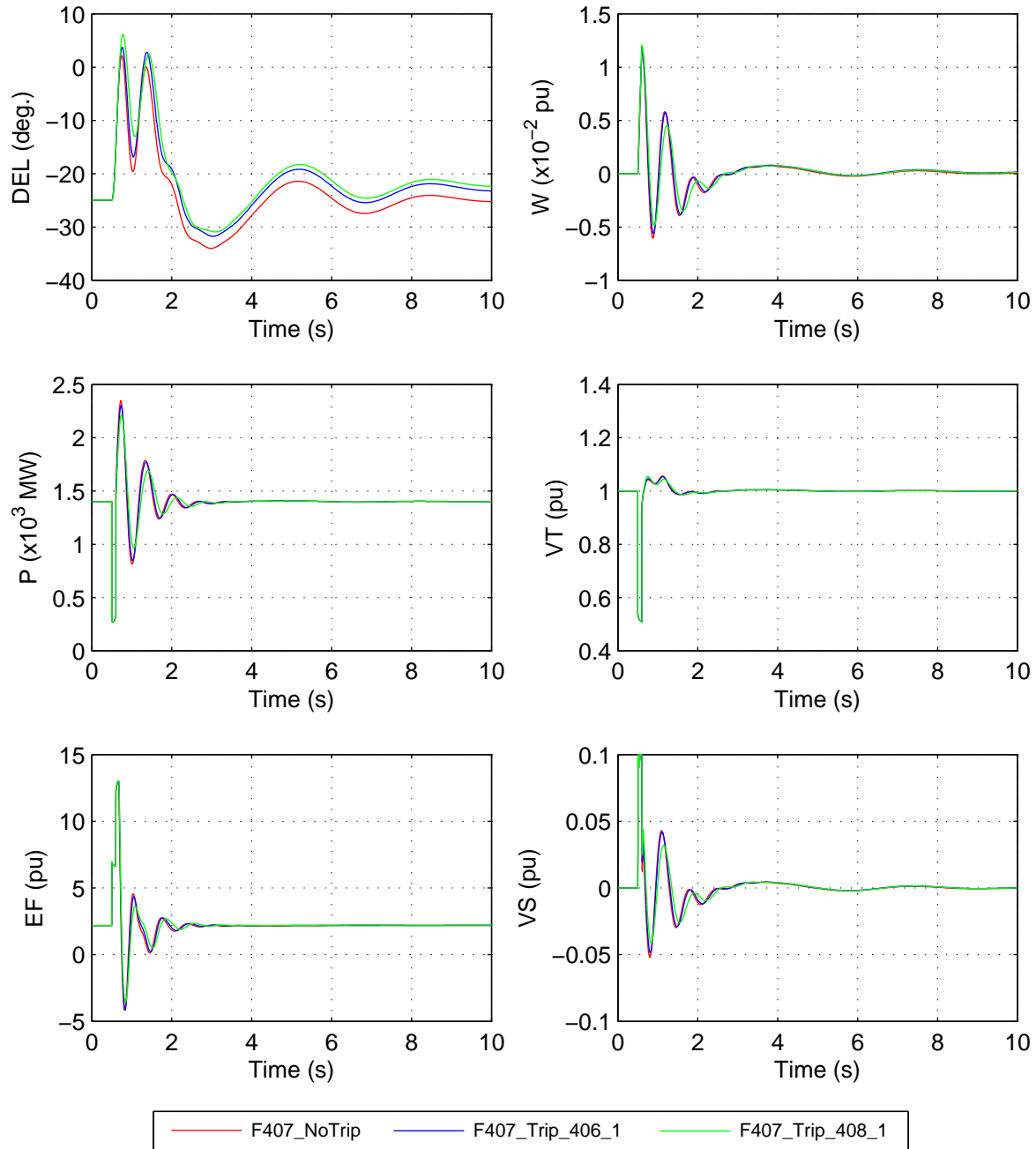


File: FaultStudy_Case02_G402_F408_G402_AllVars.eps
Mon, 17-Feb-2014 21:31:05

Figure 71 Case 2. Similar to [Figure 63](#) but for generator CPS_4 and a fault applied to bus 408.

The University of Adelaide, MudpackScripts

Simplified 14 generator model of the SE Australian power system;
Case02; Two phase to ground fault at bus 407 for 100ms; Monitor SPS_4 variables.

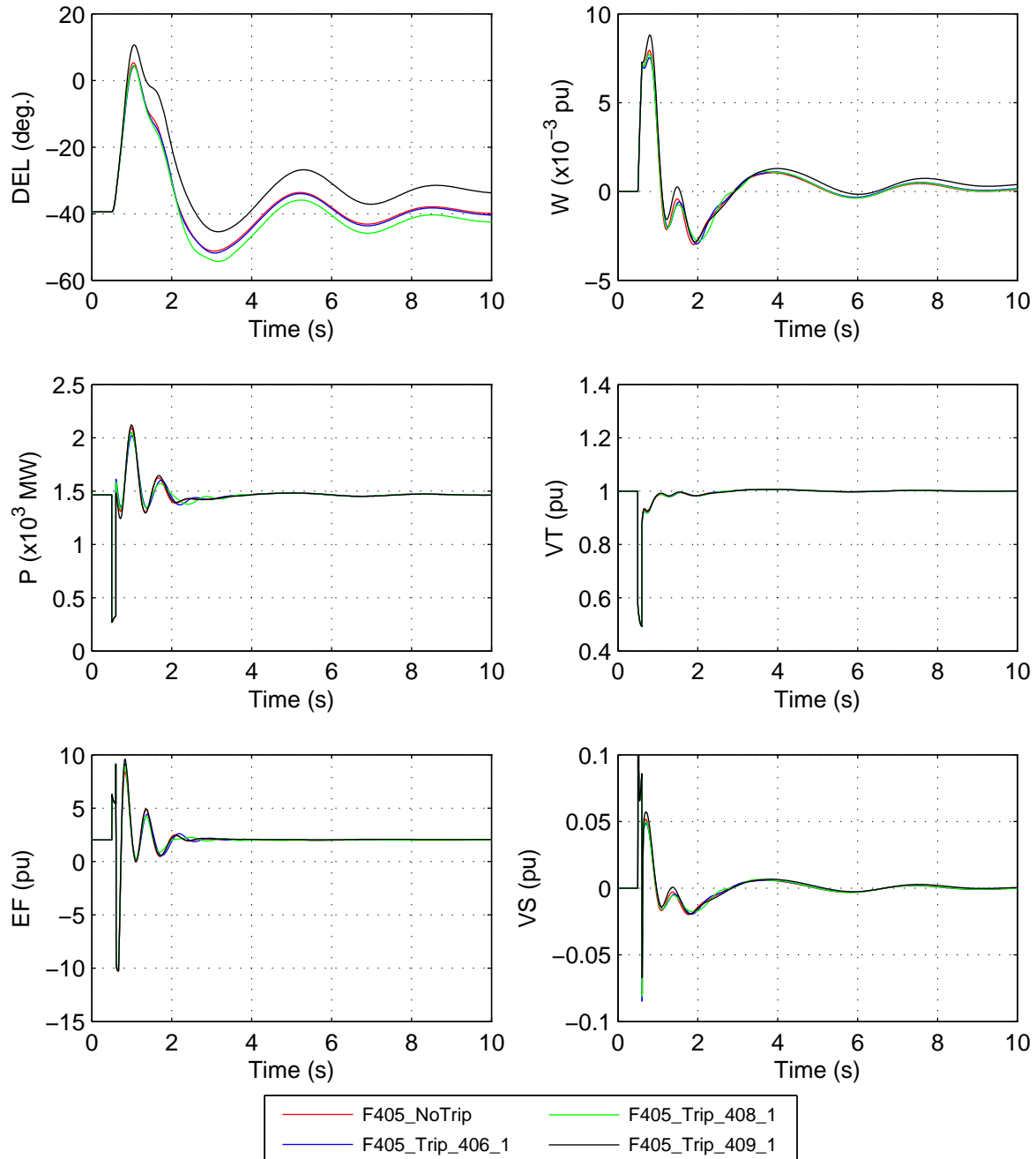


File: FaultStudy_Case02_G403_F407_G403_AllVars.eps
Mon, 17-Feb-2014 21:32:30

Figure 72 Case 2. Similar to [Figure 63](#) but for generator SPS_4 and a fault applied to bus 407.

The University of Adelaide, MudpackScripts

Simplified 14 generator model of the SE Australian power system;
Case02; Two phase to ground fault at bus 405 for 100ms; Monitor GPS_4 variables.

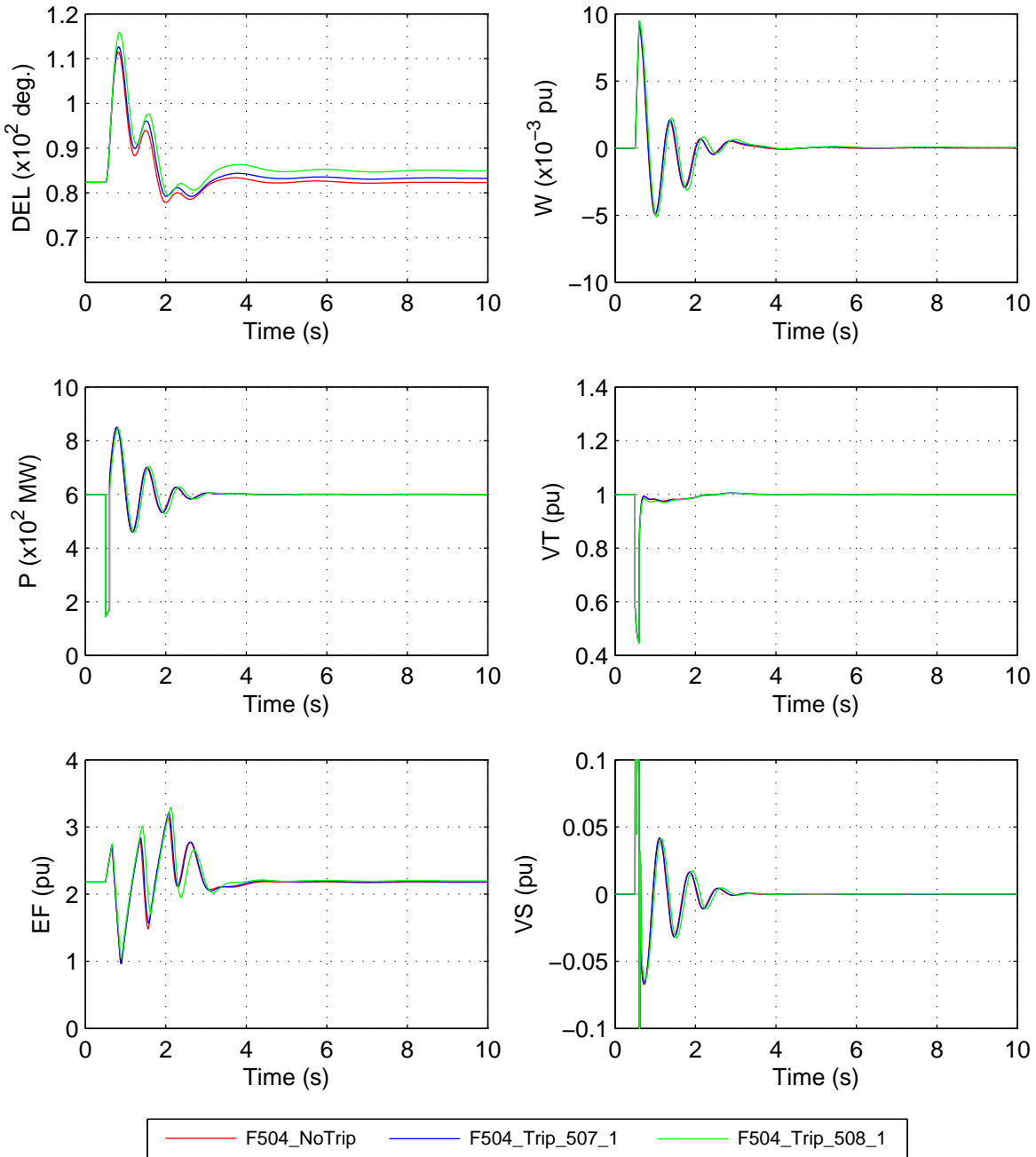


File: FaultStudy_Case02_G404_F405_G404_AllVars.eps
Mon, 17-Feb-2014 21:34:23

Figure 73 Case 2. Similar to [Figure 63](#) but for generator GPS_4 and a fault applied to bus 405.

The University of Adelaide, MudpackScripts

Simplified 14 generator model of the SE Australian power system;
Case02; Two phase to ground fault at bus 504 for 100ms; Monitor NPS_5 variables.

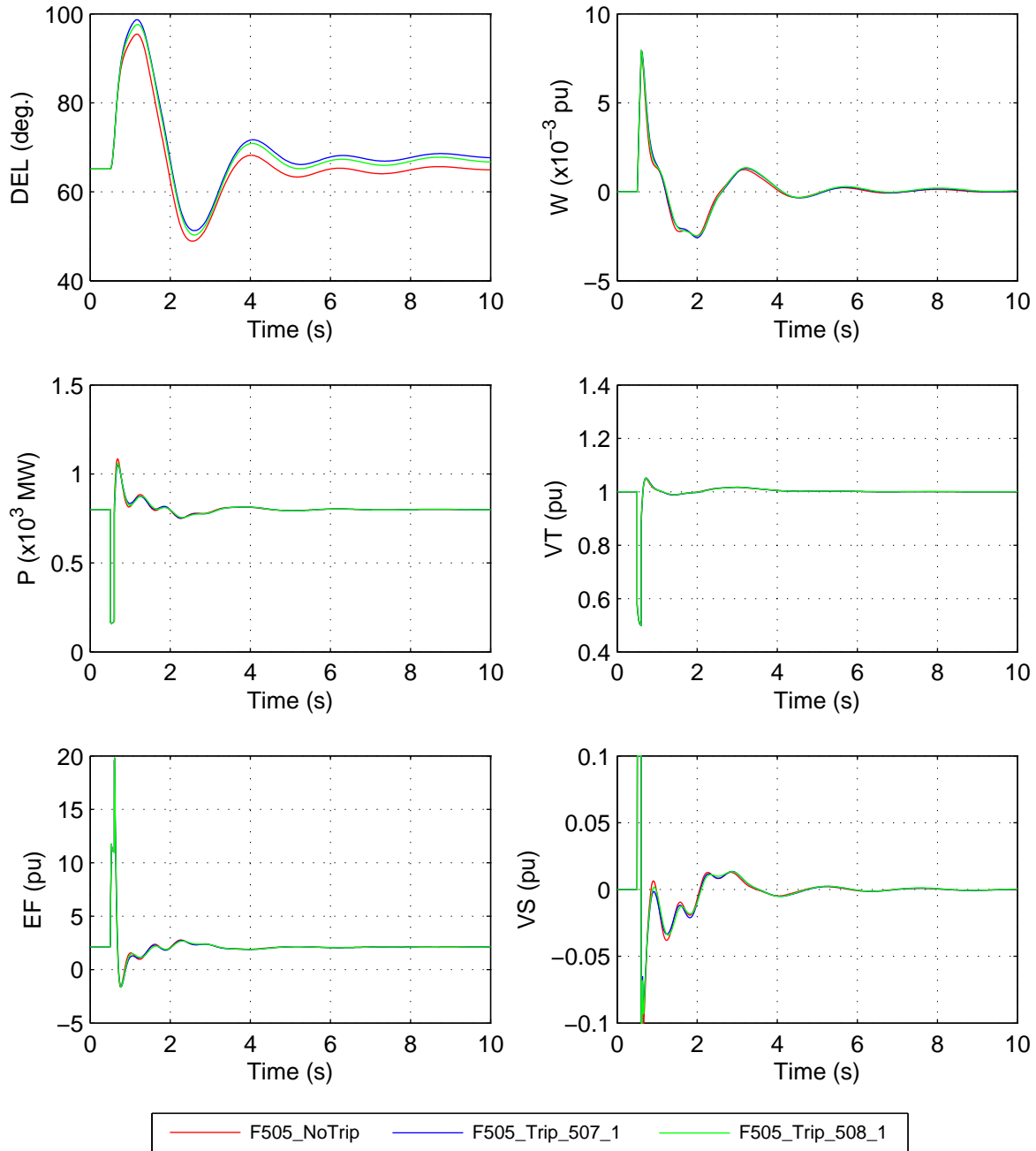


File: FaultStudy_Case02_G501_F504_G501_AllVars.eps
Mon, 17-Feb-2014 21:35:40

Figure 74 Case 2. Similar to [Figure 63](#) but for generator NPS_5 and a fault applied to bus 504.

The University of Adelaide, MudpackScripts

Simplified 14 generator model of the SE Australian power system;
Case02; Two phase to ground fault at bus 505 for 100ms; Monitor TPS_5 variables.

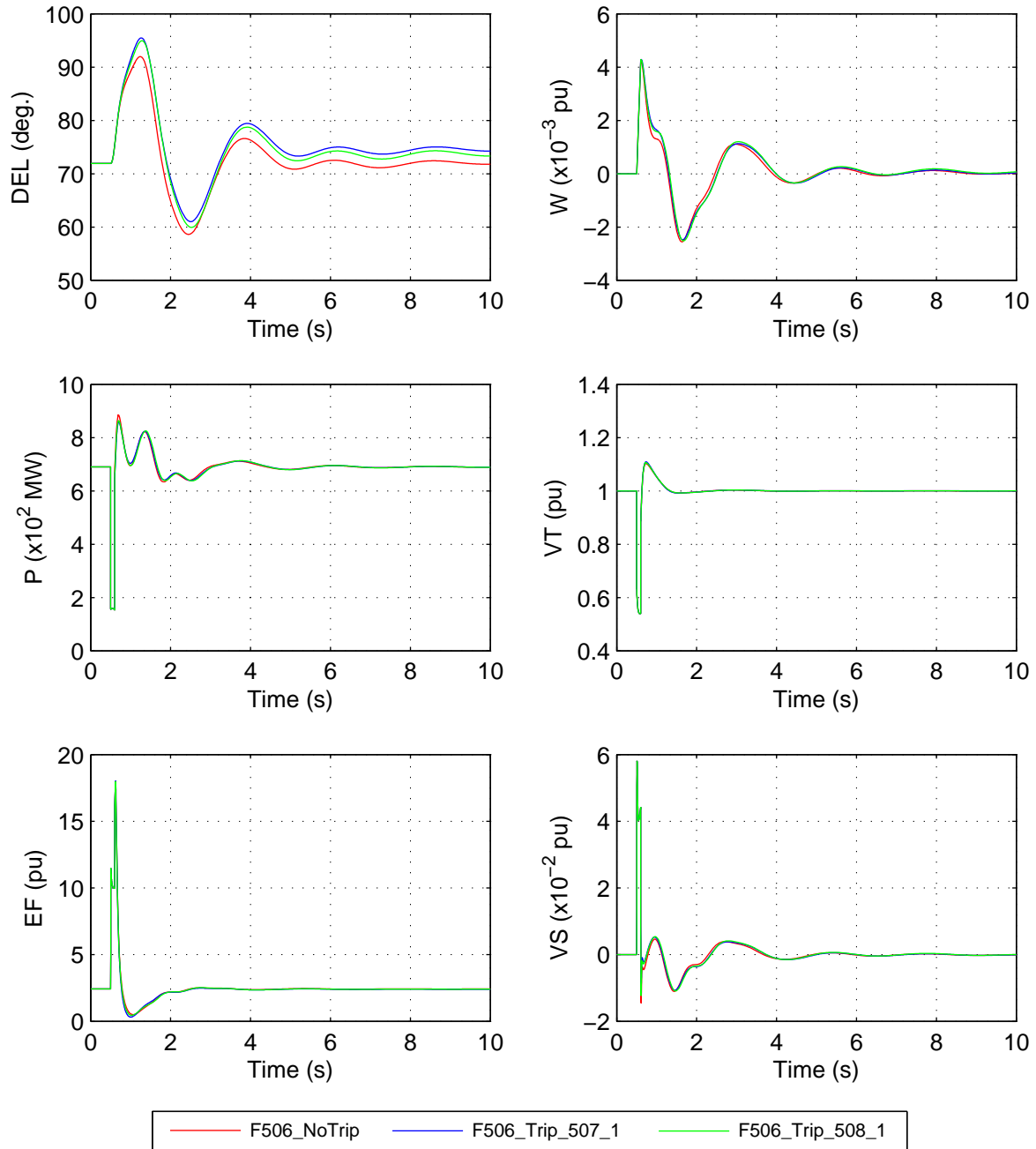


File: FaultStudy_Case02_G502_F505_G502_AllVars.eps
Mon, 17-Feb-2014 21:36:53

Figure 75 Case 2. Similar to [Figure 63](#) but for generator TPS_5 and a fault applied to bus 505.

The University of Adelaide, MudpackScripts

Simplified 14 generator model of the SE Australian power system;
Case02; Two phase to ground fault at bus 506 for 100ms; Monitor PPS_5 variables.



File: FaultStudy_Case02_G503_F506_G503_AllVars.eps
Mon, 17–Feb–2014 21:38:00

Figure 76 Case 2. Similar to [Figure 63](#) but for generator PPS_5 and a fault applied to bus 506.

IV.3 Two-phase to ground faults at other transmission system buses

Apart from the faults applied at the high-voltage terminals of the generator step-up transformers, two-phase to ground faults are similarly analysed at the other 31 nodes in the high-voltage transmission network. The only difference is in the presentation of the results. For each fault at other transmission buses the inertia-weighted rotor-angles (DEL), rotor-speed perturbations

(W) and stator-voltages (Vt) of each of the fourteen generators are displayed. Note that the inertia-weighted rotor-angles should not be relied on to provide modal information; rather divergence of this variable provides clear evidence of transient instability. For each case, studies are conducted for a total of 115 fault scenarios – 31 are bus faults which are cleared without switching a network element; and 84 are faults in which a circuit element (transmission line or transformer) is disconnected to clear the fault.

Results are presented for the following two fault scenarios in Case 2:

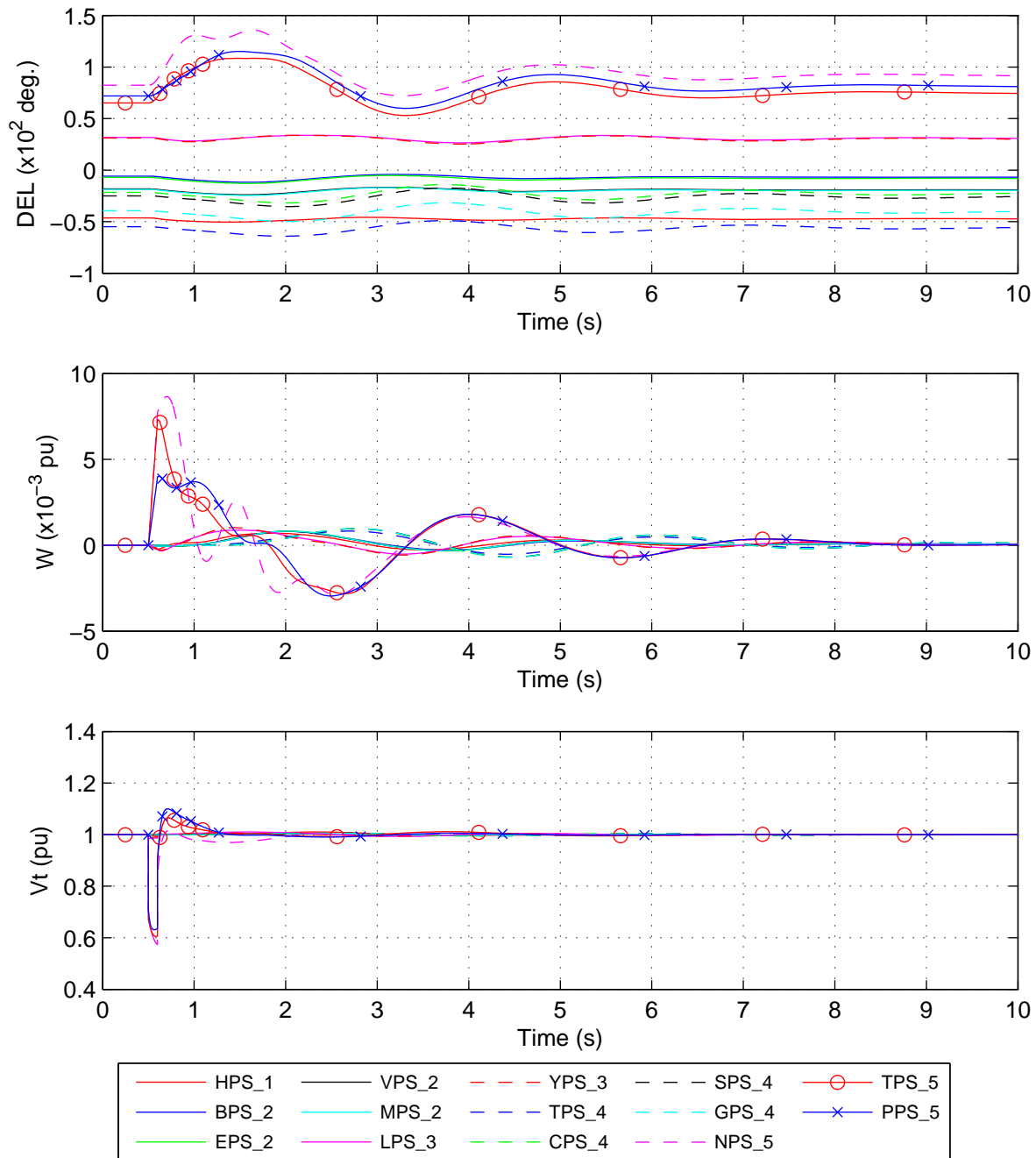
1. A two-phase to ground fault applied to the 275 kV #1 circuit between buses 507 and 509 immediately adjacent to bus 507 at time $t = 0.5$ s. The fault is cleared 100 ms later by tripping the circuit. The generator variables are displayed in [Figure 77](#). In addition, the terminal voltage, susceptance and reactive power outputs of all five SVCs are displayed in [Figure 78](#). In [Figure 79](#) the powerflow on the interconnectors from area 2 to 4 (P.LN_413_410); from area 3 to 2 (P.LN_102_217); and from area 5 to 3 (P.LN_509_315) are displayed. The system is transiently stable.
2. A two-phase to ground fault is applied to the 275 kV #1 circuit between buses 410 and 413 immediately adjacent to bus 413 at time $t = 0.5$ s. The fault is cleared 100 ms later by tripping the circuit. Results, in the same format as above, are displayed for this fault in [Figures 80 to 82](#). The system is transiently stable.

It is found that the system is transiently stable for each of the $6 \times 115 = 690$ faults analysed.

The University of Adelaide, MudpackScripts

Simplified 14 generator model of the SE Australian power system; Case02.

Two phase to ground fault at bus 507 cleared in 100ms by tripping 507–509–1.



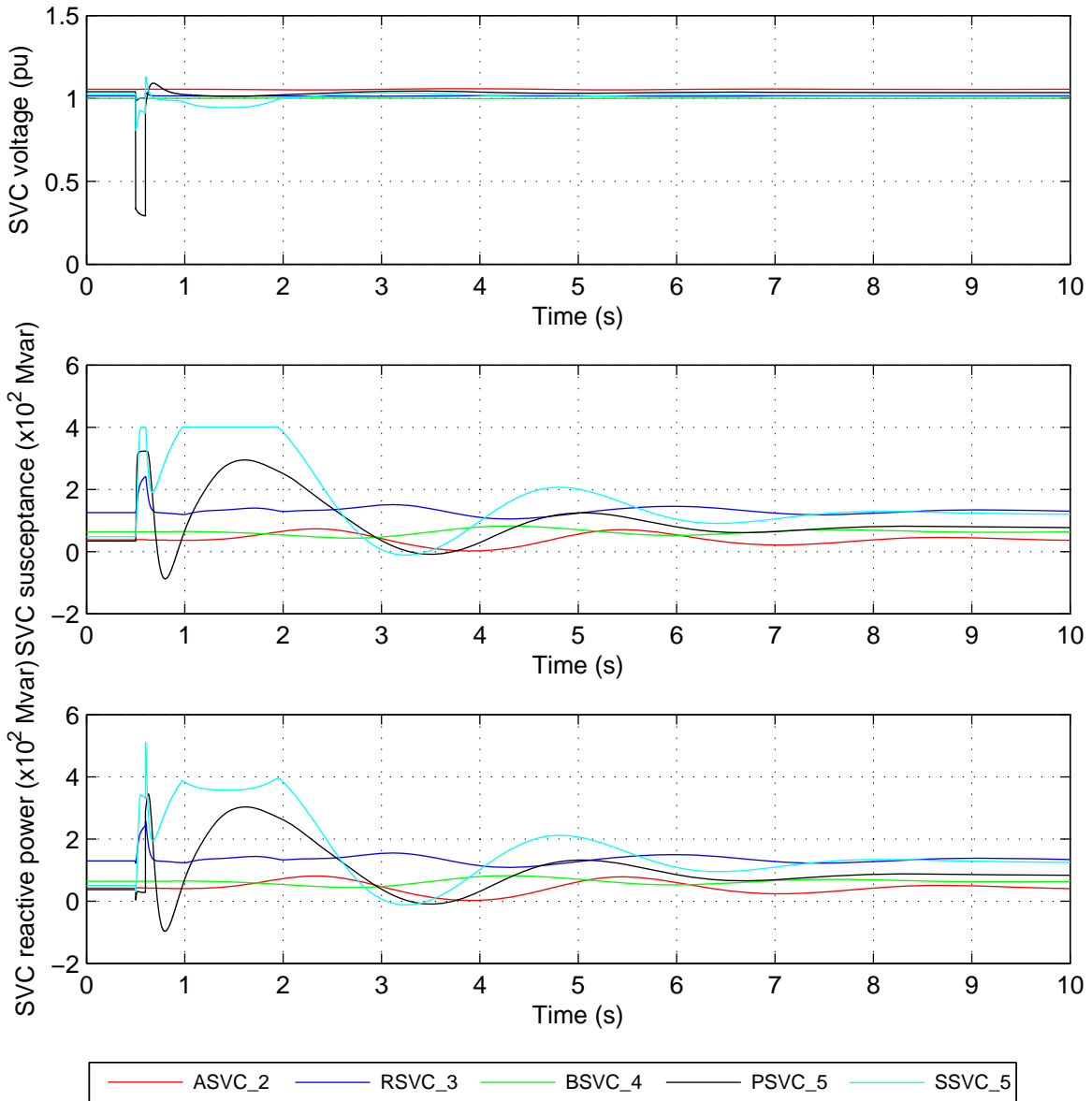
File: NetworkFaultStudy_Case02_F507_Trip_509_1_DWV.eps
Mon, 17-Feb-2014 19:11:08

Figure 77 Case 2. Two-phase to ground fault applied to the 275 kV #1 circuit between buses 507 and 509 immediately adjacent to bus 507 at time $t = 0.5$ s. The fault is cleared 100 ms later by tripping the circuit. The inertia-weighted rotor-angles (DEL), rotor-speed perturbations (W) and stator-voltages (V_t) of all 14 generators are displayed.

The University of Adelaide, MudpackScripts

Simplified 14-generator model of the SE Australian power system.

Case02; 2ph-g fault at bus 507 cleared in 100 ms by tripping 507–509–1



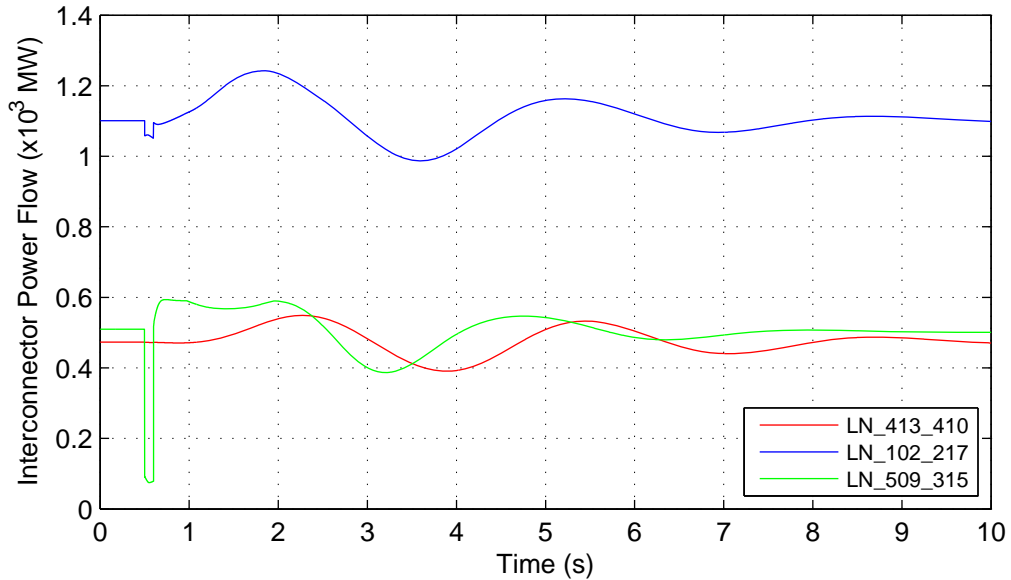
File: Case02_F507_Trip_509_1_SVCR Responses.eps
Mon, 17–Feb–2014 19:05:24

Figure 78 [Continuation of [Figure 77](#)] Case 2. Two-phase to ground fault applied to the 275 kV #1 circuit between buses 507 and 509 immediately adjacent to bus 507 at time $t = 0.5$ s. The fault is cleared 100 ms later by tripping the circuit. The terminal voltage, susceptance and reactive power output of all five SVCs are displayed.

The University of Adelaide, MudpackScripts

Simplified 14-generator model of the SE Australian power system.

Case02; 2ph-g fault at bus 507 cleared in 100 ms by tripping 507–509–1



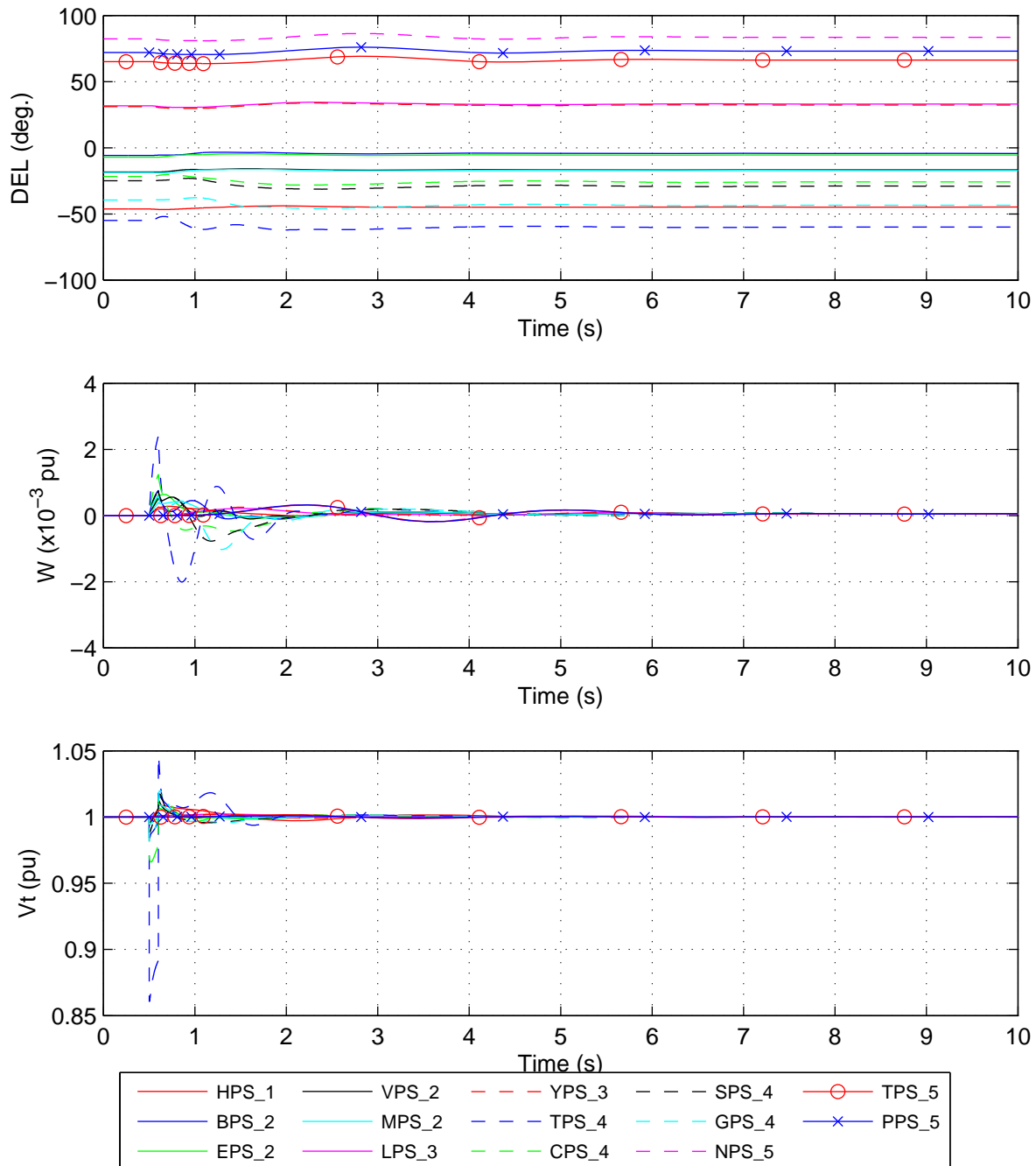
File: Case02_F507_Trip_509_1_TielineResponses.eps
Mon, 17-Feb-2014 19:08:33

Figure 79 Continuation of [Figure 77] Case 2. Two-phase to ground fault applied to the 275 kV #1 circuit between buses 507 and 509 immediately adjacent to bus 507 at time $t = 0.5$ s. The fault is cleared 100 ms later by tripping the circuit. The interconnector power flows are displayed.

The University of Adelaide, MudpackScripts

Simplified 14 generator model of the SE Australian power system; Case02.

Two phase to ground fault at bus 413 cleared in 100ms by tripping 413–410–1.



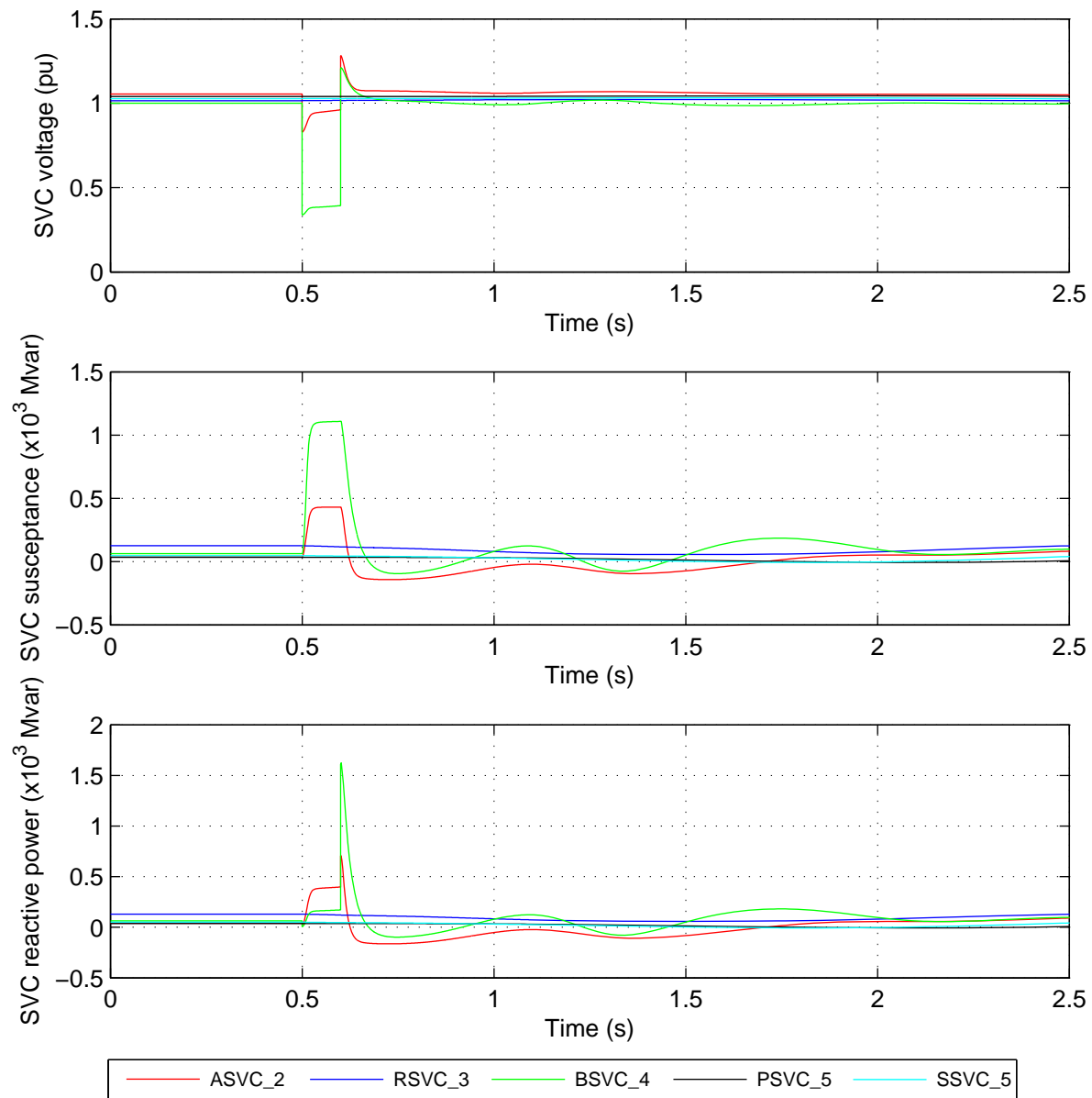
File: NetworkFaultStudy_Case02_F413_Trip_410_1_DWV.eps
Mon, 17-Feb-2014 21:07:46

Figure 80 Case 2. Two-phase to ground fault applied to the 275 kV #1 circuit between buses 410 and 413 immediately adjacent to bus 413 at time $t = 0.5$ s. The fault is cleared 100 ms later by tripping the circuit. The inertia weighted rotor angles (DEL), rotor-speed perturbations (W) and stator-voltages (V_t) of all 14 generators are displayed.

The University of Adelaide, MudpackScripts

Simplified 14-generator model of the SE Australian power system.

Case02; 2ph-g fault at bus 410 cleared in 100 ms by tripping 410–413–1



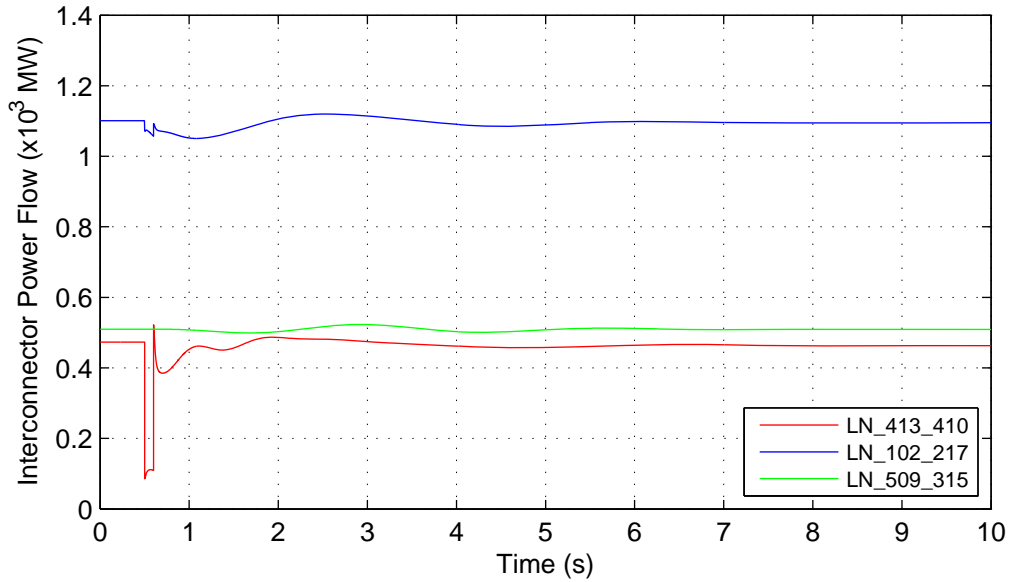
File: Case02_F410_Trip_413_1_SVCResponses.eps
Mon, 17-Feb-2014 21:04:41

Figure 81 [Continuation of [Figure 80](#)] Case 2. Two-phase to ground fault applied to the 275 kV #1 circuit between buses 410 and 413 immediately adjacent to bus 413 at time $t = 0.5$ s. The fault is cleared 100 ms later by tripping the circuit. The terminal voltage, susceptance and reactive power output of all five SVCs are displayed.

The University of Adelaide, MudpackScripts

Simplified 14-generator model of the SE Australian power system.

Case02; 2ph-g fault at bus 413 cleared in 100 ms by tripping 413–410–1



File: Case02_F410_Trip_413_1_TielineResponses.eps
Mon, 17-Feb-2014 21:02:58

Figure 82 Continuation of [Figure 80] Case 2. Two-phase to ground fault applied to the 275 kV #1 circuit between buses 410 and 413 immediately adjacent to bus 413 at time $t = 0.5$ s. The fault is cleared 100 ms later by tripping the circuit. The interconnector power flows are displayed.

Appendix V Model data and results package

V.1 Online sources of data and results

The data and results listed below are available from the following web-sites:

1. <http://www.eleceng.adelaide.edu.au/groups/PCON/PowerSystems/IEEE/AU14G/Ver04>
2. <DJV: IEEE website??>

If you have any problems downloading the data please contact David.Vowles@adelaide.edu.au.

V.2 Model data

The archive file AU14GenModelData_Ver04.zip is available for download from the websites listed in [Appendix V.1](#). It contains the loadflow data for the six study cases in PSS®/E loadflow raw data format (version 29); the dynamics model data in PSS®/E and Mudpack formats; and the network sequence data in PSS®/E compatible format and loadflow solution reports. Refer to the file AU14GenModelData_Ver04_Contents.pdf in the archive for further information on its contents.

V.3 State-space models and eigenanalysis results in Matlab format

The archive file AU14GenModel_StateSpaceAndEigen_Matlab_Ver04.zip is available for download from the websites listed in [Appendix V.1](#). It contains the following Matlab *.mat files, generated by a small-signal analysis package [14], are provided for Cases 1 & 6, (i) with no PSSs in service, and (ii) with PSSs in service:

1. the ABCD matrices of the system are in files:
 - Case#_PSSs_Off_ABCD_Rev3_Matlab.mat; and
 - Case#_PSSs_On_ABCD_Rev3_Matlab.mat;
2. the eigenvalues, the eigenvectors and participation factors are in:
 - Case#_PSSs_Off_Eigs_Rev3_Matlab.mat; and
 - Case#_PSSs_On_Eigs_Rev3_Matlab.mat,

where # is the case number, 1 or 6.

Refer to AU14GenModel_StateSpaceAndEigen_Matlab_Ver04_Contents.pdf in the archive for further information on its contents.

V.4 Small-signal time-response results

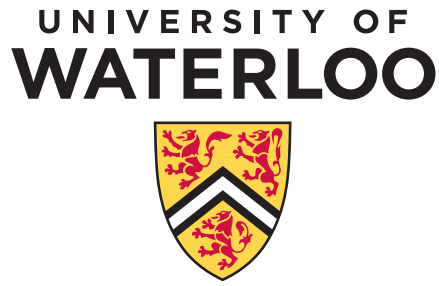
The archive file AU14GenModel_SmallSignal_TimeResponse_Results_Ver04.zip is available for download from the websites listed in [Appendix V.1](#). It contains in Matlab and CSV format time-series data from the Mudpack and PSS®/E step-response tests reported in Appendices [III.1](#) and [III.2](#). It also contains PDF files displaying the results of the step-response tests. A Matlab mfile is also provided to assist the user to graphically display time series data. Refer to the file AU14GenModel_SmallSignal_TimeResponse_Results_Ver04_Contents.pdf in the archive for further information on its contents.

V.5 PSS[®]/E transient stability analysis results

The archive file AU14GenModel_TransientStabilityResults_Ver04.zip is available for download from the websites listed in [Appendix V.1](#). It contains in Matlab and CSV format time-series data from the PSS[®]/E transient-stability tests reported in [Appendix IV](#). It also contains PDF files displaying the results of the transient-stability studies. A Matlab mfile is also provided to assist the user to graphically display time series data. Refer to the file AU14GenModel_TransientStabilityResults_Ver04_Contents.pdf in the archive for further information on its contents.

B.1

**Appendix B - Report on the Simplified Australian 14-Generator Model by
Prof. Claudio Canizares and Dr. Behnam Tamimi**



Department of Electrical and Computer Engineering

IEEE Task Force on Benchmark Systems for Stability Controls: Australian Test System

Behnam Tamimi and Claudio A. Cañizares

12 March 2015

I. Introduction

Small-perturbation and transient stability analyses are performed for a simplified model of the Australian power system using the DSA Tools [1], as part of the work of the IEEE Task Force on Benchmark Systems for Stability Controls. This report and its accompanying files¹ can serve as a benchmark for future similar studies. The DSA Tools include four components, namely, PSAT, SSAT, VSAT, and TSAT, to perform power flow, small-perturbation stability, voltage stability, and transient stability analyses, respectively.

Two other studies on this system have been reported in [2] and [3]. The focus in [2] is small-perturbation stability (eigenvalue) analysis of the system under different loading conditions, whereas time-domain simulations which examine the transient stability of the system for different disturbances are mainly reported in [3].

The report is organized as follows: First, the test system is briefly described; then, the transient stability simulations with TSAT and the studied scenarios/disturbances from [2] are presented and discussed; finally, the results of eigenvalue analyses using SSAT are described.

II. System Description

This test system represents a simplified model of the eastern and southern Australian networks [2], [3]. There are 19 generators in the system synchronized at 50 Hz. The grid includes 59 buses and 104 lines with 15 kV to 500 kV voltage levels. Six power flow cases summarized in Table 1 are considered in the following sections to examine the system performance under different loading conditions. Note that Case 6 and Case 3 have the lowest and the highest loading levels, respectively.

Table 1. Summary of the six power flow cases studied.

	Generators [MW]	Loads [MVA]
Case 1	23013.71	$22300 + j 2462$
Case 2	21568.69	$21000 + j 2251$
Case 3	25411.13	$24800 + j 2760$
Case 4	15038.15	$14806 + j 1595$
Case 5	19041.64	$18597 + j 1920$
Case 6	14828.54	$14631 + j 1595$

III. Time-domain Simulations

Time-domain simulations are carried out using TSAT, based on the data provided in [2]. All the dynamic models used in [2] are recognized by TSAT and are directly imported into its environment. However, to

¹ Available [Online], <http://www.sel.eesc.usp.br/ieee/index.htm>

avoid input data modifications, the automatic data-correction option is disabled and a small integration time-step (1 ms) is used, so that lower limits on the TSAT models' time-constants are not enforced.

Three following disturbances are simulated in the study, with a duration of 10 s for all of them:

- A. Two-phase-to-ground fault at Bus 209 at $t = 0.5$ s, and cleared in 100 ms without disconnecting any circuit elements.
- B. Two-phase-to-ground fault at Bus 303 at $t = 0.5$ s, and cleared in 80 ms without disconnecting any circuit elements.
- C. Two-phase-to-ground fault at Bus 506 at $t = 0.5$ s, and cleared in 100 ms without disconnecting any circuit elements.

Case 2 is used for the simulations, with the generator stabilizers in service. Various variables for generators, including stabilizer outputs, and SVCs are plotted and presented in the appendix, which includes sixty selected (based on the proximity of fault locations) graphs comparing TSAT and PSS/E results. The results match well with the ones reported in [2]. The differences can be attributed to some small model differences between PSS/E and TSAT. Figures 1(a) - 1(d) show the results at Bus 101 for Disturbance A.

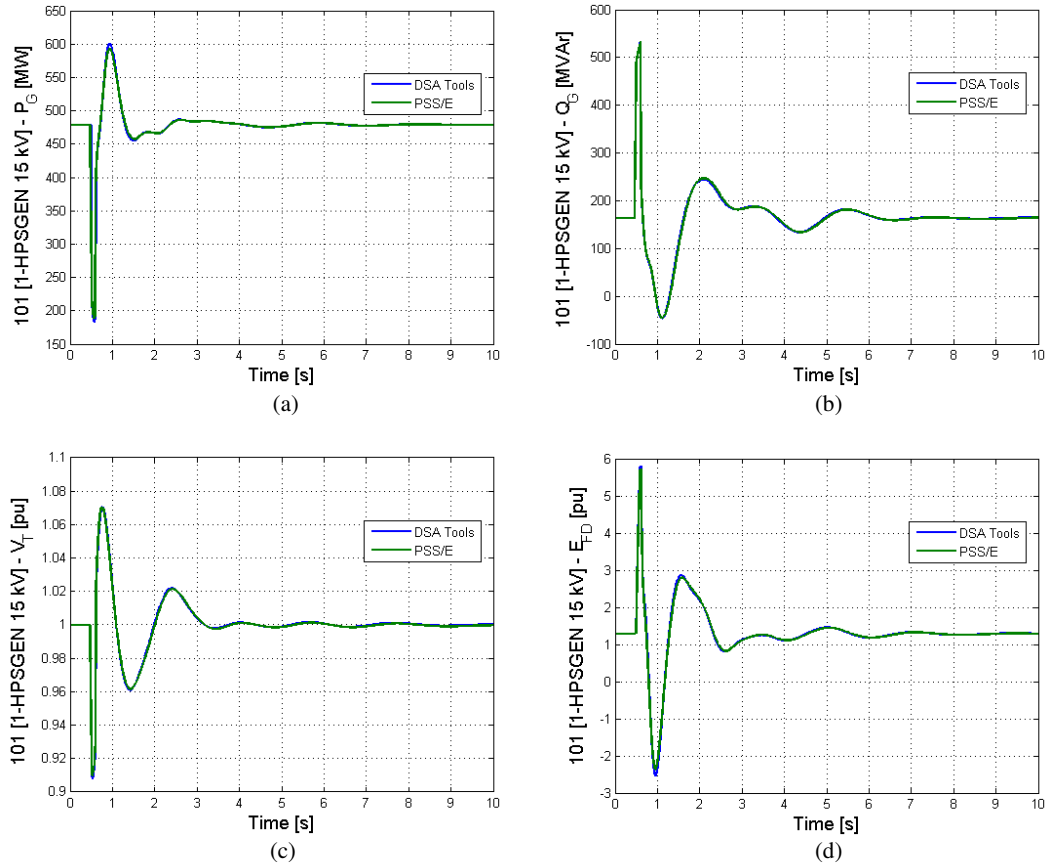


Figure 1. Time-domain simulation results at generator Bus 101 for Disturbance A.

IV. Eigenvalue Analyses

Eigenvalue analyses are performed for the system using SSAT following the studies presented in [2]. Similar to the time-domain simulation studies, all the models are imported from the files provided with [2], with SSAT recognizing all dynamic models. In SSAT, static loads are assumed to be constant power by default; in [2], on the other hand, the loads were modeled as constant impedance. However, for eigenvalue calculations, both yield the same results for the same operating point (power flow solution) since loads are static. Therefore, the default SSAT load model is used in these studies, so that the same PSS/E database can be used without changes, otherwise modifications to the input data set are required.

The examination of un-damped oscillations is of interest for these studies. Thus, a window is defined to examine the eigenvalues within a desired range, i.e. close to the imaginary axis or the right-hand side (e.g. in the range of $[-1 \dots 10, -20 \dots 20]$). Since there are six power flow cases and the PSSs can be on or off, there are $6 \times 2 = 12$ cases to be studied. The results for all the twelve cases are provided in an attached file in MS Excel format, showing the real and imaginary parts of the computed eigenvalues, as well as their damping ratios and frequencies, and associated dominant state variables. In these results, it can be observed that one or two zero (or very small) eigenvalues are present in all cases. One of these eigenvalues is due to the lack of an angle reference in the system; the other one corresponds to the rotor speeds, and is present because speed governors are not modeled and all generator damping factors are assumed to be zero [4].

The results associated with Cases 3 and 6 (highest and lowest loading levels) with and without stabilizers are shown in Figures 2 and 3, respectively. The damping effect of the stabilizers is clearly seen in both cases, as the eigenvalues “move” to the left side of the 10%-damping line due to the stabilizers. The results are almost identical to the ones presented in [2].

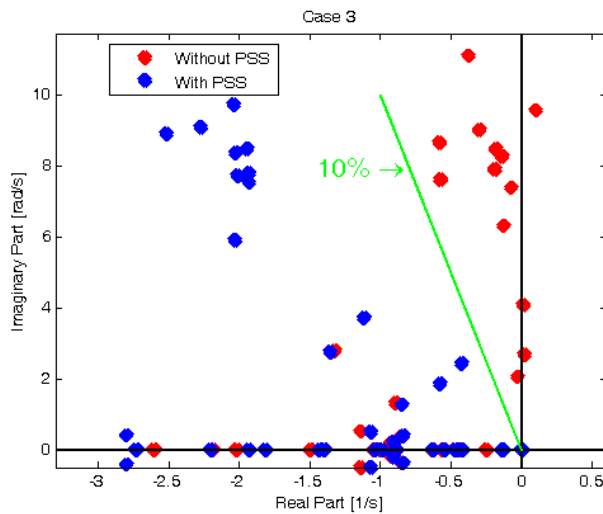


Figure 2. Case 3 eigenvalues with and without stabilizers.

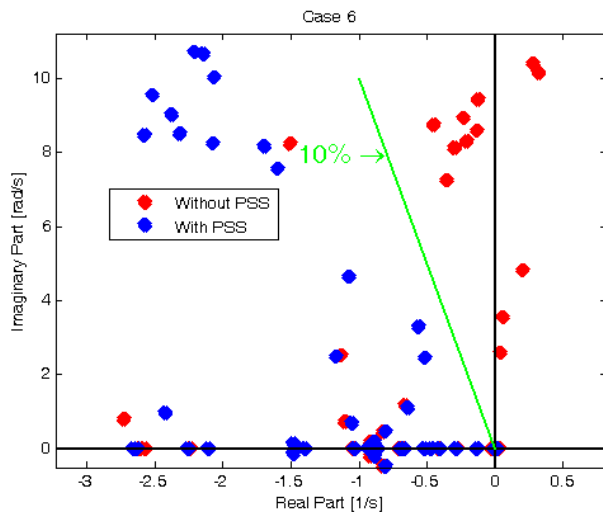


Figure 3. Case 6 eigenvalues with and without stabilizers.

V. References

- [1] *DSA Tools Reference Manual*, [online] Available: <http://www.dsatools.com> ver. 10.
- [2] Mike Gibbard and David Vowles, “*Simplified 14-generator model of the SE Australian power system*,” IEEE Task Force on Benchmark Systems for Stability Controls, June 2014.
- [3] Leonardo Lima, “*Report on the 14-generator system (Australian reduced model)*,” IEEE Task Force on Benchmark Systems for Stability Controls, June 2013.
- [4] P. Kundur, *Power System Stability and Control*, Mc Graw Hill, EPRI Power System Engineering Series, 1994.

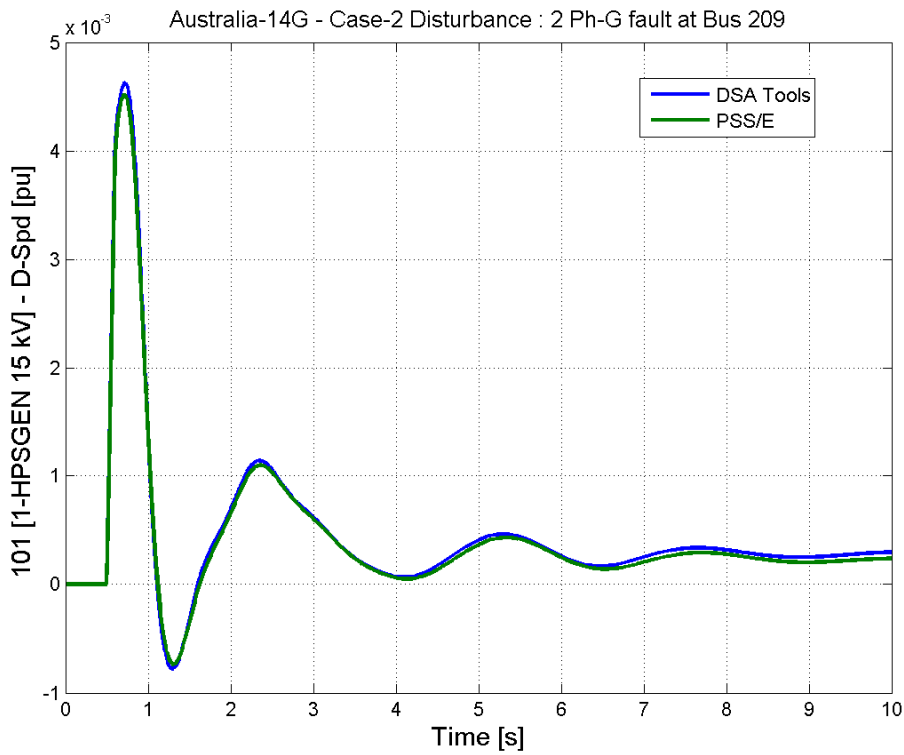


Department of Electrical and Computer Engineering

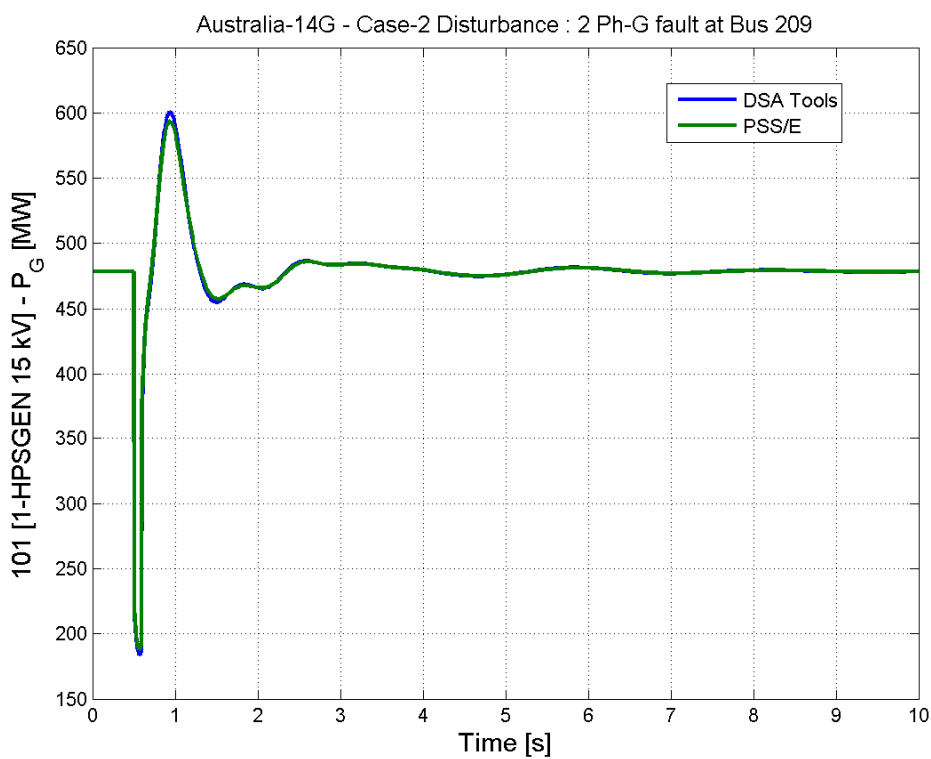
IEEE Task Force on Benchmark Systems for Stability
Controls:

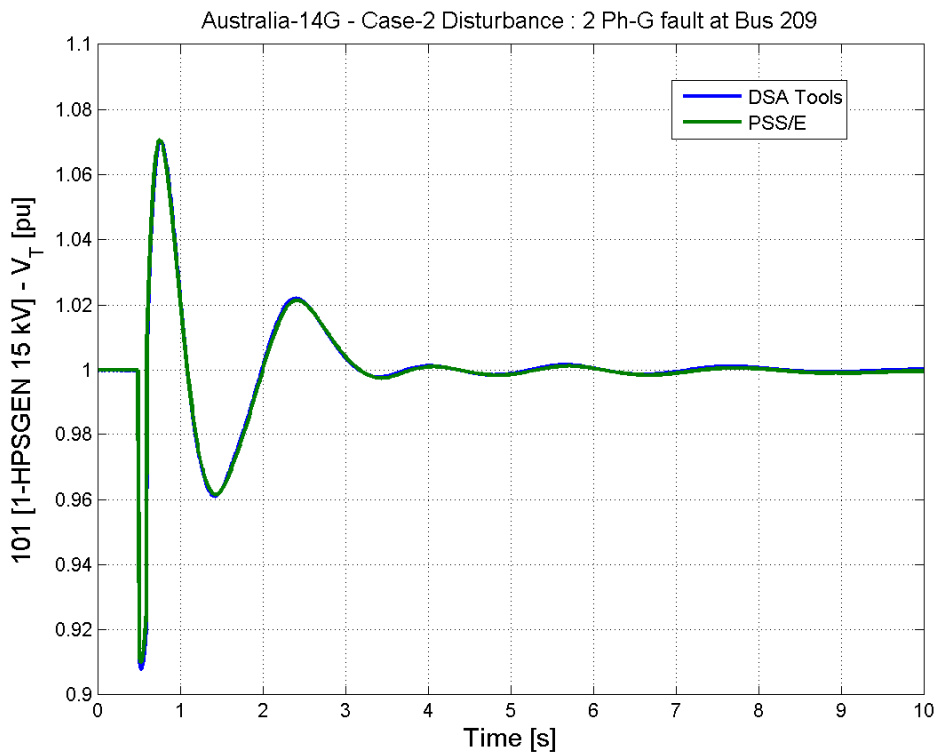
Australian Test System

Appendix: Time-domain results

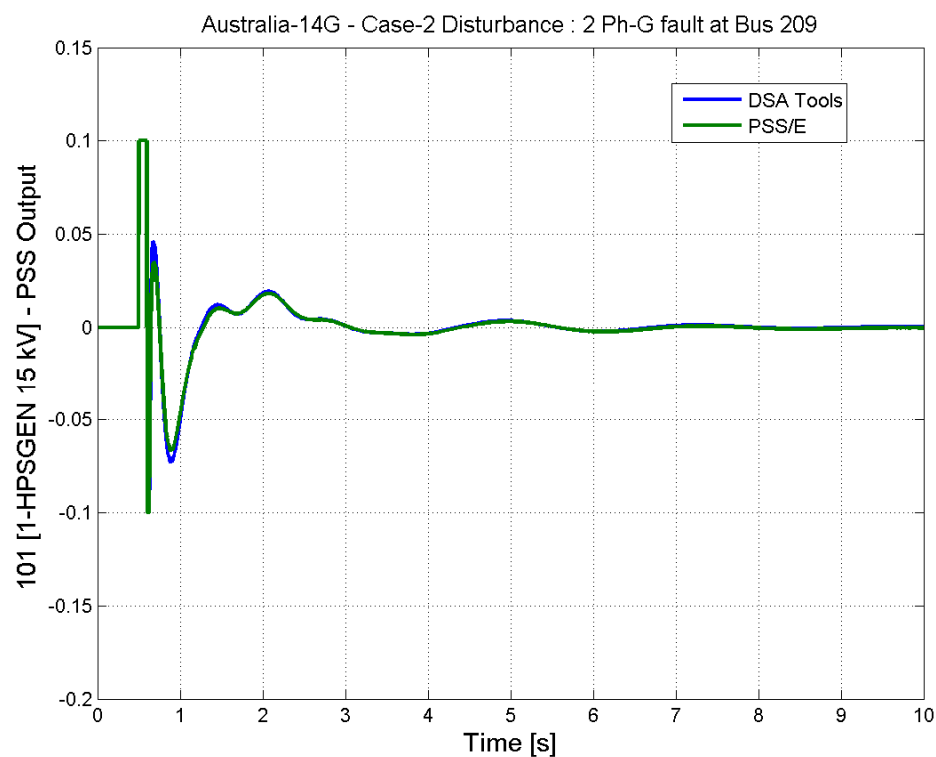


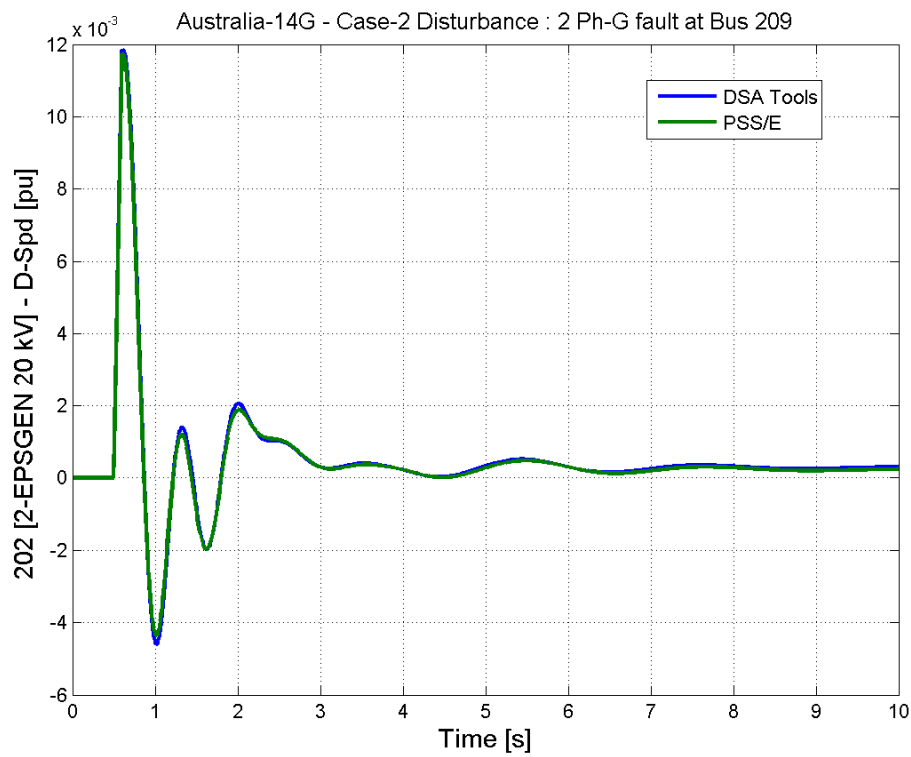
Contingency A



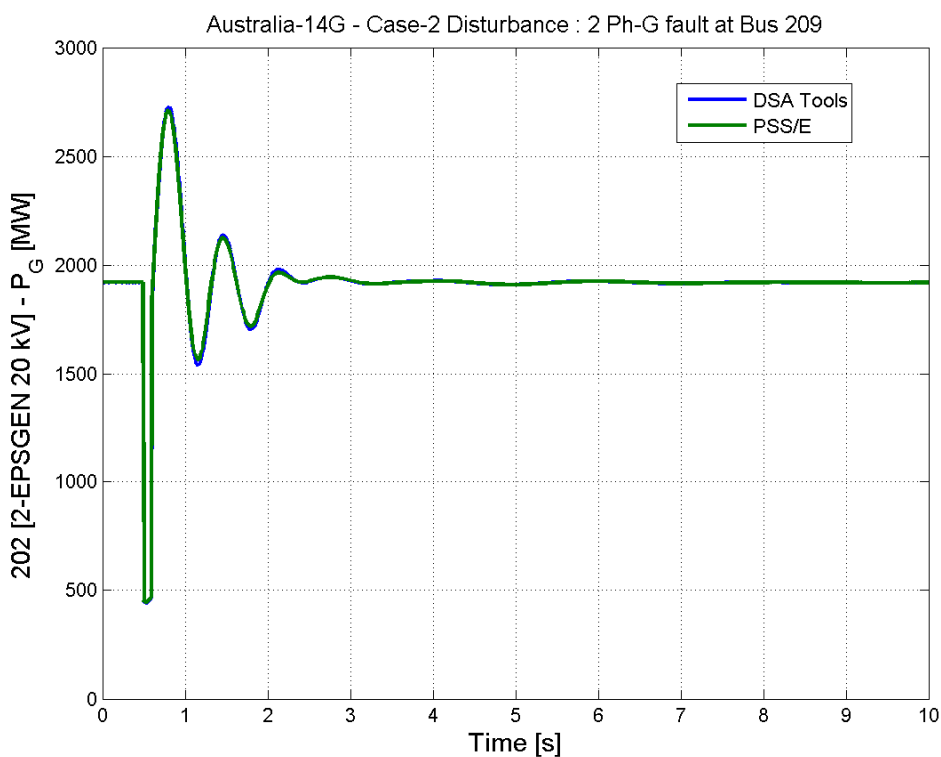


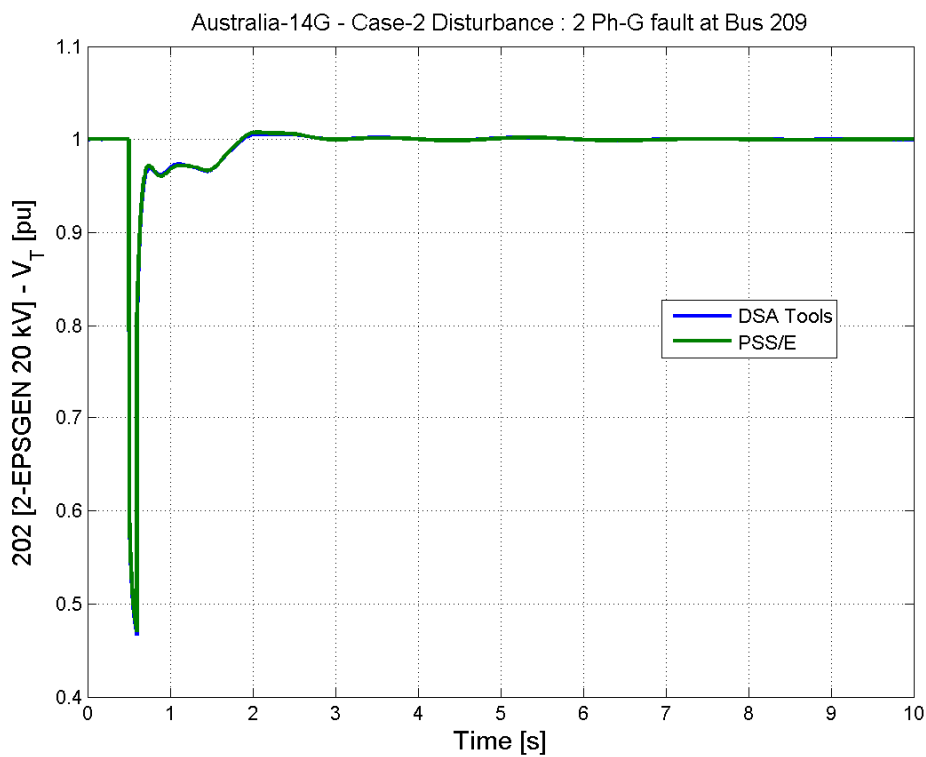
Contingency A



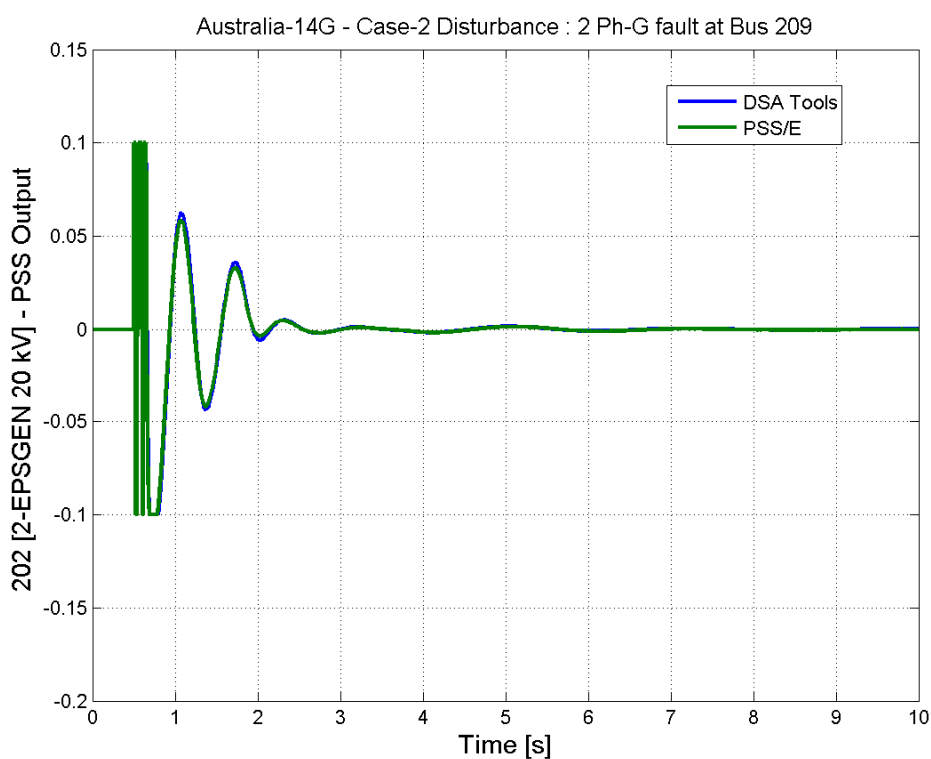


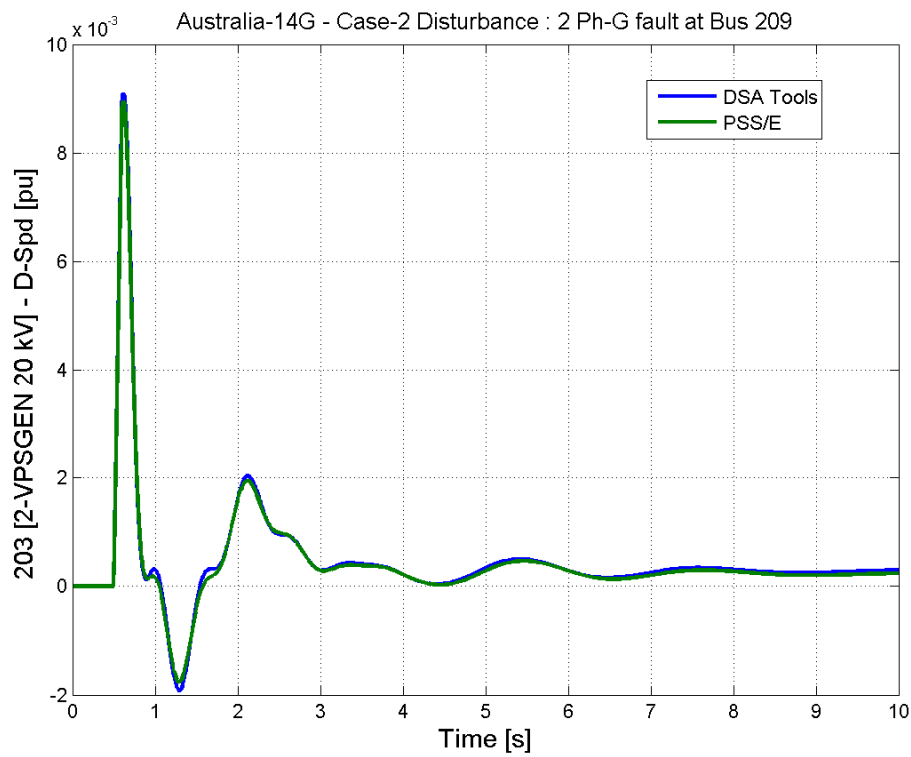
Contingency A



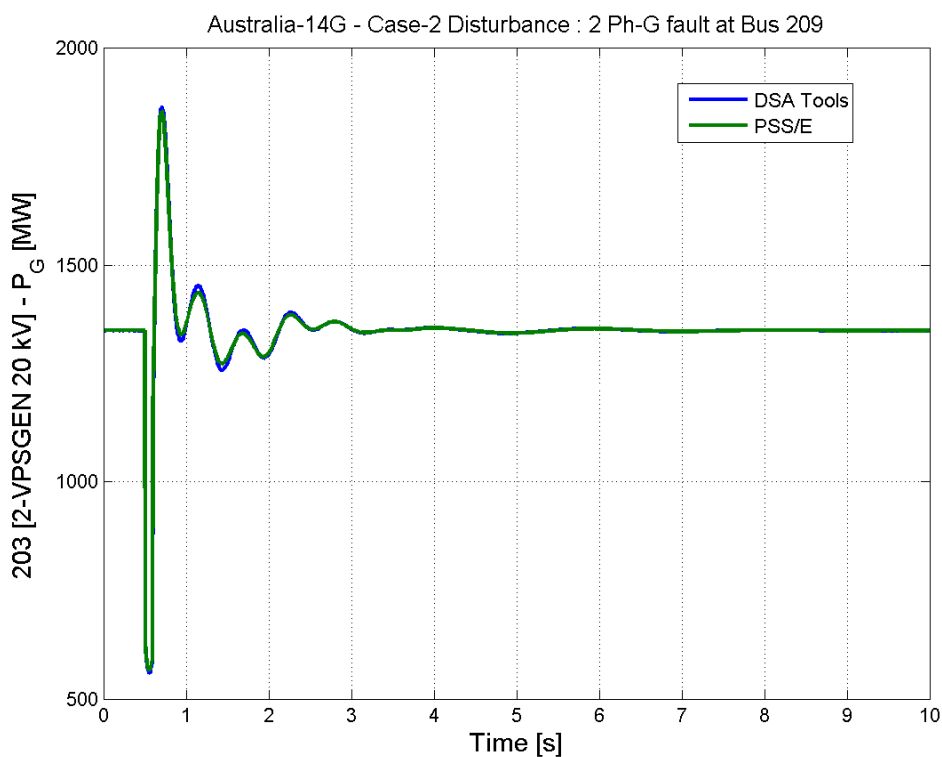


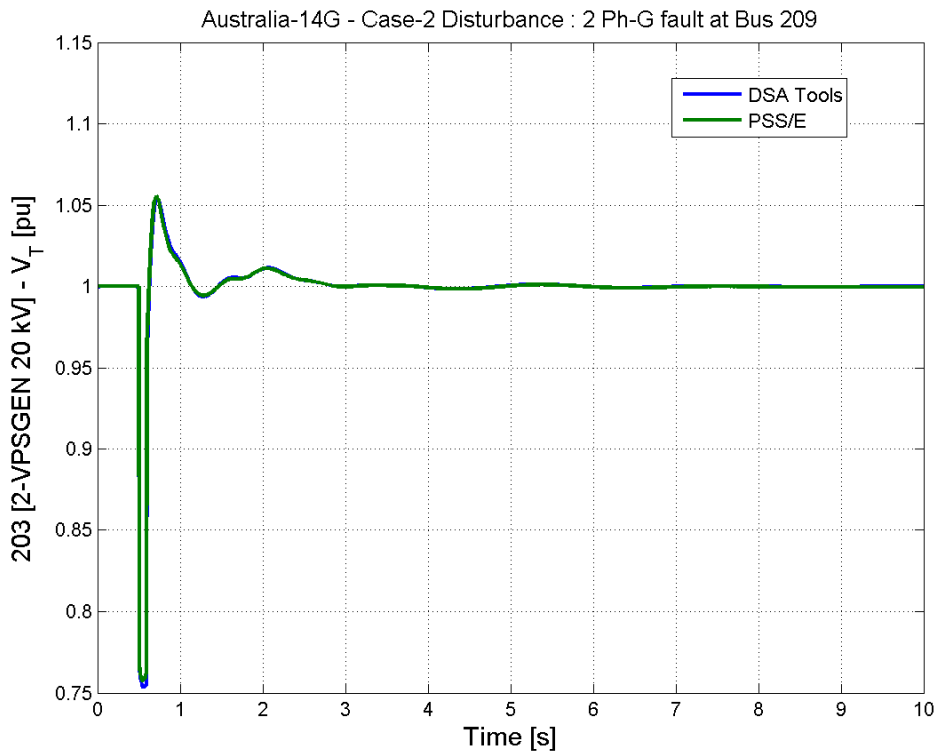
Contingency A



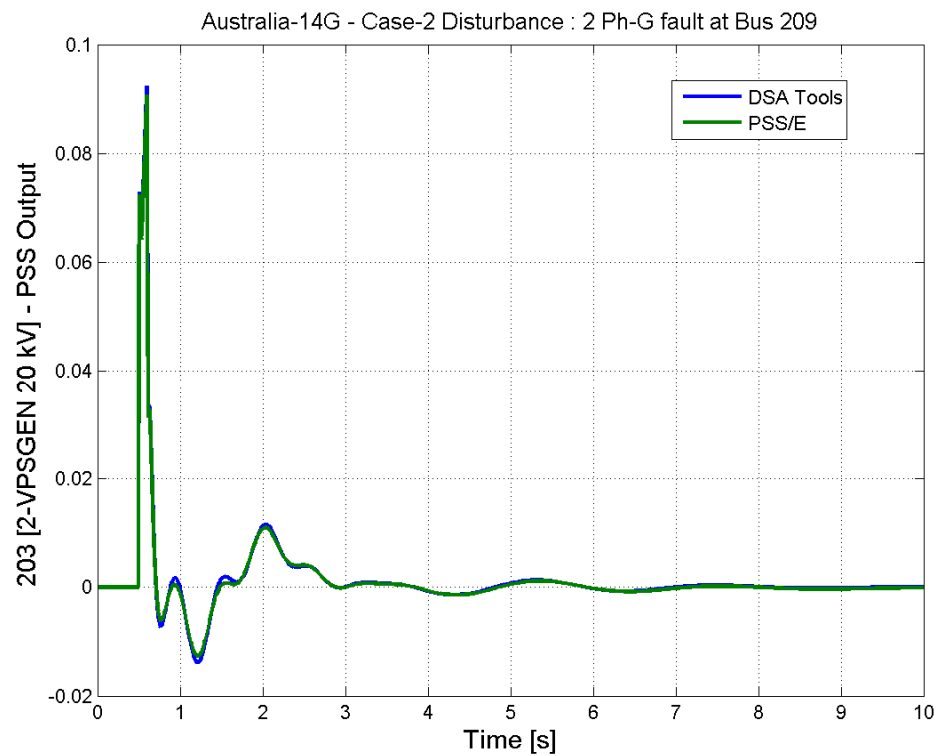


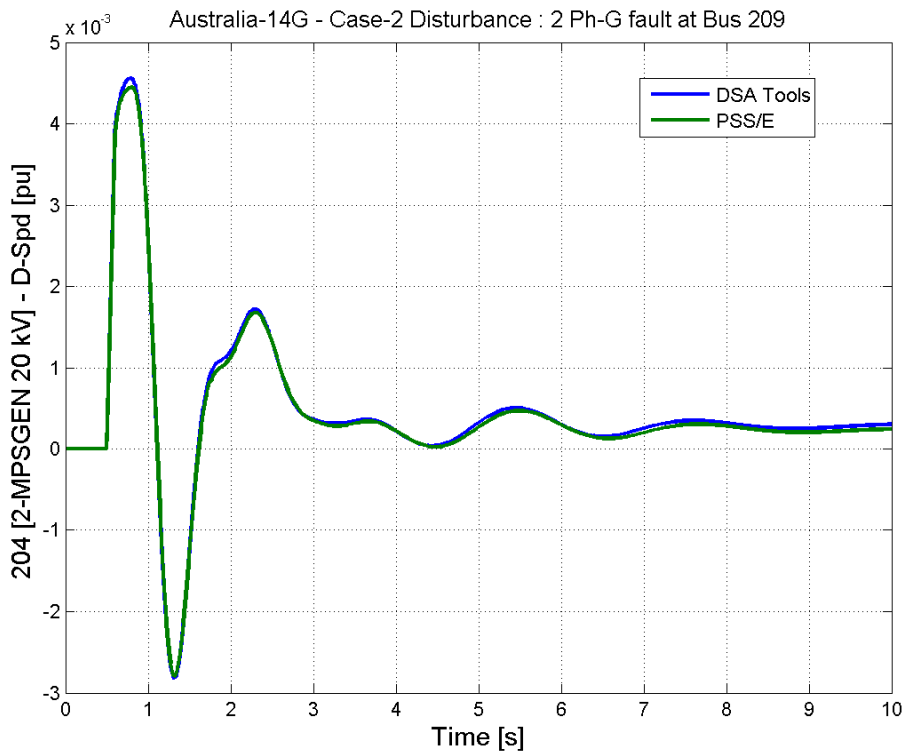
Contingency A



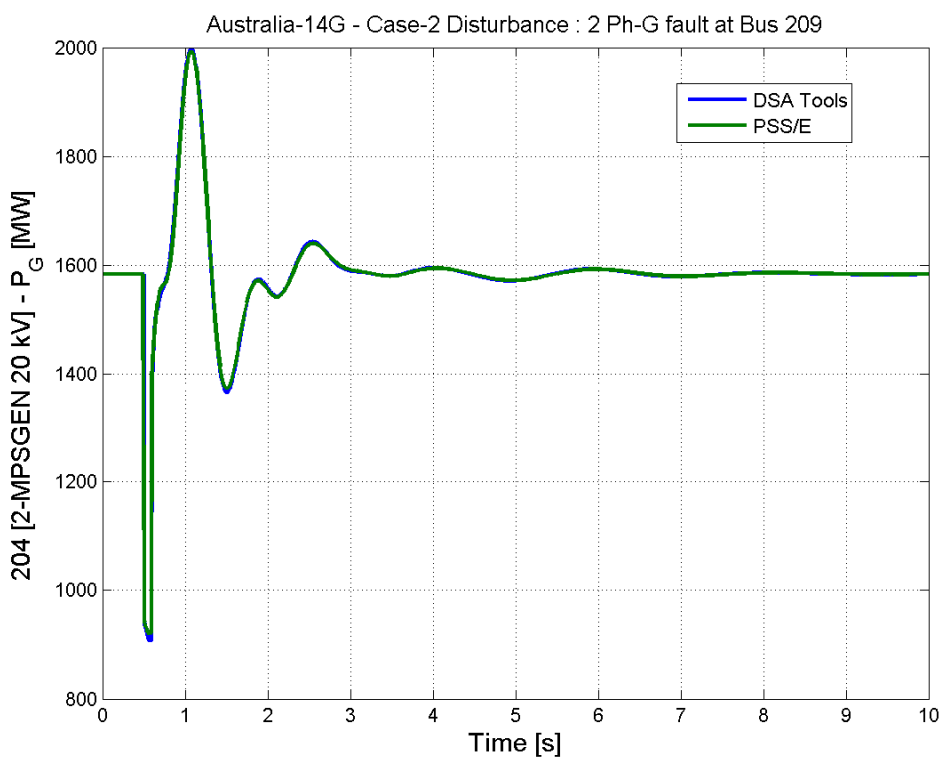


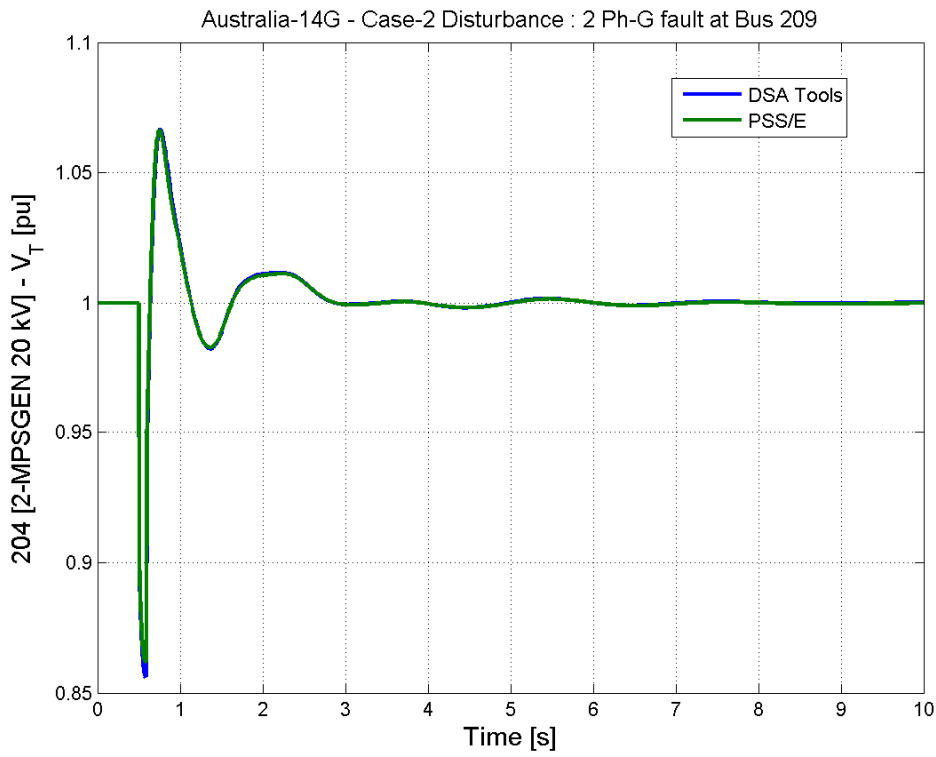
Contingency A



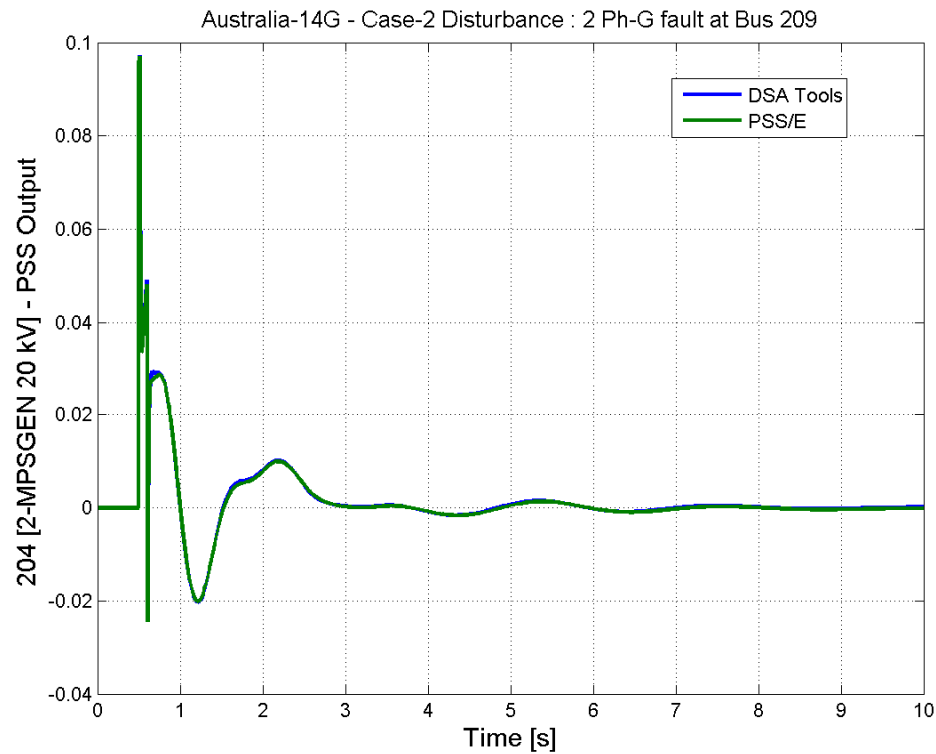


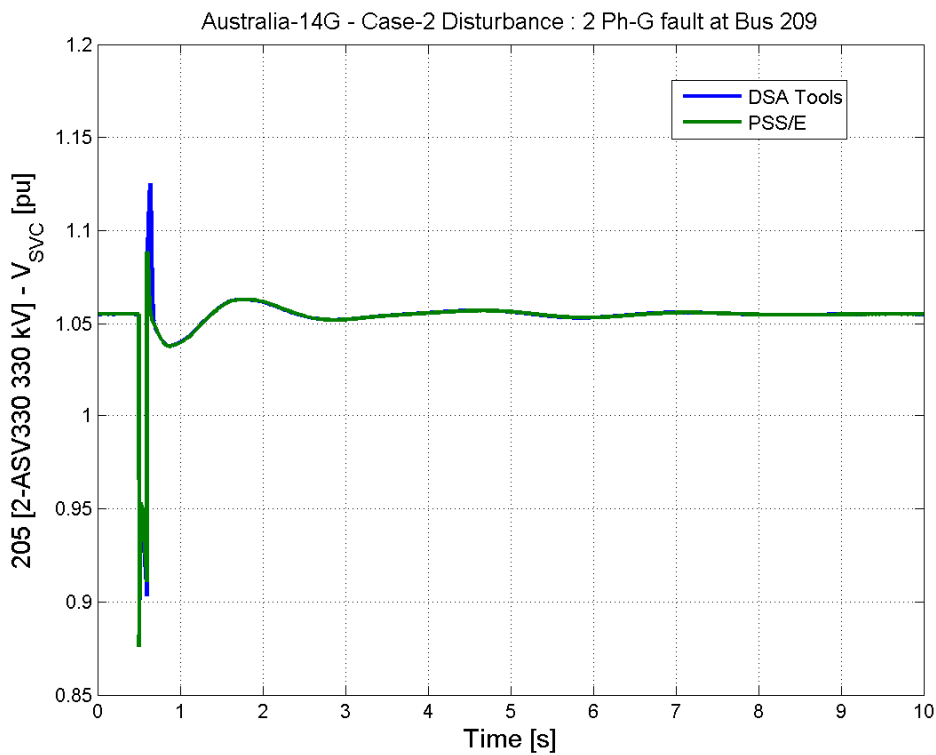
Contingency A



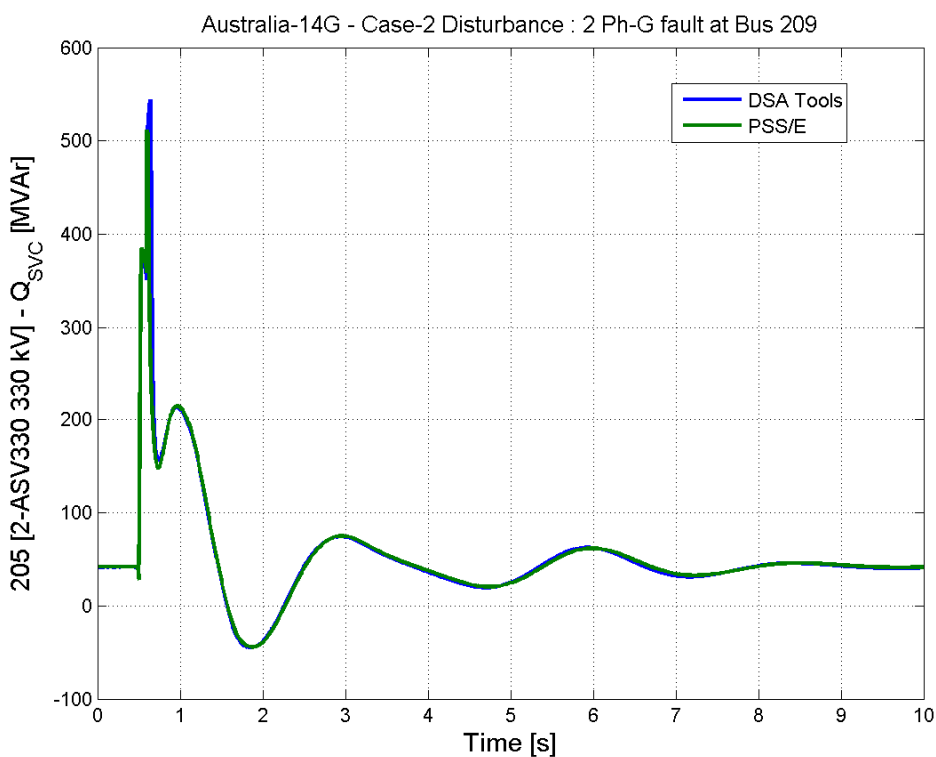


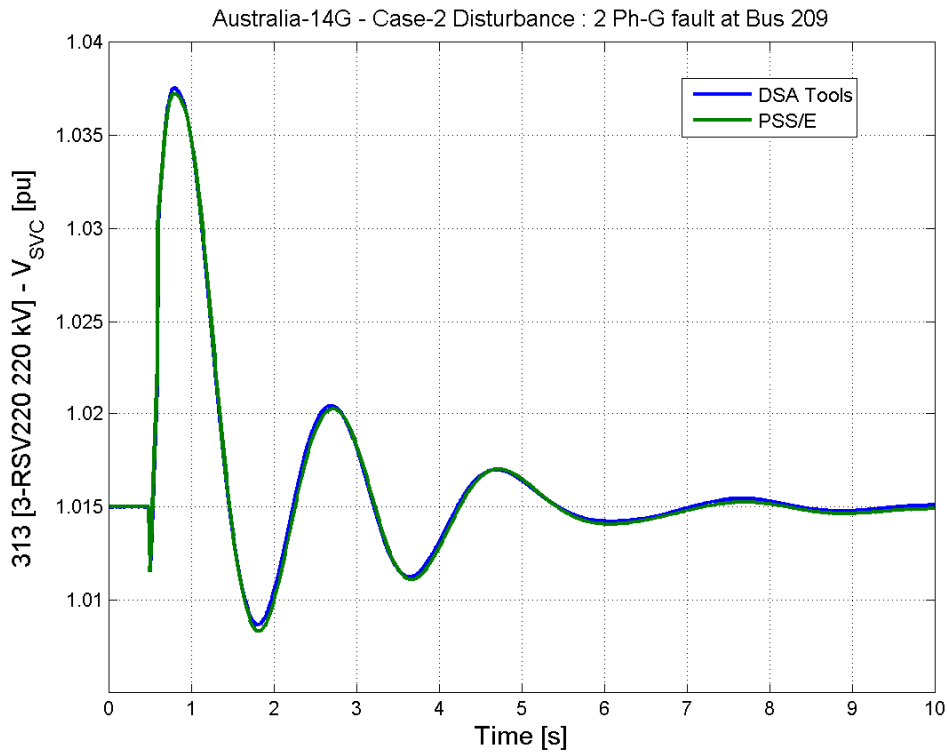
Contingency A



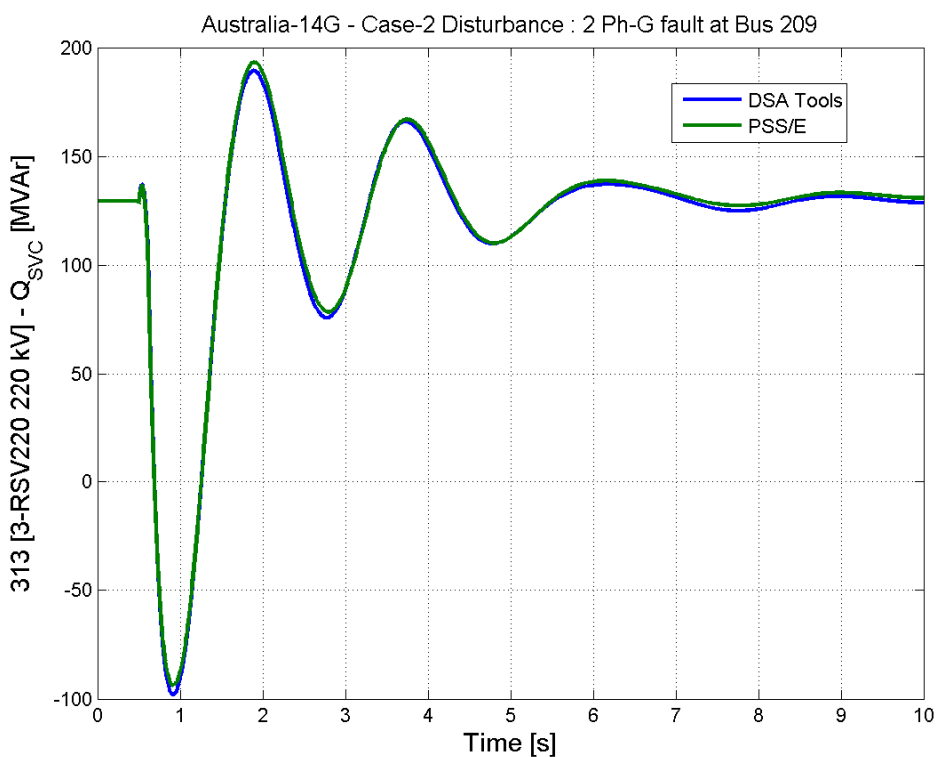


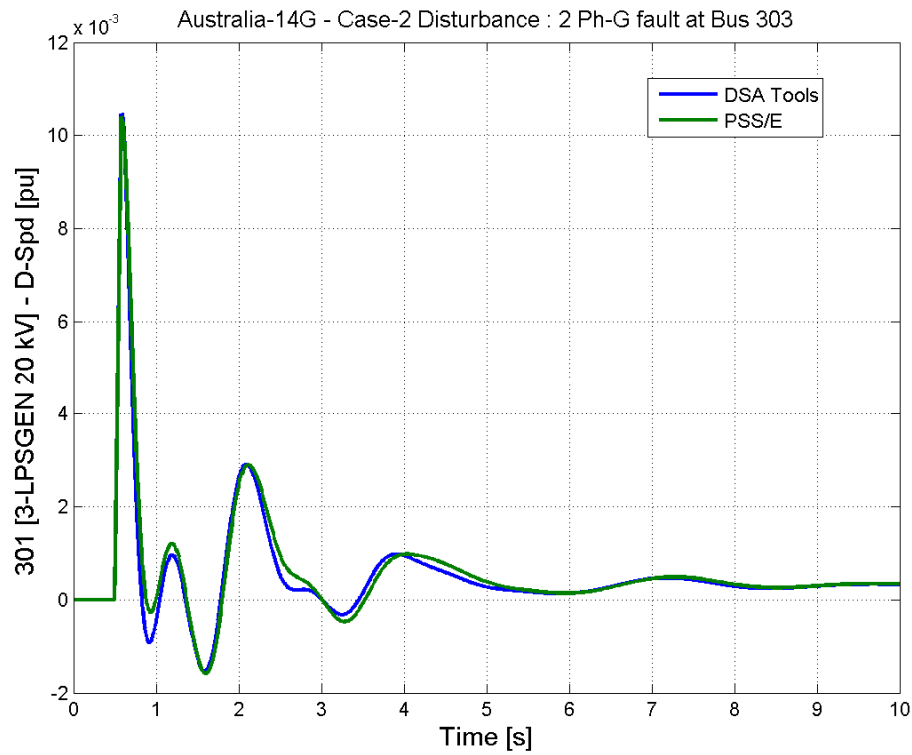
Contingency A



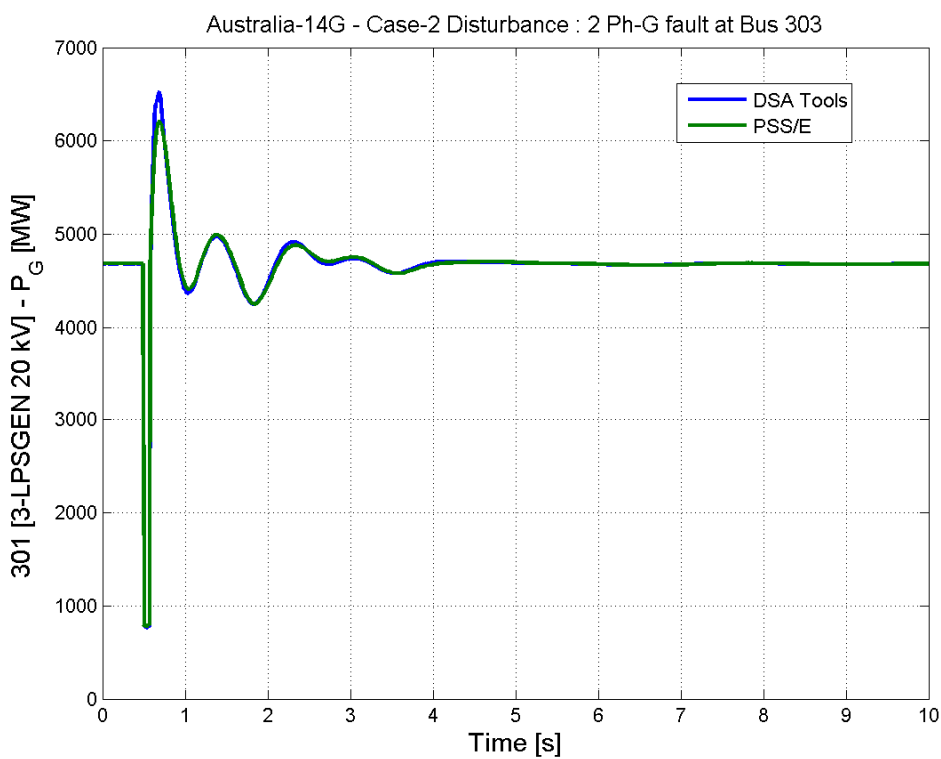


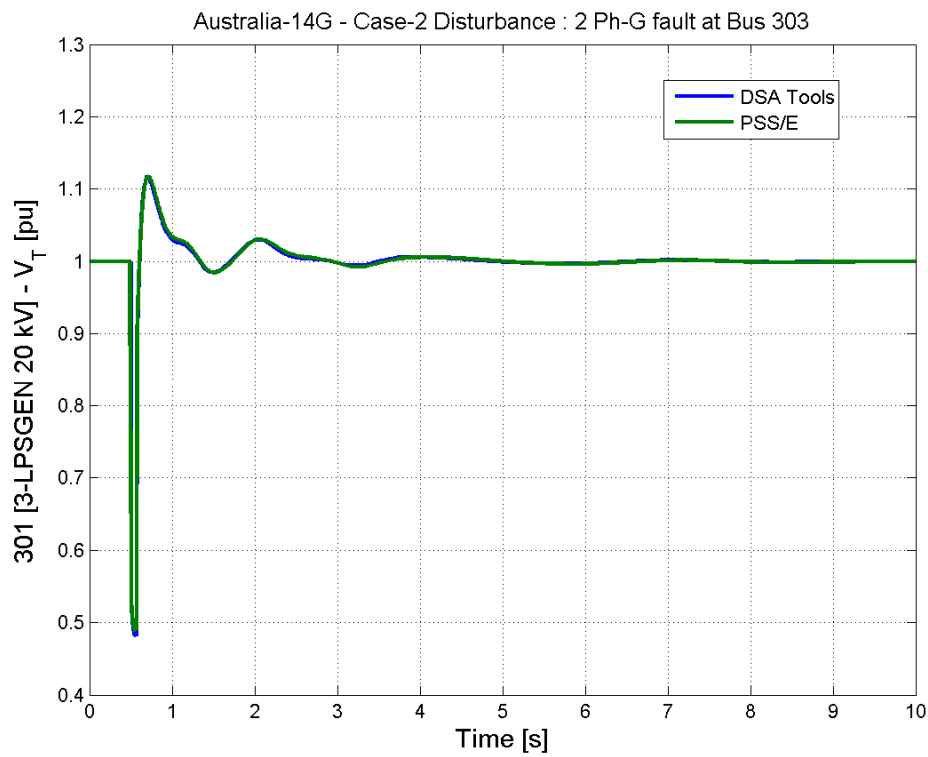
Contingency A



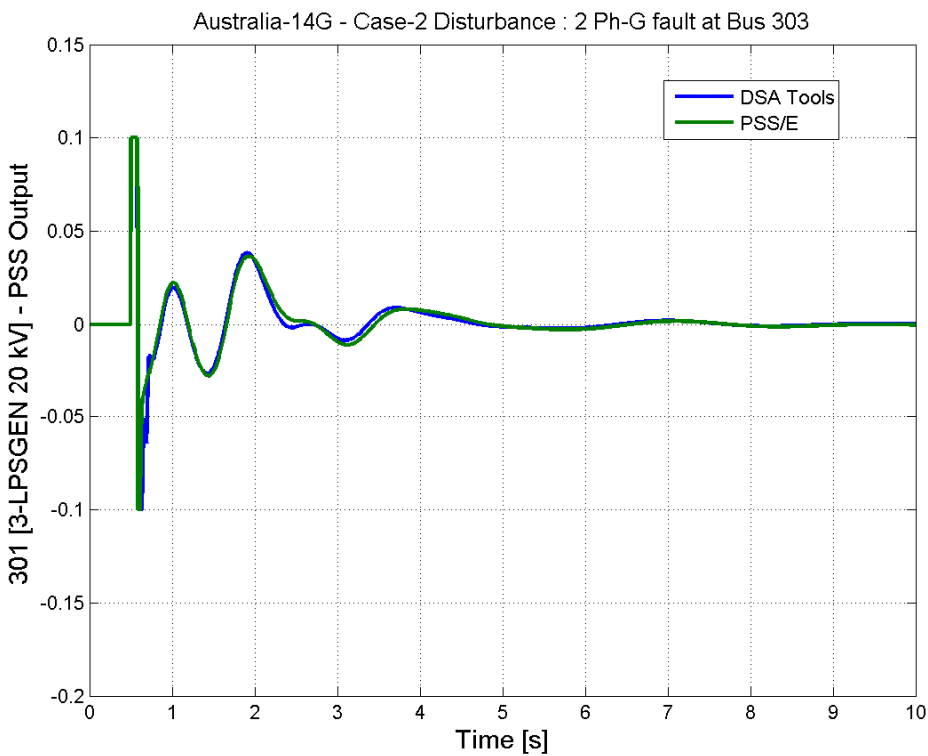


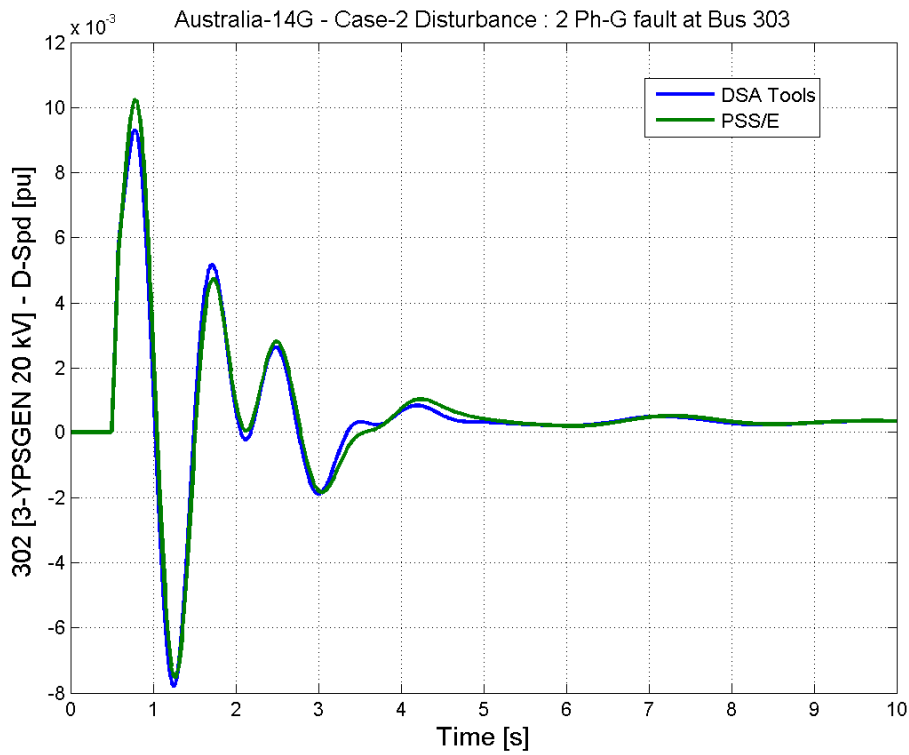
Contingency B



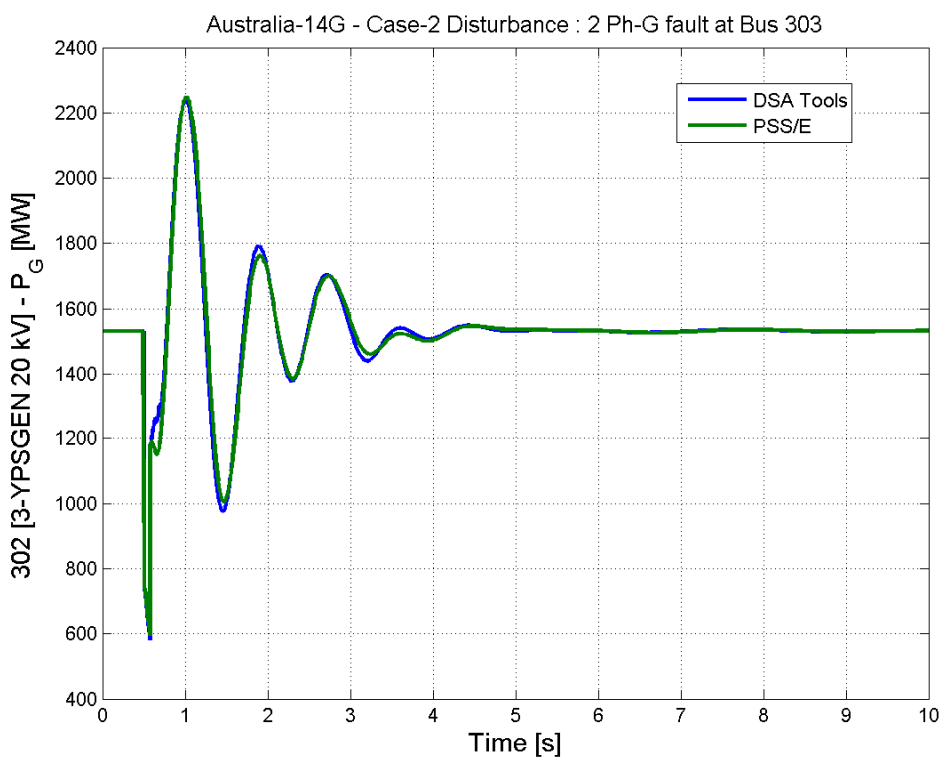


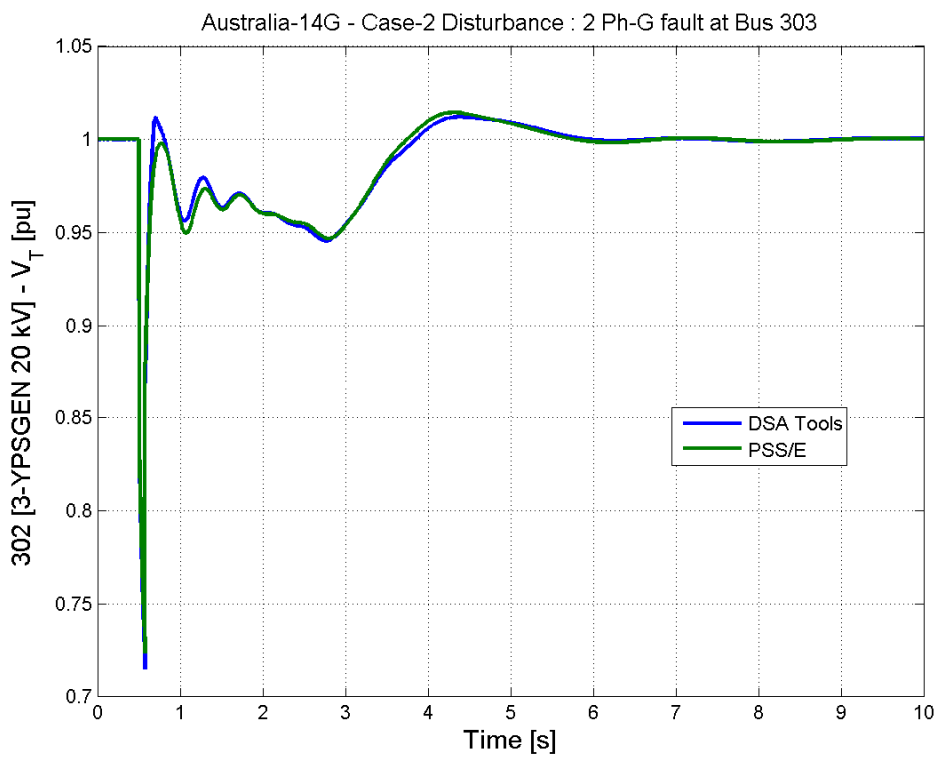
Contingency B



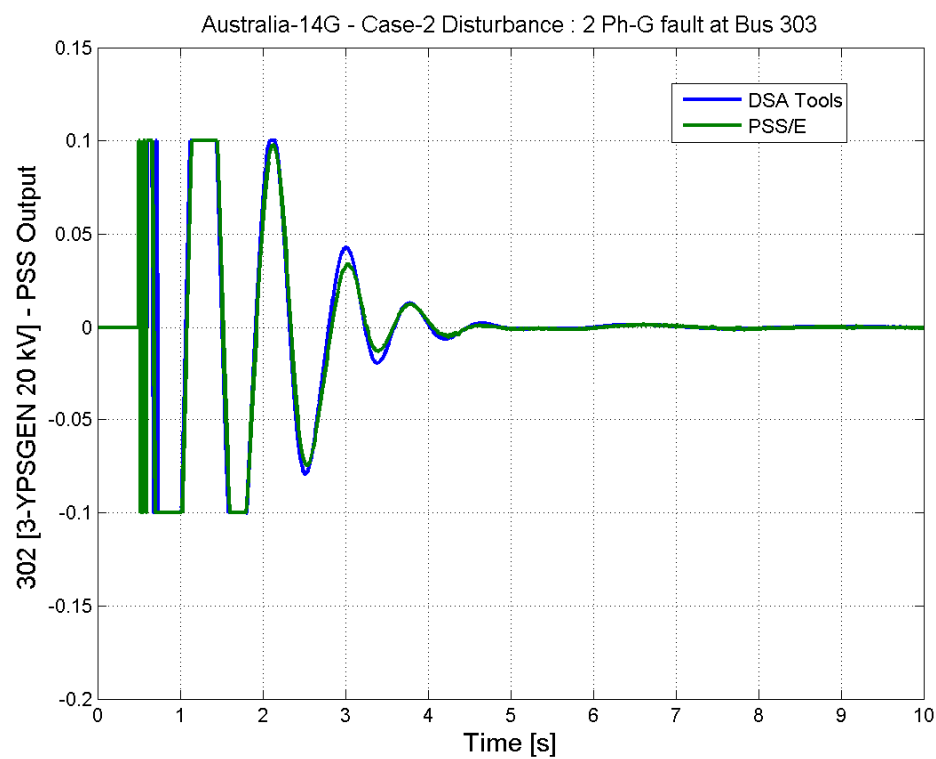


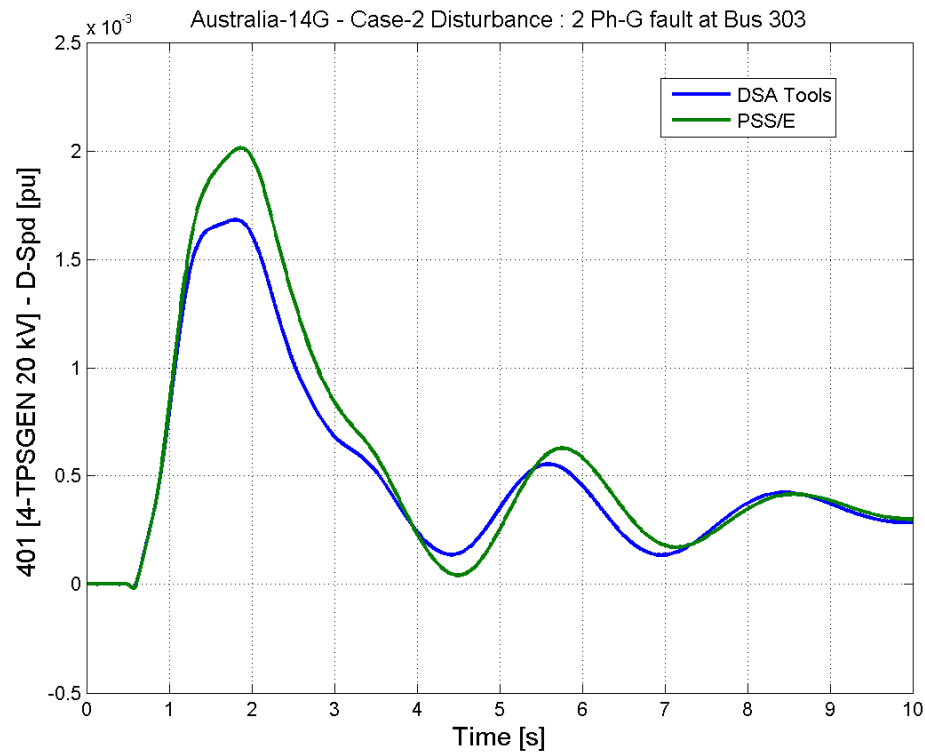
Contingency B



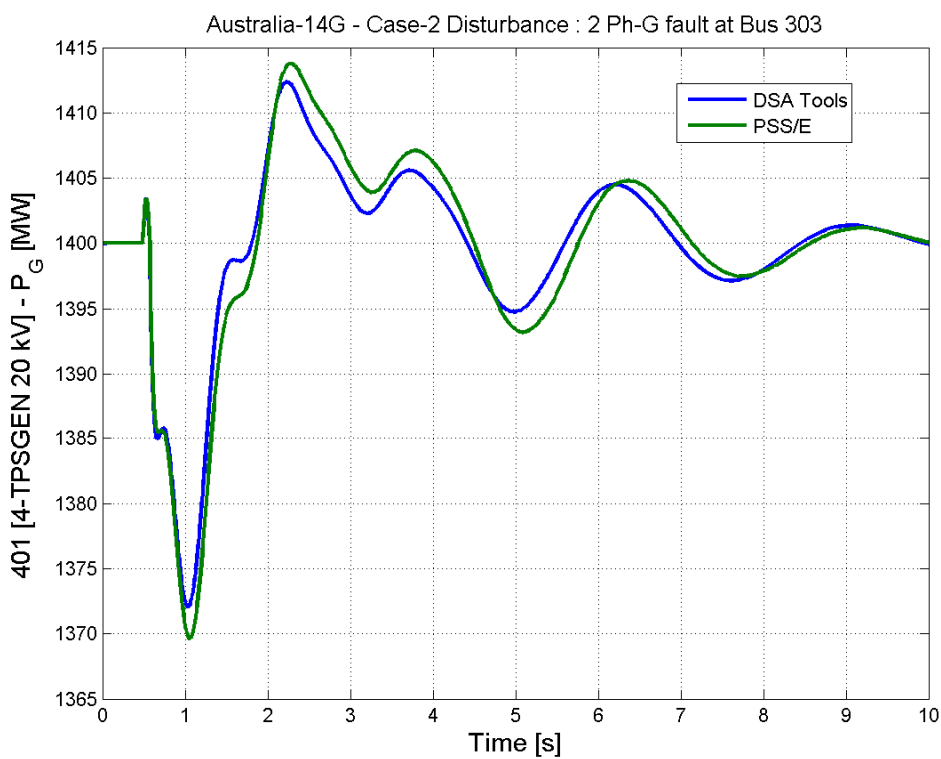


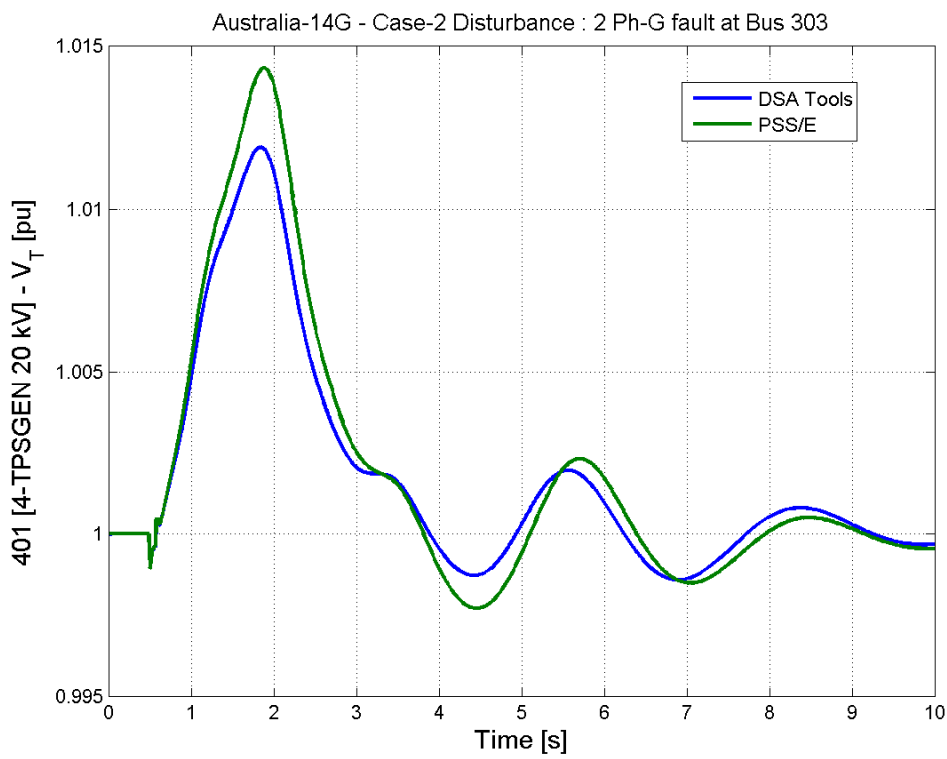
Contingency B



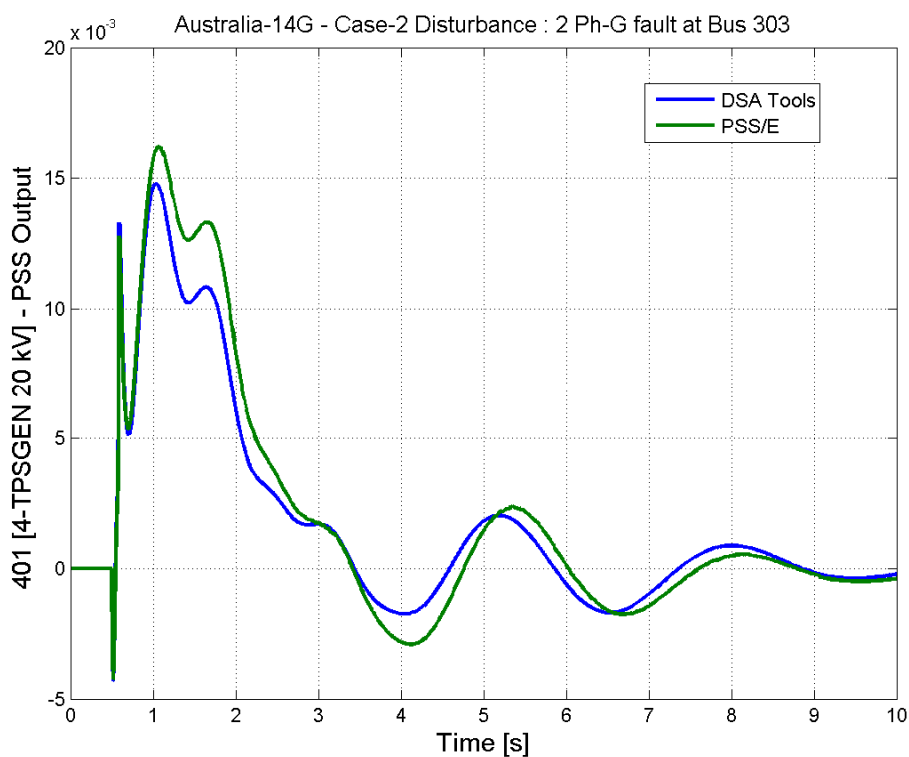


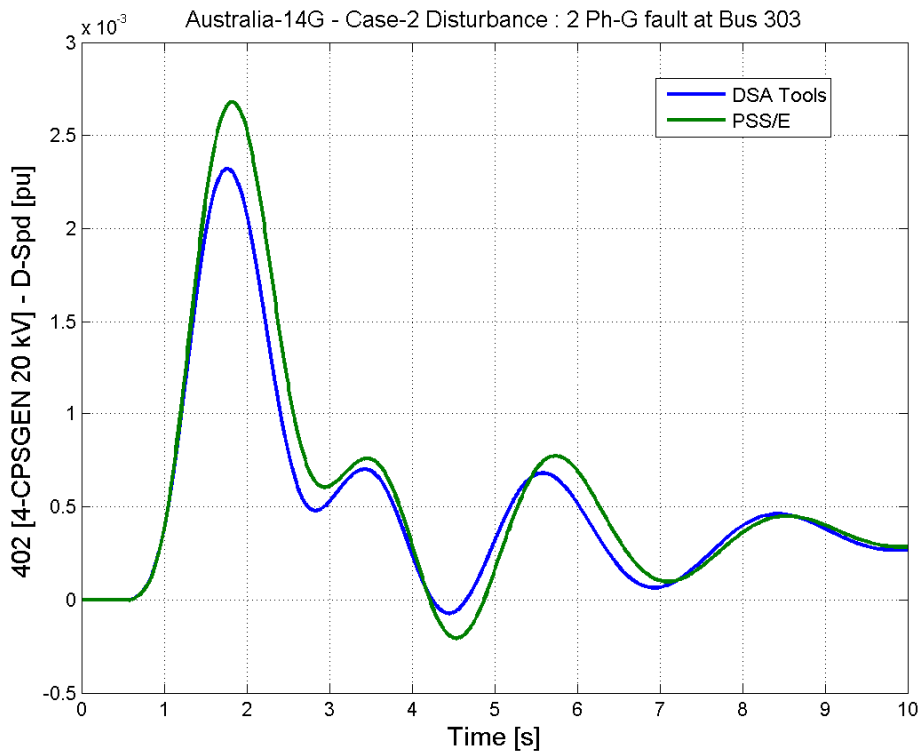
Contingency B



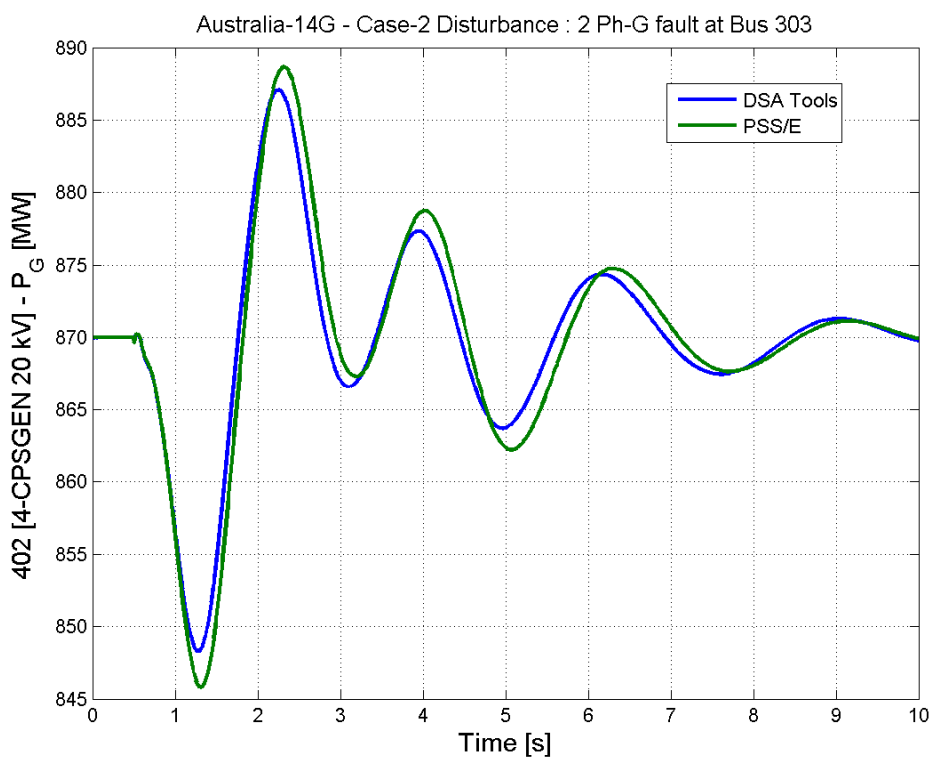


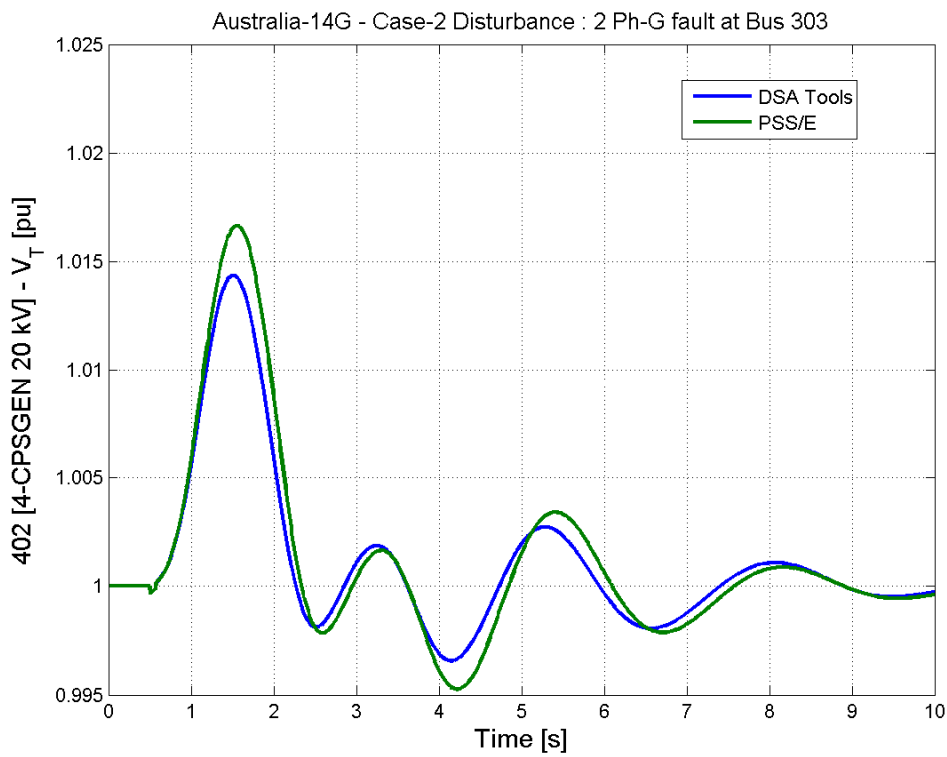
Contingency B



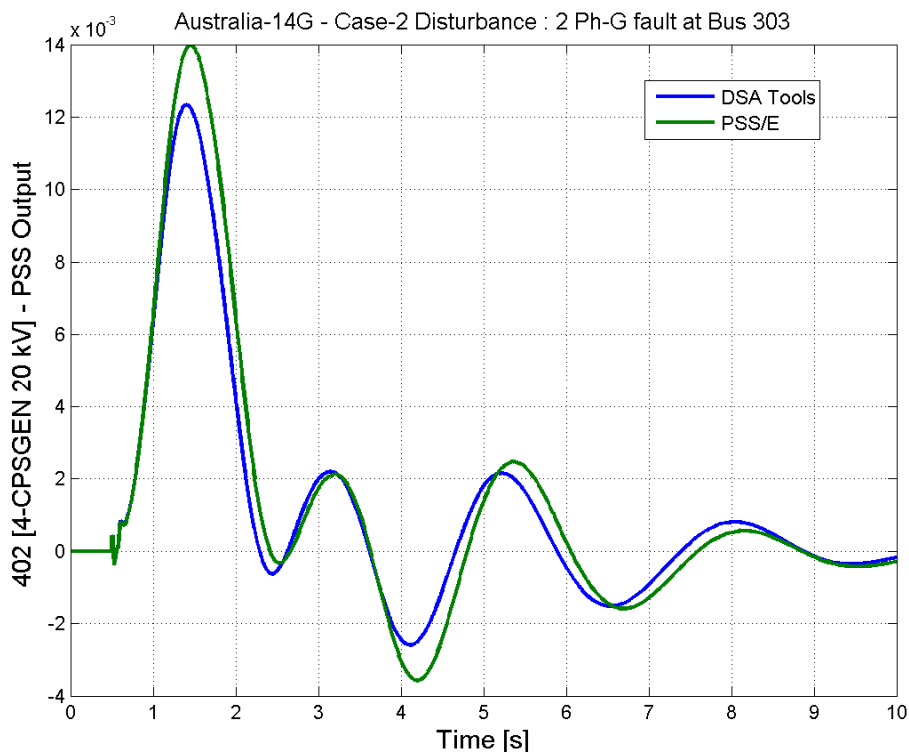


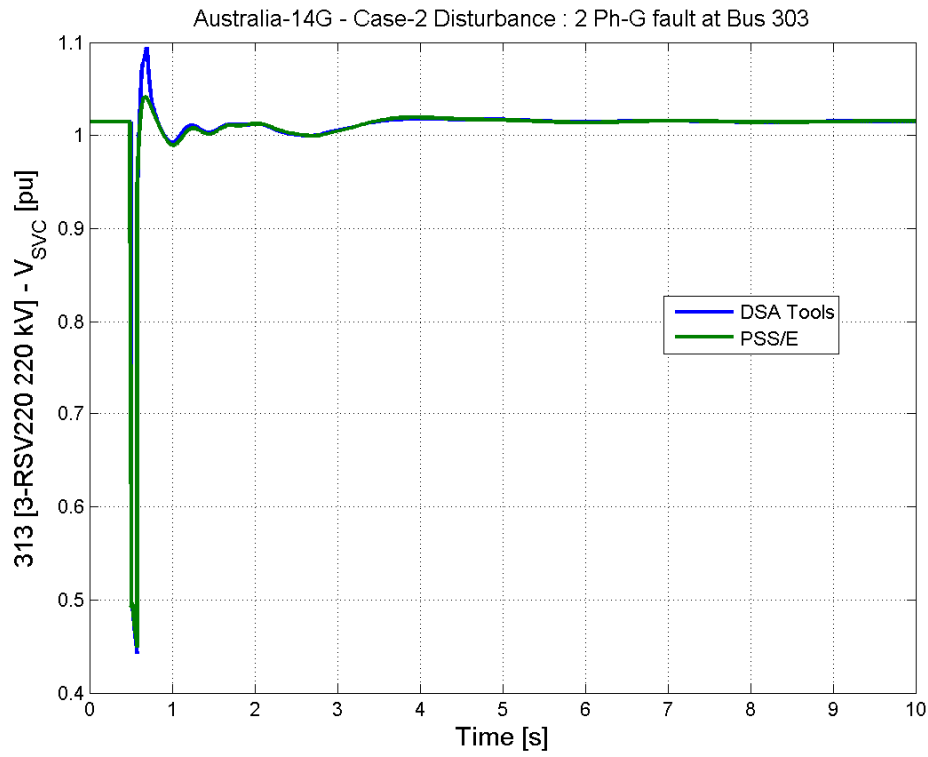
Contingency B



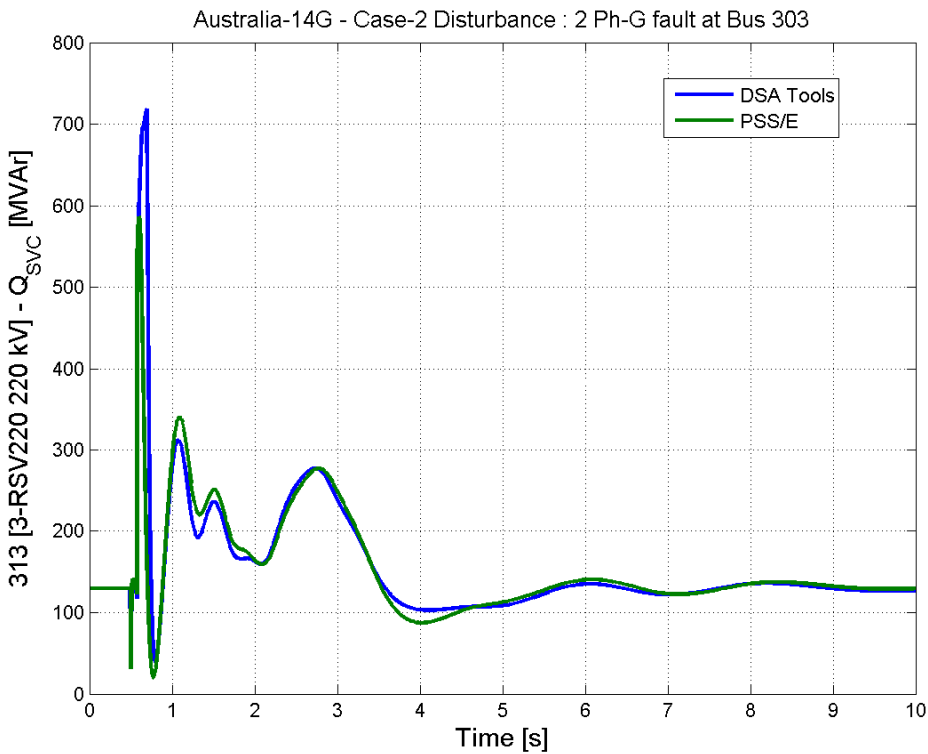


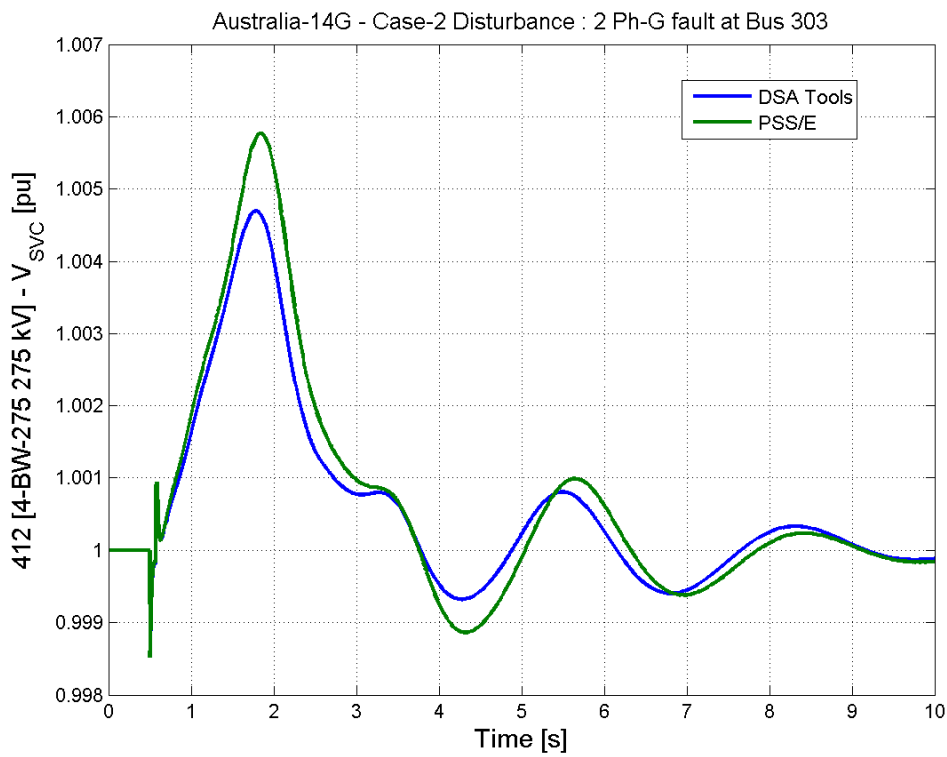
Contingency B



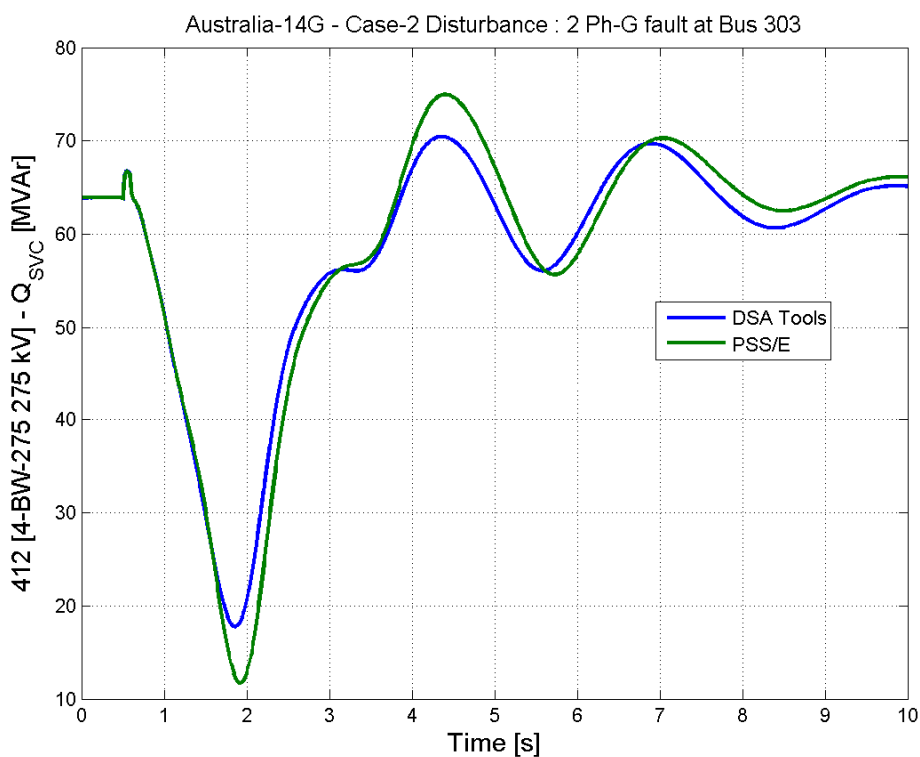


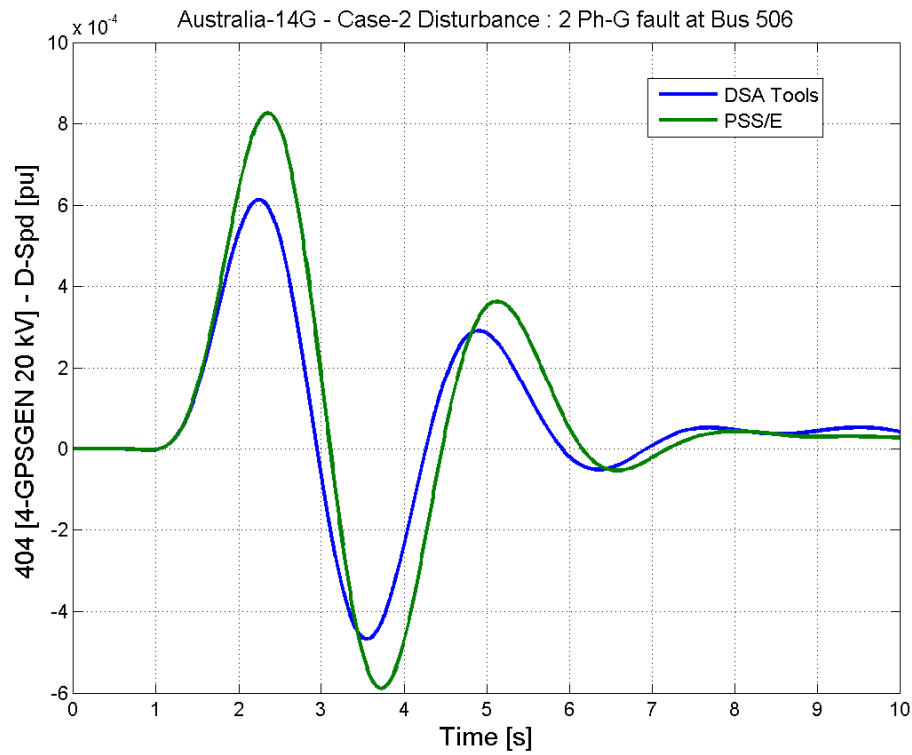
Contingency B



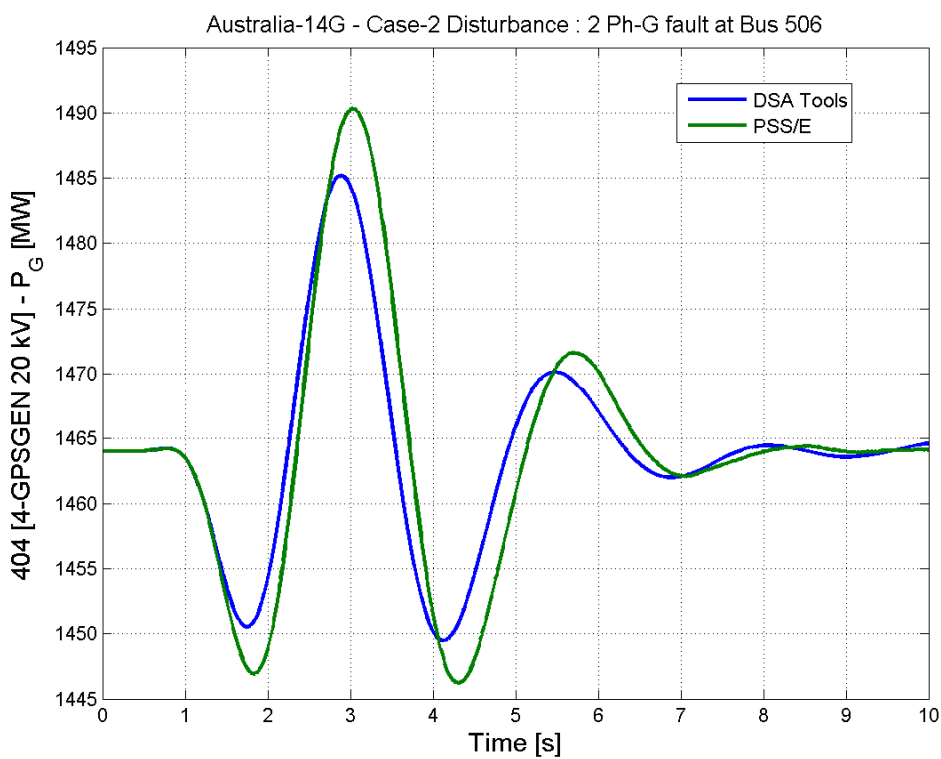


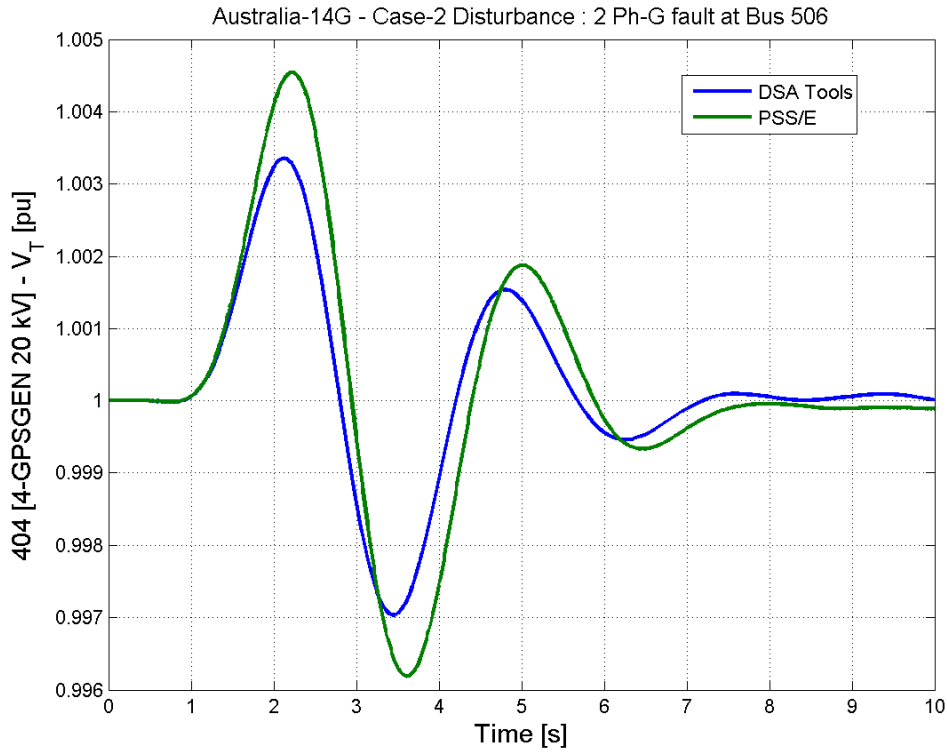
Contingency B



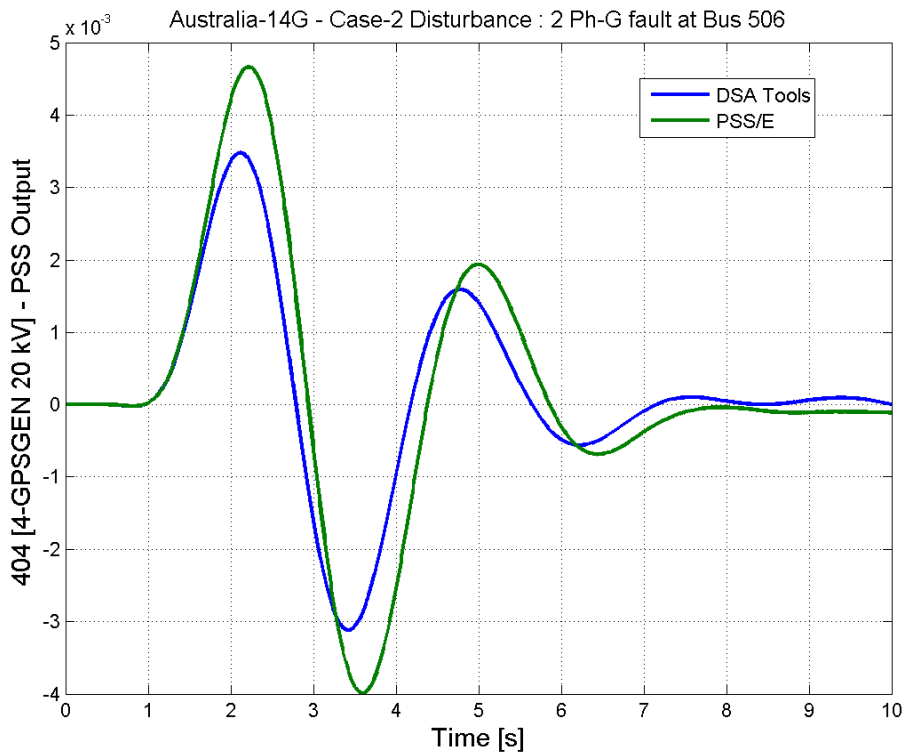


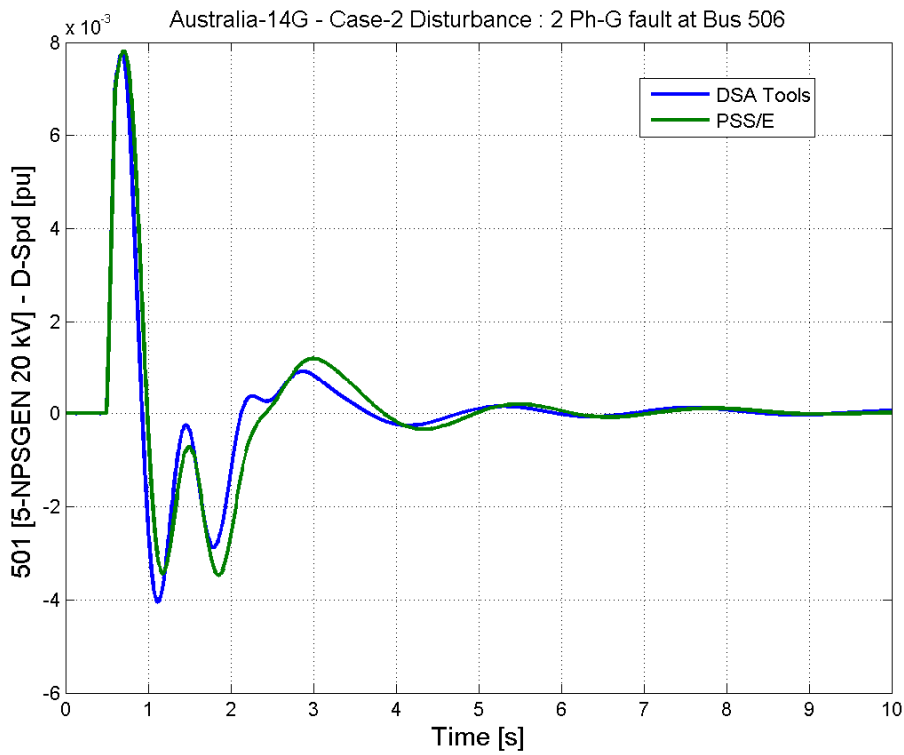
Contingency C



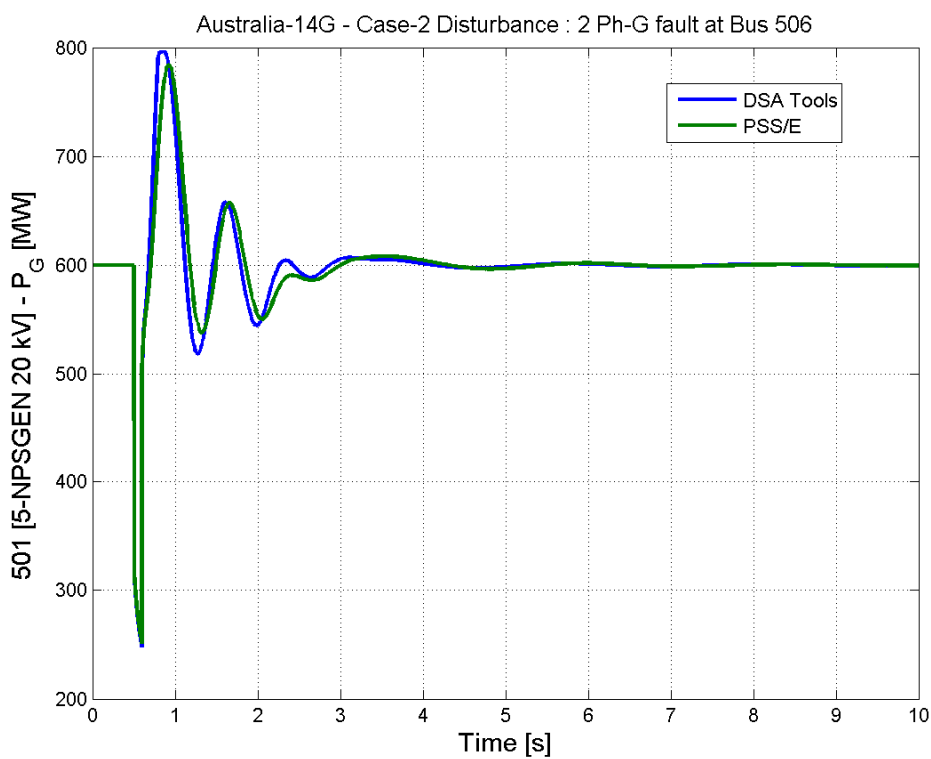


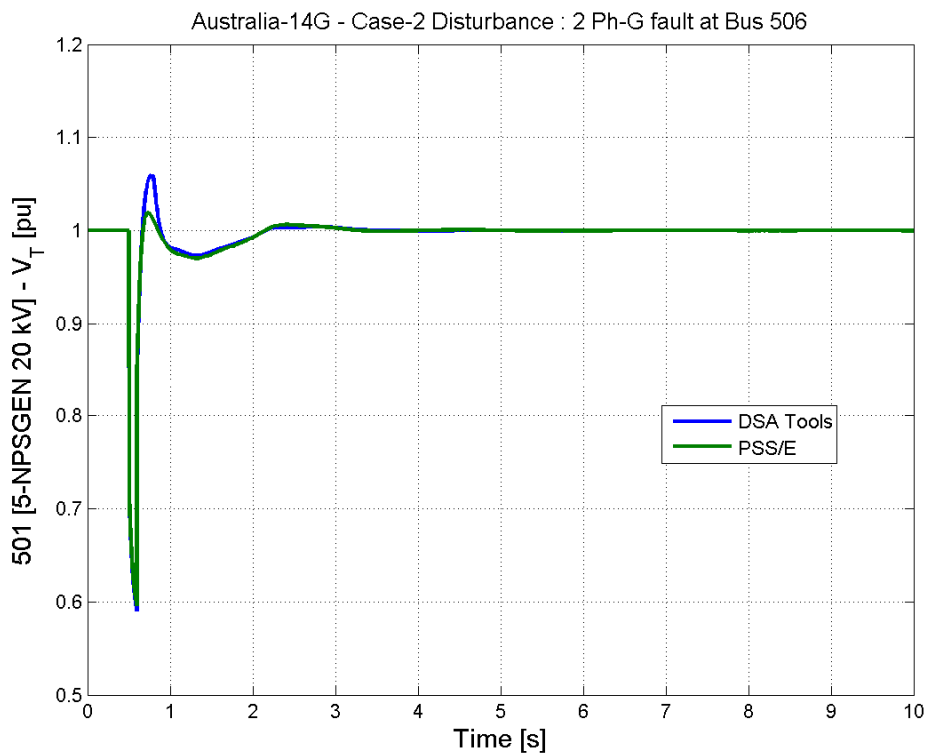
Contingency C



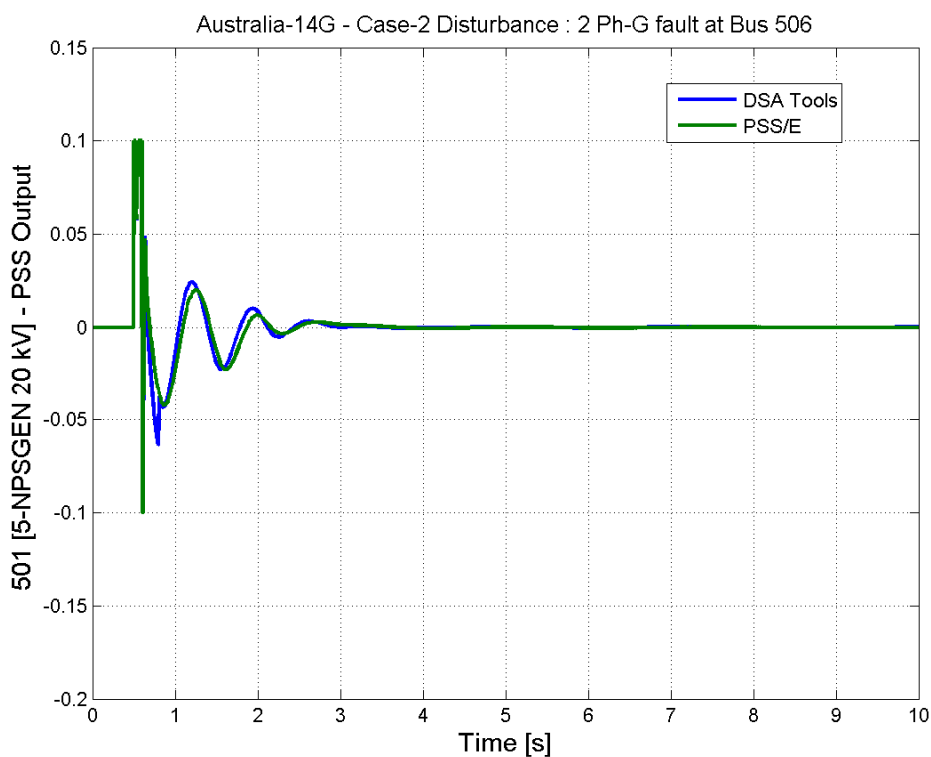


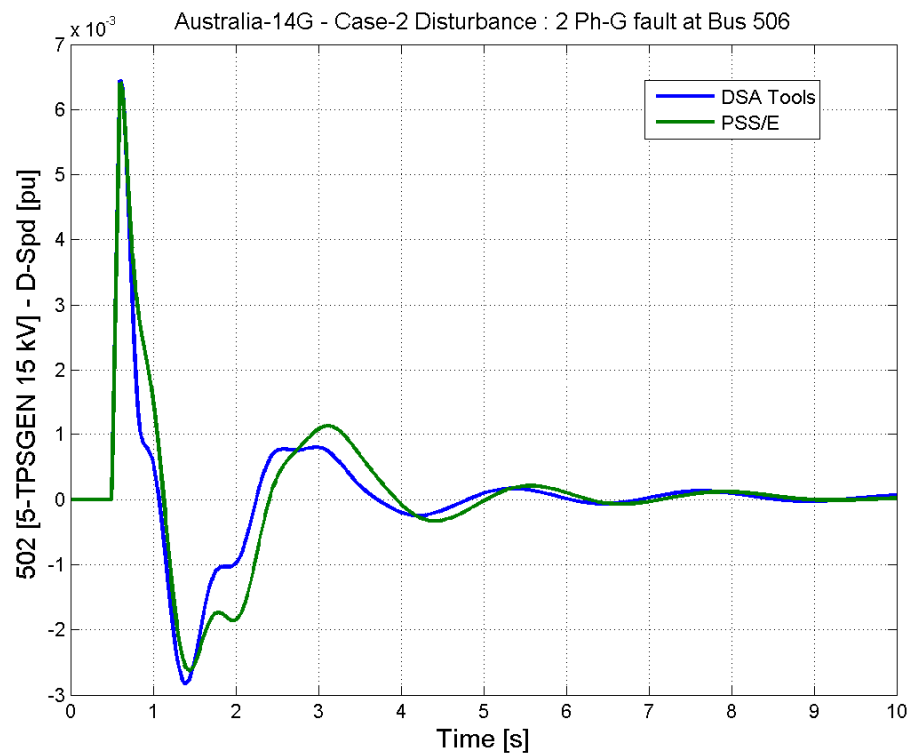
Contingency C



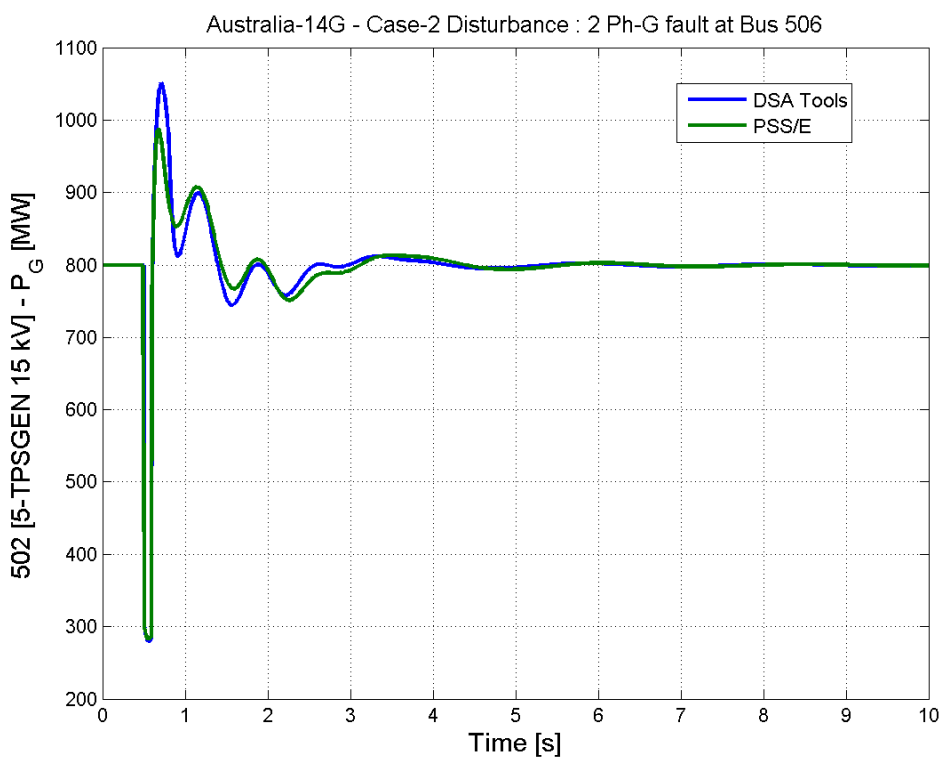


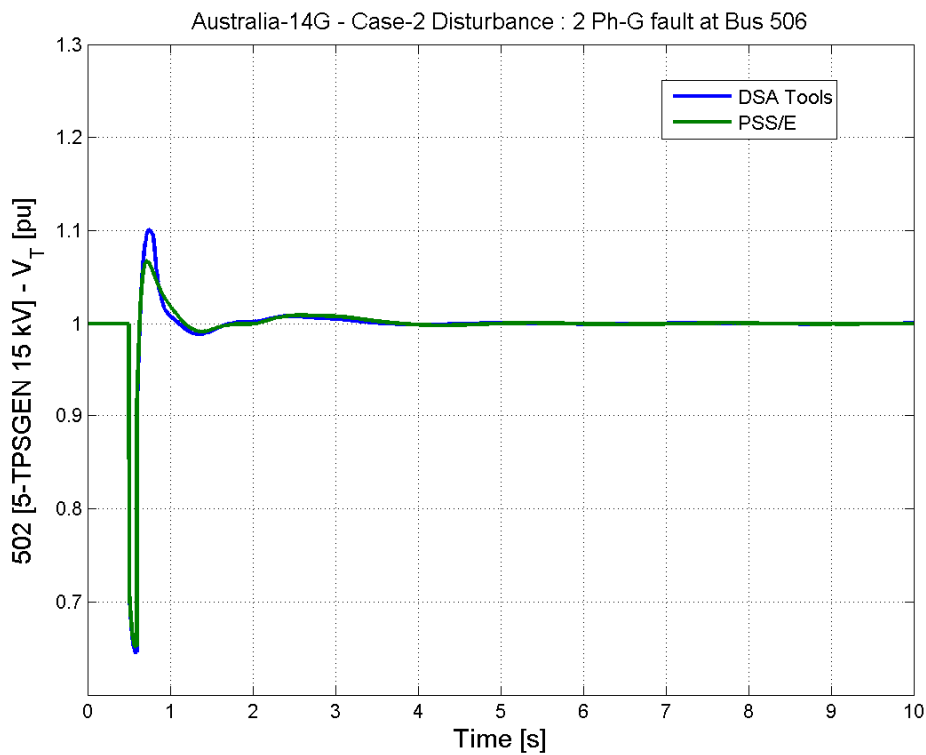
Contingency C



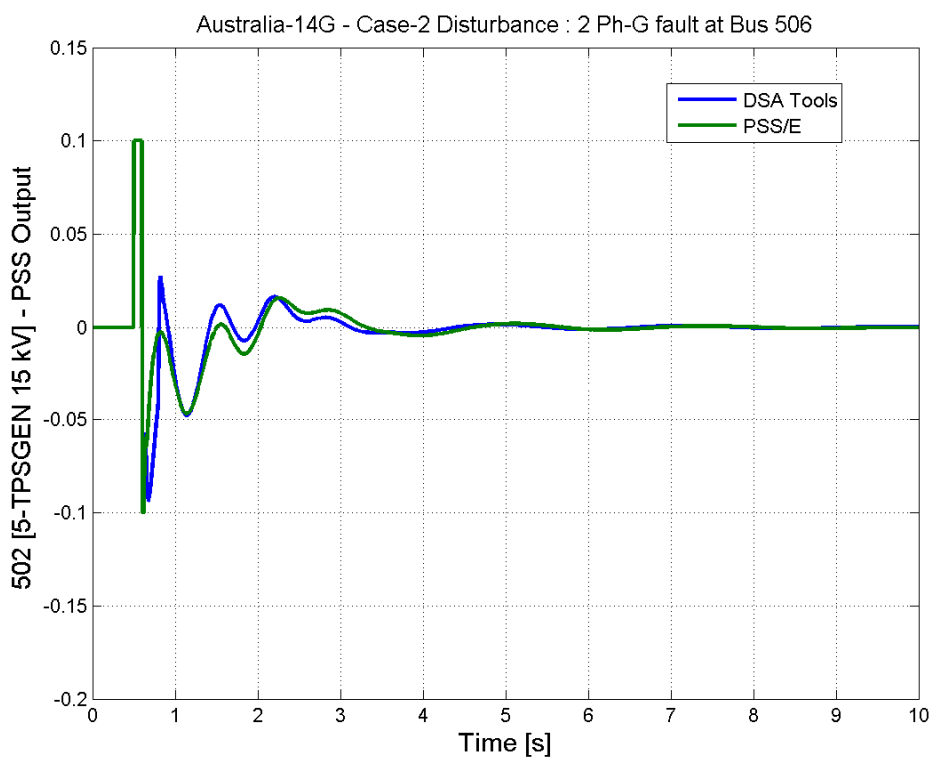


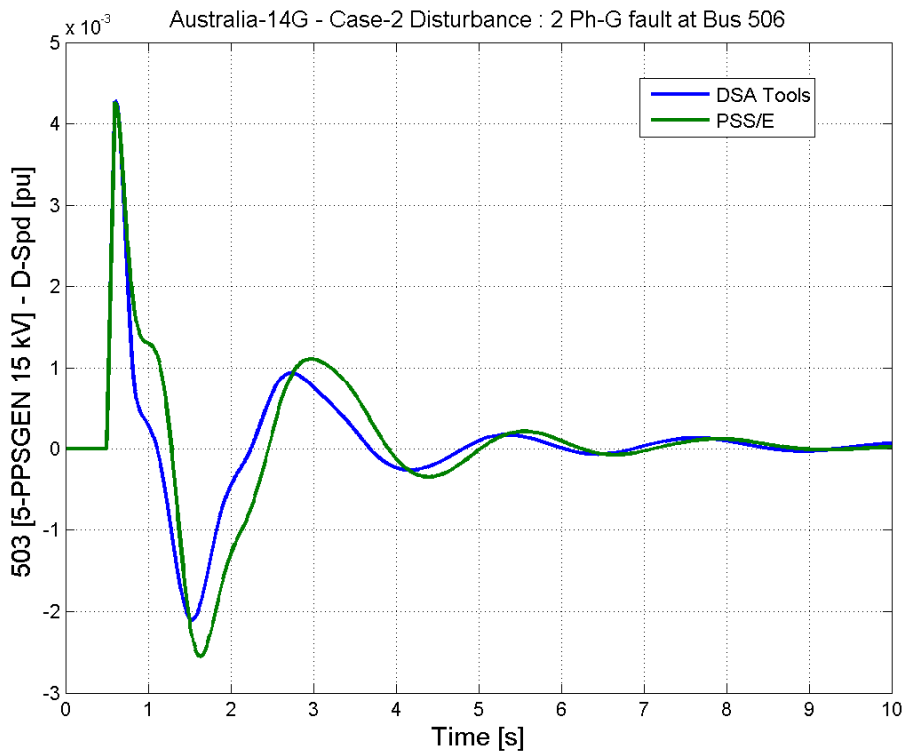
Contingency C



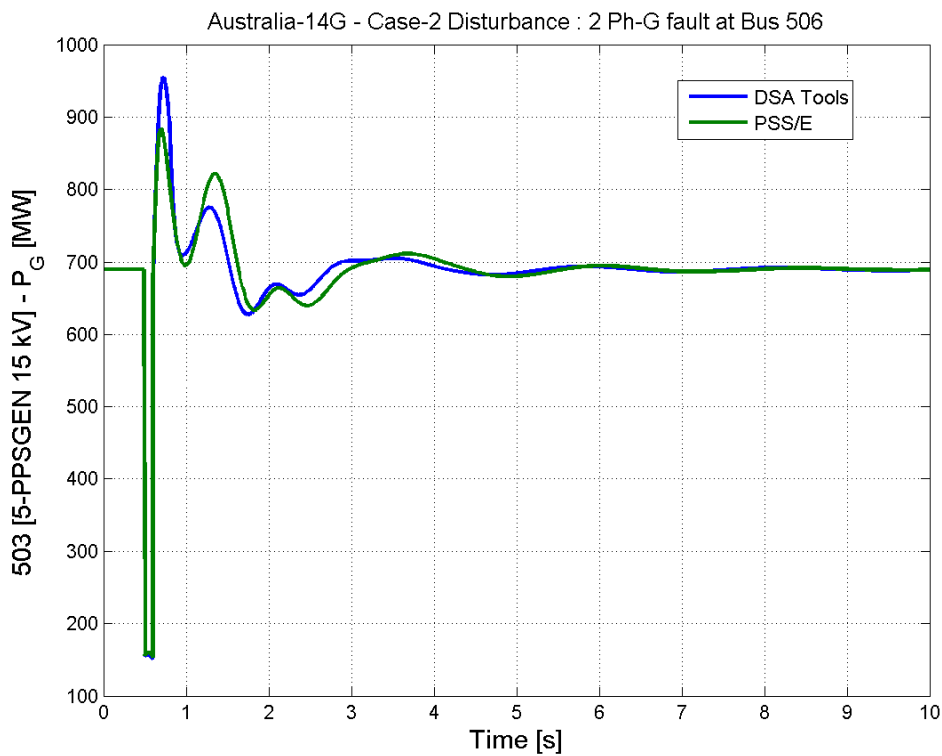


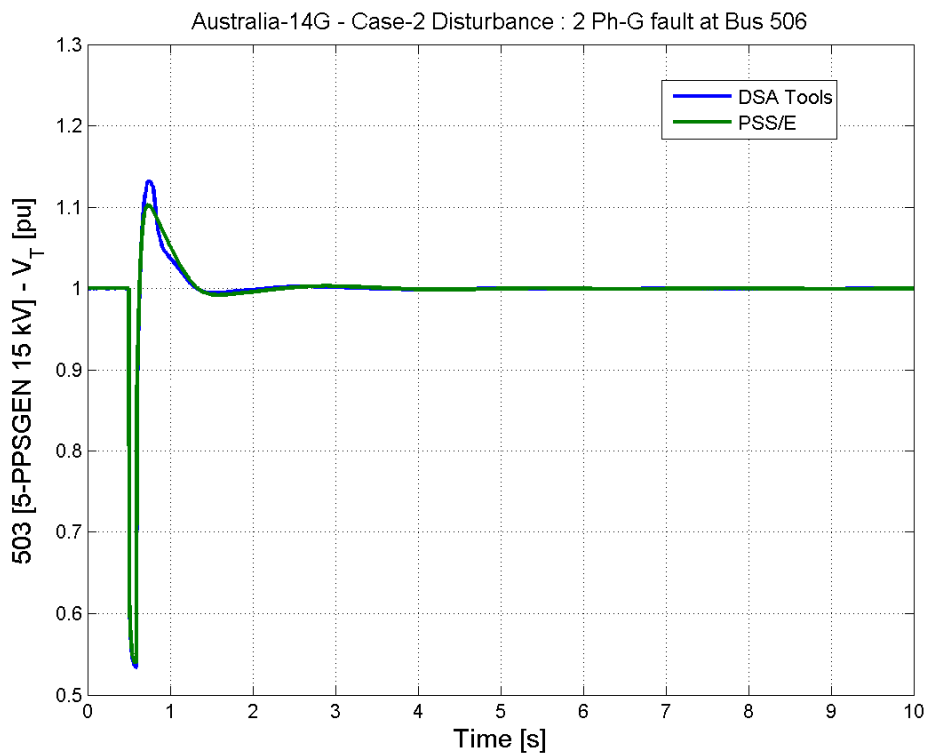
Contingency C



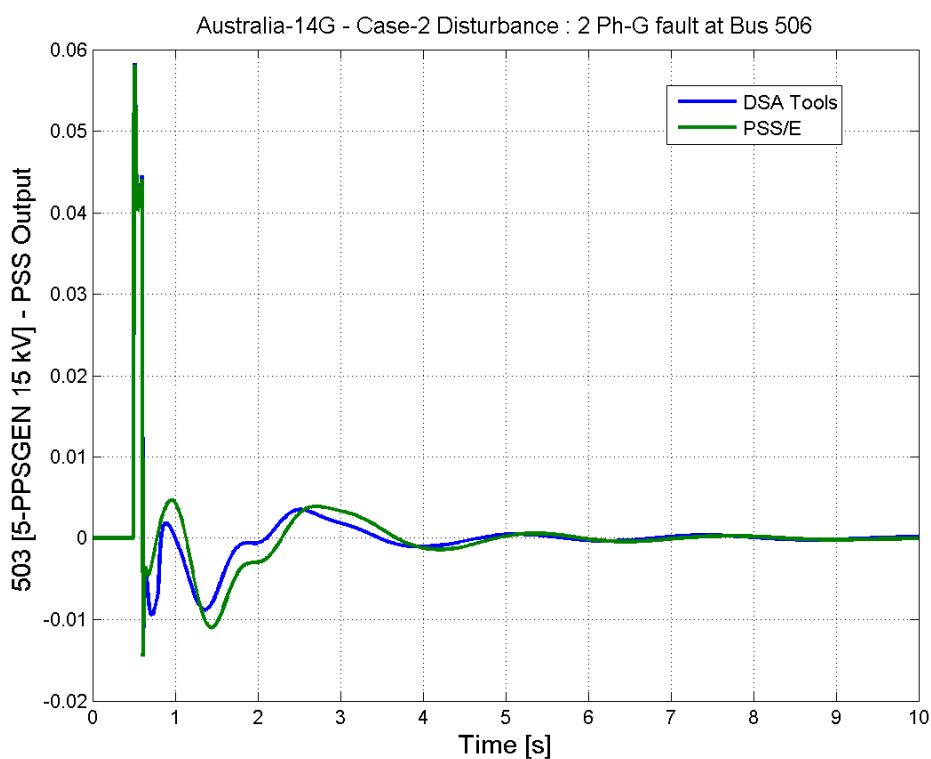


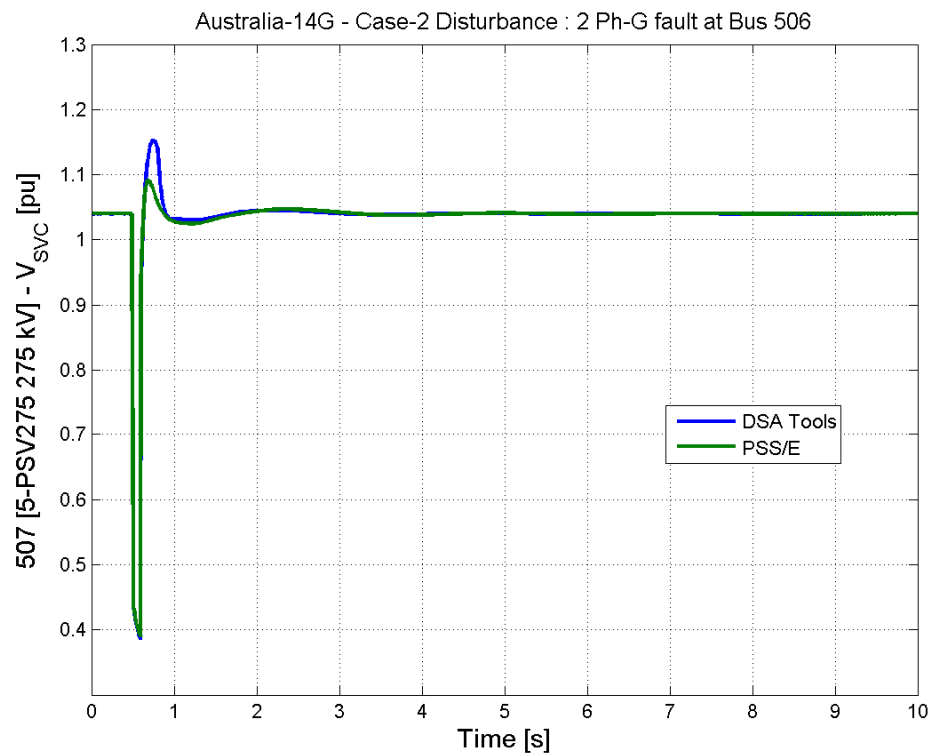
Contingency C



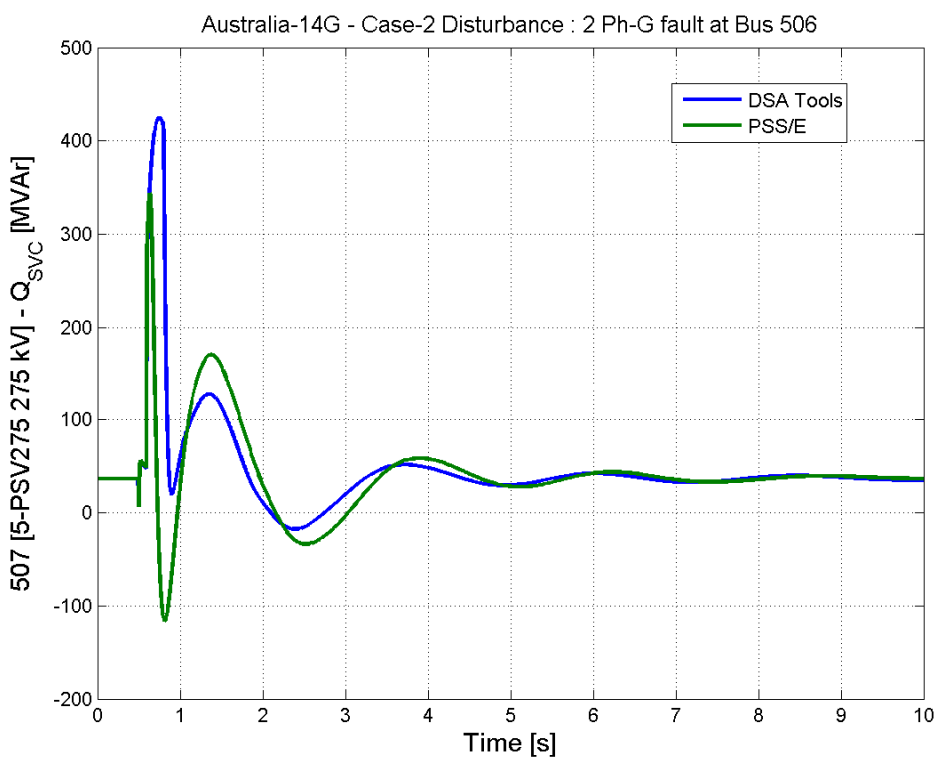


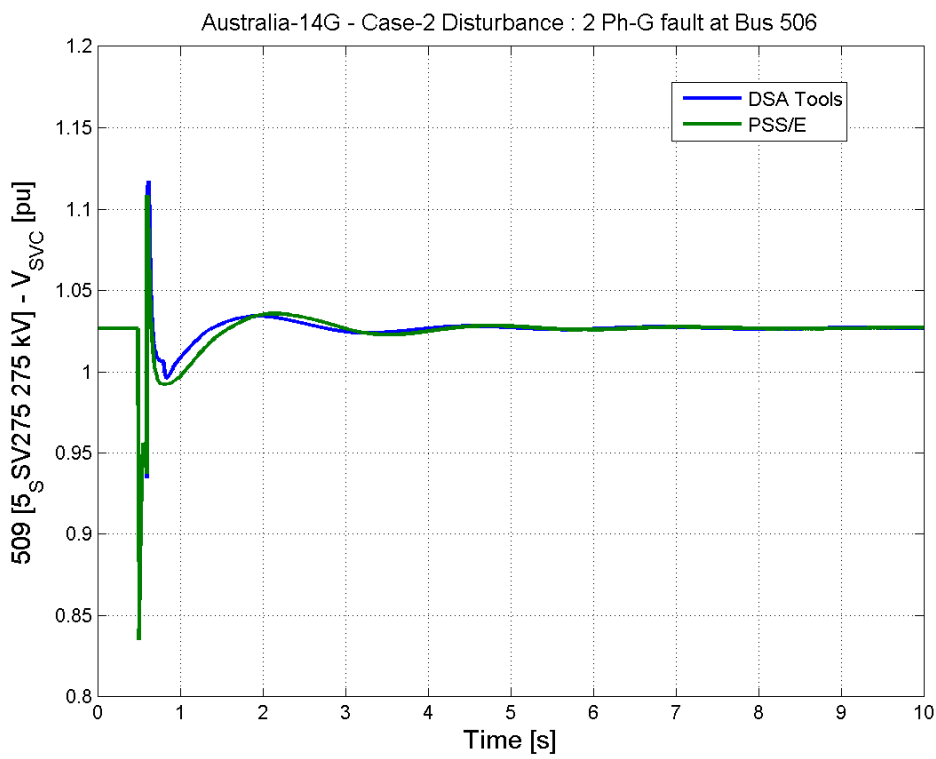
Contingency C



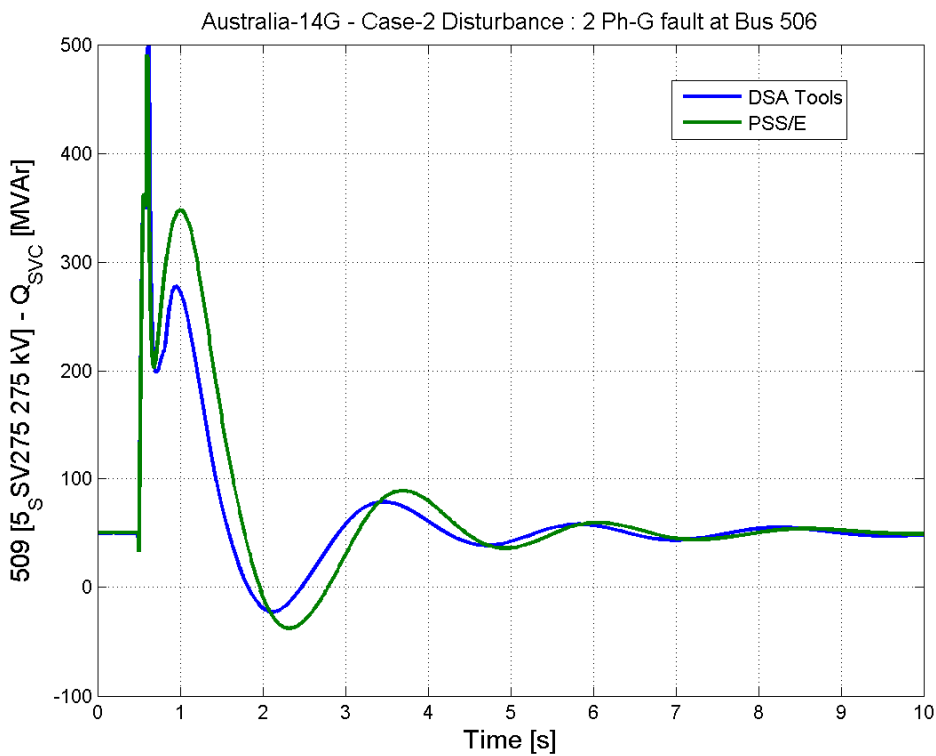


Contingency C





Contingency C



C.1

**Appendix C - Report on the 2-area (4-generator) system by Dr. Leonardo
Lima and Dinemayer Silva**

IEEE PES Task Force on Benchmark Systems for Stability Controls

Report on the 2-Areas, 4-generators system

Version 6 – July 1st, 2015

Leonardo Lima
Senior Member
Kestrel Power Engineering
leo@kestrelpower.com

Dinemayer Silva
Member
Siemens PTI
dinemayer.silva@siemens.com

Table of Contents

1.	Introduction	3
2.	Power Flow	3
3.	Dynamic Simulation Models.....	6
3.1.	Synchronous Machines	6
3.2.	Excitation Systems	9
3.3.	DC Rotating Excitation System	10
3.4.	Static Excitation System.....	10
3.5.	Power System Stabilizers	12
4.	Time Domain Simulation Results	15
4.1.	System without AVR – Constant Field Voltage	15
4.1.1.	50 MVar Reactor at Mid-Point.....	15
4.2.	ESDC1A with $K_A=20$	17
4.2.1.	50 MVar Reactor at Mid-Point.....	17
4.2.2.	Steps in V_{ref}	18
4.3.	ESDC1A with $K_A=200$	19
4.3.1.	50 MVar Reactor at Mid-Point.....	19
4.3.2.	Steps in V_{ref}	20
4.4.	ESST1A with TGR.....	21
4.4.1.	50 MVar Reactor at Mid-Point.....	21
4.4.2.	Steps in V_{ref}	22
4.5.	ESST1A without TGR	23
4.5.1.	50 MVar Reactor at Mid-Point.....	23
4.5.2.	Steps in V_{ref}	24
4.6.	ESST1A without TGR with Original PSS	25
4.6.1.	50 MVar Reactor at Mid-Point.....	25
4.6.2.	Steps in V_{ref}	26
4.7.	ESST1A without TGR with Modified PSS.....	27
4.7.1.	50 MVar Reactor at Mid-Point.....	27
4.7.2.	Steps in V_{ref}	28
5.	Modal Analysis	29
5.1.	PSS/E LSYSAN	29
5.2.	PSSPLT	39
5.3.	Impact of Generator Saturation	45
6.	References	49

1. Introduction

This report describes the data setup and nonlinear stability study carried over with the 4-generators, two-areas, system proposed in [1] using the Siemens PTI's PSS/E software [2]. The main objectives of this report are to document the data setup and to provide some validation of such data, comparing (to the extent possible) the results obtained with a time-domain nonlinear simulation with the eigenvalue analysis shown in [1].

It should be noted that simplified versions of this system have been used in the past [3-4], but the data shown in this report corresponds to that presented in Example 12.6 of [1].

2. Power Flow

The power flow solution is shown in Figure 1, with the one line diagram of the system. The bus data, including the voltage magnitudes and angles from the power flow solution, are shown in Table 1. The transmission line data is shown in Table 2. The data is provided in percent considering a system MVA base of 100 MVA. All transmission lines are 230 kV lines. The lines are represented by π sections and the charging shown in Table 2 corresponds to the total line charging.

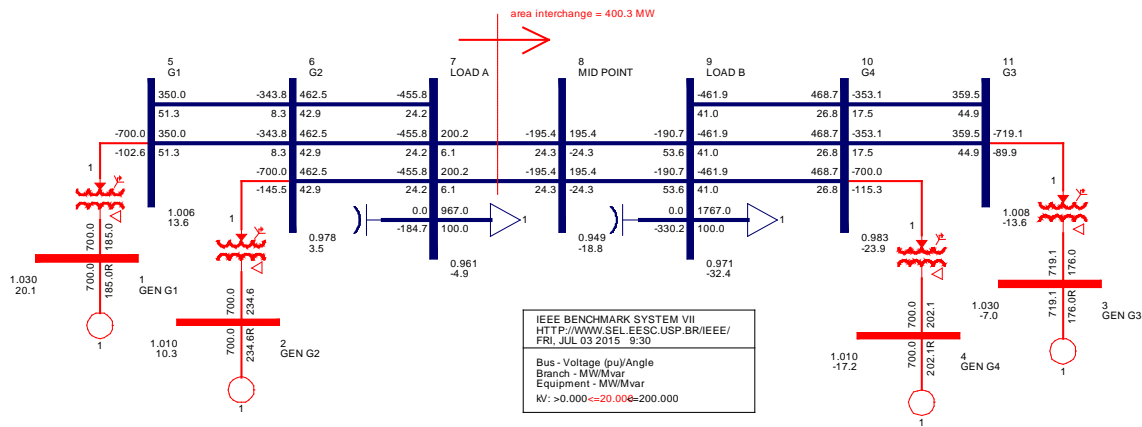


Figure 1: Case 1 Power Flow Solution

Table 1: Bus Data and Power Flow Solution

Bus Number	Bus Name	Base kV	Bus type	Voltage (pu)	Angle (deg)
1	GEN G1	20.0	PV	1.0300	20.07
2	GEN G2	20.0	PV	1.0100	10.31
3	GEN G3	20.0	swing	1.0300	-7.00
4	GEN G4	20.0	PV	1.0100	-17.19
5	G1	230.0	PQ	1.0065	13.61
6	G2	230.0	PQ	0.9781	3.52
7	LOAD A	230.0	PQ	0.9610	-4.89
8	MID POINT	230.0	PQ	0.9486	-18.76
9	LOAD B	230.0	PQ	0.9714	-32.35
10	G4	230.0	PQ	0.9835	-23.94
11	G3	230.0	PQ	1.0083	-13.63

Table 2: Transmission Line Data

From Bus	To Bus	ckt id	R (%)	X (%)	Charging (%)	Length (km)
5	6	1	0.50	5.0	2.1875	25
5	6	2	0.50	5.0	2.1875	25
6	7	1	0.30	3.0	0.5833	10
6	7	2	0.30	3.0	0.5833	10
6	7	3	0.30	3.0	0.5833	10
7	8	1	1.10	11.0	19.2500	110
7	8	2	1.10	11.0	19.2500	110
8	9	1	1.10	11.0	19.2500	110
8	9	2	1.10	11.0	19.2500	110
9	10	1	0.30	3.0	0.5833	10
9	10	2	0.30	3.0	0.5833	10
9	10	3	0.30	3.0	0.5833	10
10	11	1	0.50	5.0	2.1875	25
10	11	2	0.50	5.0	2.1875	25

The only difference regarding the data as presented in [1] is the introduction of multiple parallel circuits, so results considering weaker transmission system conditions might be investigated.

The generator step-up transformers (GSU) are explicitly represented in the case. The GSUs are all rated 900 MVA and have a leakage reactance of 15% on the transformer base. Winding resistance and magnetizing currents are neglected. Table 3 presents the GSU data.

There are two loads, directly connected to the 230 kV buses 7 and 9. The associated data is given in Table 4. These loads are represented, in the dynamic simulation, with a constant current characteristic for the active power and a constant admittance characteristic for the reactive power (100%I, 100%Z for P and Q, respectively).

Capacitor banks are also connected to the 230 kV buses 7 and 9. The values for these capacitors at nominal voltage (1.0 pu voltage) are shown in Table 5.

The complete PSS/E [2] report with all power flows for this system is given in Table 6.

Table 3: Generator Step- Up Transformer Data (on Transformer MVA Base)

From Bus	To Bus	R (%)	X (%)	MVA Base	tap (pu)
1	5	0	15	900	1
2	6	0	15	900	1
3	11	0	15	900	1
4	10	0	15	900	1

Table 4: Load Data

Bus	P (MW)	Q (MVAr)
7	967	100
9	1767	100

Table 5: Capacitor Bank Data

Bus	Q (MVAr)
7	200
9	350

Table 6: PSS/E Power Flow Results

X---- FROM BUS ---X VOLT		GEN	LOAD	SHUNT	X---- TO BUS -----X	TRANSFORMER					
BUS#	X-- NAME --X	PU/KV	ANGLE	MW/MVAR	MW/MVAR	MW/MVAR	BUS#	X-- NAME --X CKT	MW	MVAR	RATIO
1 GEN G1	1.0300	20.1	700.0	0.0	0.0	-----	5 G1	1	700.0	185.0	1.000UN
	20.600		185.0R	0.0	0.0						
2 GEN G2	1.0100	10.3	700.0	0.0	0.0	-----	6 G2	1	700.0	234.6	1.000UN
	20.200		234.6R	0.0	0.0						
3 GEN G3	1.0300	-7.0	719.1	0.0	0.0	-----	11 G3	1	719.1	176.0	1.000UN
	20.600		176.0R	0.0	0.0						
4 GEN G4	1.0100	-17.2	700.0	0.0	0.0	-----	10 G4	1	700.0	202.0	1.000UN
	20.200		202.0R	0.0	0.0						
5 G1	1.0065	13.6	0.0	0.0	0.0	-----	1 GEN G1	1	-700.0	-102.6	1.000LK
	231.49		0.0	0.0	0.0		6 G2	1	350.0	51.3	
							6 G2	2	350.0	51.3	
6 G2	0.9781	3.5	0.0	0.0	0.0	-----	2 GEN G2	1	-700.0	-145.5	1.000LK
	224.97		0.0	0.0	0.0		5 G1	1	-343.8	8.3	
							5 G1	2	-343.8	8.3	
							7 LOAD A	1	462.5	42.9	
							7 LOAD A	2	462.5	42.9	
							7 LOAD A	3	462.5	42.9	
7 LOAD A	0.9610	-4.9	0.0	967.0	0.0	-----	6 G2	1	-455.8	24.2	
	221.04		0.0	100.0	-184.7		6 G2	2	-455.8	24.2	
							6 G2	3	-455.8	24.2	
							8 MID POINT	1	200.2	6.1	
							8 MID POINT	2	200.2	6.1	
8 MID POINT	0.9486	-18.8	0.0	0.0	0.0	-----	7 LOAD A	1	-195.4	24.3	
	218.18		0.0	0.0	0.0		7 LOAD A	2	-195.4	24.3	
							9 LOAD B	1	195.4	-24.3	
							9 LOAD B	2	195.4	-24.3	
9 LOAD B	0.9714	-32.4	0.0	1767.0	0.0	-----	7 LOAD A	1	-195.4	24.3	
	223.42		0.0	100.0	-330.2		8 MID POINT	1	-190.7	53.6	
							8 MID POINT	2	-190.7	53.6	
							10 G4	1	-461.9	41.0	
							10 G4	2	-461.9	41.0	
							10 G4	3	-461.9	41.0	
10 G4	0.9835	-23.9	0.0	0.0	0.0	-----	4 GEN G4	1	-700.0	-115.3	1.000LK
	226.20		0.0	0.0	0.0		9 LOAD B	1	468.7	26.8	
							9 LOAD B	2	468.7	26.8	
							9 LOAD B	3	468.7	26.8	
							11 G3	1	-353.1	17.5	
							11 G3	2	-353.1	17.5	
11 G3	1.0083	-13.6	0.0	0.0	0.0	-----	10 G4	1	359.5	44.9	
	231.90		0.0	0.0	0.0		10 G4	2	359.5	44.9	

3. Dynamic Simulation Models

The models and associated parameters for the dynamic simulation models used in this PSS/E setup are described in this Section. All generation units are considered identical and will be represented by the same dynamic models and parameters, with exception of the inertias.

3.1. Synchronous Machines

The generator model to represent the round rotor units is the PSS/E model GENROE, shown in the block diagram in Figure 2. Details about the implementation of the model are available in the software documentation [2]. This is a 6th order dynamic model with the saturation function represented as a geometric (exponential) function. Table 7 provides the parameters for this model and all data are the same for all generators in the system, with the exception of the inertia constants.

The representation of the saturation of the generators has some impact on the results of a small-signal (linearized) analysis of the system performance. On the other hand, the proper representation of saturation is extremely important for transient stability and the determination of rated and ceiling conditions (minimum and maximum generator field current and generator field voltage) for the excitation system. Figure 3 presents the calculated generator open circuit saturation curve, based on the data in Table 7. As mentioned before, the saturation function is represented by a geometric function in the PSS/E GENROE model.

The calculated rated field current for this generator model is 2.66 pu (considering 0.85 rated power factor). This calculation comprises the initialization of the generator model at full (rated) power output, considering their rated power factor. It should be noted that in PSS/E models, due to the choice of base values for generator field voltage and generator field current, these variables are numerically the same, in steady state, when expressed in per unit.

Figure 4 shows the calculated capability curve for the generators, based on the data in Table 7.

Table 7: Dynamic Model Data for Round Rotor Units (PSS/E GENROE Model)

PARAMETERS				
Description	Symbol	Value	Unit	
Rated apparent power	M _{BASE}	900	MVA	
d-axis open circuit transient time constant	T' _{do}	8.0	s	
d-axis open circuit sub-transient time constant	T'' _{do}	0.03	s	
q-axis open circuit transient time constant	T' _{qo}	0.4	s	
q-axis open circuit sub-transient time constant	T'' _{qo}	0.05	s	
Inertia	H	†	MW.s/MVA	
Speed damping	D	0	pu	
d-axis synchronous reactance	X _d	1.8	pu	
q-axis synchronous reactance	X _q	1.70	pu	
d-axis transient reactance	X' _d	0.3	pu	
q-axis transient reactance	X' _q	0.55	pu	
sub-transient reactance	X'' _d = X'' _q	0.25	pu	
Leakage reactance	X _l	0.20	pu	
Saturation factor at 1.0 pu voltage	S(1.0)	0.0392	–	
Saturation factor at 1.2 pu voltage	S(1.2)	0.2672	–	

Notes:

† Units 1 and 2 have inertias H = 6.50, while units 3 and 4 have inertias H = 6.175

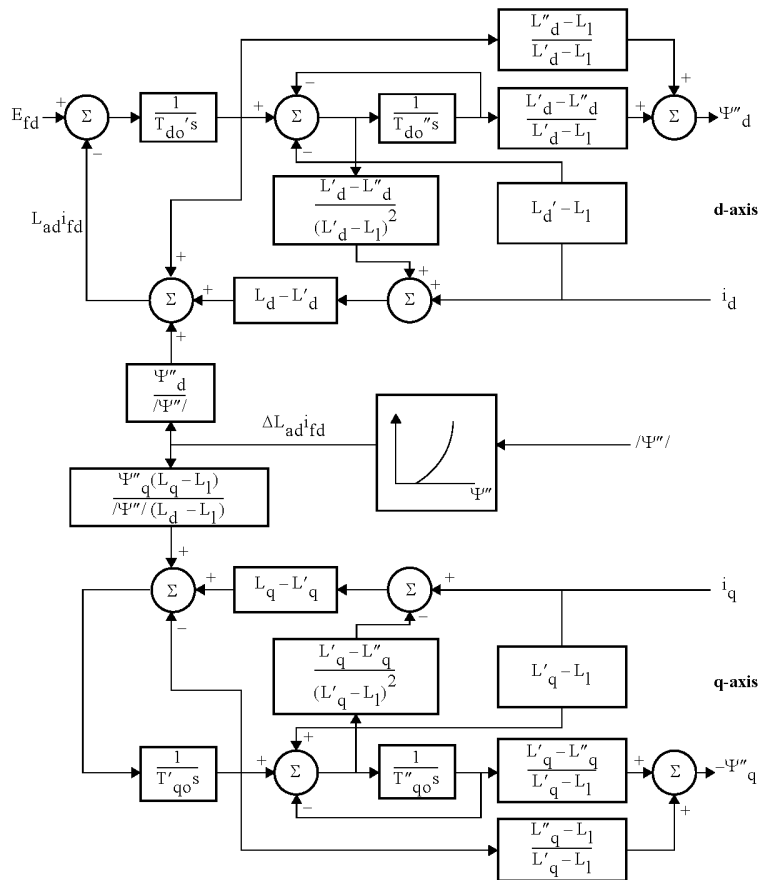


Figure 2: Block Diagram for the PSS/E Model GENROE

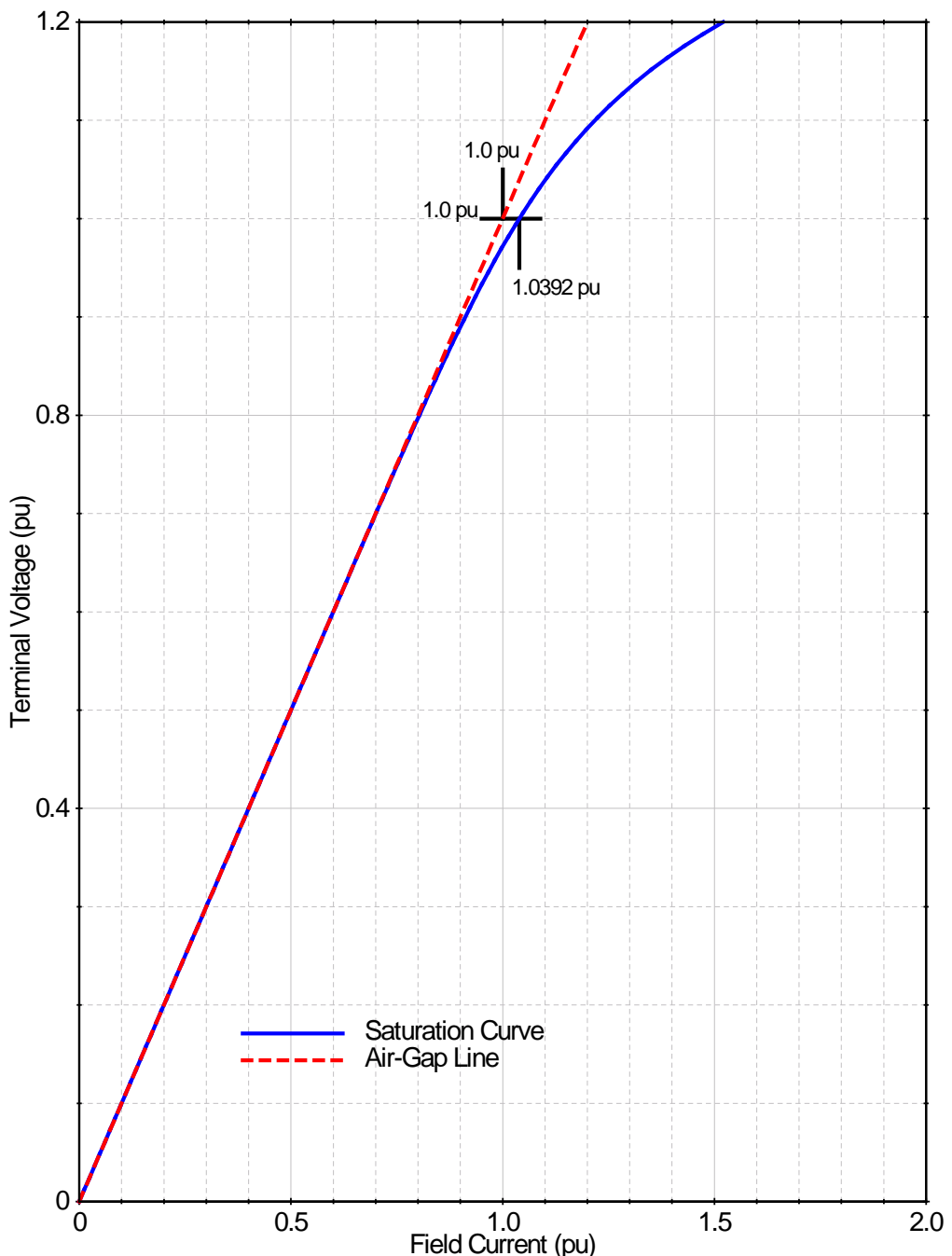


Figure 3: Generator Open Circuit Saturation Curve

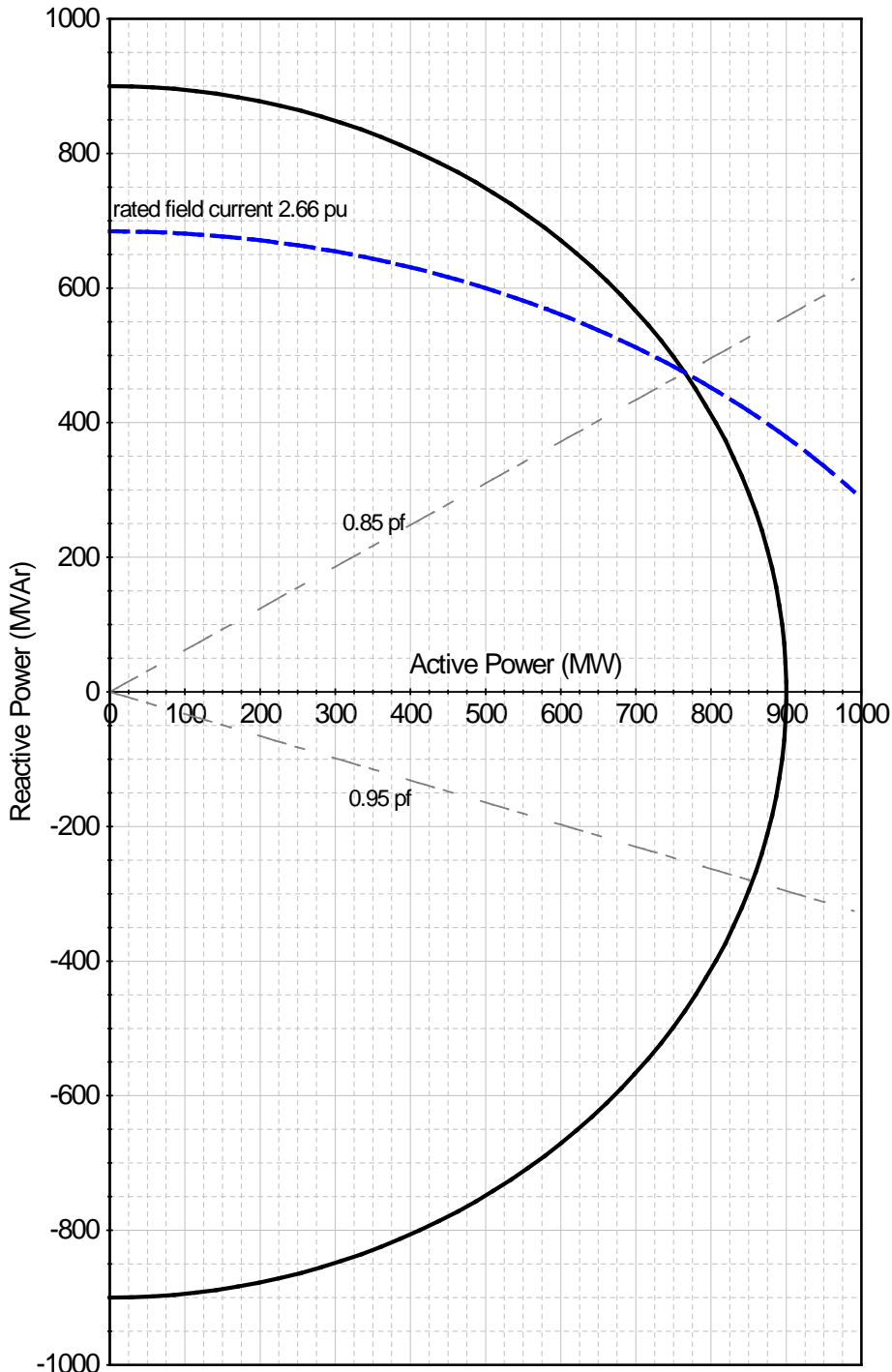


Figure 4: Generator Capability Curve

3.2. Excitation Systems

Following the results presented in [1], this report will present simulation results with different representations/models for the excitation system of the generators.

The first set of results is associated with all generators in manual control (constant generator field voltage). Therefore, in PSS/E there will be no explicit excitation system model, as PSS/E assumes constant generator field voltage when no dynamic model for the excitation system is available.

The second set of results is related to a low gain, relatively slow DC rotating exciter. This excitation system is represented by the IEEE Std. 421.5(2005) DC1A [5], corresponding to the PSS/E model ESDC1A [1]. A variation regarding the results in [1] will be introduced in this report, where the steady state gain of the AVR in this DC rotating excitation system is increased tenfold.

A relatively fast (high initial response) static excitation system will be used in the next three sets of results: an AVR with transient gain reduction, then the AVR without such transient gain reduction, and finally the AVR without transient gain reduction with an active power system stabilizer (PSS).

3.3. DC Rotating Excitation System

The block diagram of the PSS/E model ESDC1A [2] is shown in Figure 5. The parameters for the model are presented in Table 8.

3.4. Static Excitation System

The block diagram of the PSS/E model ESST1A [2] is shown in Figure 6. The transient gain reduction will be implemented by the lead-lag block with parameters T_C and T_B , so the parameters T_{C1} , T_{B1} , K_F and T_F are not applicable and have been set accordingly. Similarly, the generator field current limit represented by the parameters K_{LR} and I_{LR} is not considered in the results presented in this report. The parameters for the ESST1A model are presented in Table 9.

The limits (parameters $V_{I\max}$, $V_{I\min}$, $V_{A\max}$, $V_{A\min}$, $V_{R\max}$ and $V_{R\min}$) in the model were set to typical values corresponding to the expected ceilings of such static excitation system. These limits are irrelevant for the small-signal analysis of the system dynamic response. On the other hand, these limits are a critical part of the model and the expected response of the excitation system following large system disturbances such as faults.

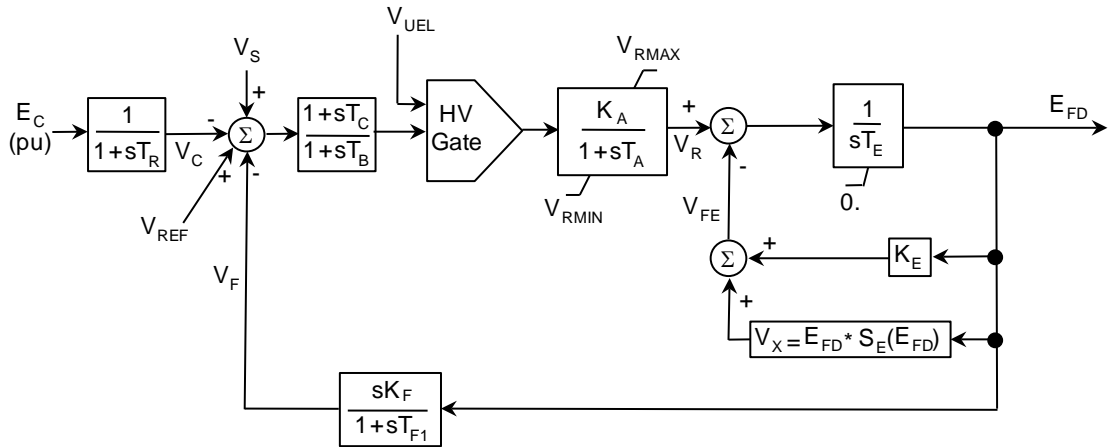


Figure 5: Block Diagram for the PSS/E Model ESDC1A

Table 8: Dynamic Model Data for DC Rotating Excitation Systems (PSS/E Model ESDC1A)

PARAMETERS			
Description	Symbol	Value	Unit
Voltage transducer time constant	T_R	0.05	s
AVR steady state gain	K_A	20^{\dagger}	pu
AVR equivalent time constant	T_A	0.055	s
TGR block 1 denominator time constant	T_B	0	s
TGR block 2 numerator time constant	T_C	0	s
Max. AVR output	V_{Rmax}	5	pu
Min. AVR output	V_{Rmin}	-3	pu
Exciter feedback time constant	K_E	1	pu
Exciter time constant	T_E	0.36	s
Stabilizer feedback gain	K_F	0.125	pu
Stabilizer feedback time constant	T_{F1}	1.8	s
Switch		$0^{\ddagger\ddagger}$	
Exciter saturation point 1	E_1	$3^{\ddagger\ddagger\ddagger}$	pu
Exciter saturation factor at point 1	$S_E(E_1)$	0.1	-
Exciter saturation point 2	E_2	4	pu
Exciter saturation factor at point 2	$S_E(E_2)$	0.3	-

Notes:

- [†] Results will be presented with gain $K_A=20$ and also $K_A=200$.
- [‡] The parameter “switch” is specific to the PSS/E implementation of this model and it is not part of the Standard definition of the DC1A model. It might not be needed in other software.
- ^{††} Saturation for the rotating DC exciter was not provided in [1]. Typical saturation values are assumed.

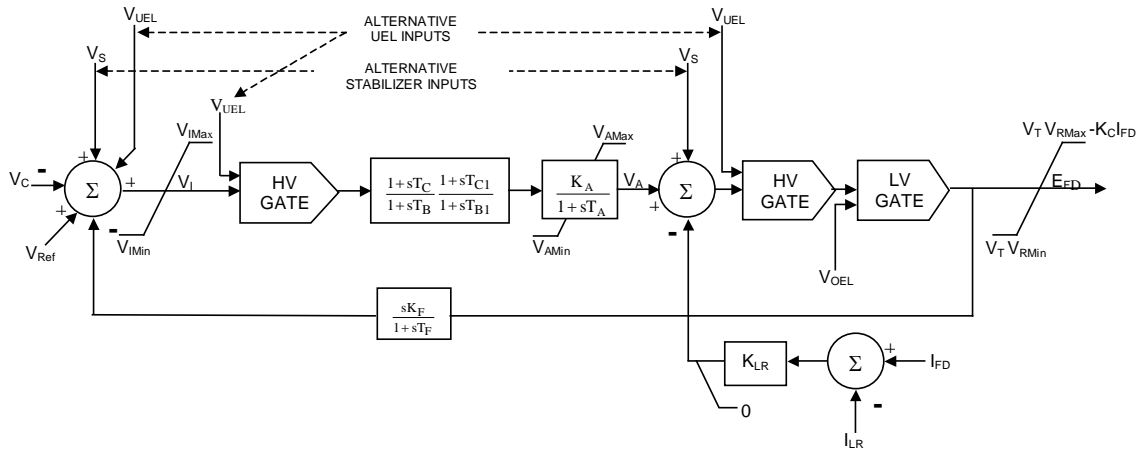


Figure 6: Block Diagram for the PSS/E Model ESST1A

Table 9: Dynamic Model Data for Static Excitation Systems (PSS/E Model ESST1A)

PARAMETERS			
Description	Symbol	Value	Unit
Voltage transducer time constant	T_R	0.01	s
Max. voltage error	$V_{I\max}$	99	pu
Min. voltage error	$V_{I\min}$	-99	pu
TGR block 1 numerator time constant	T_C	1	s
TGR block 1 denominator time constant	T_B	1^\dagger	s
TGR block 2 numerator time constant	T_{C1}	0	s
TGR block 1 denominator time constant	T_{B1}	0	s
AVR steady state gain	K_A	200	pu
Rectifier bridge equivalent time constant	T_A	0	s
Max. AVR output	$V_{A\max}$	4	pu
Min. AVR output	$V_{A\min}$	-4	pu
Max. rectifier bridge output	$V_{R\max}$	4	pu
Min. rectifier bridge output	$V_{R\min}$	-4	pu
Commutation factor for rectifier bridge	K_C	0	pu
Stabilizer feedback gain	K_F	0	pu
Stabilizer feedback time constant	T_F	1	s
Field current limiter gain	K_{LR}	0	pu
Field current instantaneous limit	I_{LR}	3	pu

Notes:

[†] This data corresponds to the case without transient gain reduction (TGR). The parameter T_B should be set to 10 seconds for the cases considering transient gain reduction.

3.5. Power System Stabilizers

The IEEE Std. 421.5(2005) model PSS1A [5] will be used to represent the power system stabilizers. The block diagram of the PSS/E model IEEEST [2] is shown in Figure 7. The parameters for the IEEEST model are presented in Table 10.

The output limits were set to $\pm 5\%$, while the logic to switch off the PSS for voltages outside a normal operation range has been ignored (parameters V_{CU} and V_{CL} set to zero).

These stabilizers are used with the excitation system represented by the ESST1A model without transient gain reduction (TGR). The PSS transfer function and, in particular, the phase compensation would have to be adjusted for application with any of the other excitation system models presented in this benchmark system.

Figure 8 presents the calculated phase requirement for the PSS (the phase characteristic of the GEP(s) transfer function [6]), and the phase characteristic of the PSS proposed in [1]. It can be seen that the original PSS does not provide sufficient phase lead, particularly at the frequencies associated with the local mode of oscillation of the generator (above 1 Hz). This is consistent with the results presented in [1], where the frequency of the local mode of oscillation increases when the PSS is in service.

A modified tuning for the PSS transfer function is proposed here, with significant more phase lead particularly in the frequency range associated with the local mode of oscillation. Figure 8 shows that this new PSS transfer function is a much closer match to the actual phase

requirement given by GEP(s), within $\pm 30^\circ$ of the actual compensation requirement as suggested in [6].

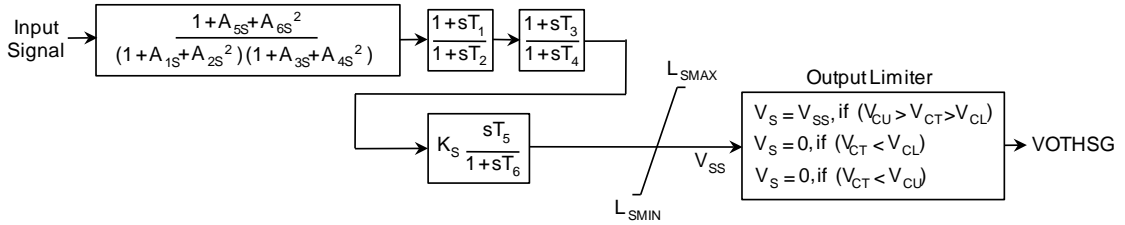


Figure 7: Block Diagram for the PSS/E Model IEEEST

Table 10: Dynamic Model Data for Power System Stabilizers (PSS/E Model IEEEST)

PARAMETERS				
Description	Symbol	Original Values	New Values	Unit
2 nd order denominator coefficient	A ₁	0	0	
2 nd order denominator coefficient	A ₂	0	0	
2 nd order numerator coefficient	A ₃	0	0	
2 nd order numerator coefficient	A ₄	0	0	
2 nd order denominator coefficient	A ₅	0	0	
2 nd order denominator coefficient	A ₆	0	0	
1 st lead-lag numerator time constant	T ₁	0.05	0.08	s
1 st lead-lag denominator time constant	T ₂	0.02	0.015	s
2 nd lead-lag numerator time constant	T ₃	3	0.08	s
2 nd lead-lag denominator time constant	T ₄	5.4	0.015	s
Washout block numerator time constant	T ₅	10	10	s
Washout block denominator time constant	T ₆	10	10	s
PSS gain	K _S	20	10	pu
PSS max. output	L _{Smax}	0.05	0.05	pu
PSS min. output	L _{Smin}	-0.05	-0.05	pu
Upper voltage limit for PSS operation	V _{Cu}	0	0	pu
Lower voltage limit for PSS operation	V _{Cl}	0	0	pu

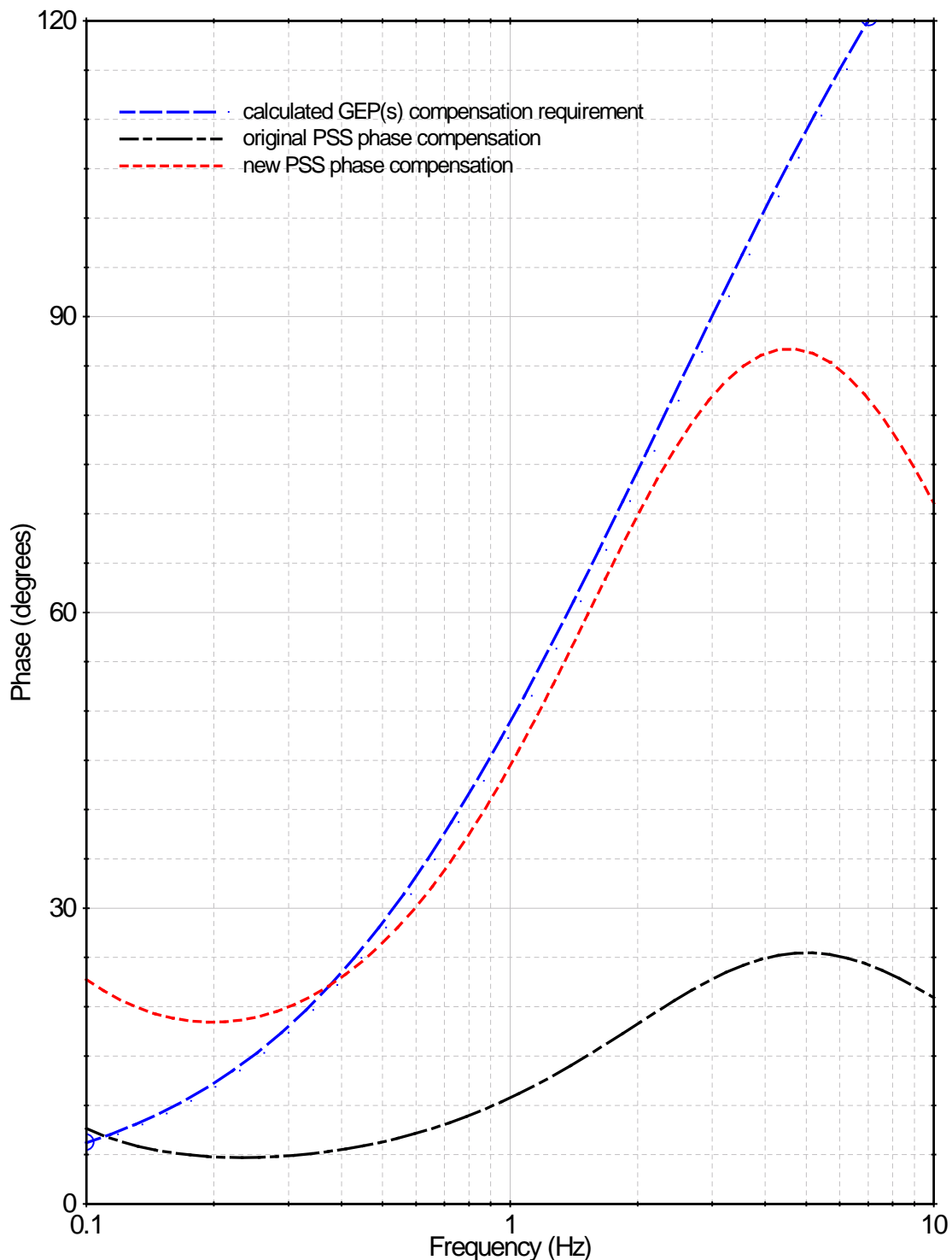


Figure 8: PSS Phase Compensation Characteristics

4. Time Domain Simulation Results

The results presented in this report correspond to time-domain simulations of different disturbances. The main objective associated with the selection of these disturbances was to assess the system damping and the effectiveness of the proposed stabilizers in providing damping to these oscillations.

The first set of simulations comprise the connection of a 50 MVar reactor at the mid-point of the system (bus #8) at $t=1.0$ second. The reactor is disconnected 100 ms later, without any changes in the system topology. This is a very small disturbance, and as such leads to results that correspond to the linear response of the system. Furthermore, given the location where the disturbance is applied, it tends to excite primarily the inter-area oscillation.

The second set of simulations correspond to simultaneous changes in voltage reference in all generator units, applied at $t=1.0$ second. The applied step changes are as follows:

GENERATOR	STEP IN V_{ref}
G1	+3%
G2	-1%
G3	-3%
G4	+1%

These changes in voltage reference were selected in order to excite not only the inter-area oscillation mode but also the other electromechanical modes in the system.

4.1. System without AVR – Constant Field Voltage

The results in this Section correspond to the results in [1] with a manual excitation control. Since there is no automatic voltage regulator (AVR), the steps in voltage reference cannot be applied, so only the results corresponding to the 50 MVar reactor at the mid-point are presented.

4.1.1. 50 MVar Reactor at Mid-Point

Figure 9 presents the PSS/E results (time domain simulation) of the 50 MVar reactor disturbance, when the excitation systems are operated in manual control (constant field voltage). The results in Figure 9 are the electrical power outputs of the four machines, in per unit of the system MVA base (100 MVA).

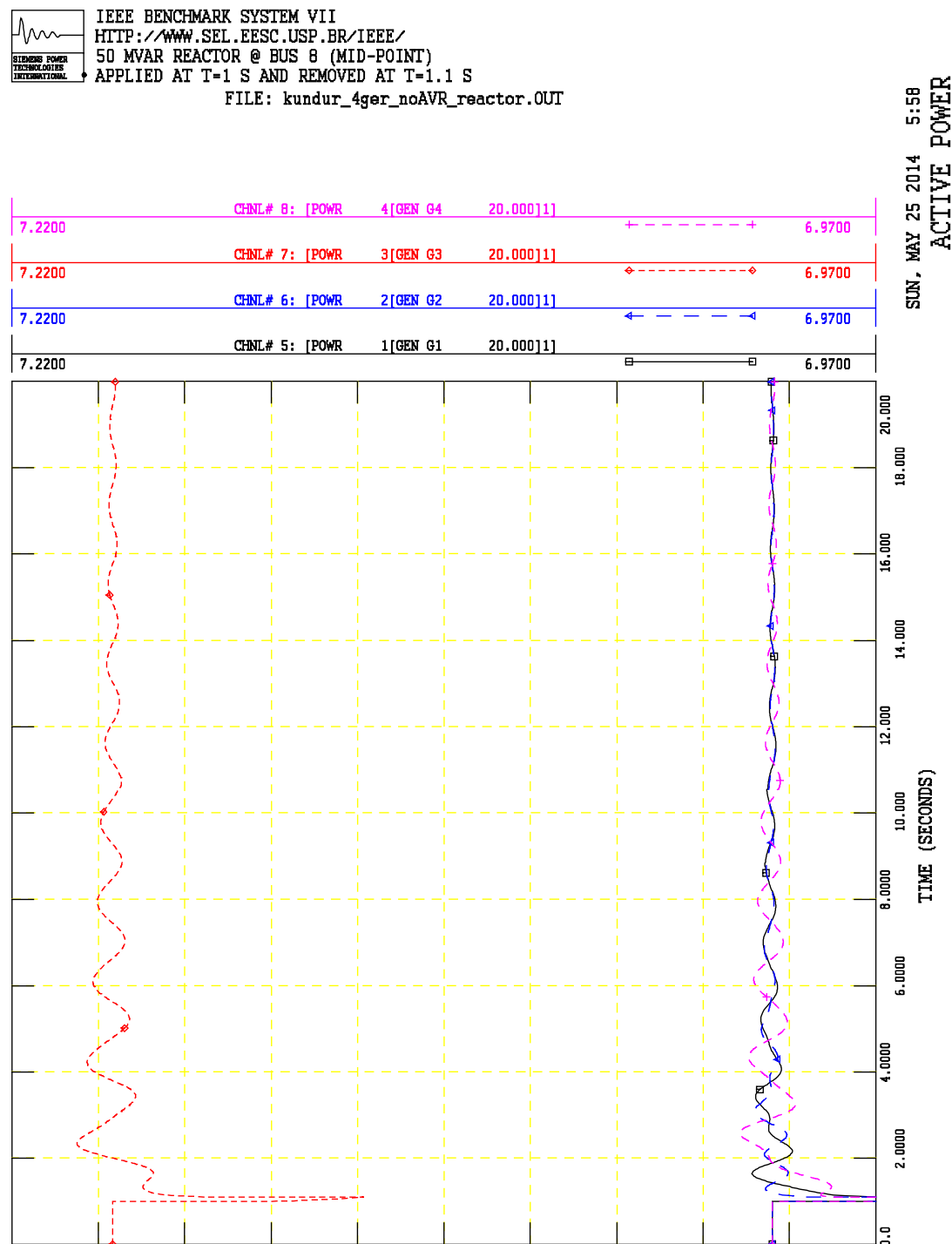


Figure 9: 50 MVar Reactor Disturbance with Manual Excitation Control

4.2. ESDC1A with $K_A=20$

The results in this Section correspond to the results in [1] with the self-excited dc exciter, represented in PSS/E by the ESDC1A model presented in Section 1.2.1 (gain $K_A=20$ pu).

4.2.1. 50 MVar Reactor at Mid-Point

Figure 10 shows the electrical power output of the generators (100 MVA base) for the 50 MVar reactor disturbance (ESDC1A model with $K_A=20$ pu).

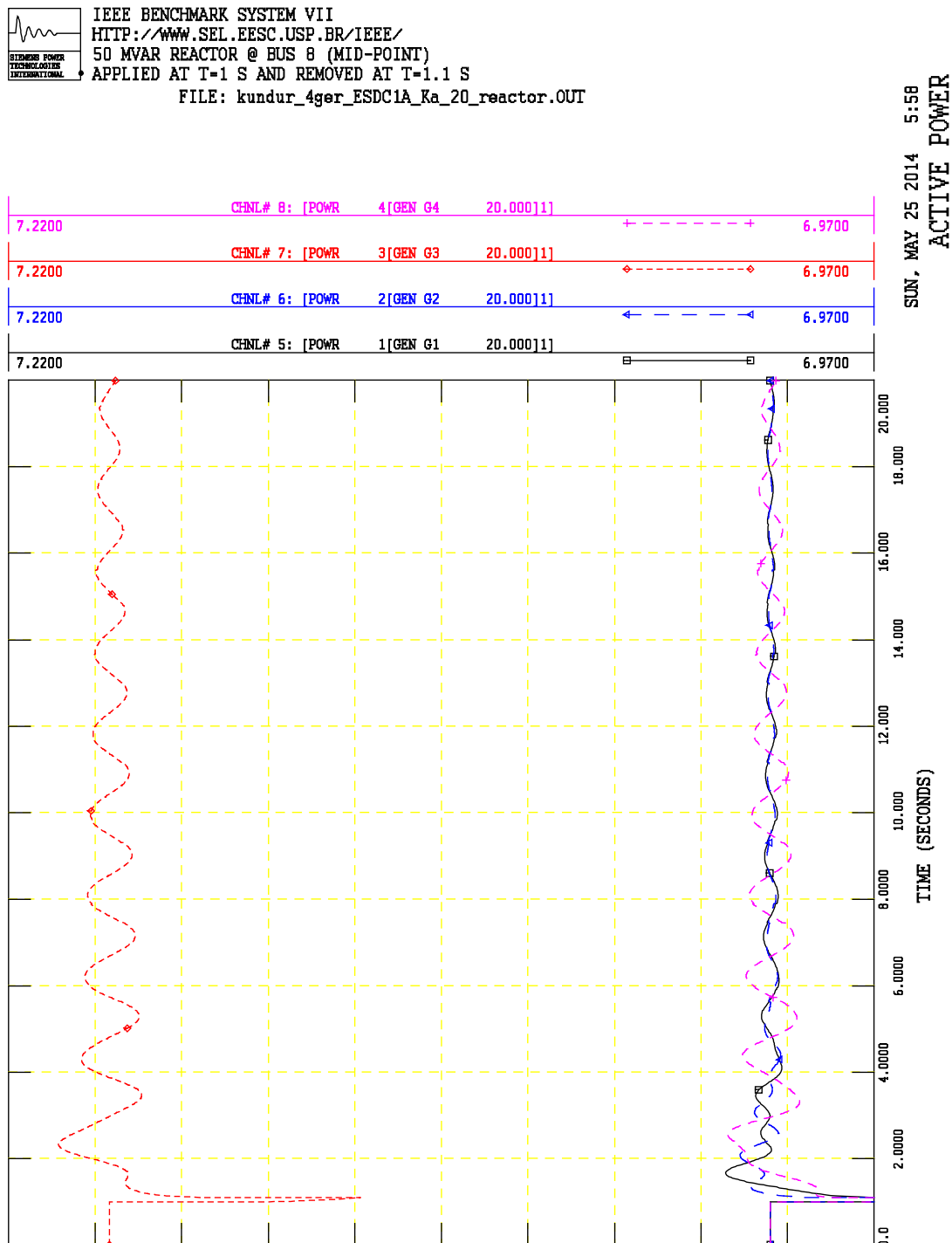


Figure 10: 50 MVar Reactor Disturbance with ESDC1A Model ($K_A=20$)

4.2.2. Steps in V_{ref}

Figure 11 shows the electrical power output of the generators (100 MVA base) for the step changes in voltage reference, when the excitation systems represented by the ESDC1A model, considering the gain $K_A=20$ pu.

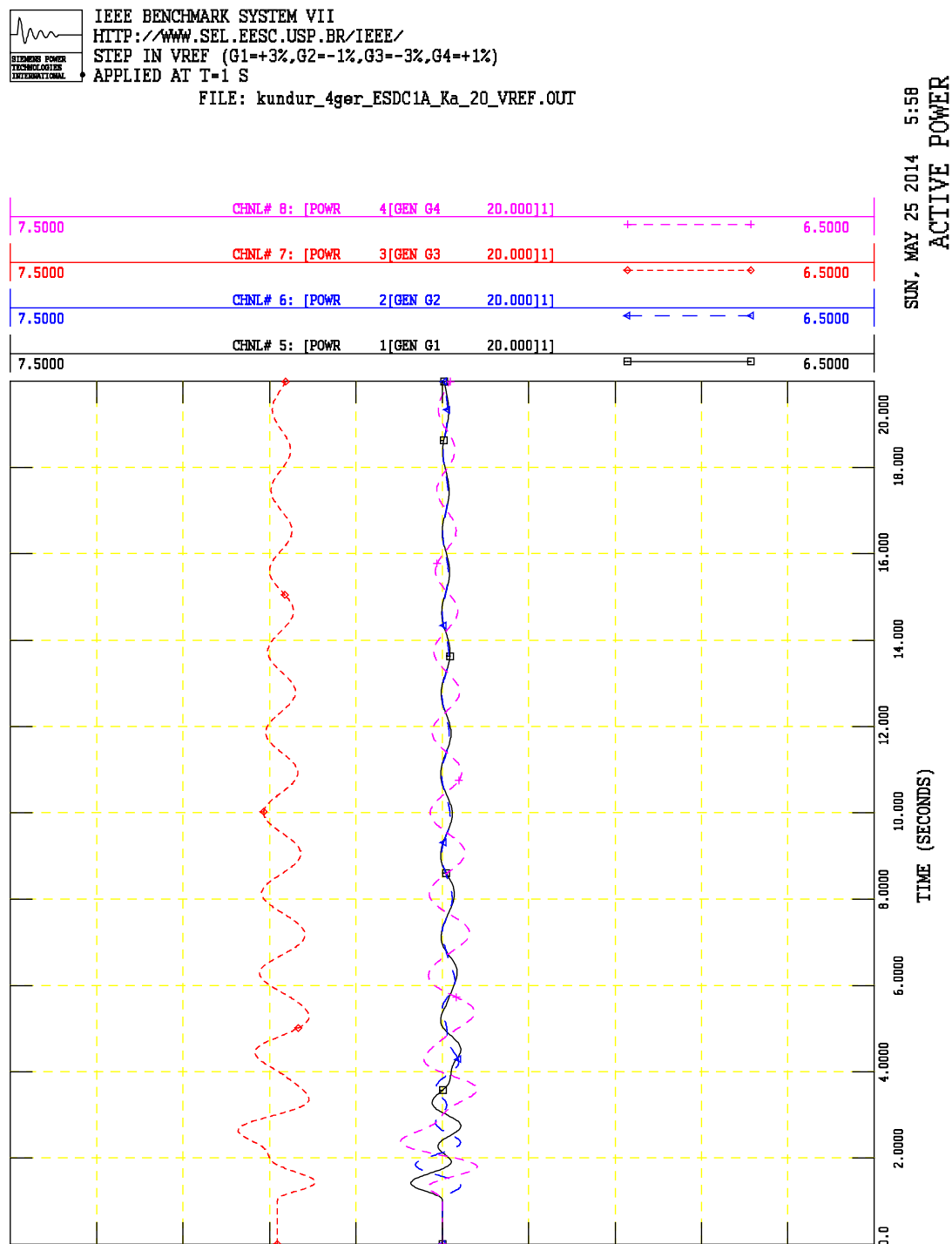


Figure 11: Step in Voltage References with ESDC1A Model ($K_A=20$)

4.3. ESDC1A with $K_A=200$

The results in this Section correspond to the results in [1] with the self-excited dc exciter, represented in PSS/E by the ESDC1A model presented in Section 1.2.1 (gain $K_A=200$ pu).

4.3.1. 50 MVar Reactor at Mid-Point

Figure 12 shows the electrical power output of the generators (100 MVA base) for the 50 MVar reactor disturbance (ESDC1A model with $K_A=200$ pu).

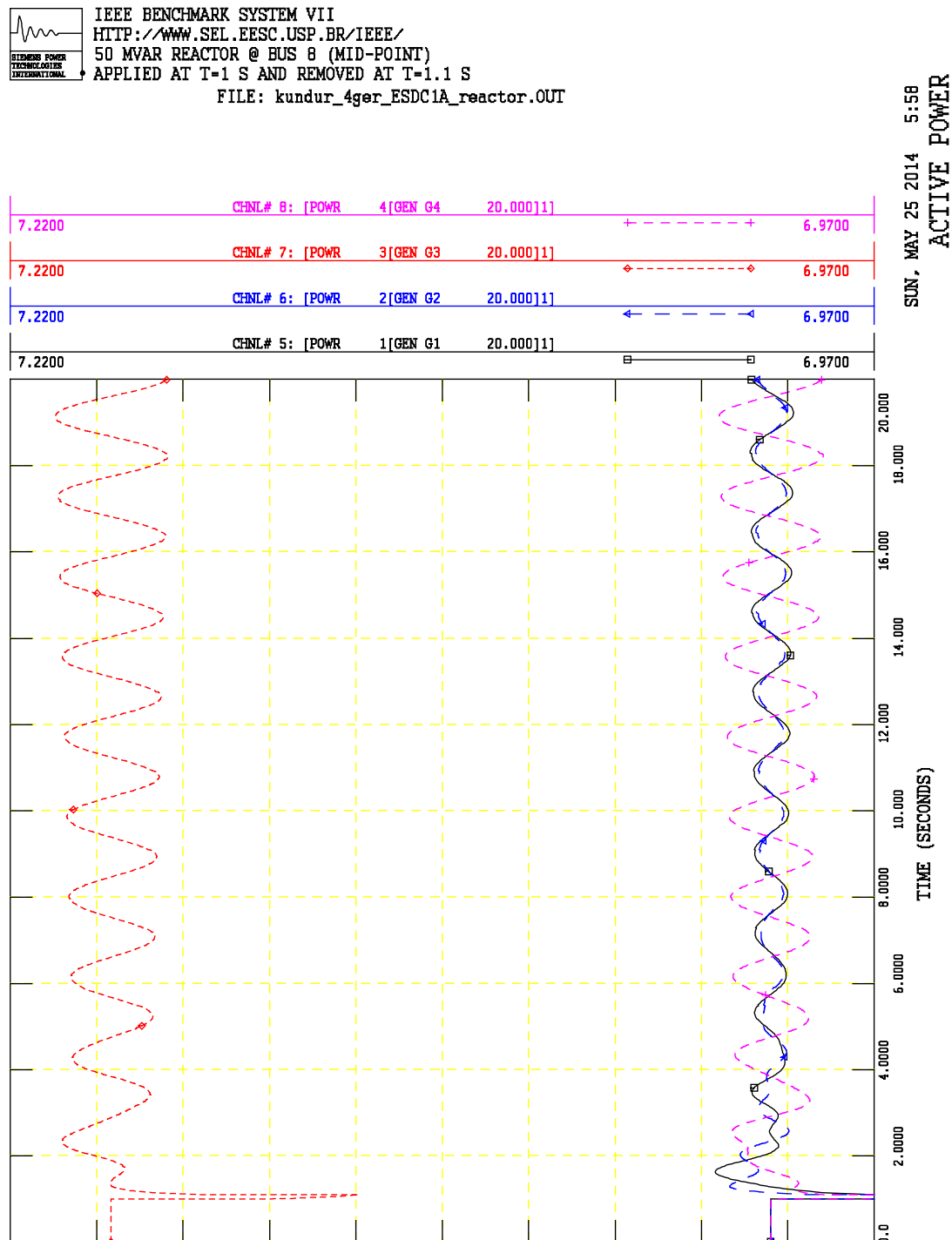


Figure 12: 50 MVar Reactor Disturbance with ESDC1A Model ($K_A=200$)

4.3.2. Steps in V_{ref}

Figure 13 shows the electrical power output of the generators (100 MVA base) for the step changes in voltage reference, when the excitation systems represented by the ESDC1A model, considering the gain $K_A=200$ pu.

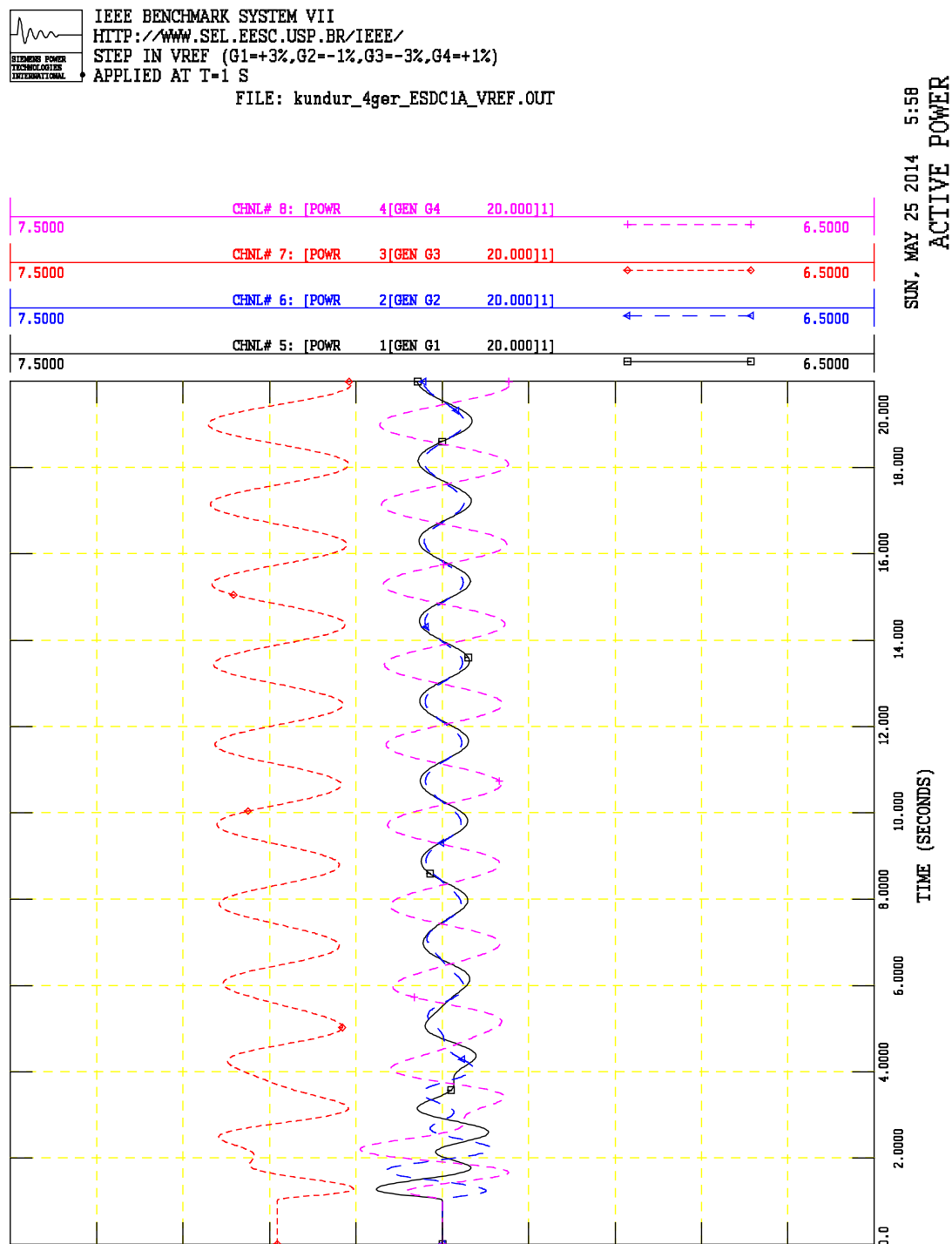


Figure 13: Step in Voltage References with ESDC1A Model ($K_A=200$)

4.4. ESST1A with TGR

The results in this Section correspond to the results in [1] with the static excitation system, represented in PSS/E by the ESST1A model presented in Section 1.2.2 (time constant $T_B=10$ s).

4.4.1. 50 MVar Reactor at Mid-Point

Figure 14 shows the electrical power output of the generators (100 MVA base) for the 50 MVar reactor disturbance (ESST1A model with $T_B=10$ s).

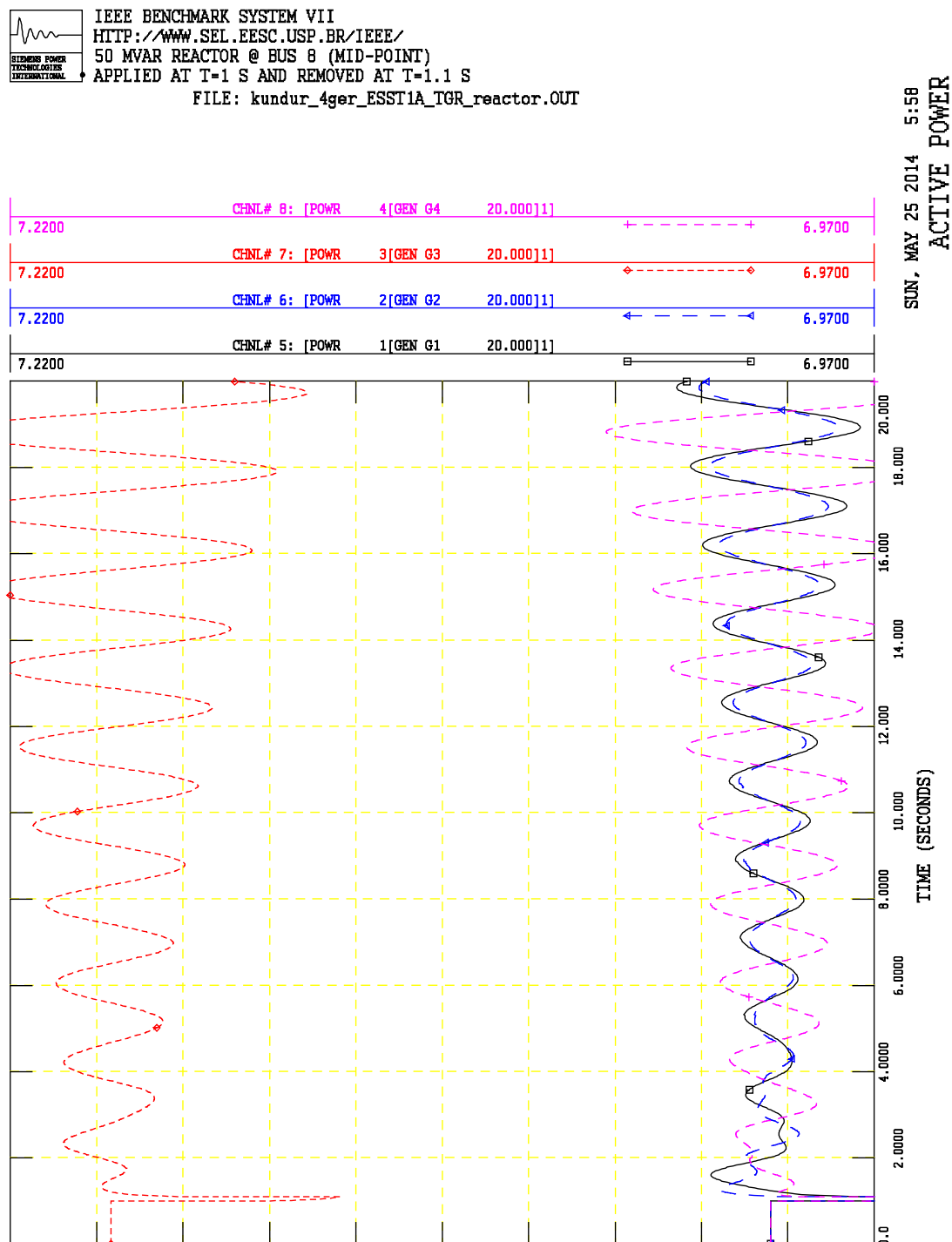


Figure 14: 50 MVar Reactor Disturbance with ESST1A Model with TGR

4.4.2. Steps in V_{ref}

Figure 15 shows the electrical power output of the generators (100 MVA base) for the step changes in voltage reference, when the excitation systems represented by the ESST1A model, considering the gain $T_B=10$ s.

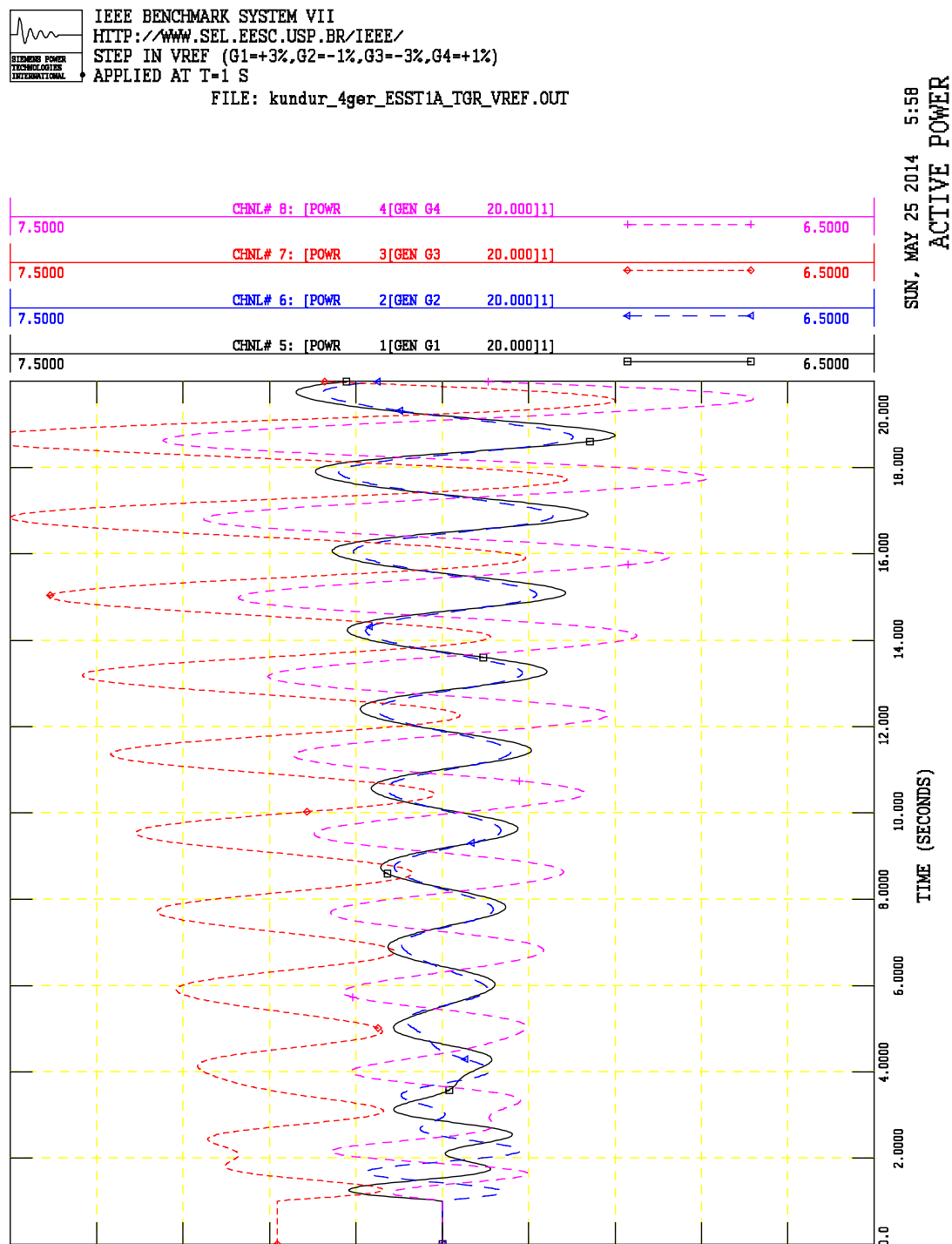


Figure 15: Step in Voltage References with ESST1A Model with TGR

4.5. ESST1A without TGR

The results in this Section correspond to the results in [1] with the static excitation system, represented in PSS/E by the ESST1A model presented in Section 1.2.2 (time constant $T_B=1$ s).

4.5.1. 50 MVar Reactor at Mid-Point

Figure 16 shows the electrical power output of the generators (100 MVA base) for the 50 MVar reactor disturbance (ESST1A model with $T_B=1$ s).

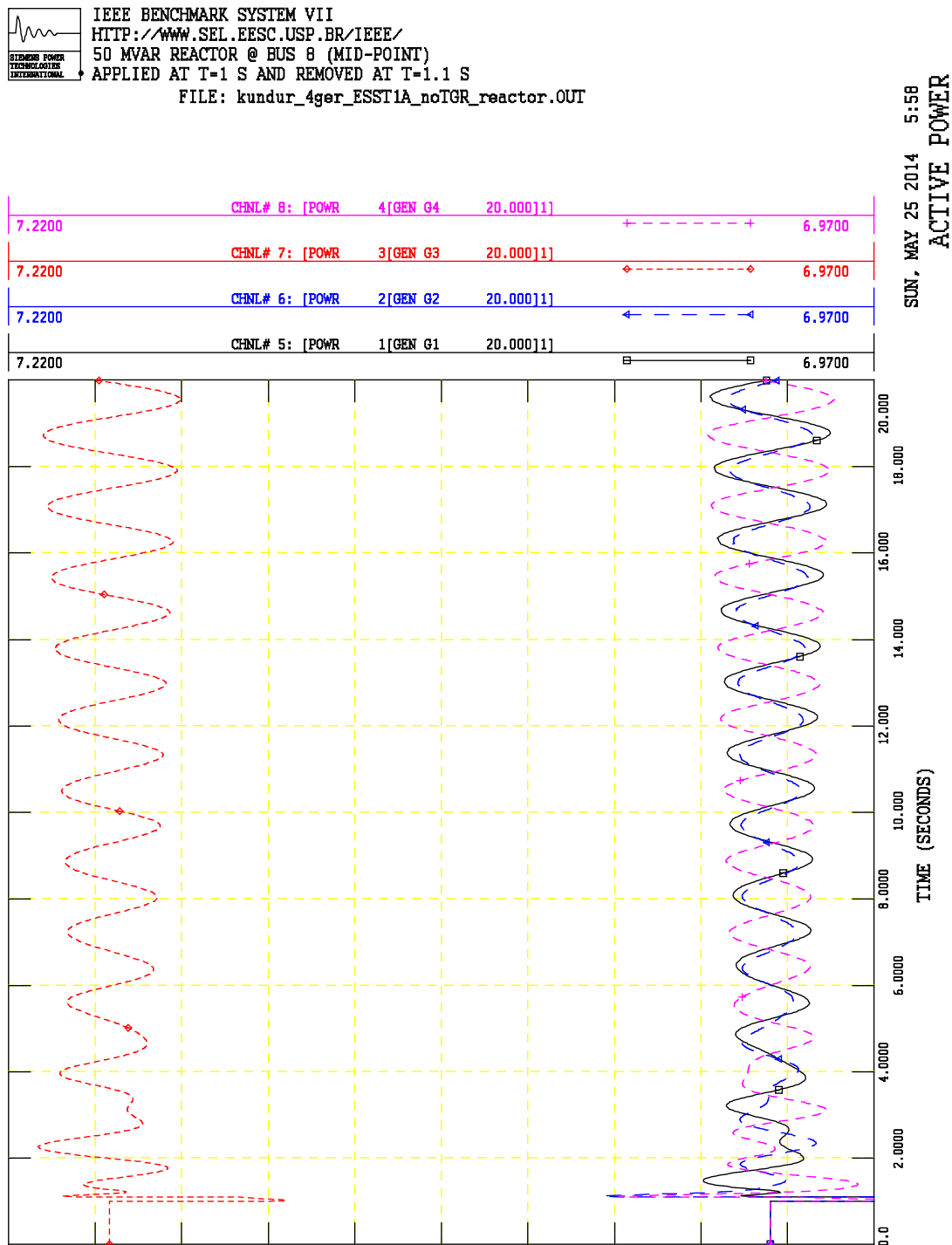


Figure 16: 50 MVar Reactor Disturbance with ESST1A Model without TGR

4.5.2. Steps in Vref

Figure 17 shows the electrical power output of the generators (100 MVA base) for the step changes in voltage reference, when the excitation systems represented by the ESST1A model, considering the gain $T_B=1$ s.

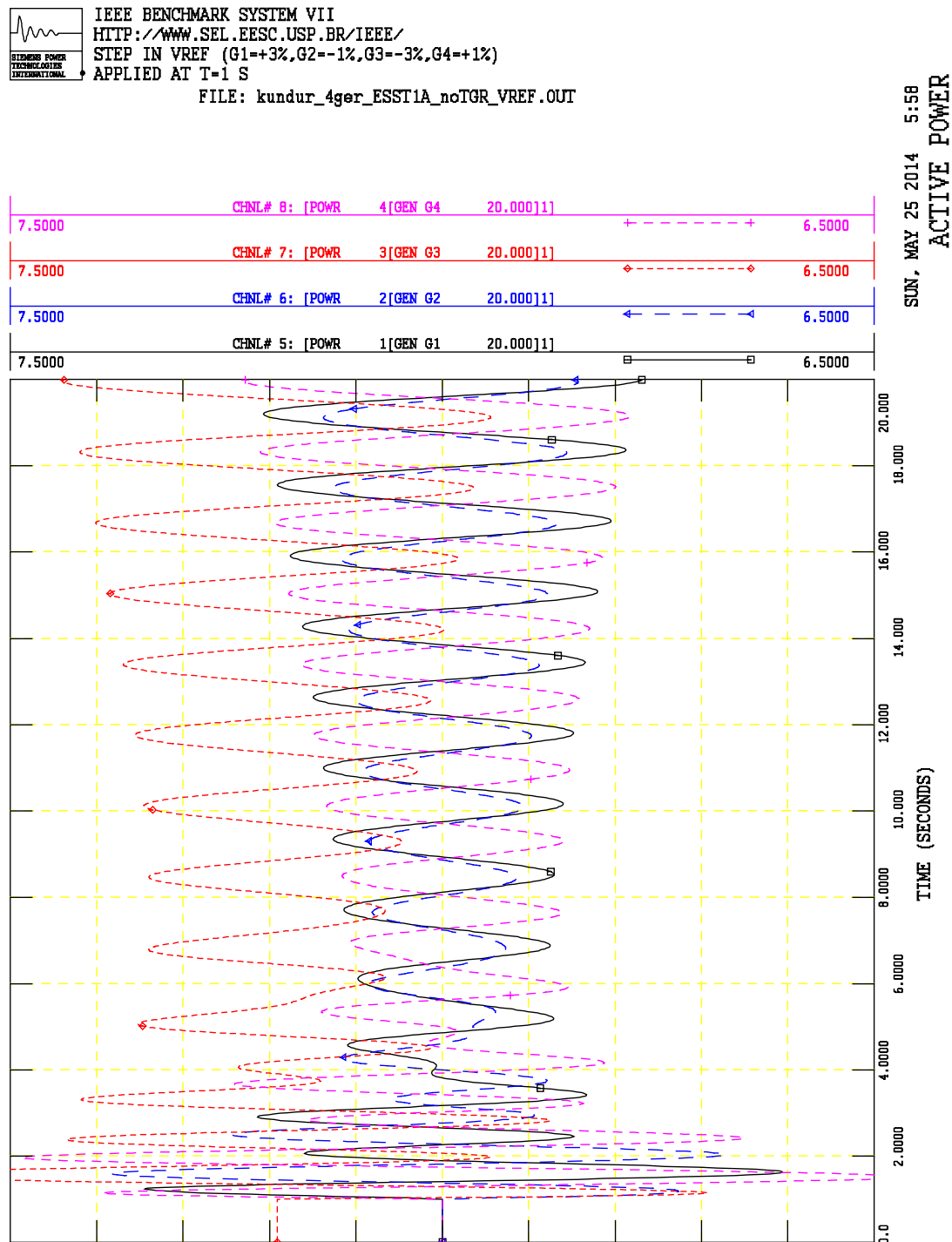


Figure 17: Step in Voltage References with ESST1A Model without TGR

4.6. ESST1A without TGR with Original PSS

The results in this Section correspond to the results in [1] with the static excitation system, represented in PSS/E by the ESST1A model presented in Section 1.2.2 (time constant $T_B=1$ s) and considering the original PSS parameters as described in Section 1.3.

4.6.1. 50 MVar Reactor at Mid-Point

Figure 16 shows the power output of the generators for the 50 MVar reactor disturbance.

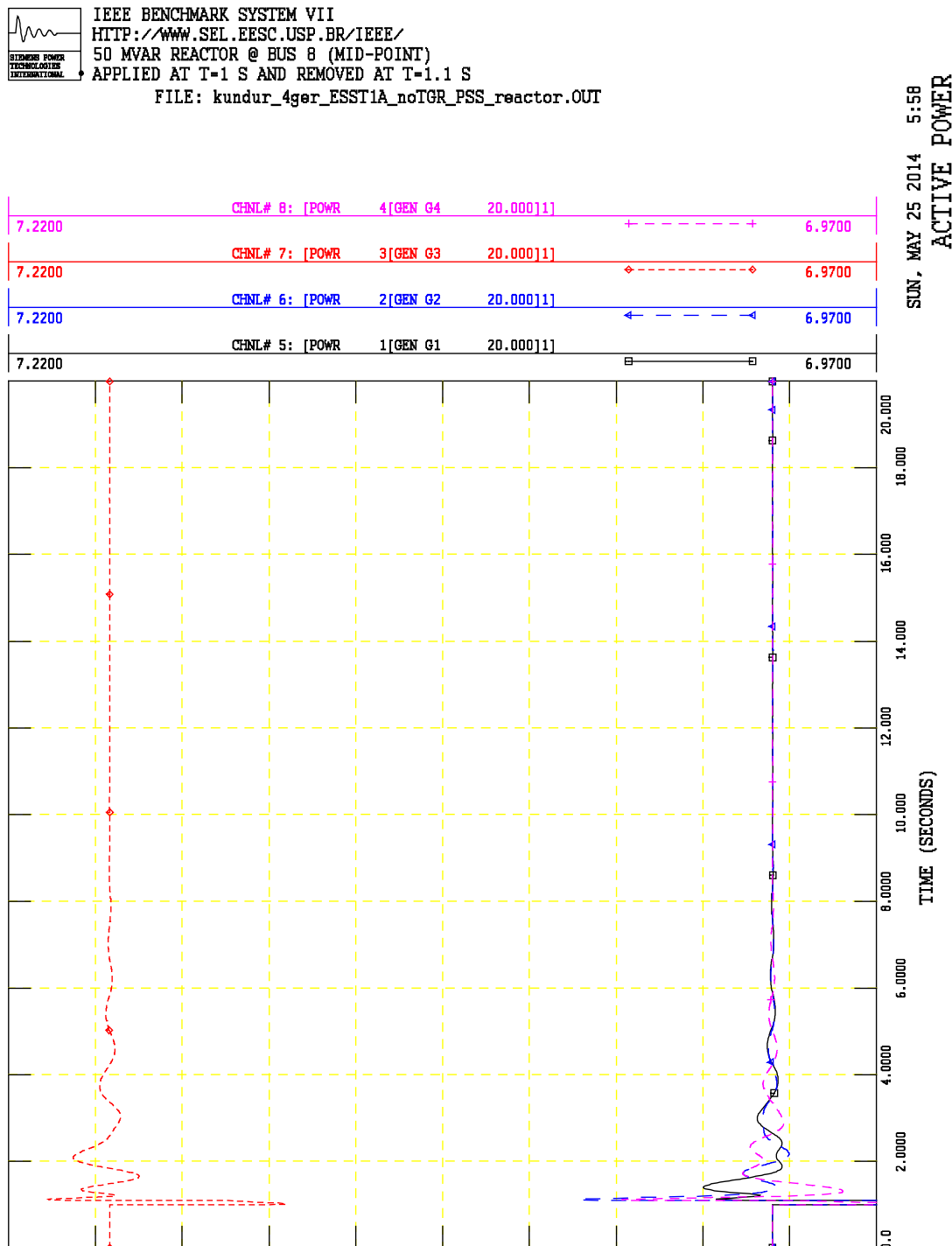


Figure 18: 50 MVar Reactor Disturbance with ESST1A Model without TGR and Original PSS

4.6.2. Steps in V_{ref}

Figure 19 shows the electrical power output of the generators (100 MVA base) for the step changes in voltage reference.

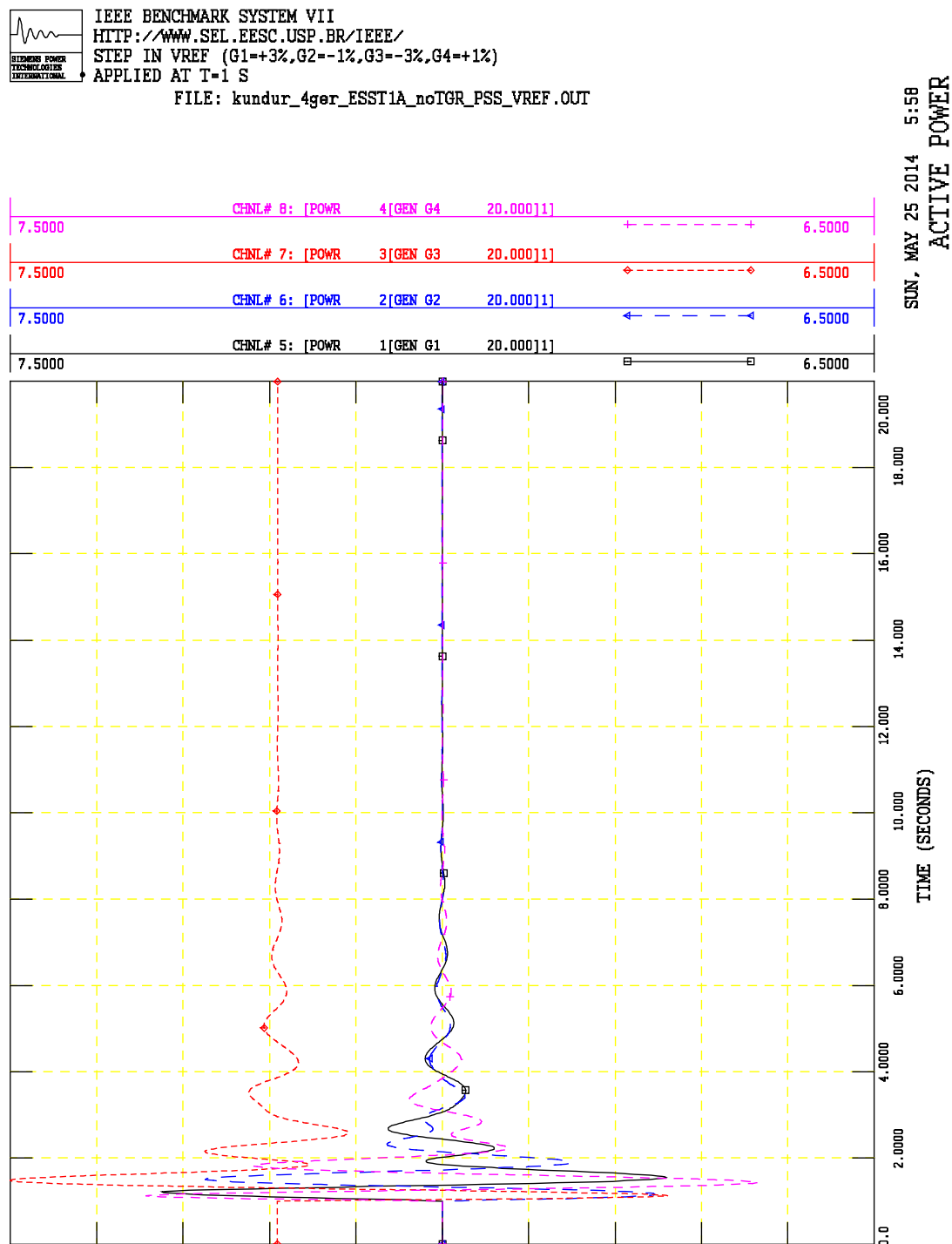


Figure 19: Step in Voltage References with ESST1A Model without TGR and Original PSS

4.7. ESST1A without TGR with Modified PSS

The results in this Section correspond to the results in [1] with the static excitation system, represented in PSS/E by the ESST1A model presented in Section 1.2.2 (time constant $T_B=1$ s) and considering the modified PSS parameters proposed in Section 1.3.

4.7.1. 50 MVar Reactor at Mid-Point

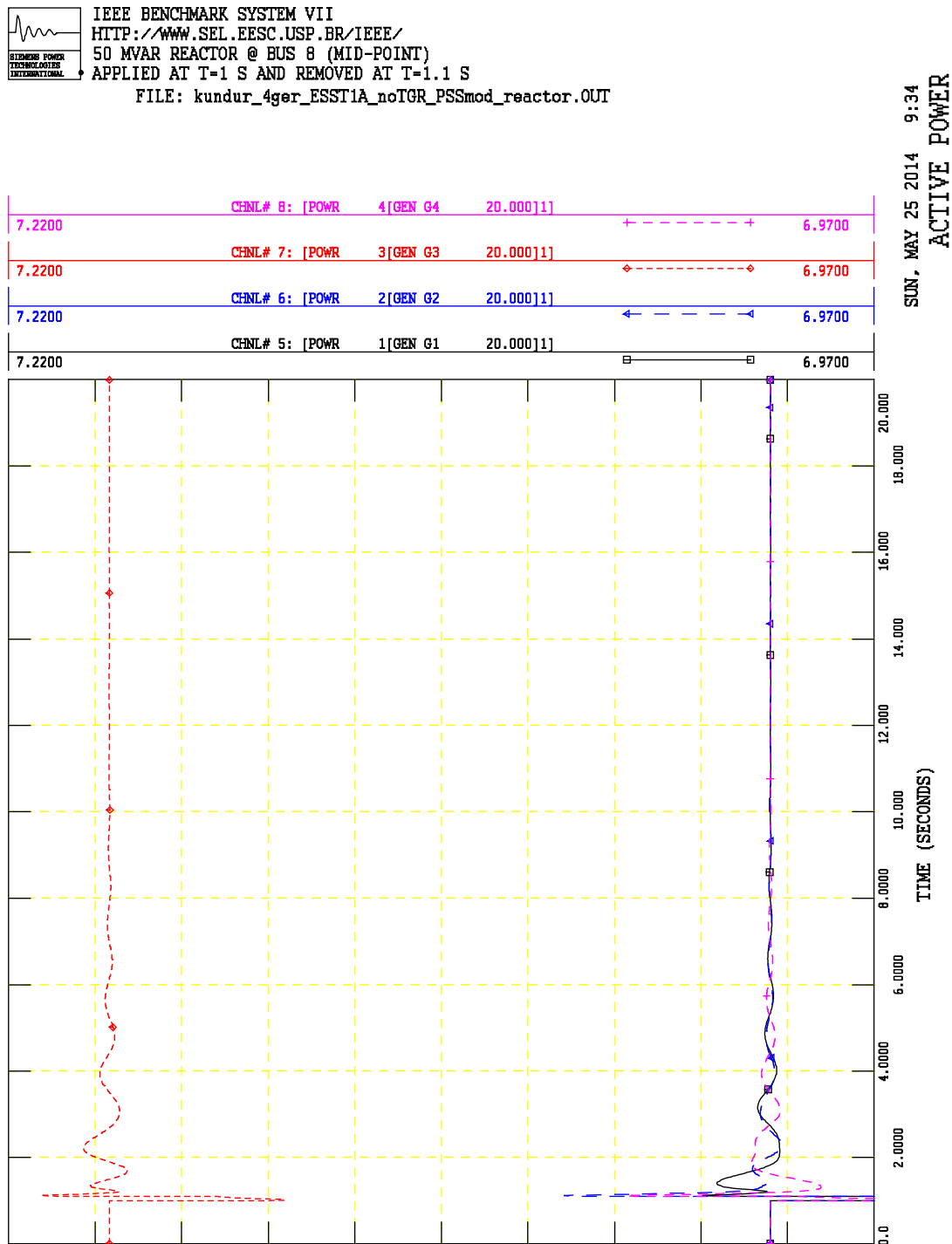


Figure 20: 50 MVar Reactor Disturbance with ESST1A Model without TGR and Modified PSS

4.7.2. Steps in Vref

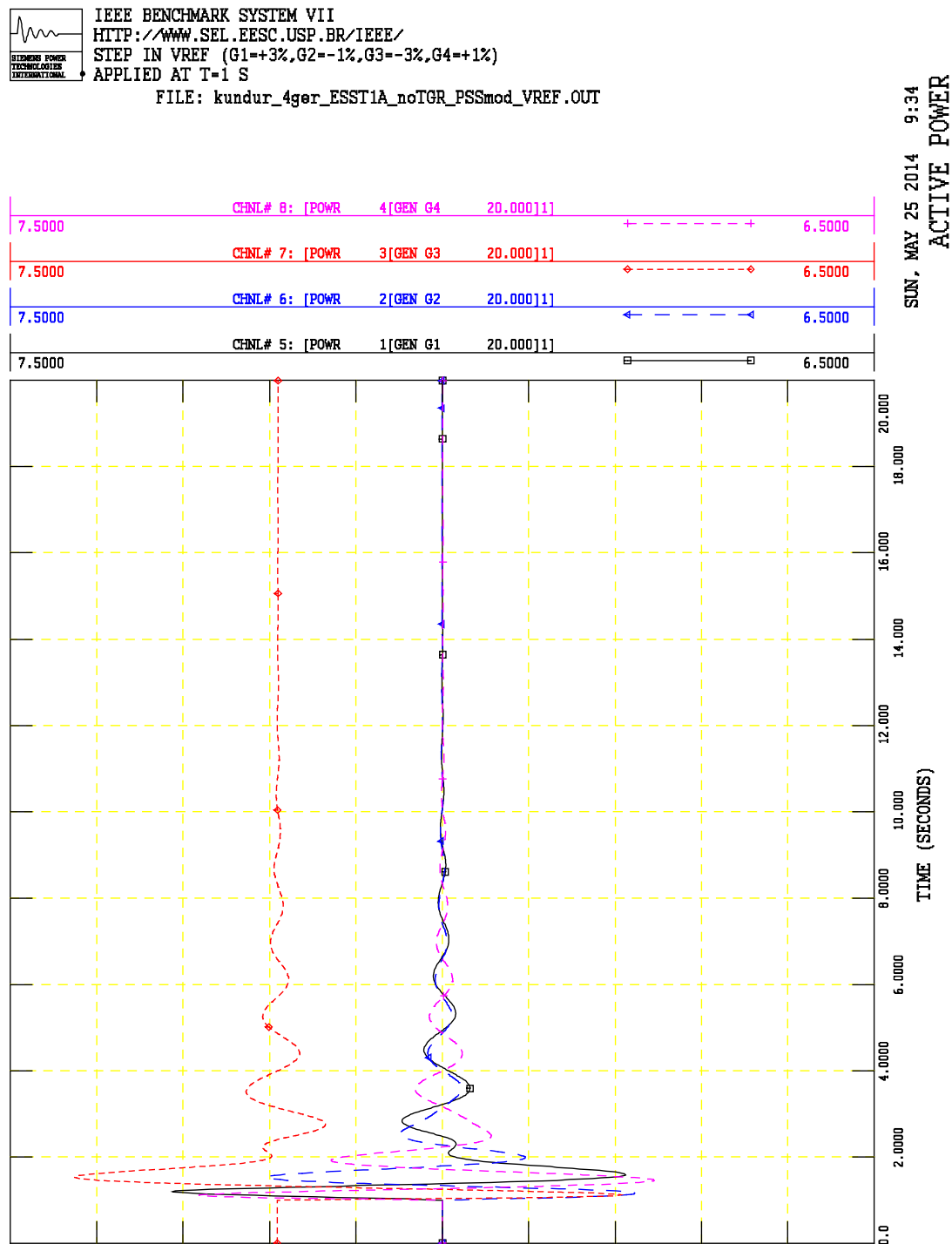


Figure 21: Step in Voltage References with ESST1A Model without TGR and Modified PSS

5. Modal Analysis

5.1. PSS/E LSYSAN

PSS/E can build a numerical approximation for the linearized system model. This approximation is obtained by numerical disturbances applied to the states of the nonlinear model, so the resulting precision of the numerical approximation is a function of the applied disturbance.

The results obtained with this tool might not be as accurate as the results that can be obtained from linearized models built with analytical linearization techniques, so the results (eigenvalues and eigenvectors) presented in this section cannot be taken as an absolute (precise) reference. On the other hand, it would be an interesting exercise to compare these results with those obtained from analytical methods.

The PSS/E activity ASTR allows the definition of the disturbance to be used, and also the state variables and input/output variables that will be used in building a (linearized) state equation for modal analysis, as shown in Figure 22.

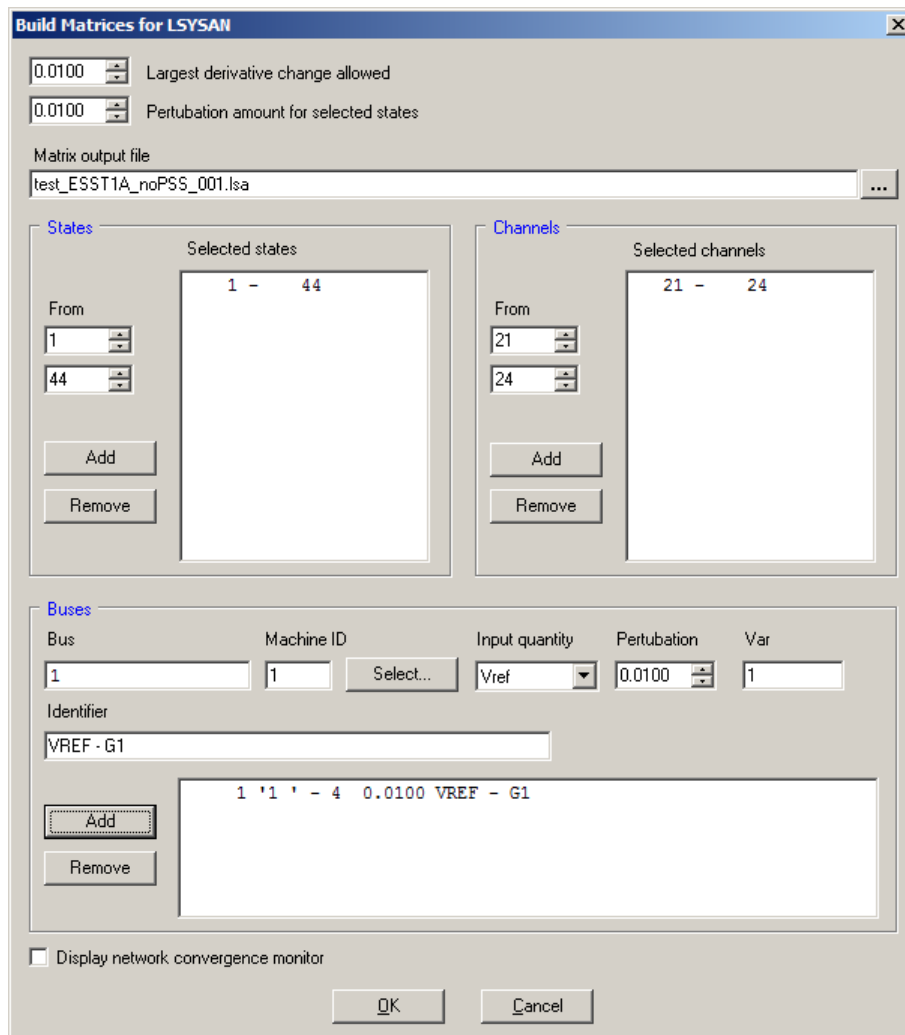


Figure 22: PSS/E Window for Activity ASTR (Linearized State Equation)

Once the linearized state equations have been numerically calculated, the auxiliary program LSYSAN¹ can be used for the modal analysis.

It should be noted that the PSS/E case associated with Section 2.5 (ESST1A model without TGR, no PSS) has 44 states, corresponding to 6 states per generator, plus 5 states per excitation system (ESST1A model). On the other hand, the data for the ESST1A model has been set (see Table 9) with $T_A=T_{C1}=T_{B1}=K_F=0$, so only two state variables in each ESST1A model are “active”, i.e., are part of the system dynamic response: the state associated with the voltage measurement time constant T_R and the state associated with the lead-lag block with parameters T_C and T_B .

The program LSYSAN was able to automatically identify (and eliminate from the linearized state equations) the state variables associated with the time constant T_A in the four ESST1A models in the system. Thus, LSYSAN calculated the eigenvalues of a linearized system of order 40, as shown Table 11. The other state variables that are redundant (not active due to the selected values for the parameters in the model) are still part of the state equations. Each of these redundant states will result in an eigenvalue equal to -1, as highlighted in Table 11 .

Also, it is important to notice that the system data does not contain an infinite bus and PSS/E uses angles referred to the synchronous frame of reference (absolute angles), not relative angles between machines, or between machines and an infinite bus. Furthermore, there are no speed governor models in the system data, so all generators are represented as having constant mechanical power from the turbine. Therefore, the linearized system model contains two eigenvalues at the origin, associated with the rigid-body motion of the system [7]. Numerical calculations, both in the determination of the linearized state equations and the EISPACK routines for the QR method, result in a pair of eigenvalues close to the origin, but not exactly zero (highlighted in Table 11). Sometimes these eigenvalues, due to the numerical issues described above, are even shown with a positive real part, which might be misinterpreted as an unstable mode. These modes should be ignored and cannot be misinterpreted as an electromechanical oscillation mode, particularly an unstable mode. All it takes is to determine the speed mode-shape for this mode (eigenvector elements associated with the rotor speed deviation of the generators) and the analyst will see that the mode-shape shows all components with the same phase and magnitude, clearly indicating that this is the rigid-body motion of the system, all units accelerating together.

Table 12 presents the eigenvector associated with mode #5 in Table 11. The components of the eigenvector associated with the rotor speed deviation of the generators (state K+4 of the model GENROE) are highlighted. It can be seen that this mode is related with machines 1 and 4 oscillating in phase opposition to machines 2 and 3. Moreover, the relative magnitudes of these eigenvector components indicate that this mode corresponds (mostly) to the oscillation between machines 3 and 4. The fact that this mode is an oscillation between machines 3 and 4 becomes obvious when looking at the relative participation factors for this mode, shown in Table 13.

Table 14 presents the eigenvector associated with mode #7 in Table 11. The components of the eigenvector associated with the rotor speed deviation of the generators (state K+4 of the

¹ Provided as part of the PSS/E installation, for users with the proper license. Consult the software vendor if you are not sure about your license.

model GENROE) are highlighted. It can be seen that this mode is (mostly) the oscillation between machines 1 and 2, as clearly shown by the participation factors in Table 15.

Table 16 presents the eigenvector associated with mode #9 in Table 11. The components of the eigenvector associated with the rotor speed deviation of the generators (state K+4 of the model GENROE) are highlighted. It can be seen that this mode is the inter-area mode, with machines 1 and 2 oscillating against machines 3 and 4. Considering the relative magnitudes of these eigenvector components, the inter-area mode is somewhat more observable in the importing area (generators 3 and 4). The relative participation factors in Table 17 show that all four units participate in this oscillation mode, with slightly more observability and controlability on the units in the importing area.

Table 18 corresponds to the eigenvector associated with mode #11 in Table 11 and it can be seen that the components of the eigenvector associated with rotor speed deviation of the generators (highlighted) have practically the same phase, the indication that this is the rigid body mode, as described above.

Table 11: Eigenvalues Calculated with PSS/E Program LSYSAN

COMPLEX EIGENVALUES:				
NO.	REAL	IMAG	DAMP	FREQ
1	-18.119	22.262	0.63124	3.5431
2	-18.119	-22.262	0.63124	3.5431
3	-19.167	16.532	0.75724	2.6311
4	-19.167	-16.532	0.75724	2.6311
5	-0.66058	7.2907	0.90236E-01	1.1604
6	-0.66058	-7.2907	0.90236E-01	1.1604
7	-0.65639	7.0881	0.92210E-01	1.1281
8	-0.65639	-7.0881	0.92210E-01	1.1281
9	0.64617E-03	3.8361	-0.16840E-03	0.61054
10	0.64617E-03	-3.8361	-0.16840E-03	0.61054
11	-0.28446E-01	0.80374E-01	0.33364	0.12792E-01
12	-0.28446E-01	-0.80374E-01	0.33364	0.12792E-01
REAL EIGENVALUES:				
NO.	REAL	TIME CONSTANT		
13	-97.447	0.10262E-01		
14	-97.389	0.10268E-01		
15	-95.600	0.10460E-01		
16	-94.467	0.10586E-01		
17	-36.297	0.27550E-01		
18	-36.200	0.27625E-01		
19	-31.617	0.31628E-01		
20	-30.678	0.32597E-01		
21	-25.254	0.39598E-01		
22	-24.357	0.41057E-01		
23	-16.818	0.59461E-01		
24	-15.953	0.62682E-01		
25	-3.6304	0.27545		
26	-3.5340	0.28296		
27	-3.3135	0.30179		
28	-3.2842	0.30449		
29	-1.0000	1.0000		
30	-1.0000	1.0000		
31	-1.0000	1.0000		
32	-1.0000	1.0000		
33	-1.0000	1.0000		
34	-1.0000	1.0000		
35	-1.0000	1.0000		
36	-1.0000	1.0000		
37	-1.0000	1.0000		
38	-1.0000	1.0000		
39	-1.0000	1.0000		
40	-1.0000	1.0000		

Table 12: Eigenvector Calculated with PSS/E Program LSYSAN for Mode #5

EIGENVALUE		5:	REAL=	-0.66058	IMAG=	7.2907						
ROW			VECTOR	ELEMENT	--X	STATE	MODEL	BUS	X-----	NAME	-----X	ID
			MAGNITUDE	PHASE								
1	0.19592E-01		0.19592E-01	-23.884		K	GENROE	1	GEN G1	20.000		1
2	0.34422E-01		0.34422E-01	-61.870		K+1	GENROE	1	GEN G1	20.000		1
3	0.12763E-01		0.12763E-01	-176.57		K+2	GENROE	1	GEN G1	20.000		1
4	0.59303E-01		0.59303E-01	-30.047		K+3	GENROE	1	GEN G1	20.000		1
5	0.33976E-02		0.33976E-02	86.700		K+4	GENROE	1	GEN G1	20.000		1
6	0.17497		0.17497	-8.4770		K+5	GENROE	1	GEN G1	20.000		1
7	0.55303E-01		0.55303E-01	-146.60		K	GENROE	2	GEN G2	20.000		1
8	0.38783E-01		0.38783E-01	102.49		K+1	GENROE	2	GEN G2	20.000		1
9	0.25895E-01		0.25895E-01	-124.26		K+2	GENROE	2	GEN G2	20.000		1
10	0.66405E-01		0.66405E-01	139.87		K+3	GENROE	2	GEN G2	20.000		1
11	0.42271E-02		0.42271E-02	-86.616		K+4	GENROE	2	GEN G2	20.000		1
12	0.21768		0.21768	178.21		K+5	GENROE	2	GEN G2	20.000		1
13	0.21400		0.21400	-175.06		K	GENROE	3	GEN G3	20.000		1
14	0.11930		0.11930	112.51		K+1	GENROE	3	GEN G3	20.000		1
15	0.54508E-01		0.54508E-01	175.54		K+2	GENROE	3	GEN G3	20.000		1
16	0.22165		0.22165	147.92		K+3	GENROE	3	GEN G3	20.000		1
17	0.17545E-01		0.17545E-01	-88.884		K+4	GENROE	3	GEN G3	20.000		1
18	0.90351		0.90351	175.94		K+5	GENROE	3	GEN G3	20.000		1
19	0.11370		0.11370	103.45		K	GENROE	4	GEN G4	20.000		1
20	0.24404		0.24404	-66.045		K+1	GENROE	4	GEN G4	20.000		1
21	0.19437		0.19437	134.07		K+2	GENROE	4	GEN G4	20.000		1
22	0.39142		0.39142	-32.350		K+3	GENROE	4	GEN G4	20.000		1
23	0.19418E-01		0.19418E-01	95.177		K+4	GENROE	4	GEN G4	20.000		1
24	1.0000		1.0000	0.0000		K+5	GENROE	4	GEN G4	20.000		1
25	0.65227E-02		0.65227E-02	-131.75		K	ESST1A	1	GEN G1	20.000		1
26	0.0000		0.0000	0.0000		K+1	ESST1A	1	GEN G1	20.000		1
27	0.0000		0.0000	0.0000		K+2	ESST1A	1	GEN G1	20.000		1
28	0.0000		0.0000	0.0000		K+4	ESST1A	1	GEN G1	20.000		1
29	0.15153E-01		0.15153E-01	117.79		K	ESST1A	2	GEN G2	20.000		1
30	0.0000		0.0000	0.0000		K+1	ESST1A	2	GEN G2	20.000		1
31	0.0000		0.0000	0.0000		K+2	ESST1A	2	GEN G2	20.000		1
32	0.0000		0.0000	0.0000		K+4	ESST1A	2	GEN G2	20.000		1
33	0.62847E-01		0.62847E-01	87.260		K	ESST1A	3	GEN G3	20.000		1
34	0.0000		0.0000	0.0000		K+1	ESST1A	3	GEN G3	20.000		1
35	0.0000		0.0000	0.0000		K+2	ESST1A	3	GEN G3	20.000		1
36	0.0000		0.0000	0.0000		K+4	ESST1A	3	GEN G3	20.000		1
37	0.24736E-01		0.24736E-01	26.409		K	ESST1A	4	GEN G4	20.000		1
38	0.0000		0.0000	0.0000		K+1	ESST1A	4	GEN G4	20.000		1
39	0.0000		0.0000	0.0000		K+2	ESST1A	4	GEN G4	20.000		1
40	0.0000		0.0000	0.0000		K+4	ESST1A	4	GEN G4	20.000		1

Table 13: Relative Participation Factors Calculated with PSS/E Program LSYSAN for Mode #5

NORMALIZED PARTICIPATION FACTORS FOR MODE				5: -0.66058		7.2907		
FACTOR	ROW	STATE	MODEL	BUS	X-----	NAME	----X	ID
1.00000	23	K+4	GENROE	4	GEN G4	20.000	1	
0.99928	24	K+5	GENROE	4	GEN G4	20.000	1	
0.82994	17	K+4	GENROE	3	GEN G3	20.000	1	
0.82930	18	K+5	GENROE	3	GEN G3	20.000	1	
0.13109	20	K+1	GENROE	4	GEN G4	20.000	1	
0.11943	13	K	GENROE	3	GEN G3	20.000	1	
0.11232	22	K+3	GENROE	4	GEN G4	20.000	1	
0.06230	19	K	GENROE	4	GEN G4	20.000	1	
0.05871	14	K+1	GENROE	3	GEN G3	20.000	1	
0.05824	16	K+3	GENROE	3	GEN G3	20.000	1	
0.04037	11	K+4	GENROE	2	GEN G2	20.000	1	
0.04034	12	K+5	GENROE	2	GEN G2	20.000	1	
0.01833	5	K+4	GENROE	1	GEN G1	20.000	1	
0.01832	6	K+5	GENROE	1	GEN G1	20.000	1	
0.01189	21	K+2	GENROE	4	GEN G4	20.000	1	
0.00880	33	K	ESST1A	3	GEN G3	20.000	1	
0.00629	7	K	GENROE	2	GEN G2	20.000	1	
0.00364	8	K+1	GENROE	2	GEN G2	20.000	1	
0.00340	37	K	ESST1A	4	GEN G4	20.000	1	
0.00340	15	K+2	GENROE	3	GEN G3	20.000	1	
0.00332	10	K+3	GENROE	2	GEN G2	20.000	1	
0.00193	2	K+1	GENROE	1	GEN G1	20.000	1	
0.00178	4	K+3	GENROE	1	GEN G1	20.000	1	
0.00111	1	K	GENROE	1	GEN G1	20.000	1	
0.00043	29	K	ESST1A	2	GEN G2	20.000	1	
0.00033	9	K+2	GENROE	2	GEN G2	20.000	1	
0.00009	25	K	ESST1A	1	GEN G1	20.000	1	
0.00008	3	K+2	GENROE	1	GEN G1	20.000	1	
0.00000	31	K+2	ESST1A	2	GEN G2	20.000	1	
0.00000	30	K+1	ESST1A	2	GEN G2	20.000	1	
0.00000	28	K+4	ESST1A	1	GEN G1	20.000	1	
0.00000	27	K+2	ESST1A	1	GEN G1	20.000	1	
0.00000	26	K+1	ESST1A	1	GEN G1	20.000	1	
0.00000	40	K+4	ESST1A	4	GEN G4	20.000	1	
0.00000	39	K+2	ESST1A	4	GEN G4	20.000	1	
0.00000	38	K+1	ESST1A	4	GEN G4	20.000	1	
0.00000	36	K+4	ESST1A	3	GEN G3	20.000	1	
0.00000	35	K+2	ESST1A	3	GEN G3	20.000	1	
0.00000	34	K+1	ESST1A	3	GEN G3	20.000	1	
0.00000	32	K+4	ESST1A	2	GEN G2	20.000	1	

Table 14: Eigenvector Calculated with PSS/E Program LSYSAN for Mode #7

EIGENVALUE		7: REAL= -0.65639		IMAG= 7.0881				
		DAMP= 0.92210E-01		FREQ= 1.1281				
ROW	X----	VECTOR	ELEMENT ---X	STATE	MODEL	BUS	X----- NAME -----X	ID
		MAGNITUDE	PHASE					
1	0.18930	-170.48		K	GENROE	1	GEN G1	20.000 1
2	0.14218	116.04		K+1	GENROE	1	GEN G1	20.000 1
3	0.33462E-01	-159.24		K+2	GENROE	1	GEN G1	20.000 1
4	0.25376	150.20		K+3	GENROE	1	GEN G1	20.000 1
5	0.17559E-01	-86.802		K+4	GENROE	1	GEN G1	20.000 1
6	0.92993	177.91		K+5	GENROE	1	GEN G1	20.000 1
7	0.10921	84.714		K	GENROE	2	GEN G2	20.000 1
8	0.23755	-65.703		K+1	GENROE	2	GEN G2	20.000 1
9	0.16242	129.42		K+2	GENROE	2	GEN G2	20.000 1
10	0.38205	-32.365		K+3	GENROE	2	GEN G2	20.000 1
11	0.18882E-01	95.291		K+4	GENROE	2	GEN G2	20.000 1
12	1.0000	0.0000		K+5	GENROE	2	GEN G2	20.000 1
13	0.42190E-01	-143.53		K	GENROE	3	GEN G3	20.000 1
14	0.22907E-01	144.52		K+1	GENROE	3	GEN G3	20.000 1
15	0.11378E-01	-152.44		K+2	GENROE	3	GEN G3	20.000 1
16	0.42333E-01	179.42		K+3	GENROE	3	GEN G3	20.000 1
17	0.34616E-02	-57.699		K+4	GENROE	3	GEN G3	20.000 1
18	0.18333	-152.99		K+5	GENROE	3	GEN G3	20.000 1
19	0.24313E-01	159.85		K	GENROE	4	GEN G4	20.000 1
20	0.31238E-01	-33.506		K+1	GENROE	4	GEN G4	20.000 1
21	0.32708E-01	166.02		K+2	GENROE	4	GEN G4	20.000 1
22	0.48241E-01	-0.40388		K+3	GENROE	4	GEN G4	20.000 1
23	0.21223E-02	130.85		K+4	GENROE	4	GEN G4	20.000 1
24	0.11240	35.564		K+5	GENROE	4	GEN G4	20.000 1
25	0.53270E-01	90.079		K	ESST1A	1	GEN G1	20.000 1
26	0.0000	0.0000		K+1	ESST1A	1	GEN G1	20.000 1
27	0.0000	0.0000		K+2	ESST1A	1	GEN G1	20.000 1
28	0.0000	0.0000		K+4	ESST1A	1	GEN G1	20.000 1
29	0.21164E-01	-0.68033		K	ESST1A	2	GEN G2	20.000 1
30	0.0000	0.0000		K+1	ESST1A	2	GEN G2	20.000 1
31	0.0000	0.0000		K+2	ESST1A	2	GEN G2	20.000 1
32	0.0000	0.0000		K+4	ESST1A	2	GEN G2	20.000 1
33	0.12050E-01	118.79		K	ESST1A	3	GEN G3	20.000 1
34	0.0000	0.0000		K+1	ESST1A	3	GEN G3	20.000 1
35	0.0000	0.0000		K+2	ESST1A	3	GEN G3	20.000 1
36	0.0000	0.0000		K+4	ESST1A	3	GEN G3	20.000 1
37	0.64398E-02	79.346		K	ESST1A	4	GEN G4	20.000 1
38	0.0000	0.0000		K+1	ESST1A	4	GEN G4	20.000 1
39	0.0000	0.0000		K+2	ESST1A	4	GEN G4	20.000 1
40	0.0000	0.0000		K+4	ESST1A	4	GEN G4	20.000 1

Table 15: Relative Participation Factors Calculated with PSS/E Program LSYSAN for Mode #7

NORMALIZED PARTICIPATION FACTORS FOR MODE							7 : -0.65639	7.0881
FACTOR	ROW	STATE	MODEL	BUS	X--	NAME	--X	ID
1.00000	11	K+4	GENROE		2	GEN G2	20.000	1
0.99926	12	K+5	GENROE		2	GEN G2	20.000	1
0.85261	5	K+4	GENROE		1	GEN G1	20.000	1
0.85199	6	K+5	GENROE		1	GEN G1	20.000	1
0.12671	8	K+1	GENROE		2	GEN G2	20.000	1
0.10786	10	K+3	GENROE		2	GEN G2	20.000	1
0.09957	1	K	GENROE		1	GEN G1	20.000	1
0.06985	2	K+1	GENROE		1	GEN G1	20.000	1
0.06596	4	K+3	GENROE		1	GEN G1	20.000	1
0.05868	7	K	GENROE		2	GEN G2	20.000	1
0.04558	17	K+4	GENROE		3	GEN G3	20.000	1
0.04554	18	K+5	GENROE		3	GEN G3	20.000	1
0.01862	23	K+4	GENROE		4	GEN G4	20.000	1
0.01861	24	K+5	GENROE		4	GEN G4	20.000	1
0.00948	9	K+2	GENROE		2	GEN G2	20.000	1
0.00703	25	K	ESST1A		1	GEN G1	20.000	1
0.00622	13	K	GENROE		3	GEN G3	20.000	1
0.00319	14	K+1	GENROE		3	GEN G3	20.000	1
0.00311	16	K+3	GENROE		3	GEN G3	20.000	1
0.00285	29	K	ESST1A		2	GEN G2	20.000	1
0.00280	20	K+1	GENROE		4	GEN G4	20.000	1
0.00228	22	K+3	GENROE		4	GEN G4	20.000	1
0.00203	19	K	GENROE		4	GEN G4	20.000	1
0.00191	3	K+2	GENROE		1	GEN G1	20.000	1
0.00045	33	K	ESST1A		3	GEN G3	20.000	1
0.00030	21	K+2	GENROE		4	GEN G4	20.000	1
0.00018	15	K+2	GENROE		3	GEN G3	20.000	1
0.00013	37	K	ESST1A		4	GEN G4	20.000	1
0.00000	31	K+2	ESST1A		2	GEN G2	20.000	1
0.00000	30	K+1	ESST1A		2	GEN G2	20.000	1
0.00000	28	K+4	ESST1A		1	GEN G1	20.000	1
0.00000	27	K+2	ESST1A		1	GEN G1	20.000	1
0.00000	26	K+1	ESST1A		1	GEN G1	20.000	1
0.00000	40	K+4	ESST1A		4	GEN G4	20.000	1
0.00000	39	K+2	ESST1A		4	GEN G4	20.000	1
0.00000	38	K+1	ESST1A		4	GEN G4	20.000	1
0.00000	36	K+4	ESST1A		3	GEN G3	20.000	1
0.00000	35	K+2	ESST1A		3	GEN G3	20.000	1
0.00000	34	K+1	ESST1A		3	GEN G3	20.000	1
0.00000	32	K+4	ESST1A		2	GEN G2	20.000	1

Table 16: Eigenvector Calculated with PSS/E Program LSYSAN for Mode #9

EIGENVALUE		9 : REAL= 0.64617E-03 IMAG= 3.8361									
ROW		VECTOR	ELEMENT	STATE	MODEL	BUS	NAME	ID			
		MAGNITUDE	PHASE								
1	0.15161	173.09		K	GENROE	1	GEN G1	20.000	1		
2	0.16606E-01	14.014		K+1	GENROE	1	GEN G1	20.000	1		
3	0.95891E-01	165.58		K+2	GENROE	1	GEN G1	20.000	1		
4	0.17763E-01	81.067		K+3	GENROE	1	GEN G1	20.000	1		
5	0.83922E-02	-100.94		K+4	GENROE	1	GEN G1	20.000	1		
6	0.82473	169.07		K+5	GENROE	1	GEN G1	20.000	1		
7	0.25589	158.66		K	GENROE	2	GEN G2	20.000	1		
8	0.82312E-01	-64.728		K+1	GENROE	2	GEN G2	20.000	1		
9	0.19836	144.92		K+2	GENROE	2	GEN G2	20.000	1		
10	0.95749E-01	-53.104		K+3	GENROE	2	GEN G2	20.000	1		
11	0.59052E-02	-89.479		K+4	GENROE	2	GEN G2	20.000	1		
12	0.58033	-179.47		K+5	GENROE	2	GEN G2	20.000	1		
13	0.30072E-01	90.912		K	GENROE	3	GEN G3	20.000	1		
14	0.82204E-01	-51.165		K+1	GENROE	3	GEN G3	20.000	1		
15	0.55905E-01	134.61		K+2	GENROE	3	GEN G3	20.000	1		
16	0.12286	-32.017		K+3	GENROE	3	GEN G3	20.000	1		
17	0.10176E-01	89.990		K+4	GENROE	3	GEN G3	20.000	1		
18	1.0000	0.0000		K+5	GENROE	3	GEN G3	20.000	1		
19	0.73132E-01	130.31		K	GENROE	4	GEN G4	20.000	1		
20	0.10633	-56.573		K+1	GENROE	4	GEN G4	20.000	1		
21	0.10084	134.98		K+2	GENROE	4	GEN G4	20.000	1		
22	0.15149	-38.018		K+3	GENROE	4	GEN G4	20.000	1		
23	0.93171E-02	87.142		K+4	GENROE	4	GEN G4	20.000	1		
24	0.91562	-2.8485		K+5	GENROE	4	GEN G4	20.000	1		
25	0.24354E-01	70.038		K	ESST1A	1	GEN G1	20.000	1		
26	0.0000	0.0000		K+1	ESST1A	1	GEN G1	20.000	1		
27	0.0000	0.0000		K+2	ESST1A	1	GEN G1	20.000	1		
28	0.0000	0.0000		K+4	ESST1A	1	GEN G1	20.000	1		
29	0.42509E-01	59.639		K	ESST1A	2	GEN G2	20.000	1		
30	0.0000	0.0000		K+1	ESST1A	2	GEN G2	20.000	1		
31	0.0000	0.0000		K+2	ESST1A	2	GEN G2	20.000	1		
32	0.0000	0.0000		K+4	ESST1A	2	GEN G2	20.000	1		
33	0.14633E-02	19.536		K	ESST1A	3	GEN G3	20.000	1		
34	0.0000	0.0000		K+1	ESST1A	3	GEN G3	20.000	1		
35	0.0000	0.0000		K+2	ESST1A	3	GEN G3	20.000	1		
36	0.0000	0.0000		K+4	ESST1A	3	GEN G3	20.000	1		
37	0.10261E-01	49.336		K	ESST1A	4	GEN G4	20.000	1		
38	0.0000	0.0000		K+1	ESST1A	4	GEN G4	20.000	1		
39	0.0000	0.0000		K+2	ESST1A	4	GEN G4	20.000	1		
40	0.0000	0.0000		K+4	ESST1A	4	GEN G4	20.000	1		

Table 17: Relative Participation Factors Calculated with PSS/E Program LSYSAN for Mode #9

NORMALIZED PARTICIPATION FACTORS FOR MODE							9 : 0.64617E-03	3.8361
FACTOR	ROW	STATE	MODEL	BUS	X--	NAME	--X	ID
1.00000	18	K+5	GENROE		3	GEN G3	20.000	1
0.99986	17	K+4	GENROE		3	GEN G3	20.000	1
0.84740	24	K+5	GENROE		4	GEN G4	20.000	1
0.84729	23	K+4	GENROE		4	GEN G4	20.000	1
0.84029	6	K+5	GENROE		1	GEN G1	20.000	1
0.84018	5	K+4	GENROE		1	GEN G1	20.000	1
0.52350	12	K+5	GENROE		2	GEN G2	20.000	1
0.52344	11	K+4	GENROE		2	GEN G2	20.000	1
0.11696	7	K	GENROE		2	GEN G2	20.000	1
0.05480	1	K	GENROE		1	GEN G1	20.000	1
0.05069	20	K+1	GENROE		4	GEN G4	20.000	1
0.04270	14	K+1	GENROE		3	GEN G3	20.000	1
0.03779	8	K+1	GENROE		2	GEN G2	20.000	1
0.03522	22	K+3	GENROE		4	GEN G4	20.000	1
0.03111	16	K+3	GENROE		3	GEN G3	20.000	1
0.02695	19	K	GENROE		4	GEN G4	20.000	1
0.02143	10	K+3	GENROE		2	GEN G2	20.000	1
0.00927	13	K	GENROE		3	GEN G3	20.000	1
0.00878	2	K+1	GENROE		1	GEN G1	20.000	1
0.00587	9	K+2	GENROE		2	GEN G2	20.000	1
0.00485	29	K	ESST1A		2	GEN G2	20.000	1
0.00458	4	K+3	GENROE		1	GEN G1	20.000	1
0.00241	21	K+2	GENROE		4	GEN G4	20.000	1
0.00225	3	K+2	GENROE		1	GEN G1	20.000	1
0.00220	25	K	ESST1A		1	GEN G1	20.000	1
0.00112	15	K+2	GENROE		3	GEN G3	20.000	1
0.00094	37	K	ESST1A		4	GEN G4	20.000	1
0.00011	33	K	ESST1A		3	GEN G3	20.000	1
0.00000	31	K+2	ESST1A		2	GEN G2	20.000	1
0.00000	30	K+1	ESST1A		2	GEN G2	20.000	1
0.00000	28	K+4	ESST1A		1	GEN G1	20.000	1
0.00000	27	K+2	ESST1A		1	GEN G1	20.000	1
0.00000	26	K+1	ESST1A		1	GEN G1	20.000	1
0.00000	40	K+4	ESST1A		4	GEN G4	20.000	1
0.00000	39	K+2	ESST1A		4	GEN G4	20.000	1
0.00000	38	K+1	ESST1A		4	GEN G4	20.000	1
0.00000	36	K+4	ESST1A		3	GEN G3	20.000	1
0.00000	35	K+2	ESST1A		3	GEN G3	20.000	1
0.00000	34	K+1	ESST1A		3	GEN G3	20.000	1
0.00000	32	K+4	ESST1A		2	GEN G2	20.000	1

Table 18: Eigenvector Calculated with PSS/E Program LSYSAN for Mode #11

EIGENVALUE	11:	REAL=	-0.28446E-01	IMAG=	0.80374E-01	DAMP=	0.33364	FREQ=	0.12792E-01		
ROW	X----	VECTOR	ELEMENT	--X	STATE	MODEL	BUS	X-----	NAME	-----X	ID
	MAGNITUDE			PHASE							
1	0.58873E-02	-0.62087			K	GENROE	1	GEN G1	20.000		1
2	0.40065E-02	178.61			K+1	GENROE	1	GEN G1	20.000		1
3	0.52644E-02	-0.90546			K+2	GENROE	1	GEN G1	20.000		1
4	0.49813E-02	178.96			K+3	GENROE	1	GEN G1	20.000		1
5	0.22615E-03	109.48			K+4	GENROE	1	GEN G1	20.000		1
6	1.0000	0.0000			K+5	GENROE	1	GEN G1	20.000		1
7	0.68345E-02	-0.59659			K	GENROE	2	GEN G2	20.000		1
8	0.45170E-02	178.61			K+1	GENROE	2	GEN G2	20.000		1
9	0.60773E-02	-0.87527			K+2	GENROE	2	GEN G2	20.000		1
10	0.56001E-02	178.96			K+3	GENROE	2	GEN G2	20.000		1
11	0.22550E-03	109.49			K+4	GENROE	2	GEN G2	20.000		1
12	0.99714	0.50360E-03			K+5	GENROE	2	GEN G2	20.000		1
13	0.24227E-02	-0.68215			K	GENROE	3	GEN G3	20.000		1
14	0.16116E-02	178.68			K+1	GENROE	3	GEN G3	20.000		1
15	0.21571E-02	-0.93353			K+2	GENROE	3	GEN G3	20.000		1
16	0.19979E-02	179.04			K+3	GENROE	3	GEN G3	20.000		1
17	0.22589E-03	109.49			K+4	GENROE	3	GEN G3	20.000		1
18	0.99877	-0.71651E-02			K+5	GENROE	3	GEN G3	20.000		1
19	0.12133E-02	-0.49801E-02			K	GENROE	4	GEN G4	20.000		1
20	0.87161E-03	179.38			K+1	GENROE	4	GEN G4	20.000		1
21	0.10347E-02	-0.19490			K+2	GENROE	4	GEN G4	20.000		1
22	0.11019E-02	179.76			K+3	GENROE	4	GEN G4	20.000		1
23	0.22592E-03	109.48			K+4	GENROE	4	GEN G4	20.000		1
24	0.99892	-0.92475E-02			K+5	GENROE	4	GEN G4	20.000		1
25	0.11317E-03	-170.09			K	ESST1A	1	GEN G1	20.000		1
26	0.0000	0.0000			K+1	ESST1A	1	GEN G1	20.000		1
27	0.0000	0.0000			K+2	ESST1A	1	GEN G1	20.000		1
28	0.0000	0.0000			K+4	ESST1A	1	GEN G1	20.000		1
29	0.78409E-04	-163.16			K	ESST1A	2	GEN G2	20.000		1
30	0.0000	0.0000			K+1	ESST1A	2	GEN G2	20.000		1
31	0.0000	0.0000			K+2	ESST1A	2	GEN G2	20.000		1
32	0.0000	0.0000			K+4	ESST1A	2	GEN G2	20.000		1
33	0.43968E-04	-169.49			K	ESST1A	3	GEN G3	20.000		1
34	0.0000	0.0000			K+1	ESST1A	3	GEN G3	20.000		1
35	0.0000	0.0000			K+2	ESST1A	3	GEN G3	20.000		1
36	0.0000	0.0000			K+4	ESST1A	3	GEN G3	20.000		1
37	0.18509E-04	-167.22			K	ESST1A	4	GEN G4	20.000		1
38	0.0000	0.0000			K+1	ESST1A	4	GEN G4	20.000		1
39	0.0000	0.0000			K+2	ESST1A	4	GEN G4	20.000		1
40	0.0000	0.0000			K+4	ESST1A	4	GEN G4	20.000		1

5.2. PSSPLT

The plotting package PSSPLT provided with the PSS/E installation [2] has a modal analysis function that can be used to obtain a numerical approximation of the oscillation modes observed in a time domain curve, such as the time domain simulation results from PSS/E. This modal analysis tool has a Prony method as well as a least square curve fit. The user has to select a time domain curve to be used for the analysis, as well as the time interval for the analysis and the order of the approximation, via the window shown in Figure 23.

The least square methods allow a scan for different orders of linear approximation, a useful tool to determine the best possible approximation. Figure 23 shows the options to be selected to determine the best fit from a 15th order equivalent to a 45th order equivalent, while Figure 24 presents the options related with the modal analysis calculation for the chosen equivalent system order.

Table 19 shows the results of the modal analysis scan, searching for the best fit as a function of the order of the equivalent system. It can be seen that the minimum error is associated with a 36th-order system.

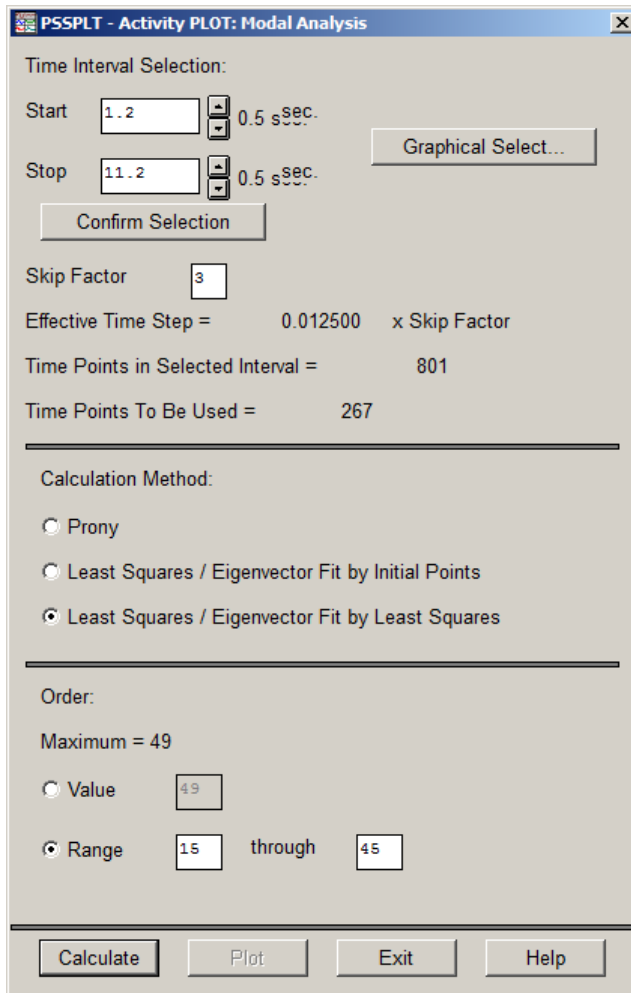


Figure 23: PSSPLT Window for Modal Analysis Scan to Determine Order of Best Equivalent

Table 20 shows the results of the modal analysis calculations with a given equivalent system order, usually the best fit determined by as shown above.

The user should always remember that this is a numerical approach, therefore the results are sensitive to numerical issues and user selections. The mode highlighted in blue is a good example, as it is associated with a pole in the origin, representing a step function in the time domain. This mode is always present, when the initial and final points of the selected curve, in the given time window (time range) are not identical. The curve fit procedure would understand (and represent) this change as a step change in the response and, as such, introduce this mode at the origin, with the appropriate magnitude to match the difference between the values of initial and final points. This mode should be disregarded, for all practical purposes.

The two modes highlighted in yellow are reasonable (numerical) approximations to the modes #5 and #9, obtained with LSYSAN and shown in Table 11. It is also notable that mode #7 in Table 11 is not present in these results: generator G1 has limited participation in that mode, thus the observability of that mode in the electrical power output of generator G1 (selected trace for this analysis) is quite small.

The remaining modes have relatively small magnitudes, with exception of the the 3rd component. This 3rd component has a relatively high frequency (above 3 Hz) and is very well damped, corresponding to a time domain response that disappears very fast.

The time domain response of the equivalent system can be generated and plotted on top of the original curve, the selected curve for the modal analysis. Figure 25 shows the PSSPLT interface for selecting the modes for plotting. In this example, only the highlighted modes in Table 20 were selected. Figure 26 presents the time domain response of the reduced order equivalent system (5th order system) in blue, with the original trace from the nonlinear time domain simulation in PSS/E shown in black. It is a very good match, with some error introduced at the very beginning of the plot (less than 0.5 seconds).

Despite the difficulties associated with numerical methods, particularly potential inaccuracies, the results obtained with these tools are quite consistent and provide the correct qualitative information regarding oscillation frequencies, damping or these modes, and relative participation factors.

Table 19: PSSPLT Scan of Modal Equivalents

NUMBER OF SELECTED DATA POINTS IS 801 AND TIME STEP IS 0.012		
SELECT AN NPLT OF 8 TO REDUCE THE NUMBER OF POINTS TO ABOUT 100		
EFFECTIVE NUMBER OF DATA POINTS IS 267 AND EFFECTIVE TIME STEP IS 0.037		
ORDER	% ERROR	SIGNAL/NOISE
15	93.71	0.07
16	82.46	1.54
17	78.88	1.63
18	56.34	4.47
19	40.91	7.08
20	25.30	11.07
21	14.17	14.99
22	19.40	12.96
23	8.716	20.20
24	11.22	18.00
25	11.89	17.58
26	5.465	24.58
27	9.238	20.06
28	3.963	27.85
29	4.116	26.95
30	7.888	21.71
31	3.037	30.04
32	14.31	16.65
33	9.399	20.08
34	7.099	22.73
35	3.631	28.64
36	2.112	32.61
37	3.826	27.42
38	3.258	29.38
39	3.287	29.30
40	9.174	20.37
41	2.163	32.41
42	6.183	23.84
43	4.771	26.03
44	3.276	29.35
45	2.317	32.61

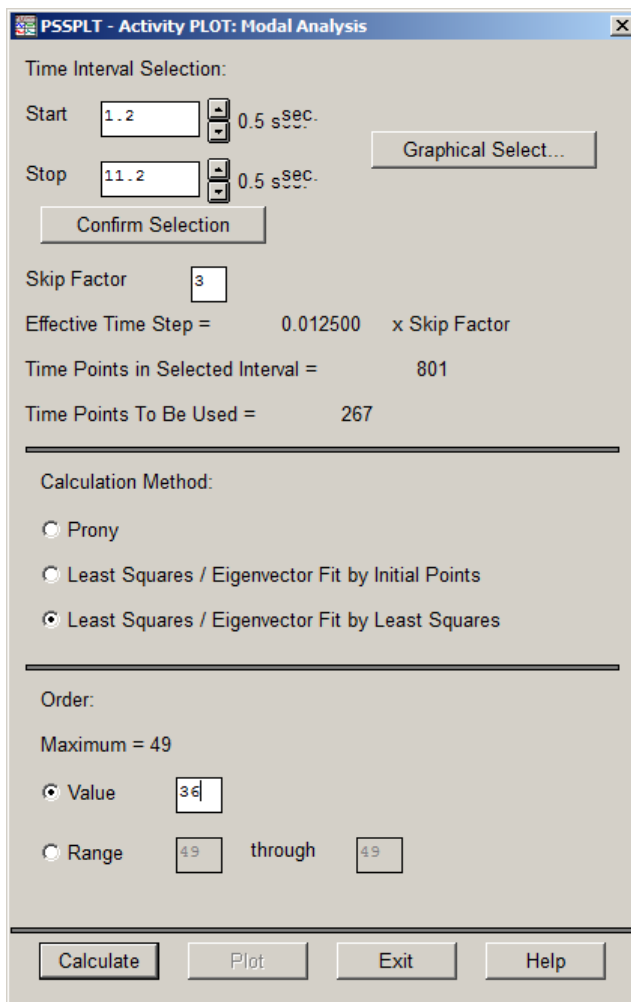


Figure 24: PSSPLT Window for Modal Analysis Calculation with a Specific Equivalent System Order

Table 20: Results of the Modal Analysis Calculations with the Equivalent System of 36th Order

MODAL COMPONENTS					
COMP. NO	EIGENVALUE		EIGENVECTOR		
	REAL	IMAGINARY	MAGNITUDE	ANGLE	REMARKS
1	0.635793E-05	--	6.9996	--	
2	-0.575326	7.05087	0.12623E-01	-112.24	FREQ.: 1.122 HZ.
3	-15.1229	19.9601	0.91841E-02	97.49	FREQ.: 3.177 HZ.
4	0.376434E-01	3.82388	0.87685E-02	-67.89	FREQ.: 0.609 HZ.
5	-1.88157	13.5899	0.26695E-03	60.48	FREQ.: 2.163 HZ.
6	-1.96054	24.1774	0.15576E-03	-63.89	FREQ.: 3.848 HZ.
7	-0.999003	29.2507	0.56638E-04	51.75	FREQ.: 4.655 HZ.
8	-1.53119	19.2763	0.52868E-04	-166.83	FREQ.: 3.068 HZ.
9	-0.669758	34.8902	0.31107E-04	143.42	FREQ.: 5.553 HZ.
10	-1.15286	41.5950	0.17379E-04	-150.87	FREQ.: 6.620 HZ.
PERC. ERROR: 2.112					
SIGNAL/NOISE: 32.61					
METHODS: EIGENVALUE - LEAST SQUARE, EIGENVECTOR - LEAST SQUARE					
ORDER: 36					

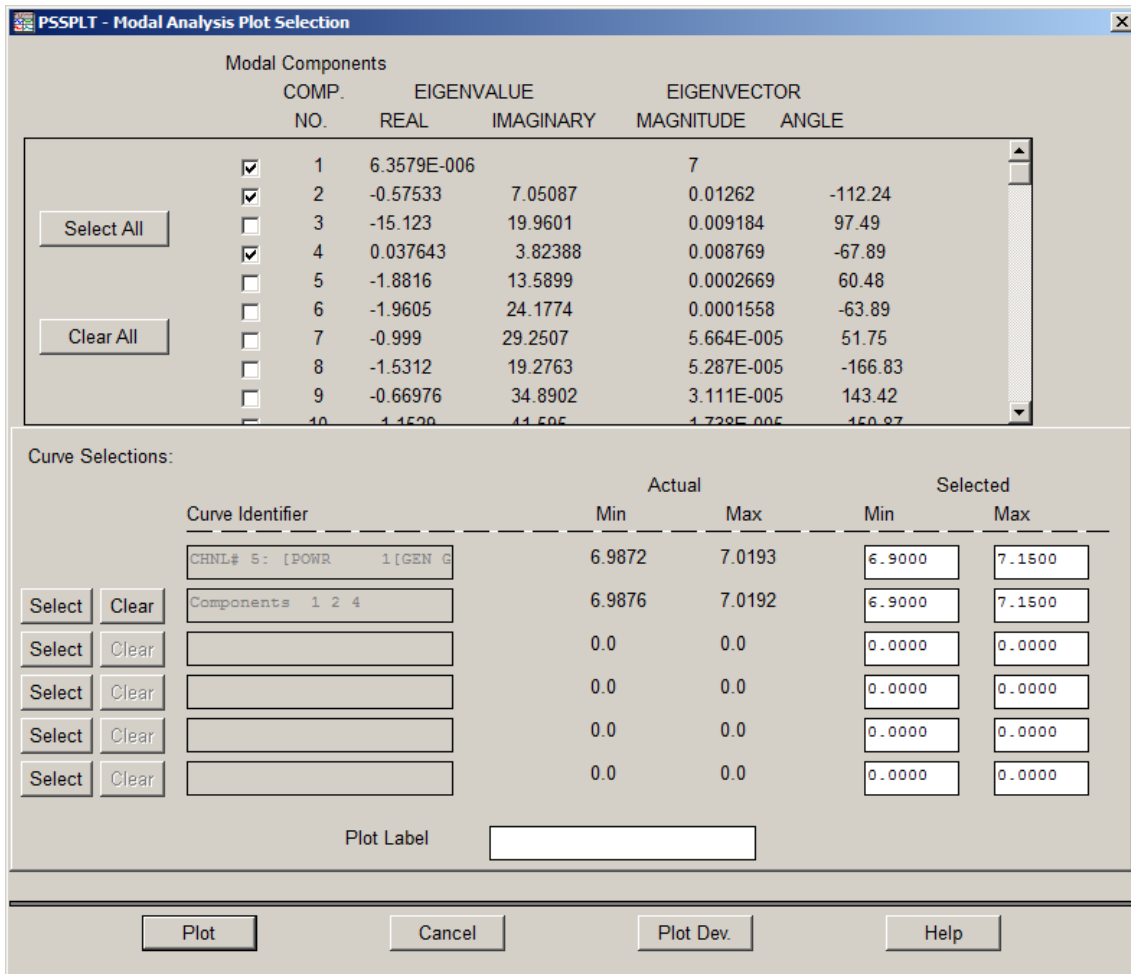


Figure 25: PSSPLT Window for Time Domain Plot of Modal Analysis Equivalent Response

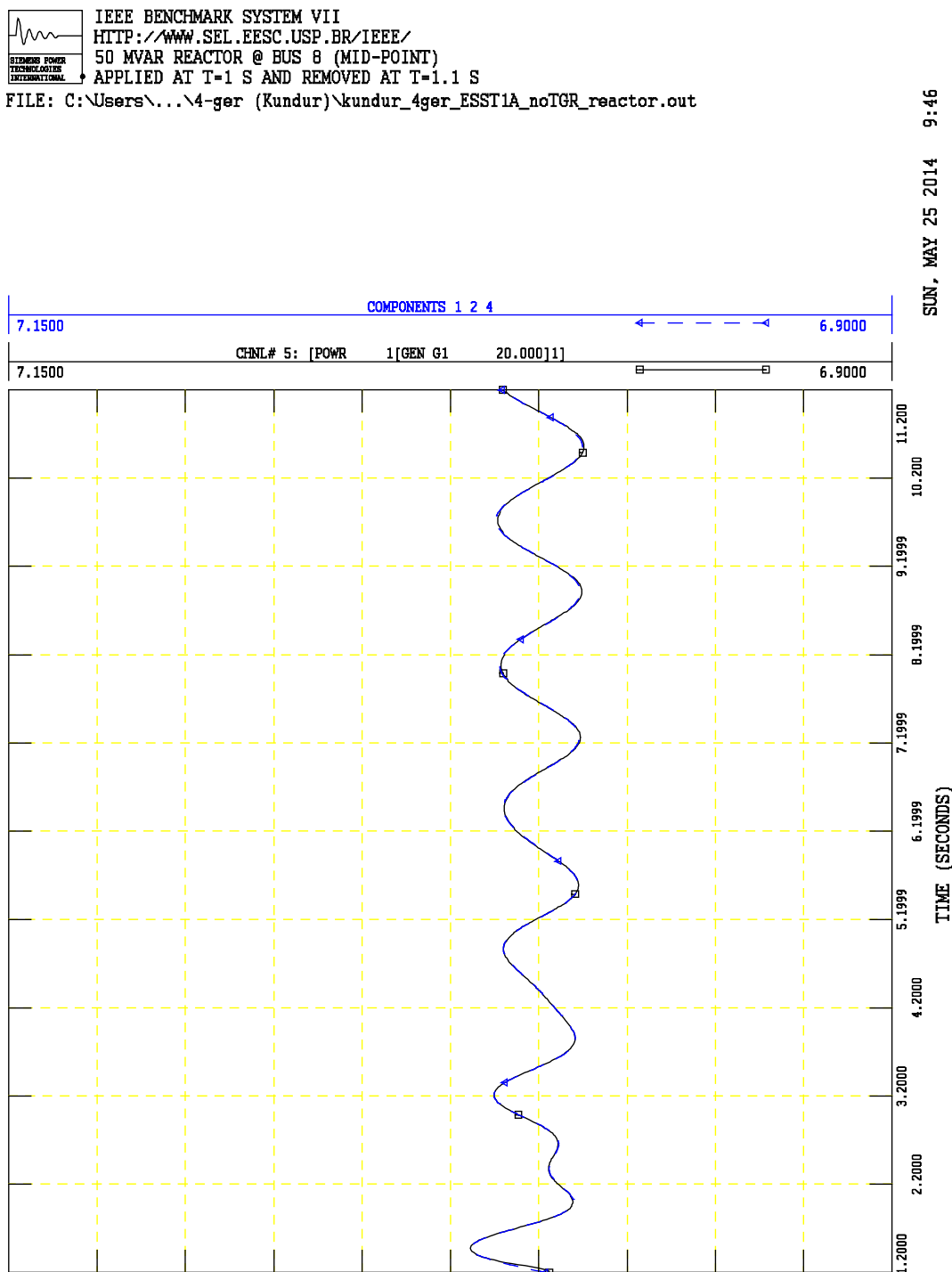


Figure 26: Time Domain Plot of Original Curve and Modal Analysis Equivalent Response

5.3. Impact of Generator Saturation

As mentioned in Section 1.1, the representation of the magnetic saturation in the synchronous machine impacts the small-signal stability results.

To show the impact of the magnetic saturation in the small-signal stability results, the simulations with the ESST1A model without TGR (see Sections 2.5, 2.6, and 2.7) were repeated with the magnetic saturation of the generator models being ignored.

Figure 27 presents the electrical power output of the four generators in the case, for the disturbance considering the 50 MVA reactor applied at the mid-point of the system, for the case without PSS (see Section 2.5.1). The black traces correspond to the original simulation, considering the magnetic saturation as described in Section 1.1. The blue traces are the simulation results when the magnetic saturation is neglected on all machines. It can be seen that the damping and even the frequency of the inter-area electromechanical mode of oscillation has been affected by this modeling decision. This impact is even more visible in the rotor speed deviations shown in Figure 28.

On the other hand, the impact of neglecting magnetic saturation almost vanishes in the case where the PSS are in service. The power output of the generators following the step changes in voltage references, for the case where the PSS are in service (see Section 2.6.2), is shown in Figure 29.

Thus, two basic conclusions can be drawn:

- a) Modeling differences, such as the representation of the magnetic saturation in the synchronous machine, will have some impact on the small-signal stability results. This impact is more visible and significant for unstable or poorly damped oscillation modes (critical modes), as relatively small differences in the damping ratio of the oscillation will have more pronounced effect on the time domain results;
- b) These differences in modeling, leading to differences in numerical values for the calculated eigenvalues, do not affect the overall conceptual analysis (relative mode-shapes and participation factors, for instance) and do not significantly impact the tuning and performance of the PSS. With properly tuned PSS, resulting in better damping for all electromechanical modes, the modeling differences are practically negligible.

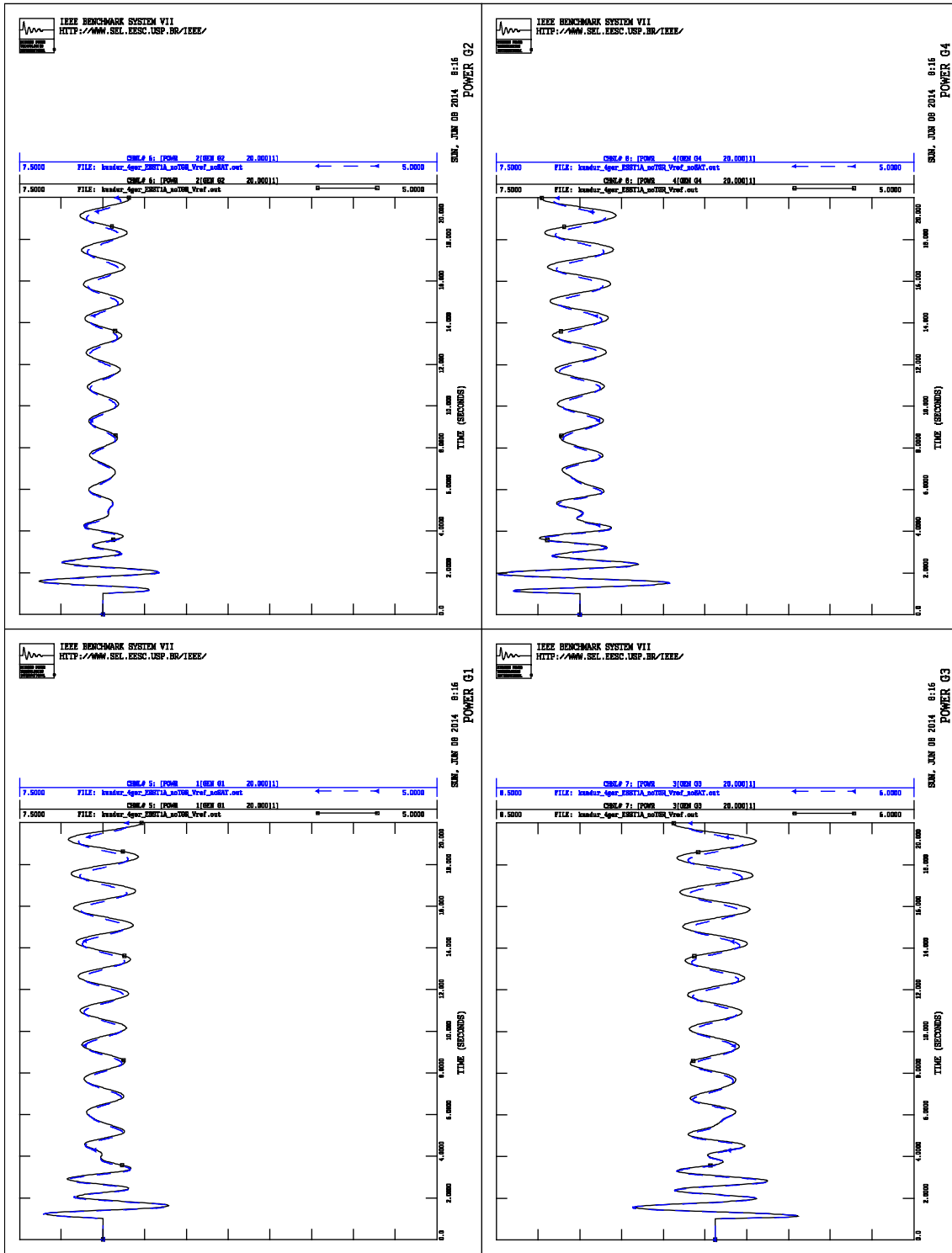


Figure 27: Electrical Power Output Comparison (50 MVAr Reactor Disturbance)

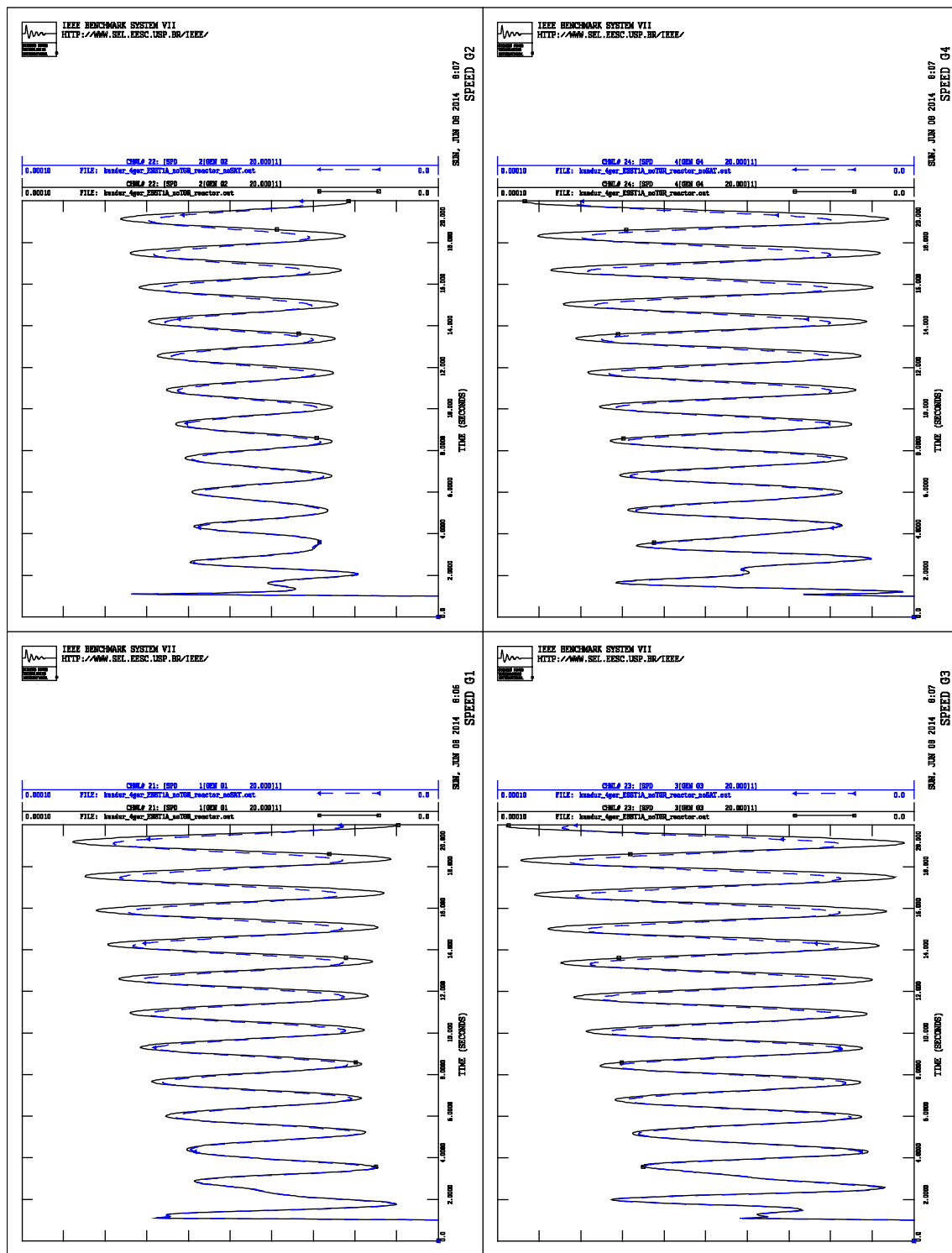


Figure 28: Speed Deviation Comparison (50 MVar Reactor Disturbance)

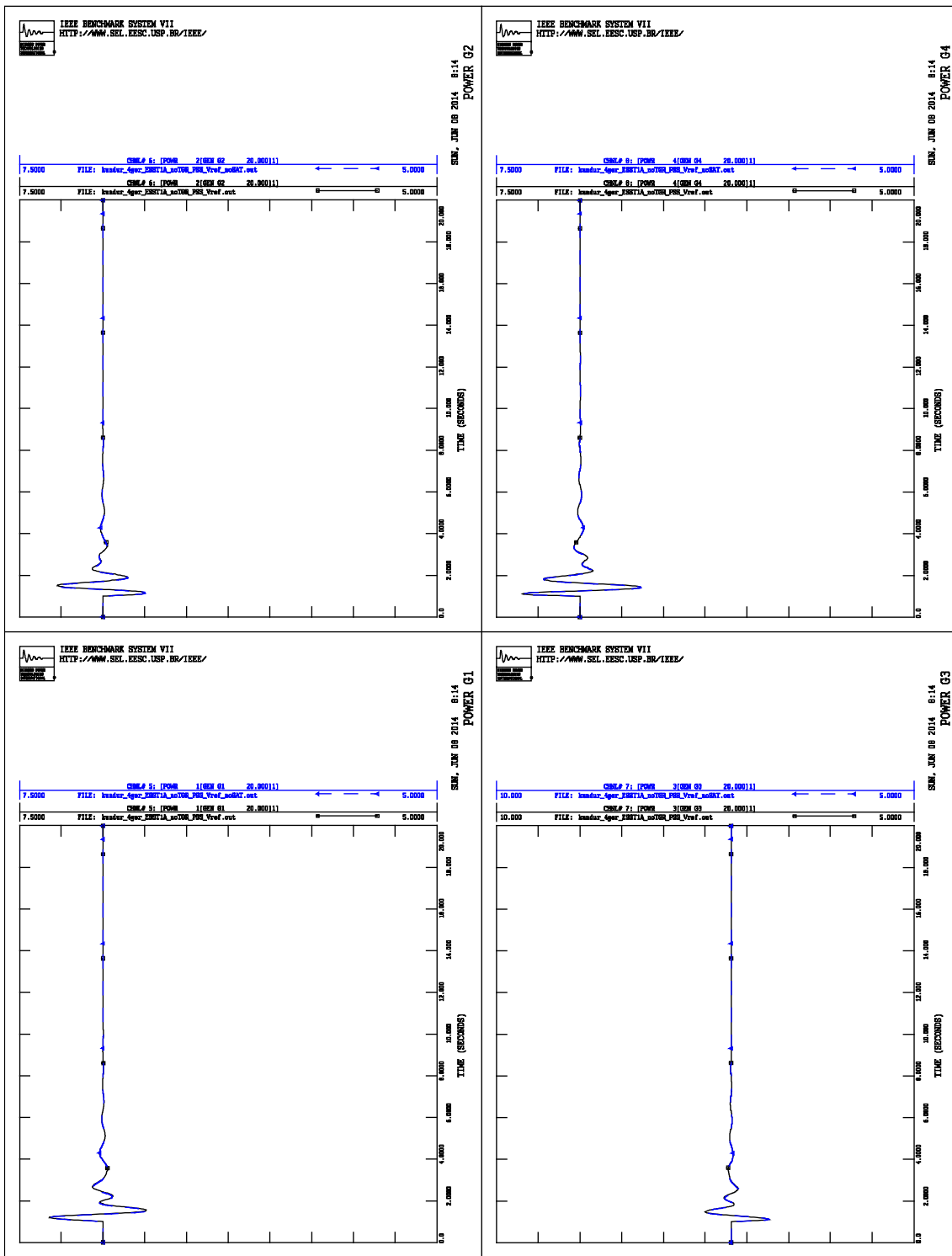


Figure 29: Electrical Power Output Comparison with PSS (Voltage Reference Disturbance)

6. References

- [1] P. Kundur, *Power System Stability and Control*, McGraw Hill, 1994.
- [2] Siemens PTI, “*PSS/E 32.0 Online Documentation*”, June 2009.
- [3] M. Klein, G. J. Rogers and P. Kundur, “*A Fundamental Study of Inter-Area Oscillations*”, IEEE Trans. On Power Systems, vol. 6, no. 3, pp. 914-921, August 1991.
- [4] M. Klein, G. J. Rogers, S. Moorty and P. Kundur, “*Analytical Investigation of Factors Influencing Power System Stabilizers Performance*”, IEEE Trans. On Energy Conversion, vol. 7, no. 3, pp. 382-390, September 1992.
- [5] *IEEE Recommended Practice for Excitation System Models for Power System Stability Studies*, IEEE Standard 421.5(2005), April 2006.
- [6] F. P. de Mello and C. Concordia, “*Concepts of Synchronous Machine Stability as Affected by Excitation Control*,” IEEE Trans. On Power Apparatus and Systems, vol.PAS-88, no.4, pp.316-329, April 1969.
- [7] N. Martins and L. Lima, “*Eigenvalue and Frequency Domain Analysis of Small-Signal Electromechanical Stability Problems*”, in Eigenanalysis and Frequency Domain Methos for System Dynamic Performance, IEEE Special Publication 90TH0292-3-PWR, 1989.

D.1

**Appendix D - Report on the New England Test System by Prof. Ian Hiskens
and Jonas Kersulis**

IEEE PES Task Force on Benchmark Systems for Stability Controls

Ian Hiskens

November 19, 2013

Abstract

This report summarizes a study of an IEEE 10-generator, 39-bus system. Three types of analysis were performed: load flow, small disturbance analysis, and dynamic simulation. All analysis was carried out using MATLAB, and this report's objective is to demonstrate how to use MATLAB to obtain results that are comparable to benchmark results from other analysis methods. Data from other methods may be found on the website www.sel.eesc.usp.br/ieee.

Contents

1 System Model	3
1.1 Generators	3
1.1.1 State Variable Model	3
1.1.2 Model Parameters	3
1.1.3 AVR Model	4
1.1.4 AVR Parameters	5
1.1.5 PSS Model	5
1.1.6 PSS Parameters	6
1.1.7 Governor Model	6
1.2 Loads	7
1.2.1 Load Model	7
1.2.2 Load Parameters	7
1.3 Lines and Transformers	8
1.4 Power and Voltage Setpoints	10
2 Load Flow Results	11
3 Small Disturbance Analysis	12
4 Dynamic Simulation	13
5 Appendix	15
5.1 Accessing Simulation Data with MATLAB®	15
5.1.1 Variable Indexing	15
5.1.2 Example Application	16
5.2 Contents of file <code>39bus.out</code>	18

List of Figures

1 IEEE 39-bus network	2
2 AVR block diagram	4
3 PSS block diagram	6
4 Graphical depiction of Eigenvalues	12
5 δ (in radians) versus time for generators	13

6	ω (in percent per-unit) for generators	14
7	Contents of file 39bus.out (Page 1 of 4)	19

List of Tables

1	Generator inertia data	3
2	Generator data	4
3	Generator AVR parameters	5
4	Generator PSS parameters	6
5	Generator setpoint data	7
6	Active and reactive power draws for all loads at initial voltage	8
7	Network data	9
8	Power and voltage setpoint data	10
9	Power flow results	11
10	Eigenvalues calculated through small disturbance analysis	12
11	Mapping from MATLAB® files to simulation data	15

The IEEE 39-bus system analyzed in this report is commonly known as "the 10-machine New-England Power System." This system's parameters are specified in a paper by T. Athay et al[1] and are published in a book titled 'Energy Function Analysis for Power System Stability'[2]. A diagram of the system is shown in Figure 1, and system models and parameters are introduced in the following section.

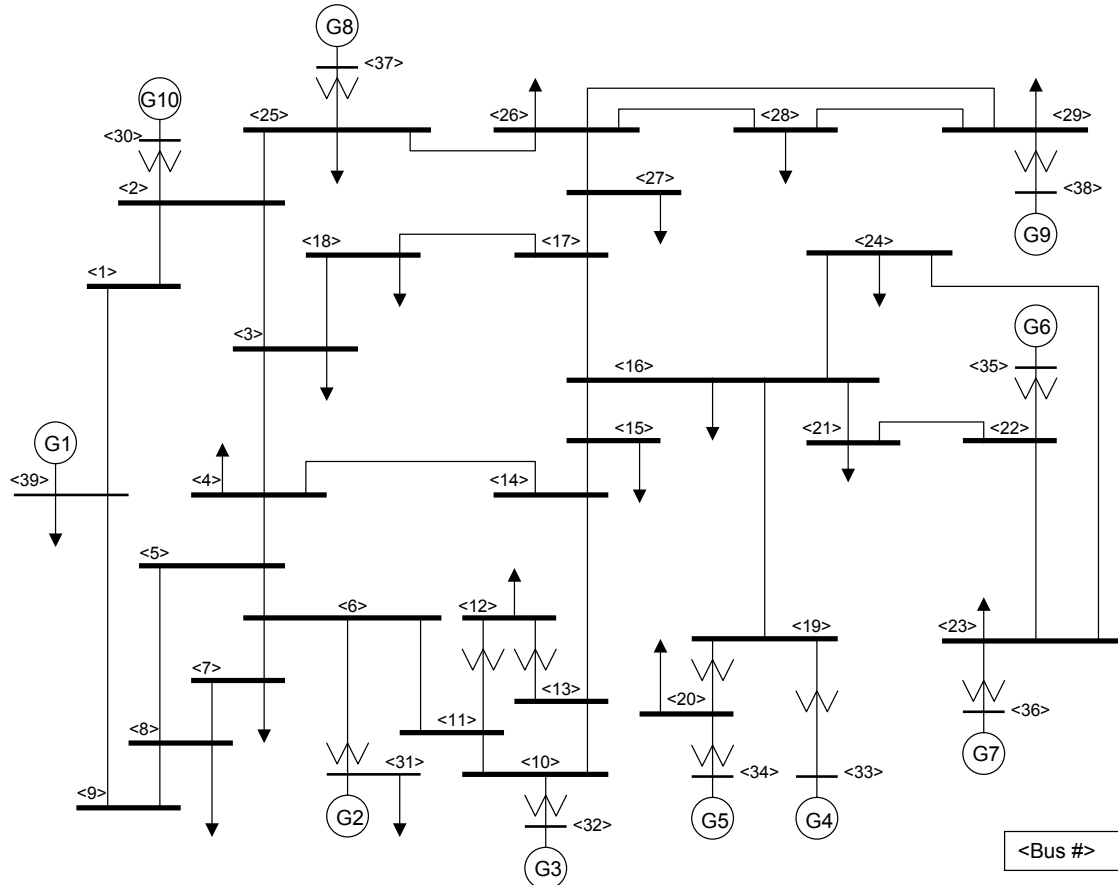


Figure 1: IEEE 39-bus network

1 System Model

1.1 Generators

1.1.1 State Variable Model

Generator analysis was carried out using a fourth-order model, as defined in the equations below. Equations 1 through 4 model the generator, while the remaining equations relate various parameters. Parameter values for the model are shown in Table 2 on the system base MVA. For more information on this generator model and its parameters, refer to Sauer and Pai pages 101-103 [3].

$$\dot{E}'_q = \frac{1}{T'_{do}}(-E'_q - (x_d - x'_d)I_d + E_{fd}) \quad (1)$$

$$\dot{E}'_d = \frac{1}{T'_{qo}}(-E'_d + (x_q - x'_q)I_q) \quad (2)$$

$$\dot{\delta} = \omega \quad (3)$$

$$\dot{\omega} = \frac{1}{M}(T_{mech} - (\phi_d I_q - \phi_q I_d) - D_\omega) \quad (4)$$

$$0 = r_a I_d + \phi_q + V_d \quad (5)$$

$$0 = r_a I_q - \phi_d + V_q \quad (6)$$

$$0 = -\phi_d - x'_d I_d + E'_q \quad (7)$$

$$0 = -\phi_q - x'_q I_q - E'_d \quad (8)$$

$$0 = V_d \sin \delta + V_q \cos \delta - V_r \quad (9)$$

$$0 = V_q \sin \delta - V_d \cos \delta - V_i \quad (10)$$

$$0 = I_d \sin \delta + I_q \cos \delta - I_r \quad (11)$$

$$0 = I_q \sin \delta - I_d \cos \delta - I_i \quad (12)$$

1.1.2 Model Parameters

Generator inertia data is given in Table 1. Note that the per unit conversion for M associated with ω is in radians per second. Also, we changed the value of T'_{qo} for Unit 10 from 0.0 to 0.10.

Table 1: Generator inertia data

Unit No.	M=2*H
1	$2 \cdot 500.0 / (120\pi)$
2	$2 \cdot 30.3 / (120\pi)$
3	$2 \cdot 35.8 / (120\pi)$
4	$2 \cdot 28.6 / (120\pi)$
5	$2 \cdot 26.0 / (120\pi)$
6	$2 \cdot 34.8 / (120\pi)$
7	$2 \cdot 26.4 / (120\pi)$
8	$2 \cdot 24.3 / (120\pi)$
9	$2 \cdot 34.5 / (120\pi)$
10	$2 \cdot 42.0 / (120\pi)$

All other generator parameters are set according to Table 2.

Table 2: Generator data

Unit No.	H	R_a	x'_d	x'_q	x_d	x_q	T'_{do}	T'_{qo}	x_l
1	500	0	0.006	0.008	0.02	0.019	7	0.7	0.003
2	30.3	0	0.0697	0.17	0.295	0.282	6.56	1.5	0.035
3	35.8	0	0.0531	0.0876	0.2495	0.237	5.7	1.5	0.0304
4	28.6	0	0.0436	0.166	0.262	0.258	5.69	1.5	0.0295
5	26	0	0.132	0.166	0.67	0.62	5.4	0.44	0.054
6	34.8	0	0.05	0.0814	0.254	0.241	7.3	0.4	0.0224
7	26.4	0	0.049	0.186	0.295	0.292	5.66	1.5	0.0322
8	24.3	0	0.057	0.0911	0.29	0.28	6.7	0.41	0.028
9	34.5	0	0.057	0.0587	0.2106	0.205	4.79	1.96	0.0298
10	42	0	0.031	0.008	0.1	0.069	10.2	0	0.0125

1.1.3 AVR Model

All generators in the system are equipped with automatic voltage regulators (AVRs). We chose to use static AVRs with E_{fd} limiters. The model for this controller is shown in Figure 2 below.

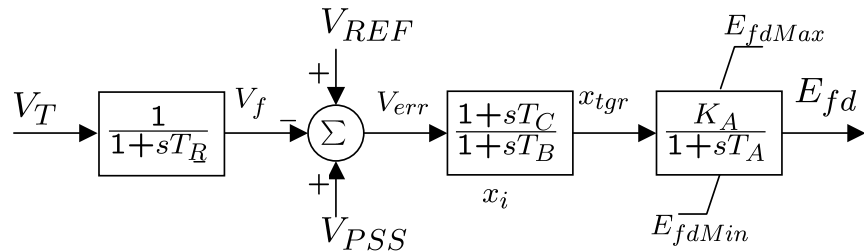


Figure 2: AVR block diagram

AVR parameters are related according to equations 13 to 24.

$$\dot{V}_f = \frac{1}{T_R} (V_T - V_f) \quad (13)$$

$$\dot{E}_{fd} = \frac{1}{T_A} (K_A x_{tgr} - E_{fd}) \quad (14)$$

$$\dot{x}_i = x_{err} - x_{tgr} \quad (15)$$

$$\dot{V}_{REF} = \begin{cases} 0 & \text{when } t > 0 \\ V_T - V_{\text{setpoint}} & \text{when } t < 0 \end{cases} \quad (16)$$

$$0 = V_T^2 - (V_r^2 + V_i^2) \quad (17)$$

$$0 = T_B x_{tgr} - T_C x_{err} - x_i \quad (18)$$

$$0 = x_{err} - (V_{REF} + V_{PSS} - V_f) \quad (19)$$

$$0 = E_{fd} - E_{fd} \quad (20)$$

$$\text{Upper Limit Detector} < 0 \begin{cases} 0 = \text{Upper Limit Switch} - 1 \\ 0 = \text{Upper Limit Detector} - E_{fd} - E_{fd,\text{Max}} \end{cases} \quad (21)$$

$$\text{Upper Limit Detector} > 0 \begin{cases} 0 = \text{Upper Limit Switch} \\ 0 = \text{Upper Limit Detector} - (K_A x_{tgr} - E_{fd}) \end{cases} \quad (22)$$

$$\text{Lower Limit Detector} > 0 \begin{cases} 0 = \text{Lower Limit Switch} - 1 \\ 0 = \text{Lower Limit Detector} - E_{fd} - E_{fd,\text{Min}} \end{cases} \quad (23)$$

$$\text{Lower Limit Detector} < 0 \begin{cases} 0 = \text{Lower Limit Switch} \\ 0 = \text{Lower Limit Detector} - (K_A x_{tgr} - E_{fd}) \end{cases} \quad (24)$$

1.1.4 AVR Parameters

AVR parameters, as defined in the previous section, are specified in Table 3.

Table 3: Generator AVR parameters

Unit No.	T_R	K_A	T_A	T_B	T_C	V_{setpoint}	$E_{fd,\text{Max}}$	$E_{fd,\text{Min}}$
1	0.01	200.0	0.015	10.0	1.0	1.0300	5.0	-5.0
2	0.01	200.0	0.015	10.0	1.0	0.9820	5.0	-5.0
3	0.01	200.0	0.015	10.0	1.0	0.9831	5.0	-5.0
4	0.01	200.0	0.015	10.0	1.0	0.9972	5.0	-5.0
5	0.01	200.0	0.015	10.0	1.0	1.0123	5.0	-5.0
6	0.01	200.0	0.015	10.0	1.0	1.0493	5.0	-5.0
7	0.01	200.0	0.015	10.0	1.0	1.0635	5.0	-5.0
8	0.01	200.0	0.015	10.0	1.0	1.0278	5.0	-5.0
9	0.01	200.0	0.015	10.0	1.0	1.0265	5.0	-5.0
10	0.01	200.0	0.015	10.0	1.0	1.0475	5.0	-5.0

1.1.5 PSS Model

Each generator in the system is equipped with a δ and ω type PSS with two phase shift blocks. The model for this PSS is shown in Figure 3 below.

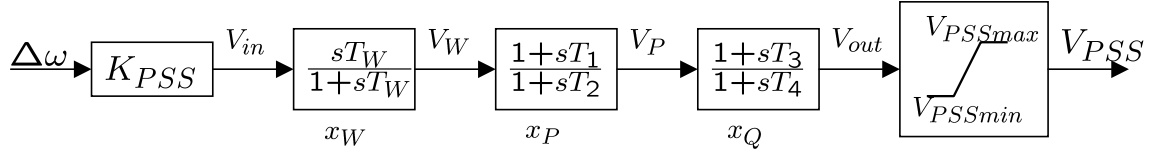


Figure 3: PSS block diagram

PSS parameters are related according to equations 25 to 33.

$$\dot{x}_W = \frac{V_W}{T_W} \quad (25)$$

$$\dot{x}_P = V_W - V_P \quad (26)$$

$$\dot{x}_Q = V_P - V_{out} \quad (27)$$

$$0 = \omega K_{PSS} - V_W - x_W \quad (28)$$

$$0 = V_P T_2 - V_W T_1 - x_P \quad (29)$$

$$0 = V_{out} T_4 - V_P T_3 - x_Q \quad (30)$$

$$0 = x_{PSS,Max} - V_{out} - (V_{PSS,Max} - V_{out}) \quad (31)$$

$$0 = V_{out} - x_{PSS,Min} - (V_{out} - V_{PSS,Min}) \quad (32)$$

$$0 = \begin{cases} V_{PSS} - x_{PSS,Max} & \text{when } (V_{PSS,Max} - V_{out}) < 0 \\ V_{PSS} - x_{PSS,Min} & \text{when } (V_{out} - V_{PSS,Min}) < 0 \\ V_{PSS} - V_{out} & \text{otherwise} \end{cases} \quad (33)$$

1.1.6 PSS Parameters

PSS parameters defined in the previous section are specified according to Table 4.

Table 4: Generator PSS parameters

Unit No.	K	T_W	T_1	T_2	T_3	T_4	$V_{PSS,Max}$	$V_{PSS,Min}$
1	$1.0/(120\pi)$	10.0	5.0	0.60	3.0	0.50	0.2	-0.2
2	$0.5/(120\pi)$	10.0	5.0	0.40	1.0	0.10	0.2	-0.2
3	$0.5/(120\pi)$	10.0	3.0	0.20	2.0	0.20	0.2	-0.2
4	$2.0/(120\pi)$	10.0	1.0	0.10	1.0	0.30	0.2	-0.2
5	$1.0/(120\pi)$	10.0	1.5	0.20	1.0	0.10	0.2	-0.2
6	$4.0/(120\pi)$	10.0	0.5	0.10	0.5	0.05	0.2	-0.2
7	$7.5/(120\pi)$	10.0	0.2	0.02	0.5	0.10	0.2	-0.2
8	$2.0/(120\pi)$	10.0	1.0	0.20	1.0	0.10	0.2	-0.2
9	$2.0/(120\pi)$	10.0	1.0	0.50	2.0	0.10	0.2	-0.2
10	$1.0/(120\pi)$	10.0	1.0	0.05	3.0	0.50	0.2	-0.2

1.1.7 Governor Model

No governor dynamics are included in our analysis, and each generator's mechanical torque is assumed to be constant. Since Unit 2 is the angle reference and resides at the swing node, P_{set} point is determined by the

power flow initialization. The value of $P_{\text{set point}}$ is given for each generator in Table 5 on the system base of 100 MVA.

Table 5: Generator setpoint data

Unit No.	$P_{\text{set point}}$
1	10.00
2	-
3	6.50
4	6.32
5	5.08
6	6.50
7	5.60
8	5.40
9	8.30
10	2.50

1.2 Loads

1.2.1 Load Model

We use a constant impedance load model in our analysis. Loads modeled this way are voltage dependent and behave according to the following equations.

$$\begin{cases} 0 = P_0 + V_r I_r + V_i I_i \\ 0 = Q_0 + V_i I_r - V_r I_i \\ V = (V_r^2 + V_i^2)^2 \end{cases} \quad \text{(34)}$$

$$\begin{cases} 0 = P_0 \left(\frac{V}{V_0} \right)^\alpha + V_r I_r + V_i I_i \\ 0 = Q_0 \left(\frac{V}{V_0} \right)^\beta + V_i I_r + V_r I_i \\ V = (V_r^2 + V_i^2)^2 \end{cases} \quad \text{(35)}$$

1.2.2 Load Parameters

Table 6 contains load behavior at initial voltage. Due to the voltage dependence discussed above, these values may not be accurate after voltages change.

Table 6: Active and reactive power draws for all loads at initial voltage

Bus	Load	
	P [PU]	Q [pu]
1	0.000	0.000
2	0.000	0.000
3	3.220	0.024
4	5.000	1.840
5	0.000	0.000
6	0.000	0.000
7	2.338	0.840
8	5.220	1.760
9	0.000	0.000
10	0.000	0.000
11	0.000	0.000
12	0.075	0.880
13	0.000	0.000
14	0.000	0.000
15	3.200	1.530
16	3.290	0.323
17	0.000	0.000
18	1.580	0.300
19	0.000	0.000
20	6.280	1.030
21	2.740	1.150
22	0.000	0.000
23	2.475	0.846
24	3.086	-0.920
25	2.240	0.472
26	1.390	0.170
27	2.810	0.755
28	2.060	0.276
29	2.835	0.269
31	0.092	0.046
39	11.040	2.500

1.3 Lines and Transformers

Network data for the system is shown in Table 7. As with generator data, all values are given on the system base MVA at 60 Hz.

Table 7: Network data

Line Data					Transformer Tap	
From Bus	To Bus	R	X	B	Magnitude	Angle
1	2	0.0035	0.0411	0.6987	-	-
1	39	0.001	0.025	0.75	-	-
2	3	0.0013	0.0151	0.2572	-	-
2	25	0.007	0.0086	0.146	-	-
3	4	0.0013	0.0213	0.2214	-	-
3	18	0.0011	0.0133	0.2138	-	-
4	5	0.0008	0.0128	0.1342	-	-
4	14	0.0008	0.0129	0.1382	-	-
5	6	0.0002	0.0026	0.0434	-	-
5	8	0.0008	0.0112	0.1476	-	-
6	7	0.0006	0.0092	0.113	-	-
6	11	0.0007	0.0082	0.1389	-	-
7	8	0.0004	0.0046	0.078	-	-
8	9	0.0023	0.0363	0.3804	-	-
9	39	0.001	0.025	1.2	-	-
10	11	0.0004	0.0043	0.0729	-	-
10	13	0.0004	0.0043	0.0729	-	-
13	14	0.0009	0.0101	0.1723	-	-
14	15	0.0018	0.0217	0.366	-	-
15	16	0.0009	0.0094	0.171	-	-
16	17	0.0007	0.0089	0.1342	-	-
16	19	0.0016	0.0195	0.304	-	-
16	21	0.0008	0.0135	0.2548	-	-
16	24	0.0003	0.0059	0.068	-	-
17	18	0.0007	0.0082	0.1319	-	-
17	27	0.0013	0.0173	0.3216	-	-
21	22	0.0008	0.014	0.2565	-	-
22	23	0.0006	0.0096	0.1846	-	-
23	24	0.0022	0.035	0.361	-	-
25	26	0.0032	0.0323	0.513	-	-
26	27	0.0014	0.0147	0.2396	-	-
26	28	0.0043	0.0474	0.7802	-	-
26	29	0.0057	0.0625	1.029	-	-
28	29	0.0014	0.0151	0.249	-	-
12	11	0.0016	0.0435	0	1.006	0
12	13	0.0016	0.0435	0	1.006	0
6	31	0	0.025	0	1.07	0
10	32	0	0.02	0	1.07	0
19	33	0.0007	0.0142	0	1.07	0
20	34	0.0009	0.018	0	1.009	0
22	35	0	0.0143	0	1.025	0
23	36	0.0005	0.0272	0	1	0
25	37	0.0006	0.0232	0	1.025	0
2	30	0	0.0181	0	1.025	0
29	38	0.0008	0.0156	0	1.025	0
19	20	0.0007	0.0138	0	1.06	0

1.4 Power and Voltage Setpoints

Table 8 contains power and voltage setpoint data, specified on the system MVA base. Note that Generator 2 is the swing node, and Generator 1 represents the aggregation of a large number of generators.

Table 8: Power and voltage setpoint data

Bus	Type	Voltage [PU]	Load		Generator		
			MW	MVar	MW	MVar	Unit No.
1	PQ	-	0	0	0	0	
2	PQ	-	0	0	0	0	
3	PQ	-	322	2.4	0	0	
4	PQ	-	500	184	0	0	
5	PQ	-	0	0	0	0	
6	PQ	-	0	0	0	0	
7	PQ	-	233.8	84	0	0	
8	PQ	-	522	176	0	0	
9	PQ	-	0	0	0	0	
10	PQ	-	0	0	0	0	
11	PQ	-	0	0	0	0	
12	PQ	-	7.5	88	0	0	
13	PQ	-	0	0	0	0	
14	PQ	-	0	0	0	0	
15	PQ	-	320	153	0	0	
16	PQ	-	329	32.3	0	0	
17	PQ	-	0	0	0	0	
18	PQ	-	158	30	0	0	
19	PQ	-	0	0	0	0	
20	PQ	-	628	103	0	0	
21	PQ	-	274	115	0	0	
22	PQ	-	0	0	0	0	
23	PQ	-	247.5	84.6	0	0	
24	PQ	-	308.6	-92	0	0	
25	PQ	-	224	47.2	0	0	
26	PQ	-	139	17	0	0	
27	PQ	-	281	75.5	0	0	
28	PQ	-	206	27.6	0	0	
29	PQ	-	283.5	26.9	0	0	
30	PV	1.0475	0	0	250	-	Gen10
31	PV	0.982	9.2	4.6	-	-	Gen2
32	PV	0.9831	0	0	650	-	Gen3
33	PV	0.9972	0	0	632	-	Gen4
34	PV	1.0123	0	0	508	-	Gen5
35	PV	1.0493	0	0	650	-	Gen6
36	PV	1.0635	0	0	560	-	Gen7
37	PV	1.0278	0	0	540	-	Gen8
38	PV	1.0265	0	0	830	-	Gen9
39	PV	1.03	1104	250	1000	-	Gen1

This completes the description of the system and its model. The remainder of this report focuses on the three analyses performed on the system: load flow, small signal stability assessment via Eigenvalue calculation, and numerical simulation. The results of load flow analysis are presented in the next section.

2 Load Flow Results

Load flow for the system was calculated using MATLAB. The results are in Table 9. Note that all voltages, active power values, and reactive power values are given in per unit on the system MVA base.

For a more complete description of power flow, including flow on each line, see Section 5.2 in the Appendix.

Table 9: Power flow results

Bus	V	Angle [deg]	Bus Total		Load		Generator		
			P	Q	P	Q	P	Q	Unit No.
1	1.0474	-8.44	0	0	0	0			
2	1.0487	-5.75	0	0	0	0			
3	1.0302	-8.6	-322	-2.4	-322	-2.4			
4	1.0039	-9.61	-500	-184	-500	-184			
5	1.0053	-8.61	0	0	0	0			
6	1.0077	-7.95	0	0	0	0			
7	0.997	-10.12	-233.8	-84	-233.8	-84			
8	0.996	-10.62	-522	-176	-522	-176			
9	1.0282	-10.32	0	0	0	0			
10	1.0172	-5.43	0	0	0	0			
11	1.0127	-6.28	0	0	0	0			
12	1.0002	-6.24	-7.5	-88	-7.5	-88			
13	1.0143	-6.1	0	0	0	0			
14	1.0117	-7.66	0	0	0	0			
15	1.0154	-7.74	-320	-153	-320	-153			
16	1.0318	-6.19	-329	-32.3	-329	-32.3			
17	1.0336	-7.3	0	0	0	0			
18	1.0309	-8.22	-158	-30	-158	-30			
19	1.0499	-1.02	0	0	0	0			
20	0.9912	-2.01	-628	-103	-628	-103			
21	1.0318	-3.78	-274	-115	-274	-115			
22	1.0498	0.67	0	0	0	0			
23	1.0448	0.47	-247.5	-84.6	-247.5	-84.6			
24	1.0373	-6.07	-308.6	92.2	-308.6	92.2			
25	1.0576	-4.36	-224	-47.2	-224	-47.2			
26	1.0521	-5.53	-139	-17	-139	-17			
27	1.0377	-7.5	-281	-75.5	-281	-75.5			
28	1.0501	-2.01	-206	-27.6	-206	-27.6			
29	1.0499	0.74	-283.5	-26.9	-283.5	-26.9			
30	1.0475	-3.33	250	146.16			250	146.16	10
31	0.982	0	511.61	193.65	-9.2	-4.6	520.81	198.25	2
32	0.9831	2.57	650	205.14			650	205.14	3
33	0.9972	4.19	632	109.91			632	109.91	4
34	1.0123	3.17	508	165.76			508	165.76	5
35	1.0493	5.63	650	212.41			650	212.41	6
36	1.0635	8.32	560	101.17			560	101.17	7
37	1.0278	2.42	540	0.44			540	0.44	8
38	1.0265	7.81	830	22.84			830	22.84	9
39	1.03	-10.05	-104	-161.7	-1104	-250	1000	88.28	1

3 Small Disturbance Analysis

Small signal stability was assessed by calculating Eigenvalues of the system. To find Eigenvalues, we first calculated reduced A matrices as follows:

$$\begin{array}{l} \dot{x} = f(x, y) \mid 0 = g(x, y) \\ \text{Differential eq.} \quad \text{Algebraic eq.} \end{array}$$

Linearize:

$$\Delta\dot{x} = f_x\Delta x + f_y\Delta y \mid 0 = g_x\Delta x + g_y\Delta y$$

Eliminate algebraic equations:

$$\Delta\dot{x} = (f_x - f_yg_y^{-1}g_x)\Delta x$$

Reduced A matrices

Eigenvalues, which correspond to machine oscillatory modes, are calculated from the reduced A matrices. Some Eigenvalues of our system are given in Table 10 below. To access all Eigenvalues calculated in our analysis, see Section 5.1 in the Appendix.

Table 10: Eigenvalues calculated through small disturbance analysis

Index	Real part	Imaginary part
27	-2.553	j10.566
29	-1.8494	j10.028
31	-1.5817	j8.5503
33	-2.5633	j8.6706
35	-1.8626	j7.4388
37	-1.3118	j7.1081
39	-1.8437	j7.0812
41	-1.523	j6.3180
57	-2.9563	j2.5076

The Eigenvalues in Table 10 are plotted in Figure 4.

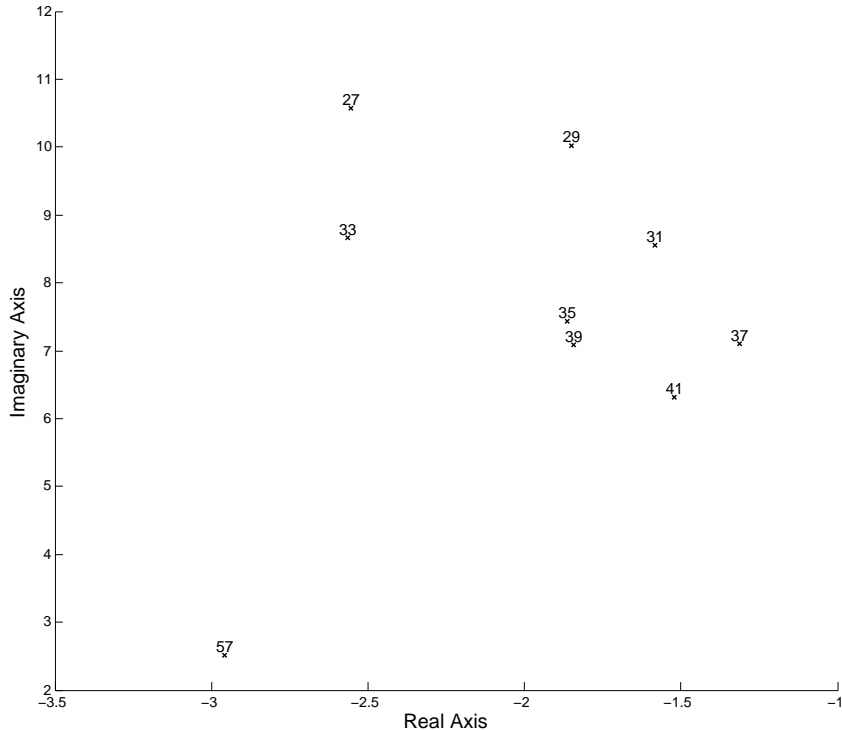


Figure 4: Graphical depiction of Eigenvalues

4 Dynamic Simulation

Dynamic simulation was performed for a three-phase fault at Bus 16 occurring at $t = 0.5\text{s}$. The fault impedance is 0.001 PU, and it is cleared at $t = 0.7\text{s}$. The simulation method used was numerical trapezoidal integration with a time step of 20 ms.

Figure 5 shows the generator state δ as a function of time for the ten generators, with Unit 1 as the angle reference. Figure 6 on the following page shows the generator state ω as a function of time for the ten generators.

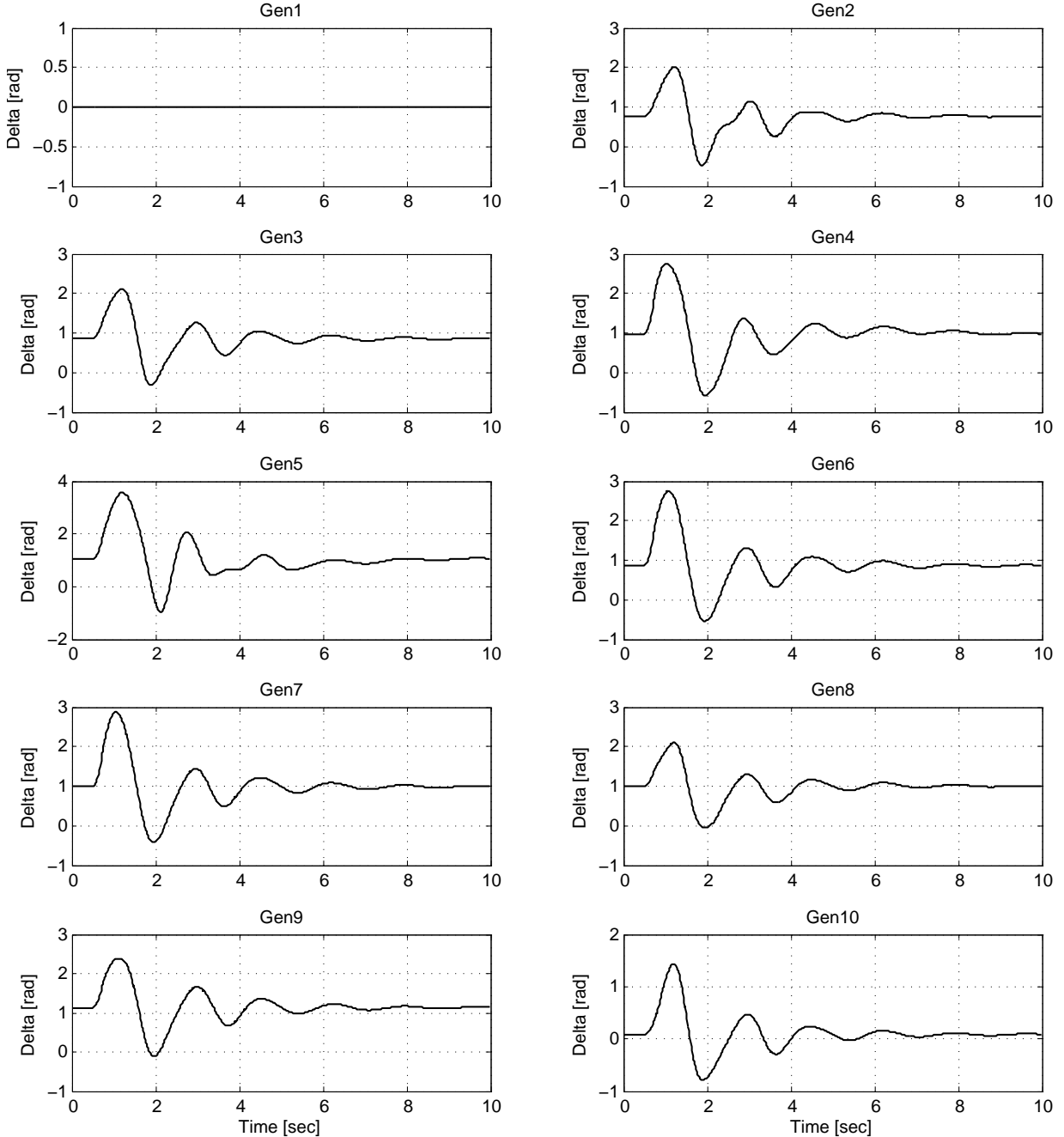
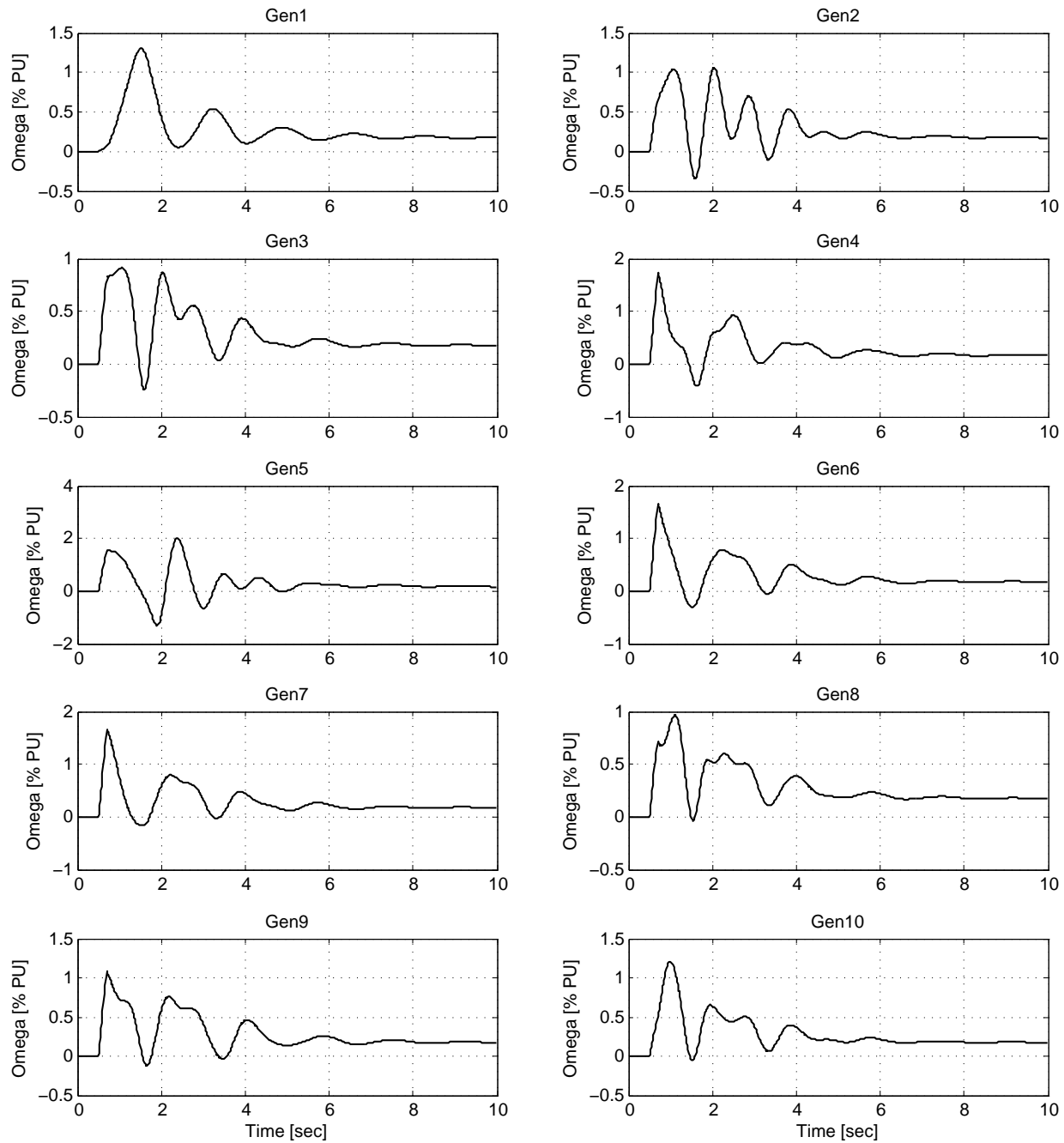


Figure 5: δ (in radians) versus time for generators

Figure 6: ω (in percent per-unit) for generators

To generate these and other figures from the MATLAB files available on the website, see "Accessing Simulation Data with MATLAB" in the appendix.

5 Appendix

5.1 Accessing Simulation Data with MATLAB®

There are seven MATLAB®.mat files available for download. Each .mat file has a csv counterpart for those who prefer to work with Excel or another CSV-friendly program (the procedure described here may be adapted for such programs). Each file is described below.

- **time.mat** is a row vector with 677 elements. This vector represents the simulation time period with increments of 20ms. To observe the variation of any model variable with respect to time, simply plot the corresponding row of **x.mat** or **y.mat** versus **time.mat**.
- **x.mat** contains 209 row vectors, each corresponding to a model state variable. See Table 11.
- **x0.mat** contains 209 elements corresponding to initial values of model state variables. It is indexed the same as **x.mat**.
- **y.mat** contains 617 row vectors, each corresponding to a non-state variable in the model. See Table 11.
- **y0.mat** contains 617 elements corresponding to initial values of non-state variables. It is indexed the same as **y.mat**.
- **Aeig.mat** contains 209 complex elements corresponding to system Eigenvalues. To obtain any entry of Table 10, one need only extract the element of **Aeig** corresponding to that entry's Index. Of course, there are many more Eigenvalues stored in **Aeig** than those listed in Table 10, and all Eigenvalues may be easily plotted so long as care is taken in isolating the real and imaginary parts.
- **Ared.mat** is a 209-by-209 variable containing reduced *A* matrix data for the system. (Reduced *A* matrices are discussed in Section 3.)

Model state variables are stored in **x.mat** while non-state variables are located in **y.mat**. Table 11 maps from these files to specific model variables by specifying the range of variables corresponding to each component of the model. The order of variables within a component's range is discussed in the next five subsections.

Table 11: Mapping from MATLAB®files to simulation data

Model	Model ID	x range from	x range to	y range from	y range to	Description
Generator	G1	1	4	1	13	4 x states and 13 y variables
	G10	37	49	118	130	
AVR	G1	110	114	438	448	5 x states and 11 y variables
	G10	155	159	537	547	
PSS	G1	160	164	548	554	5 x states and 7 y variables
	G10	205	209	611	617	
Load	Bus1	47	48	303	306	2 x states and 4 y variables (x states are real and reactive power)
	Bus39	107	108	423	426	
Network	Bus1			131	134	4 y variables
	Bus39			283	286	

5.1.1 Variable Indexing

This section defines all variables contained in the MATLAB files. When writing code to extract specific variables, refer to this section to determine which indices to use.

Generator Variables (See Section 1.1.1)

	y_1	:	V_r		
	y_2	:	V_i		
	y_3	:	I_r		
	y_4	:	I_i		
x_1	:	E'_q	y_5	:	V_d
x_2	:	E'_d	y_6	:	V_q
x_3	:	δ	y_7	:	I_d
x_4	:	ω	y_8	:	I_q
			y_9	:	ψ_d
			y_{10}	:	ψ_q
			y_{11}	:	E_{fd}
			y_{12}	:	ω
			y_{13}	:	T_{mech}

AVR Variables (See Section 1.1.3)

	y_1	:	V_r		
	y_2	:	V_i		
	y_3	:	V_T		
x_1	:	V_f	y_4	:	V_{PSS}
x_2	:	E_{fd}	y_5	:	x_{err}
x_3	:	x_i	y_6	:	x_{tgr}
x_4	:	V_{REF}	y_7	:	E_{fd}
			y_8	:	Upper Limit Detector
			y_9	:	Lower Limit Detector
			y_{10}	:	Upper Limit Switch
			y_{11}	:	Lower Limit Switch

PSS Variables (See Section 1.1.5)

	y_1	:	ω (input)		
	y_2	:	V_W		
x_1	:	x_W	y_3	:	V_P
x_2	:	x_P	y_4	:	V_{out}
x_3	:	x_Q	y_5	:	V_{PSS}
			y_6	:	$V_{PSS,Max} - V_{out}$
			y_7	:	$V_{out} - V_{PSS,Min}$

Load Variables (See Section 1.2.1)

x_1	:	P	y_1	:	V_r
x_2	:	Q	y_2	:	V_i
			y_3	:	I_r
			y_4	:	I_i

Network Variables (See ??) Network variables are indexed in the MATLAB files as follows:

5.1.2 Example Application

The code below will generate Figures 5 and 6. By modifying or adapting this code, the reader may plot or manipulate any variables in `x.mat` and `y.mat`.

(Note: The placeholders "TIMEPATH", "XPATH", and "YPATH" should be replaced with paths to the respective files on your computer.)

```

%% Import Data
% Import time.mat
newData = load('-mat', 'TIMEPATH\time.mat');

% Create new variables in the base workspace from those fields.
vars = fieldnames(newData);
for i = 1:length(vars)
    assignin('base', vars{i}, newData.(vars{i}));
end

% Import x.mat
newData = load('-mat', 'XPATH\x.mat');

% Create new variables in the base workspace from those fields.
vars = fieldnames(newData);
for i = 1:length(vars)
    assignin('base', vars{i}, newData.(vars{i}));
end

% Import y.mat
newData = load('-mat', 'YPATH\y.mat');

% Create new variables in the base workspace from those fields.
vars = fieldnames(newData);
for i = 1:length(vars)
    assignin('base', vars{i}, newData.(vars{i}));
end

clear newData, clear vars

%% Plot x or y vs. time
% Plot omega vs time
figure('name','Generator Omega vs Time')
for i = 1:10
    subplot(5,2,i);
    p = plot(time,x(i*4 - 0,:)/4,'k'); % Note factor of 1/4
    set(p,'LineWidth',1);
    figtitle = strcat('Gen',num2str(i));
    title(figtitle)
    if or(i==9,i==10)
        xlabel('Time [sec]')
    end
    ylabel('Omega [% PU]')
    grid on
end

% Plot delta vs time
figure('name','Generator Delta vs Time')
for i = 1:10
    subplot(5,2,i);
    p = plot(time,x(i*4 - 1,:)-x(3,:),'k'); % Subtract Unit 1 (angle reference)
    set(p,'LineWidth',1);

```

```
figtitle = strcat('Gen',num2str(i));
title(figtitle)
if or(i==9,i==10)
    xlabel('Time [sec]')
end
ylabel('Delta [rad]')
grid on
end
```

5.2 Contents of file 39bus.out

The next four pages show the contents of the file 39bus.out. This file contains power flow data with enough granularity to observe flows on all lines.

39bus.out													
IEEE 39 bus test system													
BUS	Bus	1.	0.0474PU	-8.44	CKT	MW	MVAR	MVA	MW(NOM)	MVR(NOM)	MW(LOSS)	MVAR(LOSS)	TAP
BUS	Bus1	100.0	1.0474PU	-8.44	TO Bus2	100.0	1	-124.34	-28.32	127.52	0.50	-70.92	
		104.7KV			TO Gen39	100.0	1	124.34	28.32	127.52	0.18	-76.30	
BUS	Bus10	100.0	1.0172PU	-5.43	CKT	MW	MVAR	MVA	MW(NOM)	MVR(NOM)	MW(LOSS)	MVAR(LOSS)	TAP
		101.7KV			TO Bus11	100.0	1	365.25	70.36	371.96	0.54	-1.74	
					TO Bus13	100.0	1	284.75	38.65	287.37	0.32	-4.07	
					TO Gen32	100.0	1	-650.00	-109.01	659.08	0.00	96.14	1.0700FX
BUS	Bus11	100.0	1.0127PU	-6.28	CKT	MW	MVAR	MVA	MW(NOM)	MVR(NOM)	MW(LOSS)	MVAR(LOSS)	TAP
		101.3KV			TO Bus6	100.0	1	364.76	29.01	365.92	0.92	-3.43	
					TO Bus10	100.0	1	-364.71	-72.10	371.77	0.54	-1.74	
					TO Bus12	100.0	1	-0.06	43.09	43.09	0.03	0.79	1.0060UN
BUS	Bus12	100.0	1.0002PU	-6.24	CKT	MW	MVAR	MVA	MW(NOM)	MVR(NOM)	MW(LOSS)	MVAR(LOSS)	TAP
		100.0KV			LOAD						0.03	0.79	1.0060FX
					TO Bus11	100.0	1	0.09	-42.30	42.30			
					TO Bus13	100.0	1	-7.59	-45.70	46.32			
BUS	Bus13	100.0	1.0143PU	-6.10	CKT	MW	MVAR	MVA	MW(NOM)	MVR(NOM)	MW(LOSS)	MVAR(LOSS)	TAP
		101.4KV			TO Bus10	100.0	1	-284.43	-42.72	287.62	0.32	-4.07	
					TO Bus14	100.0	1	276.81	-3.92	276.84	0.67	-10.16	
					TO Bus12	100.0	1	7.62	46.64	47.26	0.03	0.94	1.0060UN
BUS	Bus14	100.0	1.0117PU	-7.66	CKT	MW	MVAR	MVA	MW(NOM)	MVR(NOM)	MW(LOSS)	MVAR(LOSS)	TAP
		101.2KV			TO Bus4	100.0	1	271.01	42.41	274.31	0.59	-4.47	
					TO Bus13	100.0	1	-276.14	-6.23	276.21	0.67	-10.16	
					TO Bus15	100.0	1	5.14	-36.17	36.54	0.01	-37.53	
BUS	Bus15	100.0	1.0154PU	-7.74	CKT	MW	MVAR	MVA	MW(NOM)	MVR(NOM)	MW(LOSS)	MVAR(LOSS)	TAP
		101.5KV			LOAD								
					TO Bus14	100.0	1	320.00	153.00	354.70	0.01	-37.53	
					TO Bus16	100.0	1	-5.13	-1.36	5.31	1.04	-7.02	
BUS	Bus16	100.0	1.0318PU	-6.19	CKT	MW	MVAR	MVA	MW(NOM)	MVR(NOM)	MW(LOSS)	MVAR(LOSS)	TAP
		103.2KV			LOAD								
					TO Bus15	100.0	1	329.00	32.30	330.58	1.04	-7.02	
					TO Bus17	100.0	1	315.91	144.63	347.45	0.36	-9.78	
					TO Bus19	100.0	1	230.04	-43.63	234.14			
					TO Bus21	100.0	1	-502.68	-48.08	504.97	3.81	13.54	
					TO Bus24	100.0	1	-329.60	13.03	329.85	0.82	-13.26	
											0.03	-6.68	
BUS	Bus17	100.0	1.0336PU	-7.30	CKT	MW	MVAR	MVA	MW(NOM)	MVR(NOM)	MW(LOSS)	MVAR(LOSS)	TAP
		103.4KV			TO Bus16	100.0	1	-229.68	33.85	232.16	0.36	-9.78	
					TO Bus18	100.0	1	210.66	9.73	210.88	0.29	-10.63	
					TO Bus27	100.0	1	19.02	-43.58	47.55	0.01	-34.32	
BUS	Bus18	100.0	1.0309PU	-8.22	CKT	MW	MVAR	MVA	MW(NOM)	MVR(NOM)	MW(LOSS)	MVAR(LOSS)	TAP
		103.1KV			LOAD								
					TO Bus3	100.0	1	158.00	30.00	160.82	0.03	-22.36	
					TO Bus17	100.0	1	52.36	-9.64	53.24	0.29	-10.63	
BUS	Bus19	100.0	1.0499PU	-1.02	CKT	MW	MVAR	MVA	MW(NOM)	MVR(NOM)	MW(LOSS)	MVAR(LOSS)	TAP
		105.0KV			TO Bus16	100.0	1	506.49	61.62	510.22	3.81	13.54	
					TO Gen33	100.0	1	-629.10	-51.14	631.18	2.90	58.76	1.0700FX
					TO Bus20	100.0	1	122.62	-10.48	123.06	0.11	2.13	1.0600FX
BUS	Bus2	100.0	1.0487PU	-5.75	CKT	MW	MVAR	MVA	MW(NOM)	MVR(NOM)	MW(LOSS)	MVAR(LOSS)	TAP
		104.9KV			TO Bus1	100.0	1	124.83	-42.60	131.90	0.50	-70.92	
					TO Bus3	100.0	1	364.26	92.24	375.76	1.70	-8.02	
					TO Bus25	100.0	1	-239.09	82.68	252.98	4.16	-11.08	
					TO Gen30	100.0	1	-250.00	-132.32	282.86	0.00	13.83	1.0250FX
BUS	Bus20	100.0	0.9912PU	-2.01	CKT	MW	MVAR	MVA	MW(NOM)	MVR(NOM)	MW(LOSS)	MVAR(LOSS)	TAP
		99.1KV			LOAD								

Figure 7: Contents of file 39bus.out (Page 1 of 4)

39bus.out										
		TO Gen34	100.0 1	-505.49	-115.61	518.54		2.51	50.16	1.0090FX
		TO Bus19	100.0 1	-122.51	12.61	123.15	0.11	2.13	1.0600UN	
BUS Bus21	100.0 1.0318PU 103.2KV	-3.78	CKT	MW	MVAR	MVA	MW(NOM) MVR(NOM)	MW(LOSS)	MVAR(LOSS)	TAP
	LOAD		274.00	115.00	297.15					
	TO Bus16	100.0 1	330.42	-26.29	331.46		0.82	-13.26		
	TO Bus22	100.0 1	-604.42	-88.71	610.89		2.79	21.00		
BUS Bus22	100.0 1.0498PU 105.0KV	0.67	CKT	MW	MVAR	MVA	MW(NOM) MVR(NOM)	MW(LOSS)	MVAR(LOSS)	TAP
	TO Bus21	100.0 1	607.21	109.71	617.04		2.79	21.00		
	TO Bus23	100.0 1	42.80	41.97	59.94		0.02	-19.85		
	TO Gen35	100.0 1	-650.00	-151.68	667.46		0.00	60.73	1.0250FX	
BUS Bus23	100.0 1.0448PU 104.5KV	0.47	CKT	MW	MVAR	MVA	MW(NOM) MVR(NOM)	MW(LOSS)	MVAR(LOSS)	TAP
	LOAD		247.50	84.60	261.56					
	TO Bus22	100.0 1	-42.77	-61.82	75.17		0.02	-19.85		
	TO Bus24	100.0 1	353.84	0.51	353.84		2.53	1.15		
	TO Gen36	100.0 1	-558.57	-23.30	559.05		1.43	77.88	1.0000FX	
BUS Bus24	100.0 1.0373PU 103.7KV	-6.07	CKT	MW	MVAR	MVA	MW(NOM) MVR(NOM)	MW(LOSS)	MVAR(LOSS)	TAP
	LOAD		308.60	-92.20	322.08					
	TO Bus16	100.0 1	42.71	91.56	101.04		0.03	-6.68		
	TO Bus23	100.0 1	-351.31	0.64	351.31		2.53	1.15		
BUS Bus25	100.0 1.0576PU 105.8KV	-4.36	CKT	MW	MVAR	MVA	MW(NOM) MVR(NOM)	MW(LOSS)	MVAR(LOSS)	TAP
	LOAD		224.00	47.20	228.92					
	TO Bus2	100.0 1	243.25	-93.76	260.70		4.16	-11.08		
	TO Bus26	100.0 1	71.09	-17.04	73.10		0.15	-55.58		
	TO Gen37	100.0 1	-538.34	63.60	542.09		1.66	64.04	1.0250FX	
BUS Bus26	100.0 1.0521PU 105.2KV	-5.53	CKT	MW	MVAR	MVA	MW(NOM) MVR(NOM)	MW(LOSS)	MVAR(LOSS)	TAP
	LOAD		139.00	17.00	140.04					
	TO Bus25	100.0 1	-70.94	-38.54	80.73		0.15	-55.58		
	TO Bus27	100.0 1	262.95	68.67	271.77		0.96	-16.09		
	TO Bus28	100.0 1	-140.83	-21.69	142.49		0.79	-77.51		
	TO Bus29	100.0 1	-190.18	-25.44	191.88		1.91	-92.68		
BUS Bus27	100.0 1.0377PU 103.8KV	-7.50	CKT	MW	MVAR	MVA	MW(NOM) MVR(NOM)	MW(LOSS)	MVAR(LOSS)	TAP
	LOAD		281.00	75.50	290.97					
	TO Bus17	100.0 1	-19.01	9.26	21.14		0.01	-34.32		
	TO Bus26	100.0 1	-261.99	-84.76	275.36		0.96	-16.09		
BUS Bus28	100.0 1.0501PU 105.0KV	-2.01	CKT	MW	MVAR	MVA	MW(NOM) MVR(NOM)	MW(LOSS)	MVAR(LOSS)	TAP
	LOAD		206.00	27.60	207.84					
	TO Bus26	100.0 1	141.61	-55.82	152.22		0.79	-77.51		
	TO Bus29	100.0 1	-347.61	28.22	348.76		1.56	-10.67		
BUS Bus29	100.0 1.0499PU 105.0KV	0.74	CKT	MW	MVAR	MVA	MW(NOM) MVR(NOM)	MW(LOSS)	MVAR(LOSS)	TAP
	LOAD		283.50	26.90	284.77					
	TO Bus26	100.0 1	192.10	-67.24	203.53		1.91	-92.68		
	TO Bus28	100.0 1	349.17	-38.88	351.33		1.56	-10.67		
	TO Gen38	100.0 1	-824.77	79.23	828.56		5.23	102.07	1.0250FX	
BUS Bus3	100.0 1.0302PU 103.0KV	-8.60	CKT	MW	MVAR	MVA	MW(NOM) MVR(NOM)	MW(LOSS)	MVAR(LOSS)	TAP
	LOAD		322.00	2.40	322.01					
	TO Bus2	100.0 1	-362.56	-100.26	376.16		1.70	-8.02		
	TO Bus4	100.0 1	92.89	110.58	144.42		0.29	-18.17		
	TO Bus18	100.0 1	-52.33	-12.72	53.86		0.03	-22.36		
BUS Bus4	100.0 1.0039PU 100.4KV	-9.61	CKT	MW	MVAR	MVA	MW(NOM) MVR(NOM)	MW(LOSS)	MVAR(LOSS)	TAP
	LOAD		500.00	184.00	532.78					
	TO Bus3	100.0 1	-92.60	-128.75	158.59		0.29	-18.17		
	TO Bus5	100.0 1	-136.98	-8.37	137.24		0.15	-11.16		
	TO Bus14	100.0 1	-270.41	-46.88	274.45		0.59	-4.47		
BUS Bus5	100.0 1.0053PU 100.5KV	-8.61	CKT	MW	MVAR	MVA	MW(NOM) MVR(NOM)	MW(LOSS)	MVAR(LOSS)	TAP
	TO Bus4	100.0 1	137.13	-2.79	137.16		0.15	-11.16		
	TO Bus6	100.0 1	-454.42	-55.95	457.85		0.41	0.99		
	TO Bus8	100.0 1	317.29	58.74	322.68		0.83	-3.14		

39bus.out													
BUS	Bus	100.0	1.0077PU	-7.95	CKT	MW	MVAR	MVA	MW(NOM)	MVR(NOM)	MW(LOSS)	MVAR(LOSS)	TAP
		100.8KV			TO Bus5	100.0 1	454.84	56.94	458.39		0.41	0.99	
					TO Bus7	100.0 1	420.62	91.57	430.47		1.10	5.53	
					TO Bus11	100.0 1	-363.85	-32.44	365.29		0.92	-3.43	
					TO Gen31	100.0 1	-511.61	-116.07	524.61		0.00	77.58	1.0700FX
		100.0	0.9970PU	-10.12	CKT	MW	MVAR	MVA	MW(NOM)	MVR(NOM)	MW(LOSS)	MVAR(LOSS)	TAP
		99.7KV			LOAD	233.80	84.00	248.43					
					TO Bus6	100.0 1	-419.52	-86.04	428.25		1.10	5.53	
					TO Bus8	100.0 1	185.72	2.04	185.73		0.14	-6.15	
		100.0	0.9960PU	-10.62	CKT	MW	MVAR	MVA	MW(NOM)	MVR(NOM)	MW(LOSS)	MVAR(LOSS)	TAP
		99.6KV			LOAD	522.00	176.00	550.87					
					TO Bus5	100.0 1	-316.46	-61.88	322.45		0.83	-3.14	
					TO Bus7	100.0 1	-185.58	-8.19	185.76		0.14	-6.15	
					TO Bus9	100.0 1	-19.96	-105.94	107.80		0.18	-36.06	
		100.0	1.0282PU	-10.32	CKT	MW	MVAR	MVA	MW(NOM)	MVR(NOM)	MW(LOSS)	MVAR(LOSS)	TAP
		102.8KV			TO Bus8	100.0 1	20.15	69.88	72.73		0.18	-36.06	
					TO Gen39	100.0 1	-20.15	-69.88	72.73		0.00	-126.98	
		100.0	1.0475PU	-3.33	CKT	MW	MVAR	MVA	MW(NOM)	MVR(NOM)	MW(LOSS)	MVAR(LOSS)	TAP
		104.8KV			GENERATION	250.00	146.16	289.59	(250.00	0.00)			
					TO Bus2	100.0 1	250.00	146.16	289.59		0.00	13.83	1.0250UN
		100.0	0.9820PU	0.00	CKT	MW	MVAR	MVA	MW(NOM)	MVR(NOM)	MW(LOSS)	MVAR(LOSS)	TAP
		98.2KV			LOAD	9.20	4.60	10.29					
					GENERATION	520.81	198.25	557.27	(0.00	0.00)			
					TO Bus6	100.0 1	511.61	193.65	547.03		0.00	77.58	1.0700UN
		100.0	0.9831PU	2.57	CKT	MW	MVAR	MVA	MW(NOM)	MVR(NOM)	MW(LOSS)	MVAR(LOSS)	TAP
		98.3KV			GENERATION	650.00	205.15	681.60	(650.00	0.00)			
					TO Bus10	100.0 1	650.00	205.15	681.60		0.00	96.14	1.0700UN
		100.0	0.9972PU	4.19	CKT	MW	MVAR	MVA	MW(NOM)	MVR(NOM)	MW(LOSS)	MVAR(LOSS)	TAP
		99.7KV			GENERATION	632.00	109.91	641.49	(632.00	0.00)			
					TO Bus19	100.0 1	632.00	109.91	641.49		2.90	58.76	1.0700UN
		100.0	1.0123PU	3.18	CKT	MW	MVAR	MVA	MW(NOM)	MVR(NOM)	MW(LOSS)	MVAR(LOSS)	TAP
		101.2KV			GENERATION	508.00	165.76	534.36	(508.00	0.00)			
					TO Bus20	100.0 1	508.00	165.76	534.36		2.51	50.16	1.0090UN
		100.0	1.0493PU	5.63	CKT	MW	MVAR	MVA	MW(NOM)	MVR(NOM)	MW(LOSS)	MVAR(LOSS)	TAP
		104.9KV			GENERATION	650.00	212.41	683.83	(650.00	0.00)			
					TO Bus22	100.0 1	650.00	212.41	683.83		0.00	60.73	1.0250UN
		100.0	1.0635PU	8.32	CKT	MW	MVAR	MVA	MW(NOM)	MVR(NOM)	MW(LOSS)	MVAR(LOSS)	TAP
		106.4KV			GENERATION	560.00	101.17	569.07	(560.00	0.00)			
					TO Bus23	100.0 1	560.00	101.17	569.07		1.43	77.88	1.0000UN
		100.0	1.0278PU	2.42	CKT	MW	MVAR	MVA	MW(NOM)	MVR(NOM)	MW(LOSS)	MVAR(LOSS)	TAP
		102.8KV			GENERATION	540.00	0.44	540.00	(540.00	0.00)			
					TO Bus25	100.0 1	540.00	0.44	540.00		1.66	64.04	1.0250UN
		100.0	1.0265PU	7.81	CKT	MW	MVAR	MVA	MW(NOM)	MVR(NOM)	MW(LOSS)	MVAR(LOSS)	TAP
		102.6KV			GENERATION	830.00	22.84	830.31	(830.00	0.00)			
					TO Bus29	100.0 1	830.00	22.84	830.31		5.23	102.07	1.0250UN
		100.0	1.0300PU	-10.05	CKT	MW	MVAR	MVA	MW(NOM)	MVR(NOM)	MW(LOSS)	MVAR(LOSS)	TAP
		103.0KV			LOAD	1104.00	250.00	1131.95					
					GENERATION	1000.00	88.28	1003.89	(1000.00	0.00)			
					TO Bus1	100.0 1	-124.15	-104.61	162.35		0.18	-76.30	
					TO Bus9	100.0 1	20.15	-57.10	60.56		0.00	-126.98	

SYSTEM TOTALS

39bus.out

	MW	MVAR
GENERATION	6140.81	1250.37
LOAD	6097.10	1408.90
LOSSES	43.71	-158.52
BUS SHUNTS	0.00	0.00
LINE SHUNTS	0.00	0.00
SWITCHED SHUNTS		0.00
IMSMATCH	0.00	0.01

BASE MVA : 100.0
TOLERANCE: 0.000100 PU

SLACK BUSES

Gen31 100.0

References

- [1] T. Athay, R. Podmore, and S. Virmani. "A Practical Method for the Direct Analysis of Transient Stability". In: *IEEE Transactions on Power Apparatus and Systems* PAS-98 (2 Mar. 1979), pp. 573–584.
- [2] M. A. Pai. *Energy function analysis for power system stability*. The Kluwer international series in engineering and computer science. Power electronics and power systems. Boston: Kluwer Academic Publishers, 1989.
- [3] Peter W Sauer and M. A Pai. *Power system dynamics and stability*. English. Champaign, IL.: Stipes Publishing L.L.C., 2006.

E.1

Appendix E - Report on the New England Test System by Luc Gerin-Lajoie

IEEE PES Task Force on Benchmark Systems for Stability Controls

Report on the EMTP-RV 39-bus system

(New England Reduced Model)

Version 1.5 - Mars 04, 2015

Author: Luc Gérin-Lajoie

Contributor: O. Saad, J. Mahseredjian

The present report refers to a small-signal stability study carried over the New England reduced order model using the EMTP-RV package. This report has the objective to show how the simulation of this system must be done using this package in order to get results that are comparable (and exhibit a good match with respect to the electromechanical modes). To facilitate the comprehension, this report is divided in three sections (according to the software to be used):

- Load Flow ;
- Time Domain Simulation of the Nonlinear Model;

To use the EMTP-RV software, a GUI (EMTPWorks) is requiring to entering data. All components as line, transformer, load, machine and AVR have them own data forms.

Transformer and synchronous machines use mainly units in pu. Line, load and all others S.I. unit (Ω , H, F, W, VAR or Wb). Consequently some assumptions for impedance translations are required.

1. Models and parameters

1.1 Line

Two line components are used in this benchmark: Constant Parameter Line (Ω/km) and PI(Ω). Both use direct and zero sequence impedance; CP line require length. From the p.u. unit, the flowing assumptions are defined for these two components in EMTP.

$$R_0/R_1=10, L_0/L_1=3, B_0/B_1=0,6 \text{ and } L_1(\text{ohm})/\text{km} = 0,373$$

For simplification aspect, except one or two all the 500kV lines use the same Z_1 and Z_0 / km based on the line2-3; only the lengths are different to respect de X_1 parameter. The parameters are documented in Appendix A.

1.2 Generator transformers

The transformer rated power and impedances are change as following. The voltages ratio are 500/20 kV for all transformers of the machines and 500/25 kV for the two 450MVA transformers of the loads.

		Rated Power	R	X	Rated Power	R	X
12	11	100	0.0016	0.0435	450	0.0072	0.196
12	13	100	0.0016	0.0435	450	0.0072	0.196
6	31	100	0	0.025	1000	0	0.250
10	32	100	0	0.02	1000	0	0.200
19	33	100	0.0007	0.0142	1000	0.007	0.142
20	34	100	0.0009	0.018	600	0.0054	0.108
22	35	100	0	0.0143	1000	0	0.143
23	36	100	0.0005	0.0272	1000	0.005	0.272
25	37	100	0.0006	0.0232	1000	0.006	0.232
2	30	100	0	0.0181	1000	0	0.181
29	38	100	0.0008	0.0156	1000	0.008	0.156
19	20	100	0.0007	0.0138	1400	0.0098	0.1932

1.3 Loads

In time-domain, this load model is an exponential load [1]. A controlled current source gives power in parallel of the R-L component to satisfy the equations bellow.

$$P(t) = P_{ic} \left(\frac{V(t)}{V_{ic}} \right)^{K_{pv}} (1 + K_{pf} \Delta f) \frac{(1 + T_{p1}s)}{(1 + T_{p2}s)}$$

Load39

$$Q(t) = Q_{ic} \left(\frac{V(t)}{V_{ic}} \right)^{K_{qv}} (1 + K_{qf} \Delta f) \frac{(1 + T_{q1}s)}{(1 + T_{q2}s)}$$

Expon  LF

The parameters are unique for all loads:

// Static behavior

Kpv = 1, Kqv = 1.8, Kpf = 0, Kqf = 0

// Dynamic behavior

Tp1 = 0, Tp2 = 0, Tq1 = 0, Tq2 = 0

1.4 Generators

The 39-bus system is composed by 10 generators, and all of them are represented by a synchronous machine (SM). The help document of this component is given in Appendix. The connection in the drawing between the LF-device, SM and theirs AVR is as bellow. The power ratings of the machine are changed. The 100MVA value cannot be used in time-domain when LF-device asks 500MW. The table 3 indicates the news values.

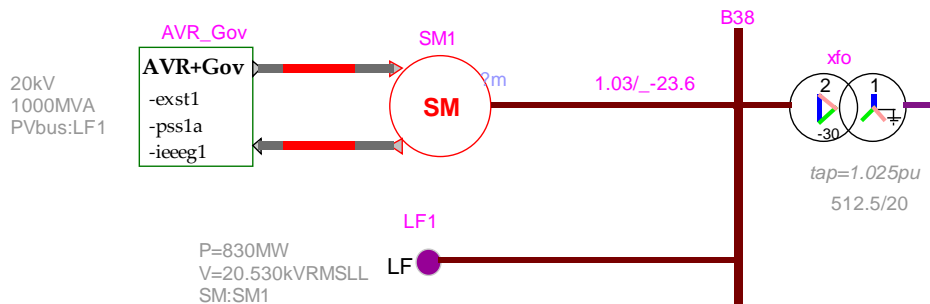


Figure 1- Connection in EMTPWorks for LF-device, SM/AVR and transformer

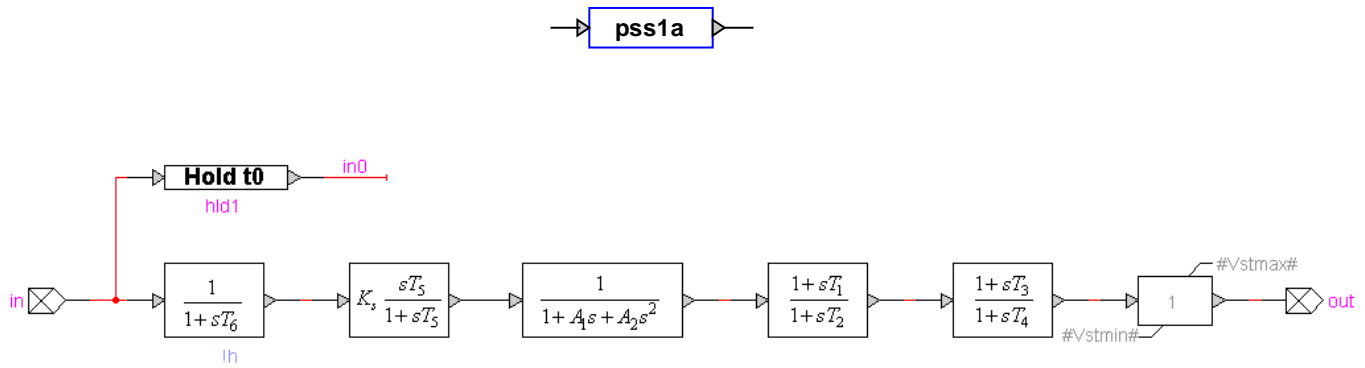
Table 3: Generator parameters

Unit No.	Rated Power	H	R _a	x' _d	x' _q	x _d	x _q	T' _{do}	T' _{qo}	x _l
1	10000	5.000	0.000	0.600	0.800	2.000	1.900	7.000	0.700	0.300
2	1000	3.030	0.000	0.697	1.700	2.950	2.820	6.560	1.500	0.350
3	1000	3.580	0.000	0.531	0.876	2.495	2.370	5.700	1.500	0.304
4	1000	2.860	0.000	0.436	1.660	2.620	2.580	5.690	1.500	0.295
5	600	4.333	0.000	0.792	0.996	4.020	3.720	5.400	0.440	0.324
6	1000	3.480	0.000	0.500	0.814	2.540	2.410	7.300	0.400	0.224
7	1000	2.640	0.000	0.490	1.860	2.950	2.920	5.660	1.500	0.322
8	1000	2.430	0.000	0.570	0.911	2.900	2.800	6.700	0.410	0.280
9	1000	3.450	0.000	0.570	0.587	2.106	2.050	4.790	1.960	0.298
10	1000	4.200	0.000	0.310	0.080	1.000	0.690	10.200	0.000	0.125

1.5 Controllers

All generators in this system are equipped with automatic voltage regulators [2], power system stabilizers [2] and governor [3]. The governor doesn't change the mechanical power P_m during fault and after. They will work only if perturbation is a load or generator disconnection. These generators use the same controller model, only altering the corresponding parameter values according to the specifications given in the website.

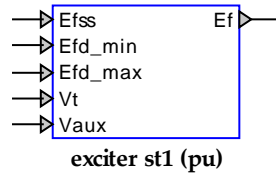
1.5.1 PSS – pss1a



Reference : IEEE std 421.5 1992, chap. 8 Power System Stabilizers PSS1A

Figure 2- PSS1a control schema in EMTPWorks

1.5.2 Voltage regulator (exc ST1)



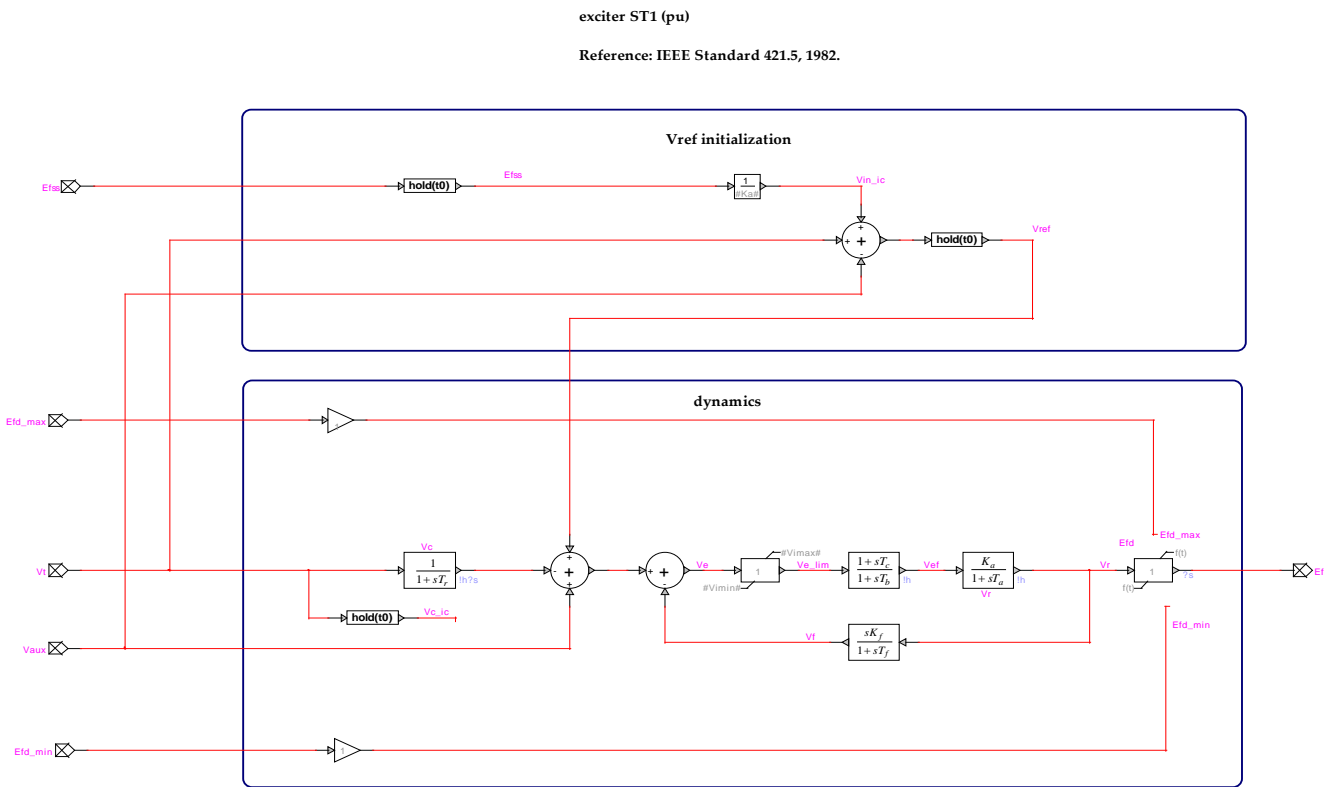


Figure 3– EXCST1 control schema in EMTPWorks

1.5.3 Governor – ieeeg1

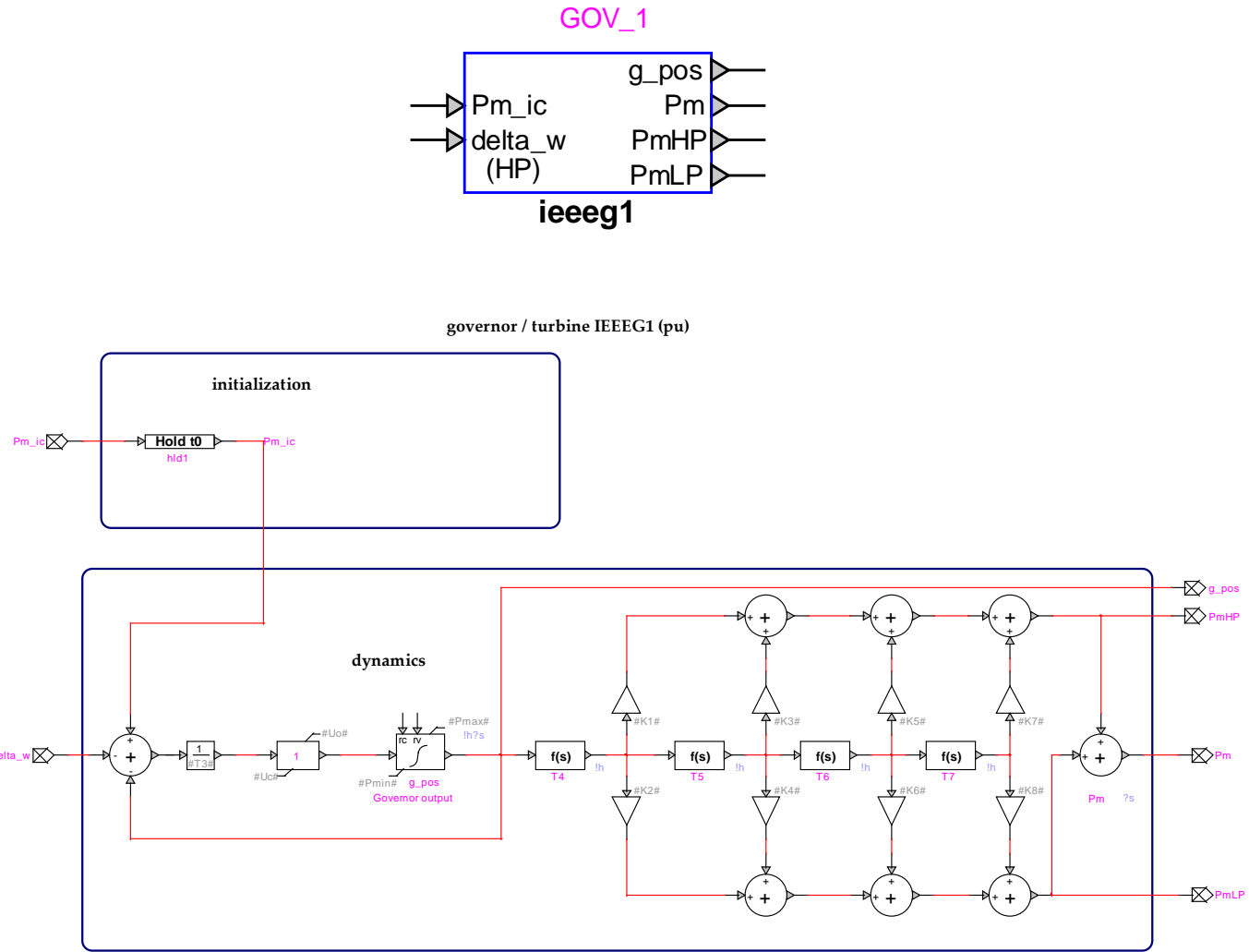


Figure 4– IEEEG1 control schema in EMTPWorks

1.5.4 AVR/GOV parameters

The parameters are documented in Appendix B. The governor parameters-set is unique for all machines.

2. Results

2.1 Load Flow

The load flow of the 39-bus system was calculated using the EMTP-RV software. The electrical network equations are solved using complex phasors. The active (source) devices are only the Load-Flow devices (LF-devices). They could be Slack, PQ or PV. A load device is used to enter PQ load constraint equations, np and nq could be set between 0 and 2. For the present case, np=nq=0 (constant power).

2.1.1 Generator

Table 1: Results of the load flow calculation for the generators

Reference Case			EMTP			
Unit No.	P(MW)	V(pu)	P(MW)	V(kVRMSLL)	Q(MVAR)	Bus id
1	1000.0	1.030	1000.00	1.03	222.0	39
2 (slack)	520.8	0.982	539.41	0.98	254.0	31
3	650.0	0.983	650.00	0.98	260.0	32
4	632.0	0.997	632.00	1.00	147.0	33
5	508.0	1.012	508.00	1.01	203.0	34
6	650.0	1.049	650.00	1.05	255.0	35
7	560.0	1.064	560.00	1.06	135.0	36
8	540.0	1.028	540.00	1.03	38.0	37
9	830.0	1.027	830.00	1.03	76.0	38
10	250.0	1.048	250.00	1.04	178.0	30

2.1.2 Bus

The results obtained by this load flow calculation can be analyzed from 2. It is shows on the drawing too. When comparing these results to the ones provided in the website, it is possible to observe a very good match between them. Note the 30° differences caused by the Yd transformers.

Table 2: Results of the load flow calculation for the bus.

Bus	Reference Case		EMTP	
	V [PU]	Angle [deg]	V1 [PU]	Angle [deg]
1	1.047	-8.44	1.04	-9.8
2	1.049	-5.75	1.04	-7.1
3	1.030	-8.60	1.01	-9.9
4	1.004	-9.61	0.98	-10.8
5	1.005	-8.61	0.99	-9.6
6	1.008	-7.95	0.99	-8.9
7	0.997	-10.12	0.98	-11.2
8	0.996	-10.62	0.98	-11.7
9	1.028	-10.32	1.02	-11.6
10	1.017	-5.43	1.00	-6.4
11	1.013	-6.28	1.00	-7.2
12	1.000	-6.24	0.97	-37.3
13	1.014	-6.10	1.00	-7.1
14	1.012	-7.66	0.99	-8.8
15	1.015	-7.74	1.00	-9.1
16	1.032	-6.19	1.02	-7.6
17	1.034	-7.30	1.02	8.7
18	1.031	-8.22	1.01	-9.6
19	1.050	-1.02	1.04	-2.4
20	0.991	-2.01	0.98	-3.4
21	1.032	-3.78	1.02	-5.1
22	1.050	0.67	1.04	-0.7
23	1.045	0.47	1.04	-0.9
24	1.037	-6.07	1.02	-7.5
25	1.058	-4.36	1.05	-5.7
26	1.052	-5.53	1.04	-6.9
27	1.038	-7.50	1.02	-8.9
28	1.050	-2.01	1.04	-3.4
29	1.050	0.74	1.04	-0.7

2.2 Time-domain solution

Steady-state solution. The electrical network equations are solved using complex phasors. All devices are given a lumped circuit model. This option can be used in the stand-alone mode or for initializing the time-domain solution. The control system devices are disconnected and not solved. Some nonlinear devices are linearized or disconnected. All devices have a specific steady state model.

Time-domain solution. The electrical network and control system equations are solved using a numerical integration technique. All nonlinear devices are solved simultaneously with network equations. A Newton method is used when nonlinear devices exist. The solution can optionally start from the steady-state solution for initializing the network variables and achieving quick steady-state conditions in time-domain waveforms. The steady-state conditions provide the solution for the time-point $t=0$. The user can also optionally manually initialize state-variables. The first time-domain solution is found at $t = \Delta t$ or $t = \Delta t / 2$ depending on the selected numerical integration method explained below.

The time-domain solution in EMTP-RV is performed after the Load-flow solution and the Steady-State Solution. That give a perfect three phases solution at $0+$. The total simulation time was 20 s and the integration step was $100 \mu\text{s}$

2.2.1 Perturbation

The applied perturbation was a three-phase-to-ground fault at bus 16, on $t = 0.5$ s, with a fault impedance of 1.0Ω and a duration of 0,1 s.

2.2.2 Output request

The angle of generator 1 (placed at bus 39) was taken as a reference for angle differences. Electric power (P_e), Field voltage (E_{fd}), the output of PSS (Vaux) and Omega are also showed.

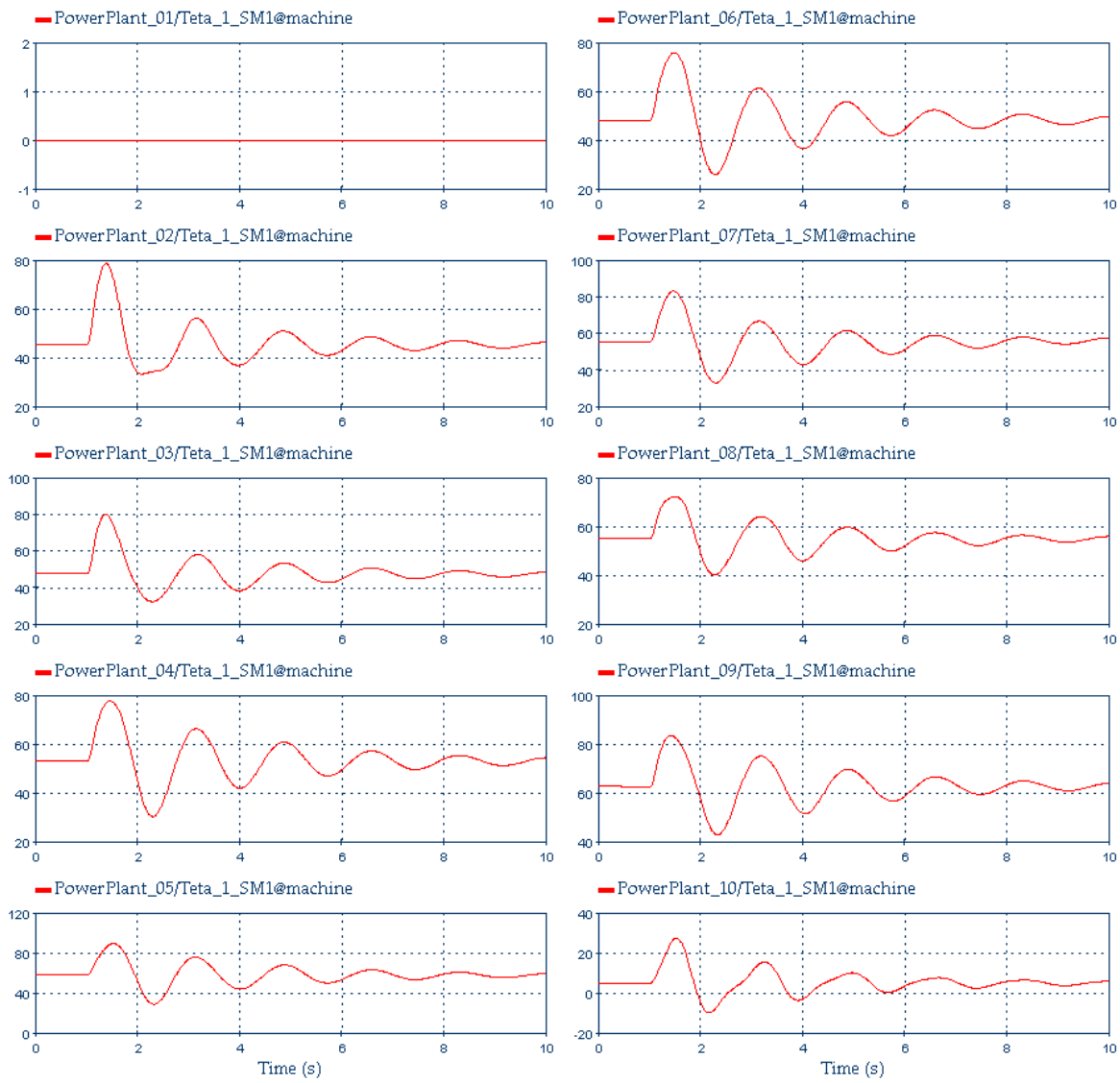


Figure 5 - Rotor angles of generators 1 to 10 respectively, referenced to generator 1.

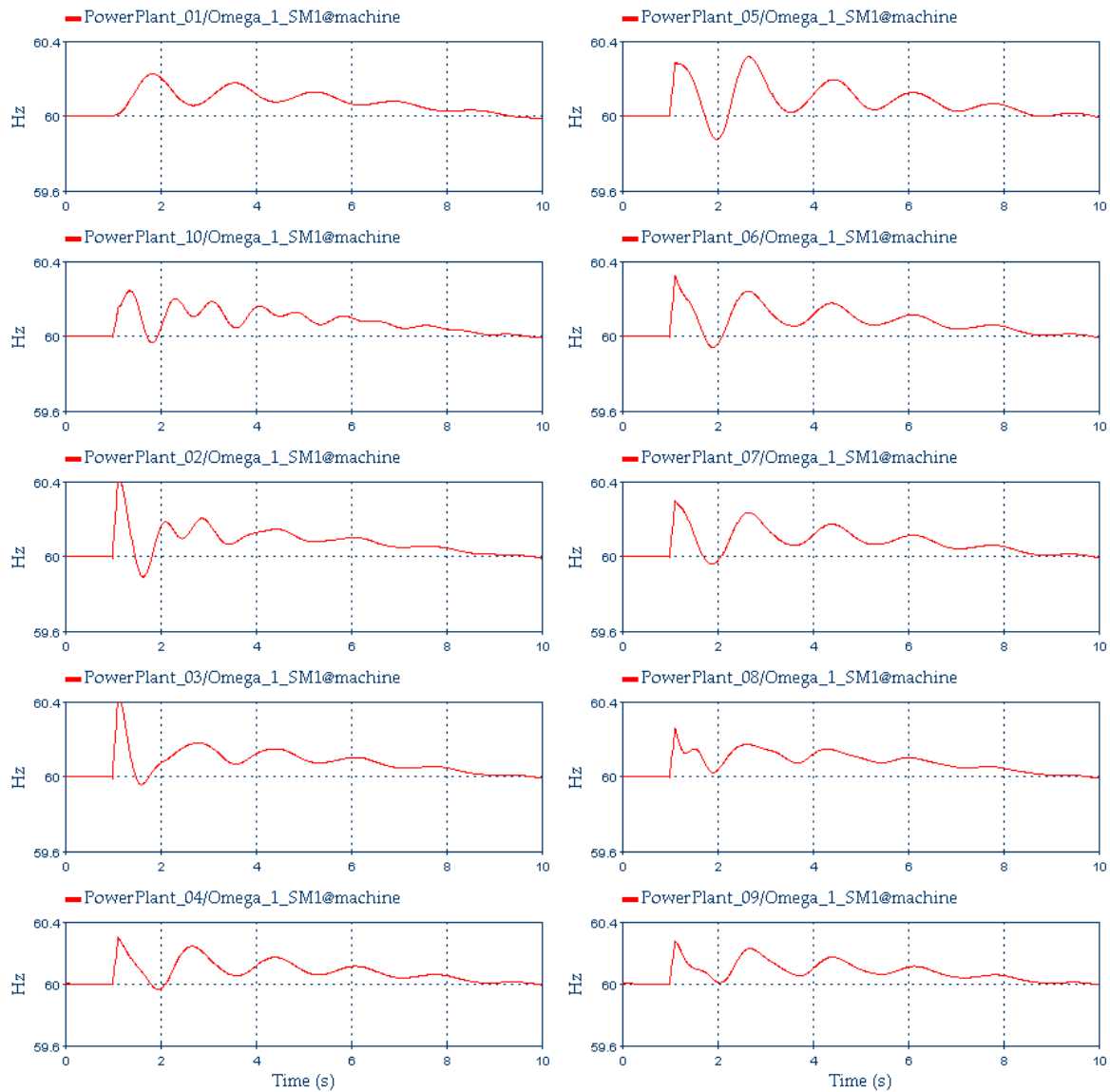


Figure 6 - Rotor speed.

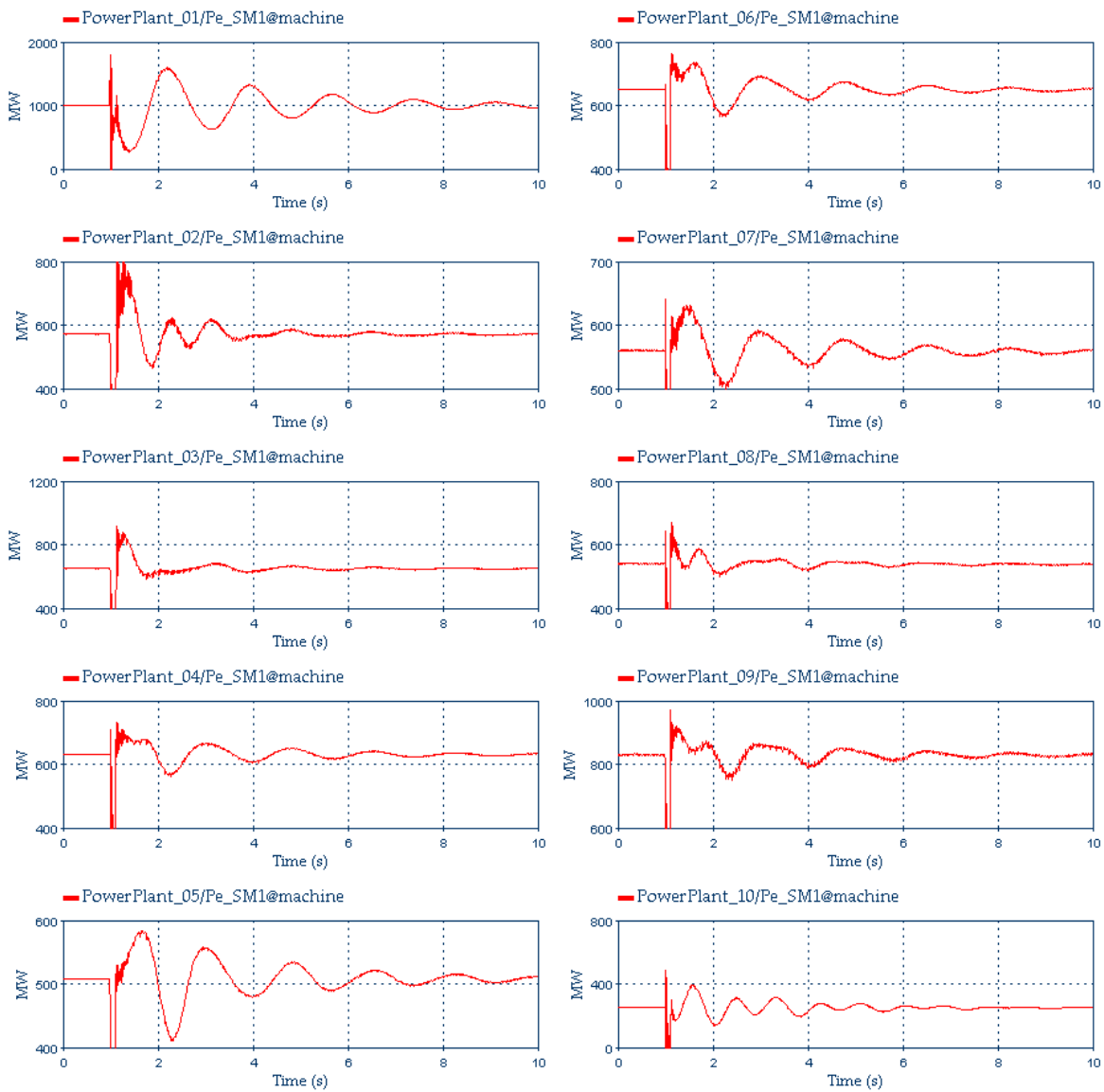


Figure 7 – Total electric power.

2.3 Modal analysis

The modal analysis is performed for the number of ten synchronous machines from small-signal perturbations results in time-domain [1]. These curves were imported in MATLAB to perform $[A, B, C, D]$ state-space matrices with minimum acceptable error. The input V_s (PSS output) which is added to V_{ref} and the output P_e are the transfer function of the state-space system. The superimposed results below confirms the *quality* in term of calibration of the state-space matrices. Note that the system is not a total of ten individual SISO (Single Input Single Output) but one MIMO (Multiple Input Multiple Output) including oscillations mode between synchronous machines.

With the validated state-space matrices, for each synchronous machine a Bode Diagram is generated as shown in the Figure 9. Afterword for each main oscillations mode, eight in this case, the polar plots are generated according to the observable and controllable vectors (see Figure 10). These plots indicate which machine take the lead in term of effect on the oscillation mode.

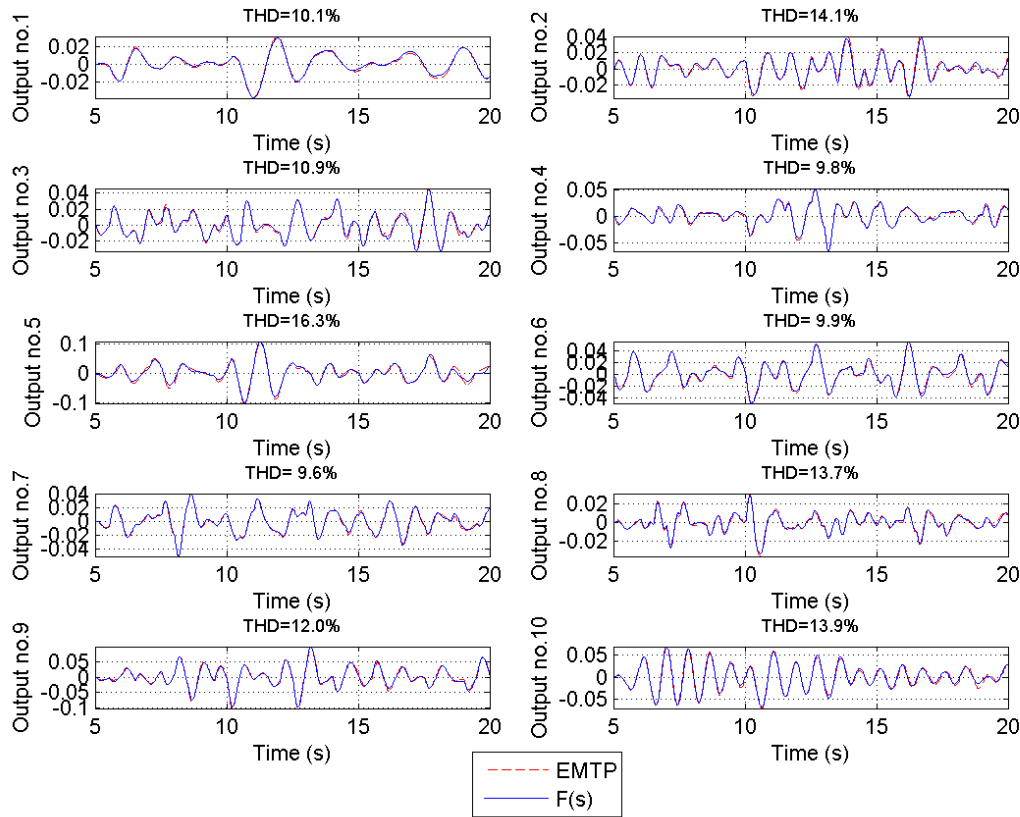
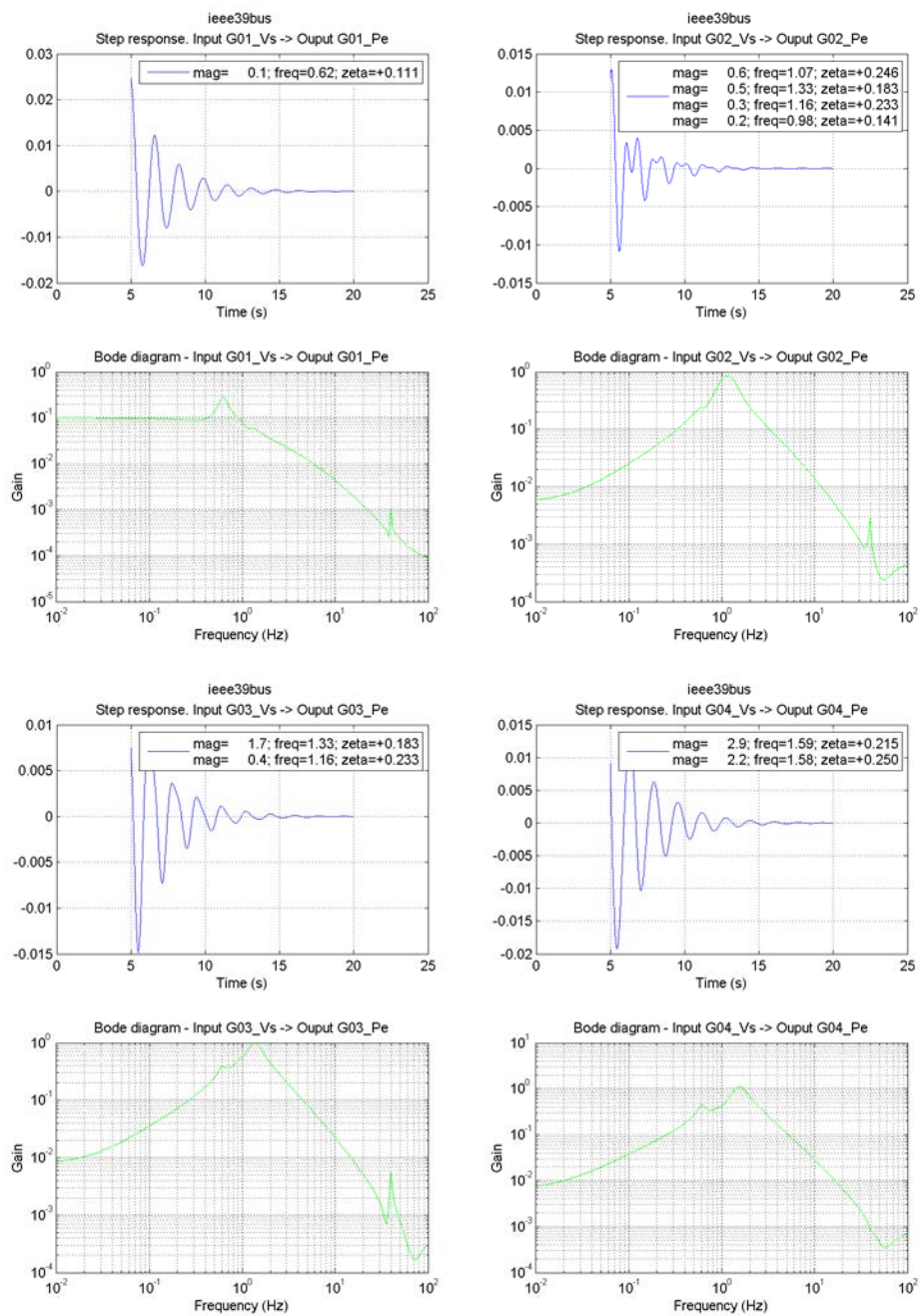
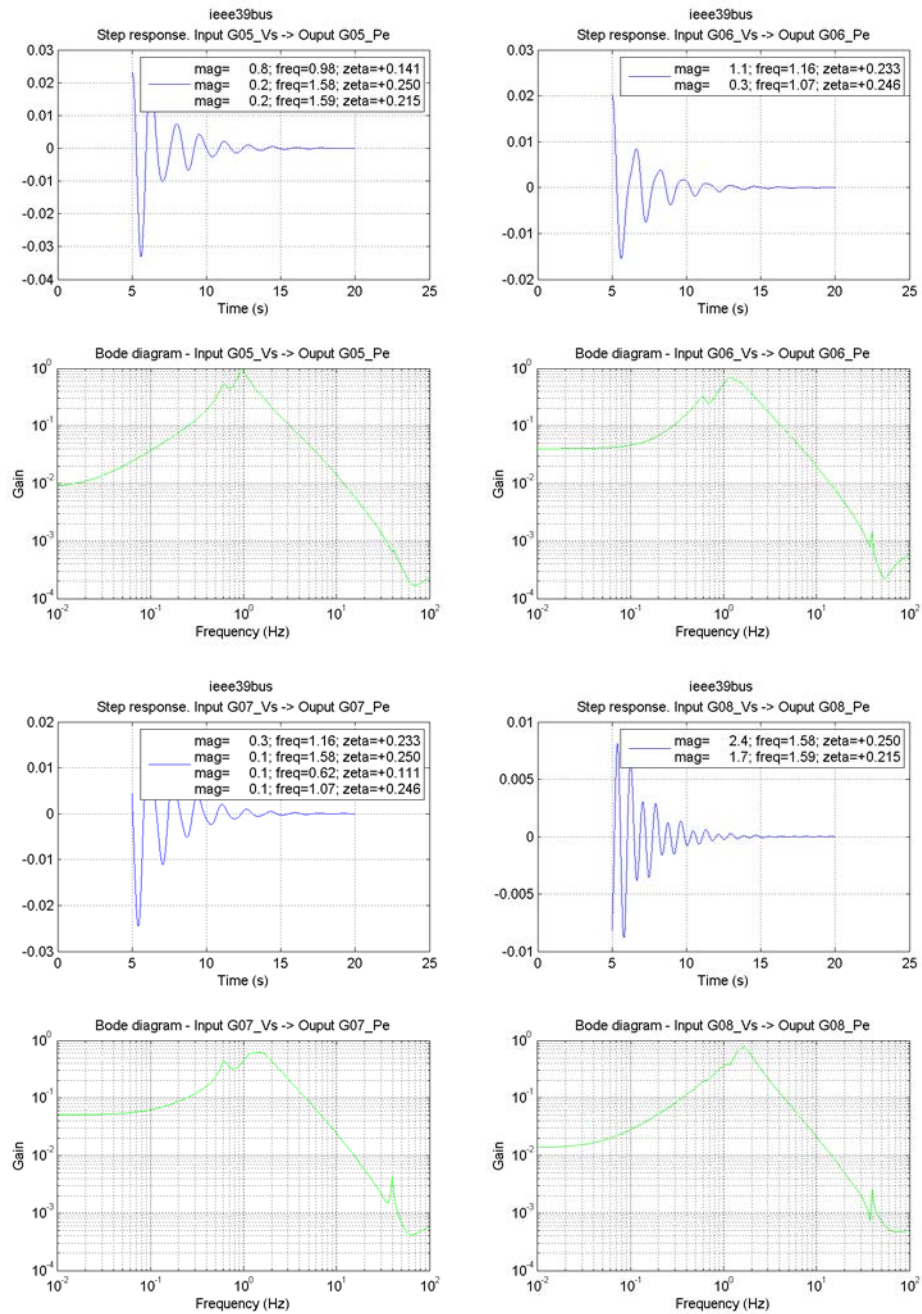


Figure 8 – Comparison of EMTP and state-space matrices

1. L. Gérin-Lajoie. *Plant Identification and tuning controls – An EMTP case*. Presented at the Internal Conference on Power Systems Transient (IPST'09) in Kyoto, Japan, 2009.





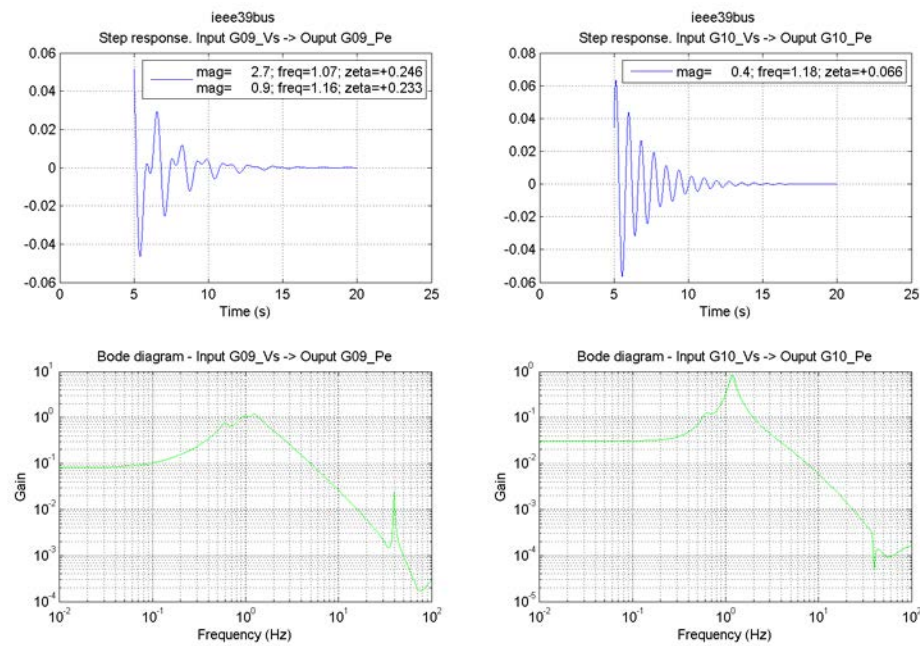
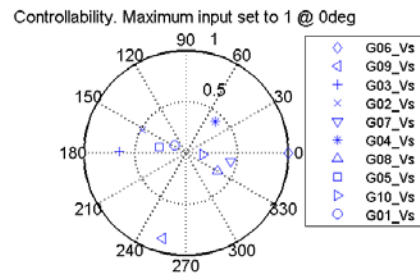
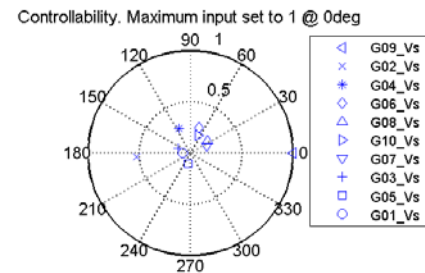
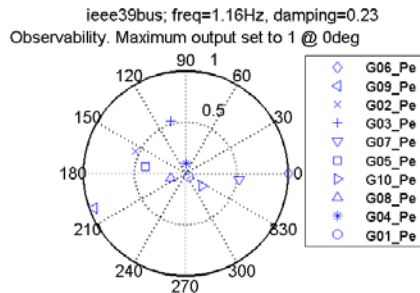
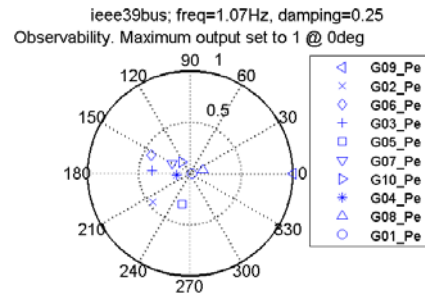
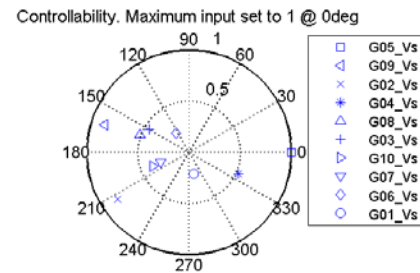
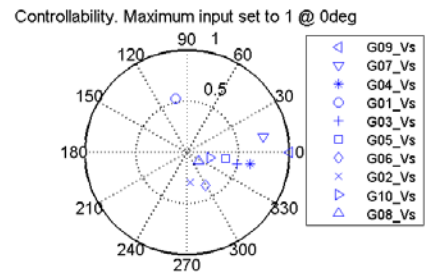
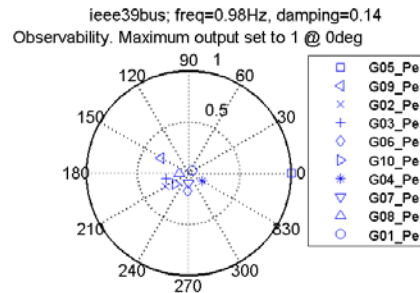
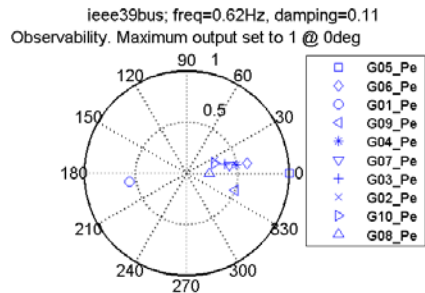


Figure 9 – Impulse response and Bode diagram for each generator.



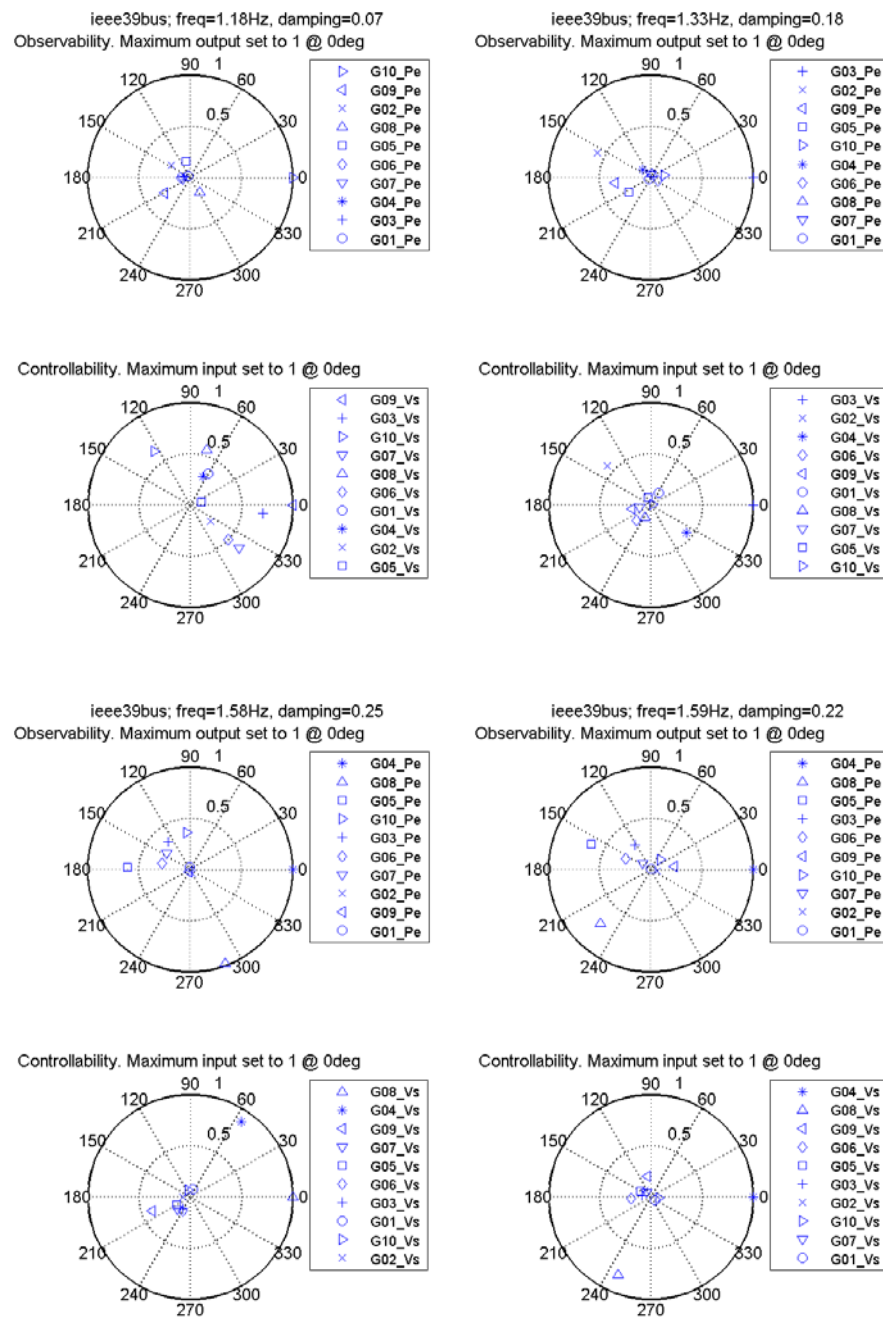


Figure 10 – Polar observability and controllability plots for the principal modes.

3. Conclusions

A benchmark of the 39bus system in EMTP-RV was developing for this TF. The results seem very close to the originals dynamics results.

This benchmark in EMTP-RV / EMTPWorks may perform all these study type:

- Drawing, what you see is what you get.
- Power device
- Control device
- Load-Flow
- Stability with the three sequence admittance
- Short-circuit analysis

Appendix A – lines data

		R1(pu)	X1(pu)	B1(pu)	km	R1(ohm/km)	X1(ohm/km)	B1(uS/km)	R0(ohm/km)	X0(ohm/km)	B0(uS/km)
1	2	0.0035	0.0411	0.6987	275.5	0.032	0.373	1.015	0.318	1.119	0.609
1	39	0.001	0.025	0.75	167.6	0.015	0.373	1.790	0.149	1.119	1.074
2	3	0.0013	0.0151	0.2572	101.2	0.032	0.373	1.017	0.321	1.119	0.610
2	25	0.007	0.0086	0.146	57.6	0.304	0.373	1.013	3.036	1.119	0.608
3	4	0.0013	0.0213	0.2214	142.8	0.023	0.373	0.620	0.228	1.119	0.372
3	18	0.0011	0.0133	0.2138	89.1	0.031	0.373	0.959	0.308	1.119	0.576
4	5	0.0008	0.0128	0.1342	85.8	0.023	0.373	0.626	0.233	1.119	0.375
4	14	0.0008	0.0129	0.1382	86.5	0.023	0.373	0.639	0.231	1.119	0.384
5	6	0.0002	0.0026	0.0434	17.4	0.029	0.373	0.996	0.287	1.119	0.598
5	8	0.0008	0.0112	0.1476	75.1	0.027	0.373	0.786	0.266	1.119	0.472
6	7	0.0006	0.0092	0.113	61.7	0.024	0.373	0.733	0.243	1.119	0.440
6	11	0.0007	0.0082	0.1389	55.0	0.032	0.373	1.011	0.318	1.119	0.607
7	8	0.0004	0.0046	0.078	30.8	0.032	0.373	1.012	0.324	1.119	0.607
8	9	0.0023	0.0363	0.3804	243.3	0.024	0.373	0.625	0.236	1.119	0.375
9	39	0.001	0.025	1.2	167.6	0.015	0.373	2.865	0.149	1.119	1.719
10	11	0.0004	0.0043	0.0729	28.8	0.035	0.373	1.012	0.347	1.119	0.607
10	13	0.0004	0.0043	0.0729	28.8	0.035	0.373	1.012	0.347	1.119	0.607
13	14	0.0009	0.0101	0.1723	67.7	0.033	0.373	1.018	0.332	1.119	0.611
14	15	0.0018	0.0217	0.366	145.4	0.031	0.373	1.007	0.309	1.119	0.604
15	16	0.0009	0.0094	0.171	63.0	0.036	0.373	1.086	0.357	1.119	0.651

16	17	0.0007	0.0089	0.1342	59.7	0.029	0.373	0.900	0.293	1.119	0.540
16	19	0.0016	0.0195	0.304	130.7	0.031	0.373	0.930	0.306	1.119	0.558
16	21	0.0008	0.0135	0.2548	90.5	0.022	0.373	1.126	0.221	1.119	0.676
16	24	0.0003	0.0059	0.068	39.5	0.019	0.373	0.688	0.190	1.119	0.413
17	18	0.0007	0.0082	0.1319	55.0	0.032	0.373	0.960	0.318	1.119	0.576
17	27	0.0013	0.0173	0.3216	116.0	0.028	0.373	1.109	0.280	1.119	0.666
21	22	0.0008	0.014	0.2565	93.8	0.021	0.373	1.093	0.213	1.119	0.656
22	23	0.0006	0.0096	0.1846	64.3	0.023	0.373	1.148	0.233	1.119	0.689
23	24	0.0022	0.035	0.361	234.6	0.023	0.373	0.616	0.234	1.119	0.369
25	26	0.0032	0.0323	0.513	216.5	0.037	0.373	0.948	0.370	1.119	0.569
26	27	0.0014	0.0147	0.2396	98.5	0.036	0.373	0.973	0.355	1.119	0.584
26	28	0.0043	0.0474	0.7802	317.7	0.034	0.373	0.982	0.338	1.119	0.589
26	29	0.0057	0.0625	1.029	418.9	0.034	0.373	0.983	0.340	1.119	0.590
28	29	0.0014	0.0151	0.249	101.2	0.035	0.373	0.984	0.346	1.119	0.590

Appendix B – AVR parameters

Machine no1.

```
// Exciter ST1
st1_Tr = 0.01          // voltage meter time constant [s]
st1_Vimax = 0.1        // control error high limit [pu(V_base)]
st1_Vimin = -0.1       // control error low limit [pu(V_base)]
st1_Tc = 1              // transient filter lead time constant [s]
st1_Tb = 10             // transient filter lag time constant [s]
st1_Ka = 200            // regulator gain (incl base conv V_base/Efd_base)
st1_Ta = 0.015          // regulator time constant [s]
st1_Vrmax = 5           // regulator high limit
st1_Vrmin = -5          // regulator low limit
st1_Kc=0                // transformer fed systems
st1_Kf = 0.0             // feedback gain (incl base conv Efd_base/V_base)
st1_Tf = 1.0             // feedback time constant [s]

// Stabilizer Input selection
// 1 - rotor speed deviation (SM device Omega_1 only)
// 2 - bus frequency deviation
// 3 - electrical power
// 4 - accelerating power
pss1a_InputSelec=1
pss1a_T1 = 5.0          // lead time constant no1
pss1a_T2 = 0.6           // lag time constant no1
pss1a_T3 = 3.0           // lead time constant no2
pss1a_T4 = 0.5           // lag time constant no2
pss1a_T5 = 10             // washout time constant
pss1a_T6 = 0.0             // transducer time constant
pss1a_Ks = 1               // gain
pss1a_Vstmax = 0.20      // Maximum output limit
pss1a_Vstmin = -0.20     // Minimum output limit
pss1a_A1=0,pss1a_A2=0      // High frequency filter coefficients
```

```
// Governor-turbine parameters (IEEEG1)
ieeeeg1_K      = 20      //
ieeeeg1_T1     = 0.0     //
ieeeeg1_T2     = 0       //
ieeeeg1_T3     = 0.075   //
ieeeeg1_Uo     = 0.6786  //
ieeeeg1_Uc     = -1.0    // gate min closing speed (pu@SM_MVABASE)
ieeeeg1_Pmax   = 0.90   //
ieeeeg1_Pmin   = 0.0     //
ieeeeg1_T4     = 0.3     // Steam flow time cst(s)
ieeeeg1_K1     = 0.2     // Fraction of LP mech power
ieeeeg1_K2     = 0       // Fraction of HP mech power
ieeeeg1_T5     = 10      // First reheater time cst
ieeeeg1_K3     = 0.4     // Fraction of LP mech power
ieeeeg1_K4     = 0       // Fraction of HP mech power
ieeeeg1_T6     = 0.6     // Second reheater time cst
ieeeeg1_K5     = 0.4     // Fraction of LP mech power
ieeeeg1_K6     = 0       // Fraction of HP mech power
ieeeeg1_T7     = 0       // Crossover reheater time cst
ieeeeg1_K7     = 0       // Fraction of LP mech power
ieeeeg1_K8     = 0       // Fraction of HP mech power
```

Machine no.2

```

// Exciter ST1
st1_Tr = 0.01          // voltage meter time constant [s]
st1_Vimax = 0.1         // control error high limit [pu(V_base)]
st1_Vimin = -0.1        // control error low limit [pu(V_base)]
st1_Tc = 1               // transient filter lead time constant [s]
st1_Tb = 10              // transient filter lag time constant [s]
st1_Ka = 200             // regulator gain (incl base conv V_base/Efd_base)
st1_Ta = 0.015            // regulator time constant [s]
st1_Vrmax = 5             // regulator high limit
st1_Vrmin = -5            // regulator low limit
st1_Kc=0                 // transformer fed systems
st1_Kf = 0.0              // feedback gain (incl base conv Efd_base/V_base)
st1_Tf = 1.0                // feedback time constant [s]

// Stabilizer Input selection
// 1 - rotor speed deviation (SM device Omega_1 only)
// 2 - bus frequency deviation
// 3 - electrical power
// 4 - accelerating power
pss1a_InputSelec=1
pss1a_T1 = 5.0           // lead time constant no1
pss1a_T2 = 0.4            // lag time constant no1
pss1a_T3 = 1.0            // lead time constant no2
pss1a_T4 = 0.1            // lag time constant no2
pss1a_T5 = 10             // washout time constant
pss1a_T6 = 0.0            // transducer time constant
pss1a_Ks = 0.5            // gain
pss1a_Vstmax = 0.20       // Maximum output limit
pss1a_Vstmin = -0.20      // Minimum output limit
pss1a_A1=0,pss1a_A2=0      // High frequency filter coefficients

```

Machine no.3

```

// Exciter ST1
st1_Tr = 0.01          // voltage meter time constant [s]
st1_Vimax = 0.1         // control error high limit [pu(V_base)]
st1_Vimin = -0.1        // control error low limit [pu(V_base)]
st1_Tc = 1               // transient filter lead time constant [s]
st1_Tb = 10              // transient filter lag time constant [s]
st1_Ka = 200             // regulator gain (incl base conv V_base/Efd_base)
st1_Ta = 0.015            // regulator time constant [s]
st1_Vrmax = 5             // regulator high limit
st1_Vrmin = -5            // regulator low limit
st1_Kc=0                 // transformer fed systems
st1_Kf = 0.0              // feedback gain (incl base conv Efd_base/V_base)
st1_Tf = 1.0                // feedback time constant [s]

// Stabilizer Input selection
// 1 - rotor speed deviation (SM device Omega_1 only)
// 2 - bus frequency deviation
// 3 - electrical power
// 4 - accelerating power
pss1a_InputSelc=1
pss1a_T1 = 3.0           // lead time constant no1
pss1a_T2 = 0.2           // lag time constant no1
pss1a_T3 = 2.0           // lead time constant no2
pss1a_T4 = 0.2           // lag time constant no2
pss1a_T5 = 10             // washout time constant
pss1a_T6 = 0.0           // transducer time constant
pss1a_Ks = 0.5           // gain
pss1a_Vstmax = 0.20       // Maximum output limit
pss1a_Vstmin = -0.20      // Minimum output limit
pss1a_A1=0,pss1a_A2=0     // High frequency filter coefficients

```

Machine no4

```

// Exciter ST1
st1_Tr = 0.01          // voltage meter time constant [s]
st1_Vimax = 0.1         // control error high limit [pu(V_base)]
st1_Vimin = -0.1        // control error low limit [pu(V_base)]
st1_Tc = 1               // transient filter lead time constant [s]
st1_Tb = 10              // transient filter lag time constant [s]
st1_Ka = 200             // regulator gain (incl base conv V_base/Efd_base)
st1_Ta = 0.015            // regulator time constant [s]
st1_Vrmax = 5             // regulator high limit
st1_Vrmin = -5            // regulator low limit
st1_Kc=0                 // transformer fed systems
st1_Kf = 0.0              // feedback gain (incl base conv Efd_base/V_base)
st1_Tf = 1.0                // feedback time constant [s]

```

```

// Stabilizer Input selection
// 1 - rotor speed deviation (SM device Omega_1 only)
// 2 - bus frequency deviation
// 3 - electrical power
// 4 - accelerating power
pss1a_InputSelec=1
pss1a_T1 = 1.0          // lead time constant no1
pss1a_T2 = 0.1          // lag time constant no1
pss1a_T3 = 1.0          // lead time constant no2
pss1a_T4 = 0.3          // lag time constant no2
pss1a_T5 = 10           // washout time constant
pss1a_T6 = 0.0          // transducer time constant
pss1a_Ks = 2             // gain
pss1a_Vstmax = 0.20     // Maximum output limit
pss1a_Vstmin = -0.20    // Minimum output limit
pss1a_A1=0,pss1a_A2=0   // High frequency filter coefficients

```

Machine no.5

```

// Exciter ST1
st1_Tr = 0.01           // voltage meter time constant [s]
st1_Vimax = 0.1          // control error high limit [pu(V_base)]
st1_Vimin = -0.1         // control error low limit [pu(V_base)]
st1_Tc = 1                // transient filter lead time constant [s]
st1_Tb = 10               // transient filter lag time constant [s]
st1_Ka = 200              // regulator gain (incl base conv V_base/Efd_base)
st1_Ta = 0.015            // regulator time constant [s]
st1_Vrmax = 5             // regulator high limit
st1_Vrmin = -5            // regulator low limit
st1_Kc=0                  // transformer fed systems
st1_Kf = 0.0               // feedback gain (incl base conv Efd_base/V_base)
st1_Tf = 1.0               // feedback time constant [s]

// Stabilizer Input selection
// 1 - rotor speed deviation (SM device Omega_1 only)
// 2 - bus frequency deviation
// 3 - electrical power
// 4 - accelerating power
pss1a_InputSelec=1
pss1a_T1 = 1.5          // lead time constant no1
pss1a_T2 = 0.2          // lag time constant no1
pss1a_T3 = 1.0          // lead time constant no2
pss1a_T4 = 0.1          // lag time constant no2
pss1a_T5 = 10           // washout time constant
pss1a_T6 = 0.0          // transducer time constant
pss1a_Ks = 1             // gain
pss1a_Vstmax = 0.20     // Maximum output limit
pss1a_Vstmin = -0.20    // Minimum output limit
pss1a_A1=0,pss1a_A2=0   // High frequency filter coefficients

```

Machine no.6

```

// Exciter ST1
st1_Tr = 0.01          // voltage meter time constant [s]
st1_Vimax = 0.1         // control error high limit [pu(V_base)]
st1_Vimin = -0.1        // control error low limit [pu(V_base)]
st1_Tc = 1               // transient filter lead time constant [s]
st1_Tb = 10              // transient filter lag time constant [s]
st1_Ka = 200             // regulator gain (incl base conv V_base/Efd_base)
st1_Ta = 0.015            // regulator time constant [s]
st1_Vrmax = 5             // regulator high limit
st1_Vrmin = -5            // regulator low limit
st1_Kc=0                 // transformer fed systems
st1_Kf = 0.0              // feedback gain (incl base conv Efd_base/V_base)
st1_Tf = 1.0              // feedback time constant [s]

// Stabilizer Input selection
// 1 - rotor speed deviation (SM device Omega_1 only)
// 2 - bus frequency deviation
// 3 - electrical power
// 4 - accelerating power
pss1a_InputSelec=1
pss1a_T1 = 0.5           // lead time constant no1
pss1a_T2 = 0.1           // lag time constant no1
pss1a_T3 = 0.5           // lead time constant no2
pss1a_T4 = 0.05          // lag time constant no2
pss1a_T5 = 10             // washout time constant
pss1a_T6 = 0.0             // transducer time constant
pss1a_Ks = 4               // gain
pss1a_Vstmax = 0.20       // Maximum output limit
pss1a_Vstmin = -0.20      // Minimum output limit
pss1a_A1=0,pss1a_A2=0     // High frequency filter coefficients

```

Machine no.7

```

// Exciter ST1
st1_Tr = 0.01          // voltage meter time constant [s]
st1_Vimax = 0.1         // control error high limit [pu(V_base)]
st1_Vimin = -0.1        // control error low limit [pu(V_base)]
st1_Tc = 1               // transient filter lead time constant [s]
st1_Tb = 10              // transient filter lag time constant [s]
st1_Ka = 200             // regulator gain (incl base conv V_base/Efd_base)
st1_Ta = 0.015            // regulator time constant [s]
st1_Vrmax = 5             // regulator high limit
st1_Vrmin = -5            // regulator low limit
st1_Kc=0                 // transformer fed systems
st1_Kf = 0.0              // feedback gain (incl base conv Efd_base/V_base)
st1_Tf = 1.0              // feedback time constant [s]

```

```

// Stabilizer Input selection
// 1 - rotor speed deviation (SM device Omega_1 only)
// 2 - bus frequency deviation
// 3 - electrical power
// 4 - accelerating power
pss1a_InputSelec=1
// Stabilizer PSS1A
pss1a_T1 = 0.2          // lead time constant no1
pss1a_T2 = 0.02         // lag time constant no1
pss1a_T3 = 0.5          // lead time constant no2
pss1a_T4 = 0.1          // lag time constant no2
pss1a_T5 = 10           // washout time constant
pss1a_T6 = 0.0          // transducer time constant
pss1a_Ks = 7.5          // gain
pss1a_Vstmax = 0.20     // Maximum output limit
pss1a_Vstmin = -0.20    // Minimum output limit
pss1a_A1=0,pss1a_A2=0   // High frequency filter coefficients

```

Machine no8

```

// Exciter ST1
st1_Tr = 0.01           // voltage meter time constant [s]
st1_Vimax = 0.1          // control error high limit [pu(V_base)]
st1_Vimin = -0.1         // control error low limit [pu(V_base)]
st1_Tc = 1                // transient filter lead time constant [s]
st1_Tb = 10               // transient filter lag time constant [s]
st1_Ka = 200              // regulator gain (incl base conv V_base/Efd_base)
st1_Ta = 0.015             // regulator time constant [s]
st1_Vrmax = 5              // regulator high limit
st1_Vrmin = -5             // regulator low limit
st1_Kc=0                  // transformer fed systems
st1_Kf = 0.0                // feedback gain (incl base conv Efd_base/V_base)
st1_Tf = 1.0                // feedback time constant [s]

// Stabilizer Input selection
// 1 - rotor speed deviation (SM device Omega_1 only)
// 2 - bus frequency deviation
// 3 - electrical power
// 4 - accelerating power
pss1a_InputSelec=1
pss1a_T1 = 1.0            // lead time constant no1
pss1a_T2 = 0.2             // lag time constant no1
pss1a_T3 = 1.0             // lead time constant no2
pss1a_T4 = 0.1             // lag time constant no2
pss1a_T5 = 10              // washout time constant
pss1a_T6 = 0.0              // transducer time constant
pss1a_Ks = 2                // gain
pss1a_Vstmax = 0.20        // Maximum output limit
pss1a_Vstmin = -0.20       // Minimum output limit

```

```
pss1a_A1=0, pss1a_A2=0      // High frequency filter coefficients
```

Machine no.9

```
// Exciter ST1
st1_Tr = 0.01          // voltage meter time constant [s]
st1_Vimax = 0.1        // control error high limit [pu(V_base)]
st1_Vimin = -0.1       // control error low limit [pu(V_base)]
st1_Tc = 1              // transient filter lead time constant [s]
st1_Tb = 10             // transient filter lag time constant [s]
st1_Ka = 200            // regulator gain (incl base conv V_base/Efd_base)
st1_Ta = 0.015          // regulator time constant [s]
st1_Vrmax = 5           // regulator high limit
st1_Vrmin = -5          // regulator low limit
st1_Kc=0                // transformer fed systems
st1_Kf = 0.0            // feedback gain (incl base conv Efd_base/V_base)
st1_Tf = 1.0             // feedback time constant [s]
```

```
// Stabilizer Input selection
// 1 - rotor speed deviation (SM device Omega_1 only)
// 2 - bus frequency deviation
// 3 - electrical power
// 4 - accelerating power
pss1a_InputSelec=1
pss1a_T1 = 1.0          // lead time constant no1
pss1a_T2 = 0.5          // lag time constant no1
pss1a_T3 = 2.0          // lead time constant no2
pss1a_T4 = 0.1          // lag time constant no2
pss1a_T5 = 10            // washout time constant
pss1a_T6 = 0.0          // transducer time constant
pss1a_Ks = 2              // gain
pss1a_Vstmax = 0.20     // Maximum output limit
pss1a_Vstmin = -0.20    // Minimum output limit
pss1a_A1=0, pss1a_A2=0      // High frequency filter coefficients
```

Machine no.10

```
// Exciter ST1
st1_Tr = 0.01          // voltage meter time constant [s]
st1_Vimax = 0.1        // control error high limit [pu(V_base)]
st1_Vimin = -0.1       // control error low limit [pu(V_base)]
st1_Tc = 1              // transient filter lead time constant [s]
st1_Tb = 10             // transient filter lag time constant [s]
st1_Ka = 200            // regulator gain (incl base conv V_base/Efd_base)
st1_Ta = 0.015          // regulator time constant [s]
st1_Vrmax = 5           // regulator high limit
st1_Vrmin = -5          // regulator low limit
st1_Kc=0                // transformer fed systems
st1_Kf = 0.0            // feedback gain (incl base conv Efd_base/V_base)
st1_Tf = 1.0             // feedback time constant [s]
```

```
// Stabilizer Input selection
// 1 - rotor speed deviation (SM device Omega_1 only)
// 2 - bus frequency deviation
// 3 - electrical power
// 4 - accelerating power
pss1a_InputSelec=1
pss1a_T1 = 1.0          // lead time constant no1
pss1a_T2 = 0.05         // lag time constant no1
pss1a_T3 = 3.0          // lead time constant no2
pss1a_T4 = 0.5          // lag time constant no2
pss1a_T5 = 10           // washout time constant
pss1a_T6 = 0.0           // transducer time constant
pss1a_Ks = 1             // gain
pss1a_Vstmax = 0.20      // Maximum output limit
pss1a_Vstmin = -0.20     // Minimum output limit
pss1a_A1=0,pss1a_A2=0    // High frequency filter coefficients
```

Appendix C – Reference

- [1] IEEE Task Force on Load Representation for Dynamic Performance. Load Representation for Dynamic Performance Analysis. IEEE Transactions on Power Systems, Vol. 8, No. 2, May 1993
- [2] IEEE Standard 421.5, 1982.
- [3] HYDRAULIC TURBINE AND TURBINE CONTROL MODELS FOR SYSTEM PYNAMIC STUDIES. Working Group on Prime Mover and Energy Supply. Models for System Dynamic Performance Studies. Transactions on Power Systems, Vol. 7, NO. 1, February 1992